50272-101

REPORT DOCUMENTATION PAGE	1. REPORT NO. NSF/ENG-92003	2.	3. PB93-223709
4. Title and Subtitle "Earthquake Engineering Research at Berkeley-1992"			5. Report Date October 1992 6.
7. Author(s)			8. Performing Organization Rept. No. UCB/EERC-92/13
9. Performing Organization Name and Address Earthquake Engineering Research Center University of California, Berkeley 1301 So. 46th Street Richmond, Calif. 94804			10. Project/Task/Work Unit No. 11. Contract(C) or Grant(G) No. (C) (G) BCS-9013334
12. Sponsoring Organization Name and Address National Science Foundation 1800 G Street, N.W. Washington, D.C. 20550	Earthquake Engineering Research Cent. University of California at Berkeley 1301 S. 46th Street Richmond, Calif. 94804		13. Type of Report & Period Covered 14.
15. Supplementary Notes			

16. Abstract (Limit: 200 words)

Twenty-five papers by faculty participants and research personnel associated with the Earthquake Engineering Research Center of the University of California at Berkeley were presented at the Tenth World Conference on Earthquake Engineering held in Madrid, Spain, July 19-24, 1992. The papers have been compiled in this report to illustrate some of the research work in earthquake engineering being conducted at the University of California at Berkeley.

17. Document Analysis a. Descriptors

b. Identifiers/Open-Ended Terms

c. COSATI Field/Group

18. Availability Statement: Release Unlimited	19. Security Class (This Report) unclassified	21. No. of Pages 218
	20. Security Class (This Page) unclassified	22. Price

(See ANSI-Z39.18) See Instructions on Reverse OPTIONAL FORM 272 (4-77) (Formerly NTIS-35)

PB93-223709

REPORT NO.
UCB/EERC-92/13
OCTOBER 1992

EARTHQUAKE ENGINEERING RESEARCH CENTER

EARTHQUAKE ENGINEERING RESEARCH AT BERKELEY – 1992

Papers presented by faculty participants and research personnel associated with the Earthquake Engineering Research Center at the Tenth World Conference on Earthquake Engineering, Madrid, Spain, July 1992.

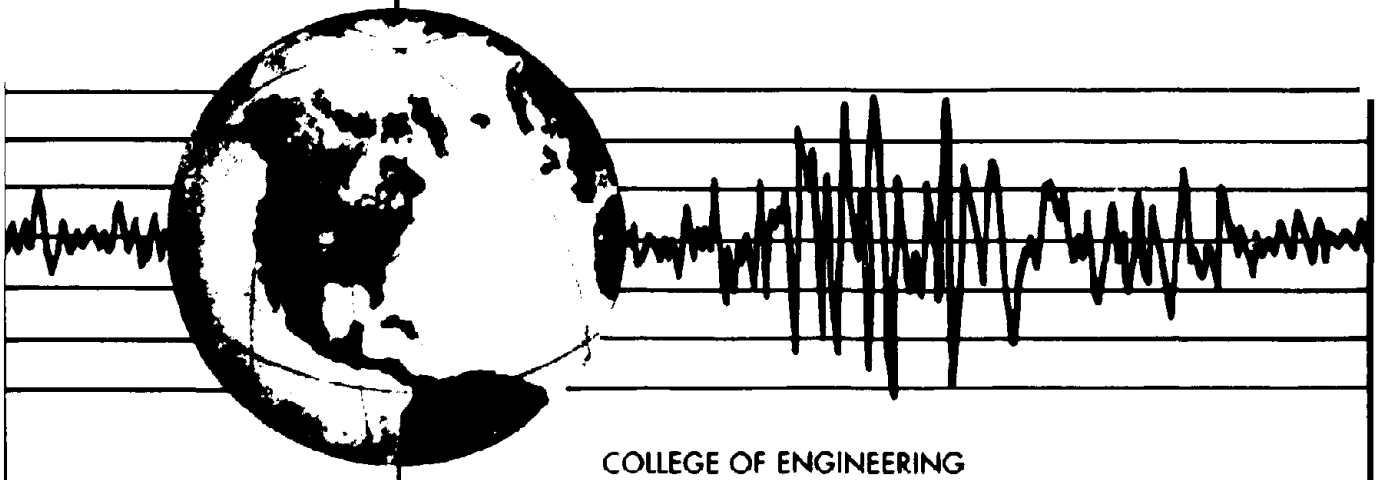

COLLEGE OF ENGINEERING

UNIVERSITY OF CALIFORNIA AT BERKELEY

For sale by the National Technical Information Service, U.S. Department of Commerce, Springfield, Virginia 22161

See back of report for up to date listing of EERC reports.

DISCLAIMER

Any opinions, findings, and conclusions or recommendations expressed in this publication are those of the authors and do not necessarily reflect the views of the Sponsors or the Earthquake Engineering Research Center, University of California at Berkeley.

EARTHQUAKE ENGINEERING RESEARCH AT BERKELEY — 1992

Papers by faculty participants and research personnel
associated with the Earthquake Engineering Research Center,
presented at the Tenth World Conference on Earthquake Engineering
Madrid, Spain
July 1992

Report No. UCB/EERC-92/13
Earthquake Engineering Research Center
College of Engineering
University of California at Berkeley

October 1992

FOREWORD

Twenty-five papers by faculty participants and research personnel associated with the Earthquake Engineering Research Center of the University of California at Berkeley were presented at the Tenth World Conference on Earthquake Engineering held in Madrid, Spain, July 19-24, 1992. The papers have been compiled in this report to illustrate some of the research work in earthquake engineering being conducted at the University of California at Berkeley. The research has been sponsored by the following agencies:

National Science Foundation
American Institute of Steel Construction
County of Los Angeles Department of Public Works
CUREe-Kajima
Harza Engineering Company
U.S. Bureau of Reclamation
U.S.-China Protocol on Earthquake Studies
U.S. Corps of Engineers

Table of Contents

Workshop — Learning from Earthquakes

Major issues and future directions in earthquake-resistant design

V.V. Bertero
Nishkian Professor Emeritus of Structural Engineering and Research Engineer at the Earthquake Engineering Research Center at the University of California at Berkeley, USA

ABSTRACT: After general remarks about the nature of the earthquake (EQ) problem, the conditions that determine the occurrence of an EQ disaster, and the resulting seismic risks in our urban and rural areas, the role and importance of EQ Engineering, particularly EQ-Resistant Design (EQRD) and EQ-Resistant Construction (EQRC) in the overall problem of controlling these risks are discussed. The need for EQ preparedness programs is emphasized. Analysis of events of the last four years since the 1988 WCEE shows that seismic risks have increased rather than decreased. Evaluation of the lessons learned from recent EQs and research results provides reasons for this increase, points out that the lessons learned are quickly forgotten or not taken seriously, and indicates the need for EQ preparedness to control these risks. This will require control of the built environment, which is a complex problem requiring integration of knowledge and collaboration of experts from many different disciplines. In a brief evaluation of the state of the knowledge and particularly the state of the practice in EQRD of new structures and seismic upgrading of existing facilities, major issues and pressing problems requiring short-term solutions are identified. Emphasis is placed on identifying the main issues in the formulation and application of seismic code procedures in EQRD, particularly regarding the establishment of reliable design EQs. Solutions are suggested based on an energy approach. A conceptual methodology for the numerical design part of EQRD is proposed. This methodology is based on well-established fundamental principles of structural dynamics, mechanical behavior of entire facility systems and comprehensive design, and is in compliance with the world-wide accepted philosophy of EQRD. The main advantages of this conceptual methodology are discussed. The lecture concludes with pleas, first to all of the experts in the different disciplines that are involved in solving the EQ problem to collaborate closely toward a timely solution to this problem; and secondly to all of the participants in this 10th WCEE to screen the research and development (R&D) results that are presented at this conference and disseminate in their communities those that can be applied immediately, and also to collaborate in the preparation and implementation of EQ preparedness programs.

1 INTRODUCTION

1.1 *Introductory remarks*

Thank you very much, Dr. Blásquez, for your kind introduction. Professor Grandori, president of the International Association for Earthquake Engineering (IAEE), members of the Steering Committee for the Tenth World Conference, officers and national delegates for the IAEE, distinguished guests, fellow participants, ladies and gentlemen:

It is a privilege to attend this Tenth World Conference on Earthquake Engineering (10th WCEE), and a great honor for me to participate through this keynote lecture in this significant event. This gathering of more than 1,500 leading researchers and practitioners from so many countries, with its impressive technical program, gives clear evidence of the remarkable progress in this so important field since the first WCEE in 1956. It is indeed a great pleasure every four years to see and renew relationships that I have had over the years with so many colleagues around the world and with my ex-students and research associates working in the field of EQ engineering. It is heartening to see so many young engineers and scientists getting together with those of us who have been working for many years in this field, because all of these young researchers and practitioners will be conducting the needed research and development (R&D) and implementing the results of such R&D in the field to reduce the seismic risks in our urban and rural areas. The importance of implementation cannot be overemphasized: there cannot be reduction of seismic risks without implementation of research results and developments in the field. This in turn requires transfer of knowledge to practitioners and to government officials who manage the natural disaster programs. It would be of great interest to know how many of the 1,500 participants are practitioners and government officials, because they are the ones who will make possible the so-needed improvement in seismic risk reduction by implementing the results of R&D. To achieve this implementation it will be necessary to formulate and implement massive and comprehensive education programs. This lecture, which has the main objectives and scope outlined below, will emphasize the need for such education and implementation programs.

1.2 *Objectives and scope of the lecture*

When I was approached to prepare and deliver this keynote lecture, my first intention as a teacher and researcher was to prepare a technical lecture on "*Major issues and future directions in Earthquake-Resistant Design (EQRD) of new structures and seismic upgrading of existing hazardous facilities.*" Then a series of events, including recent EQs and my participation in a series of committees on EQ hazard reduction, led me to change my mind and start looking more deeply at the main objective of the IAEE, which is: "*To promote international cooperation among scientists and engineers in the field of EQ engineering through the interchange of knowledge, ideas and the results of research and practical experience.*" I questioned whether this is all that the IAEE expects, and I questioned the purpose of promoting interchange. The answer is in the definition of

EQ Engineering: *"EQ Engineering is the branch of engineering that encompasses the practical efforts to reduce, and ideally to avoid, EQ hazards."*

Clearly, EQ Engineering is of great importance to human life and welfare. I decided to look at the role and importance of EQ Engineering, particularly EQRD and EQRC, not only as a researcher, but also from a humanistic viewpoint. I decided to present a lecture with the following main objectives and scope:

(1) To make some general remarks about the nature of the EQ problem and the resulting seismic risks in our urban and rural areas.

(2) To review the role and importance of EQ Engineering, particularly EQRC of existing and new facilities, within the overall problem of reducing seismic risks in our urban and rural areas to acceptable levels, which should be the ultimate goal of EQ Engineering.

(3) To discuss briefly where we are in our knowledge and particularly our practice in the EQRD of new structures and the seismic upgrading of existing constructions. (This discussion will be based on lessons learned from recent EQs and associated research. Most of these lessons are discussed in the "Primera Conferencia International Torroja," 1989 by the lecturer, whose publication has been distributed to the participants of this 10WCEE). This will involve: (a) an attempt to identify the pressing problems requiring reliable solutions in the short term; and (b) suggestions for future directions for our R&D and practice for finding and implementing such required solutions.

(4) To conclude with: (a) first, a brief discussion of the need for a massive and comprehensive education program to transmit our present knowledge, permitting implementation of EQ preparedness programs and results of R&D in EQRD and EQRC, which will lead quickly to reduction to acceptable levels of the seismic risks in urban and rural areas; and (b) a plea to experts in the different disciplines involved in solving the EQ problem to collaborate closely toward a timely solution.

It should be noted that all that I will say has been said in previous WCEEs. The only difference is in the things that I believe should be emphasized so that seismic risk can be reduced quickly to a socially and economically acceptable level. These emphases will be on: *first*, a thorough assessment of the results of EQ Engineering R&D that has been conducted and can be immediately applied to improve the state of the practice in this field through formulation of better seismic codes (format and regulations) for EQRD and EQRC of new structures and upgrading of existing hazardous facilities than those that are presently enforced. This will require collaboration of experts from the many disciplines involved in EQ Engineering. *Second*, comprehensive EQ preparedness programs must be formulated; and *third*, there is a need for a massive and comprehensive education program to facilitate systematic and strict implementation of preparedness programs and new codes.

2. THE NATURE OF THE EQ PROBLEM; OCCURRENCE OF AN EQ DISASTER; AND CONTROL OF SEISMIC RISKS

2.1 *The nature of the EQ problem*

The nature of this problem has been very well defined by Press (1984): "Earthquakes are a very special type of natural hazard in the sense that they are very rare, low-probability events, whose consequences, when they do occur, are very large in terms of destruction and suffering." Hazards with these characteristics create the difficult public policy problem of how to sustain public interest and involvement and attract adequate government resources for mitigation programs. Only countries with recent catastrophes become concerned and organize national programs. Unfortunately, a few years after the catastrophe, efforts to implement these programs usually decrease and fall into neglect. It is a high duty for a civilized society to anticipate and control, rather than react only after, a disaster.

EQs are natural disasters whose feature is that most of the human and economic losses are not due to the EQ mechanisms, but to failures of human-made facilities: buildings and lifelines, such as dams, bridges, transportation systems, etc., which supposedly were designed and constructed for the comfort of human beings. Although this is depressing, it is also fortunate and encouraging, because it tells us that in the long run the EQ problem is in principle solvable.

With sufficient resources for R&D, formulation of *EQ preparedness programs*, and *education* needed for the *implementation* of the results of this R&D. EQs are hazards to which it is in our power to respond effectively. We can reduce their threat over time by as much as we want. We can learn where not to build and how to build so that facilities will not fail. On the average, more than 10,000 EQs are recorded each year, of which about 60 are significant (producing significant damages or having a magnitude M≥6.5). Between 1890 and 1978, an average of more than 10,000 people died in EQs per year (Fig. 1) and nearly 500,000 people were left homeless. Economic losses due to physical damage amount to about $10 billion per year.

The psychological impact on millions of people who experience major EQs is an enormous, complex fear that remains a nightmare to them for many years. Thus, it is of importance that we engineers and scientists attempt to find the reasons for EQ disasters and to eliminate or reduce the potentially catastrophic consequences of major EQs.

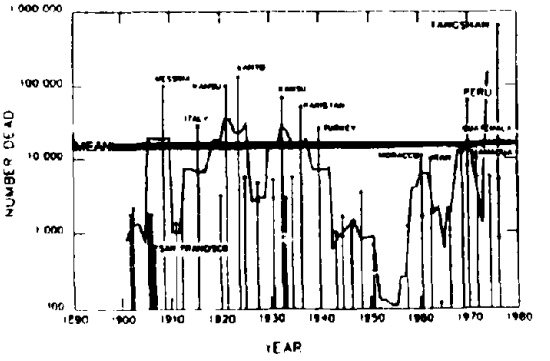

Figure 1. Loss of life caused by major EQs (after Hiroo Kanamori, 1978)

2.2 *Occurrence of an EQ disaster*

2.2.1 *EQ disaster potential*. Four conditions determine the occurrence of an EQ disaster. The first is the

magnitude of the EQ, since a small-magnitude EQ will not induce ground-shaking severe enough to produce extensive damage. Secondly, the EQ source must be sufficiently close to the urban area, because at greater distances the ground-shaking attenuates to below the level required to induce serious damage [it should be noted that EQ disasters can occur at distances from the source considerably greater than the 160 to 240 km at most which has usually been assumed: 400 km (in the 1957 and 1985 Mexico EQs) and over 900 km (in the 1972 Caucete (Argentina) EQ]. These experiences show that under special conditions damage can occur at epicentral distances even larger than 400 km. Thirdly, the size and distribution of the population and the economic development (high-technology industries); and fourthly, the degree of EQ preparedness, determine the possibility of disaster. Obviously, *the potential disaster becomes greater the larger and nearer the EQ is to an urban center, the larger the population, the greater the economic development, and the poorer the preparation.*

Clearly, EQ hazard depends not only on the seismicity of the region, but also on its population density, economic development, and degree of preparedness. In this respect, EQ hazards are becoming more important each year. Even though seismicity remains constant, the uncontrolled and rapid increase in population, urbanization and economic development of our urban areas are not being counterbalanced by an increase in preparedness. For example, in terms of population and economic development, disaster potential in California is now at least ten times what it was at the time of the 1906 San Francisco EQ [Committee on EQ Engineering Research, 1982].

In 1988, in Tokyo, during the 9thWCEE, Professor Hudson [1988], in the conclusion to his excellent keynote address, questioned the overall effectiveness of the IAEE's work on the following questions: *(1) To what extent have our efforts helped to reduce the threat of EQs? (2) How far along the way are we to preventing EQs from becoming disasters?*

Professor Hudson's conclusion was, *"We must hasten to admit that we are very far from our goal."*

There is no doubt that there has been an impressive increase in knowledge in EQ Engineering, particularly in the seismic upgrading of existing hazardous facilities. However, if today at the 10thWCEE, we ask, *"How effective has this increase in knowledge been in reducing the seismic risks in our urban and rural areas?"* we will have to give practically the same answer. *We are very far from our main goal, which is the reduction of seismic risks in our urban and rural areas. Why is this so?* An answer to this question can be obtained through the following analysis.

2.2.2 *Analysis of what has happened in the four years since the 1988 9th WCEE due to significant EQs.* As previously defined, significant EQs are those events which either produce significant damage or have magnitudes M≥6.5. The main results obtained in this analysis are given in Table 1. The loss of life during this period (1988-1991) is illustrated in the plot of Figure 2.

To summarize, this analysis has shown that the average number of deaths per year has increased, in spite of the fact that the largest magnitudes, M_b and M_s (surface wave), of all of the recorded EQs do not exceed 6.8 and 7.7, respectively. The total number of

Table 1. Effects of significant EQs during 1988-1992

	No. OF SIGNIFICANT EQs	MAX. M_b	MAX. M_S	No. DEAD	No. HOMELESS
1988	60	6.8	7.5	27,000 to 32,000	800,000
1989	60	6.5	7.4	600	210,000
1990	73	6.7	7.7	42,000 to 52,000	500,000
1991	61	6.5	7.4	3,300	209,000
1992*	26		7.4	522 to 840	50,000

*UP TO JULY 1992

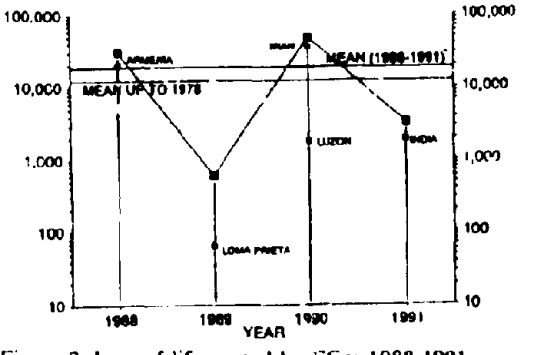

Figure 2. Loss of life caused by EQs: 1988-1991

people left homeless by EQs during this last four years exceeded 1.7 million, i.e., an average of 425,000 per year. A brief description of the main EQs that occurred during this four-year period follows.

• *The Armenian EQ of December 7, 1988* [Wyllie et al. (1989) and Bommer and Ambraseys (1988)]: The main shock of this EQ, with a body wave magnitude of M_b=6.3 and corresponding to a surface wave magnitude M_s=6.8, occurred at 11:41 am local time near the relatively new town of Spitak (population about 20,000), which is located midway between the cities of Leninakan (population about 290,000) and Kirovakan (population about 170,000), located about 60 km east of Leninakan. This main shock, with a focus (hypocenter) estimated at 15 km and with strong motion lasting nearly 30 seconds, caused catastrophic damage, and was followed four minutes later by an aftershock with M_b=5.9, which caused significant additional damage. Although the exact number of people killed is not known, official reports placed it at about 28,000 (ranging from 25,000 to 30,000) and unofficial reports gave a death toll ranging from 45,000 to 60,000. It has been estimated that about 130,000 people were injured, of whom 18,000 required hospital care. The mortality among the injured was also high, especially among those who remained buried alive for long periods of time. The number of people left homeless was estimated at between 500,000 and 700,000. The Armenian EQ was one of the most lethal

(a) Collapsed and damaged 9-story precast RC frame buildings

(b) Collapsed 6-story precast frame-panel apartment building

(c) Collapsed precast frame panel building (foreground), standing precast panel buildings (background)

(d) Failure of infill walls and planks of a precast concrete frame building

Figure 3. 1988 Armenia EQ. Photos illustrating collapsed modern precast RC frame buildings [EERI Slide Library]

(a) Village completely demolished

(c) Large boulders that rolled down the mountains caused significant damage to buildings

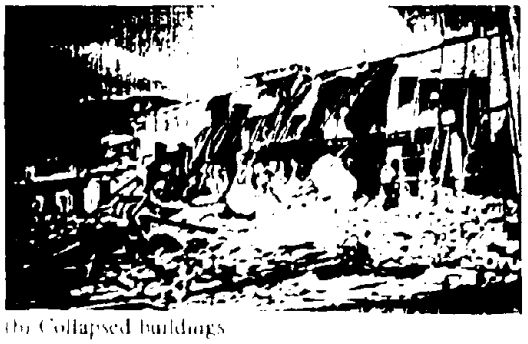

(b) Collapsed buildings

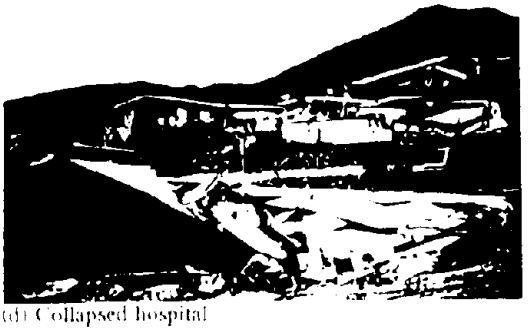

(d) Collapsed hospital

Figure 4. 1990 Manjil-Rudbar Iran EQ. Photos illustrating damage of buildings (courtesy of A.H. Astaneh)

of the decade, but an even more important lesson from this M_s=6.8 EQ is that most of its losses resulted from the collapse of modern buildings (Figure 3).

• *The Manjil-Rudbar, Iran, EQ of June 21, 1990* [Astaneh (1990)]: The magnitudes of this EQ, which occurred in the northern part of Iran at 0:30 (local time), were M_b=6.8 and M_s=7.6. It has been estimated that more than 35,000 (up to 50,000) persons were killed and that about 400,000 persons became homeless. Hundreds of towns and villages were destroyed [Figure 4(a)], and more than 130,000 homes and commercial buildings were damaged [Figure 4(b)]. A very severe aftershock of Richter M=6, which occurred 12 hours after the main shock on June 21, contributed to the collapse of many structures that had been damaged during the main shock. The Manjil-Rudbar EQ also caused severe damage to transportation facilities and lifeline structures. Almost all of the damage appears to have been the result of poor seismic design, construction and maintenance.

• *The Luzon, Philippines EQ of July 16, 1990:* This EQ, with a magnitude of 7.7, affected a large area. More than 2,000 were killed and 3,500 were injured. About 22,000 buildings were destroyed, and the number of persons who were evacuated was estimated at 1,600,000. In Baguio City, more than 50 multi-story RC buildings collapsed or were severely damaged, including several hotels. The hotel shown in Figure 5(a) was designed using seismic code regulations that were practically identical to those of the UBC in the U.S.A. In the city of Dagupan, numerous buildings suffered significant damage owing to soil liquefaction [Figure 5(c)]. A large number of major roads were blocked by numerous landslides.

• *The Loma Prieta EQ of October 17, 1989.* A clear example of the increased seismic risk in California is given by analysis of what occurred during the Loma Prieta EQ. In spite of the fact that the number of injured (around 3,000) and particularly the number who lost their lives (about 65) were surprisingly low, it is clear from analyzing the seismological and engineering aspects of the Loma Prieta EQ that the effects of this EQ have been devastating, producing what has been evaluated as one of the largest natural disasters in U.S. history. Estimates of economic losses due to physical damage alone [i.e., the costs of replacing physical facilities (structures) that were damaged] reach $8 billion. Further EQ consequences that can and will affect people's lives are "functional and indirect damage." Functional damage includes psychological stress and disruption of everyday routine caused by functional disorder of urban facilities; indirect damage denotes the loss of business opportunities. When these are added to the physical damage, total losses will exceed $10 billion.

The economic losses of the Loma Prieta disaster were of the same order as those of the great 1906 San Francisco EQ. This is somewhat surprising, because while the magnitude (M) of the 1906 San Francisco EQ was estimated at M_{SF}=8.3, the surface wave magnitude of the Loma Prieta EQ (M_{LP}) was estimated originally at 6.9 and then upgraded to 7.1. It is clear that the energy, E_{LP}, released by this EQ was significantly lower

(a) Collapsed modern hotel

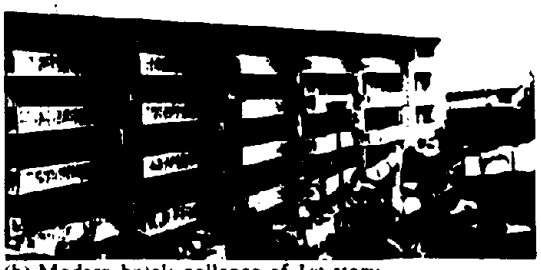

(b) Modern hotel: collapse of 1st story

(c) Tilted corner building

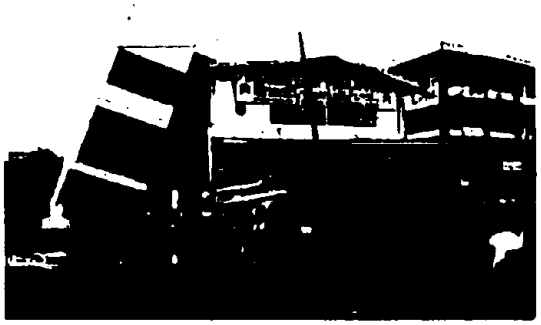

(d) Tilted slender building

Figure 5. 1990 Luzon EQ: photos illustrating collapsed and damaged buildings

than the energy, E_{SF}, released by the San Francisco EQ. In fact,

$$\frac{E_{SF}}{E_{LP}} = 63 \qquad (1)$$

Furthermore, because the epicenter was more than 90 km from Oakland and San Francisco (Figure 6), this EQ cannot properly be considered a Bay Area EQ. Then why was the 1989 Loma Prieta disaster as great as the 1906 San Francisco disaster? Does the greater economic loss mean that our knowledge of how to design and construct EQ-resistant structures has not advanced since 1906? No, that is not the case: even though EQ Engineering is a relatively new branch of engineering research, advances in this field have already played a significant role in reducing seismic hazard through the improvement of the built environment, making possible the design and construction of EQ-resistant civil engineering structures (highway structures, dams, pipelines, critical facilities, high-rise buildings, etc.), and improving the seismic safety of non-engineered construction.

Rather, the answer can be found in the following circumstances. *First*, numerous studies have shown that the greatest current threat to life and safety arising from moderate to severe EQs occurring near urban areas is posed by existing hazardous structures. Many hazardous structures and facilities exist in the U.S., because many buildings were constructed when EQ Engineering was in its infancy. Furthermore, although EQ resistance requirements in building codes have become more stringent and improved significantly, even current codes are not infallible. *Second*, this problem of existing hazardous civil engineering structures has become markedly exacerbated by continuous uncontrolled population growth, increased urbanization, and the development of high-technology industries in our urban areas. The growth of San Francisco and the concomitant increase in EQ risk are illustrated in the photos of Figure 7. In 1906 there were very few medium-rise buildings. There were no bridges and elevated highways connecting San Francisco with the other cities of the Bay Area. This confirms the statement made previously that the disaster potential in California is now significantly higher than it was in 1906.

The Loma Prieta EQ might be called "*the transportation and geotechnical engineers' EQ*," because of: (1) the large number of damaged highways, roads and bridges, and the damage to several facilities at the Oakland airport and harbor; (2) the spectacular failures of one span of the Bay Bridge (Figure 8) and the Cypress Street double-decker viaduct (Figure 9), and the economic impact of these failures; (3) the many failures related to geotechnical effects; and (4) the wealth of strong motion records which permit study of these effects. Although the spectacular failures cannot be considered unexpected, because similar failures have occurred before (Figures 10-13), they do emphasize that either we very quickly forget the lessons learned in previous EQs or we do not take the warnings seriously.

Although the collapse of freeway structures (particularly overpasses) taught the most important lesson learned from the effects of the 1971 San Fernando (or Sylmar) EQ (Figure 10), there is no doubt that the dramatic collapse of the Cypress Street double-deck viaduct (Figure 9) is the first observed collapse of

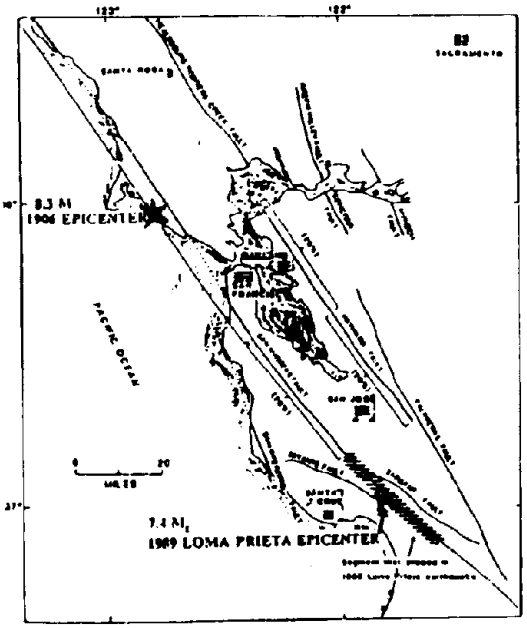

Figure 6. Map showing locations of the 1906 San Francisco and 1989 Loma Prieta EQs

(a) Immediately following the 1906 EQ

(b) San Francisco today

Figure 7. Views of San Francisco

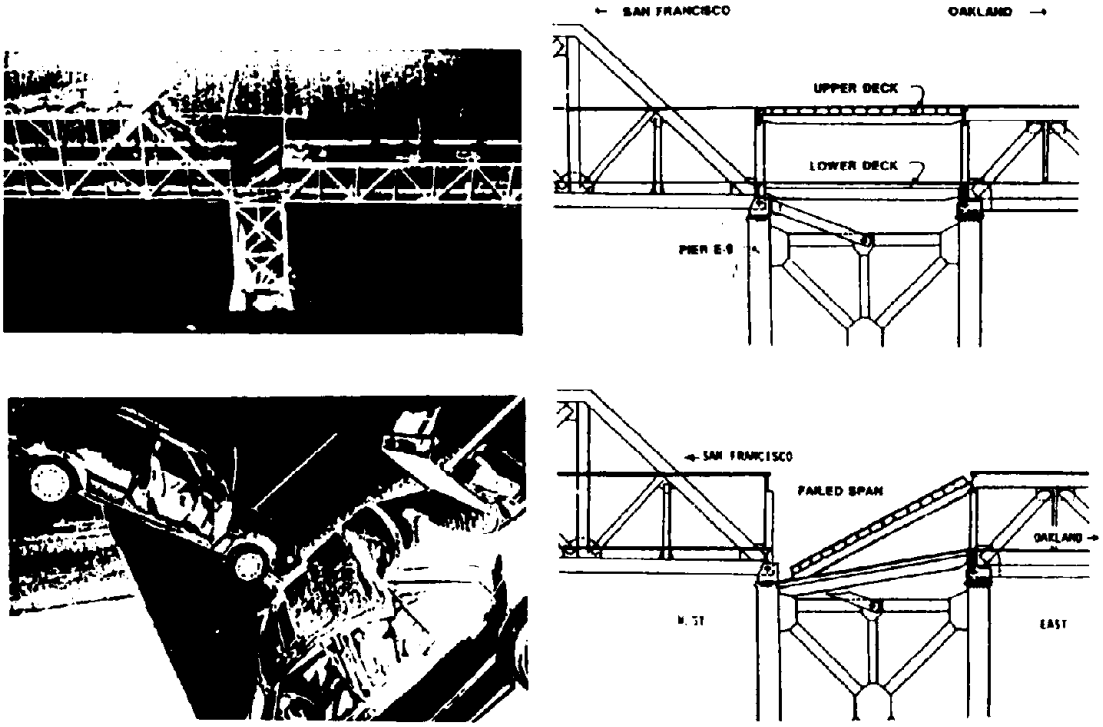

Figure 8. Failure of one span of the upper deck of the San Francisco Bay Bridge [Astaneh et al., 1989]

(a) Part that survived the EQ

(b) Part that collapsed

Figure 9. Cypress Street double-deck viaduct

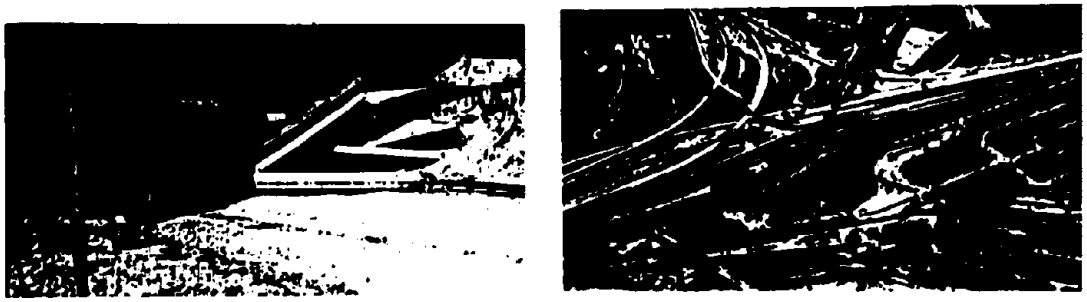

Figure 10. Freeway structures that collapsed during the 1971 San Fernando EQ

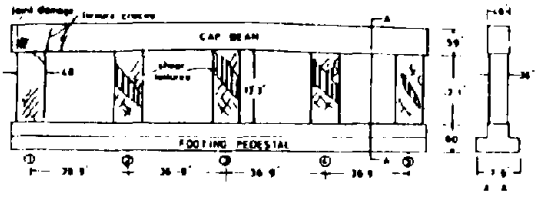

Figure 11. Illustration of the dimensions of and damage to bent 6 of a major freeway overpass [Priestley 1988]

Figure 12. Overview of the collapse of a bridge at Nigata, Japan in 1964

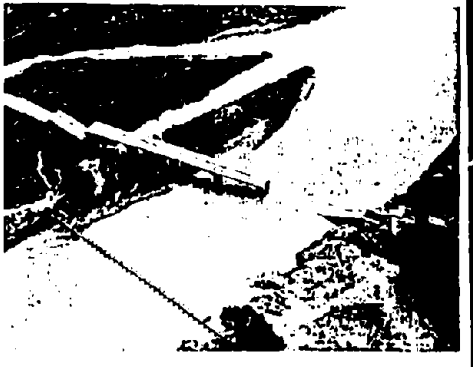

Figure 13. Collapse of the Lo-Gallardo Bridge during the 1985 Chile EQ [EERI 1986]

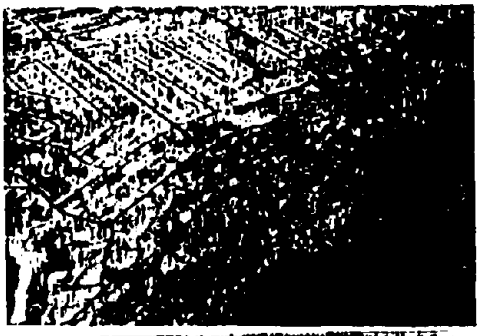

Figure 14. Effects of liquefaction of soil in Anchorage, Alaska (Turnagain Heights area)

Nigata, Japan, 1964

Oakland, U.S., 1989

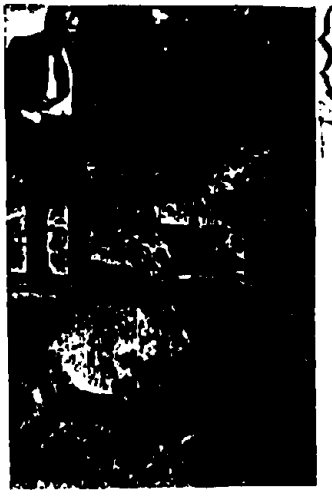

Figure 15. Sand boils

this particular type of freeway structure. Because it was designed and constructed between 1951 and 1957, when very little knowledge existed about EQ-resistant construction of this type of structure, its dramatic collapse clearly points out the need for conducting vulnerability assessments of this type of hazardous existing structure, and for immediate reliable upgrading of similar existing structures. It appears that the lessons learned from the 1971 EQ and the reminder given by the failure of the piers in one bent of a major freeway overpass during the 1988 Whittier Narrows EQ (Figure 11) were not taken seriously.

The collapse of the upper deck of the Bay Bridge (Figure 8) points out that it is necessary to conduct reliable analyses of the possible relative movement between two adjacent and different structures, in the case of long multi-span bridges subjected to moderate or severe EQGMs, as well as the necessity of learning how to upgrade such structures. Again, this is not a new lesson. Analysis of what happened in the 1964 Nigata EQ (Figure 12) and in the 1985 Chile EQ (Figure 13) again underscores the fact that we forget very quickly the lessons learned in previous EQs and do not take seriously their warnings of the urgent need to perform assessments of the vulnerability of similar important transportation facilities in our urban areas.

The dramatic collapse of several buildings in San Francisco's Marina District during the Loma Prieta EQ does not teach a new lesson. The collapses were, in most cases, consequences of a combination of the following factors: liquefaction of the soil, inadequate foundations, "soft" first stories, and poor structure conditions (woods rotten or infected or both due to poor maintenance). The importance of the effects of liquefaction has been taught by many previous EQs. The occurrence of liquefaction in general is not a surprise. In the Nigata (Japan) and Alaska EQs of 1964 (see Figure 14), many buildings subsided, inclined, overturned, and in some cases were translated very large distances by landslides as a consequence of liquefaction of saturated sand. Comparison of the photos shown in Figure 15, taken in 1964 in Nigata, to the photo taken at the Oakland Airport in 1989 shows that the sand boils observed at the Oakland Airport are nothing new. Furthermore, there is evidence that in San Francisco during the Great San Francisco EQ of 1906, liquefaction occurred in the same areas in which it was observed in 1989. A significant and surprising feature of the 1989 EQ is that liquefaction occurred at large epicentral distances (100 km), and after very few seconds of strong motion (less than seven seconds in the Bay Area). It appears that if the strong motions had lasted a few seconds longer, the amount of liquefaction, and hence the amount of damage, would have increased dramatically. There are major areas throughout the San Francisco Bay Area with liquefiable sites unsuitable for EQRC on standard foundation types which remain at considerable risk in large EQs.

More than 105,000 homes and 320 apartment buildings were damaged by the 1989 Loma Prieta EQ. It is estimated that the number of people displaced from their homes exceeded 14,000. Sheltering those displaced by the EQ was a major problem, especially in Watsonville and other small communities in the epicentral region. This large number of houses damaged and people displaced clearly points out not only the need to improve non-engineered construction of dwellings through improved design practices and codes, but also the urgent need to develop effective and economical techniques for the seismic upgrading of existing hazardous dwellings.

2.2.3 *The issue of EQ preparedness.* It has been stated previously that "*the poorer the preparedness, the greater the disaster.*" A country with poor preparedness will suffer more than a country with good preparedness. Preparedness is necessary. A comprehensive program of reduction of any natural hazard should include attempts to prevent the event creating the hazard, i.e., *prevention of the event.* If this is not possible, the program should include the possibility of *prediction of the event* using a *probabilistic* approach (analysis), and *prevention of the disaster* by *preparedness* through a comprehensive hazard reduction plan.

Because of this content, such a comprehensive program could be called the 4P program (Prevention, Probability, Prediction and Preparedness). Note that prevention usually implies prediction. In the case of EQs, prevention or control of the event may never be achieved, at least not in the near future, and prediction is uncertain in the near future and may never be achieved for certain faults. The only effective way to prevent an EQ disaster is to reduce the consequences of EQ effects through a comprehensive preparedness program, effectively implemented. The *ideal solution of the EQ problem will be through prediction of the event and hazard reduction through preparedness.* Prediction research should be continued, but should not interfere with efforts to solve the present and pressing problems through an adequate *preparedness program.*

To summarize: EQs are inevitable, but the fault rupture generating the EQ does not itself kill people or induce great economic losses. What causes most of the injuries and losses is *the interaction of the EQGMs with the built environment.* What is needed is to control seismic risk in our urban areas by controlling the built environment, which should be the main point of the EQ preparedness program.

2.3 *Control of seismic risks*

In order to learn how to control seismic risk, it is necessary to define it. According to the glossary of the EQ Engineering Research Institute's Committee on Seismic Risk [1984], seismic risk is "*the probability that social or economic consequences of EQs will equal or exceed specified values at a site, at various sites, or in an area, during a specified exposure time.*" According to Dowrick [1987], seismic risk is an outcome of seismic hazards, as described in the following relationship, which is also illustrated in the flow chart of Figure 16.

$$\textit{Seismic Risk} = (\textit{Seismic Hazard})(\textit{Vulnerability})(\textit{Value}) \qquad (2)$$

A *seismic hazard* is any EQ-related physical phenomenon (e.g., ground-shaking, ground failure) that may produce adverse effects on human activities. As indicated in Figure 16, seismic hazards at any site or region are consequences of the interaction of the *sources of potential EQ hazards* (created by the local *seismic activity*) with the degree of *vulnerability* of the *built environment. Built environment* denotes the different

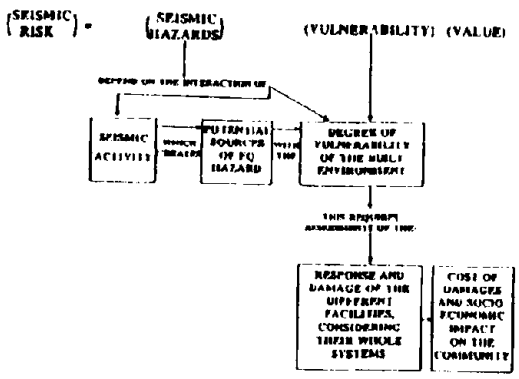

Figure 16. Flow chart for assessing seismic risk

facilities (engineered or non-engineered) such as buildings, transportation and communication systems, dams or lifelines in general, and equipment, that are located on a site or in an area. *Vulnerability* is the amount of damage induced by a given degree of hazard, expressed as a fraction of the value of the damaged item or facility. Therefore, to assess the degree of vulnerability of the built environment, it is necessary to assess the response (performance) of whole systems (i.e., soil, foundation, superstructure and nonstructural components and contents) of the facilities in the built environment.

From the above considerations, it is clear that to control seismic risk at any give site it is necessary to estimate seismic risk, which requires the following.

- First, *estimation of the seismic activity* at the site, which requires *identification* of all sources of EQGMs that could affect the built environment, i.e., that could induce damage. Once the sources of various potential seismic hazards created by the seismic activity have been identified, it is necessary to determine whether the EQs will be single or multi-events, and to estimate their moment magnitudes, recurrence periods, and the attenuations of the intensities of their EQGMs with distance.
- Second, *prediction* of whether the EQ faulting originating the EQGMs could induce any of the following potential seismic hazards at the site or the surrounding region: surface fault ruptures, tsunamis, seiches, landslides, floods and ground failure.
- Third, *prediction* of the time history of the six components of the EQGM at the site and at the foundation of each facility.
- Fourth, *prediction* of whether the predicted EQGMs can induce ground failure, i.e., liquefaction, settlement, subsidence, differential compaction, loss of bearing and shearing strength, lateral spreading, landsliding and/or lurching.
- Fifth, *assessment* for any given facility of the mechanical behavior (performance) of the whole facility system under the predicted six components of the EQGM at its foundation, estimating the degree of damage and losses, considering the possibility of fire, flood, and other consequent or indirect sources of seismic hazards.
- Sixth, *evaluation* of the economic consequences of the losses and the socio-economic impact on the community. The costs and benefits of seismic upgrading of existing hazardous facilities should be estimated.

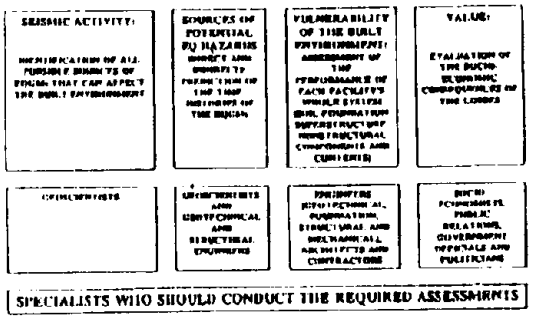

Table 2. Experts needed to perform seismic risk assessment

Analysis of Table 2, which summarizes the experts needed to perform the required assessments indicates that: (1) the estimation of the seismic activity should be conducted by geoscientists (geologists and seismologists); (2) the prediction of possible sources of potential EQ hazards should be conducted by geoscientists and geotechnical engineers; (3) the prediction of EQGMs at the site and at the foundation of the facility should be conducted by geoscientists and geotechnical engineers in consultation with structural engineers; (4) the prediction of the ground failures that can be induced by EQGMs at the site has to be done by geotechnical engineers; (5) the assessment of the mechanical behavior of the whole system of any given facility when subjected to the predicted EQGMs requires the collaboration of geotechnical, foundation, structural, construction and mechanical engineers, in consultation with architects and contractors; and (6) the evaluation of the economic consequences of the losses and the socio-economic impact on the community requires the collaboration of engineers, architects, contractors, socio-economists, government officials and politicians. *From this analysis it is clear that reduction and control of seismic risk in any given urban area is a complex problem, requiring the integration of knowledge and the collaboration of experts from many disciplines.*

Furthermore, the problem of seismic risk reduction will not be solved just by the acquisition of the required knowledge through research. Research must be accompanied by the necessary technological developments and the implementation of the knowledge and the developments in practice. *What is needed is a translation of current engineering and architectural know-how into simplified options which can answer the socio-political and economic concerns. This will require not only a multi-disciplinary approach, but also a comprehensive educational program, not only for owners and future users but also for all of the different audiences that in one way or another are involved in the implementation of the seismic risk reduction measures.* This education program should emphasize the importance of EQ disaster preparedness, including preparing for fires, control of panic, etc.

Until now, most of the emphasis has been on (1) trying to predict EQs based on probabilistic approaches, and (2)

gaining knowledge of the mechanical behavior (performance) of different facilities. While these are necessary, prediction alone will not solve the problems. What is necessary is to *improve the preparedness* of the public against EQ disaster. There is an urgent need to coordinate the acquisition, processing, evaluating and synthesizing of the research results already available, and the knowledge gained through lessons learned in past EQs. This integrated knowledge must then be converted into action. *There is a need for multi-disciplinary groups of researchers, practicing professionals, users, government officials, etc., who will develop and ensure the implementation of reliable and suitable policies and strategies which will help to reduce and control seismic risks to acceptable levels, which is what is needed.*

2.4 *Concluding remarks regarding the control of seismic risks, the need for EQ preparedness, and future directions toward a solution*

During the 1984 8th WCEE Press [1984] stated that, *"Good government management is the key factor in preparedness, and therefore government performance is a major controllable factor influencing the impact of a disaster."* There is no doubt that if government does not assume its proper role of hazard management after being provided with the required assessments by competent professionals, seismic risk reduction to an acceptable level will not occur. With all of the possibilities for reducing EQ hazards by controlling the built environment (through reliable assessment of risks, seismic codes and construction standards, land use, and criteria for identification of existing hazardous facilities and upgrading them), one wonders why we have not found proper solutions to the following issues:

- *Why have we not progressed very much in the reduction of seismic risks in our urban and rural areas?*
- *Why are there not adequate preparedness programs in most countries?*

While the lack of preparedness against EQ disasters can be justified in countries that are very poor, it is difficult to understand the short-sightedness of some industrialized countries. There are many parts of the world that are particularly prone to EQs but have not had the advantages of risk assessment for their regions and the development and/or implementation of EQ preparedness programs. The importance of the need for developing and implementing comprehensive EQ preparedness programs is clearly demonstrated by what has happened in the past in the following cities.

- *San Juan, Argentina.* In 1944, this city was destroyed by an EQ. A very simple seismic code was formulated, with very specific recommendations regarding the use of masonry and concrete in the construction of buildings. Through the strict enforcement of this code, the city was rebuilt and survived, without any significant damage and without loss of life, an EQ in 1977 with characteristics similar to that of the 1944 EQ.
- *El Asnam, Algeria.* This city was practically destroyed during an EQ in 1954. A new, modern seismic code was developed, but was not properly enforced or implemented in the rebuilding of the city, particularly in the large number of buildings built in the 1970s. During the 1980 EQ, most of those buildings collapsed.
- *Erzincan, Turkey.* This city was destroyed by an EQ of magnitude M=8.0 in 1939, and was warned again by a moderate EQ of M=5.6 in 1983 which damaged several buildings. In 1992, the city was severely damaged by an EQ of M=6.8. More than 2,100 buildings collapsed or were heavily damaged. This last EQ also affected about 70 villages and towns, in most of which 40% of the houses collapsed or were damaged beyond repair. The total number of people left homeless was estimated at about 120,000. Most of the buildings that failed in the city were modern buildings of four or more stories (Figure 17) designed and, particularly, constructed without compliance with seismic code regulations. The history of the effects of EQs in Erzincan demonstrates again that either we very quickly forget the lessons learned, or we do not take their warnings seriously.

It is clear from the above examples and from the lessons learned in many other recent EQs that the potentially destructive EQGMs will not wait for our knowledge to be transferred to the practitioners and government officials in charge of EQ hazards management by osmosis from the R&D publications on their shelves. There is an urgent need to educate not only practitioners involved in EQ Engineering (particularly EQRD and EQRC), but also government officials, politicians, and the public in general.

To summarize: the main issue confronting all of us interested in EQ Engineering is the need to control the seismic risks in our urban and rural areas. The solution is controlling the vulnerability of the built environment, because this allows us to control the potential sources of EQ hazards, which are consequences of the interaction of seismic activity (which we cannot control) with the vulnerability of the built environment.

3. ROLE AND IMPORTANCE OF EQ ENGINEERING IN THE OVERALL PROBLEM OF CONTROLLING SEISMIC RISK IN URBAN AND RURAL AREAS

3.1 *Role and importance of EQ Engineering*

3.1.1 *Definition and objectives of EQ Engineering.* As stated previously, EQ engineering is the branch of engineering that encompasses the practical efforts to avoid EQ hazards. It is a relatively new field of engineering: in the U.S. it is not more than 65 years old. Even so, EQ engineering has already played a significant role in mitigating seismic hazards around the world. Significant advances in analysis of the seismic response of mathematical models of structures and even in the understanding of real structures have been made. Nevertheless, there has not been a corresponding improvement in the reliability with which new structures and facilities are designed, constructed and maintained, nor in how existing structures are seismically upgraded to resist effectively the seismic hazards to which they may be exposed in their service lives. Therefore, it is not surprising that, as mentioned earlier, most human injury and economic losses from moderate to severe EQGMs are caused by the failure of engineered facilities. One main reason for this is that the state of the practice in EQ Engineering, and particularly in EQRD, as reflected by present seismic codes, is based on zonation maps which do not reliably depict the real seismic hazards of the sites on which facilities are built. The slow rate of

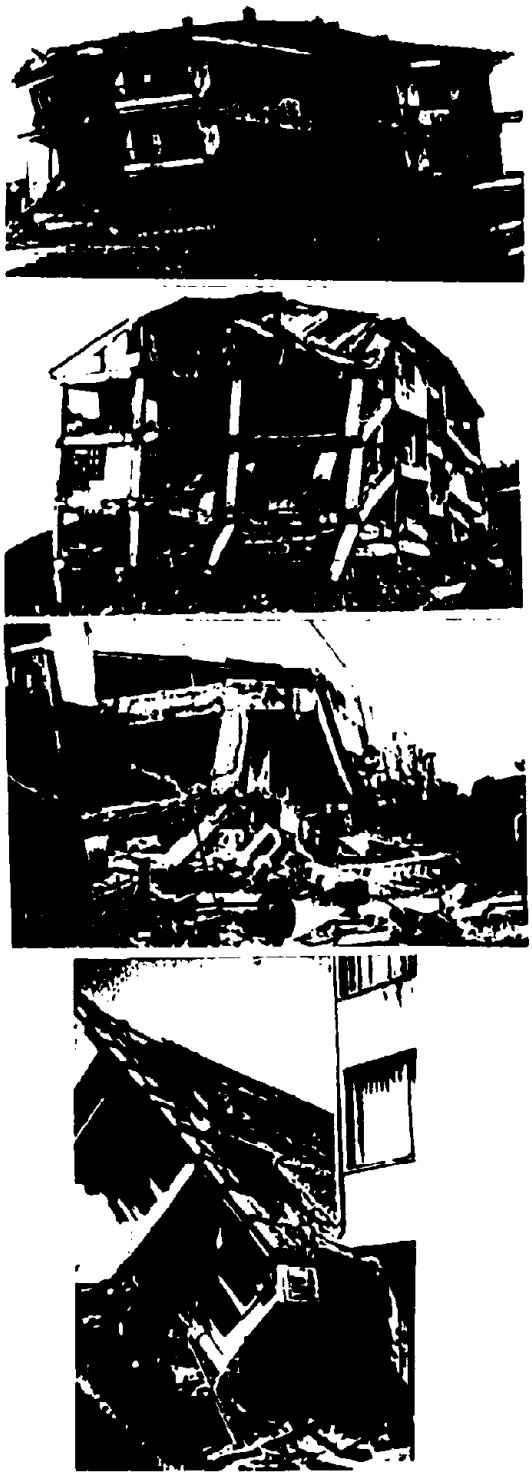

Figure 17. 1992 Erzincan, Turkey, EQ: photos illustrating damage to modern RC buildings

improvement in EQ hazard reduction has been a consequence of the tardy introduction of advances in zonation and microzonation into EQ engineering and particularly into EQRD codes [Bertero, 1991 (Seismic Zonation)].

As pointed out above, the evaluation of the EQ hazards to which a facility may be subjected is a complex task, requiring not only probabilistic consideration of the EQ occurrence and the physical effects of the source, propagation path, and local site geology, but also the interaction of the ground-shaking with the whole soil-foundation-superstructure-and-nonstructural components and contents system of the facility to be designed. Unfortunately, most of the research on these different areas has been concerned with isolated areas of each specialized discipline. There have not been serious attempts to integrate the knowledge and the requirements of the various disciplines involved in the general problem of EQ hazard reduction. The engineers are perhaps not asking the geoscientists the right questions, and the geoscientists are perhaps more interested in trying to predict EQs than in the problems involved in the EQRD of engineered facilities. These attitude have to be changed.

3.1.2 *Role and importance of EQRD of structures.* From previous discussion, it is clear that EQRD of structures is at present the key element in the problem of EQ hazard reduction. As has been mentioned, one of the most effective ways to mitigate the destructive effects of EQs is to improve and develop more reliable methods than are now available for designing, constructing and maintaining and monitoring new structures and seismically upgrading existing hazardous facilities. In order to find out what information is necessary for the realization of such improvements, it is convenient to analyze the main issues. These can be expressed as questions about what went wrong in the past (why are there so many hazardous facilities?), what is happening at present (where do we stand right now?), and where should we go (what are the directions for short-term and long-term solutions?).

Because the design and construction of most EQ-resistant facilities (particularly buildings) in practice generally follow seismic code provisions, it is convenient to examine these provisions briefly and to scrutinize what has been done and what should be done to improve the present state of the practice. Before examining present seismic codes, it is convenient to review briefly the problems involved in EQRD and EQRC, and the general philosophy of EQRD.

3.2 *Problems involved in EQRD and EQRC.*

The general aspects and problems involved in EQRD and EQRC for buildings (on which the following discussion will concentrate) have been discussed by Bertero [1982], and from analysis of these general aspects it is clear that seismic codes should regulate:

(1) Selection of building sites, siting restrictions, land use, and building site suitability analysis;
(2) establishment of design EQs, EQRD criteria, and design methodology;
(3) restrictions and/or guidelines regarding proper selection of building configuration, foundation, structural layout, structural system, structural

material and nonstructural components;

(4) estimation of demands on a structure and its contents at the different levels of design EQs;

(5) estimation of the supplied capacities to a structure; and

(6) analysis of the performance of a designed structure under different established levels of design EQs. This should be done visualizing the mechanical characteristics that the real constructed facility will have.

(7) Construction (supervision), use and maintenance of the constructed facility.

As will be discussed in more detail later, review of the results conducted on the importance and effects of the general aspects of EQRD of structures indicates that the principal issues that remain to be resolved for the improvement of such design are related to the following three basic elements: *EQ input, demands on the structure*, and *supplied capacities to the structure*. After a brief review of how seismic codes in the U.S. have been developed and have attempted to resolve these three issues, this lecture will focus on the first of these, the EQ input element, which involves the following interrelated issues: *Design EQs, design criteria*, and *selection of design methodology*. The importance of proper establishment of the design EQs is reflected by *the need to know against what we have to design the structure*.

Design criteria should reflect in a transparent way the general philosophy of EQRD, which has been well established and is accepted world-wide. However, as will be discussed below, current code design methodologies in the U.S. fall short of realizing the goals and objectives of this philosophy [Bertero and Bresler (1977), Bertero (1986)].

The problems encountered in EQRD are complex, and therefore in general their solutions are also complex. In order to keep code design procedure as simple as possible, as it should be, it is necessary to specify very severe and restrictive regulations regarding the siting of facilities and the selection of their configurations, structural layouts, structural systems, structural materials and nonstructural components. This is the best way to avoid creating complex problems (soil-structure interaction, foundation movements, P-Δ effects, torsional effects, etc.). When these restrictive regulations are not followed, the code needs to specify that simple code procedure should be complemented with dynamic linear and nonlinear analyses and design procedures, which should be subjected to peer review.

3.2.1 *General philosophy of EQRD*. What can be considered the general philosophy of EQRD of buildings sheltering other than essential and hazardous facilities was introduced in the U.S. for the first time in the Commentary of the 1967 edition of the Structural Engineers' Association of California (SEAOC) Blue Book [1967], and it has changed very little since then. Essentially, this EQRD philosophy states that the design should accomplish the following objectives:

1. Prevent nonstructural damage in minor EQ ground shakings, which may occur frequently during the service life of the structure.
2. Prevent structural damage and minimize nonstructural damage during moderate EQ ground shakings, which may occasionally occur.
3. Avoid collapse or serious damage during severe EQ ground shakings, which may rarely occur.

3.2.2 *Ideal philosophy of EQRD*. Recognizing first that the acceleration and deformations that can be developed during the responses of building systems to severe and even to moderate EQGMs are very high, and secondly that there are many uncertainties in the estimation of demands and supplies, the ideal philosophy should attempt to realize all of the objectives of the above general philosophy by providing all the needed stiffness, strength and energy dissipation capacity that can be accomplished with the minimum possible extra cost in initial construction and/or the slightest possible sacrifice in the architectural features that would be required for the design of the building for just gravity loads.

The above general philosophy is in complete accord with the concept of comprehensive design. However, current code design methodologies, at least in the U.S., fall short of realizing the goals and objectives of this philosophy.

Although in the commentary of the 1988 SEAOC Blue Book recommendations it is stated that structures designed in conformity with these recommendations should, in general, be able to accomplish the objectives of the above general philosophy, *they are primarily intended to safeguard against major failure and loss of life, not to limit damage, maintain functions, or provide for easy repair. In few words, current code design methodology is based on a one-level design EQ*. Moreover, the SEAOC commentary states that, "*the protection of life is reasonably provided but not with complete assurance*." To summarize, the primary goal of the U.S. seismic provisions is to protect life. *The secondary goal is to reduce (not eliminate) property damage*. The questions that need to be answered are: First, *does the application of current seismic code provisions accomplish the above goals?*; and second, *are these goals sufficient?* Before attempting to answer these questions, it is convenient to review the philosophy of building codes, particularly seismic codes, and to review the history and development of these codes.

3.2.3 *U.S. code philosophy*. Building codes are primarily technical legal requirements, adopted by government agencies, specifying *minimum standards* for the design, manufacture, installation and use of building materials and components. Although the primary function of a building code is *to provide minimum standards to assure public safety*, it usually has other objectives as well. For example, the intention of the 1991 UBC is clearly stated in its Section 1 02·

> The purpose of this code is to provide minimum standards to safeguard life or limb, health, properties, and public welfare by regulating and controlling the design, construction, quality of materials, use and occupancy, location and maintenance of all building and structures within this jurisdiction and certain equipment specifically regulated therein.

In view of the above code purpose, it is not surprising that SEAOC has established a seismic code philosophy that is in accordance with the above purpose of building codes. *Thus, the basic philosophy of the SEAOC seismic code, as well as most of the other seismic codes, has been to protect the public in and about buildings from*

Table 3. History of seismic design codes in the United Sates.

Date	Code or Provisions
Post-1906	San Francisco rebuilt to 30 psf wind
1927	First seismic design appendix in Uniform Building Code: V=CW (C=0.075 to 0.10)
1933	Los Angeles City Code: V=CW, (C=0.08) First enforced seismic code.
1943	Los Angeles City Code: V=CW, [C=60/(N+4.5)] N greater than 13 stories.
1952	ASCE-SEAONC: $(C=K_1/T_1)$, $(K_1=0.015\text{-}0.025)$
1959	SEAOC: V=KCW, $[C=0.05/(T)_{1/3}$
1974	SEAOC: V=ZIKCSW
1976	UBC: V=ZIKCSW
1977	ATC-3 Tentative Recommendations: $V=Z_aW$, $C_s=1.2\ A_v\ S/RT \leq 2.5\ A_a/R$
1988	SEAOC and UBC: $V=ZIC\ W/R_w$, $C=1.25\ S/T^{2/3} \leq 2.75$, $C/R_w \geq 0.075$

NOTE: *W=weight of building; V=base shear; T=period of vibration; N=number of stories; Z,K,I and S=numerical coefficients (C was originally a seismic design coefficient but in codes later that 1943 a numerical coefficient dependent on T; Z=factor dependent on the zone in a seismic risk map; I=occupancy importance factor; and S=site-structural response or soil-profile coefficient); C_s=seismic coefficient; A_v=effective peak-velocity acceleration; R=response modification factor; and R_w=numerical coefficient (called system quality factor).*

loss of life and serious injury during major EQs. However, some owner-sponsored codes have gone further than this. For example, in 1975 the Titles 17 and 21 of the California Administrative Code related to the design and construction of hospitals and public school buildings includes, as its added purpose, the protection of property. At present, Title 24 of the California Administrative Code regarding hospitals has the additional purpose that hospitals remain operational after an EQ.

3.2.4 *History of seismic design codes.* The 1980 edition of the SEAOC Blue Book describes the history of EQ codes in California. Table 3 summarizes the history of seismic design codes and their provisions in the U.S. [Committee on EQ Engineering Research, 1982].

The first EQ design requirements appeared in the 1927 edition of the Uniform Building Code. Although these provisions were never put into effect in any city, they required all buildings over twenty feet in height to be designed for a lateral force applied at each floor level and at the roof level generally parallel to the two main axes of the structure. The force required was a percentage of the total dead and live loads, with the exception of buildings with a live load not over 50 pounds per square foot, for which only a percentage of the dead load was required to be used. Structures on soils with a bearing value of two or more tons per square foot were to be designed for 7.5% of their vertical loads, and those with lesser soil bearing value and those on piles were to be designed for 10% of their vertical loads.

When seismic requirements first appeared in building codes and were put into effect, practically nothing was known about EQ Engineering. The 1933 L.A. Building Code, for example, merely stated that a building should be designed to withstand a steady horizontal thrust equal to 8% of its weight, in effect treating EQ forces as wind pressures. In recent years, understanding of EQ Engineering problems and EQRD has undergone remarkable development. In the U.S. this was made possible largely by research after World War II on military protective structures, and after 1960 by EQ Engineering research programs conducted in several countries.

Building codes to which ordinary buildings are designed have also developed impressively, so that they are now much better suited to guide realistic design against EQ forces. Clearly, present U.S. methods of EQRD are an outstanding improvement over methods available 20 or even 10 years ago, particularly in regard to sizing and detailing of superstructures of ordinary buildings. To elaborate on this, it is convenient to classify seismic code provisions into the following two main groups.

1. *EQ-resistant criteria.* This group covers the basis for design and specifications of minimum lateral forces and related effects (estimation of seismic demands).
2. *Material code specifications.* This group regulates sizing and detailing of the structure.

In the last two decades there have been tremendous improvements in the code specifications for the sizing and detailing of structural members and their connections and supports. Figure 18 illustrates the changes in the spacing of ties in the EQRD of RC columns. Although the importance of providing the structure with large *ductility* was already recognized in the 1959 SEAOC-recommended requirements, special provisions regarding the EQRD of RC structures first appeared in the 1971 edition of the ACI code. Because the amounts of detailing and transverse reinforcement for achieving high ductility demands depart somewhat from the requirements of the ordinary practice in RC design and construction, the cost is higher for EQRC. This higher cost has caused some concern and the complaint that there may have been too much emphasis on creating ductility for ductility's sake [Dowrick (1987)]. This has also raised the following valid question: *"How do we design less ductile structures which are sufficiently reliable against EQs?"*

Regarding these complaints and questions, the lecturer believes that ductility requirements should not be relaxed in EQRD, at least until the results of new and reliable research and developments become available to justify such relaxation. *These stringent requirements for sizing, and particularly for detailing, have been the blessing of*

the current code requirements for EQRD. The reasons for this are that there are many uncertainties involved in the estimation of the demands and supplies for EQRD procedure. As discussed below, the present code specifications for estimating seismic lateral forces and their effects are far from reliable. It is for this reason that *the lecturer believes that stringent sizing and detailing requirements, rather than complex numerical analyses conducted to comply with code formulae for estimating demands, have permitted many buildings to survive recent moderate-to-severe EQGMs.*

3.2.5 *U.S. code EQ resistant criteria: estimation of demands.* The several sources of uncertainty in the estimation of demands can be grouped into two categories: 1) specified seismic forces, and 2) methods used to estimate responses to these seismic forces.

(1) *Estimation of seismic forces.* For regular buildings, the lateral seismic forces can be derived as follows.

(a) Base Shear

$$V = C_s W = \frac{C_{sp} W}{R} \tag{3}$$

where V is base shear, C_s is defined as the design seismic coefficient, W is the weight of the reactive mass (i.e., the mass that can induce inertial forces), C_{sp} is the seismic coefficient equivalent to a linear elastic response spectral acceleration, S_a, ($C_{sp}=C_sR=S_a/g$), and R is the reduction factor.

(b) Distribution of base shear over the height of the structure.

$$V = F_t + \sum_{i=1}^{n} F_i \tag{4}$$

where F_t is concentrated force at the top and represents the effects of higher modes (whiplash effect) and.

$$F_i = \frac{(V - F_t) w_i h_i}{\sum_{i=1}^{n} w_i h_i} \tag{5}$$

is the force at level *i* (usually the floor level, w_i is the portion of W located at or assigned to level *i*, and h_i is the height above the base to level *i*.

(2) *Estimation of structural response to seismic forces.* Structural response can be estimated using linear elastic analyses, either directly using the above statically equivalent lateral forces (Eqs. 4 and 5), or multiplying them by load factors, depending on whether the design will use allowable (service) stress or strength method.

The uncertainties involved in the estimation of base shear and its distribution over the height of the structure, as well as the reliability of the procedures and values specified by present U.S. seismic codes, have been discussed in detail by Bertero, V.V. [1982 and 1986].

A review of the history of how the values for the base shear resistance (Table 3) have been computed clearly shows that the equation recommended for its evaluation has become more and more sophisticated and requires more and more empirical numerical coefficients. However, what is really surprising is that the code

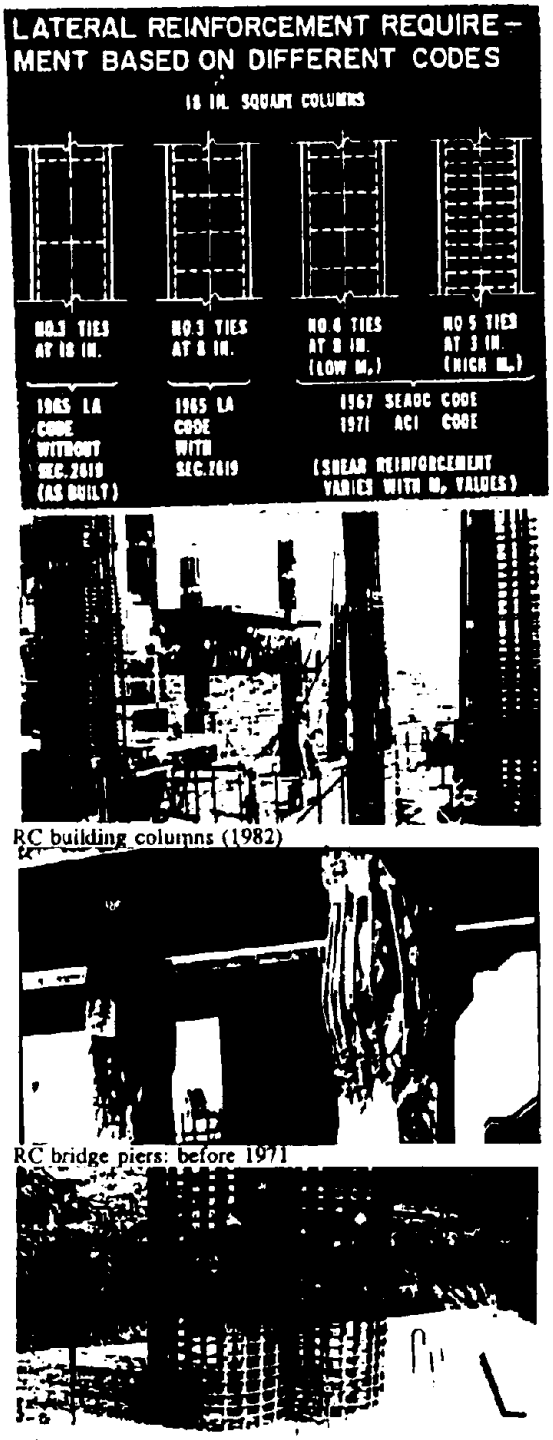

Figure 18. Illustration of the changes in RC lateral reinforcement requirements

requirement for basc shear resistance remains practically the same as the first seismic code in 1927, and has even been reduced, as is shown by comparing Tables 3 and 4. This is surprising, because the building technology of the 1930's was quite different from the present one, and although it resulted in buildings with smaller ductility, these buildings usually had higher overstrength.

As indicated in Tables 3 and 4, SEAOC introduced significant changes into their code recommendations in 1988 by adopting some of the 1977 ATC-3 recommendations. The new SEAOC recommendations have been adopted in the 1988 UBC. Although these recent codes and recommendations recognize the severity of seismic hazard for different seismic zones in the U.S. and incorporate modern seismic design philosophies and approaches, they continue to place too much emphasis on designing for a yielding strength capacity which is the same as or even less than that which resulted from applying the provisions of the first U.S. seismic code regulations in 1927.

The lecturer has recently analyzed present trends in EQRD and EQRC of buildings in the U.S. and has made the following observations.

(1) Recent code recommendations recognize the probable occurrence of very severe EQGMs at a given site in a region of high seismicity (high intensity and long duration of EQGMs). In spite of this and the significant changes in construction technology, there has been very little change in the overall seismic coefficient for which buildings must be designed.
(2) The code continues to place too much emphasis on strength design based on fictitious seismic forces and linear elastic analyses of their effects.
(3) Because of economic pressures, designers try hard to comply with just the code minimum requirements for strength.
(4) The development and use of computer programs based on optimal design of members of a structure will lead to final designs with very little overstrength with respect to the code-required minimum strength. This problem is exacerbated by the use of taller and slenderer buildings.
(5) The use of very light and weak nonstructural elements (walls, partitions, claddings, etc.) which, furthermore, are built such that their performance will not interfere with the deformation of the structure, results in buildings whose strength and stiffness are just those of the bare structural system.

All of the above developments and trends result in the construction of buildings with very little overstrength beyond the minimum code-required strength. There is an urgent need for calibration of the real strength and stiffness of buildings that have been designed and constructed according to present codes. *There can be no improvement in the EQRD of new buildings, in seismic performance evaluation of existing buildings, or in vulnerability assessment and upgrading of hazardous buildings, if there is no improvement in predicting stiffness, strength, and energy absorption and dissipation capacities of real building systems (soil-foundation-superstructure and nonstructural components).*

In recent years there has been an increasing amount of research on design concepts based on probabilistic approaches. This activity has resulted in a re-examination of past data, a close analysis of design concepts, and a formulation of design provisions to make the latter more logical for practitioners. Much remains to be done to apply such research to assessments of seismic risk, particularly in areas of low seismic activity, and to adapt such research to practical design and construction.

Table 4. Comparison between:

(1) Expressions for effective seismic coefficient, $C_s=V/W$, specified by the 1985 UBC, ATC-3 and the 1988 SEAOC recommendations.

UBC	ATC	SEAOC
$ZIKCS$	$\frac{1.2\,A_v\,S}{RT^{2/3}}$	$\frac{ZIC}{R_w}$
$C=\frac{1}{15\sqrt{T}}$		$C=\frac{1.25\,S}{T^{2/3}}$
$\frac{ZIKS}{15\sqrt{T}}$	$\frac{1.2A_v\,S}{RT^{2/3}}$	$\frac{1.25ZIS}{R_wT^{2/3}}$

(2) The values of C_s for ductile moment-resisting space frames, DMRSF, in regions of high seismic risk.

	UBC	ATC	SEAOC
	(K=0.7)	(R=8)	(R_w=12)
	$\frac{0.51\,S}{12\sqrt{T}}$	$\frac{0.060\,S}{T^{2/3}}$	$\frac{0.042\,IS}{T^{2/3}}$
	For I = 1 and T = 1 sec.		
V	0.045 S	0.060 S	0.042 S
Vu	0.063 S	0.060 S	0.059 S

3.2.6 *Comparison of current seismic code provisions.* Analysis of comparisons of U.S. codes with the present seismic codes of Europe, Chile, Japan, Mexico D.F. and New Zealand makes it clear that there are some significant discrepancies among the seismic provisions of the current codes [Bertero et al. (1991)]. It is believed that this is a consequence of the fact that seismic codes, of necessity, are generalized oversimplifications of the very complex real EQRD problem. *Modern building codes, which try to reflect great advances in knowledge and understanding in a very simple way, are not transparent about the expected level of performance of the whole building system (soil-foundation-superstructure and nonstructural components). Expected level of performance has become an implicit, rather than an explicit, part of the codes through a series of empirical factors and detailing requirements which obscure the true nature of the EQRD problem: building performance.*

Current seismic codes lack transparency in their provisions regarding: the reliable establishment of critical EQGMs for the desired performance of the whole

building system at the different limit states through which it can go during its service life; and also the real expected response of the resulting designed and constructed building system to real critical EQGMs (not just to code-specified motions). Although there have not been enough moderate and severe EQGMs in urban areas to permit analyses and judgements of the performance of building systems designed according to current seismic codes, the observed behavior of some modern buildings in recent EQs, particularly in Mexico City during the 1985 Michoacan EQ and in the Bay Area during the 1989 Loma Prieta EQ, and also in the 1990 Luzon, Philippines and the 1992 Erzincan, Turkey EQs, indicates the need for improvement of the current U.S. EQRD code approach.

The slow rate of improvement in our seismic codes is not surprising because, as pointed out by Housner (1984), the code is a legal document that specifies a minimum level of design that must be attained by facilities and because it has a large socio-economic impact, substantial changes in code requirements are made slowly and cautiously. In addition, because building codes affect so many agencies, groups, individuals, etc., there is a great inertia against change, and therefore developments in building codes tend to lag behind developments in research, as will be discussed in more detail below. Unfortunately, needed changes in the code are usually deferred until the occurrence of a destructive EQ.

4 MAIN ISSUES REGARDING PRESENT EQRD SEISMIC CODE PROCEDURES

4.1 *Introductory remarks*

From the analysis and discussion presented in section 3.2, it can be concluded that current codes in the U.S. and most other countries have as primary goals the protection of human life, and that the second goal is to reduce (not eliminate) property damage. However, as these codes are based on just a one-level design EQ, the main issues that remain to be answered regarding present seismic code regulations and their implementation are:

(1) Does the implementation of current seismic code provisions accomplish the above primary and secondary goals of these codes?
(2) Are these goals sufficient?

As previously discussed, structures designed in conformance with present seismic code regulations can not guarantee the accomplishment of the above main goals, and particularly the objectives of EQRD philosophy. In order to be able to accomplish such goals and objectives, seismic codes should define clearly: the damages to the entire facility system that can result from the sources of potential seismic hazards originated by all of the possible EQs affecting the region of the structure site; and then what constitutes acceptable damage, i.e., what constitutes acceptable risks. As already discussed, facility damage may result from different seismic effects, which may be classified into two main groups: direct effects and indirect effects. The direct effects are: (1) ground failures due to fault ruptures or to the effects of seismic waves; (2) vibrations transmitted from the ground to the structure; and (3) seismic sea waves (tsunamis) and tsunami-like disturbances in lakes (seiches). The indirect, or consequential, effects result from other EQ phenomena, such as fires and floods caused by dam failures and landslides. Thus, the first and perhaps the main step in a comprehensive design approach should be to conduct a reliable assessment of the above seismic hazards and to analyze the suitability of the selected building site. This requires reliable seismic microzonation of urban areas. Regarding this matter, the commentary of the SEAOC Blue Book [1988] states:

> It is to be understood that the damage due to the earth slides such as those that occurred in Anchorage, Alaska or due to earth consolidation such as occurred in Nigata, Japan, would not be prevented by conformance with the SEAOC Code. The SEAOC Code has been prepared to provide minimum required resistance to typical EQ ground shaking, without slides, subsidence, or faulting in the immediate vicinity of the structure.

The seismic effect that usually concerns the structural engineer and is accounted for in EQRD provisions of building codes is the response (vibration) of a building to ground shaking that might occur at its foundation. In most cases, damage due to other effects exceeds that due to the vibration of the building. Nonetheless, procedures for gauging the probability of such hazards and coping with them are normally outside the scope of the structural engineering discipline, and so are not included in the codes. Generally, the only way to avoid damage from most of these effects is by changing the building site, a decision which rests with government officials. In spite of this, the engineer should be aware of the different seismic hazards and should advise the client of potential dangers involved in constructing buildings at certain sites.

As stated in section 3.2.2, according to the commentary of the SEAOC recommendations, structures designed in conformance with these recommendations, which are based on a one-level design EQ approach, should, in general, be able to attain the three objectives of the general philosophy. This is not only questionable, but indeed the code seismic design provisions have been developed to satisfy only the criteria involved in Objective 3 of the above philosophy. Apparently, this has been done under the assumption that if Objective 3 were met, Objectives 1 and 2 would automatically be satisfied. Recent studies show that this is not the case.

Uang and Bertero (1991) have shown that the UBC-(or SEAOC) specified seismic design procedure cannot adequately control the general demands that can be imposed by service EQGMs. Furthermore, the lecturer believes that it will be very difficult to satisfy the criteria for all three objectives of seismic design philosophy by keeping the present building code design methodology, which requires only one level of design EQ (life-safety level). *It is believed that the time has arrived to move from the current code one-level design EQ methodology to a code design methodology based on at least two distinct levels of design EQs: the service-level (functional adequacy) and the life-safety level EQs.*

It should be noted that the above proposed two-level design EQ methodology does not necessarily mean that the preliminary design of any EQ-resistant building system should have to be carried out considering simultaneously the specified two-level design EQs.

Although this would be highly desirable, the above proposed two-level design methodology really means that the EQRD process would have to be conducted in two phases. In the first phase, the preliminary design of the building system would conform to what is considered to be the *critical or controlling* level design EQ. This would require thorough comparison and analysis of the two specified level design EQs. In the second phase, the preliminary design of the building would be analyzed and detailed to ensure compliance with the dual criteria involved in the two levels of design EQ, i.e., satisfactory performance at both the service level and the life-safety level EQGMs.

The idea of using two levels of design EQ is not new. In the U.S., its application and introduction into seismic codes were discussed in the 1960's [Degenkolb (1972) and Bertero (1975)]. A survey of the seismic design codes of other nations [Bertero et al. (1991)] and the World List of EQ-Resistant Regulations (1988) reveals that the 1981 Japanese Building Standard Law (BSL) explicitly specifies a *two-level design EQ: moderate EQGMs*, which would occur several times during the service life of the building with almost no damage, and *severe EQGMs*, which would occur less than once during the use of the building and would not cause collapse or harm to human lives. While buildings not higher than 31 m (102 ft.) can be designed under just moderate EQGMs, buildings higher than 31 m must be designed for the two-level EQGMs.

4.2 *Principal issues in the improvement of EQRC.*

As discussed in section 2.1, it is well-recognized that most human injuries and economic losses due to moderate or severe EQGMs are caused by the failures of facilities, particularly buildings, many of which were presumed to have been engineered, i.e., designed and constructed, to provide protection against natural hazards and comfort to human beings. This has been dramatically confirmed during recent EQs around the world (the 1985 Chile, the 1985 Mexico, the 1986 San Salvador, the 1987 Whittier Narrows, the 1989 Loma Prieta, the 1990 Iran, the 1990 Philippines, and the 1992 Erzincan, Turkey, EQs. *Therefore, one of the most effective ways to mitigate the destructive effects of EQs is to improve existing methods or develop new and better methods of designing, constructing and maintaining new structures and of repairing and upgrading (retrofitting) existing seismically hazardous facilities.*

The seismic response of any facility (structure), and therefore the degree of damage that it will suffer, depends on the whole building system (soil-foundation-superstructure and nonstructural components and contents) when the EQ occurs: i.e., response depends not only on how the building has been designed and constructed, but also on how it has been maintained up to the time that the EQ strikes. Thus, the principal issues that need to be considered in order to improve EQRC, and therefore to reduce the seismic risks in our urban areas, are the ones grouped into the following categories.

- Improvement of the EQRD of the whole facility system (soil, foundation, superstructure, and nonstructural components and contents).
- Improvement of the construction of the foundation, the superstructure and the nonstructural components.
- Improvement of the maintenance (monitoring and preservation) of the whole system.

In what follows, only the main issues regarding the improvement of the EQRD of the whole system of any given facility (particularly the building system) will be discussed in detail. The main reason for this is that while issues concerning field construction and maintenance vary not only from one country to the next but even from one region to another in a given country (because they reflect the building technology available in each region), the basic problems created by EQGMs in the EQRD of our facilities are the same. However, before identifying and discussing the main issues that need to be resolved for an improvement in the EQRD of whole facility sy[illegible] the importance of proper field construction [illegible]QRC) and maintenance must be briefly discussed.

4.3 *Importance of proper EQRC and monitoring and maintenance of facilities.*

While a sound EQRD of any given structure is necessary, it is not sufficient to ensure a satisfactorily EQ resistant structure. As discussed above, the seismic response, and therefore the performance of any facility under the effects of EQGMs, depends on how the whole system of this facility has been constructed, how its function has been monitored, and how it has been maintained. A design can only be effective is the model used to engineer the design can be and is constructed and maintained [Bertero (1975), (1982) and (1986)]. Although the importance of construction and maintenance in the seismic performance of structures has been recognized, insufficient effort has been made to improve them (e.g., through improving supervision and inspection). Design and construction are intrinsically interrelated. If good workmanship is to be achieved, the detailing of members and their supports must be simple. Field inspection has revealed that a great deal of damage and failure is due to poor quality control of structural materials and/or poor workmanship - *problems that would not have arisen if the building had been properly inspected during construction.* The photos in Figure 19 illustrate the severe damage that occurred in one half of a building during the 1985 Chile EQ (the two halves, divided from each other by an expansion joint, were built by two different contractors), while no damage occurred in the other half. The concrete in the severely damaged half had a compressive strength of only 100 kg/cm^2. One of the main factors in the failures of several buildings during the 1985 Mexico, 1986 San Salvador, 1990 Philippines and 1992 Erzincan EQs was the poor quality of concrete and the poor workmanship in the detailing and placing of the reinforcement. Poor workmanship in the connections was the main reason for the failure of many industrialized (prefabricated) buildings during the 1988 Armenia EQ (Figure 20).In many other cases, damage may be attributed to improper monitoring of the function of the building, as in the case of several buildings during the 1985 Mexico EQ (Figure 21). Some of these buildings were built for offices or as residences, but were later used to shelter lightweight industries. Similarly, many observed failures of buildings have been due to improper maintenance during their service lives. Inappropriate alteration, repair, and

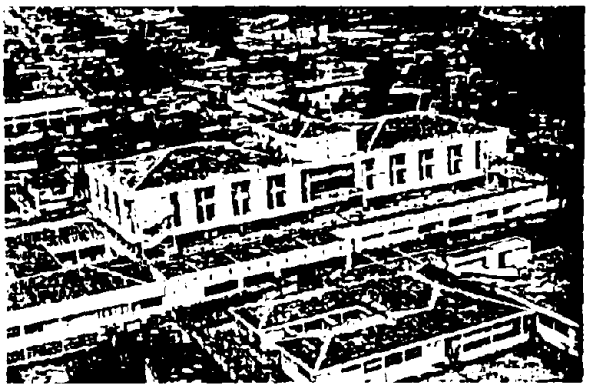

Overview of a 4-story building:
one half of the building was damaged

Damaged RC columns

Figure 19. Illustration of damage due to poor quality control of material [*Earthquake Spectra*, EERI February 1986]

Poorly-connected precast elements

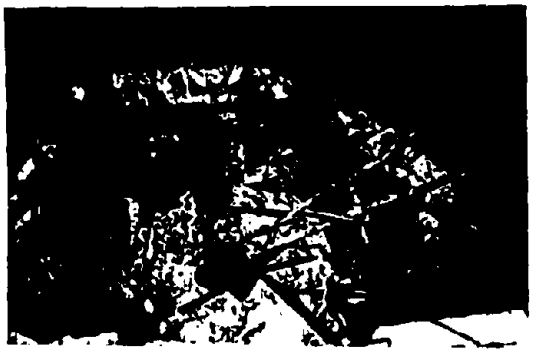

Poor detailing and workmanship of ties and welding of main bars

Figure 20. Illustration of damage to a precast concrete frame building due to poor detailing and workmanship [EERI Slide Library]

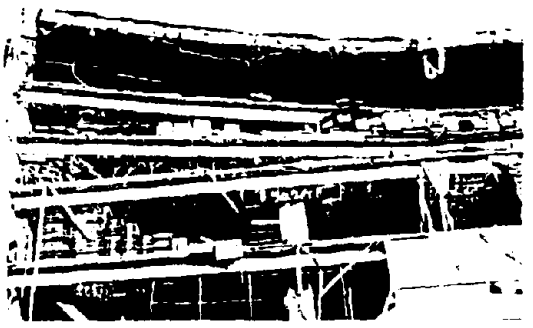

An office building used as a clothing factory

Overloaded commercial building

Figure 21. Illustrations of buildings that have collapsed due to excessive live load

retrofitting of the structure and nonstructural components can lead to severe damage during major EQ shaking. *Strict enforcement of seismic codes should be included in the EQ preparedness programs, and enforcement of seismic code regulations should not be lax under any circumstances.*

4.4 *Principal issues in the improvement of EQRD of structures*

4.4.1 *Differences between design and analysis.* In trying to identify the problems whose solutions need improvement in order to achieve an efficient EQRD of a facility, it is necessary to recognize clearly the differences between analysis and design. While usually (particularly for the design of engineered facilities) in order to achieve an efficient final design it is necessary to conduct analyses, in order to conduct analyses it is necessary to have a preliminary design. Design is thus more than just analysis. In order to distinguish clearly between analysis and design and at the same time to identify problems inherent in the design of EQ-resistant structures, it is convenient to analyze the main steps involved in satisfying what can be called the *basic design equation.*

DEMAND	≤	SUPPLY	(6)
on		of	
Stiffness		Stiffness	
Strength		Strength	
Stability		Stability	
Energy absorption and dissipation capacities		Energy absorption and dissipation capacities	

Evaluation of the *demand* and prediction of the *supply* are not straightforward, particularly for EQ-resistant facilities. Determination of the *demand*, which is usually done by numerical analyses of mathematical models of the entire soil-foundation-building system, depends not only on the interaction of the system as a whole with the different excitations that originate from changes in the environment, but also on *the intrinsic interrelation between demand and supply itself.*

In the last three decades, our ability to analyze mathematical models of structures subjected to EQ ground shaking has improved dramatically. Sophisticated computer programs have been developed and used in the numerical analyses of linear as well as nonlinear seismic responses of three-dimensional models of the bare structures of facilities to certain assumed EQGMs (*EQ input*). The time is ripe to take advantage of these improvements in analysis in the seismic design of structures. In general, however, these analyses have failed to predict the responses of real facilities, particularly at ultimate limit states. As a consequence of this, and also of the lack of reliable models to predict *supplies to real structures*, there has not been a corresponding improvement in the design of EQ-resistant structures. There is an urgent need to improve mathematical modeling of the whole systems of real facilities, which in turn requires integrated analytical and experimental research.

The proportioning (sizing) and detailing of the structural elements of a structure is usually done through equations derived from the theory of mechanics of continuous solids or by using empirical formulae. Except in the case of pure flexure, a general theory with reliable equations which can accurately predict energy absorption and dissipation capacities of structural elements and of so-called nonstructural elements, in the case of real buildings, has not been developed. Improving this situation will require integrated analytical and experimental research in the field (through intensive instrumenting of buildings) and in experimental laboratories (through the use of pseudo-dynamic or EQ simulator facilities or both).

4.4.2 *Main issues that remain to be resolved for the improvement of the EQRD of structures.* As discussed in section 3.2, the information needed to improve EQRD by improving prediction of EQ responses of structures can be grouped into the following three basic elements: *EQ input, demands on the structure, and supplied capacities to the structure.* These three basic elements of the EQ response problem are discussed briefly below.

- *EQ input: specification (establishment) of design EQs and design criteria.* The design EQs depend on the design criteria, or *the limit states controlling the design.* Conceptually, the design EQ should be that EQGM, out of all probable EQGMs that can occur at the site, which will drive a structure to its critical response. In practice, the application of this simple concept meets with serious difficulties because, firstly, there are great difficulties in predicting the main dynamic characteristics of ground EQGMs which have yet to occur at the building site, and, secondly, because even the critical response of a specific structural system will vary according to the various limit states which could control the design.

Seismic codes specify design EQs in terms of a building code zone, a site intensity factor, or a peak site acceleration. Reliance on these indices, however, is generally inadequate, and methods using *ground motion spectra (GMS), and Smoothed Linear Elastic Design Response Spectra (SLEDRS)* based on *effective peak acceleration (EPA)* have been recommended. While this has been a major improvement conceptually, great uncertainties regarding appropriate values for EPA and GMS, as well as for other parameters that have been recommended, persist.

- *Estimation of reliable demands.* The major uncertainties in the estimation of reliable demands (usually done by numerical analysis) are due to difficulties in predicting the following: (1) critical seismic loading during the service life of the structure (lack of properly established design EQs); (2) the state of the entire soil-foundation-superstructure-nonstructural components and contents system when the critical EQGM occurs [proper selection of the mathematical model(s) to be analyzed]; (3) internal forces, deformation, stresses and strains induced in the model (structural and stress analysis); and (4) realistic supplies of stiffness, strength, stability, and capacity to absorb and dissipate energy (i.e., realistic hysteretic behavior) of the entire facility system.
- *Prediction of supplies.* The supplies to a facility depend not only on supplies to its bare superstructural system, but also on supplies that result from the interaction of the bare superstructural system with the soil-foundation and the so-called *nonstructural components* of the facility. For example, masonry walls or partitions (or both) tightly packed as infill into the

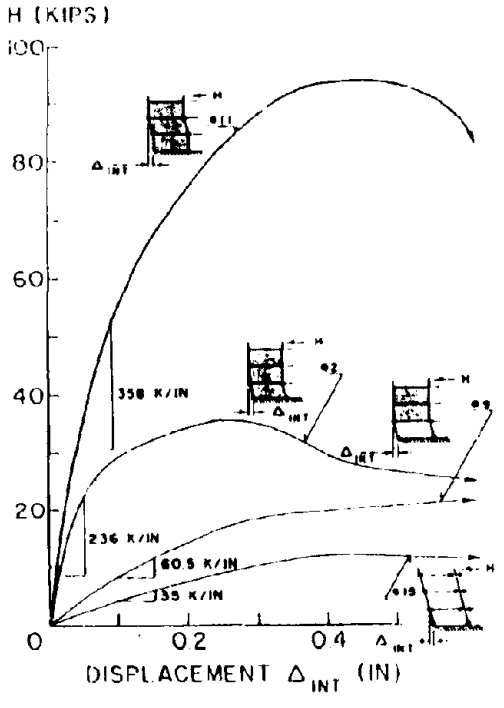

Figure 22. Effects of addition of infills on the initial parts of the lateral load (H) vs. interstory drift (Δ_{INT}) relationship for moment-resisting frames

moment-resisting frames of a building introduce significant changes into the dynamic characteristics of that building. Changes in stiffness, strength, and deformation capacities are illustrated in Figure 22. An evaluation of the test results illustrated in this figure and implications of these results are discussed by Brokken and Bertero [1981]. It is obvious that when interaction occurs between structural and nonstructural components, *neglecting such interaction in the selection of numerical characteristics for the design of the structure could lead to completely unrealistic evaluation of the demands, and consequently could result in a poor final design of the entire building system.* This observation is confirmed by the fact that many RC moment-resistant space frame buildings infilled with unreinforced masonry performed poorly during the 1985 Mexico EQ. Similarly, a large percentage of the buildings that collapsed during the 1988 Armenia EQ were RC frames infilled with stone.

In considering the basic general design equation, the designer might be tempted to increase supplies in order to overcome the problems created by the uncertainties in the values of *demands*. However, supply must be increased very carefully, because it may contribute to and considerably increase the demand.

4.5 *Directions toward solutions of the main issues in establishment of design EQs*

4.5.1 *General remarks regarding the need for site seismic hazard assessment.* Before embarking on the design of any structure to be constructed at any given site, it is necessary to conduct *an analysis of the seismic suitability of the selected site* and to define the *design events*, i.e., what is needed is a reliable site seismic hazard assessment. Recent EQs have indicated that in order to improve the reliability of this analysis and definition, it is necessary to: first, improve the *identification of all possible sources of EQs* that can affect the site; second, *to describe fully and reliably the dynamic characteristics of the ground motions at the source*; third, to quantify how the source ground motions are modified (attenuated or amplified) as they are propagated from the source to the site (i.e., *to improve the so-called Attenuation Law*); fourth, to identify the types of EQ hazards at the selected site; and finally, to estimate the return periods of EQGMs at different intensity levels.

■ *Identification of EQ sources. There is a need to improve identification of all possible EQ sources (faults) that can cause hazards at the site.* This has been confirmed by the experience of the 1976 Tangshan EQ and the Diablo Canyon Nuclear Power Plant Studies. It will require better zonation maps. Studies conducted after the 1985 Mexico EQ show that for sites located in Mexico City it is necessary to distinguish at least four sources: local EQs; continental place EQs; intermediate depth EQs; and subduction EQs, which can be located up to 400 km (250 miles) from the city [Rosenblueth, 1989]. It should be noted that, until a few years ago, cities and sites located at rather remote distances, say, 150 km (93 miles), had little concern about EQs. However, in the last two decades, with the advent of taller and slenderer structures, some instances of alarming and dangerous sway have occurred in the long natural period structures in cities which were located considerably more than 150 km from the epicenter.

For example, the sway and cracking of many slender (particularly soft first story) medium-to-high rise buildings in Buenos Aires, Argentina, caused dramatic panic among the occupants during the 1977 El Caucete (San Juan) EQ, whose epicenter was located more than 950 km (590 miles) from Buenos Aires. Furthermore, a tall, slender steel water tank near Buenos Aires collapsed during this EQ. It can be concluded from this that:

- *EQ disaster can occur at distances from the EQ source that are considerably greater that those usually assumed and reflected in present seismic zonation maps and codes.* This statement is substantiated by observations of damages during the following EQs: 1957 Mexico, 1977 Caucete (San Juan, Argentina), 1985 Chile and Mexico and 1990 Philippines.

■ *Dynamic characteristics of ground motions at the source*

- There is a need to consider the possibility of multi-events, i.e., two or more separate fault ruptures (not necessarily in the same fault), leading not only to overlapping ground motions originating from each fracture, but also, and even more importantly, the probability of a significant increase in the duration of strong motions at the epicentral region and at large distances from the epicenter. This is implied in the recorded EQGMs from the following EQs: 1985 Chile, 1985 Mexico and 1990 Philippines.
- *There is a need for a more reliable definition of the total strength of an EQ at the source than is given by magnitude.* This has resulted in the introduction of the

concept and definition of *Seismic Moment*, which is related directly to the energy released to the source and to its use in what has been defined as *Moment Magnitude* [Hanks and Kanamori, 1979].

■ *Attenuation laws: ground motions at the site*

• While significant improvement has been achieved in the accuracy of predicting the attenuation of peak acceleration with distance from the epicenter, focus or fault when seismic waves travel through rock or firm soil, the same cannot be said for the travel of waves through very soft soils. Peak ground accelerations are a function of both the source mechanism and the properties of the travel path. The EQGMs recorded during the 1985 Chile and Mexico EQs, and particularly those recorded during the Loma Prieta EQ, show that:

(1) Due to combinations of special geological settings and local soil conditions, EQs that at their sources have the same moment magnitude as those contemplated in present seismic codes can generate EQGMs of the damaging intensity specified by the codes at considerably greater distances that those usually reflected in present seismic zonation maps.

(2) Due to variations in soil conditions (soil profile), the dynamic characteristics of the induced EQGMs can differ significantly even for sites located at the same large epicentral distances.

(3) The *frequency content* of EQGMs not only varies with epicentral distance, but also is a complex function of source mechanism, focal depth, nature of travel path and site soil topography and profile. Higher frequencies attenuate more rapidly that low ones do.

(4) Duration of strong motion generated by multiple events is longer than that caused by single events. Furthermore, this duration tends to increase with moment magnitude, source distance, and soil deposits when compared to rock.

(5) *Directivity*. Recent studies have shown that peak acceleration can vary by a factor of 10 depending on the direction from the epicenter, and that peak velocity can vary by a factor of about 5 depending on the fault rupture process.

■ *Types of EQ hazards at the selected site*. As discussed in section 4.1, damage to human-made facilities may result from different seismic effects (hazards). They have been classified into two main groups: (1) direct effects and (2) indirect, or consequential, effects. Although present U.S. codes have been prepared to provide minimum EQ resistance against the vibration effects of typical EQ shaking, the damage during the following EQs has shown that the economic losses due to other effects can exceed those due to the vibration of buildings: 1964 Alaska (in Anchorage) and Japan (in Nigata), the 1989 Loma Prieta in San Francisco (in the Marina District), and particularly the 1990 Philippines. There is an urgent need for government officials and designers to pay more attention to these and other EQ hazards. The seismic risk resulting from these other physical phenomena should be taken into consideration through reliable regional zonation maps and microzonation of urban areas.

■ *EQ return period, or EQ recurrence relationship*. For any given site, establishing what constitutes an *acceptable seismic risk* (i.e., an acceptable probability of social or economic consequences due to EQs) requires statistical information regarding the seismic activity in the region where the site is located. For each of the different levels of moment magnitude (or, even better, level of ground motion) that needs to be considered in the design of the structure (design event and design EQGM), it is necessary to establish a relationship between the damage potential of the particular motion and its frequency, i.e., the rate of occurrence of such a motion. At present, there is great uncertainty in predicting such recurrence relationships.

4.5.2 *Establishment of design events and the corresponding design EQ*. As discussed in sections 3.3.2 and 4.1, for any given building to be constructed on a selected site, present U.S. codes define just one level of hazard (EQGM). From analyses of the damages resulting from recent EQs, particularly the 1984 Morgan Hill, the 1987 Whittier Narrows and the 1989 Loma Prieta, it becomes clear that there is a need to consider more than one level of EQGMs for the design of structures (as is clearly spelled out in the adopted general seismic design philosophy discussed earlier). Before establishing the design EQGMs at the site, it is necessary to define the design events causing such motions.

• *Design events*. According to the EERI Committee on Seismic Risk, the design event(s) is defined as "a specification of one or more EQ source parameters, and of the location of energy with respect to the site of interest used for the EQRD of a structure." Although it is common to define a design event simply by specifying just a magnitude and a slant (focal) distance, a reliable definition of such an event requires the specification of: moment magnitude, return period, epicentral distance, focal depth, fault position, fault type and rupture area (length and depth).

• *Design EQ*. For each of the possible design events (i.e., EQs at the sources that can control the design), it is necessary to define the damage potential of the EQGMs that can be generated at the facility site, or, even better, at the facility foundation. As discussed before, seismic codes specify design EQs in terms of one or two variables. Reliance on these parameters is generally inadequate. To have a reliable definition of a design EQ, it is necessary to specify: its effective peak acceleration, velocity and displacement, its frequency content (particularly the dominant period of the shaking), and the duration of the strong motion. *What is important is to have a reliable definition of each of the possible EQGMs at the facility site*. The above parameters, as well as other engineering parameters, have been used to define the damage potential of EQGMs.

Since damage involves nonlinear response (inelastic deformation), the only way to estimate damage and the actual behavior of a facility under severe EQ excitation is to consider its inelastic behavior. Guided by this basic concept and by the fact that the damage potential of any given EQ ground shaking at the foundation of a structure depends on the interaction of the intensity, the frequency content, and the duration with the dynamic characteristics of the structure, the lecturer believes that one of the most reliable ways to define the damage potential of an EQ ground shaking is to compute its energy input, E_I, to the foundation of the structure together with the other associated parameters [Bertero, 1991].

Recent EQs, particularly the 1989 Loma Prieta, clearly indicate that the level of "acceptable damage" should

vary with the *function* (occupancy category) of the structure. For certain occupancies, there is an urgent need for code specifications that require damage control. To achieve this, it will be necessary to specify at least two of the following levels of design EQs.

- *Service-level design EQs.* During this frequent type of EQ the entire soil-foundation-superstructure-and-nonstructural components and contents system should remain elastic (i.e., without any damage).
- *Functional or operational-level design EQs.* During this type of occasional EQ, the entire building could undergo some degree of nonstructural as well as structural damage (small yielding) which will not disrupt the operation of the facility.
- *Safety or survival-level design EQ.* Under this rare circumstance, the building should not collapse or suffer serious damage that can jeopardize human life.

For a reliable definition of the design EQ, it is necessary to *specify at least the three translational components* of the critical EQGMs at the site. This need has been clearly identified through observations of damage during the following EQs: 1979 Imperial Valley and 1985 Chile and Mexico. It has also been confirmed by experiments conducted on models of building structures using EQ simulator as well as pseudo-dynamic testing facilities [Bertero, 1986].

As pointed out previously, while the introduction of GMS and SLEDRS based on an EPA has been a major improvement conceptually (particularly for the design of essential facilities which should remain practically in their elastic range even under the extreme EQGMs), great uncertainties regarding appropriate values for EPA, GMS and SLEDRS, as well as for other parameters that have been recommended to improve this situation, persists [Bertero, V.V., 1991, Kunming, P.R. China and Bertero, V.V., 1991, Int'l Conf. on Seismic Zonation]. The uncertainties are even greater in the case of standard facilities in which structural damage under extreme EQs is acceptable. The lecturer believes that a promising engineering parameter for improving selection of proper design EQs, particularly when structural damage is acceptable and it is necessary to define the Smoothed Inelastic Design Response Spectra is the concept of Energy Input, E_I, of the EQGM, and its associated parameters, which can be obtained through the use of energy concepts.

5 USE OF ENERGY CONCEPTS

5.1 *General remarks*

Traditionally, displacement ductility has been used as a criterion to establish *Inelastic Design Response Spectra (IDRS)* for EQRD of buildings [Bertero and Uang, 1992]. The minimum required *strength* (or capacity for lateral force) of a building is then based on the selected IDRS. As an alternative to this traditional design approach, an energy-based design method was proposed by Housner [1956]. Although estimates have been made of input energy to SDOFS [Berg and Thomaides, 1960], and even of MDOFS, (steel structures designed in the 1960s for some of the existing recorded EQGMs) [Anderson and Bertero, 1969], it is only recently that this approach has gained extensive attention [Akiyama, 1985]. This design method is based on the premise that the *energy demand* during an EQ (or an ensemble of EQs) can be predicted, and that the *energy supply* of a structural element (or structural system) can be established. In a satisfactory design, the energy supply is larger than the energy demand.

To develop reliable design methods based on an energy approach, it is necessary to derive the energy equations. Although real structures are usually MDOFS, to facilitate the analysis and understanding of the physical meaning of the energy approach, it is convenient first to derive the energy equations for SDOFS and then to derive these equations for MDOFS.

5.2 *Derivation of energy equations.*

Uang and Bertero [1988] give a detailed discussion of the derivation of the two basic energy equations starting directly from Eq. 7 for a given viscous damped SDOFS subjected to an EQGM.

$$m\ddot{v}_t + c\dot{v} + f_s = 0 \qquad (7)$$

where: m=mass; c=viscous damping coefficient; f_s=restoring force (if k=stiffness, f_s=kv for a linear elastic system); v_t=v+v_g = absolute (or total) displacement of the mass; v=relative displacement of the mass with respect to the ground; and v_g=EQ ground displacement.

5.2.1 *Derivation of "absolute" energy equation.* Integrating Eq. 7 with respect to v from the time that the EQ excitation starts, and considering that $v=v_t-v_g$, it can be shown that

$$\frac{m(\dot{v}_t)^2}{2} + \int c\dot{v}dv + \int f_s dv = \int m\ddot{v}_t dv_g \qquad (8)$$

$$E_K + E_\xi + E_s = E_I \qquad (9)$$

"Absolute" Kinetic Energy | Damping Energy | Absorbed Energy | "Absolute" Input Energy

Considering that E_s is composed of recoverable Elastic Strain Energy, E_s, and of irrecoverable Hysteretic Energy, E_H, Eq. 9 can be rewritten as

$$E_I = E_K + E_s + E_\xi + E_H \qquad (10)$$

E_I is defined as the *"absolute input energy"* because it depends on the absolute acceleration, $\ddot{v}_t$. Physically, it represents the inertia force applied to the structure. This force, which is equal to the restoring force plus damping force (see Eq. 7), is the same as the total force applied to the structure foundation. Therefore, E_I represents the work done by the total base shear at the foundation on the foundation displacement, v_g.

5.2.2 *Derivation of "relative" energy equation.* Eq. 7 can be rewritten as

$$m\ddot{v}+c\dot{v}+f_s=-m\ddot{v}_g \qquad (11)$$

Integrating Eq. 11 with respect to v leads to:

$$\frac{m(\dot{v})^2}{2} + \int c\dot{v}dv + \int f_s dv = -\int m\ddot{v}_g dv \quad (12)$$

$$E_K' + E_\xi + E_a = E_I' \quad (13)$$

"Relative" Kinetic Energy — Damping Energy — Absorbed Energy — "Relative" Input Energy

As $E_a=E_s+E_H$, Eq. 13 can be rewritten as

$$E_I' = E_K' + E_s + E_\xi + E_H \quad (14)$$

The E_I' that is defined as the *"Relative Input Energy"* represents the work done by the static equivalent external force ($m\ddot{v}_g$) on the equivalent fixed-base system: that is, it neglects the effect of the rigid body translation of the structure.

5.2.3 *Difference between input energies from different definitions.* Uang and Bertero [1988] discuss in detail the differences between the values of the input energies E_I and E_I'. Although the profiles of the energy time histories calculated by the absolute energy equation (8) differ significantly from those calculated by the conventional relative equation (12), the maximum values of E_I and E_I' for a constant displacement ratio are very close in the period range of practical interest for buildings, which is 0.3 to 5.0 secs.

5.2.4 *Input energy to MDOFS.* The E_I for an N-story building can be calculated as follows [Uang and Bertero, 1988]:

$$E_I = \int (\sum_{i=1}^{N} m_i \ddot{v}_{ti}) dv_g \quad (15)$$

Where: m_i is the lumped mass associated with the i-th floor, and $\ddot{v}_{ti}$ is the total acceleration at the i-th floor. In other works, E_I is the summation of the work done by the total inertia force ($m_i\ddot{v}_{ti}$) at each floor through the ground displacement v_g. Analysis of results obtained from experiments conducted on medium rise steel dual systems indicates that the E_I to a multi-story building can be estimated with sufficient practical accuracy by calculating the E_I of a SDOFS using the fundamental period of the multi-story structure.

5.3 *Advantages of using energy concepts in seismic design of structures.*

Equation (10) can be rewritten as

$$E_I = E_E + E_D \quad (16a)$$

$$E_I = E_K + E_s + E_\xi + E_H \quad (16b)$$

where E_E can be considered as the stored elastic energy and E_D the dissipated energy. Comparing this equation with the design equation (6), it becomes clear that E_I represents the *demands*, and the summation of $E_E + E_D$ represents the *supplies*. Equation (16a) points out clearly to the designer that to obtain an efficient seismic design, the first step is to have a good estimate of the E_I for the critical EQGM. Then the designer has to analyze if it is possible to balance this demand with just the elastic behavior of the structure to be designed or will it be convenient to attempt to dissipate as much as possible some of the E_I, i.e., using E_D. As revealed by Eq. (16b), there are three ways of increasing E_D: one is to increase E_ξ by increasing the linear viscous damping, E_ξ; another is to increase the hysteretic energy, E_H; and the third is a combination of increasing E_ξ and E_H. At present it is common practice to just try to increase the E_H as much as possible through inelastic (plastic) behavior of the structure, which implies damage of the structural members. Only recently it has been recognized that it is possible to increase significantly the E_H and control damage throughout the structure through the use of *energy dissipation devices*. Furthermore, as discussed by Bertero [1992] in a paper presented at this conference (in a discussion of the use of an energy equation for rational selection of seismic upgrading strategies for existing hazardous structures), increasing E_D by increasing E_ξ has the great advantage that it can control the behavior of the structure under both safety and service levels of EQGMs.

If technically or economically (or both) it is not possible to balance the required E_I either through E_E alone or E_E+E_D, the designer has the option of attempting to control (decrease) the E_I to the structure. This can be done by *base isolation techniques*. A combination of controlling (decreasing) the E_I by base isolation techniques and increasing the E_D by the use of energy dissipation devices is a very promising strategy not only for achieving efficient EQRD and EQRC of new structures, but also for the seismic upgrading of existing hazardous structures [Bertero and Whittaker, 1989]. To use this energy approach reliably, it is essential to be able to select the critical EQGM (design EQ); in other words, the ground motion that has the largest damage potential for the structure being designed. Although many parameters have been and are being used to establish design EQs, most of them are not reliable for assessing the damage potential of EQGMs. As mentioned previously, a promising parameter for assessing damage potential of these motions is the E_I. However, as will be discussed below, this parameter alone is not sufficient to evaluate (visualize) the E_D (particularly E_H) that has to be supplied to balance the E_I for any specified acceptable damage. Additional information is needed.

5.4 *Information needed to conduct reliable EQRD.*

5.4.1 *General remarks.* It has been pointed out previously that the first and fundamental step in EQRD of structures is the reliable establishment of the design EQs. This requires a reliable assessment of the damage potential of all the possible EQGMs that can occur at the site of the structure. Currently, for structures that can tolerate a certain degree of damage, the *Safety or Survival-Level Design EQ* is defined through *Smoothed Inelastic Design Response Spectra, SIDRS*. Most of the SIDRS that are used in practice (seismic codes) have been obtained directly from SEDRS, through the use of the *displacement ductility ratio, μ*, or *reduction factors, R*. The validity of such procedures has been questioned, and it is believed that at present such SIDRS can be obtained directly as the mean or the mean plus different values of standard deviation of the *Inelastic Response*

Spectra, IRS, corresponding to all the different time histories of the severe EQGMs that can be induced at the given site from EQs that can occur at all of the possible sources affecting the site [Bertero, 1991, Seismic Zonation].

While the above information is *necessary* to conduct reliable design for safety, i.e., to avoid collapse and or serious damage that can jeopardize human life, it is *not sufficient*. Although the IRS takes into account the effects of duration of strong motion in the required strength, these spectra do not give an appropriate idea of the amount of energy that the whole facility system will dissipate through hysteretic behavior during the critical EQGM. They give only the value of maximum global ductility demand. In other words, *the maximum global ductility demand by itself does not give an appropriate definition of the damage potential of EQGMs*. As discussed previously, it has been shown that a more reliable parameter than those presently used in assessing damage potential is the E_I. As is clearly shown by Eq. (8), this damage potential parameter depends on the dynamic characteristics of both the shaking of the foundation and the whole building system (soil-foundation-superstructure and nonstructural components). Now the question is: Does the use of the SIDRS for a specified global μ and the corresponding E_I of the critical EQGM give sufficient information to conduct a reliable seismic design for safety?

Although the use of E_I can identify the damage potential of a given EQGM and, therefore, permits selection, amongst all the possible motions at a given site, of that which will be the critical one for the response of the structure, it does not provide sufficient information to design for safety level. From recent studies [Uang and Bertero, 1988; Bertero, 1991, Seismic Zonation] it has been shown that the energy dissipation capacity of a structural member, and therefore of a structure, depends upon both the loading and deformation paths. Although the energy dissipation capacity under monotonic increasing deformation may be considered as a lower limit of energy dissipation capacity under cyclic inelastic deformation, the use of this lower limit could be too conservative for EQRD. This is particularly true when the ductility deformation ratio, say μ, is limited, because of the need to control damage of nonstructural components or other reasons, to low values compared to the ductility deformation ratio reached under monotonic loading. Thus, effort should be devoted to determining experimentally the energy dissipation capacity of main structural elements and their basic subassemblages as a function of the maximum deformation ductility that can be tolerated, and the relationship between energy dissipation capacity and loading and/or deformation history.

From the above studies, it has also been concluded that damage criteria based on the simultaneous consideration of E_I and μ (given by SIDRS), and the E_{II} (including *Accumulative Ductility Ratio*, μ_a, and *Number of Yielding Reversals, NYR*, and *Number of Equivalent Yielding Cycles at* μ_{max}, $NEYC_{\mu_{max}}$) are promising parameters for defining rational EQRD procedures. The need for considering all of these engineering parameters rather than just one will be justified below by a specific example. From the above discussion, it is clear that when significant damage can be tolerated, *the search for a single parameter to characterize the EQGM or the design EQ for safety is doomed to fail.*

5.4.2 *Importance of simultaneously considering the* E_I, *IDRS, and* E_{II} *(including* μ_a *and NYR) for defining the safety-level design EQ*. Figures 23-27 permit comparison of the values of these different engineering parameters for two recorded EQGMs San Salvador (SS) and Chile (CH). Table 5 summarizes approximate maximum values for these parameters corresponding to each of these two different recorded EQGMs. The importance and, actually, the need for simultaneously considering all the above parameters in selecting the critical EQGMs and, therefore, for defining the safety-level design EQ, is well illustrated by analyzing the values of these parameters for these two records.

San Salvador (SS) vs. Chile (CH) Records. From analyses of the values of *Peak Ground Acceleration (PGA), Effective Peak Acceleration (EPA)*, and *Effective Peak Velocity (EPV)* given in Table 5, which are values presently used to define the seismic hazard zoning maps, it might be concluded that the damage potential of these EQGMs is quite similar. One can arrive at a similar conclusion if the values of the required *Yielding Strength Coefficient*, $C_y=V_y/W$, for different values of μ are compared or, in other words, if the IRS for different μ are compared (Fig. 23). However, a completely different picture is obtained when the values of the E_I, E_{II}, μ_a, and NYR for different values of μ are compared. The E_I for the CH record can be as much as 5 times the E_I for the SS record (Fig. 24). The E_{II} [represented by the equivalent hysteretic velocity, $V_H=(2E_H/m)^{1/2}$, in Fig. 25] for the CH record is more than 3 times the E_{II} for the SS record when the period, T, is about 0.5 secs. and nearly 2 times when the T varies from 0.5 secs. up to 1.5 secs. The μ_a for the CH record are 2 to 4 times higher than those of the SS record (Fig. 26). The NYR for the CH record and for a μ=6 and T<0.5 seconds are more than 10 times the NYR for the SS record (Fig. 27). For a μ=4 and T≥0.5, the NYR for the CH record are more than 5 times those of the SS record.

From the above comparison, it is clear that the damage potential of the CH recorded EQGM is significantly (at least 3 times) greater than that of the SS record in spite of the fact that PGA, EPA, EPV, ERS (IRS for μ=1) and even the IRS for different values of μ are very similar. Thus, the importance of evaluating the E_I and E_{II} (represented herein by V_H, μ_a and NYR spectra) which are functions of the duration of strong ground motions, t_d, becomes very clear. While the t_d for the CH records is 36 secs., the t_d for the SS record is only 4.3 secs. (see Table 5). The importance of t_d in judging damage control is discussed in by Bertero [1991, 4th Zonation Conference]. While the above spectra are very helpful in preliminary design, for the final design (detailing of members), the ideal would be to have the time history of the E_H, i.e., the time history of the load-deformation relationship of the designed structure.

The assembly of all the above spectra and time histories can be considered the ideal information for making reliable decisions regarding the critical EQGMs and, therefore, for reliable establishment of design EQs and design criteria. Thus, this basic information should be gathered in order to improve seismic codes as well as for the design of important facilities. It should be noted that all of the above spectra can be computed by an engineer who is provided with the time history of all possible EQGMs at the site of the structure.

Table 5. Parameters corresponding to the Chile (CH) and San Salvador (SS) EQGMs

EQ GROUND MOTION PARAMETERS / EQ RECORD	PGA (g)	CPA (g)	APV (in/s)	t_d (secs)	μ = 2				μ = 4				μ = 6			
					C_y	E_y/m $\frac{in^2}{sec^2}$	μ_s	HYS	C_y	E_y/m $\frac{in^2}{sec^2}$	μ_s	HYS	C_y	E_y/m $\frac{in^2}{sec^2}$	μ_s	HYS
CHILE (CH)	0.67	0.57	16	35.8	0.95	11,200	11	28	0.70	9,600	33	53	0.67	8,800	133	122
SAN SALVADOR (SS)	0.69	0.54	17	4.3	1.04	2,400	5	6	0.69	1,900	12	9	0.69	1,700	28	9

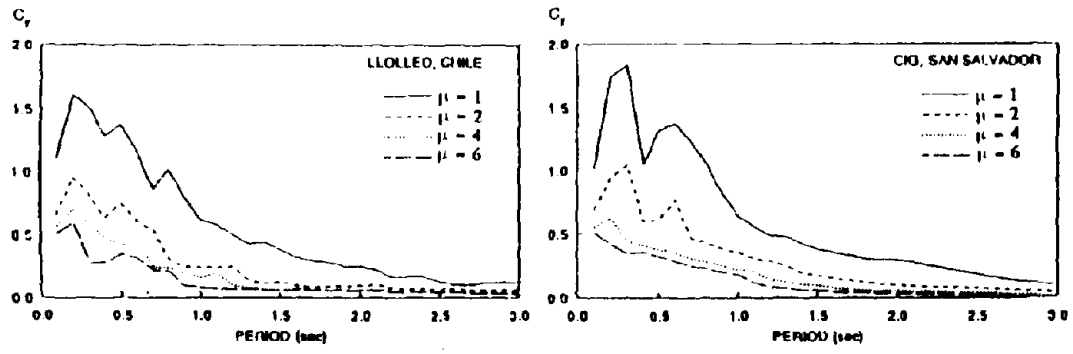

Figure 23. Yielding strength spectra (C_y) for CH and SS records (5% damping)

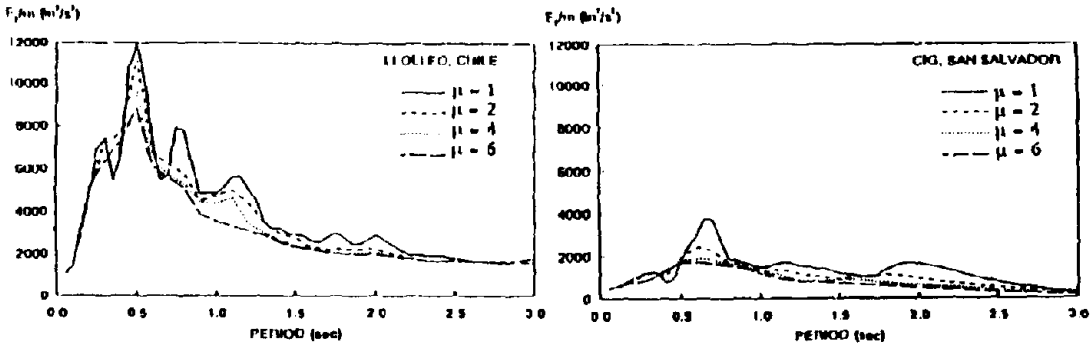

Figure 24. Input energy (E_y/m) for CH and SS records (5% damping)

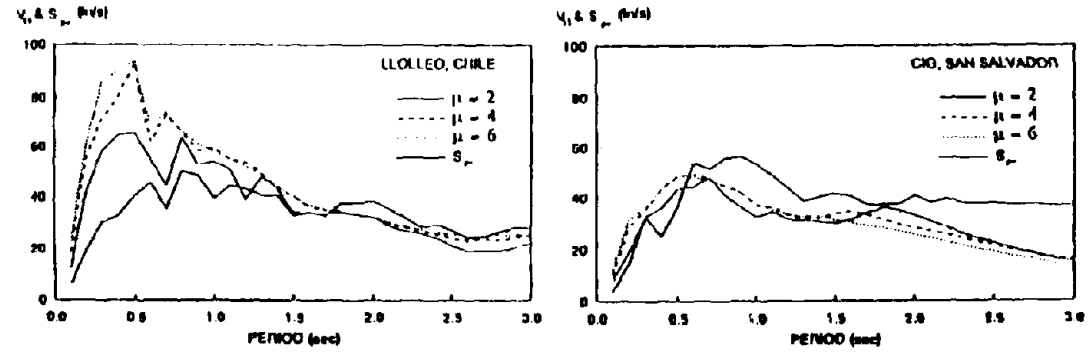

Figure 25. Hysteretic energy equivalent velocity (V_H) spectra for CH and SS records (5% damping)

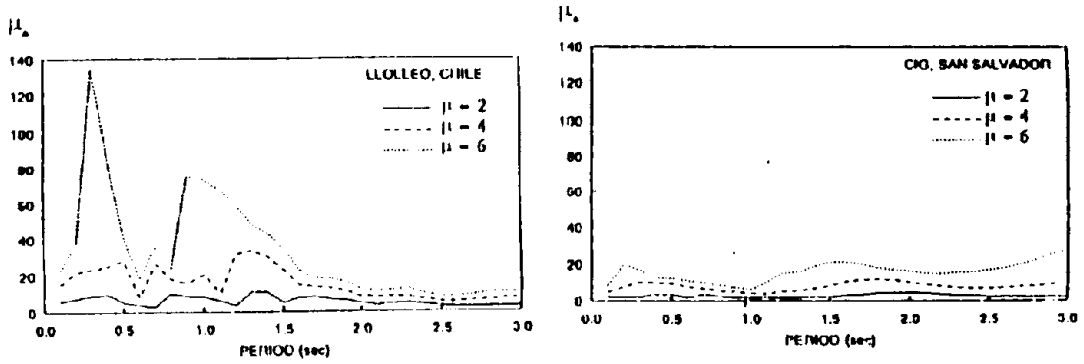

Figure 26. Cumulative displacement ductility ratio (μ_s) spectra for CH and SS records (5% damping)

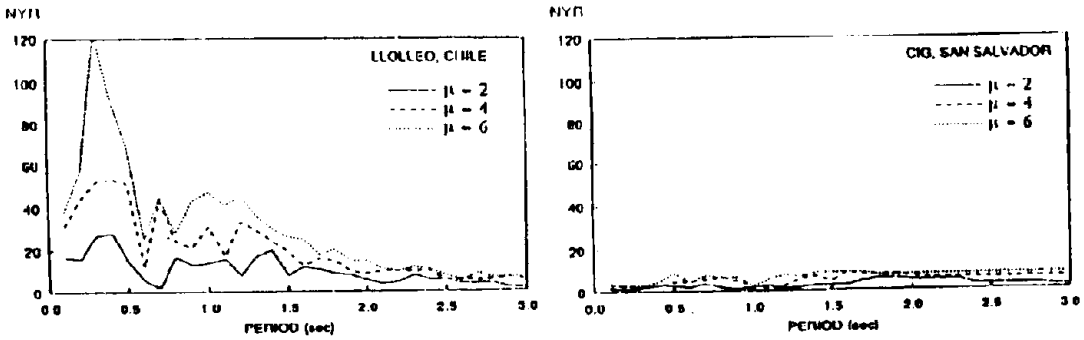

Figure 27. Number of yielding reversal (NYR) spectra for CH and SS records (5% damping)

It has to be recognized that, for practical preliminary design of most standard facilities, it will be convenient to specify the minimum possible information to keep it simple. It is believed that, for a given structural site, this minimum could be the E_I and the SIDRS for strength and displacement of all the possible EQGMs at that site. The E_I would permit selection of the type of critical EQGM, i.e., the one that will induce the largest damage. The SIDRS, corresponding to the type of critical EQGM can be used to conduct the preliminary design of the structure. Once a preliminary design is completed, it will be possible to obtain all the other information, i.e., the E_H, μ_s, NYR and NEYCμ_{max} for different μ_s, from nonlinear, dynamic time history analyses, taking advantage of the significant advances achieved in the development of computer programs for such analysis. This will permit checking the adequacy of the preliminary design. While a nonlinear analysis of the preliminary design using a static approach (i.e., equivalent static lateral force) can give an idea of the strength and deformation capacities as well as a lower limit of the available E_H and therefore it should be used if no time history of the critical EQGMs is possible, this type of analysis will not supply any information regarding the μ_s, NYR, NEYCμ_{max} or the sequence of damage.

From the above discussion, it becomes clear that, *if future codes perpetuate simple procedures for seismic design specifying only smoothed strength response spectra, it will be necessary to place more stringent limitations on the type of structural systems that could be used and on how such procedures can be applied, and to have very conservative regulations in the sizing and detailing for ductility and in the maximum acceptable deformations.*

6. NEED FOR FORMULATION OF A CONCEPTUAL METHODOLOGY FOR EQRD OF STRUCTURES

6.1 *Introductory remarks.*

As discussed previously, present seismic codes fall short of the goals and objectives of the worldwide accepted philosophy of EQRD. Furthermore, these codes, in their attempt to be simple (as they should be), have tried hard to simplify the complex problem of EQRD by developing design procedures based on just one parameter. The result is codes that are not transparent, i.e., codes whose regulations do not present in a visible way the basic concepts which govern the EQRD of structures.

Although it is generally recognized that damage is due to deformation, there is no agreement regarding the main criterion for preliminary EQRD of structures. Perhaps as a consequence of past and present code requirements, present practice emphasizes the use of strength in the preliminary design of structures. More specifically, in most of the present codes, the preliminary design is based only on base shear strength, with a requirement to check the drift by elastic analysis. The insistence on using only strength as primary criterion is perhaps a consequence of the following two reasons: first, it allows the practice of trying to design for ultimate or safety

limit state by reducing the actual inelastic design to one at working stress where linear elastic analysis can be used; and second, there is an assumption that there is a unique relation between strength and stiffness. This assumption ignores the fact that, particularly in the case of RC structures, it is possible to change the strength of a structure significantly without changing its stiffness.

While preliminary design based just on base shear strength could be justified for design where serviceability (elastic response) controls, it cannot be accepted where the design is controlled by the ultimate (safety) limit state, where large plastic deformation is accepted: at this limit state, base shear strength of a given designed structure is insensitive to variation of deformation and, therefore, to damage. Once structures yield and deform as mechanisms, the base shear strength remains constant, while the deformation can take any value, from its yielding value up to the maximum value, at which collapse (sudden significant drop in resistance) occurs. In view of the above insensitivity of the base shear strength to damage in the inelastic (plastic) range of response, it is perhaps unfortunate that in the past most of the efforts in improving EQRD have been expended in designing for strength only, without proper consideration of the role of deformation. Damage is a consequence of deformations. For any structure that is responding in the inelastic (plastic) range under practically a constant strength, the degree or level of damage depends upon the amount of the plastic deformation that the structure undergoes. Thus, to control damage it is necessary to control deformations. The question is how to achieve such control at the different levels of EQ shaking that can occur during the life of the structure. Bertero et al. [1991] discuss in detail the issues involved in achieving such control at the serviceability and safety limit states, pointing out the need for ductility and drift control. The need for drift control can be summarized by the following statement.

While displacement ductility factors generally provide a good indication of structural damage, they do not usually adequately reflect the damage to nonstructural elements. This is an important limitation in EQRD of buildings, since a significant portion of the hazard to occupants and of the total cost of repairing EQ damage is a consequence of nonstructural damage. Nonstructural damage is more dependent on the relative displacements (drift) than on the overall displacements. To obtain a reliable measure of nonstructural damage, maximum drifts must remain unnormalized or be divided by the value of drift corresponding to the damage threshold. Nonstructural damage estimates based on drift ductility ratios may be misleading. For example, nonstructural damage for relatively rigid structures may be small even for large values of displacement, since the yield displacement may be well below the nonstructural damage threshold. On the other hand, the nonstructural damage and lateral displacements for flexible structures may become intolerably large even before significant yielding develops.

To produce serviceable, safe and economical facilities, EQRD methods must incorporate drift (damage) control in addition to lateral displacement ductility as design constraints.

The control of the drift of a structural system under EQ excitation is important for at least three different reasons: (1) to maintain architectural integrity, thereby avoiding unacceptable damage to nonstructural components; (2) to limit structural damage and avoid structural instability (P-Δ) problems; and (3) to avoid human discomfort under frequent minor or even occasional moderate EQ shaking.

Story drifts and drift ductility factors may also be useful in providing information on the distribution of structural damage. Unfortunately, conventionally computed story drifts may not adequately reflect the potential structural or nonstructural damage to multistory buildings. In some structures, a substantial portion of the horizontal displacements results from axial deformations in the columns. Story drifts due to these deformations are not usually a source of damage [Fig. 28a].

A better index of both structural and nonstructural damage is the tangential story drift index, R_T. As schematically indicated in Fig. 28b, the intent of this index is to measure the shearing distortion within a story. For the displacement components shown in Fig. 28c and assuming that floor diaphragms are rigid in their own plane, the average tangential drift index is equal to

$$R_T = \frac{1}{H}(u_1 - u_l) + \frac{1}{L}(u_6 + u_8 - u_2 - u_4) \qquad (17)$$

in which L is the bay width and H is the story height. This first term on the right-hand side of Eq. 17 is the conventional story drift index, and the second is a correction applied for each bay accounting for the slope of the floors above and below the story. It may not be appropriate to average the values of R_T for a story when the pattern of axial column deformations varies greatly across the structure (e.g., frames with structural walls). In recognition of the noted weakness of present seismic code EQRD procedures based on base shear strength, which is insensitive to damage in the inelastic (plastic) range, there have been proposals that preliminary design be based only on lateral stiffness, i.e., only on controlling interstory drift.

6.2 *Recommended practical methods for designing considering IDI*

A simplified method for estimating lateral drift of RC structures has been suggested by Sozen [1983]. The method is intended to be used for interpreting experience and evaluating relative merits of different structural schemes and member sizes on the basis of a tolerable damage criterion. The method is conveniently used in preliminary evaluation by simple estimates of the base shear capacity coefficient.

Shimazaki [1984 and 1988] investigated the effects of strength and stiffness and of the type of EQGM on nonlinear displacement response of SDOF systems. *The results obtained show that the nonlinear displacement response is equal to the linear response spectral values if the system has a certain strength which is determined by dimensionless parameters for strength, initial period, and type of EQGM.*

Recently Qi and Moehle [1991] and Moehle [1992] developed two simple and practical EQRD procedures based on displacement (drift) information. One uses displacement information directly, and the other, a ductility-ratio approach, uses it indirectly, establishing ductility requirements as a function of the provided strength and the strength required for elastic response.

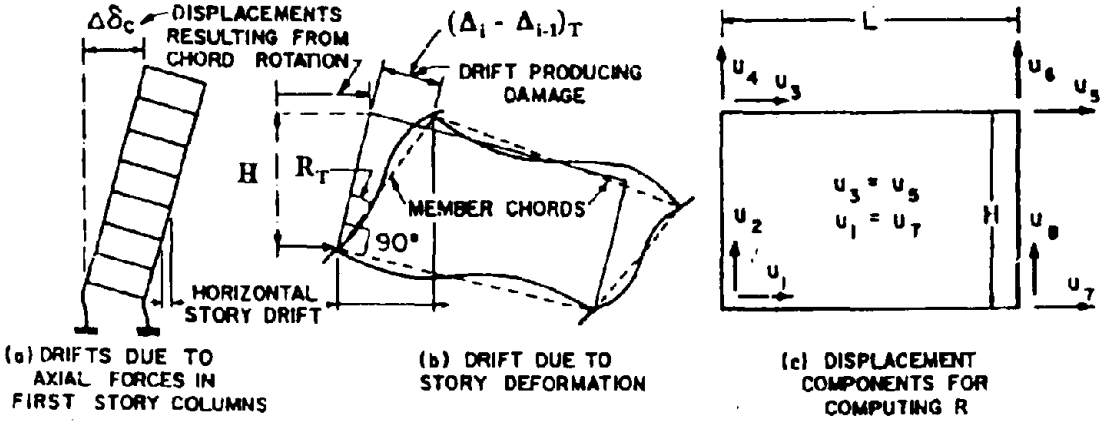

Figure 28. Computation of tangential interstory drift index (IDI)

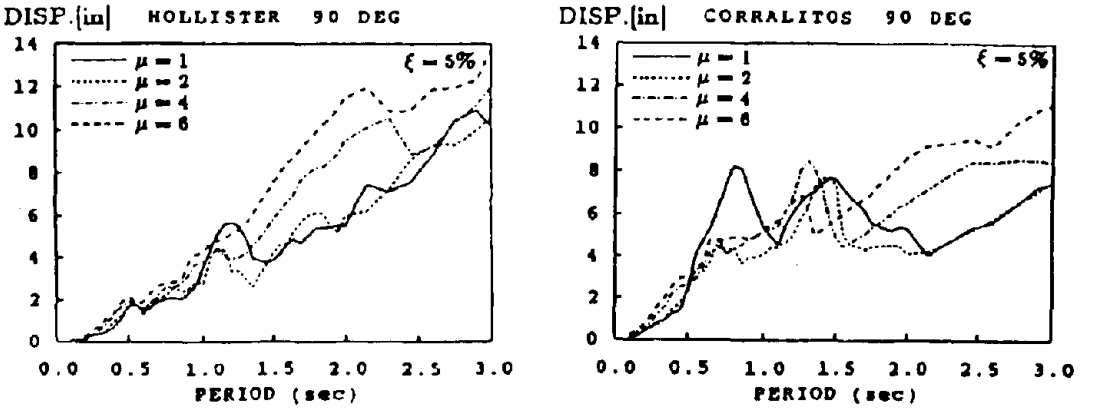

Figure 29. Nonlinear displacement response spectra

Results obtained by Miranda [1991] have shown that the nonlinear displacements are very sensitive to the dynamic characteristics of the EQGMs and in some cases the displacement can be significantly higher than those computed from a linear elastic response, particularly if high μ_s are used in the derivation of the yielding strength (see Fig. 29 for the case of Corralitos and Hollister EQGMs recorded during the 1989 Loma Prieta EQ). This observation agrees with the results obtained by Kappos [1990]. These observations also agree with results reported by Hwang and Jaw [1990], which recommend the use of the following empirical formula for estimating the deflection amplification factor C_d (defined as the ratio of absolute maximum interstory displacement to the corresponding value from a linear time history analysis).

$$\ln C_d = 0.414(\ln \mu_m) \qquad (18)$$

where μ_m is the maximum story ductility ratio.

Hatamoto et al. [1990] propose a newly automated seismic design method for RC frames which aims at uniform energy dissipation throughout the building frame, so that the resulting damage is uniformly distributed as much as possible over all elements.

Because of the limitations involved (due to the assumptions made to simplify the design procedure) in applying each of the practical methods on the basis of the use of just one parameter, whether strength (as in the present code), or lateral drift, and because of the difficulties in specifying very clearly the limitations on the application of these proposed methods, the lecturer believes that a more rational approach to EQ-resistant preliminary design is one that recognizes from the beginning of the EQRD process the importance of strength and stiffness (control of deformation) and which also recognizes that these two factors, while strongly interrelated in the case of elastic response, clearly have a weaker relation to each other in the case of inelastic response. In this last case, the lateral deformation at ultimate limit state depends on the yielding strength provided to the structure. To control inelastic deformation, it is necessary to provide the structure with a minimum yielding strength. Therefore, to achieve an efficient preliminary EQRD, there is a need to consider two requirements simultaneously: the *strength* (based on rational use of μ_s and ξ), and the *deformation* (based on the limitation of IDI), and their combined effect on the

energy capacity of the whole facility system.

The above need for a rational and transparent approach to the issue of improving EQRD procedure for new facilities and for upgrading existing hazardous facilities has motivated the lecturer and his research associates to attempt to develop and apply what can be called a conceptual methodology for EQRD of structures.

6.3 *Conceptual methodology for EQRD* [Bertero, R., and Bertero, V., 1992]

This proposed conceptual methodology is in compliance with the worldwide accepted EQRD philosophy and is based on well-established fundamental principles of structural dynamics, the mechanical behavior of the entire facility system, and comprehensive design. It takes into account from the very beginning of the EQRD procedure (i.e., from the preliminary design on) the simultaneous demands for *strength, deformation and their combined effects* on the demanded and supplied *energy capacities* of the entire facility system. The proposed conceptual methodology leads to a rational and transparent EQRD procedure, which is divided for convenience into two main phases. The *first phase* covers the acquisition and processing of the data needed to establish reliable design EQs for at least two limit states: serviceability and safety. The *second phase* is devoted to the design of the structure for the design EQs: it consists of an iterative procedure, starting with an efficient preliminary design followed by an analysis of the preliminary design, ending with a final design.

The main advantage of this proposed conceptual methodology is that, notwithstanding the great uncertainties in the quantification of some of the concepts involved in its codification, the numerical quantification of some of the concepts can be improved without changing the format of this codified methodology as new and more reliable data are acquired.

This conceptual methodology has been developed to improve EQRD by improving the numerical design phase of the whole EQRD procedure. Thus, this conceptual methodology should not be confused with what the lecturer [Bertero 1980 and 1982] has defined as "conceptual design," i.e., the avoidance or minimization of problems created by the effects of seismic excitation through applying the understanding of mechanical behavior (performance) of the entire soil-foundation-building system rather than using numerical computations. Illustrations of this definition and guidelines for its application to improve EQRD and EQRC are given in the above references, which conclude that, *"Because of large uncertainties in estimating the demands and real supplies in the EQRD of buildings, it is of paramount importance to pay more attention to 'conceptual' than to 'numerical' design."* By proper selection of building configuration, structural layout, structural system, structural material and nonstructural components and their materials, and by proper proportioning and detailing of the structural and nonstructural components, it is possible to reduce and control the uncertainties in the demands and supplies. Thus, sophistication in these selections and proportionings and detailings is more important that sophistication in numerical analysis of mathematical models to estimate demands and supplies.

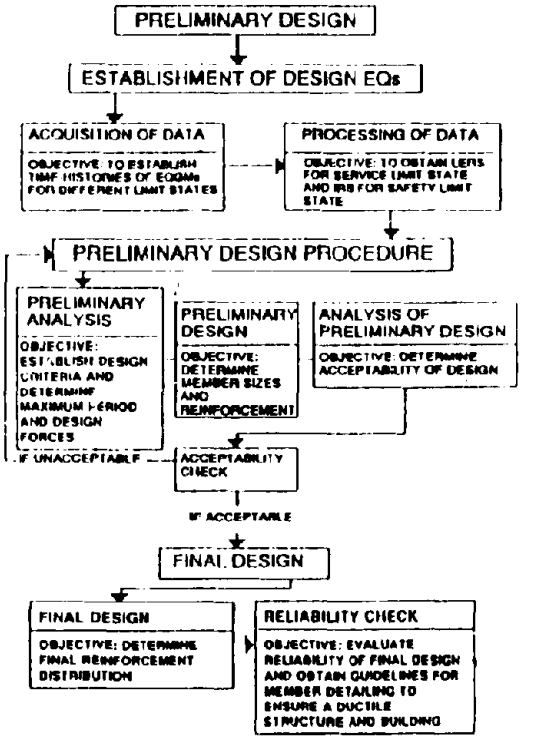

Figure 30. Flow chart for EQRD procedure

The "conceptual methodology phase" (numerical design) should be applied after the "conceptual design phase" of the overall EQRD and EQRC problems has already been conducted. Thus, from the point of view of the numerical design phase, the formulation and solution of the EQRD problem can be summarized as follows.

GIVEN: • Function of building; site of building; and general configuration of building, structural layout (including foundation), structural system, structural material and nonstructural components and contents.

REQUIRED: • An efficient (optimum) EQRD of the entire building.

SOLUTION: • A technically efficient and economical final solution requires an iterative procedure, starting with an efficient preliminary EQRD.

The iterative procedure required for the solution of the EQRD problem is illustrated in Figure 30. In order to attain an efficient EQRD of a structure, it is necessary that the procedure at our disposal be rational, transparent and reliable. Present seismic code design procedures do not satisfy these requirements. As illustrated in Figure 30, it is convenient in the formulation of such procedures to divide the formulation into two main phases: the *establishment of design EQs* and the *development of an efficient and reliable design procedure* for the building against the design EQs. Although it would be ideal for the designer to be involved in both of these phases, in general it is not necessary, because the design EQs can be established for different site types by a group of experts.

6.3.1 *First phase: establishment of design EQs.* This phase covers the acquisition and processing of data needed for the establishment of the design EQs. As discussed previously, the establishment of reliable design EQs is the key step in achieving a reliable EQRD, because to achieve any reliable prediction of the demands on a structure, it is necessary to have a reliable definition of the EQGMs against which the structure has to be designed.

■ *Acquisition of data.* The needed data and the problems involved in their acquisition can be summarized as follows.

GIVEN: • The site of the building (soil profile and topography).

REQUIRED: • Return periods of the different levels of EQGMs that my occur at the site of the building and their damage potential for the entire building system for at least its service and safety limit states.

SOLUTION: • Conduct a reliable analysis of the site (soil profile and topography); identify all of the possible sources of EQs from which the EQGMs that could affect the building could be originated; define the seismic activity at the site due to all possible EQ sources in the form of time histories of the possible EQGMs and their recurrence periods (T_r); select T_r for the service and safety limit states.

Ideally, the acquisition of the needed data should be based on EQGM records from the site. If there are not enough recorded EQGMs for the site, the needed data can be obtained either from recorded EQGMs at sites with similar soil profile and topography or by using numerical synthesis to generate several probable EQGM time histories.

Processing of data. The main objective of this key step in the establishment of the design EQs is to process the data about the probable future EQGMs at the site to facilitate the reliable selection of the design EQs. According to the discussions presented above in sections 4 and 5, the problems involved in this step and their solutions can be summarized as follows.

GIVEN: • Time histories of probable EQGMs for at least service and safety limit states.

REQUIRED: • For serviceability limit state: the Smoothed Linear Elastic Design Response Spectra (SLEDRS) for strength (C_s) and for displacement (S_d).
• For Safety limit state: the SLEDRS and Smoothed Inelastic Design Response Spectra (SIDRS) (for different values of μ) for C_s, S_d, for the spectra of parameters for evaluation of the cumulative damage caused for cyclic load reversals [input energy (E_I), hysteretic energy (E_H), cumulative ductility ratio (μ_e), Number of Yielding Reversals (NYR) and Number of Equivalent Yielding Cycles ($NEYC\mu_{max}$)].

SOLUTION: • Computation of the LERS and the Inelastic Response Spectra (IRS) (for different values of μ) for C_s and for S_d for each of the possible EQGMs that can be originated at the site from the different EQ sources. From statistical studies of the LERS, find the SLEDRS and SIDRS. In smoothing the LERS and IRS, careful consideration should be given to the standard deviation, σ, as well as to the uncertainties regarding the dynamic characteristics of future EQGMs. To obtain the critical EQGMs that are to be considered for safety level where some level of damage is tolerated (i.e., $\mu>1$), conceptually it is necessary to compute for each EQGM the following spectra: E_I, E_H, μ_e, NYR and $NEYC\mu_{max}$, as well as the hysteretic behavior history. Selection of critical EQGMs can be simplified by using recently proposed damage indices.

For practical application of this solution, R. Bertero and V. Bertero [1992] have used the suggestion of Fajfar et al. [1992], who have introduced the concept of an equivalent reduced ductility factor, μ_e, to account for the effect of cumulative damage caused by cyclic load reversals, as discussed in section 5.4.2. Three different damage models were used. The first two models, which are based on maximum displacements and dissipated energy, respectively, yield upper and lower limits for the equivalent reduced μ_e. The third model is based in the Park-Ang [1984] damage model, DM, which can be written in the following form:

$$DM = \frac{\delta}{\delta_u} + \beta \frac{E_H}{F_y \delta_u} = \frac{\mu}{\mu_u} + \beta \frac{E_H}{F_y \delta_y \mu_u} \qquad (19)$$

where β is a parameter that depends on structural characteristics.

Using the Park-Ang model together with the dimensionless parameter γ, introduced by Fajfar et al. [1992], the following equation for μ_e has been obtained for SDOFS

$$\mu_e = \frac{\sqrt{1 + 4(DM)\beta\gamma^2\mu_u} - 1}{2\beta\gamma^2} \qquad (20)$$

This equation points out that the reduction due to low cyclic fatigue is controlled by the parameters β and γ and the desired (or permissible). As pointed out previously, although it would be highly desirable that the designer be involved in the data acquisition and processing for establishing the design EQs, in general this is unnecessary; for any given urban area, a group of geoscientists, geotechnical engineers and structural engineers can establish the design EQs for different limit states (at least service and safety) according to the different site conditions in each urban area.

6.3.2 *Second phase: design procedure.* This second phase of the proposed conceptual methodology is devoted to the design (sizing and detailing of the members and their connections and supports) of the entire building system against the critical combination of the established design EQs with other excitations that can act on the building according to its site location. As illustrated in Fig. 30, in order to arrive at the desired final design it is necessary to start with a preliminary design procedure.

■ *Preliminary design procedure.* The main objective of this phase is a design which is as close as possible to the

desired final design. As illustrated in Fig. 30, the preliminary design phase consists of three main groups of steps: (1) preliminary analysis, (2) preliminary design, and (3) analysis of preliminary design.

1. Preliminary analysis. The objective of this first group of steps is the establishment of the design criteria and the estimation of the acceptable maximum fundamental period (T) and the design forces (critical combinations among all of the forces that can be induced). In the conceptual methodology, preliminary analysis of the design problem can be formulated thus:

GIVEN: • Function of building; • general configuration of the building, structural layout, structural system, structural materials and nonstructural components and contents; • gravity, wind, snow and other possible loads or excitations; and • SLEDRS and SIDRS for EQGMs expected at service and safety limit states.

REQUIRED: • Establishment of the design criteria, the minimum stiffness (or maximum T) acceptable to control the damage (maximum deformation of the building), the design seismic forces and the critical load combinations.

SOLUTION: • Based on a transparent approach that takes into account from the beginning that: the structure is a Multi-Degree-of-Freedom System (MDOFS); there can be important torsional effects even under service EQGMs (i.e., in the linear elastic response) and that for safety EQGMs these effects can be different; and it is necessary to consider the desired damage index (control of damage) for selecting appropriate μ that can be used as well as the expected overstrength.

Figure 31 shows a flow chart of the steps involved in the preliminary analysis to estimate the design seismic forces. Note that although the main purpose of this step is analysis of the problem involved [i.e., what is given (general configuration, structural layout, structural system, structural material, and nonstructural components and contents), what is known (SLEDRS and SIDRS for service and safety limit state), and what is needed (to find the maximum period and design forces)], it is clear that a preliminary design of member sizes is in fact necessary in order to satisfy the deformation demand and obtain the fundamental period of the building, T_1, to be used for estimating the design forces. A more detailed description of the problems confronted by the designer in carrying out this preliminary analysis is offered by Bertero R. and Bertero V. [1992].

2. Preliminary Design. The preliminary design step (assuming that preliminary sizing for stiffness was done in the preliminary analysis phase) can be as follows for a RC building.

GIVEN: • Gravity, wind, snow and seismic-design loads for service and safety limit states; critical load combinations; mechanical characteristics of the structural and nonstructural materials.

REQUIRED: • Beam and columns sizes and their flexural reinforcement.

SOLUTION: • Based on the application of linear optimization theory, the beams and columns of each story are designed to minimize the volume of flexural reinforcement, using practical requirements as well as the service bending moments as constraints so that the preliminary design simultaneously considers the demands for serviceability and safety.

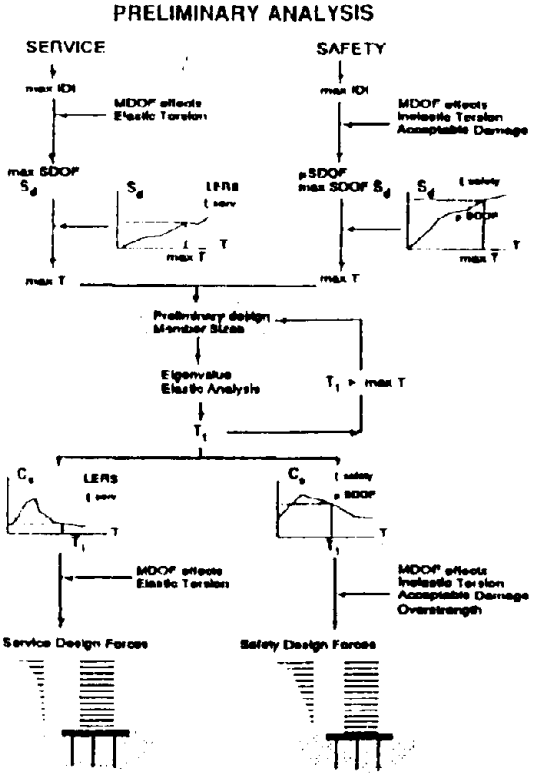

Figure 31. Preliminary analysis: flow chart of the steps required to estimate the design seismic forces

3. Analysis of preliminary design. This may be stated as follows:

GIVEN: • General configuration of building, structural layout, structural system, structural material and its mechanical characteristics, and nonstructural components and their materials and mechanical characteristics; • beams and columns sizes and flexural reinforcement; and • design EQs, critical load combinations and possible critical EQGMs for service and safety limit states.

REQUIRED: • A determination of the acceptability of the preliminary design, i.e., check whether it satisfies the established design criteria.

SOLUTION: • Check inter-story drift index (IDI), stress-ratios, shear stresses in the members and joints, adequacy of the foundation, and local damage index (DM)

under critical GMs for each limit state using static and dynamic load analyses.

6.3.3 *Discussion of the preliminary design procedure.*

■ *Preliminary analysis.* In the numerical design of a structure, one of the most important data for attaining a reliable design is the reliable quantification of the excitations against which the structure is to be designed. Thus, the proper selection of the design EQs is an important and at the same time one of the most difficult tasks in efficient preliminary EQRD of a structure. As summarized above under "Establishment of design EQs," it is necessary to compute a series of spectra. At present most of these spectra are computed just for SDOFSs. Because a real building generally is a MDOF, as is indicated in Figure 31 it is necessary to modify the obtained SDOFS spectra. Furthermore, additional modifications are necessary from the beginning of the EQRD process to include the effects of torsion and overstrength (which in turn depends on the design method). These modifications are necessary in order to arrive at a preliminary design that is as close as possible to the desired final design.

· *Modifications to account for design method.* Because in EQRD the critical regions of the members and therefore the members themselves are usually provided with a large local μ, structures designed using elastic methods usually result in strength higher than that for which they were designed. The result is a designed and usually a constructed structure with significant lateral overstrength with respect to code-required strength. This overstrength varies with the T_1 of the structure. The taller the building (the larger the T_1) and the fewer structural bays, the smaller the overstrength will be. It should be noted that if the designer tailors the main reinforcement so that all of the critical regions of each of the members reach their demanded strength simultaneously, the resulting structure's overstrength will be reduced. Thus it is not only difficult, but even dangerous, to attempt to codify just one constant value for such overstrength. Similarly, if the designer uses the ACI code strength method with the redistribution due to plastic deformation allowed by this code, the overstrength will also be reduced. If the designer uses inelastic design method, i.e., methods that account for plastic redistribution of the internal forces that are demanded elastically from the structure, the resulting overstrength will decrease. However, the degree of decrease depends on how the design is conducted. If the design is based on optimization, proceeding as those suggested herein, the overstrength will be reduced to a minimum, but can still be significant. The actual dynamic overstrength during the dynamic response to recorded EQGMs is even higher than that estimated under equivalent static load (pushover test). It should be noted that in specifying the possible reduction that can be made in the ordinates of the SIDRS for C_s due to overstrength, it is necessary to look not only to the possible overstrength, but also to its effect on maximum IDI. The increase in IDI beyond the acceptable limit can control the reduction. From this discussion it is clear that the final design will generally have a maximum yielding strength larger than that required by the adopted yielding strength spectra (C_s), and therefore that the response ordinates of such SIDRS can be reduced by a factor R_{OVS}. The problem is, how much can the value of R_{OVS} be? As this value depends on many variables (design method, dynamic effects, T_1 and T_1/T_i, etc.), at present its selection requires seasoned judgement and should be done conservatively, at least until needed research produces the required calibration data for its proper selection.

· *Modifications due to torsional effects.* Due to torsion, the demanded strength and IDI at certain parts of the structure increase over those required by just the translational deformation. The larger the eccentricity between the center of rigidity and the center of mass, the larger the effects of torsion. These effects will be different under service EQGMs from what they would be under safety EQGMs. At the safety level involving inelastic behavior, the effects of torsion can significantly increase depending on the initial location of the center of torsional resistance (strength) and how this center and the resulting yielding resistance eccentricity are changing in the yielding of the structure [Sedarat and Bertero, 1990]. The torsional effects are currently taken into account in the estimation of the seismic design forces by modifying the distribution of the computed total design base shear and average IDI obtained from the design spectra, or even later, in the analysis of the preliminary design. As illustrated in Fig. 31, in the proposed conceptual methodology the torsional effects are considered from the beginning by direct modification of the value obtained from the spectra. A series of practical equations for doing this have been developed [Bertero, R. and Bertero, V. 1992].

■ *Preliminary design.* As was briefly stated in the summary of the preliminary design steps, in order to attain the required sizing of the structural elements and the amount of their reinforcement it is proposed to do this story by story, starting from the roof, and to use plastic design and optimization theory, using as an objective function the minimization of the flexural reinforcement, and introducing as constraints all practical requirements as well as the axial-flexural strength required by the service design EQ, so that the preliminary design will satisfy the demands imposed by both the service and the safety design EQs.

■ *Analysis of preliminary design.* As indicated in the flow chart of Fig. 30 and in the summary presented previously, the main objective of this step is to determine if the preliminary design is acceptable according to the adopted design criteria. To do so it is necessary to conduct a series of analyses of the demanded values for the main response parameters used in the establishment of the design criteria, considering the main limit states through which the whole facility system could pass during its service life. The main parameters are: total weight (W); IDI; the stress ratio; shear stresses in the members and their joints; the global, story and local μ; and the local damage index (DI). These should be done for the critical EQGMs for each different limit state considered in the design criteria. To carry out the above checks it is necessary to conduct linear and nonlinear analyses. The ideal would be to conduct a 3-D dynamic analysis which would consider all of the components of the critical EQGMs acting simultaneously, or at least their two horizontal components. While at present this can be done easily for the serviceability limit state because it requires the use of dynamic linear analysis, checking the safety limit state is more difficult because of the lack of reliable 3-D dynamic nonlinear analysis computer programs that can be used in practice for multistory buildings. The use of

available general 3-D dynamic nonlinear computer programs demands the use of large computers and significant amounts of computer time. Therefore, at present, attempts should be made to conduct the 3-D analysis using the static lateral load (pushover) method with a proper load pattern, or, even better, considering the probable bounds of such a pattern. If 3-D analysis programs are not available or can not be used because of the powerful computers required or computer costs, then attempts should be made to use Pseudo-3-D programs. The disadvantages of these Pseudo-3-D programs, such as DRAIN-2DX, is that they cannot estimate the effects of torsion and of multidirectional input.

Recent studies note that while the static pushover method can give an idea of the first (local) and maximum (global) yielding strengths, it can significantly underestimate the actual dynamic global yielding strength. Furthermore, the results of such pushover analysis can significantly underestimate the local cumulative plastic rotation and will not reveal the possibility of a shakedown problem, particularly in very slender, tall RC buildings. Thus, efforts should be devoted to developing practical and reliable 3-D dynamic nonlinear analysis computer programs that will enable 3-D time-history analyses to be conducted on the response of the buildings when subjected to the time-history components of the critical EQGMs.

6.4 *Concluding remarks*

The conceptual methodology for EQRD that has been summarized herein has been developed for the main purpose of attaining a transparent procedure, based on fundamental principles of structural dynamics and comprehensive design, that can be used as a basis for the formulation of EQRD procedure for a new generation of seismic codes which SEAOC envisions for the year 2000. It has been applied successfully to the design of a 30-story RC building which has also been designed using the 1991 edition of the UBC [Bertero, R. and Bertero, V., 1992]. Comparison of the two designs shows the weakness of present UBC regulations when applied to tall buildings. It should be clearly noted that it is not the intention to propose that such a methodology as has been presented be implemented in the code for all kinds of structures. What has been proposed is that such a conceptual methodology be used for the design of irregular buildings, tall buildings, and particularly buildings on abnormal sites. For regular buildings located on standard sites, this methodology can be used to carry out case studies whose results can be used to formulate seismic code regulations that are simpler, but still more transparent and reliable, than present ones.

7 CONCLUSIONS, RECOMMENDATIONS AND PLEAS

7.1 *Conclusions*

- Earthquakes are a very special type of natural hazard in the sense that they are very rare, low-probability events that can result in disasters in which most of the human and economic losses are due not to the EQ mechanism (fault rupture) but to the failures of human-made facilities. Thus, although EQs are inevitable, it is in our hands to reduce their consequences to acceptable limits by controlling the built environment. This should be the key point in the formulation of an EQ preparedness program.
- Analysis of what happened during 1988-1992 shows that even though the seismic activity (seismicity) of any urban area remains constant, and in spite of the impressive increase in knowledge in the field of EQ Engineering, the seismic risks in our urban areas have increased rather than decreased. This increase is due to fact that the rapid and uncontrolled growth in population, urbanization, and the development of high technology industries in our urban areas has not been counterbalanced by a needed increase in EQ preparedness.
- We are far from the main goal of the work of the IAEE, which is the reduction of seismic risks in our urban and rural areas. It is taking too long to transfer knowledge gained through research and experience to the practitioners working in EQRD and EQRC of the facilities of the built environment and to the government officials in charge of the management of EQ hazard reduction programs.
- Review of what has happened during recent significant EQs reveals that either we very quickly forget the lessons learned in previous EQs or we do not take seriously their warnings regarding: (1) where not to build, and how to build so that new facilities will not fail; and (2) the urgent need to perform reliable assessments of the vulnerability of facilities similar to those that have been observed to fail.
- *The issue of EQ preparedness.* "The poorer the EQ preparedness, the greater the EQ disaster." The ideal solution of the EQ problem will be through prediction of the event and hazard reduction through preparedness. Prediction research should be continued, but should not interfere with efforts to solve the present and pressing problems of our built environment through the formulation and implementation of adequate EQ preparedness programs.
- The main issue confronting all of us interested in EQ Engineering is the need to control the seismic risks in our urban and rural areas. The solution lies in controlling the vulnerability of the built environment, because this allows us to control the potential sources of EQ hazards, which are consequences of the interaction of seismic activity (which we cannot control) with the vulnerability of the built environment.
- From analysis of the aspects involved in the assessment of seismic risks and the experts needed to perform such assessment, it is clear that control and reduction of seismic risks in any given urban area is a complex problem requiring the integration of knowledge and the collaboration of experts from many disciplines.
- The problem of seismic risk reduction will not be solved just by the acquisition of the required knowledge through research. Research must be accompanied by the necessary technological developments and the implementation of the knowledge and the developments in practice. What is needed is a translation of current engineering and architectural know-how into simplified options which

can answer the socio-political and economic concerns. This will require not only a multi-disciplinary approach, but also a comprehensive educational program, not only for owners and future users but also for all of the different audiences that in one way or another are involved in the implementation of seismic risk reduction measures.

- Good government is the key factor in preparedness, and therefore government performance is a major controllable factor influencing the impact of a disaster.
- There have not been serious attempts to integrate the knowledge and the requirements of the various disciplines involved in the general problem of EQ hazard reduction. The engineers are perhaps not asking the geoscientists the right questions, and the geoscientists are perhaps more interested in trying to predict EQs than in the problems involved in the EQRD of facilities. These attitudes have to be changed.
- The most effective way to mitigate the destructive effects of EQs is to improve and develop more reliable methods than those presently used for designing, constructing and maintaining and monitoring new structures and seismically upgrading existing hazardous facilities. Therefore, EQRD is at present the key element in coping with the problems of EQ hazard reduction.
- The principal issues that remain to be resolved for the improvement of the EQRD of structures are related to the following three basic elements: EQ input, demands on the structure, and supplied capacities to the structure.
- The EQ input element involves the following interrelated issues: design EQs, design criteria, and selection of design methodology.
- Design criteria should reflect in a transparent way the general philosophy of EQRD, which has been well established and is accepted world-wide. EQRD in practice generally follows seismic code provisions. Unfortunately, most present code EQRD methods fall short of realizing the goals and objectives of the general EQRD methodology.
- Most current seismic codes are primarily intended to safeguard against major failure and loss of life, and not to limit damage, maintain function, or provide for easy repair. In few words, current code design methodology is based on a one-level design EQ. Moreover, "the protection of life is reasonably provided, but not with complete assurance." The time has arrived to move from the current code one-level design EQ methodology to a code design methodology based on at least two distinct levels of design EQs: the service-level (functional adequacy) and the life-safety level EQs.
- Modern building codes, which try to reflect great advances in knowledge and understanding in a very simple way, are not transparent about the expected level of performance of the whole building system (soil foundation-superstructure and nonstructural components). Expected level of performance has become an implicit, rather than an explicit, part of the codes through a series of empirical factors and detailing requirements which obscure the true nature of the EQRD problem: building performance.
- A promising engineering parameter for improving selection of proper design EQs, particularly when structural damage is acceptable and it is necessary to define the Smoothed Linear Elastic Design Response Spectra, is the energy input, E_I, of the EQGM, and its associated parameters.
- A conceptual methodology for EQRD of facilities is proposed. It is based on well-established fundamental principles of structural dynamics, the mechanical behavior of the entire facility, and comprehensive design. It takes into account from the very beginning of the EQRD procedure (i.e., from the preliminary design on) the simultaneous demands for *strength, deformation, and their combined effects* on the demanded and supplied *energy capacities* of the entire facility system. The proposed conceptual methodology leads to a rational and transparent EQRD procedure. The main advantage of this proposed conceptual methodology is that, notwithstanding the great uncertainties involved in the quantification of some of the concepts involved in its codification, the numerical quantification of some of the concepts can be improved without changing the format of this codified methodology as new and more reliable data are acquired.

7.2 *Recommendations and pleas*

- Considering that most structural engineers receive their education in the EQ problem through the code, which they have to apply in practice in the design of ordinary (standard) facilities which compose the bulk of modern construction, I believe that the decision on the part of the IAEE to undertake in the period 1980-1984, through international collaboration, the formulation of "Basic Concepts of Seismic Codes," which was accomplished with the publication of Part I, "Basic Concepts of Seismic Codes," in 1980 and Part II, "Basic Concepts for the Development of Seismic Design Criteria on Engineered Construction," in 1982, was a very good single decision. However, it is considered that the time has come to review these publications, introducing the new knowledge acquired and published in the 8th, 9th and now this 10th WCEE. The concepts of EQRD are universal. They should reflect the world-wide adopted EQRD philosophy, which is unique. Therefore, it is suggested that the IAEE, in collaboration with the United Nations as a part of this International Decade for Natural Disaster Reduction (IDNDR), appoint an international group of experts from the different fields of knowledge which are required for the formulation of the basic concepts and format in which a conceptual code for EQRD of new structures and upgrading of existing structures should be based. Then, based on these concepts and code format together with the digestion and screening of present knowledge, an exemplary code should be formulated for a certain ideal or real seismic region.

  Based on the formulated conceptual code, each country, according to its seismic hazards, the education of its engineers, its building technology and its socio-economic conditions, could decide on specific quantifications of the conceptual seismic code. The main advantages of this approach are, first, that, as the acquisition of reliable information continues, it would be easy to change the numerical values of the coefficients in the formulas given in the conceptual code so that it will not be necessary to

give a new empirical approach and formulations which will confuse the engineers. Secondly, it will facilitate the interpretation of the codes for different countries, which will be very healthy for the improvement of all codes in general.

- The IAEE should do whatever is possible to encourage more practitioners and government officials working in the field of EQ Engineering to participate in the world conferences. Furthermore, an attempt should be made to find a format for the technical sessions that is better than the present format of many simultaneous sessions, in order to encourage the interchange of knowledge and ideas among the experts and practitioners from the different disciplines.
- The IAEE should encourage the development of EQ preparedness programs and of the massive educational program which is so needed for the dissemination of knowledge and the implementation of the EQ preparedness program.

The following pleas are made: firstly, to all of the experts in the different disciplines involved in solving the EQ problem, that they collaborate closely toward a timely solution to this problem; secondly, to each author of a paper to be presented to this conference, that they devote efforts to identify, among the research and/or development results that they have obtained, those that can be applied immediately in the field to reduce future EQ hazards; and thirdly, to all of the participants, that they disseminate in their communities what they learn during this conference, and collaborate in the preparation and implementation of EQ preparedness program.

ACKNOWLEDGEMENTS

Most of the material presented in this lecture has been obtained from studies supported by grants from the National Science Foundation and lately by CUREe-Kajima. These financial supports are gratefully acknowledged. The lecturer would also like to express his deepest gratitude to all of the graduate students and research associates who carried out the studies whose results have been discussed in this lecture. Thanks are also due to Brad Young, who edited and typed this lecture.

REFERENCES

Akiyama, H. 1985. *Earthquake resistant limit-state design for buildings*. University of Tokyo Press.

American Concrete Institute, 1971. *Building code requirements for reinforced concrete - ACI 318-71*. Detroit, Michigan. A later (1989) edition exists.

Anderson, J.C. and Bertero, V.V. 1969., Seismic behavior of multi-story frames by different philosophies. *Report No. UCB/EERC-69/11*. Earthquake Engineering Research Center, University of California at Berkeley.

Astaneh, A.H. 1990. The Manjil, Iran, earthquake of June 21, 1990. *EERI Newsletter*: 24: 5-13

Astaneh, A.H. 1989. Preliminary report on the seismological aspects of the October 17, 1989 Santa Cruz (LOMA PRIETA) earthquake. *Report No. UCB/EERC-89/14*, Earthquake Engineering Research Center, University of California at Berkeley.

Berg, G.V. and Thomaides, S.S. 1960. Energy consumption by structures in strong-motion earthquakes. *Proc.*, 2nd WCEE: 2: 681-696.

Bertero, V.V. 1975. Identification of research needs for improving aseismic design of building structures. *Report No. UCB/EERC-75/27*. Earthquake Engineering Research Center, University of California at Berkeley.

Bertero, V.V. and Bresler, B. 1977. Design and engineering decisions: failure criteria (limit states). *Proc.*, 6th WCEE: 1: 77-88.

Bertero, V.V. 1980, Strength and deformation capacities of buildings under extreme environments. *Structural Engineering and Structural Mechanics*, ed. K. Pister. Prentice-Hall: 188-237.

Bertero, V.V. 1980. Lessons learned from structures damaged in recent earthquakes. *Proc.*, 7th WCEE: 4: 257-264.

Bertero, V.V. 1982. State of the art in earthquake-resistant construction of structures. *Proc.*, 3rd Int'l EQ Microzonation Conf.: 2: 767-808.

Bertero, V.V. 1982. State of the art in seismic resistant construction of structures. *Proc.*, 3rd Int'l Microzonation Conf.: II: 767-808.

Bertero, V.V. 1986. Implications of recent earthquakes and research on earthquake-resistant design and construction. *Report No. UCB/EERC-86/03*, Earthquake Engineering Research Center, University of California at Berkeley.

Bertero, V.V. and Whittaker, A.S. 1989. Seismic upgrading of existing buildings. *5as Jornadas Chilenas de Sismologia e Ingenieria Antisismica*: 1: 27-46.

Bertero, V.V. 1991. Structural engineering aspects of seismic zonation. *Proc.*, 4th Int'l Conf. on Zonation: 1: 261-321.

Bertero, V.V. et al. 1991. Design guidelines for ductility and drift limits: review of state-of-the-practice and state-of-the-art in ductility and drift-based earthquake-resistant design of buildings. *Report No. UCB/EERC-91/15*, Earthquake Engineering Research Center, University of California at Berkeley.

Bertero, V.V. 1991. Earthquake-resistant code regulations: implications of recent earthquakes and research. *Proc. Int'l Symposium on Bldg. Technology and EQ Hazard Mitigation:* 1-35. Nagoya, Japan.

Bertero, V.V. and Uang, C.-M. 1992. *Nonlinear seismic analysis and design of reinforced concrete buildings*, ed. P. Fajfar and H. Krawinkler. Elsevier Applied Science.

Bertero, V.V. 1992. Seismic upgrading of existing structures. *Proc.*, 10th WCEE: 9: 5101-5106.

Bertero, R. and Bertero, V.V. 1992. Tall reinforced concrete building: development of conceptual seismic -resistant design methodology. *Report No. UCB/EERC-992/16*. Earthquake Engineering Research Center, University of California at Berkeley.

Bommer, J.J. and Ambraseys, N.N 1989. The Spitak (Armenia USSR) earthquake of 7 December 1988: a preliminary engineering seismology report. *ESEE/EFTU Research Report No. 8911*. Civil Engineering Dept., Imperial College of Science and Technology.

Brokken, S.T. and Bertero V.V. 1981. Studies on the effects of infills in seismic resistant construction. *Report No. UCB/EERC-81/12*, Earthquake

Engineering Research Center, University of California at Berkeley.

Committee on Earthquake Engineering Research 1982. Earthquake engineering research - 1982. *Report No. CETS-CEER 001B*. Nat. Acad. Sci., Washington D.C.

Degenkolb, E. 1972. Basic design criteria of the recommended lateral force requirements and commentary. ASCE *Journal of the Structural Division*: 98: ST9: 1913-1922.

Dowrick, O.J. 1987. *Earthquake resistant design for engineers and architects*. John Wiley & Sons, Ltd.: New York.

Earthquake Engineering Research Institute Committee on Seismic Risk, H.C. Shah, Chair. 1984. Glossary of terms for probabilistic seismic risk and hazard analysis. *Earthquake Spectra*: 1: 1: 33-40.

Earthquake-resistant regulations: a world list - 1988. IAEE, Tokyo.

Fajfar, P. et al. 1992. On energy demands in SDOF systems. *Nonlinear seismic analysis and design of reinforced concrete buildings*. Elsevier Applied Science Publishers, Ltd.: 41-62.

Hanks, T.C. and Kanamori, H. 1979. A Moment magnitude scale. *Journal of Geophysical Research*: 84: B5: 2348-2350.

Hatamoto, H. et al. 1990. Seismic capacity enhancement of R/C frames by means of damage control design. *Proc.*, 4th U.S. Nat'l Conf. on EQ Engineering: 2: 279-288.

Housner, G.W. 1956. Limit design of structures to resist earthquakes. *Proc.*, 1st WCEE: 5.1-5.13.

Housner, G. 1984. Conference lecture: Historical view of earthquake engineering. *Proc.*, 8th WCEE Post-conference volume: 25-39.

Hudson, D. 1988. Nine milestones on the road to earthquake safety. *Proc. 9th WCEE*: 2: II.3-II.11.

Hwang, H. and Jaw, J.W. 1990. Statistical evaluation of reflection amplification factors for reinforced concrete structures. *Proc.*, 4th U.S. Nat'l Conf. on EQ Engineering: 2: 937-944.

International Conference of Builkling Officials, 1927-91. *Uniform Building Code*. Whittier, California.

Kanamori, H. 1978. Quantification of earthquakes. *Nature*: 271, Feb. 2.

Kappos, A.J. 1990. Sensitivity of calculated seismic response to input motion characteristics. *Proc.*, 4th U.S. Nat'l Conf. on EQ Engineering: 2: 25-34.

Miranda, E. 1991. Seismic evaluation and upgrading of existing buildings. Ph.D. thesis, University of California at Berkeley.

Moehle, J.P. 1992. Displacement based design of RC structures. *Proc.*, 10th WCEE: 8: 4297-4302.

Park, Y.J., Ang, A.H. and Wen, Y.K. 1984. Damage-limiting aseismic design of buildings. *Earthquake Spectra*: 3: 1.

Priestley, M.J.N. 1988. The Whittier Narrows earthquake of October 1, 1987, *Earthquake Spectra*: 4: 1, Feb. 1988 and Vol. 2, May 1988.

Press, F. 1981. Keynote address: the role of science and engineering in mitigating natural hazards. *Proc. 8th WCEE*: 1: 13-24.

Qi, X., and Moehle, J.P. 1991. Displacement design approach for reinforced concrete structures subjected to earthquakes. *Report No. UCB/EERC-91/02*. Earthquake Engineering Research Center, University of California at Berkeley.

Rosenblueth, E., et al. 1989. The Mexico earthquake of September 19, 1985 - design spectra for Mexico's Federal District. *Earthquake Spectra*, Earthquake Engineering Research Institute: 5: 1: 273-291.

SEAOC Seismology Committee, 1957-90. *Recommended lateral force requirements and commentary*. Structural Engineers' Association of Northern California, San Francisco [SEAOC Blue Book].

Sedarat, H., and Bertero, V.V. 1990. Effects of torsion on the nonlinear elastic seismic response of multi-story structures. *Proc.*, 4th U.S. Nat'l Conf. on EQ Engineering. EERI, Oakland, California.

Shimizaki, K. and Sozen, M.A. 1984. Seismic drift of reinforced concrete structures. Technical Research Report, Hazama-Gumi, Ltd.: 145-166.

Shimizaki, K. 1988. Strong motion drift and base shear coefficient for R/C structures. *Proc.*, 9th WCEE: V: 165-170.

Sozen, M.A. 1983. Lateral drift of reinforced concrete structures subjected to strong ground motions. University of Illinois, Urbana.

Uang, C.-M. and Bertero, V.V. 1988. Use of energy as a design criterion in earthquake-resistant design. *Report No. UCB/EERC-88/18*. Earthquake Engineering Research Center, University of California at Berkeley.

Wyllie, L.A., et al. 1989. Armenia earthquake reconnaissance report. *Earthquake Spectra: Special Supplement to ES 89-01*.

The state of the art in synthesis of strong ground motion for earthquake engineering

Bruce A. Bolt
Department of Geology and Geophysics and Department of Civil Engineering, University of California, Berkeley, California, U.S.A.

ABSTRACT: The engineering demand for realistic seismic wave inputs for design and response studies has shifted emphasis in recent years. The effectiveness of building codes and ground intensity zoning maps has been tested in a number of recent large earthquakes, such as Loma Prieta, 1989, Erzincan, 1992, and Landers, California, 1992. The observational basis for seismic strong motion variability is much firmer after the addition of many new accelerograms from California, Japan, Europe, and elsewhere. As a result, engineering requirements have expanded from simple spectrum scaling, using (high frequency) peak-ground accelerations, to emphasis on full seismograms, frequency-dependent intensity mapping, spectral attenuation and appropriate seismological wave phasing. For critical structures, checks for nonlinear responses now involve analysis in both the time and frequency domain. Multi-supported and base-isolated structures and soil-structure interaction adjustments require the incorporation of ground displacement histories and coherency functions in the synthetic inputs. The main methods of ground motion synthesis at present are fourfold: record selection and scaling, statistical spectral generation, elastic dislocation theoretics, and matched estimated parameterization. These methods will be briefly reviewed with emphasis on the nonlinear algorithms involved in the last procedure. The strengths and weaknesses of finite element path and source modelling and the Green's function empirical construction will be discussed. Recent illustrations of iterations to match target parameters will be given from the predicted ground motions for long bridges and viaducts in the San Francisco Bay Area.

1 INTRODUCTION

Although analysis of strong earthquake motion is a relatively vigorous part of present day seismological research, there are many aspects which remain undeveloped. The reason is the continued lack of actual closely-spaced measurements of large amplitude seismic motions near to large seismic sources. There are, for example, as yet few records of ground accelerations recorded by strong motion instruments in the near field of earthquakes above magnitude 7.5. An important set of accelerograms (see Figure 1) was obtained in Central California in the 1989 Loma Prieta earthquake (MS = 7.1, ML = 6.7). These have provided a starting point for studies of the seismic response of San Francisco Bay bridges now being undertaken.

On the theoretical side, it has been demonstrated that reasonably accurate synthetic seismograms can be computed using appropriate Green's functions (Irikura, 1983; Hartzell, 1985; Hutchings, 1991; Somerville et al., 1991) or records of small earthquakes as impulse responses. Recently, a valuable introduction to this problem has been given by Mikumo & Miyatake (1987). These authors point out that for predicting strong motions from a large earthquake, the complex dynamic rupture processes of the fault, the heterogeneous crustal structures along the source propagation path and near the recording site must be allowed for. Because of the difficulty, in situations where these details are unknown, of incorporating a full theoretical description into the synthesis process, another approach is to combine theory and the limited observational measurements. This paper is concerned mainly with this semi-empirical method (Spudich & Archuleta, 1987).

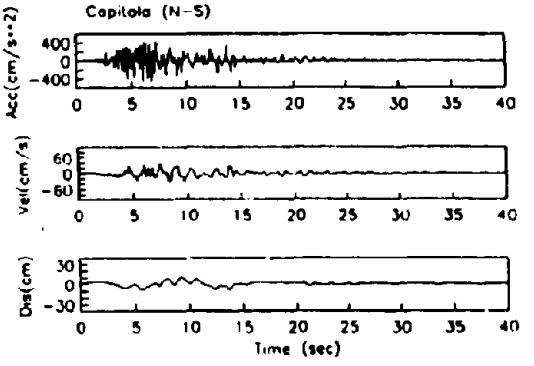

Figure 1. Ground motions recorded at Capitola, California, in the 1989 Loma Prieta earthquake.

The contribution of strong motion seismology is to explain high amplitude seismic waves near a seismic source and to use such measured motions to infer pro-

perties of the source, propagation path and predict ground motions at the recording site (Hartzell & Heaton, 1983; Boatwright, 1988; Hartzell & Mendoza, 1991). An important part of such research is directly applicable to seismic risk assessment and earthquake engineering. The final synthesis must be carefully defined if it is to be used in the construction of realistic seismic inputs to analyze critical structures. For example, advanced engineering studies now incorporate the *phase* of seismic wave motions that shake structures.

Specifically, structures with multiple supports respond so as to average the free-field accelerations incident upon the supports. Hence, dynamic analysis of these structures requires suitably phased time histories applied at each support or a modal response analysis with complete phase information appropriate to the local tectonic zone. In the past, the usual engineering response spectrum described only the amplitude of the oscillatory motion and did not define the phase behavior. In reality, for viaducts, large bridges, and dams, out-of-phase wave motions over inter-support distances cause differential ground accelerations and differential rotations along the base of the structure. Thus, complex spectral representation must be used.

The most obvious case arises for non-vertically propagating seismic waves which produce systematic phase shifts between support points with significant incoherency. These travel-time lags are reinforced by the mixing of out-of-phase motions produced in other ways such as wave scattering.

Recently the measurement of such effects has become feasible from dense strong motions arrays with absolute times. The array recordings have provided opportunities to study phase changes and coherency in seismic ground motions over various distances and to estimate their effects on large engineering structures (Bolt et al., 1982). Phasing may be incorporated through the definition of a response phase spectrum which is consistent with the response (amplitude) spectrum. This method allows the routine calculation of the response phase spectrum for ground acceleration, ground velocity, and ground displacement (Abrahamson & Bolt, 1985).

At the present time, the use of coherency in engineering practice has been limited and is probably necessary only in critical cases. Nevertheless, the importance of the relevant engineered structures suggests that the methodology will expand into practice because of the reduction in vulnerability and overall construction costs. The incorporation of phase shifts generally, but not always, leads to a reduction in structural response relative to in-phase input motions and hence reduces nonlinear structural effects.

2 SEISMIC WAVE PATTERNS

Strong ground motion consists of a mix of seismic waves as described by elastic wave mechanics. Seismic shaking at a site arises from the superposition of different elastic wave types, with time as an independent variable. An earthquake is rarely stationary in time but varies in amplitude A, frequency ω (radians per sec), and wavelength λ, from time window to time window. This motion can often be represented by the sum of simple
harmonic (advancing) plane waves. Each wave can be signified by a wave number, k, where $k = 2\pi/\lambda$.

The standard assumption in multiple support or array analysis is that the record consists of a deterministic signal plus noise. For example,

$$u_j(t) = u(\mathbf{x}_j,t) = s(t) + \varepsilon(\mathbf{x}_j,t), \tag{1}$$

where $u_j(t)$ is the output (acceleration, velocity, or displacement) of the jth accelerometer at position $\mathbf{x}_j$, $s(t)$ is the deterministic signal, and $\varepsilon(\mathbf{x}_j,t)$ is the noise. The form of equation (1) assumes that the signal arrives simultaneously at each station. This condition is satisfied by introducing a delay τ_j to the output of the jth accelerometer. For a plane wave, the delay is

$$\tau_j = \mathbf{k}.\mathbf{x}_j \,/\, \omega, \tag{2}$$

where $\mathbf{k}$ is the vector wave number and ω is the frequency of the plane wave.

In some analyses it is sufficient to consider a single harmonic component of the strong motion record

$$s(\mathbf{x},t) = A \cos(\mathbf{k}.\mathbf{x} - \omega t + \delta), \tag{3}$$

where A and δ are constants. The wave velocity is $c = \omega/|\mathbf{k}|$.

In equation (3) the angle δ is called the phase angle because $s = A \cos\delta$ represents ($\mathbf{x} = 0$, $t = 0$) an advance (or delay) of the constituent wave harmonic. In computing phased synthetics, the phase angles δ are key parameters.

Alternatively, the time domain representation given by equation (3) is transformed to an equivalent frequency description. The wave field is then expressed as a three-dimensional Fourier transform. Because a Fourier transform is a complex variable, the complete representation of a time history requires an amplitude spectrum plus a phase spectrum. The different phase spectra of often-used accelerograms are sometimes used to generate an artificial but more suitable time history by interchange of phase spectra. This substitution procedure preserves the amplitude spectra and maximum motions but varies the duration and phasing pattern. As mentioned earlier, in engineering applications to structures with a rigid base or single input point, the response phase spectrum is usually unimportant and is ignored.

The construction of synthetic time histories requires the correct inclusion of different types of seismic waves with their theoretical interrelationship (see Bullen & Bolt, 1985, for a full description). In most applications, three types of seismic waves need consideration: compressional (P) waves, shear (S) waves, and surface (Love and Raleigh) waves. As P, S, or surface waves propagate through the rock or soil strata, one type of wave may generate waves of another

type, and phase shifts δ occur as waves are reflected or refracted.

The seismic zone is highly significant because the location, size, and type of seismic source and the propagation path may affect the total motion strongly. If the waves all emerged from a point source, then phasing, or order of arrival, at a series of support points would depend only upon the particular wave velocity. In fact, earthquake waves are radiated from many points along an extended fault slip and depend on the type of slip involved. In the 1989 Loma Prieta earthquake in California, this slipped area was about 40 km long and 20 km deep (Steidl et al., 1991; Wald et al., 1991). Waves from different parts of the ruptured fault are thus delayed by various amounts due to the different distances that they travel from their source points to the station. Inhomogeneity of geological structures near the site also causes significant wave scattering.

It follows that between seismogenic zones a set of strong motion seismograms, constructed as boundary conditions at the various structural input points, will not in general be alike. A measure of the *likeness* of two wave trains is given the technical name *coherency*, and quantitative measures can be obtained in the time domain (through simple cross-correlation) or in the frequency domain. In the frequency domain, the (complex) coherency between sites 1 and 2 is

$$\delta_{12}(\omega) = S_{12}(\omega) / [S_{11}(\omega)\, S_{22}(\omega)]^{1/2} , \qquad (4)$$

where S_{ij} is the cross-spectral matrix.

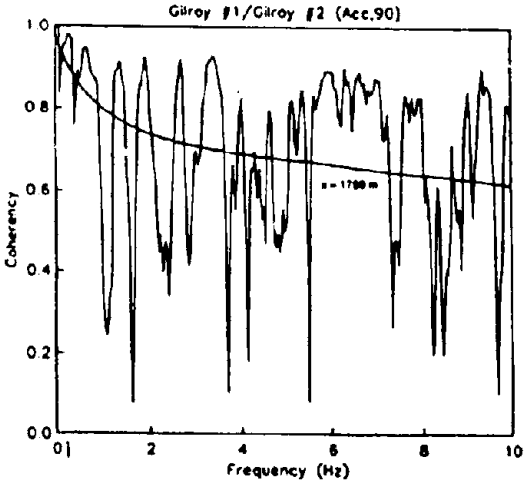

Figure 2. The coherency function (equation (4)) computed from adjacent (1750 m separation) recordings of strong motion in the Gilroy strong motion array during the 1989 Loma Prieta main shock. The heavy line is a smooth representation of the coherency effect.

Studies of the coherency of strong ground motions have now been published (see Abrahamson & Bolt, 1987), and a few have been incorporated into structural response analyses for critical structures as part of soil-structure interaction calculations. When numerically modelling with realistic synthetic sets, a test of coherency attributes is recommended.

3 NUMERICAL SYNTHESIS OF STRONG MOTIONS

Numerous methods and examples of synthesizing seismograms in the near field of a large seismic source have been published (see, for example, the book *Seismic Strong Motion Synthetics*, 1987). A numerical construction process for prediction of semi-empirical but realistic strong ground motions is now outlined. The computation of such site dependent and phased time histories is not unique, and a number of alternative methods are available (see, e.g., Joyner & Boore, 1988; Vidale & Helmberger, 1987; Cohee et al., 1991).

The first step is to define, from geological and seismological information, the appropriate earthquake sources for the site of interest. The source selection may be deterministic or probabilistic and may be decided on grounds of acceptable risk (Bolt, 1991). Next, specification of the propagation path distance is needed, as well as the P, S, and surface wave velocities in the zone. These speeds allow calculation of the appropriate wave propagation attenuation (Abrahamson & Litehiser, 1989) and delays between support points and the angles of approach of the incident waves.

The construction of realistic motions proceeds as a series of iterations from the most appropriate observed strong motion record already available to a set of more specific time histories which incorporate the seismologically defined wave patterns. Where feasible, strong motion accelerograms are chosen which satisfy the seismic source (dip-slip, etc.) and path specifications for the seismic zone in question.

The iterative process is controlled by applying seismological (Kanamori & Anderson, 1975) and engineering constraints. For example, the response amplitude spectra should fall within one standard error of a specified target spectrum obtained, say, from previous data analysis or an earthquake building code (Lilhanand & Tseng, 1988). Similarly, each seismogram must maintain prespecified peak-ground accelerations, velocities, and displacements within statistical bounds. The durations of each wave section (mainly P, S, and surface wave portions) of each time history must also satisfy prescribed source, path, and site conditions. At the present, automatic convergent algorithms are not available for reliable constructions, so that experience with observed seismograms and knowledge of seismic wave theory are needed.

3.1 *Illustration from San Francisco Bay*

After the damage to the San Francisco Bay Bridge and the I-880 elevated roadway in the 1989 Loma Prieta earthquake, new considerations were given to the appropriate design criteria for large structures in high seismic hazard zones. The California Department of

Transportation, for example, initiated thorough ground motion studies for its existing and future bridges and viaducts in the San Francisco Bay Area and elsewhere.

The large size of such structures focused attention on relatively long period seismic motions, i.e., from 2 Hz to 5 sec or more. It should be remembered that for energetic S wave components (see equation (3)) of period about 1 sec, the wave lengths λ incident on the supports are of the same order as key structural dimensions. Hence, specifications for these studies required consideration of coherency factors. The studies have challenged the state of modelling knowledge. First, no strong motion records were available for large near-earthquakes in the Bay Area that measure the spatial variation of shaking over distances of many hundreds of meters (e.g., long spans for the Bay Bridge and the Golden Gate Bridge). Secondly, compatible ground velocity and displacement time histories, essential input for structural analysis, were also unavailable.

As an example, let us consider construction of a synthetic set of phased ground motions (horizontal component) suitable for structural seismic response analysis of the eastern section of the San Francisco Bay Bridge. The bridge is about 3 km long with its eastern end situated about 5 km from the active strike-slip Hayward fault. This fault ruptured last in 1868, producing a magnitude 7.2 earthquake. The required design motions are chosen to represent a repetition of this even.

Let us now choose two neighbouring input points for the Bay Bridge, called E23 and E17, a distance of 613 meters apart, with peak-ground accelerations of 0.55g and 0.53g, respectively, after allowance for distance attenuation. The bridge supports are actually almost all located on recent sediments of varying depth, but in the following, rock sites will be assumed. (Allowance for the soils can be made at a later stage by soil engineering methods.)

The initial accelerogram chosen for site E23 is horizontal ground motion recorded at Capitola on firm ground, 10 km from the fault source of the 1989 Loma Prieta earthquake. The ground accelerations, velocities, and displacements are shown in Figure 1. These records are then scaled to the required peak acceleration for E23 and the 5 percent damped response spectrum calculated (Figure 3). In Figure 3, a design spectrum developed for the extensions to the Bay Area Rapid Transit System (BART) is compared with that of this initially assumed ground motion. A ratio function between these two response spectra is then used to iterate the Fourier spectrum so that compatibility with this smoothed target spectrum is achieved (Figure 4). This non-linear process produces a realistic motion for site E23 (Figure 5). This synthetic motion has a wave pattern, duration, amplitude, and spectrum that meet the seismological and engineering criteria for a source, site, and structure of the kind involved.

Next, incoherency must be introduced for the adjacent input point, E17. The first step is simply to lag the phase at each wavelenth of the E23 record to allow for the wave propagation. Because no coherency function

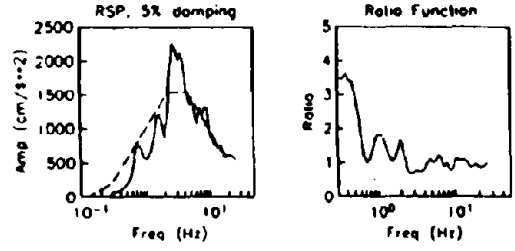

Figure 3. Response spectrum for the Capitola motion (Figure 1) compared with a target code spectrum. On the right, the ratio of frequency components is shown.

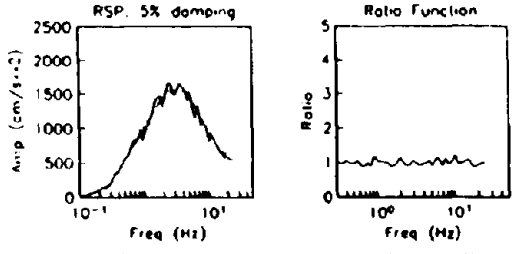

Figure 4. Four iterations of the Fourier amplitude spectrum (phase fixed) of the Capitola record produced the compatibility shown.

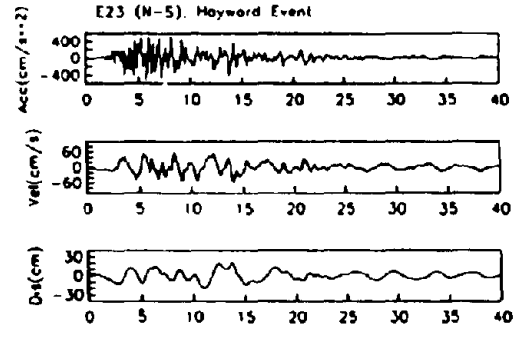

Figure 5. The synthesized ground motions for site E23 (on rock) for a magnitude 7.2 earthquake, generated by shallow fault rupture about 5 km away.

(equation (4)) has been measured for the geological region around the Bay Bridge (see Bolt et al., 1982), an acceptable substitute function is required. This function was computed from two horizontal-component ground accelerations at neighbouring sites near Gilroy (Figure 2), also from the 1989 Loma Prieta earthquake. (The interstation distance of 1750 m was the shortest available.) The smooth line in Figure 2 represents a target which the coherency function between motions at E23 and E17 should achieve.

The process was to adjust the Fourier phase spectrum for the E23 record in Figure 5 pointwise by a suitable shape function until the target coherency function was matched within reasonable bounds. The modified Fourier complex spectrum was then

formed back to the time domain and the time history rescaled to the specified peak-ground acceleration (0.53g). The resulting phased accelerogram is reproduced in Figure 6.

In this example, because the intersite distance (613 m) is not large relative to the wave lengths of most engineering interest (corresponding to 5 to 0.5 Hz), the differences between the E23 and E17 motions are not great. Over many bridge spans, however, the dynamical effects become significant.

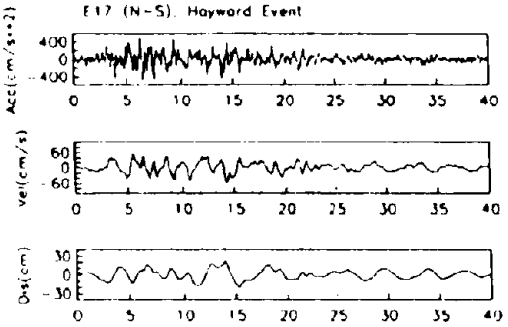

Figure 6. The phased synthetic ground motion for site E17 (on rock) which is compatible with the motion (given in Figure 4) at E23.

4 CONCLUDING REMARKS

The verification of artificial ground motions is impossible in many cases because no relevant recorded seismograms are available. Acceptability for engineering design purposes is enhanced by minimizing the range of extrapolation from records of moderate magnitude earthquakes such as Loma Prieta, 1989, and Erzincan, 1992, to the larger design earthquake. Records from the recent Landers, California, earthquake (M_S = 7.5) will fill a gap. The case of synthesizing realistic ground motions for earthquakes from blind thrust faulting remains a special challenge.

The discussion here does not take up the difficult question of effects of non-linear soil response at the site (Darragh & Shakal, 1991). When two-dimensional soil structure response is involved, the problem is to provide the different types of seismic waves separately in the rock synthetics.

REFERENCES

Abrahamson, N.A. & B.A. Bolt 1985. The spatial variation of the phasing of seismic strong ground motion. *Bull. Seismol. Soc. Am.* 75: 1247-1264.

Abrahamson, N.A. & B.A. Bolt 1987. Array analysis and synthesis mapping of strong seismic motion. In: *Seismic Strong Motion Synthetics*, B.A. Bolt, ed. New York: Academic Press.

Abrahamson, N.A. & J.J. Litehiser 1989. Attenuation of vertical peak acceleration. *Bull. Seismol. Soc. Am.* 79: 549-580.

Boatwright, J. 1988. The seismic radiation from composite models of faulting. *Bull. Seismol. Soc. Am.* 78: 489-508.

Bolt, B.A., C.H. Loh, J. Penzien, Y.B. Tsai & Y.T. Yeh 1982. Preliminary report on the SMART 1 strong ground motion array in Taiwan. *Earthquake Engineering Research Inst. Report* 82/13.

Bolt, B.A. 1991. Balance of risks and benefits in preparation for earthquakes. *Science* 251: 169-172.

Bullen, K. & B.A. Bolt 1985. *An Introduction to the Theory of Seismology*. New York: Academic Press.

Cohee, B., P.G. Somerville & N. Abrahamson 1991. Simulated ground motions for hypothesized M_w = 8 subduction earthquakes in Washington and Oregon. *Bull. Seismol. Soc. Am.* 81: 28-56.

Darragh, R.B. & A.F. Shakal 1991. The site response of two rock and soil station pairs to strong and weak ground motion. *Bull. Seismol. Soc. Am.* 81: 1885-1899.

Hartzell, S. 1985. The use of small earthquakes as Green's functions. *Strong ground motion simulation and earthquake engineering application. Earthquake Engineering Research Inst. Report* 85-02 22: 1-7.

Hartzell, S. & T. Heaton 1983. Inversion of strong ground motion and teleseismic waveform data for the fault rupture history of the 1979 Imperial Valley, California, earthquake. *Bull. Seismol. Soc. Am.* 73: 1553-1583.

Hartzell, S. & C. Mendoza 1991. Application of an iterative least-squares waveform inversion of strong ground motion and teleseismic records to the 1978 Tabas, Iran, earthquake. *Bull. Seismol. Soc. Am.* 81: 305-331.

Hutchings, L. 1991. "Prediction" of strong ground motion for the 1989 Loma Prieta earthquake using empirical Green's functions. *Bull. Seismol. Soc. Am.* 81: 1813-1837.

Irikura, K. 1983. Semi-empirical estimation of strong ground motions during large earthquakes. *Bull. Disaster Prevention Res. Inst. (Kyoto Univ.)* 33: 63-104.

Joyner, W.B. & D.M. Boore 1988. Measurement, characterization, and prediction of strong ground motion. In: *Earthquake engineering and soil dynamics II. Recent advances in ground motion evaluation*. Am. Soc. Civil Engin. Special Geotechnical Publication 20: 43-102.

Kanamori, H. & D. Anderson 1975. Theoretical basis of some empirical relations in seismology. *Bull. Seismol. Soc. Am.* 65: 1073-1095.

Lilhanand, K. & W.S. Tseng 1988. Development and application of realistic earthquake time histories compatible with multiple-damping design spectra. *Proc. 9th World Conference on Earthquake Engineering* 2: 819-824. Tokyo-Kyoto, Japan.

Mikumo, T. & T. Miyatake 1987. Numerical modeling of realistic fault rupture process. In: *Seismic Strong Motion Synthetics*, B.A. Bolt, ed. New York: Academic Press.

Somerville, P., M. Sen & B. Cohee 1991. Simulation of strong ground motions recorded during the 1985 Michoacan, Mexico, and Valparaiso, Chile, earthquakes. *Bull. Seismol. Soc. Am.* 81: 1-27.

Spudich, P. & R.J. Archuleta 1987. Techniques for earthquake ground-motion calculation with applications to source parameterization to finite faults. In: *Seismic Strong Motion Synthetics*, B.A. Bolt, ed. New York.

Steidl, J.H., R.J. Archuleta & S.T. Hartzell 1991. Rupture history of the 1989 Loma Prieta, California, earthquake. *Bull. Seismol. Soc. Am.* 81: 1573-1602.

Vidale, J. & D.V. Helmberger 1987. Path effects in strong ground motion seismology. *Strong motion synthetics*. New York: Academic Press.

Wald, D.J., D.V. Helmberger & T.H. Heaton 1991. Rupture model of the 1989 Loma Prieta earthquake from the inversion of strong-motion and broadband teleseismic data. *Bull. Seismol. Soc. Am.* 81: 1540-1572.

Structural reliability methods for seismic safety assessment

Armen Der Kiureghian
University of California, Berkeley, CA 94720, U.S.A.

ABSTRACT: Recent developments in the area of probabilistic methods and structural reliability that are relevant to earthquake engineering problems are reviewed. The paper begins with a discussion of types of uncertainties and methods for their quantification and analysis. The mathematical formulation of the structural reliability problem and existing methods for computation of failure probabilities are then reviewed. Included are methods based on first and second-order approximations, simulation, and various hybrid methods. The topics of reliability sensitivity, updating of reliability, and analysis of reliability uncertainties are discussed. An account of recent developments that combine these probabilistic methods with finite element analysis concludes the paper.

1 INTRODUCTION

Perhaps no other discipline within engineering has to deal with as much uncertainty as the field of earthquake engineering. The randomness in the occurrence of earthquakes in time and space, the vast uncertainty in predicting intensities of resulting ground motions, and our inability to accurately assess capacities of structures under cyclic loading all compel us to make use of probabilistic methods in order to consistently account for the underlying uncertainties and make quantitative assessments of structural safety. While the need for probabilistic methods in earthquake engineering has long been recognized, their use in practice has been limited because of the analytical and computational difficulties that these methods impose on the design and evaluation process. This paper aims at presenting a brief review of recent developments in the field of structural reliability that hopefully will facilitate a wider use of probabilistic methods in earthquake engineering.

The final objective in earthquake engineering often is decision on design specifications. This usually requires risk analysis, involving the assessment of probabilities as well as costs associated with each design alternative and the corresponding consequences, should structural failure occur. A simpler, more practical framework is provided by probabilistic design codes, which implicitly account for the underlying uncertainties and optimize (albeit in an approximate manner) the expected utility derived from each design. The topics of risk analysis and probabilistic codes are not addressed in this paper. However, probabilistic methods that are reviewed are essential elements of any such risk analysis and form the basis upon which probabilistic codes are developed.

Any review on probabilistic methods has to begin with a discussion on the nature of uncertainties and methods for their modeling and analysis. The Bayesian approach for this purpose is reviewed in the following section. Special emphasis is placed on model uncertainty, an important problem in earthquake engineering which, in the opinion of the writer, has not received adequate attention. In Section 3, general formulations for the structural reliability problem are presented. These include formulations for component and system reliability problems, time-variant reliability problems, and a discussion of reliability measures under conditions of statistical and model uncertainty. Section 4 describes a number of methods for computation of probabilities that are particularly relevant to the structural reliability problem. These include the first- and second-order reliability methods, various simulation methods, the response surface method, and the nested reliability method. Sections 5 and 6 discuss the important topics of probability sensitivity measures and updating of reliability, which are of particularly interest in design and planning of systems. The newly emerging field of finite element reliability analysis is briefly reviewed in Section 7, where two numerical examples relevant to earthquake engineering are also presented.

2 MODELING AND ANALYSIS OF UNCERTAINTIES

2.1 Types of Uncertainty

Three types of uncertainty are dominant in structural engineering: (a) inherent randomness, which arises from intrinsic variabilities in materials and in environmental effects, such as loads and support movements; (b) statistical uncertainty, which arises in the course of estimating parameters of probability distributions from observational samples of limited size; and (c) model uncertainty, which arises from the imperfection of

mathematical models used to describe complex physical phenomena, such as models describing loads and capacities of soils or structures. Whereas the uncertainty due to inherent randomness is irreducible, statistical and model uncertainties can be reduced, the former by collection of additional samples and the latter by use of more refined models (see Ditlevsen 1981, 1988; Der Kiureghian 1989). This distinction between the three types of uncertainties is fundamental and deserves careful attention, particularly in connection with developing design codes (Der Kiureghian 1989; Maes 1991). Other sources of uncertainty, such as measurement error and human error, also deserve attention but are not discussed here. Approaches for treatment of these uncertainties may be found in Ditlevsen (1981,1988), Grigoriu (1984) and Nowak (1986).

A unified approach to the analysis of statistical and model uncertainties is provided by the well known Bayesian updating rul (Box and Tiao 1973)

$$f''(\boldsymbol{\theta}) = c\, L(\boldsymbol{\theta})\, f'(\boldsymbol{\theta}) \tag{1}$$

where $\boldsymbol{\theta} = \{\theta_1, \theta_2, \cdots\}$ denotes a vector of model parameters, $f'(\boldsymbol{\theta})$ is its prior distribution incorporating subjective information, such as an expert's opinion, $L(\boldsymbol{\theta})$ denotes the likelihood function and incorporates the information gained from observations, $c = \left[\int L(\boldsymbol{\theta})\, f(\boldsymbol{\theta})\, d\boldsymbol{\theta}\right]^{-1}$ is a normalizing factor, and $f''(\boldsymbol{\theta})$ denotes the posterior distribution of $\boldsymbol{\theta}$ that incorporates both the prior (subjective) information as well as the information gained from the observed (objective) data. For a given observation, the likelihood function is proportional to the conditional probability of making the observation given the parameters. This formula has been used extensively in earthquake engineering for the analysis of statistical uncertainties, but it has seldom been used for model uncertainty analysis. The main difficulties arise in formulating the likelihood function and in evaluating integrals needed to compute the normalizing factor c and the statistics of $\boldsymbol{\theta}$, such as its joint moments and marginal distributions. Examples in the following two subsections demonstrate the use of this formula for statistical and model uncertainty analysis.

2.2 Analysis of Statistical Uncertainty

Let $f(\mathbf{x}|\boldsymbol{\theta})$ denote the joint probability density function (PDF) of $\mathbf{x}$ expressed in terms of the unknown parameters $\boldsymbol{\theta}$. If the observation is a set of measured values $\mathbf{x}_1, \mathbf{x}_2, \cdots, \mathbf{x}_N$ from a random sampling of $\mathbf{x}$, then the likelihood function is

$$L(\boldsymbol{\theta}) = \prod_{i=1}^{N} f(\mathbf{x}_i|\boldsymbol{\theta}) \tag{2}$$

If the sampling is not random, then one has to use the joint distribution of the sampled values to formulate the likelihood function. In some applications one observes equality or inequality constraints on $\mathbf{x}$ instead of directly measuring $\mathbf{x}$. For example, one may observe $h_i(\mathbf{x}_i) \le 0$ for $i = 1, 2, \cdots, N$, where $h_i(.)$ are constraint functions. One special case is observing bounds on individual elements of $\mathbf{x}$. If the sampling is random, i.e., $\mathbf{x}_i$ are statistically independent, then

$$L(\boldsymbol{\theta}) = \prod_{i=1}^{n} P\left[h_i(\mathbf{x}_i) \le 0 | \boldsymbol{\theta}\right] \tag{3}$$

where $P[.]$ denotes the probability. For the special case of observing bounds, the above probability term is expressed in terms of cumulative distribution functions.

As an example application relevant to earthquake engineering, consider estimation of the mean rate of earthquakes in a region. Let the Poisson model

$$p(n, t) = \frac{(\theta t)^n}{n!} \exp(-\theta t) \qquad n = 0, 1, 2, \cdots \tag{4}$$

describe the occurrences, where $p(n, t)$ denotes the probability of n occurrences in the interval $(0, t)$, and θ denotes the unknown mean rate which is to be estimated. Suppose the available observation indicates x occurrences in the past τ years. Using Eq. 2, the likelihood function then is

$$L(\theta) = \frac{(\theta\tau)^x}{x!} \exp(-\theta\tau) \tag{5}$$

If the prior on θ is gamma distributed with mean μ' and standard deviation σ' (this is the so called conjugate distribution for the Poisson model, see Ang and Tang 1975), the posterior $f''(\theta)$ is also gamma with the mean and variance

$$\mu'' = \frac{\mu'^2 + x\sigma'^2}{\mu' + \tau\sigma'^2} \quad \text{and} \quad \sigma''^2 = \frac{(\mu'^2 + x\sigma'^2)\,\sigma'^2}{(\mu' + \tau\sigma'^2)} \tag{6}$$

We note that a large prior variance ($\sigma'^2 \to \infty$) produces $\mu'' = x/\tau$ and $\sigma''^2 = x/\tau^2$, which are the data-based estimates of θ, and a small observation period ($\tau, x \to 0$) produces $\mu'' = \mu'$ and $\sigma''^2 = \sigma'^2$, which are the prior estimates. For intermediate cases, the posterior mean is somewhere in between the prior and data based means and the posterior variance is usually smaller than either the prior or the data based variance due to the cumulation of information. The posterior distribution of θ reflects our current state of information and uncertainty about θ. Methods for incorporating this kind of uncertainty in reliability analysis are discussed in Section 3.3.

2.3 Analysis of Model Uncertainty

In general, a mathematical model $g(\mathbf{x}, \boldsymbol{\theta}) = 0$ describes a relation between a set of observable variables $\mathbf{x} = \{x_1, x_2, \cdots\}$ through an operator $g(., \boldsymbol{\theta})$ with parameters $\boldsymbol{\theta} = \{\theta_1, \theta_2, \cdots\}$. The operator might be algebraic, differential or integral in form. Missing variables in the model, incorrect form of the operator, errors in measuring $\mathbf{x}$ in the process of model identification, or limited samples to estimate $\boldsymbol{\theta}$ are possible sources of model uncertainty. More generally, the model might consist of a set of operators $g_i(\mathbf{x}, \boldsymbol{\theta}) = 0$, $i = 1, 2, \cdots$, that describe multiple relations between the variables. The process of formulating the likelihood function depends on the types of model uncertainty present and the form of the model (Bard 1974; Der Kiureghian 1990). In the following, the formulation of the likelihood function for a model used to predict liquefaction in soils is presented.

Motivated by an earlier work of Seed et al. (1985),

Liao et al. (1988) have proposed the following model for the liquefaction of soils under seismic loading:

$$g(N, S, \theta) = \theta_1 N - \theta_2 \ln S + \theta_3 \quad (7)$$

where N represents the standard penetration resistance of soil, S denotes the normalized cyclic stress ratio, and θ_1, θ_2 and θ_3 are parameters. According to this model, liquefaction occurs when $g(N, S, \theta) \le 0$ and it does not occur when $g(N, S, \theta) > 0$. The boundary between the two regions, $g(N, S, \theta) = 0$, in the terminology of structural reliability theory, is known as the limit-state surface. It describes the relation between N and S at the onset of liquefaction. Obviously a simple formula such as the above cannot precisely describe as complex a phenomenon as liquefaction. In particular, many variables other than S and N, such as the pore pressure and the soil grain size, may influence the liquefaction potential but are not included in the model. As a result, for any selected θ, one may observe events that violate the above rule. That is, one may predict $g < 0$ where liquefaction does not occur, and $g > 0$ where liquefaction does occur. Data points in the paper by Seed et al. (1985) clearly show such inconsistencies. As a result of this uncertainty, one cannot precisely determine θ, regardless of the amount of data available.

Suppose a set of measurements (N_k, S_k) at $k = 1, \cdots, N$ sites is available where it is known whether liquefaction has or has not occurred. Let the true limit-state function for the k-th observation be $g_{true} = g(N, S, \theta) + \gamma_k$, where γ_k is a random correction term that accounts for possible incorrectness of the model form and the effect of all missing variables. If γ_k are assumed to be statistically independent and normally distributed with zero mean (for an unbiased model) and standard deviation σ, the likelihood function for the stated observation is (Der Kiureghian 1990)

$$L(\theta, \sigma) = \prod_{\substack{\text{liquefied} \\ \text{sites}}} \left[1 - \Phi\left(\frac{g(N_k, S_k, \theta)}{\sigma}\right)\right] \times \prod_{\substack{\text{non-liquefied} \\ \text{sites}}} \Phi\left(\frac{g(N_k, S_k, \theta)}{\sigma}\right) \quad (8)$$

where $\Phi(.)$ denotes the standard normal cumulative distribution function. Note that the parameter σ is also considered unknown and is included as an argument of the likelihood function. If γ_k are deemed to be correlated, then the likelihood function involves the multinormal distribution, where the correlation coefficients may also be regarded unknown and included in the argument list of the likelihood function.

The above likelihood function together with a prior distribution can be used in Eq. 1 to derive the posterior distribution of θ and σ. This distribution reflects the uncertainty inherent in the model. The occurrence of liquefaction at a given site can now be predicted probabilistically. Specifically, if the values of N and S for the site are known,

P [liquefaction | N, S] =

$$\int_{g(N,S,\theta)/\gamma \le 0} f''(\theta, \sigma)\, \phi\left(\frac{\gamma}{\sigma}\right) d\theta\, d\sigma\, d\gamma \quad (9)$$

and if N and S are unknown,

P [liquefaction] =

$$\int_{g(N,S,\theta)/\gamma \le 0} f(N, S)\, f''(\theta, \sigma)\, \phi\left(\frac{\gamma}{\sigma}\right) d\theta\, d\sigma\, d\gamma\, dN\, dS \quad (10)$$

where $\phi(.)$ denotes the standard normal density and $f(N, S)$ denotes the joint PDF of N and S.

As described in the following section, the integrals in Eqs. 9 and 10 are typical of many structural reliability problems. Methods for efficient computation of these integrals are described in Section 4. Other integrals are involved in the evaluation of the Bayesian updating rule, such as the one required for computing the normalizing factor c. Numerical methods for computation of such integrals are reviewed by Geyskens et al. (1991). Approaches to incorporating the model uncertainty in reliability analysis are discussed in Section 3.3.

3 FORMULATION OF STRUCTURAL RELIABILITY

3.1 Time-Invariant Problems

The essence of the structural reliability problem is the probability integral

$$P_f = \int_D f(\mathbf{x})\, d\mathbf{x} \quad (11)$$

where P_f denotes the "failure" probability, $f(\mathbf{x})$ denotes the PDF of a vector of random variables $\mathbf{x}$ that represent time-invariant uncertain quantities influencing the state of the structure, and D denotes a subset of the outcome space where failure occurs. By "failure," usually the exceedance of a prescribed serviceability or safety limit state is implied. A related measure of interest is the "generalized reliability index", defined by

$$\beta_g = \Phi(1 - P_f) \quad (12)$$

where $\Phi^{-1}(.)$ denotes the inverse of the standard normal cumulative probability. This measure offers certain advantages over the probability measure, particularly in connection with developing codified design rules.

For mathematical analysis, it is necessary to describe the failure domain D in an analytical form. A "component" reliability problem is defined when D is described through a single function, i.e., $D = \{\mathbf{x} \mid g(\mathbf{x}) \le 0\}$, where $g(\mathbf{x})$ is known as the limit-state function. The boundary of D is defined by $g(\mathbf{x}) = 0$ and is known as the limit-state surface. These definitions are shown in Fig. 1 for the special case of two variables. A "system" reliability problem is defined when D is described as the union and/or intersection of several subsets. In particular, a "series system" reliability problem is defined by $D = \{\mathbf{x} \mid \bigcup_i g_i(\mathbf{x}) \le 0\}$, and a "parallel

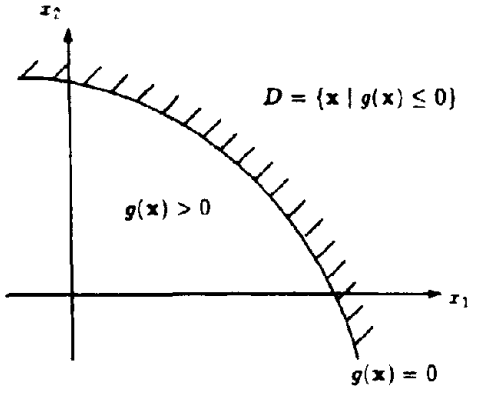

Figure 1. Component reliability problem.

system" reliability problem is defined by $D = \{x \mid \bigcap_i g_i(x) \le 0\}$, where $g_i(x)$ denote componental limit-state functions (see Fig. 2). "General system" problems are defined by a cut-set or link-set formulation. The cut-set formulation is defined by $D = \{x \mid \bigcup_k \bigcap_{i \in C_k} g_i(x) \le 0\}$, where C_k denotes the k-th cut set

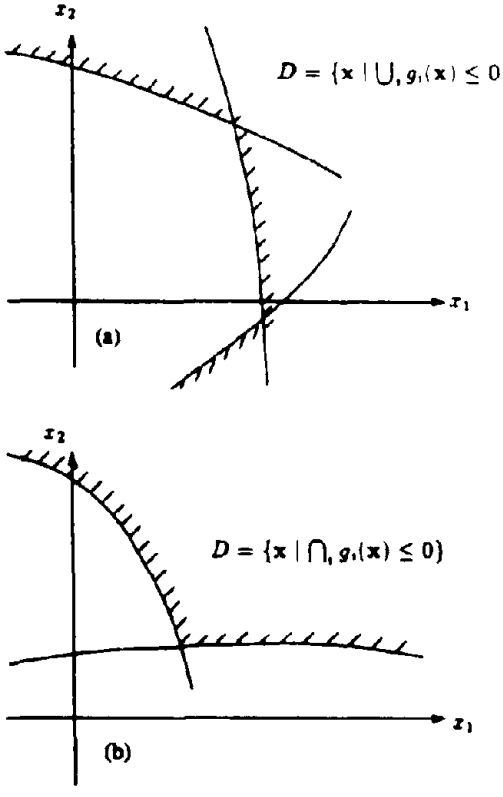

Figure 2. System reliability problems: (a) series system, (b) parallel system.

representing a set of componental limit-states whose joint exceedance constitutes failure of the system. The link-set formulation defines the complement of the failure domain as $\bar{D} = \{x \mid \bigcup_k \bigcap_{i \in L_k} g_i(x) > 0\}$, where L_k denotes the k-th link set representing a set of components whose joint survival constitutes survival of the system. Usually, statically determinate structures and elasto-plastic structures with ductile failure modes are modeled as series systems, whereas structures with brittle members require modeling as non-series systems.

The main issue in time-invariant reliability problems is the computation of the probability integral in Eq. 11. Methods available for this purpose are reviewed in Section 4.

3.2 Time-Variant Problems

A reliability problem is said to be time-variant when the limit-state function depends on time, t. One important case is when some of the uncertain variables are stochastic in nature, as in $g(x, y(t))$, where $y(t)$ denotes a vector of stochastic processes. For example, x may denote uncertain mass, stiffness or damping properties of a structure, which are usually time-invariant, and $y(t)$ may denote ground acceleration processes at the support points of the structure. For this class of reliability problems, the failure event constitutes the outcrossing of the vector process $y(t)$ through the limit-state surface $g(x, y) = 0$, as shown in Fig. 3. Usually it is necessary to solve this problem by conditioning on x, i.e.,

$$P_f = \int P\left[\min_{0<t<T} g(x, y(t)) \le 0 \mid x\right] f(x)\, dx \qquad (13)$$

where T denotes the structure lifetime. The conditioned failure probability for given x is solved by the methods of stochastic process theory (Lin 1967), and the integral is evaluated by one of the methods described in Section 4. The nested reliability method described in Subsection 4.3 is particularly suitable for this purpose.

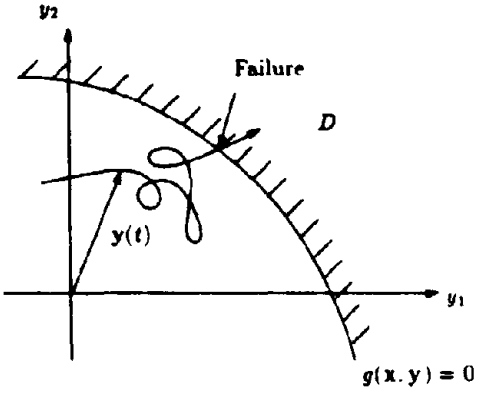

Figure 3. Time-variant reliability problem involving stochastic processes.

The exact solution of the outcrossing probability unfortunately is not available even for the special case of a linear limit-state function and stationary Gaussian processes. For small failure probabilities, however, the following upper bound provides a good approximation (Shinozuka 1964)

$$P\left[\min_{0\le t\le T} g(\mathbf{x}, \mathbf{y}(t)) \le 0 \mid \mathbf{x}\right] \le P\left[g(\mathbf{x}, \mathbf{y}(0)) \le 0\right] + \int_0^T \nu(\mathbf{x}, t)\, dt \qquad (14)$$

where $\nu(\mathbf{x}, t)$ denotes the mean rate of outcrossing of $\mathbf{y}(t)$ for given $\mathbf{x}$. The first term on the right-hand side is a time-invariant reliability problem of the type defined in Eq. 11. The main difficulty is in computing the mean outcrossing rate and considerable effort in recent years has been devoted to finding exact or approximate solutions to this problem. For a linear limit-state surface, the outcrossing problem can be converted to a scalar process upcrossing problem for which a well known solution by Rice (1944) is available. For a nonlinear limit-state surface, a generalization of the Rice formula is available that requires integration over the surface (Belyaev 1968). Based on this formula, solutions of the outcrossing rate for special cases of the limit-state surface (e.g., polyhedral or ellipsoid surfaces) have been derived (Veneziano et al. 1977; Ditlevsen 1983, Hohenbichler and Rackwitz 1986b). These solutions are rather involved and require considerable amount of computation. Another idea has been to linearize the limit-state surface at an appropriate point (either the point of maximum mean outcrossing rate or the point of maximum likelihood) and convert the problem into an upcrossing-rate problem (Pearce and Wen 1985). Various choices for the linearization point have been discussed by Ditlevsen (1987). Recently, it has been possible to convert the outcrossing problem into a parallel system sensitivity problem, for which the methods described in Sections 4 and 5 are applicable (Hagen and Tvedt 1991). In spite of these achievements, this area is still in need of research and development before general and effective tools of analysis become available.

Another class of time-variant reliability problems is defined by a limit-state function which is a direct function of time, i.e., of the form $g(\mathbf{x}, t)$. For example, an uncertain structure subjected to a time-varying deterministic load belongs to this class. In some cases it is possible to represent stochastic processes in terms of random variables and deterministic functions of time (Li and Der Kiureghian 1992). In that case, a problem defined by a limit-state function of the form $g(\mathbf{x}, \mathbf{y}(t))$ can be converted to one of the form $g(\mathbf{x}, t)$, where $\mathbf{x}$ now includes the random variables defining $\mathbf{y}(t)$. The probability of failure for this class of problems is described by the integral in Eq. 11, where the failure domain now is $D = \{\min_{0\le t\le T} g(\mathbf{x}, t) \le 0\}$. Hence, methods available for solving time-invariant reliability problems are also applicable to this class of problems. However, caution should be exercised since the limit-state surface in this case is not continuously differentiable and can be strongly nonlinear. An example application later in Section 7 demonstrates this problem.

It is easy to visualize extensions of the above formulations to space-variant reliability problems, such as those involving random fields of material properties or loads, or those where the limit-state function is explicitly dependent on a spatial coordinate. Furthermore, one can formulate problems where the limit-state function is dependent on both time and space coordinates. Methods for solution of such problems are still in early developmental stage.

3.3 Effect of Statistical and Model Uncertainties

The formulation presented in Eq. 11 only accounts for the inherent randomnesses represented by the random variables $\mathbf{x}$. To explicitly account for statistical and model uncertainties, we write the PDF of $\mathbf{x}$ as $f(\mathbf{x}|\boldsymbol{\theta})$ and the componental limit-state functions (disregarding the subscript) as $g(\mathbf{x}, \boldsymbol{\theta})$, where $\boldsymbol{\theta}$ is a vector collecting all the uncertain parameters present in the distribution function and the mathematical models describing the limit-states. The probability of failure and the generalized reliability index defined by Eqs. 11 and 12 are now dependent on $\boldsymbol{\theta}$, i.e., $P_f(\boldsymbol{\theta})$ and $\beta_g(\boldsymbol{\theta})$, and hence are uncertain. There are different views as to how these uncertainties should be treated. One view, exercised by Madsen et al. (1986) and Ditlevsen (1982) for example, is to not differentiate between the uncertainties in $\boldsymbol{\theta}$ from those in $\mathbf{x}$. The result is the expected probability of failure obtained from the total probability formulation

$$\mathrm{E}[P_f(\boldsymbol{\theta})] = \int_D f(\mathbf{x}|\boldsymbol{\theta})\, f''(\boldsymbol{\theta})\, d\mathbf{x}\, d\boldsymbol{\theta} \qquad (15)$$

where $f''(\boldsymbol{\theta})$ is the posterior distribution of $\boldsymbol{\theta}$ obtained from Bayesian updating. We note that this integral has the same form as that in Eq. 11, provided $\mathbf{x}$ and $\boldsymbol{\theta}$ are combined to form a single vector. Hence, methods used for the solution of the problem in Eq. 11 can also be used to evaluate the expected probability of failure described above.

Another approach for the analysis of uncertainties recognizes the fundamental difference between the inherent randomnesses represented by $\mathbf{x}$, which are irreducible, and the statistical and model uncertainties represented by $\boldsymbol{\theta}$, which are reducible. In this case, P_f and β_g are treated as random variables with probability distributions that reflect the effect of statistical and model uncertainties on their estimated values (Der Kiureghian 1989). The cumulative distribution function of β_g, for example, is given by

$$P[\beta_g \le \beta_o] = \int_{\beta_g(\boldsymbol{\theta}) - \beta_o \le 0} f''(\boldsymbol{\theta})\, d\boldsymbol{\theta} \qquad (16)$$

and its PDF can be seen as the sensitivity of the above probability with respect to the parameter β_o. We note that the above integral is also of the type shown in Eq. 11, except that the limit-state function here involves the conditional reliability index $\beta_g(\boldsymbol{\theta})$. The nested reliabil-

ity method described in Section 4.3 is ideal for solution of this problem.

In application, one is often interested in a simple measure to describe the effect of statistical and model uncertainties on computed P_f and β_g. One such measure is a confidence interval around the computed values with a a specified probability (or confidence). The probability distribution described above can be used to generate such intervals. Another convenient measure is the variance of $P_f(\theta)$ or $\beta_g(\theta)$ with θ regarded as random variables. These variances can also be obtained from the distribution described above. However, it is much simpler to use a first-order approximation, which for β_g leads to (Der Kiureghian 1989)

$$\mathrm{Var}[\beta_g(\theta)] \approx \nabla_\theta \beta_g \, \Sigma''_{\theta\theta} \, \nabla_\theta \beta_g^T \tag{17}$$

where $\nabla_\theta \beta_g$ is the gradient (sensitivity) vector of β_g at the mean of θ (see Section 5) and $\Sigma''_{\theta\theta}$ is the posterior covariance matrix of θ. This variance together with an assumed distribution can be used to obtain an approximate confidence interval on β_g. A similar formula for the variance of $P_f(\theta)$ can be written, which is however less accurate due to typically stronger nonlinear dependence of $P_f(\theta)$ on θ. It is better to use the confidence interval of β_g together with Eq. 12 to obtained a confidence interval on P_f.

Existing probabilistic code formats generally do not differentiate between the nature of the uncertainties in $\mathbf{x}$ and θ (Ravindra and Galambos 1978; Ditlevsen 1982). Suggestions for code formats that explicitly differentiate between the two types of uncertainties have recently been made (Der Kiureghian 1989; Maes 1991). These formats tend to penalize for the uncertainty in the computed reliability index and, hence, encourage the use of more data and refined models in engineering design.

4 PROBABILITY COMPUTATION METHODS

A great deal of effort in the past two decades has been devoted to developing efficient algorithms for computing probability integrals of the type in Eq. 11. A straightforward integration, by analytical or numerical means, usually is not possible because of the arbitrary nature of the integration domain and the typically high dimension of the problem. We note that often the size of $\mathbf{x}$ is larger than 10 and it could be as large as several hundred or thousand. Hence, indirect approaches for evaluating the integral are essential. In this section, a review of the most widely used of these methods is presented.

Several of the methods described in the following subsections require transformation of the random variables into the standard normal space. The transformation, which is necessarily nonlinear for non-Gaussian random variables, is expressed as $\mathbf{u} = \mathbf{u}(\mathbf{x})$, where $\mathbf{u}$ has the standard normal density $\phi(\mathbf{u}) = (2\pi)^{-n/2} \exp(-0.5|\mathbf{u}|^2)$, where n denotes the number of random variables. A general form of this transformation is given by Hohenbichler and Rackwitz (1981) and a more convenient form for a particular class of multi-variate distributions is given by Der Kiureghian and Liu (1986). Using this transformation, Eq. 11 is rewritten in the form

$$P_f = \int_D \phi(\mathbf{u})\, d\mathbf{u} \tag{18}$$

where D is now defined in the u space. For notational convenience, we let $G(\mathbf{u}) = g(\mathbf{x}(\mathbf{u}))$ denote the transform of the limit-state function in the u space.

4.1 First and Second-order Reliability Methods

The first- and second-order reliability methods (FORM and SORM) take advantage of the fact that the point $\mathbf{u}^* = \min(|\mathbf{u}| \mid G(\mathbf{u}) = 0)$, which is a point located on the limit-state surface with minimum distance from the origin, has the highest probability density among all failure points in the standard normal space. This point is known as the "design point" or the "most likely failure point". It is readily evident that probability densities in the standard normal space are rotationally symmetric and decay exponentially with the square of distance in both radial and tangential directions from $\mathbf{u}^*$. It follows that the major contribution to the probability integral in Eq. 18 comes from the neighborhood of $\mathbf{u}^*$, provided the surface is not strongly nonlinear and there is only one significant design point. These conditions are satisfied for most structural component reliability problems. Based on this, the limit-state surface in the neighborhood of the design point is approximated by a first- or second-order surface for which the solution of the probability integral is available. Specifically, in FORM, the limit-state surface is replaced by the tangent hyperplane at $\mathbf{u}^*$ and the first-order approximation of the failure probability is given by

$$P_f \approx P_{f1} = \Phi(-\beta) \tag{19}$$

where $\beta = \alpha \mathbf{u}^*$, known as the (first-order) reliability index, is the distance from the origin and α denotes the unit normal at the design point directed towards the failure set (Fig. 4). In SORM, the limit-state surface is fitted with a second-order surface (usually a paraboloid) at $\mathbf{u}^*$, and the second-order approximation of the fail-

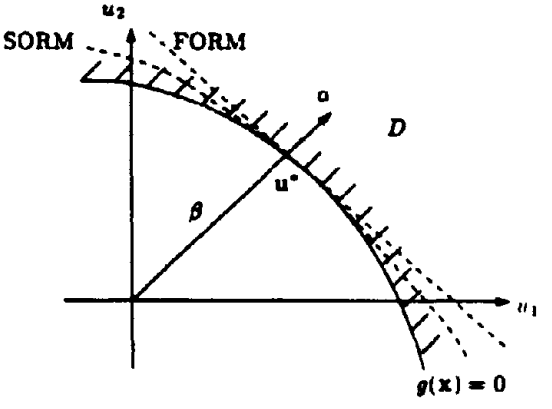

Figure 4. FORM and SORM approximations.

ure probability is given in terms of β and the principal curvatures, κ_i, of the paraboloid. The exact expression of this probability is given in terms of a single-fold integral, which must be evaluated numerically (Tvedt 1990). A simpler approximation is (Breitung 1984)

$$P_f = P_{f2} = \Phi(-\beta) \prod_{i=1}^{n-1} (1 + \beta \kappa_i)^{-1/2} \tag{20}$$

Various methods for selecting the approximating paraboloid and computing the principal curvatures are available (Fiessler et al. 1979; Der Kiureghian et al. 1987; Tvedt 1990; Der Kiureghian and DeStefano 1991; Geyskens et al. 1991). An alternative SORM approach has also been suggested by Breitung (1991), where an approximation of the probability by maximizing the log-likelihood in the space of the original variables, $\mathbf{x}$, is obtained.

An important step in FORM/SORM is the determination of the design point. This requires the solution of a constrained optimization problem. Most algorithms construct a converging sequence of points according to the rule $\mathbf{u}_{k+1} = \mathbf{u}_k + \lambda_k \mathbf{d}_k$, $k = 0, 1, \cdots$, where $\mathbf{d}_k$ denotes the search direction vector at step k and λ_k denotes the step size. In most efficient algorithms $\mathbf{d}_k$ is expressed in terms of the gradient of the constraint function, ∇G. For example, in an algorithm widely used in reliability analysis,

$$\mathbf{d}_k = \left[\frac{\nabla G}{|\nabla G|} \mathbf{u}_k - \frac{G(\mathbf{u}_k)}{|\nabla G|} \right] \frac{\nabla G^{\mathrm{T}}}{|\nabla G|} + \mathbf{u}_k \tag{21}$$

and λ_k is selected such that $m(\mathbf{u}_{k+1}) < m(\mathbf{u}_k)$, where $m(.)$ is a merit function. A comparative evaluation of this and several other algorithms used in reliability analysis is presented Liu and Der Kiureghian (1990).

When the limit-state surface in the standard normal space is strongly nonlinear, which may arise from strong nonlinearity of $g(\mathbf{x})$ or from strong nonnormality of the the basic variables $\mathbf{x}$, multiple design points on the surface may occur with significant neighborhood densities. For such cases, an improved approximation may be obtained by fitting first- or second-order approximations at all significant local design points followed by a series system analysis as described below, provided certain convexity conditions are satisfied. Finding these local design points, however, is a challenge by itself since it is difficult to prevent convergence of the optimization algorithm to the global design point. An algorithm for sequentially finding these points for a special class of reliability problems has recently been developed and an example is presented in Section 7.1.

A general formulation for a first-order system reliability analysis is presented by Hohenbichler and Rackwitz (1983). In this approach, each componental limit-state surface is linearized at an appropriate point (the minimum-distance point either on the surface or its intersection with other surfaces) and the probability of system failure is approximated by the probability content in the resulting polyhedral set. It is shown that the first-order approximation for series systems is $P_{f1} = 1 - \Phi_n(\boldsymbol{\beta}, \mathbf{A}\mathbf{A}^{\mathrm{T}})$, where $\boldsymbol{\beta} = [\beta_1, \beta_2, \cdots]$ is the vector of componental reliability indices, $\mathbf{A} = [\boldsymbol{\alpha}_1\ \boldsymbol{\alpha}_2 \cdots]$ is the matrix of unit normals at the linearization points, and $\Phi_n(., \mathbf{R})$ denotes the n-dimensional cumulative normal probability with correlation matrix $\mathbf{R}$. For parallel systems, the approximation is $P_{f1} = \Phi_n(-\boldsymbol{\beta}, \mathbf{A}\mathbf{A}^{\mathrm{T}})$. Both results require the standard multi-normal probability over polyhedral sets. An approximate method for computing this probability has been developed by Gollwitzer and Rackwitz (1988). Second-order system reliability methods that employ second-order approximations of the componental limit-states have also been developed (Madsen et al. 1986; Hohenbichler et al. 1987, Lin and Der Kiureghian 1987).

For series systems, first-order bounds on the system failure probability in terms of individual componental (or modal) failure probabilities and cross-modal correlation coefficients (represented by the product $\mathbf{A}\mathbf{A}^{\mathrm{T}}$) have been developed by Ditlevsen (1979). These bounds are easy to compute and essentially require a simple component reliability analysis for each failure mode. These bounds can also be used for computing first-order probabilities for general systems defined in terms of cut sets or link sets (Hohenbichler and Rackwitz 1983).

The major advantage of FORM/SORM is that the probability integral is computed with relatively small number of computations of the limit-state function and its gradient. Typically, for FORM the number of computations of each G and ∇G is of order 10 to 100, and for SORM, depending on the method used, extra computations of G of order $10n$ or n^2 are required to determine the principal curvatures, where n denotes the number of random variables. Note that these numbers are independent of the magnitude of the failure probability. These methods have the additional advantage of providing the coordinates of the most likely failure point and, in SORM, the shape of the limit-state surface in the neighborhood of the design point. Furthermore, as will be described in Section 5, FORM readily provides the sensitivities of the failure probability, which are important in many applications.

4.2 Simulation Methods

A widely used method for computing probabilities is the Monte Carlo simulation method (Rubenstein 1981; Ang and Tang 1984). To apply this method to the structural reliability problem, the integral in Eq. 11 is written in the form

$$P_f = \int I(\mathbf{x}) f(\mathbf{x}) d\mathbf{x} \tag{22}$$

where $I(\mathbf{x})$ is an indicator function defined by

$$I(\mathbf{x}) = 1 \quad \text{if } \mathbf{x} \in D \tag{23}$$
$$= 0 \quad \text{if } \mathbf{x} \notin D$$

Consider a sampling $\mathbf{x}_1, \mathbf{x}_2, \cdots, \mathbf{x}_N$ of the random variables according to the density $f(\mathbf{x})$ and let

$$p_i = I(\mathbf{x}_i) f(\mathbf{x}_i), \qquad i = 1, \cdots, N \tag{24}$$

A mean estimate of the probability of failure, then, is

$$E[\hat{P}_f] = \frac{1}{N}\sum_{i=1}^{N} p_i \tag{25}$$

where N denotes the sample size. A measure of the error in the estimate is given by the variance

$$\mathrm{Var}[\hat{P}_f] = \frac{1}{N(N-1)}\sum_{i=1}^{N}(p_i - E[\hat{P}_f])^2 \tag{26}$$

As N approaches infinity, the variance diminishes and the estimate in Eq. 25 approaches the exact failure probability P_f, provided, of course, that the sampling is truly random and representative of the distribution $f(\mathbf{x})$.

Aside from difficulties in producing truly random numbers in accordance with a specified distribution, the main disadvantage of the Monte Carlo simulation method lies in its large computational requirement. Roughly speaking, in order to obtain reasonably accurate probability estimates, it is necessary to have a sample size at least as large as $100/P_f$. In structural reliability problems P_f is typically small, e.g., of order 10^{-2} to 10^{-7}, and the direct Monte Carlo method normally requires tens or hundreds of thousands of repeated computations of the limit-state function. For many engineering applications this is impractical and, hence, attention has been focused on developing more efficient simulation methods. These methods are commonly aimed at reducing the variance of the probability estimate for a given number of simulations, N.

For the structural reliability problem, the most promising variance reduction technique appears to be the importance sampling method (Shinozuka 1983; Harbitz 1986). This method reduces the variance of the estimate by sampling more frequently from inside the failure set. Eqs. 22 and 24 are rewritten in the form

$$P_f = \int I(\mathbf{x})\frac{f(\mathbf{x})}{h(\mathbf{x})}h(\mathbf{x})\,d\mathbf{x} \tag{27}$$

$$p_i = I(\mathbf{x}_i)\frac{f(\mathbf{x}_i)}{h(\mathbf{x}_i)}, \qquad i = 1, \cdots, N \tag{28}$$

where $h(\mathbf{x})$ is the new sampling density. The ideal choice for $h(\mathbf{x})$ is $I(\mathbf{x})f(\mathbf{x})/P_f$. For this choice, the mean of the estimate is identical to P_f and the variance is zero for any N. However, it is not practical to sample from this ideal density since it would require the same number of g-function computations as the conventional Monte Carlo method. Instead, a sampling density that closely approximates this ideal density but does not require computation of $g(\mathbf{x})$ is employed. Knowledge of the design point(s) from FORM analysis can be particularly helpful in choosing an appropriate sampling density (Harbitz 1986; Schueller and Stix 1987; Melchers 1987). For example, when the safe set is known to be concave, sampling over the half space defined by $\boldsymbol{\alpha}\mathbf{x} \geq \beta$, where β is the reliability index and $\boldsymbol{\alpha}$ is the unit normal at the design point, can be performed. If the safe set is known to be a closed space, then sampling outside of the β-sphere defined by $|\mathbf{x}| \geq \beta$ is a good choice (Harbitz 1986). When the shape of the limit-state surface is not known in advance, then sampling with a normal density centered at each design point is a good choice and has been advocated by a number of investigators (Melchers 1987). Adaptive importance sampling techniques, where the sampling density is modified during the course of sampling, have also been suggested (Bucher 1988).

It is important to realize that the importance sampling method may converge to a wrong probability estimate if the sampling density is not properly selected. For example, if a zero density is assigned to a subset of D over which $f(\mathbf{x})$ is not zero, then no points will be sampled from that subset and a wrong estimate would be obtained. Hence, it is critical to exercise good judgment in the selection of the sampling density.

Other variance-reduction techniques include the method of antithetic variates, where the variance in the estimate is reduced by creating negative correlation between p_i (Rubenstein 1981), and the method of stratified sampling, and in particular the Latin hypercube sampling, where the number of simulations is reduced by sampling within equally likely intervals of the outcome space (McKay et al. 1979). The latter method, while effective for computing means and variances of functions, is not very effective for computing small probabilities that are typical of reliability problems.

Another class of efficient simulation methods is based on the concept of conditioning. Assume the vector of random variables is partitioned in the from $\mathbf{x} = (\mathbf{y}, \mathbf{z})$ and rewrite Eq. 11 in the total probability form

$$P_f = \int P\left[g(\mathbf{y}, \mathbf{z}) \leq 0 \;\middle|\; \mathbf{z}\right] f(\mathbf{z})\,d\mathbf{z} \tag{29}$$

Advantage is achieved if an efficient method is available to compute the conditional probability inside the integral. If this is possible, then simulation can be performed to compute the integral over $\mathbf{z}$. Note that the integral essentially represents the mean value of the conditional probability with respect to the random variables $\mathbf{z}$. Hence, the number of required simulations will be small if the conditional probability has a small variance with respect to $\mathbf{z}$.

One simulation method by conditioning is the so called directional simulation method (Bjerager 1988). The simulation in this method is performed in the standard normal space. The vector of standard variates, $\mathbf{u}$, is written in the form $\mathbf{u} = R\,\mathbf{a}$, where $R = |\mathbf{u}|$ denotes the length of the vector and $\mathbf{a} = \mathbf{u}/|\mathbf{u}|$ denotes the unit directional vector. By conditioning on $\mathbf{a}$, the probability integral is written in the form

$$P_f = \int P\left[G(R\mathbf{a}) \leq 0 \;\middle|\; \mathbf{a}\right]\frac{f(\mathbf{a})}{h(\mathbf{a})}h(\mathbf{a})\,d\mathbf{a} \tag{30}$$

where $f(\mathbf{a})$ is the density of $\mathbf{a}$, which is uniform on the unit sphere centered at the origin, and $h(\mathbf{a})$ is an appropriate sampling density. Since $R^2 = |\mathbf{u}|^2$ has the chi-square distribution with n degrees of freedom, the conditional probability is given by

$$P\left[G(R\mathbf{a}) \leq 0 \mid \mathbf{a}\right] = 1 - \chi_n^2(r^2) \tag{31}$$

where r is the root of $G(r\mathbf{a}) = 0$, i.e., is the distance from the origin to the limit-state surface along the direction $\mathbf{a}$. For a set of simulations $\mathbf{a}_1, \mathbf{a}_2, \cdots, \mathbf{a}_N$ of $\mathbf{a}$ according to the sampling density $h(\mathbf{a})$, the estimates of

the probability of failure are given by Eqs. 25 and 26, where p_i now is

$$p_i = P[G(R\mathbf{a}_i) \le 0] \frac{f(\mathbf{a}_i)}{h(\mathbf{a}_i)} \tag{32}$$

Various choices for the sampling density using the knowledge of design point(s) from FORM analysis are suggested by Bjerager (1988) and Melchers (1990).

The directional simulation method is effective when the dimension n of $\mathbf{u}$ is not too large and when the root r_i for each simulated direction $\mathbf{a}_i$ is easily obtained. In some cases, it is convenient to replace the actual surface by an approximating surface to facilitate the root finding process (Lin and Der Kiureghian 1987). Another, non-radial, directional simulation method has been suggested by Hohenbichler and Rackwitz (1988), which is aimed at improving probability estimates based on FORM and SORM.

4.3 Nested Reliability Analysis

Consider the reliability problem defined in the conditional form in Eq. 29. It can be shown (Wen and Chen 1987) that this problem is identical to a reliability problem of the form in Eq. 11 when the limit-state function is taken to be

$$g(u, \mathbf{z}) = u + \beta_g(\mathbf{z}) \tag{33}$$

where $\beta_g(\mathbf{z})$ is the conditional generalized reliability index for given $\mathbf{z}$ and u is a standard normal variate independent of $\mathbf{z}$. This formulation suggests a nested reliability analysis involving an inner reliability problem for determining $\beta_g(\mathbf{z})$, and an outer reliability problem defined by the above limit-state function and including the random variables $\mathbf{z}$ and u. The inner problem involves the variables $\mathbf{y}$, which in general can be stochastic processes or random fields.

The above formulation offers an advantage in certain reliability problems when different methods must be used to solve the inner and outer problems. For example, in a time-variant reliability problem involving stochastic processes $\mathbf{y}(t)$, $\beta_g(\mathbf{z})$ may be obtained from random vibration analysis by considering the outcrossing problem associated with $\mathbf{y}(t)$ with $\mathbf{z}$ fixed, whereas the outer reliability problem involving u and $\mathbf{z}$ may be solved by any of the methods described in this section, including FORM and SORM (Wen and Chen 1989; Madsen and Tvedt 1990). This approach has been used for reliability analysis of uncertain systems subjected to stochastic excitation (Igusa and Der Kiureghian 1988). An example in Section 7.1 demonstrates such an application.

4.4 The Response Surface Method

An alternative approach for computing probabilities of the type in Eq. 11 is to replace the integration boundary by an approximating "response" surface and then perform the integration by an appropriate means (e.g., FORM, SORM, simulation) without having to engage the actual limit-state function. This approach is particularly useful when the limit-state function is algorithmic in form (e.g., requires finite element computations) and its gradient, which is necessary in FORM and SORM analysis, is difficult to compute (Faravelli 1989). To construct the response surface, one typically computes $g(\mathbf{x})$ at a number of points $\mathbf{x} = \mathbf{x}_i$, $i = 1, 2, \cdots, N$, and then fits a polynomial surface to the points by the least squares method. If a second-order polynomial is used, calculations at at least $N^2/2 + 3N/2 + 1$ points are necessary, which is a formidable number for large N. To reduce this number the use of polynomial functions excluding cross terms has been suggested (Schueller and Stix 1987). Another suggestion is to reduce the number of random variables by collecting less important variables into a single error term, which is then analyzed by ANOVA (Faravelli 1989). One important consideration in using the response surface methodology is the selection of the "experiment" points, $\mathbf{x}_i$. There are a number of standard experiment plans for this purpose. For the structural reliability problem, it is clear that these points should be selected in the neighborhood of the design point, which unfortunately is usually unknown in advance.

5 RELIABILITY SENSITIVITY MEASURES

Analysis of probability sensitivities with respect to parameters defining a given problem is an important part of reliability analysis. Parameters, denoted $\boldsymbol{\theta}$, might be those defining the probability distribution function $f(\mathbf{x}|\boldsymbol{\theta})$, or those defining the limit-state models $g(\mathbf{x}, \boldsymbol{\theta})$. With respect to a given parameter θ, the sensitivity of the probability of failure is the partial derivative $\partial P_f/\partial\theta$. Collection of these terms in a row vector forms the gradient with respect to $\boldsymbol{\theta}$, $\nabla_{\boldsymbol{\theta}} P_f = [\partial P_f/\partial\theta_1 \;\; \partial P_f/\partial\theta_2 \;\; \cdots]$. Owing to the definition in Eq. 12, this is related to the gradient of the generalized reliability index by

$$\nabla_{\boldsymbol{\theta}} P_f = -\phi(\beta_g) \nabla_{\boldsymbol{\theta}} \beta_g \tag{34}$$

where $\phi(\,)$ denotes the standard normal density.

Sensitivity measures are useful in reliability analysis in a number of ways. They provide relative measures of importance of the random variables, are needed in search algorithms for reliability-based optimization or nested reliability analysis (see Section 4.4), are used in reliability uncertainty analysis (Eq. 17), are fundamental to reliability upgrading as discussed in Section 6, and in general are valuable in gaining insight into a problem or in making decisions.

As measures of importance of random variables, it is most useful to compute the gradients with respect to the means, $\boldsymbol{\mu} = \{\mu_1, \mu_2, \cdots\}$, and standard deviations, $\boldsymbol{\sigma} = \{\sigma_1, \sigma_2, \cdots\}$, of the random variables. When scaled by the diagonal matrix of standard deviations, these sensitivity vectors, $diag[\boldsymbol{\sigma}]\nabla_{\boldsymbol{\mu}}\beta$ and $diag[\boldsymbol{\sigma}]\nabla_{\boldsymbol{\sigma}}\beta$, represent dimensionless measures of variation in β with respect to equally likely variations in the mean and standard deviation of each variable. The elements within each of these vectors can be compared regardless of the nature of each variable or the units used to represent it. The former vector gives the relative importance of the random variables with respect to their central values, whereas the latter gives the relative importance

with respect to their variabilities. When the variability in a random variable has a relatively small influence on β, then that variable can be replaced with a deterministic quantity, thus reducing the size of the reliability problem. When used in this context, sensitivity vectors are known as omission sensitivity factors (Madsen 1988b).

One important advantage of FORM is that it provides the sensitivity gradients as a byproduct of the algorithm for finding the design point. If θ represents distribution parameters, then (Hohenbichler and Rackwitz 1986a)

$$\nabla_\theta \beta = -\frac{\nabla G}{|\nabla G|} \nabla_\theta \mathbf{u}(\mathbf{x}^*) \tag{35}$$

and if θ represents parameters in the limit-state function of a component reliability problem, then

$$\nabla_\theta \beta = \frac{1}{|\nabla G|} \nabla_\theta g(\mathbf{x}^*) \tag{36}$$

where $\mathbf{x}^*$ denotes the design point in the original space and ∇G is the gradient in the standard normal space evaluated at the design point. The latter is usually available from the algorithm used for finding the design point and, hence, one only needs the gradients of $\mathbf{u}(\mathbf{x})$ and $g(\mathbf{x})$ at the design point, which are easy to compute. For system reliability analysis, the derivative of the unit normal at each linearization point is also required. This involves the second derivative of the limit-state function (Bjerager and Krenk 1989). Reliability sensitivity measures for FORM analysis of series and parallel systems are obtained by Bjerager and Krenk (1989) and Madsen (1988a).

Reliability sensitivities can also be obtained by simulation (Ditlevsen and Bjerager 1988; Karamchandani et al. 1988). For this purpose, it is necessary to compute the gradient $\nabla_\theta p_i$ for each simulation of p_i in accordance with Eq. 24, 28 or 32. For example, with the importance sampling method, the gradient with respect to the distribution parameters is

$$\nabla_\theta p_i = I(\mathbf{x}_i) \frac{\nabla_\theta f(\mathbf{x}_i|\theta)}{h(\mathbf{x}_i)}, \qquad i = 1, \cdots, N \tag{37}$$

Note that the gradient computation is necessary only when $I(\mathbf{x}_i) = 1$, i.e., when the simulated point is inside the failure domain. Unfortunately, derivatives with respect to limit-state parameters cannot be derived with this method because of the non-differential nature of the indicator function $I(\mathbf{x})$. For such parameters, the directional simulation method is applicable, for which (Ditlevsen and Bjerager 1989)

$$\nabla_\theta p_i = \frac{2r}{\nabla G\, \mathbf{a}_i} \nabla_\theta G(r\mathbf{a}_i, \theta) \tag{38}$$

The mean and variance estimates of the sensitivities are computed by using the above two derivatives in place of p_i in Eqs. 25 and 26, respectively. One should note, however, that the optimal sampling density for the probability sensitivity in general differs from that which is optimum for the probability itself. Therefore, care must be exercised in the choice of the sampling density if it is used for both the probability and its sensitivity.

6 RELIABILITY UPDATING

Often it is of interest to update the estimated reliability of a structure in light of newfound information. For example, it might be of interest to update the reliability after in situ testing of material strengths. In recent years, this topic has become of particular interest in developing optimum inspection and maintenance strategies for offshore platforms (Madsen 1987; Jiao and Moan 1990).

In general an observation can be one of two basic types: (a) inequality observation, or (b) equality observation. The first occurs when a bound is observed, or the occurrence or non-occurrence of an event is observed. Mathematically, this can be expressed as $h(\mathbf{x}) \le 0$. For example, the observation that the first member of $\mathbf{x}$ is less than 100 can be expressed as $h(x_1) = x_1 - 100 \le 0$. If an event is observed, such as the initiation of cracks at a point in the structure, then the above formulation applies with $h(\mathbf{x})$ denoting the limit-state function for the initiation of cracks at that location. The equality observation usually is the result of a measurement and it can be mathematically expressed as $h(\mathbf{x}) = 0$. For example, the observation that $x_1 + x_2$ is measured to be 100 is expressed as $h(x_1) = x_1 + x_2 - 100 = 0$.

For the inequality-type observation, the updated reliability can be obtained from the conditional probability law

$$P[g(\mathbf{x}) \le 0 \mid h(\mathbf{x}) \le 0] = \frac{P[g(\mathbf{x}) \le 0 \cap h(\mathbf{x}) \le 0]}{P[h(\mathbf{x}) \le 0]} \tag{39}$$

The numerator on the right-hand side defines a parallel-system reliability problem involving the componental limit-states $g(\mathbf{x})$ and $h(\mathbf{x})$, whereas the denominator defines a component reliability problem with the limit-state function $h(\mathbf{x})$. Thus, methods available for component and system reliability analysis are readily applicable to the above updating problem. Generalization of the above formula to the case of several inequality observations $h_i(\mathbf{x}) \le 0$, $i = 1, 2, \cdots$, should be obvious.

It can be shown (Madsen 1987) that updating with equality observation is equivalent to

$$P[g(\mathbf{x}) \le 0 \mid h(\mathbf{x}) = 0] = \frac{P[g(\mathbf{x}) \le 0 \cap h(\mathbf{x}) = 0]}{P[h(\mathbf{x}) = 0]} = \frac{\frac{\partial}{\partial \varepsilon} P[g(\mathbf{x}) = 0 \cap h(\mathbf{x}) - \varepsilon \le 0]_{\varepsilon = 0}}{\frac{\partial}{\partial \varepsilon} P[h(\mathbf{x}) - \varepsilon \le 0]_{\varepsilon = 0}} \tag{40}$$

In this case, the probability sensitivities with respect to the dummy parameter ε for the parallel system problem in the numerator and the component problem in the denominator are required. Methods for computation of parallel-system sensitivities are described by Madsen (1988a). Other updating formulations can be found in Jiao and Moan (1990).

7 FINITE-ELEMENT RELIABILITY METHODS

The idea of combining probabilistic methods with finite elements has been around for some time (see Vanmar-

cke et al., 1986, and Der Kiureghian et al., 1991, for recent reviews). Since most structural analysis these days is carried out by finite elements, it is natural that the methods of structural reliability also employ this computational technique. In the context of structural reliability theory described in this paper, the main reason for needing the finite element method is that the limit-state function $g(\mathbf{x})$ is usually an implicit function of $\mathbf{x}$ and can only be evaluated by a numerical algorithm, such as a finite element code. For example, in structural analysis $g(\mathbf{x})$ is often described in terms of load effects such as stresses and deformations, while $\mathbf{x}$ represents elementary input quantities, such as loads and material property constants. Since the relation between load effects and loads and material property constants is usually implicit, the use of a numerical algorithm, such as a finite element code, to evaluate the $g(\mathbf{x})$ function is necessary. Another reason for using the finite element method is to address problems involving random fields of material properties or loads. In this approach, the random field over the domain of interest is discretized and represented by random variables in much the same way as the conventional finite element discretization method. Random-variable reliability methods are then used to compute probabilities of interest. Li and Der Kiureghian (1992) have recently reviewed several methods for discretization of random fields in this context.

An important advantage of combining reliability methods with finite elements is that one gains access to state-of-the-art models of mechanical behavior for reliability analysis. This is particularly important in structural safety studies, where attention naturally is focused on extreme states of a structure and, hence, consideration must be given to grossly nonlinear behavior. A key issue in this regard is the ability to combine the reliability and finite element codes without too much interference in either so that periodic updates in either code can be made. In the experience of the author, the best way is for the reliability code to act as a shell program that runs the finite element code. This approach has been implemented in the CALREL-FEAP finite element reliability code developed by the author and his colleagues at the University of California (see Liu and Der Kiureghian 1991).

Theoretically speaking, any of the reliability computation methods described in Section 4 can be used for finite element reliability analysis. However, there are impediments in straightforward implementation each of these methods. For example, for direct implementation of FORM and SORM, it is necessary to develop efficient and accurate algorithms to compute the response gradients, which typically are not available in existing finite element codes. In recent years notable successes have been achieved in developing such algorithms for both linear and nonlinear structures (Vanmarcke et al. 1986; Santos 1991, Zhang and Der Kiureghian 1991). The conventional simulation method, while appropriate for computing low-order moments of response quantities, usually is prohibitively costly for computing small probabilities that are typical of reliability problems. More efficient methods, such as directional simulation or simulation by importance sampling, are also difficult to implement. In the directional simulation method, the solution of the root r_i for each simulated direction requires repeated finite element solutions and the number of required computations rapidly grows with the number of random variables. In the importance sampling method, the main issue is in identifying a proper sampling density, which may not be easy if the design point(s) are not known from a previous FORM analysis. The response surface method is easy to implement, since it does not require the response gradients or the selection of a sampling density (Faravelli 1989). However, the challenge here is in selecting informative fitting points (which should be points near the design point) without knowing the actual shape of the limit-state surface. As mentioned earlier, this approach is also restrictive for large number of random variables, since the number of required fitting points (equal to the number of required finite element computations) rapidly grows with the number of random variables. Developments in this field are continuing and improved results and methods should be expected.

In the following subsection we present two examples employing finite element reliability analysis in conjunction with FORM and SORM. These examples are intended to demonstrate the kind of results one may obtain from such analysis. More details on the the data and methods of analysis used can be found in the cited references.

7.1 Example Applications

The first example concerns the first-excursion probability of the horizontal displacement at the top of a three-story, three-bay structure, which has uncertain properties and is subjected to the El Centro 1940 earthquake motion at its base. The girders and columns are modeled by beam elements with elasto-perfectly plastic moment-rotation relations at their ends with the yield moments described as random variables. The problem, hence, is a time-variant reliability problem with a limit-state function of the form

$$g(\mathbf{x}, t) = u_0 - u(\mathbf{x}, t) \tag{41}$$

where u_0 is the allowable displacement threshold, u is the displacement at the top, and the vector $\mathbf{x}$ represents the set of 21 random yield moments at all girder and column ends. As mentioned earlier, the limit-state surface for this type of a problem can be strongly nonlinear with possibly more than one significant design point (see Section 3.2). To solve problems of this type, an active-set gradient projection method has been developed, which is capable of sequentially finding the local design points in the order of their distance from the origin of the standard normal space (Zhang and Der Kiureghian 1992). Application of this algorithm in conjunction with the CALREL-FEAP finite-element reliability program yields two significant design points with first-order reliability indices $\beta_1 = 1.68$ and $\beta_2 = 1.78$. Each design point represents one failure mode of the structure relative to the specified threshold.

The configuration of the structure at each design point is shown in Fig. 5 together with the corresponding time history of the displacement at the top. Solid dots in this figure represent hinges that are in fully plastic state, and open dots represent hinges that have yielded in the past but at the time of failure are in elastic state due to load reversals. These two modes represent the two most likely configurations through which the displacement at the top may exceed the specified threshold. Linearizing the surface at these points and using a series-system reliability analysis for the union of the two failure modes, the generalized reliability index $\beta_g = 1.38$ is obtained, which gives $P_f = 0.083$.

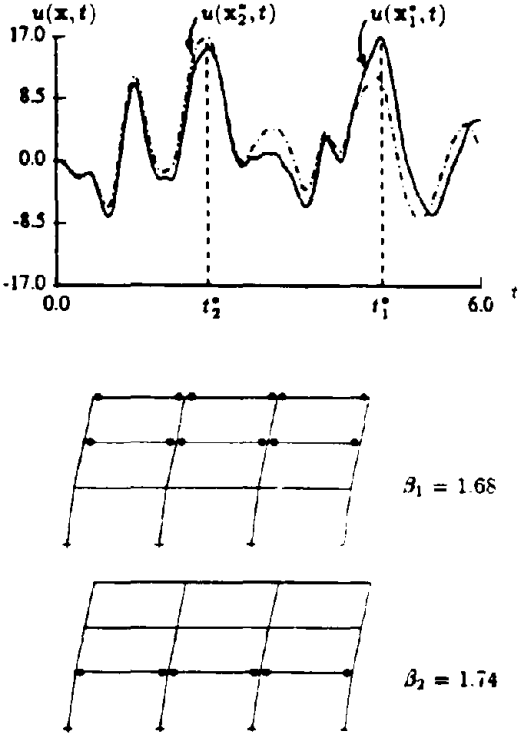

Figure 5. Design point configurations.

The second example, taken from Igusa and Der Kiureghian (1988), examines the influence of uncertainties in structural properties on the response of a tuned primary-secondary system subject to stochastic input. The system, shown in Fig. 6, consists of a 3-degree-of-freedom primary subsystem to which is attached an 8-degree-of-freedom light secondary subsystem. (The primary subsystem has rigid floors and all vertical displacements are ignored.) The mass, damping and stiffness properties of the system are modeled as random variables. The subsystems are designed such that, for the mean values of the properties, the first and third frequencies of the primary are closely tuned to the first and third-fourth frequencies of the secondary, respectively, and hence resonance and amplification of the secondary response are expected. Attention is focused on the base shear response of the primary and the peak bending moment response of the secondary to an earthquake input modeled as a white noise process. This defines a time-variant reliability problem with a limit-state function of the form

$$g(\mathbf{x}, y(t)) = s_o - s(\mathbf{x}, y(t)) \tag{42}$$

where $\mathbf{x}$ denotes the random system properties, $y(t)$ is the stochastic input, $s(\mathbf{x}, y(t))$ is the response of interest (primary base shear or secondary bending moment), and s_o is the appropriate threshold. For an "acceptable" probability of $P_f = 0.025$, Table 1 lists the normalized required design threshold for each subsystem. Each threshold is normalized with respect to the required threshold in a deterministic system having the mean properties. These results are computed by nested reliability analysis involving random vibrations (inner problem) and SORM (outer problem) analysis. It is evident that the uncertainty in the system properties has a negligible influence on the primary response (only 7% increase in the required design threshold), but a significant influence on the secondary response, i.e., an increase of 45% in the required design threshold. Further sensitivity analysis has shown that, whereas for the primary subsystem the uncertainty in damping is relatively more important, for the secondary subsystem the uncertainties in the mass and stiffness properties of both subsystems is much more important than the uncertainty in damping.

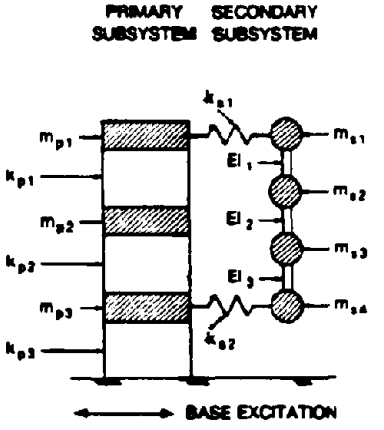

Figure 6. Example primary-secondary system.

Table 1. Normalized thresholds for $P_f = 0.025$

Primary subsystem	1.07
Secondary subsystem	1.45

The above two examples serve to demonstrate useful applications of reliability methods to problems of relevance to earthquake engineering. The domain of application of the methods reviewed in this paper, how-

ever, is much wider than presented by these examples. It is hoped that this paper will serve to stimulate a greater interest in probabilistic methods and their application for improved practice of earthquake engineering.

10 BIBLIOGRAPHY

Ang, A. H-S., and W-H. Tang (1975). *Probability concepts in engineering planning and design, vol. I - basic principles*. John Wiley & Sons, New York, N.Y.

Ang, A. H-S., and W-H. Tang (1984). *Probability concepts in engineering planning and design, vol. II - decision, risk and reliability*. John Wiley & Sons, New York, N.Y.

Bard, Y. (1974). *Nonlinear parameter estimation*. Academic Press, Orlando, Florida.

Belyaev (1968). On the number of exits across the boundary of a region by a vector stochastic process. *Theory of Probability Applications*, 13, 320-324.

Bjerager, P. (1988). Probability integration by directional simulation. *J. Eng. Mech.*, ASCE, 114(8), 1285-1302.

Bjerager, P., and S. Krenk (1989). Parametric sensitivity in first-order reliability theory. *J. Eng. Mech.*, ASCE, 115(7), 1577-1582.

Box, G. E. P., and Tiao, G. C. (1973). *Bayesian inference in statistical analysis*. Addison-Wesley, Reading, Mass.

Breitung, K. (1984). Asymptotic Approximations for multinormal integrals. *J. Eng. Mech.*, ASCE, 110(3), 357-366.

Breitung, K. (1991). Probability approximations by log likelihood maximization. *J. Eng. Mech.*, ASCE, 117(3), 457-477.

Bucher, C.G. (1988) Adaptive sampling -- an iterative fast Monte Carlo procedure. *Struc. Safety*, 5(2), 119-126.

Der Kiureghian, A. (1989). Measures of structural safety under imperfect states of knowledge. *J. Struct. Eng.*, ASCE, 115(5), 1119-1140.

Der Kiureghian, A. (1990). Bayesian analysis of model uncertainty in structural reliability. In *Reliability and Optimization of Structural Systems*, A. Der Kiureghian and P. Thoft-Christensen Eds., Lecture Notes in Engineering 61, Springer-Verlag, Germany, 211-222.

Der Kiureghian, A., and M. DeStefano (1991). Efficient algorithm for second-order reliability analysis. *J. Eng. Mechanics*, ASCE, 117(12), 2904-2923.

Der Kiureghian, A., C-C. Li and Y. Zhang (1991). Recent Developments in Stochastic Finite Elements. In *Reliability and Optimization of Structural Systems*, R. Rackwitz and P. Thoft-Christensen Eds., Lecture Notes in Engineering 76, Springer-Verlag, Germany, 19-38.

Der Kiureghian, A., H.-Z. Lin, and S.-J. Hwang (1987). Second-order reliability approximations. *J. Eng. Mech.*, ASCE, 113(8), 1208-1225.

Der Kiureghian, A., and P-L. Liu (1986). Structural reliability under incomplete probability information. *J. Eng. Mech.*, ASCE, 112(1), 85-104.

Ditlevsen, O. (1979). Narrow reliability bounds for structural systems. *J. Struct. Mech.*, 7(4), 453-472.

Ditlevsen, O. (1981). *Uncertainty modeling*. McGraw-Hill, New York, NY.

Ditlevsen, O. (1982). Model uncertainty in structural reliability. *Struc. Safety*, 1(1), 73-86.

Ditlevsen, O. (1983). Gaussian outcrossings from safe convex polyhedrons. *J. Eng. Mech.*, ASCE, 109(1), 127-148.

Ditlevsen, O. (1987). On the choice of expansion point in FORM or SORM. *Struc. Safety*, 4(3), 243-245.

Ditlevsen, O. (1988). Uncertainty and structural reliability. Hocus pocus or objective modeling. *Report No. 226*, Department of Civil Engineering, Technical University of Denmark, Lyngby 1988.

Ditlevsen, O., and P. Bjerager (1988). Plastic reliability analysis by directional simulation. *J. Eng. Mech.*, ASCE, 115(6), 1347-1362.

Faravelli, L. (1989). Response surface approach for reliability analysis. *J. Eng. Mech.*, ASCE, 115(12), 2763-2781.

Fiessler, B., H.J. Neumann and R. Rackwitz (1979). Quadratic limit states in structural reliability. *J. Eng. Mech.*, ASCE, 105(4), 661-676.

Geyskens, P., A. Der Kiureghian, and P. Monteiro (1991). Bayesian model assessment: methods and case studies. In *Reliability and Optimization of Structural Systems*, R. Rackwitz and P. Thoft-Christensen Eds., Lecture Notes in Engineering 76, Springer-Verlag, Germany, 229-238.

Geyskens, Ph., A. Der Kiureghian and G. De Roeck (1991). SORM analysis using quasi-Newton optimization. In *Computational Stochastic Mechanics*, P.D. Spanos and C.A. Brebbia Eds., Elsevier Science Publishers, Barking, Essex, UK, 89-100.

Gollwitzer, S., and R. Rackwitz (1988). An efficient numerical solution to the multinormal integral. *Probab. Eng. Mech.*, 3(2), 98-101.

Grigoriu, M. (ed.) (1984). *Risk, structural engineering and human error*. Univ. of Waterloo Press, Waterloo, Canada.

Hagen, O., and L. Tvedt (1991). Vector process outcrossing as parallel system sensitivity measure. *J. Eng. Mech.*, ASCE, 117(10), 2201-2220.

Harbitz, A. (1986). An efficient sampling method for probability of failure calculation. *Struc. Safety*, 3(2), 109-115.

Hohenbichler, M., S. Gollwitzer, W. Kruse and R. Rackwitz (1987). New light on first- and second-

order reliability methods. *Struc. Safety*, 4(4), 267-284.

Hohenbichler, M., and Rackwitz, R. (1981). Non-normal dependent vectors in structural safety. *J. Eng. Mech.*, ASCE, 107(6), 1227-1238.

Hohenbichler, M., and Rackwitz, R. (1983). First-order concepts in system reliability. *Struc. Safety*, 1(3), 177-188.

Hohenbichler, M., and Rackwitz, R. (1986a). Sensitivity and importance measures in structural reliability. *Civil Eng. Systems*, 3, 203-210.

Hohenbichler, M., and Rackwitz, R. (1986b). Asymptotic crossing rate of Gaussian vector processes into intersections of failure domains. *Probab. Eng. Mech.*, 1(3), 177-179.

Hohenbichler, M., and Rackwitz, R. (1988). Improvement of second-order reliability estimates by importance sampling. *J. Eng. Mech.*, ASCE, 114(12), 2195-2199.

Igusa, T., and A. Der Kiureghian (1988). Response of uncertain systems to stochastic excitation. *J. Eng. Mechanics*, ASCE, 114(5), 812-832.

Jiao, G., and T. Moan (1990). Methods of reliability model updating through additional events. *Struc. Safety*, 9(2), 139-153.

Karamchandani, A., P. Bjerager and C.A. Cornell (1988). Methods to estimate parametric sensitivity in structural reliability analysis. *Proc., 5th ASCE-EMD Specialty Conf.*, Blacksburg, VA, May, 86-89.

Li, C.-C., and A. Der Kiureghian (1992). An optimal discretization of random fields. *Report UCB/SEMM-92/04*, Department of Civil Engineering, University of California, Berkeley, CA., March.

Liao, S.S.C., D. Veneziano and R. Withman (1988). Regression models for evaluating liquefaction probability. *J. Geotech. Eng.*, ASCE 115(5), 1119-1140.

Lin, Y-K. (1967). *Probabilistic theory of structural dynamics*. McGraw-Hill, New York, NY.

Lin, H.-Z., and A. Der Kiureghian (1987). Second-order system reliability using directional simulation. *Proc. Fifth Int. Conf. Applic. Stat. Prob. in Soil and Struct. Eng.*, Vancouver, Canada, 2, 930-938.

Liu, P.-L., and A. Der Kiureghian (1990). Optimization algorithms for structural reliability. *Struct. Safety*, 9(3), 161-177.

Liu, P.-L., and A. Der Kiureghian (1991). Finite-element reliability of geometrically nonlinear uncertain structures. *J. Eng. Mech.*, ASCE, 117(8), 1806-1825.

Madsen, O. (1987). Model updating in reliability theory. *Proc. Fifth Int. Conf. Applic. Stat. Prob. in Soil and Struct. Eng.*, Vancouver, Canada, 1, 564-577.

Madsen, H.O. (1988a). Sensitivity factors for parallel systems. *Tech. Note 88-1*, Danish Engineering Academy, Lyngby, Denmark.

Madsen, H.O. (1988b). Omission sensitivity factors. *Struct. Safety*, 5(1) 35-45.

Madsen, H. O., S. Krenk and N. C. Lind (1986). *Methods of structural safety*. Prentice-Hall, Englewood Cliffs, NJ.

Madsen, H.O., and L. Tvedt (1990). Methods for time-dependent reliability and sensitivity analysis. *J. Eng. Mech.*, ASCE, 116(10), 2118-2135.

Maes, M.A., (1991). Codification of design load criteria subject to modeling uncertainty. *J. Struct. Eng.*, ASCE, 117(10), 2988-3007.

McKay, M.D., R.J. Beckman and W.J. Conover (1979). A comparison of three methods for selecting values of input variables in the analysis of output from a computer code. *Technometrics*, 21(2).

Melchers, R.E. (1987). *Structural reliability -- analysis and prediction*. Halsted Press, New York, NY.

Melchers, R.E. (1990). Radial importance sampling for structural reliability. *J. Eng. Mech.*, ASCE, 116(1), 189-203.

Nowak, A. S. (ed.) (1986). *Modeling human error*. ASCE, New York, NY.

Pearce, H.T., and Y-K. Wen (1985). On linearization points for nonlinear combination of stochastic load processes. *Struct. Safety*, 2(3), 169-176.

Ravindra, M. K. and Galambos, T. V. (1978). Load and resistance factor design for steel. *J. Struc. Eng. Div.*, ASCE, 104(9), 1337-1353.

Rice, O.C (1944). Mathematical analysis of random noise. *Bell System Tech. J.*, 23, 282-332 and 24, 46-156.

Rubenstein, R.Y. (1981). *Simulation and the Monte Carlo method*. J. Wiley, New York, NY.

Santos, J.L.T., (1991). Numerical techniques for design sensitivity analysis of structural systems. In *Reliability and Optimization of Structural Systems*, R. Rackwitz and P. Thoft-Christensen Eds., Lecture Notes in Engineering 76, Springer-Verlag, Germany, 83-98.

Schueller, G. I., Bucher, C. G., Bourgund, U., and W. Ouypornprasert (1987). On efficient computational schemes to calculate structural failure probabilities. In *Stochastic structural mechanics*, Y. K. Lin and G. I. Schueller, eds. Lecture notes in engineering, No. 31, Springer-Verlag, Germany, 388-410.

Schueller, G.I., and R. Stix (1987). A critical appraisal of methods to determine failure probabilities. *Struct. Safety*, 4(4), 293-309.

Seed, H.B., et al. (1985). Influence of SPT procedures in soil liquefaction resistance evaluations. *J. Geotech. Eng.*, ASCE 111(12), 1425-1445.

Shinozuka, M. (1964). Probability of failure under random loading. *J. Eng. Mech.*, ASCE, 90(5), 147-171.

Shinozuka, M. (1983). Basic analysis of structural safety. *J. Struc. Eng.*, ASCE, 109(3), 721-740.

Tvedt, L. (1990). Distribution of quadratic forms in normal space -- application to structural reliability. *J. Eng. Mech.*, ASCE, 116(6), 1183-1197.

Vanmarcke, E., M. Shinozuka, S. Nakagiri, G.I. Schueller, and M. Grigoriu (1986). Random fields and stochastic finite elements. *Struct. Safety*, 3(3+4), 143-166.

Veneziano, D., M. Grigoriu and C.A. Cornell (1977). Vector process models for system reliability. *J. Eng. Mech.*, ASCE, 103(3), 441-460.

Wen, Y.K., and H.C. Chen (1987). On fast integration for time variant structural reliability. *Probab. Eng. Mech.*, 2(3), 156-162.

Zhang, Y. and A. Der Kiureghian (1991). Dynamic response sensitivity of inelastic structures. *Report No. UCB/SEMM-91/06*, Department of Civil Engineering, University of California, Berkeley, CA.

Zhang, Y., and A. Der Kiureghian (1992). First-excursion probability of uncertain structures. *Proc. ASCE Specialty Conf. on Prob. Mechanics and Struct. and Geotech. Reliab.*, Denver, CO, July, 531-534.

The implementation of base isolation in the United States

James M. Kelly
Earthquake Engineering Research Center, University of California at Berkeley, USA

ABSTRACT: The concept of base isolation as an innovative means of providing earthquake resistance to structural systems was met initially with a great deal of skepticism by the engineering community. Today, however, it is on the cutting edge of seismic resistance engineering, as evidenced by the rapidly increasing number of buildings, both new construction and retrofit, using this earthquake resistant technique. It is now generally accepted that a base-isolated building will perform better than a conventional fixed-base building in moderate or strong earthquakes. In the structures in which it has been used so far, the major benefit has been to reduce the effects of seismic forces on contents and internal equipment, more than justifying the increased cost of isolated construction. This review will mainly cover the development and application of base isolation to buildings in the United States. The acceptance of this approach has been slow, but as a result of the 1989 Loma Prieta earthquake there is an increasing interest in its use for repair of buildings damaged in that earthquake and for the retrofit of historic buildings that are considered vulnerable to earthquake loading.

1 INTRODUCTION

The application of base isolation to address the problem of providing earthquake resistance to structural systems is a radical departure from the traditional approaches used by structural engineers. In conventional fixed-base design, efforts to strengthen the structural system to provide superior seismic performance lead to a stiffer structure, and thus will attract more force to the structure and its contents. A fixed-base building tends to amplify the ground motion. In order to minimize this amplification, the structural system must be either extremely rigid or provided with high levels of damping. At best, rigidity leads to the contents of the building experiencing the accelerations of the ground motion which may be too high for sensitive internal equipment and contents. The alternative of providing high levels of damping into the system generally leads to damage of the structural system or to structural forms.

Isolation allows the engineer to design a system that can function without damping, yet protects the building and its contents with relatively simple and low-cost structural systems. The concept has been long in gestation, but is now being used enthusiastically in many countries. At the present time, there are several types of isolation systems in use, many variants of existing systems are being developed, and new systems are being proposed and tried.

When I first presented a review of seismic isolation at the 2nd U.S. National Conference on Earthquake Engineering at Stanford University in 1979 (Kelly 1979), it was the only paper on base isolation in the entire conference. Although a few papers on base isolation had been submitted, the organizers felt that there was not enough interest in the subject to justify accepting more than one paper and these were compressed into one. At the 8WCEE in San Francisco in 1984, there was only one session devoted to base isolation; in 1988 at the 9WCEE there were four sessions, were dominated by Japanese researchers who were, by then, the leaders in this area; at the 10th WCEE in 1992, there were four sessions each day with the lecture hall overflowing with people.

To press the point even further, in 1985, I collected all the papers on isolation (in English) that I could find; this totaled about 180. By mid-1990, the updated version totaled 390 publications, by mid-1992 I would estimate that the total would be in the thousands. In this year, 1992, there are more symposia, workshops, and specialist meetings on base isolation in the United States alone than there were published papers in 1982.

Obviously, the wealth of publications on base isolation indicate that to date, research is being widely conducted on a large variety applications. However, are the results of this research being transferred into general engineering practice? Since the use of base isolation is a radical change in the way engineers think of providing earthquake protection, the implementation is most visible in its application to buildings. Most research is transferred into practice in an incremental way and may not be very visible. The straightforward manner in which the eccentrically-

seismic isolation system was completed in 1985 and was publicized in national engineering magazines and visited by a great many engineers and architects from the United States and around the world. However, it was several years before the second base-isolated building was begun. The acceptance of isolation as an anti-seismic design approach for some classes of buildings has clearly been slowed in the United States by lack of a code covering base-isolated structures.

The Structural Engineers Association of Northern California (SEAONC) created a working group in 1980 to develop design guidelines for isolated buildings. A brief document was produced and became the starting point for a sub-committee of the SEAONC Seismology Committee that was formed in early 1985. The Seismology Committee of the Structural Engineers Association of California (SEAOC) has been responsible for the development of provisions for the earthquake resistant design of structures, published as Recommended Lateral Design Requirements and Commentary, generally referred to as the "Blue Book" (SEAOC 1985). This has served as the basis for the various editions of the Uniform Building Code (UBC), published by the International Conference of Building Officials (ICBO), and which is the most widely used code for earthquake design. The SEAONC sub-committee produced a document entitled "Tentative Seismic Isolation Design Requirements" (SEAONC 1986) which was published by SEAONC in September 1986 as a supplement to the fourth edition of the Blue Book. The approach and layout of the 1986 document was chosen to parallel the Blue Book as far as possible. Emphasis was placed on equivalent lateral force procedures, and as in the Blue Book, the level of seismic input was that required for the design of fixed-base structures a level of ground motion that has a 10% change of being exceeded in a 50-year period. As in the Blue Book, dynamic methods of analysis are permitted, and for some types of structures required, but the simple statically equivalent formulas provide a minimum level for the design.

The Seismology Committee of the state-wide association (SEAOC) formed a subcommittee in 1988 to produce a isolation design document entitled "General Requirements for the Design and Construction of Seismic-Isolated Structures" (SEAOC 1989). This was published as an appendix to the fifth edition of the Blue Book in 1990 and later adopted by ICBO as an appendix to the seismic provisions in the 1991 version of the UBC (UBC 1991). The version of the code includes the static method of analysis and retains a minimum level of design based on a factor of the static analysis values, but increases the number of situations where dynamic analysis is mandatory.

A further code document has been developed for the design of base-isolated hospitals in California. The Building Safety Board (BSB) of the Office of State Architect has adopted guidelines entitled, "An Acceptable Method for Design and Review of Hospital Buildings Utilizing Base Isolation" (OSHPD 1989). These guidelines are similar to both the SEAONC requirements and the UBC code, having been developed in part by SEAONC for the BSB. The version adopted by the BSB in 1989 has subsequently been revised with some additional requirements being included in a version that was adopted in January 1992.

The UBC code differs from the SEAONC guidelines in that it explicitly requires that the design must be based on two levels of seismic input. A design basis earthquake is defined as the level of earthquake ground shaking which has a 10% probability of being exceeded in a 50-year period. For this level of input the design provisions require the structure above the isolation system to remain essentially elastic. The second level of input is defined as the maximum credible earthquake which is the maximum level of earthquake ground shaking that may be expected at the site within the known geological framework. This is taken as that earthquake ground motion that has a 10% probability of being exceeded in 250 years. The isolation system should be designed and tested for this level of seismic input and all building separations and utilities that cross the isolation interface should be designed to accommodate the forces and displacements for this level of seismic input.

Although the SEAONC and the UBC documents are very similar in many ways there is a fundamental difference between them. The first puts a premium on using static analysis and tends to force the designer toward regular superstructures with braced frames. The second on the other hand, makes dynamic analysis necessary in more situations and creates an incentive to use dynamic analysis even where it is not mandatory in order to permit reductions in the design shear for the superstructure. The SEAONC 1986 document used reduction factors (R_w) for the design of the superstructure that were one half of those used for the corresponding fixed-base structural system. The 1991 UBC document uses even more conservative reduction factors. For example, a fixed-base braced frame design would have a reduction factor of 8, whereas, if it were base isolated, it would would be allowed a reduction factor of 4 in the SEAONC code and only 2.3 in the UBC code.

These requirements for isolated buildings represent a radical departure from the code for fixed-base structures. The UBC seismic requirements for fixed-base buildings are intended to provide reasonable protection for life safety but not intended to limit damage or to maintain functionality of the structure. The fixed-base code allows the structure to be designed for forces that are very much less than those that would be developed if the structure were to remain elastic. It is implicitly assumed that inherent overstrength and ductility will prevent collapse in a large

earthquake and ensure life safety, but no check that this will be achieved is required. The requirements for isolated structures is such that the superstructure will be essentially elastic for the design basis earthquake and the isolation system will be tested and designed to be capable of sustaining the maximum credible earthquake. Since large inelastic deformations of the structure as permitted in the design of fixed-base structures can produce significant structural damage, and as a consequence, the possibility of loss of functionality, the more stringent requirements for isolated buildings will limit the level of damage that could occur and thus, these code requirements should lead to buildings which can survive severe earthquakes with little damage to structural elements, non-structural components, and with no loss of function.

In the UBC guidelines, a peer review of the design and construction of all base-isolated structures is mandatory under the code. This review is to be conducted by an independent engineering team experienced in seismic-analysis techniques and base-isolation practice whose responsibilities include reviewing both the site-specific seismic criteria and the preliminary design including design displacement and lateral forces, and overview and observation of the prototype testing and quality control program for the isolation system.

The major differences between the hospital guidelines and the UBC requirements are that no static analysis is permitted, dynamic analysis being essential. Also, site specific seismic input is required of two levels of ground motion corresponding to maximum probable and maximum credible earthquakes. Extensive testing requirements are specified and it is required that the isolation system should be monitored for the life of the building and a monitoring program must be submitted for approval with the design of the building.

3 ISOLATION SYSTEMS USED OR PROPOSED IN THE UNITED STATES

Most new or retrofit base isolation projects have made use of elastomeric isolation bearings and of these, most are in the form of lead plug bearings (LRB). The first type of bearing used for a building in the United States was the high-damping rubber bearing (HDR). Elastomeric systems are also widely used in other countries. In Japan, they are often used in conjunction with some type of steel dampers or other energy-dissipating devices. In New Zealand, there have been several buildings with LRB's and two buildings using a system based on sleeved piles (Boardman, Wood & Carr 1983) (McKay, Chapman & Kirkcaldie 1990). Aspects of elastomer technology pertinent to isolation systems have been reviewed by Taylor et al. (1992).

Sliding systems have been the subject of much recent research at NCEER, both for buildings and bridges. Additionally, the frictional characteristics of PTFE (Teflon) surfaces have been studied (Mokha, Constantinou & Reinhorn 1988) (Mokha, Constantinou & Reinhorn 1990) (Constantinou, Mokha & Reinhorn 1990). One of the systems being studied is the Frictional Pendulum System (FPS) (Zayas, Low & Mahin 1990). In this system the structure is supported on spherically shaped bearings with the load being applied through a small area covered by a high-strength composite material. The FPS has been used to retrofit an apartment building in San Francisco damaged by the Loma Prieta earthquake and will be used for the retrofit of a large U.S. Government building in San Francisco.

Many other new systems have been proposed. One example is the R-FBI (Mostaghel 1986) which uses many Teflon sliding surfaces. It has been tested on the shake table at EERC (Mostaghel, Kelly & Clark 1992). Systems that combine sliders and elastomeric bearings have been proposed and have been tested (Chalhoub & Kelly 1990) and at least one system has been used for retrofit of an historic building.

At the present time, the development of new isolation systems is extremely active and many new mechanisms are being explored. Table 1 lists only a few of the systems currently used or proposed in the United States.

Table 1. Isolation systems used/proposed in the United States

Elastomeric Systems
High-Damping Rubber Bearings (HDR), Non-Proprietary
Lead Rubber Bearings (LRB), DIS

Sliding Systems
Earthquake Barrier (EBS), M.S. Caspe
Friction-Pendulum System (FPS), EPS
Resilient Frictional Base Isolation (RFBI) N. Mostaghel

Hybrid Systems
Combined Rubber-Slider-Restrainer Systems, Fyfe Associates
Zoltan Isolator, Lorant Group
GERB Steel Springs, GERB, Gesellschaft fur Isolierung mbH & Co KG

Other Systems
Cable Suspension System, F. Garza-Tamez
Anti-Friction Isolation System, V. Shustov
Rocking Columns System, L. Li

4 BASE-ISOLATED BUILDINGS IN THE UNITED STATES

The first building in the United States to use base isolation was the Foothills Community Law and Justice Center which was begun in 1982 and completed in 1985. Further use of this approach was slow, with a few projects reaching the stage of feasibility assessment but not proceeding to construction. The next building projects using base isolation were not in California but in Salt Lake City, Utah. One was a new building for a computer manufacturing company and the purpose of the isolation system was to protect the computers and not the building. The other was the first use, in the United States and perhaps the world, of isolation as a seismic rehabilitation method for a historic building.

After this slow start, interest in the use of isolation has increased dramatically and at the present time, mid-1992, there are now many base isolation building projects in the United States either completed, under construction or in the design phase. Some of these projects are for new building, but a very large number are seismic retrofit projects. These have been stimulated by the damage to several historic buildings in San Francisco, Oakland, and the surrounding area from the 1989 Loma Prieta earthquake. It is interesting to note that the use of isolation for new buildings is, at the present time, mainly in southern California, whereas most isolation projects in northern California are for retrofits.

Tables 2, 3, and 4 list completed projects and projects that are reasonably likely to go forward to construction, both for new buildings and for retrofit. Further details on the type of isolator and the design philosophy of the completed buildings can be found in several papers and reports of which Tarics, Way and Kelly (1988), Reaveley, Mayes and Sveinsson (1988), Allen and Bailey (1988), Anderson (1989), Way and Howard (1990), Hart et al. (1991), and Asher et al. (1990) are a representative sample.

5 DEVELOPMENT OF ISOLATION SYSTEMS FOR NUCLEAR APPLICATIONS

Nuclear power plants are examples of buildings where the reduction of response of internal equipment is the primary goal. The analysis of equipment and piping systems for seismic loading is one of the most expensive parts of the design process and it is complicated by the fact that for fixed-base construction, different levels of a plant have different seismic response. Thus, it is generally necessary to use multiple support response spectrum analysis. The use of base isolation could reduce the amplification of acceleration at higher levels of a plant and would permit the use of simple design methods for equipment and piping, as well as eliminate the need for seismic restraints such as snubbers.

There are several large research programs directed toward the use of isolation for nuclear facilities. In the United States, a program funded by the Department of Energy and conducted by Argonne National Laboratory, was carried out over 1988-92. This program has covered shake table tests (Kelly 1991) and testing of a variety of potential elastomeric isolators under a wide range of loadings to determine dynamic characteristics, failure modes, fatigue resistance, and to establish failure modes. Isolators at a scale factor of two were tested under this program at EERC and full-size isolators in a large isolator test facility at the Energy Technology Engineering Center (ETEC) near Los Angeles, California. The results of these tests are detailed in Tajirian & Kelly (1988), and in conference proceedings (IAEA 1992). Under this DOE program, four different sets of isolators were obtained from four manufacturers.

The four test programs confirmed the high quality of high-damping elastomeric bearings. They were shown to be capable to extremely large shear strains before failure even under high levels of vertical pressure. It was shown that the failure mechanism is only slightly affected by pressure and that the stiffness is unaffected by pressure, while the damping is increased by pressure. The tests demonstrated that the entire search to find damping mechanisms to accompany isolation systems has been a misplaced effort. Much more important for the design of practical isolation systems is that fact that the elastomer hardens very strongly after a level of shear strain has been exceeded. If the isolators are much wider than their height, buckling is not a factor in their response and the stiffness increases by a factor of six beyond 250% shear strain. Thus, if 200% shear strain is taken as the nominal design level, at which level of base shear the superstructure is just at the yield point, then the base shear must increase by at least a factor of six before the isolation system fails. This means that the failure mechanism for the entire structure will be in the superstructure and not in the isolators. This means that conceptually , collapse of an isolated structure is no different from that of a conventional structure with, however, the proviso that the level of earthquake impact that produces the failure must be much greater for the isolated structure due to the large displacement capacity of the isolation system. The strong hardening response of the system beyond the design level means that if the system exceeds this level, the period shortens significantly and the system becomes non-resonant.

The results of these tests confirm that base-isolated nuclear facilities can be designed and built and that their performance in moderate and strong earthquakes will be superior to conventional design and that the isolation system will provide damage control to the structure and to internal equipments and contents. The performance in very strong earthquakes much beyond those assumed for design will also be superior to conventional structures, but will have the

same type of collapse mechanisms in the structure. These results should lead to increased confidence in the use of the technology for nuclear facilities and also for buildings housing sensitive internal equipment such as data centers, computer manufacturing facilities, telephone exchanges, and buildings that must be able to continue operation after strong earthquakes such as emergency control centers and hospitals.

5.1 General Electric Corp. PRISM Reactor

Interest in applying seismic isolation to nuclear plants has existed in the U.S. ever since its use by the French (Kunar & Maine 1979) (Vaidya & Eggenberger 1984). In recent years, the DOE has supported the development of two compact advanced LMR concepts, the Power Reactor Inherently Safe Module (PRISM) designed by General Electric Corp., and the Sodium Advanced Fast Reactor (SAFR) designed by Rockwell International Corp. Both concepts incorporate seismic isolation in the reference design to support plant standardization, enhance plant safety margins, permit siting in zones with higher seismicity, and thus reduce plant costs.

The selected isolation system for both concepts consists of steel-laminated elastomeric bearings. For PRISM, high-damping bearings are used to provide horizontal protection for the reactor module only, while for SAFR, the entire building is supported on bearings which provide both horizontal and vertical isolation (Tajirian, Kelly & Aiken 1990) (Aiken, Kelly & Tajirian 1989). The PRISM concept was selected by DOE for further development and has been reviewed and approved by NRC. PRISM employs a 155 MWe compact standardized LMR (Berglund, Tippets & Salerno 1988). in which the reactor module with its key safety functions of reactor shutdown, shutdown heat removal, and containment systems are isolated in the horizontal direction from potentially damaging ground motions. The reactor vessel has a diameter of 20 ft. and a height of 62 ft., and is supported from the top. The relatively small diameter of the vessel provides sufficient intrinsic resistance in the vertical direction to minimize amplifications in vertical ground motions making vertical isolation unnecessary. The entire isolated structure, which weighs approximately 5,000 tons, is supported on 20 large diameter steel-laminated elastomeric bearings, and is housed in an underground silo. The elastomeric compound used consisted of a highly filled natural rubber with high-damping (Derham, Kelly & Thomas 1985).

This particular system was selected for PRISM following a review of available hardware because it is a simple design and its dynamic response, especially at extreme loadings, is easier to characterize than some of the more nonlinear systems. Furthermore, it has sufficient inherent damping to eliminate the need for additional energy-absorbing devices which can complicate the design and the system response. Shake table tests and numerical analysis have shown that equipment response in isolated buildings is minimized when high-damping elastomeric bearings with no add-on damping elements are used, and that when frictional or elasto-plastic dampers are incorporated, they inevitably cause high-frequency response and increased accelerations in equipment (Kelly 1982) (Kelly & Tsai 1984) (Fujita et al. 1988) (Tajirian and Kelly 1987) (Skinner, Robinson & McVerry 1989) (Fan & Ahmadi 1992).

5.2 International Cooperation Programs

A cooperative program to develop design guidelines for nuclear plants using high-damping elastomeric isolators was begun in 1988 at the initiative of the Italian Agency for New Technologies, Energy and Ambient (ENEA) and General Electric Nuclear Energy and with the cooperation of ISMES in Italy and Bechtel National in the U.S. The resulting guidelines were outline at the IAEA Specialists Meeting on Seismic Isolation Technology in San Jose, California in 1992 (Martelli & Bettinali 1992).

The United Kingdom nuclear power industry has considered the application of seismic isolation to future LMR plants to potentially reduce costs, to increase margins of safety, and to facilitate standardization (Austin et al. 1989). The U.K. has been participating in a joint program with the Electric Power Research Institute (EPRI) and the Central Research Institute of Electric Power Industry (CRIEPI) of Japan to evaluate the technical feasibility of selected seismic isolation systems and their applicability in the design of large LMR plants (Gray, Rodwell & Hattori 1988) such as the European Fast Reactor (EFR). Available seismic isolation devices have been evaluated and candidate systems have been selected.

A joint U.S./Japanese program to study isolation systems for nuclear facilities has been conducted by ANL and Shimizu Corp. of Japan. As part of this program, two types of isolation systems based on high-damping rubber have been installed at the Shimizu demonstration isolation building at Tohoku University in Sendai, Japan. The first system installed at the demonstration building was closely based on the high-shape factor isolator designed for the PRISM reactor at a scale factor of approximately three. This system was monitored in the building from October 1989 to November 1990, when it was replaced by a system using a newly developed low-modulus high-damping rubber developed for application to nuclear facilities at soft-soil sites. This system is still in place at the present time. The results of the monitoring program for the two systems is given in Chang and Seidensticker (1991).

6 FUTURE DIRECTIONS IN BASE ISOLATION

It seems clear that the increasing acceptance of base isolation throughout the world will lead to many more applications of this technology. It is also clear that while elastomeric systems will continue to be used, there is a willingness to try other systems. The initial scepticism that was so prevalent when elastomeric systems were initially proposed is no longer evident, and the newer approaches which are currently being developed will benefit from this more receptive climate and lead to the development of systems based on different mechanisms and materials.

For all systems, the most important area of future research is that of the long-term stability of the mechanical characteristics of the isolator and its constituent materials. The long-term performance of isolators can best be developed from inspection and retesting of examples that have been in service for many years. Elastomeric systems in the form of non-seismic bridge bearings have been used for upwards of thirty years and a record of satisfactory performance has been established (Stevenson 1985).

Many of the completed base-isolated buildings have experienced earthquakes and so far their performance has been as predicted. The earthquakes, if close, have been small or have been moderate and distant so that the accelerations experienced have not been large. As more isolated buildings are built in earthquake-prone regions of the world, we can anticipate learning more about the behavior of such structures and it will be possible to reduce the degree of conservatism that is currently present in the design of these structures. It should be possible to bring about an alignment of the codes for fixed-base and isolated structures and have a common code based on the specified level of seismic hazard and structural performance and in this way allow the economic use of this new technology for those building types for which it is appropriate.

It is clear that the use of seismic isolation has finally achieved a level of acceptance that will ensure its continued use and its further development and that this new and radical approach to seismic design will be able to provide safer buildings at little additional cost as compared to conventional design. Additionally, base isolation will play a major role in the future in projects as diverse as advanced nuclear reactors and public housing in developing countries.

REFERENCES

Aiken, I.D., J.M. Kelly & F.F. Tajirian 1989. Mechanics of low shape factor elastomeric seismic isolation bearings. *Report No. UCB/EERC-89-13*, EERC, Univ. of Calif., Berkeley, CA.

Allen E.W. & J.S. Bailey 1988. Seismic rehabilitation of the Salt Lake City and County building using base isolation. *Proc. 9th WCEE*, p. 633-638, Tokyo-Kyoto.

Anderson, T.L. 1989. Seismic isolation for the Los Angeles County Fire Command and Control facility. *Proc. ASCE Structures Congress*, Seismic Engineering - Research and Practice, p. 615-624, San Francisco, CA.

Asher, J.W., D.R. Van Volkinburg, R.L. Mayes, T. Kelly, B.I. Sveinsson & S. Hussain 1990. Seismic isolation of the USC university hospital. *Proc. 4th U.S. Nat. Conf. on Earthq. Eng.*, 3:529-538, Palm Springs, CA.

Austin, N.M., S. Hattori, E. Rodwell & G.J. Womack 1989. UK contribution to CEGB-EPRI-CRIEPI programme on seismic isolation. *Proc. 1st Int. Sem. on Base Isolation of Nuclear Power Facilities*, San Francisco, CA.

Berglund, R.C., F.E. Tippets & L.N. Salerno 1988. PRISM, a safe, economic, and testable liquid metal fast breeder reactor plant. *ANS Topical Meeting on Safety of Next Generation Power Reactors*, Seattle, Wash.

Boardman, P.R., B.J. Wood & A.J. Carr 1983. Union house - a cross-braced structure with energy dissipators. *Bull. New Zealand Nat. Soc. Earthq. Engrg.* 16(2):83-97.

Buckle, I.G. & R.L. Mayes 1990. Seismic isolation: history, application, and performance - a world view. *Earthq. Spectra* 6(2):161-201.

Building Safety Board 1989. An acceptable method for design and review of hospital buildings utilizing base isolation. State of California, OSHPD

Chalhoub, M.S. & J.M. Kelly 1990. Sliders and tension controlled reinforced bearings combined for earthquake isolation. *J. Earthq. Engrg. Struc. Dynamics* 19(3):333-358.

Chang, Y.W. & R.W. Seidensticker 1991. Joint U.S./Japanese full-size building tests for base seismic isolation. ANL/Shimizu Corp., ANL-007.

Constantinou, M.C., A. Mokha & A.M. Reinhorn 1990. Teflon bearings in base isolation, II: modeling. *J. Struc. Engrg.* 116(2);455-474.

Derham, C.J., J.M. Kelly & A.G. Thomas 1985. Nonlinear natural rubber bearings for seismic isolation. *Nuclear Eng. Design* 84(3):417-428.

Dowrick. D.J., W.J. Cousins, W.H. Robinson & J. Babor 1992. Recent developments in seismic isolation in New Zealand. *Proc. 10th WCEE*, 4:2305-2310, Madrid.

Eisenberg J.M., A.M. Melentyev, V.I. Smirnov & A.N. Nemykin 1992. Applications of seismic isolation in the USSR. Proc. 10th WCEE, 4:2039-2046, Madrid.

Fan, F-G. & G. Ahmadi 1992. Seismic response of secondary systems in base-isolated structures. *Engrg. Structures*,, 14(1):35-48.

Fujita, S. et al. 1988. Earthquake isolation systems for buildings of industrial facilities using various types of dampers. *Proc. 9th WCEE* Tokyo-Kyoto.

Gray, S., E. Rodwell & S. Hattori 1988. EPRI/CRIEPI joint study program in support of the advancement of the liquid metal reactor (LMR). *Proc. 23rd Intersociety Energy Conversion Engrg. Conf.*, ASME, Vol. 1.

Giuliani, G.C. 1989. Design experience on seismically isolated buildings. *Proc. 1st Int. Post-SMiRT Conf. on Seismic Base Isolation of Nuclear Power Facilities*, San Francisco, CA.

Hart, G.C., D.J. Drag, W.E. Gates & R.L. Mayes 1991. Seismic strengthening of a tall concrete building incorporating base isolation. *Proc. Int. Meeting on Earthq. Protection of Buildings*, p. 57/c-76/c, Ancona, Italy.

International Conference of Building Officials (ICBO) 1991. Earthquake regulations for seismic-isolated structures. *Uniform Building Code*, Chapter 23.

Jolivet, J. & M.H. Richli 1977. Aseismic foundation system for nuclear power stations. *Proc. SMiRT-4*, Paper K.9/2, San Francisco, CA.

Kelly, J.M. 1979. Aseismic base isolation: a review. *Proc. 2nd U.S. Nat. Conf. of Earth. Engrg., EERI, Stanford University, Stanford, CA.*

Kelly, J.M. 1982. The influence of base isolation on the seismic response of light secondary equipment. *Proc. Int. Conf. Natural Rubber for Earthq. Protection of Bldgs. and Vibration Isolation*, Malaysia.

Kelly, J.M. 1986. Aseismic base isolation: review & bibliography. *Soil Dynamics and Earthq. Engrg.* 5(3):202-217.

Kelly, J.M. 1988. Base isolation in Japan, 1988. *Report No. UCB/EERC-88/20*, EERC, Univ. of Calif., Berkeley, CA.

Kelly J.M. 1991. A long-period isolation system using low-modulus high-damping isolators for nuclear facilities at soft-soil sites. *Report No. UCB/EERC-91/03*, EERC, Univ. of Calif., Berkeley, CA.

Kelly, J.M. & H.-C. Tsai 1984. Seismic response of light internal equipment in base-isolated structures. *Report No. UCB/EERC-84/17*, EERC, Univ. of Calif., Berkeley, CA.

Kunar, R.R. & T. Maine 1979. A review of seismic isolation for nuclear structures. Electric Power Research Institute, NP-1220-SR.

Lee, L. 1984. A base isolation measure for aseismic buildings in China. *Proc. 8WCEE, VI:791-798, San Francisco, CA.*

Martelli, A. & F. Bettinali 1992. Status report on activities on seismic isolation in Italy. *Proc. IAEA Specialist Meeting on Seismic Isolation Tech.*, San Jose, CA.

McKay, G.R., H.E. Chapman & D.K. Kirkcaldie 1990. Seismic isolation: New Zealand applications. *Earthq. Spectra* 6(2):203-222.

Mokha, A., M.C. Constantinou & A.M. Reinhorn 1988. Teflon bearings in aseismic base isolation: experimental studies and mathematical modeling. *Report No. NCEER 88-0038*, NCEER, Buffalo, N.Y.

Mokha, A., M.C. Constantinou & A.M. Reinhorn 1990. Teflon bearings in base isolation, I: testing. *J. Struc. Engrg.* 116(2):438-454.

Mostaghel, N. 1986. Resilient-friction base isolator (R-FBI). *Proc. ATC-17 Sem. Base Isolation and Passive Energy Dissipation*, p. 221-230, San Francisco, CA.

Mostaghel, N., J.M. Kelly & P.W. Clark 1992. Stability of R-FBI bearings: analysis and experiment. *Earthq. Spectra* 8(2)259-278.

Postollec, J-C. 1983. Les foundations antisismiques de la centrale nucleare de Cruas-Meysse. Notes du Service Etude Geni Civil d'EDF-REAM.

Proc. IAEA Specialist Meeting on Seismic Isolation Technology, 1992. San Jose, CA.

Reaveley, L.R., R.L. Mayes & B.I. Sveinsson 1988. Seismic isolation of a four-story flight simulator manufacturing facility. *Proc. 9th WCEE*, p. 79, Poster Session Paper P2A-10, Toyko-Kyoto.

Sarrazin, M. & M. Moroni 1992 Design of a base isolation confined masonry building. *Proc. 10th WCEE*, 4:2505-2508, Madrid.

Skinner, R.T., W.H. Robinson & G.H. McVerry 1989. Seismic isolation in New Zealand. *Proc. 1st Int. Sem. Seismic Base Isolation of Nuclear Power Facilities*, San Francisco, CA.

Stevenson, A. 1985. Longevity of Natural Rubber in Structural Bearings. *Plastics and Rubber Processing and Applications* 5:253.

Structural Engineers Association of California (SEAOC) 1985. Tentative lateral force requirements, Blue Book.

Structural Engineers Association of California (SEAOC) 1989. General requirements for the design and construction of seismic-isolated structures. Ad-Hoc Base Isolation Subcommittee of the Seismology Committee, Appendix to Chapter 1 of the SEAOC Blue Book.

Structural Engineers Association of Northern California (SEAONC) 1986. Tentative isolation design requirements, Yellow Book.

Taylor, A.W., A.N. Lin & J.W. Martin 1992. Performance of elastomers in isolation bearings: a literature review. *Earthq. Spectra* 8(2):279-304.

Tajirian, F.F. & J.M. Kelly 1987. Seismic and shock isolation system for modular power plants. *Proc. ASME Pressure Vessel and Piping Conf.*, ASME PVP-127.

Tajirian, F.F.& J.M. Kelly 1988. Testing of seismic Isolation bearings for advanced liquid metal reactor-prism. *2nd Symp. on Seismic, Shock and Vibration Isolation, ASME PVP-147*, ASME, Pittsburgh, Penn.

Tajirian, F.F., J.M. Kelly & I.D. Aiken 1990. Seismic isolation for advanced nuclear power stations. *Earthq. Spectra* 6(2):371-401.

Tarics, A.G., D. Way & J.M. Kelly 1984. The implementation of base isolation for the Foothill Communities Law and Justice Center. *Rept. No. RTA-84*, Reid and Tarics Assoc., San Francisco, CA.

Vaidya, N.R. & A.J. Eggenberger 1984. Feasibility evaluation of base isolation for aseismic design of structures. D'Appolonia Consulting Engineers, NSF Project No. 82-1384.

Vestroni, F., D. Capecchi, M. Meghella, G. Mazza & E. Pizzigalli 1992 Dynamic behavior of isolated buildings. *Proc. 10th WCEE*, 4:2473-2478, Madrid.

Way D. & J. Howard 1990. Seismic rehabilitation of the Mackay School of Mines, phase III, with base isolation. *Earthq. Spectra* 6(2):297-308.

Zayas, V.A., S.S. Low & S.A. Mahin 1990. A simple pendulum technique for achieving seismic isolation. *Earthq. Spectra* 6(2):317-334.

Zhou, F.L., J.M. Kelly, K.N.G. Fuller & T.C. Pan 1992. Optimal design of seismic isolation for multistoried buildings. *Proc. 10th WCEE*, 4:2449-2454, Madrid.

Table 2 Completed base isolation building projects in the United States - new construction

Fire Command and Control Facility

Location:	East Los Angeles, California
Status:	New
Owner:	County of Los Angeles
Size:	32,000 sq. ft.
Cost:	$6.3 million (excl. installed equipment)
Completed:	April 1990
Engineers:	Fluor-Daniel Engineers, Inc.
System:	HDR
Supplier:	Fyfe Assoc./Dynamic Rubber

Aircraft Simulator Manufacturing Facility

Location:	Salt Lake City, Utah
Status:	New
Owner:	Evans and Sutherland, Corp.
Size:	140,000 sq. ft.
Cost:	$8 million
Completed:	1988
Engineers:	Reavely Engineers and Assoc.; DIS
System:	LRB
Supplier:	DIS/Furon

University of Southern California Hospital

Location:	Los Angeles, California
Status:	New
Owner:	USC and National Medical Enterprises
Size:	250,000 sq. ft.
Cost:	$50 million
Completed:	1988
Engineers:	KPFF
System:	LRB
Supplier:	DIS/Furon

Foothills Communities Law and Justice Center

Location:	Rancho Cucamonga, California
Status:	New
Owner:	County of San Bernardino
Size:	230,000 sq. ft.
Total Cost:	$36 million
Completed:	1985
Engineers:	Taylor & Gaines; Reid & Tarics Assoc.
System:	HDR
Supplier:	Oil States Industries (now LTV)

Two Residences

Location:	West Los Angeles, California
Status:	New
Owner:	David Lowe
Size:	4,700 sq. ft. each
Cost:	$20,000 for each base
Completion:	1992
Engineers:	David Lowe
System:	GERB Resistant Base
Supplier:	GERB

Kaiser Computer Center

Location:	Corona, California
Status	New
Owner:	Kaiser Foundation Health Plan
Size:	120,000 sq. ft.
Cost:	$32 million
Completion:	Under construction 1992
Engineers:	Taylor & Gaines
System:	LRB & HDR
Supplier:	DIS/Furon

Titan Solid Rocket Motor Storage

Location:	Vandenburg Air Force Base, California
Status	New
Owner:	U.S. Air Force
Size:	N.A.
Cost:	N.A.
Completion:	1992
Engineers:	Bechtel Corp.
System.	HDR
Supplier:	LTV

San Bernardino Medical Center

Location:	Colton, California
Status	New
Owner:	County of San Bernardino
Size:	Five buildings, totaling 900,000 sq. ft.
Cost:	N.A.
Completion:	Design & review 1992
Engineers:	KPFF; Taylor & Gaines
System:	HDR
Supplier:	DIS

M.L. King Jr.-C.R. Drew Diagnostics Trauma Center

Location:	Watts, California
Status	New
Owner:	County of Los Angeles
Size:	140,000 sq. ft.
Cost:	$40 million
Completion:	Final design OSHPD review 1992
Engineers:	John Martin Assoc.; BIC
System:	HDR & Bronze Alloy Sliders
Supplier:	Not selected

Emergency Operations Center

Location:	East Los Angeles, California
Status	New
Owner:	County of Los Angeles
Size:	33,000 sq. ft.
Cost:	$6 million
Completion:	Construction starts 1992
Engineers:	DMJM
System:	HDR
Supplier:	Not selected

San Francisco Main Public Library

Location:	San Francisco, California
Status:	New
Owner:	City & County of San Francisco
Completed:	Design in progress 1992
Cost:	N.A.
Completion:	N.A.
Engineers:	Olmm Structural Design; Forell/Elsesser Eng.
System:	Not selected
Supplier:	N.A.

Water Control Center-Water Quality Laboratory

Location:	Portland, Oregon
Status:	New
Owner:	Portland Water Bureau
Size:	28,000 sq. ft.
Cost:	N.A.
Completion:	Design phase 1992
Engineers:	Harris Group; DIS
System:	LRB
Supplier:	DIS

Table 3 Completed base isolation building projects in the United States - retrofit

Salt Lake City and County Building

Location:	Salt Lake City, Utah
Status:	Retrofit
Owner:	Salt Lake City Corp.
Size:	170,000 sq. ft.
Cost:	$30 million (inc. non-seismic rehab.)
Completed:	1988
Engineers:	E.W. Allen and Assoc.; Forell/Elsesser Eng.
System:	LRB
Supplier:	DIS/LTV

Rockwell Seal Beach Facility

Location:	Seal Beach, California
Status:	Retrofit
Owner:	Rockwell International
Size:	300,000 sq. ft.
Cost:	$14 million
Completed:	1991
Engineers:	Englekirk & Hart
System:	LRB
Supplier:	DIS/Furon

Mackay School of Mines

Location:	Reno, Nevada
Status	Retrofit
Owner:	University of Nevada, Reno
Size:	27,000 sq. ft.
Cost:	$7 million
Completion:	Under construction 1992
Engineers:	Jack Howard and Assoc.; BIC
System:	HDR & PTEF sliders
Supplier:	Furon

Marina Apartments

Location:	San Francisco, California
Status	Retrofit
Owner:	Dr. Hawley
Size:	20,000 sq. ft.
Cost:	N.A.
Completion:	1991
Engineers:	EPS
System:	FPS
Supplier:	EPS

Table 4 Potential base isolation building projects in the United States - retrofit

Channing House Retirement Home

Location:	Palo Alto, California
Status	Retrofit
Owner:	Non-profit corporation
Size:	260,000 sq. ft.
Cost:	N.A.
Completion:	In design phase 1992
Engineers:	Renne & Peterson; DIS
System:	LRB
Supplier:	DIS

Long Beach Hospital

Location:	Long Beach, California
Status	Retrofit
Owner:	Veteran's Administration
Size:	350,000 sq. ft.
Cost:	N.A.
Completion:	Final Design 1992
Engineers:	A.C. Martin & Assoc.
System:	Not selected
Supplier:	N.A.

Hayward City Center

Location:	Hayward, California
Status	Retrofit
Owner:	City of Hayward
Size:	145,000 sq. ft.
Cost:	$7 million
Completion:	Final design 1992
Engineers:	EQE, San Francisco; C. Kircher Assoc.
System:	FPS & HDR
Supplier:	EPS & Bridgestone

U.S. Customs House

Location:	San Francisco, California
Status	Retrofit
Owner:	U.S. General Services Administration
Size:	142,000 sq. ft.
Cost:	$14 million (estimate)
Completion:	Conceptual design in progress
Engineers:	URS Blume
System:	Not selected
Supplier:	N.A.

Asian Art Museum

Location:	San Francisco, California
Status	Retrofit
Owner:	City and County of San Francisco
Size:	170,000 sq. ft.
Cost:	N.A.
Completion:	Conceptual design in progress
Engineers:	Rutherford & Chekene; C. Kircher Assoc.
System:	Not selected
Supplier:	N.A.

San Francisco City Hall

Location:	San Francisco, California
Status	Retrofit
Owner:	City and County of San Francisco
Size:	N.A.
Cost:	N.A.
Completion:	Conceptual design in progress
Engineers:	Forell/Elsesser Eng.
System:	Not selected
Supplier:	N.A.

50 United Nations Plaza

Location:	San Francisco, California
Status	Retrofit
Owner:	U.S. General Services Administration
Size:	345,000 sq. ft.
Cost:	N.A.
Completion:	Architect/Engineer selection 1992
Engineers:	N.A.
System:	N.A.
Supplier:	N.A.

Oakland City Hall

Location:	Oakland, California
Status	Retrofit
Owner:	City of Oakland
Size:	153,000 sq. ft.
Cost:	$47 million (estimate)
Completion:	Final design 1992
Engineers:	Forell/Elsesser Engineers; DIS
System:	LRB
Supplier:	DIS

State of California Justice Building

Location:	San Francisco, California
Status	Retrofit
Owner:	State of California
Size:	250,000 sq. ft.
Cost:	$40 million (est., incl. non-seismic renovation)
Completion:	Conceptual Design 1992
Engineers:	Rutherford & Chekene; C. Kircher Assoc.
System:	Not selected
Supplier:	N.A.

U.S. Court of Appeals

Location:	San Francisco, California
Status	Retrofit
Owner:	U.S. General Services Administration
Size:	350,000 sq. ft.
Cost:	N.A.
Completion:	Conceptual Design 1992
Engineers:	Skidmore, Owings & Merrill
System:	FPS
Supplier:	EPS

Kerckhoff Hall, UCLA

Location:	Los Angeles, California
Status	Retrofit
Owner:	Regents, Univ. of Calif.
Size:	100,000 sq. ft.
Cost:	$15.3 million
Completion:	December, 1994
Engineers:	Brandow & Johnston
System:	Not selected
Supplier:	N.A.

Educational Services Center

Location:	Los Angeles, California
Status	Retrofit
Owner:	L.A. Community College District
Size:	90,000 sq. ft.
Cost:	$450,000
Completion:	August 1992
Engineers:	Fleming Corp.
System:	Earthquake Barrier
Supplier:	N.A.

Seismic studies of the San Francisco-Oakland Bay bridge

A. Astaneh-Asl
University of California at Berkeley, USA

ABSTRACT: During the October 17, 1989 Loma Prieta earthquake, the San Francisco-Oakland Bay bridge sustained some damage and was closed for a month. Following the earthquake, a comprehensive research project has been underway at the University of California at Berkeley to study seismic behavior of the bridge and to formulate retrofit design recomendations. The study includes seismological, geotechnical and structural aspects. By developing realistic models of the bridge and subjecting the models to realistic ground motions, seismic deficiencies are being identified. This paper summarizes the progress of this study.

1 INTRODUCTION

The magnitude 7.1 Loma Prieta earthquake occurred on October 17, 1989 in Northern California causing damage throughout the greater San Francisco Bay area. The San Francisco- Oakland Bay bridge, shown in Figures 1 and 2 is located about 80 km north of the epicenter. The bridge sustained some seismic damage resulting in two 50-foot segments of the upper and lower decks of the bridge to drop off their support. The damage resulted in one fatality and 13 injuries and closure of the bridge for a month. Figure 3 shows summary of the damage which was mainly concentrated on the east side of the bridge.

Following the Loma Prieta earthquake, the Governor of California formed a board of inquiry to investigate the damage to the transportation facilities owned by the state. The Board in its report (Theal, 1990) among other items, recommended that comprehensive seismic studies of major bridges in California be undertaken. The research project that is summarized here (Astaneh et al, 1994) is an effort to conduct such an in-depth study of seismic behavior of the East Bay Crossing of the San Francisco- Oakland Bay Bridge.

2 THE SAN FRANCISCO OAKLAND BAY BRIDGE

The San Francisco-Oakland Bay Bridge is a 13.4 km long structure connecting cities of San Francisco and Oakland. The bridge was constructed during 1933-1937 period. Currently it carries about 250,000 commuters daily. The main structure of the steel bridge is shown in Figures 1 and 2. The West Bay Crossing of the bridge, Figure 1, consists of two suspension bridges placed in tandem. All piers as well as anchorages of the West Bay Crossing are supported on the bedrock. The East Bay Crossing, shown in Figure 2, consists of eighteen 88m span trusses, a 738m long cantilever truss and five 155m span trusses. There are eight expansion joints in the East Bay Crossing that divide the super-structure into ten segments. The expansion joints are at the location of Piers YB2, E4, E11 and E17 through E22. On the East Bay Crossing, Piers YB1, YB4, E1, and E2 are supported on the bedrock and all other piers are supported on the caissons or reinforced concrete hollow foundations and several hundred douglas fir timber piles. A typical structure of the concrete piers is shown in Figure 3 and some details of the typical cross section of the bridge is provided in Figure 4.

3 SUMMARY OF DAMAGE DUE TO 1989 LOMA-PRIETA EARTHQUAKE

Following the earthquake, the damage was documented and reported (Astaneh, 1989). Figure 5 shows a summary of the damage to the East Bay Crossing of the bridge. During the October 17, 1989 earthquake, fourteen trusses at the eastern end of the bridge had moved in the longitudinal direction of the bridge and caused structural damage and the collapse of two 17m long segments of the decks at the location of Pier E9. During the 1989 earthquake, the two 88m span trusses immediately to the east of Pier E9 appeared to have moved primarily in an east-west

direction relative to Pier E9. The main damage in this area was shear failure of forty 25mm diameter bolts connecting shoes of the trusses to the top of the steel towers. The maximum movement of shoes was estimated to have been more than 18 cm. After the quake, a residual movement of about 13 cm in longitudinal direction eastward and about 4.5 cm in transverse direction northward were measured. Due to this movement, the stringers supporting the 15m long segments of the upper and lower decks over Pier E9 came off their seat supports and collapsed.

Another area of damage was the segment of the bridge between Piers E11 and E17. The structure of the bridge between Pier E11 and E17 consists of six 88m span trusses supported on steel columns with the exception of Pier E17 which is a hollow reinforced concrete pedestal as shown in Figure 3. During the earthquake, apparently these six spans had moved together in the east-west direction about 13 cm. causing the concrete pedestals at Pier E17 to rock about their base. The rocking caused some damage to the concrete at the base of the pedestals.

The damage in the spans east of Pier E17 was failure of a number of 25mm diameter bolts connecting the truss shoes to the top of the piers. The shear failure of these bolts had resulted in release of the trusses allowing the trusses between Pier 17 and Pier 22 to move in the east-west direction along the length of the bridge.

4 SEISMIC STUDIES OF THE BAY BRIDGE

4.1 General

In the aftermath of the Loma Prieta earthquake, a research project was sponsored by the California Department of Transportation at the University of California at Berkeley to study seismic condition of the East Bay Crossing of the Bay Bridge and to develop recommendations for the retrofit. The main objective of the research project is to use the most advanced science and technology available, or to develop new scientific methods or technology if necessary, to evaluate the seismic behavior of the bridge during future maximum credible earthquakes that can occur at the nearby faults.

The methodology used in the project is shown in Figure 6 which can be summarized as follows. First, by studying the character of the nearby San Andreas and Hayward faults a series of ground motions are established at the likely hypocenters. Then by using information available on the seismological and geological characteristics of the ground, between the fault and the Bridge, bedrock acceleration time histories at a number of point beneath the bridge are established.

By using the bedrock motions and conducting dynamic analyses of the response of the soil to the bedrock motions, a series of free field ground motions are established at the site. Then by conducting soil-structure interaction studies, the free field motion is modified to include the effects of the presence of the piles, foundations and the structure. The last stage is to built a realistic computer model of the superstructure, subject the model to base excitations developed in previous stages and conduct a series of time history dynamic analyses. The process is iterated as many times as necessary until a refined and realistic model of the behavior of the bridge emerges.

Two of the challanging problems facing us at this time are slippage of soil and dynamic analyses of such a large and unprecedented model. There are three layers of soil under the bridge and these three layers can slip on each other during a moderate or strong earthquake. The slippage of the soil could be beneficial in acting as a large base isolator. However, it can also harm the piers. Although because of relatively soft soil surrounding the timber piles it is unlikely that in this case timber piles can actually shear off. The subject is currently under study by the research team.

The second issue that has developed into a very complex activity is the development of new technology for modeling and conducting three dimensional inelastic dynamic analysis of the bridge. The main part of the initial research plan was to conduct a series of realistic three- dimensional non-linear dynamic analysis. However, as the building of the structural model progressed, the structure turned out to be much more complex than a typical bridge. The complexities result from from the lack of a consistent load path for seismic forces, which require a very detailed model.

4.2 Various phases of research project

The research projects has several major inter-related areas of emphasis. These are seismological aspects, geotechnical aspects, strong motion instrumentation plans, three dimensional inelastic dynamic analysis, two-dimensional inelastic dynamic analysis, three-dimensional elastic finite element analysis of components, data base management, seismic behavior, performance and limit states of various components, evaluation of seismic deficiencies and finally development of retrofit design recommendations.

In the following, more information on the progress of the project to date are provided.

4.3 Seismological aspects

The research related to seismological studies is led by B. Bolt. Work to date has

indicated that for such a large, multi-supported, critical structure the seismological details of the expected ground motion are likely to be of great importance. There is an indication that the usual procedures of supplying one or two time histories and equivalent response spectra based on realistic maximum earthquake scenarios must be modified and extended.

The procedures to estimate the ground motions have developed in two different ways, mainly empirically with inclusion of incoherence along the bridge spans, and using numerical source and wave propagation models. The latter are necessary to allow matching realistic inputs into models developed for dynamic analyses of soil. The synthetic strong ground motions must be folded into the results of the soil-structure interaction computations and the dynamic analysis. This process must be thoroughly interactive and iterations made as necessary for the various critical ground motion parameters.

4.4. Strong motion instrumentation plans

The research related to instrumentation of the Bay Bridge is led by A. Astaneh. The instrumentation includes a dense array for the bridge and a network of instrumentation for the greater Bay Area. Figure 7 shows the proposed "Strong Motion Array for the Bay Bridge" (BBSMA) along with a sample of strong motion instrumentation for a segment of the Bay Bridge.

4.5 Geotechnical issues

This effort is led by J. Lysmer. The geotechnical studies have indicated that should a strong, but plausible, earthquake occur on the Hayward or the San Andreas fault, a horizontal failure plane may develop over most of the East Bay Crossing site at a depth of about 20m below the mud-line. This plane passes through the pile groups on which the majority of the piers of the bridge are founded. Currently no method exists for analyzing this problem. A major effort has been embarked upon to develop new methods which can (1) determine whether or not the pile groups can survive or prevent the postulated failure and, (2) produce pier motions and other parameters needed for a seismic analysis of the bridge for extreme seismic events.

Since the foundations of eastern part of the bridge are also deficient, currently several retrofit concepts are being investigated to retrofit the foundations and to protect timber piles. The challenging issue is to devise a retrofit system that will be activated during a major earthquake but will not change structural character of the initial design of the bridge.

4.6. Dynamic analysis

The main activity regarding dynamic analysis of the Bridge is to develop a realistic three dimensional, inelastic model of the entire structure and subject the model to realistic ground motions. The effort is led by G. Powell. The Bay Bridge has a very complex structural system.

In order to conduct dynamic analysis of models of this size, condensation techniques should be used aggressively to reduce the number of degrees of freedom to a few thousand. This has required the research team to develop new computational techniques and computer programs.

In addition to above-mentioned 3-D inelastic analyses, a series of 2-D inelastic and 3-D elastic analyses of the system are also being considered. This effort led by A. Astaneh is intended to establish global and local behavior by using more common structural analysis software.

4.7. Data base management

This effort is led by G. Fenves. The large number of nonlinear earthquake analyses of the Bay Bridge models generate an enormous amount of response data. A computer database was designed and implemented specifically for providing an engineering evaluation of the earthquake response of the bridge. The database includes all the information about the models (elements, nodes, etc.), static loads, ground motion analysis runs, nodal response, and components and the limit states that are to be evaluated with the capacities and the demands computed from the analyses.

4.8 Seismic condition assessment

This effort is led by A. Astaneh.

In order to ecvaluate seismic condition of the Bay Bridge, the following equation is applied to each limit state of components as well as systems of the Bay Bridge.

$$\text{Demand/Supply} \leq I \qquad (1)$$

The demand term in the equation results from dynamic analyses. The supply term is established for each limit state by studying seismic behavior of the corresponding component and or by conducting actual tests.

The term I in the above equation is an "Importance Factor" and is introduced to represent the importance of each limit state and consequences of reaching that limit state. In current design codes, for seismic design new structures, all limt states, related to member performance , are assigned the same importance. Even though a margin of safety is built into all codes, this margin of safety is due to uncertainties in load, material properties, geometry,

workmanship, modeling and computational techniques. However, in evaluating seismic performance of an existing structure, the author believes an importance factor should be assigned to each limit state based on the past performance of the component and the consequences of the occurrence of the limit state.

This philosophy of assigning Importance Factor to limit states is being implemented in seismic evaluation of the Bay Bridge. The value of "I" in equation (1) can be less than 1.0 for secondary members of the bridge, while for important members such as truss chords "I" can be as high as 1.25.

5. BEHAVIOR OF COMPONENTS

Unfortunately, the information on seismic behavior of components of steel bridges is very limited and almost non-existent. A major effort is underway to establish actual cyclic behavior of components of the Bay Bridge by conducting tests on various components and analyzing the available test data. As an example, behavior of one of the most important connections of the Bay Bridge is summarized in the following.

As shown in Figure 4, the concrete deck of the Bridge is supported on longitudinal stringers which in turn are supported by double angle connections to the web of floor plate girders. Investigation of behavior of deck system indicated that the double angle connections can experience considerable yielding due to axial push-pull when bridge moves in longitudinal direction. To study cyclic behavior of these connections comprehensive experimental and analytical studies are underway. A total of 14 test of full scale connections have been tested under simulated cyclic loading.

Figure 8 shows a typical connection and its response to the cyclic axial load. When connections were pulled, they behaved in a very flexible manner due to bending flexibility of outstanding legs of angles. When angles were pushed against the support, they exhibited very large stiffness due to the axial stiffness of the outstanding legs bearing against the support. After sufficient number of inelastic push-pull cycles, during which the shear was maintained at a constant level, the strength of outstanding legs had deteriorated so much that the connections failed due to gravity shear. This finding has extremely important design and retrofit implications. It means that connections that are designed to carry gravity shear, usually with a factor of safety of about 2.0, during severe and long duration earthquakes, can deteriorate sufficiently such that either during the quake or afterward, the connection fails under service load alone.

In addition, due to considerable cyclic inelasticity of these connections, it is necessary to model these connections as non-linear elements in the computer model and conduct the dynamic analysis of the system.

6 CONCLUSIONS

Since studies on seismic condition assessment of the Bay Bridge (6) are still ongoing, the final conclusions are not formulated yet. However, the findings of the research reported here can be summarized as:

1. Due to the very critical role of this bridge in transportation network in Northern California, the seismic performance criterion for the Bay Bridge is set at a very stringent level. The performance criteria implemented currently is that these structure should be able to survive the maximum credible earthquakes without any structural damage that will impair its full function.
2. The studies conducted so far indicate that the foundations of the eastern part of the bridge may require extensive retrofit.
3. The super-structure appears to be in better condition than the sub-structure. However, retrofit systems will be also required for the steel super-structures.
4. The main philosophy in retrofit of the Bay Bridge is try to avoid strengthening and stiffening if possible. Instead, the efforts are directed to redistribution of stiffnesses, implementing energy dissipating devices as well as additional dampers. These retrofit strategies can result in global reduction of the forces in the system which means reduction of "demand" term in Equation (1).
4. Extensive program of instrumentation is being developed.
5. The findings of this study should be considered tentative at this time.

7 ACKNOWLEDGMENTS

The damage information on the Bay Bridge summarized in the paper was primarily collected by an investigative team of the University of California headed by the author as well as by the Caltrans engineers. The study summarized here is part of a research project entitled: "Seismic Condition Assessment of the Bay Bridge", sponsored by the California Deaprtment of Transportation for which A. Astaneh is the Principal Investigator and the co-Principal Investigators are Professors B. Bolt, G. Fenves, F. Filippou, J. Lysmer, P. Monteiro and G. powell, all faculty of civil engineering at the University of California at Berkeley who also contributed to this paper. The Caltrans engineers for the project are J. Gates, L. Sheng and S. Larson. Their support is sincerely appreciated.

8 REFERENCES

Annual Report, San Francisco Oakland Bay Bridge", 6 Reports Published by Governor's Office from 1934 to 1938 and other

Caltrans documents on the Bay Bridge.

Astaneh, A. "Damage to the San Francisco Oakland Bay Bridge During October 17 1989 Earthquake", Report UCB/EERC- 89/04, Univ. of Calif. at Berkeley.

Astaneh, A., V. Bertero, B. Bolt, S. Mahin, J.P. Moehle and R. Seed 1989. "Preliminary report on the seismological and engineering aspects of the October 17, 1989 Santa Cruz (Loma Prieta) earthquake", Report UCB/EERC-89/14, EERC, Univ. of Cali.

6. Astaneh, A., Bolt, B., Fenves, G., Filippou, F., Lysmer, J., Monteiro, P. and Powell, G., "Seismic Condition Assessment of the Bay Bridge", Research Project in Progress, 90-93, University of California at Berkeley.

7. "Competing Against Time, Report to Governor George Deukmejian from The Governor's Board of Inquiry on the 1989 Loma Prieta Earthquake, Sacramento, May 1990.

8. Technical Documents and Drawings from CalTrans Files.

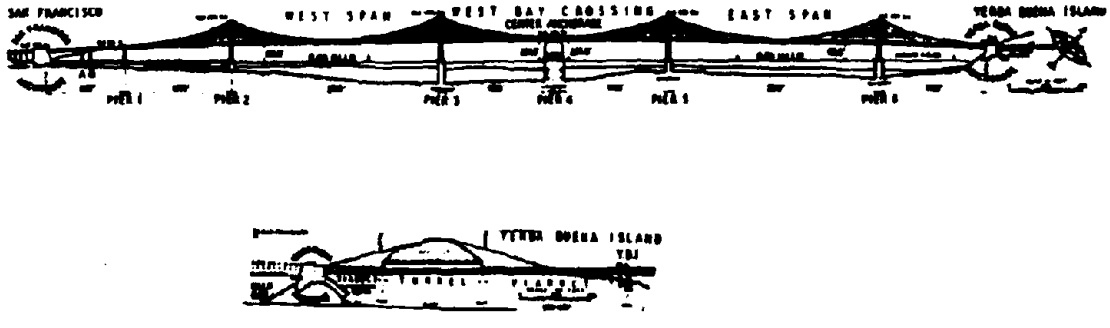

Figure 1. West Bay crossing of the San Francisco-Oakland Bay Bridge

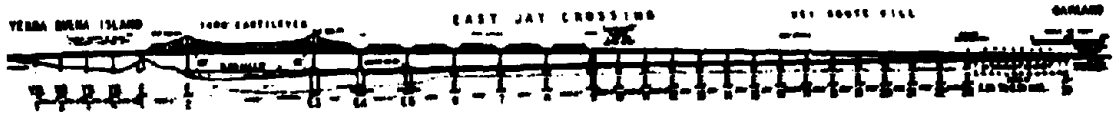

Figure 2. East Bay crossing of the San Francisco-Oakland Bay Bridge

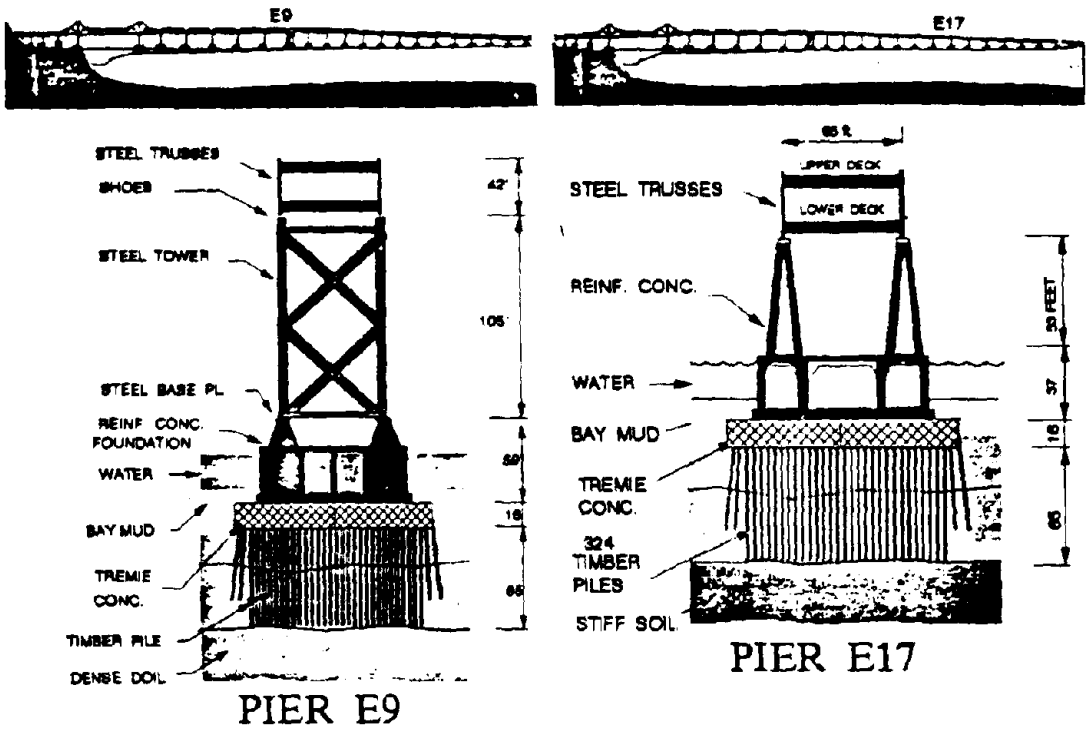

Figure 3. Typical Structures of the East Bay crossing

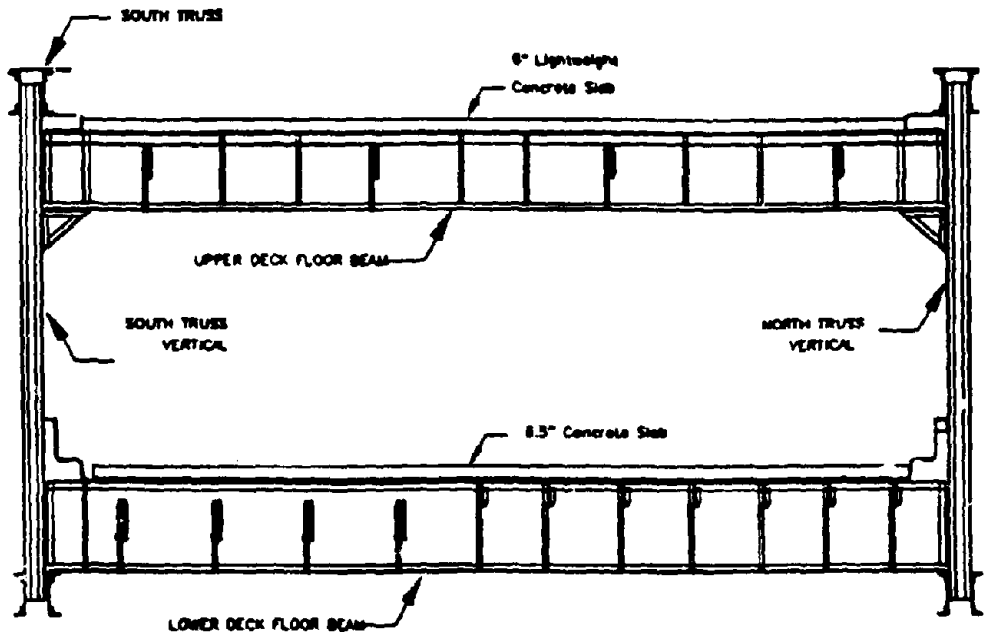

Figure 4. Typical cross section of the bridge

SEISMIC CONDITION ASSESSMENT OF THE BAY BRIDGE

BEHAVIOR DURING LOMA PRIETA EARTHQUAKE

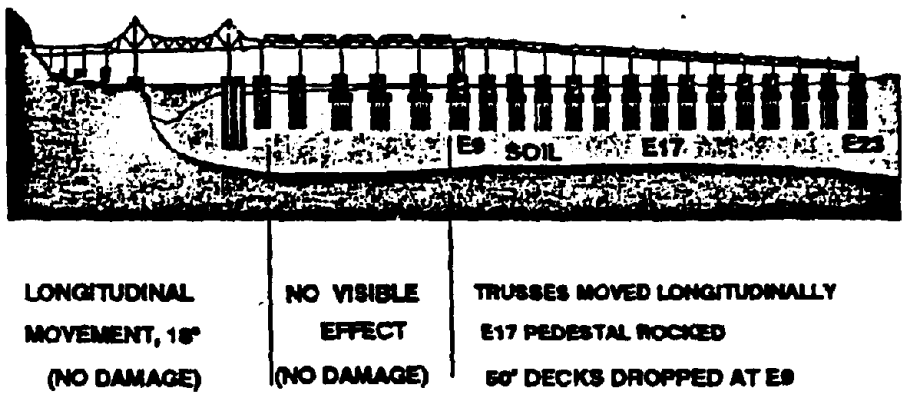

Figure 5. Summary of the damage

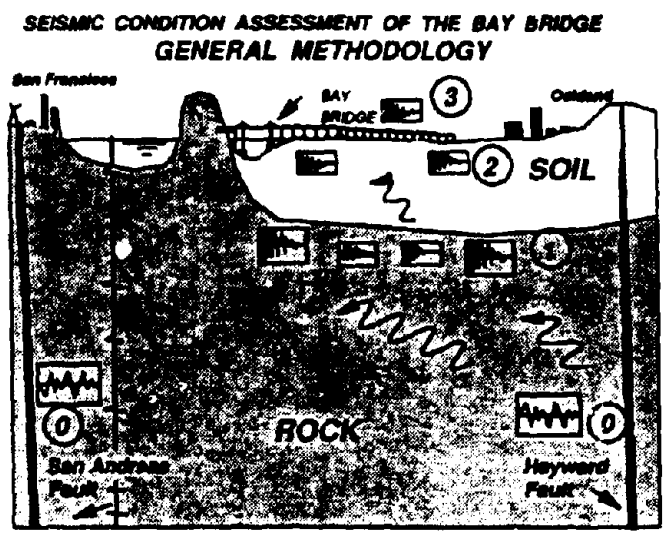

Figure 6. Research methodology

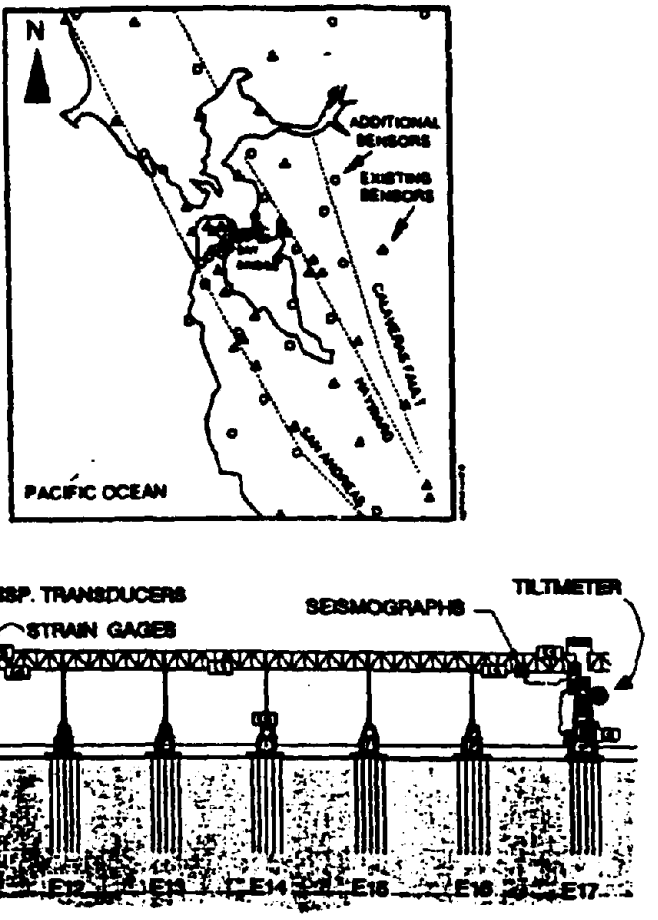

Figure 7. Proposed strong motion array for the Bay Bridge

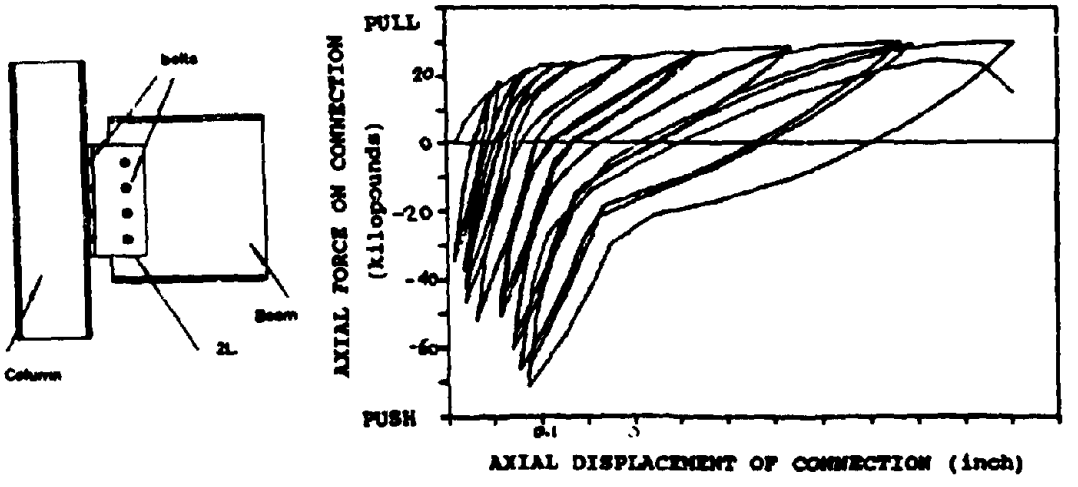

Figure 8. Behavior of angle connections subjected to cyclic axial load

Earthquake Analysis, Design, and Safety Evaluation of Concrete Arch Dams

Anil K. Chopra
University of California at Berkeley, U.S.A.

ABSTRACT: Summarized is the current state of knowledge about earthquake response analysis of concrete arch dams, and the application of this information to the earthquake-resistant design of new dams and to the seismic safety evaluation of existing dams. The limitations of the traditional design procedures are identified, the factors that should be considered in dynamic analysis are discussed, and procedures for earthquake response history analysis are summarized. The application of these linear analysis procedures to seismic design and safety evaluation of dams is discussed, followed by a brief mention of the limitations of the presently available nonlinear analysis procedures.

1 INTRODUCTION

The consequences of a large dam failing can be disastrous, so the seismic design of dams is an important part of earthquake engineering. Although no concrete dams have failed because of earthquakes, it is important to recognize that these structures have not been seriously tested--in the sense that very rarely has a large earthquake occurred close to a major concrete dam with a full reservoir. However, M6.5 earthquakes did occur close to Koyna Dam--a large concrete gravity dam--in India in 1967 and Hsinfengkiang Dam--a strengthened concrete buttress dam--in the People's Republic of China in 1962. A M7.6 earthquake occurred in 1990 near Sefidrud Dam--a large concrete buttrees--in Iran (Ahmadi and Khoshrang, 1992). All three dams were overstressed by the earthquake motions and were damaged to an alarming degree. Pacoima Dam, a concrete arch structure, sustained damage to one abutment during the 1971 San Fernando earthquake; its reservoir was only partly full at the time. The experience with the earthquake performance of these dams indicates that concrete dams are not immune to earthquake damage as had commonly been presumed. Thus, it is essential that increasing attention be given to the earthquake safety of these structures.

The ability to evaluate the effects of earthquake ground motion on concrete dams is essential to assess the safety of existing dams, to determine the adequacy of modifications planned to improve old dams, and to evaluate proposed designs for new dams to be constructed. The prediction of the performance of concrete dams during earthquakes is one of the more complex and challenging problems in structural dynamics. The following factors contribute to this complexity:

- Dams and reservoirs are of complicated shapes, as dictated by the natural topography of the site.
- The response of dams may be influenced significantly by variations in the intensity and characteristics of the ground motion over the width and height of the canyon. However, for lack of appropriate instrumental records, the spatial variations of the ground motion cannot be defined with confidence at this time.
- The response of a dam is influenced, generally to a significant degree, by the earthquake-induced motion of the impounded water; by the deformability of the foundation rock; and by the interaction of the motions of the water, foundation rock, and the dam itself.
- During intense earthquake motions, vertical construction joints may slip or open; concrete may crack; and the stored water may locally separate from the upstream face of the dam, resulting in cavitation. These phenomena are nonlinear and extremely difficult to model and account for reliably.

Realistic analyses of the seismic response of dams were not possible until the development of the finite element method, recent advances in dynamic analysis procedures, and the availability of large-capacity, high-speed computers. Thus, much of the research did not start until the mid-1960's. Initially,

all nonlinear effects, including those associated with construction-joint opening, concrete cracking and water cavitation, were ignored, and the interaction effects of the impounded water and foundation rock were either neglected or grossly simplified. Subsequently, special techniques were developed for incorporating the interaction effects in linear analyses.

The objective of this paper is to summarize the current state of knowledge about linear earthquake response analysis of concrete arch dams and how this information can be applied to the earthquake-resistant design of new dams and to the seismic safety evaluation of existing dams.

The problem of earthquake response analysis of concrete dams has been the subject of numerous research investigations in the past twenty-five years. However, no attempt is made to establish the interrelationship of the material presented in this paper to the work of other researchers. This paper is based almost exclusively on the results of studies carried out at the University of California at Berkeley during the past ten years.

2 EVALUATION OF TRADITIONAL ANALYSIS AND DESIGN PROCEDURES

2.1 Traditional analysis and design procedures

Traditionally, the dynamic response of the system has not been considered in defining the earthquake forces in the design of arch dams. For example, in a 1965 publication of the U.S. Bureau of Reclamation, it is stated:

"The occurrence of vibratory response of the earthquake, dam and water is not considered, since it is believed to be a remote possibility."

Thus, the forces associated with the inertia of the dam were expressed as the product of a seismic coefficient--which is constant over the surface of the dam with a typical value of 0.10--and the weight of the dam. Water pressures, in addition to the hydrodynamic pressure, are specified in terms of the seismic coefficient and a pressure coefficient which is based on assumptions of rigid dam, incompressible water, and a straight dam. Finally, the effects of foundation rock flexibility are not considered in computing the aforementioned earthquake forces.

The traditional design criteria require that the compressive stress should not exceed one-fourth of the compressive strength or 1000 psi, and the tensile stress should remain below 150 psi.

2.2 Limitations of traditional procedures

The seismic coefficient of 0.1 is much smaller than the ordinates of the acceleration response spectra for intense earthquakes (Figure 1). Thus, the

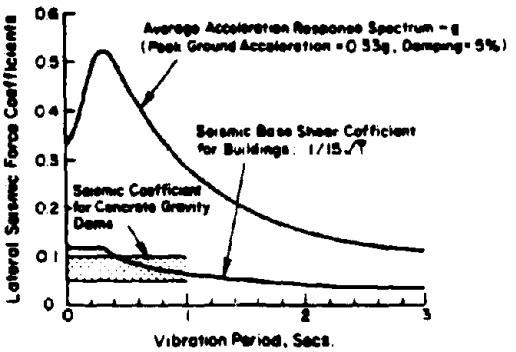

Figure 1. Comparison of earthquake response spectrum and design coefficients.

earthquake forces for arch dams are grossly underestimated in the traditional analysis procedures. It is of interest to note in Figure 1 that the seismic base shear coefficient values for dams are similar to those specified for buildings. However, building code design provisions (International Conference of Building Officials 1988) are based on the premise that buildings should be able to:

"1. Resist minor earthquakes without damage; 2. Resist moderate earthquakes without structural damage, but with some nonstructural damage; 3. Resist major earthquakes . . . without collapse but with some structural . . . damage."

Whereas these may be appropriate design objectives for buildings, major dams should be designed more conservatively and this is reflected in the aforementioned design criteria used in traditional methods for design of dams. What these traditional methods fail to recognize, however, is that in order to achieve these criteria, dams should be designed for the larger seismic coefficients corresponding to pseudoacceleration response spectra for elastic structures (Figure 1).

The effective earthquake forces on a dam due to horizontal ground motion may be expressed as the product of a seismic coefficient, which varies over the dam surface, and the weight of the dam per unit surface area. The seismic coefficient associated with earthquake forces in the first two modes of vibration of the dam (fundamental symmetric and antisymmetric modes of a symmetric dam) varies as shown in Figure 2. In contrast, traditional design procedures ignore the vibration properties of the dam and adopt a uniform distribution for the seismic coefficient, resulting in erroneous distribution of lateral forces and hence of stresses in the dam.

The traditional design loadings for concrete dams include water pressures in addition to the hydrostatic

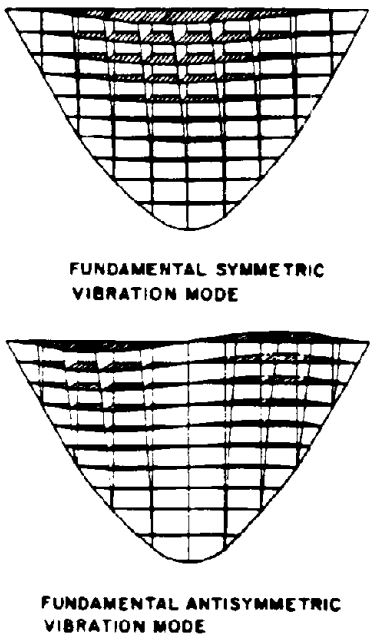

Figure 2. Distribution of seismic coefficients over the dam surface in the first two vibration modes of an arch dam (U.S. Bureau of Reclamation 1977).

pressures. A number of formulas, differing somewhat in detail and numerical values but not in the underlying assumptions, are in use (U.S. Army Corps of Engineers 1958 and U.S. Bureau of Reclamation 1966). One of these specifies the additional water pressure $p_e = C_p C_s wH$, where C_p is a pressure coefficient which varies from zero at the water surface to about 0.7 at the reservoir bottom, C_s is the seismic coefficient, w is the unit weight of water, and H is the total depth of water. For a seismic coefficient of 0.1, the additional water pressure at the base of the dam is 7 percent of the hydrostatic pressure; pressure values at higher elevations are similarly small. These small additional water pressures have little influence on the computed stresses and hence on the geometry of the dam section that satisfies the standard design criteria. However, it will be shown later that hydrodynamic effects are generally important in the response of arch dams.

Recognizing the aforementioned limitations of traditional analysis procedures, dam designers started using dynamic analysis procedures. For example, a dynamic finite-element analysis procedure, including an added mass representation of hydrodynamic effects, is described in Section 4-56 of a 1977 USBR publication. While this procedure overcomes many of the deficiencies of the traditional procedure, it does not properly consider the hydrodynamic effects or dam-foundation rock interaction effects. In particular, the added mass is computed from the analysis of hydrodynamic pressures due to upstream-downstream vibration of a straight rigid dam, neglecting water compressibility (Westergaard, 1933). The resulting added mass is taken to be valid for both "symmetric" and "antisymmetric" vibration modes of the dam, which is obviously inappropriate. It will also be shown in the next section that water compressibility effects are generally significant. Furthermore, in particular, the foundation rock is invariably idealized as massless, an assumption that ignores the important effects of foundation material and radiation damping mechanism in dam-foundation rock interaction.

3 FACTORS TO BE CONSIDERED IN DYNAMIC ANALSIS

The dynamic analysis of arch dams is especially complicated because they must be treated as three-dimensional systems. Utilizing recently developed dynamic analysis procedures, it is demonstrated that, in analyzing the earthquake response of concrete arch dams, the following factors should be considered: dam-water interaction, reservoir boundary absorption, water compressibility, and dam-foundation rock interaction. In addition, spatial variations in ground motion are expected to affect the dam response, but this factor has so far not been satisfactorily incorporated into the analysis.

3.1 Dam-water interaction

When dam-water interaction and water compressibility effects are properly considered in the analysis, the hydrodynamic effects are generally important in the response of arch dams, more so than for gravity dams. This is apparent from Figure 3 wherein the envelope values of the stresses on the upstream face

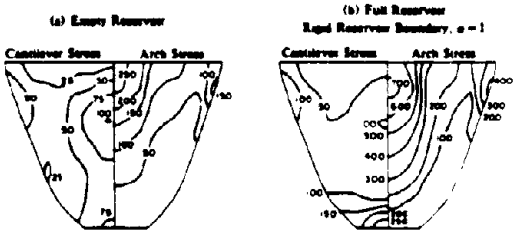

Figure 3. Hydrodynamic effects in response of Morrow Point Dam (Fok and Chopra 1986b).

of Morrow Point Dam due to the upstream component of Taf: ground motion are presented for two conditions; hydrodynamic effects were included in one and neglected in the other. It is apparent that the tensile stresses in the dam due to upstream ground motion are more than doubled when hydrodynamic effects are included; even larger increases occur in the stresses caused by the other two components of ground motion. Therefore, it is obvious that the hydrodynamic effects are grossly underestimated in the traditional design loadings.

3.2 Reservoir boundary absorption

Commonly used finite-element analysis techniques do not recognize the partial absorption of hydrodynamic pressure waves by the sediments invariably deposited at the reservoir bottom and sides, or even by the rock underlying the reservoir. These effects are demonstrated in Figure 4 where

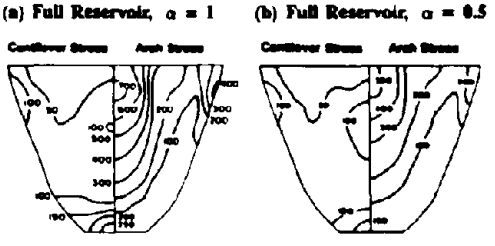

Figure 4. Reservoir boundary absorption effects in response of Morrow Point Dam (Fok and Chopra, 1986b).

envelope values of the stresses on the upstream face of Morrow Point Dam due to the upstream component of Taft ground motion are presented in for two conditions: rigid (fully reflective) reservoir boundary, $\alpha = 1$, and partially absorptive reservoir boundary, $\alpha = 0.5$, where α is the wave reflection coefficient. It is apparent that some of the stresses in the dam due to the upstream ground motion are reduced significantly because of reservoir boundary absorption; even larger decreases occur in the stresses caused by the other two components of ground motion (Fok and Chopra, 1986b). In general, assuming a non-absorptive (rigid) reservoir boundary leads to an unrealistically large response for dams with impounded water, particularly due to vertical and cross-stream ground motions.

3.3 Water compressibility

Westergaard's classical formula for the added hydrodynamic mass, commonly employed in dynamic analysis of dams, is based on three assumptions that are usually not satisfied: (1) the dam is rigid, (2) it is straight in plan and has a vertical upstream face, and (3) the water is incompressible. Although this concept has long been used in practical dam analysis, the range of conditions for which it is valid was not well understood, and during the past two decades extensive research has been devoted to this question. These studies have demonstrated that dam-water interaction arising from dam flexibility should be considered in analyzing dam response. The assumption of a straight dam with vertical upstream face obviously ignores the curvature of an arch dam which can significantly influence hydrodynamic pressures. Therefore, numerical methods considering arbitrary geometry of the upstream dam face and the reservoir were developed to determine an added hydrodynamic mass matrix to be used in conjunction with finite-element analysis of dams (Kuo, 1982). Whereas this may be an improvement over Westergaard's formula for added hydrodynamic mass, water compressibility effects were still neglected in this procedure. Although studies conducted as early as 1968 and 1970 (Chopra, 1968; Chopra, 1970) demonstrated that water compressibility effects are significant in the response of concrete gravity dams, there continues to be much interest in research (Hall, 1986) and in practical applications (Tarbox et al., 1979) to neglect water compressibility in earthquake analysis of concrete dams, primarily because such an assumption leads to considerable simplification in the analysis. However, recent research has reconfirmed earlier results and further demonstrated that water compressibility effects would be significant in the earthquake response of most concrete dams.

The key parameter that determines the significance of water compressibility in the earthquake response of dams is the frequency ratio f_{res}/f_{dam} where f_{res} is the fundamental natural frequency of the impounded water and f_{dam} is the fundamental natural frequency of the dam alone. If this ratio is large enough (e.g. greater than 2 for gravity dams), the impounded water affects the dam response essentially as an incompressible fluid (Chopra, 1968). Water compressibility effects are significant in the earthquake response of arch dams with realistic values of E_s, the elastic modulus for concrete, but negligible if E_s is small enough. This is demonstrated in Figures 5 and 6 wherein is presented the earthquake response of Morrow Point Dam, assuming its elastic modulus E_s to be 4.0 million psi--a typical value--and 0.5 million psi--an unrealistically small value--respectively. It is apparent that neglecting water compressibility would be inappropriate in the first case but would be reasonable in the latter case in determining the response of the

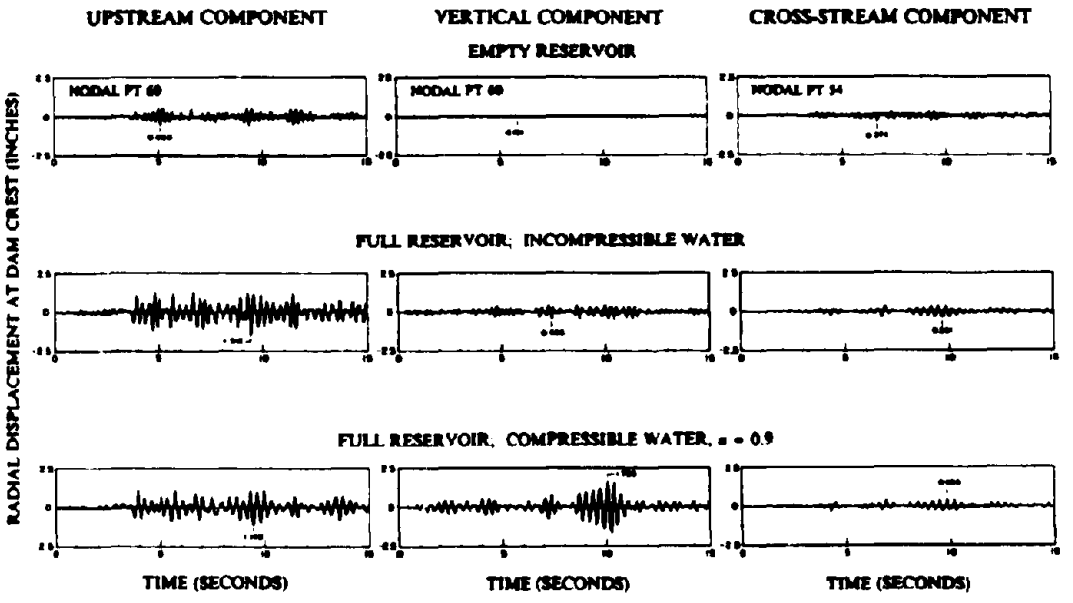

Figure 5. Displacement response of Morrow Point Dam (E_s = 4 million psi) due to upstream, vertical and cross-stream components, separately, of Taft ground motion (Fok and Chopra 1987).

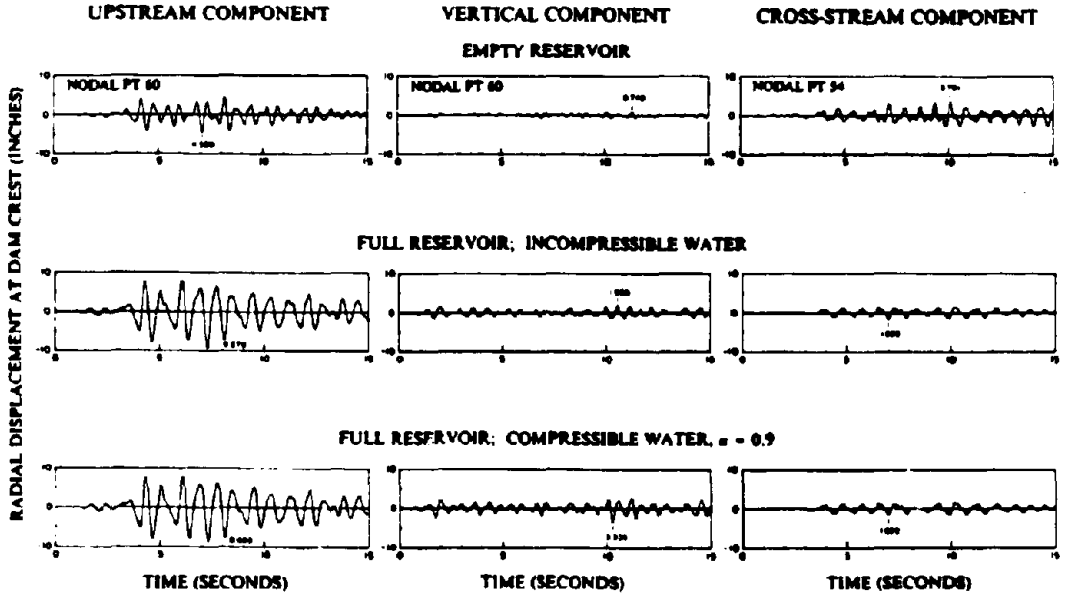

Figure 6. Displacement response of Morrow Point Dam (E_s = 0.5 million psi) due to upstream, vertical and cross-stream components, separately, of Taft ground motion (Fok and Chopra 1987).

dam to upstream or cross-stream ground motions. However, even for this unrealistically small E_s value, water compressibility has a significant influence on the response of the dam to vertical ground motion.

Water compressibility would be significant in the response of most concrete dams because E_s is generally much higher and f_{res}/f_{dam} is correspondingly smaller. Thus, the added mass representation of hydrodynamic effects, which is based on the assumption of incompressible water and is typically used in analysis of concrete dams, would generally lead to inaccurate results whether the added mass is determined from Westergaard's classical reuslt for a straight dam, as is commonly done, or from a three-dimensional analysis of the fluid domain (Kuo, 1982).

3.4 Dam-foundtion rock interaction

In standard finite element analyses the foundation rock is assumed to be massless and a portion is included in the finite element idealization of the system. This extremely simple idealization of the foundation rock, in which only its flexibility is considered but inertial and damping effects are ignored, is popular because the foundation impedance matrix (or frequency-dependent stiffness matrix) is very difficult to determine without resorting to these assumptions. Computation of this foundation impedance matrix for analysis of arch dams requires solution of a series of mixed boundary value problems governing the steady-state response of the canyon cut in a three-dimensional half-space. Such solutions have only recently been achieved (Zhang and Chopra, 1991) and have been incorporated in a substructure method for analysis of dam-water-foundation rock systems (Chopra and Tan, 1992). These very recent developments enable evaluation of the commonly used simplifications mentioned above.

Figures 7 and 8 show the envelope values of maximum tensile stresses in Morrow Point Dam with empty reservoir due to the upstream component of Taft ground motion for two conditions: only foundation flexibility effects were included in one and full dam-foundation rock effects were included in the other. Results are presented for two values of the ratio E_f/E_s where E_f and E_s are Young's moduli of foundation rock and dam concrete, respectively: E_f/E_s = 1 and 1/4, with E_s = 4 million psi. Full consideration of dam-foundation rock interaction reduces the maximum dynamic stresses by 12 to 18 percent, depending on the stress component and dam face if E_f/E_s = 1, and by 35 to 44 percent if E_f/E_s = 1/4. The stresses due to cross-stream ground motion are reduced by similar amounts and the responses due to vertical ground are reduced by up to 62 percent. Thus, it is clear that the significant reduction in dam response arising from foundation material and radiation damping is not recognized in the "standard" analyses.

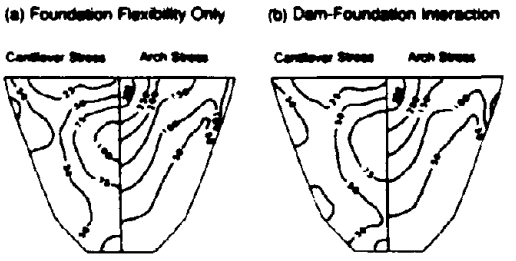

Figure 7. Dam-foundation interaction effects in response of Morrow Point Dam, E_f/E_s = 1.

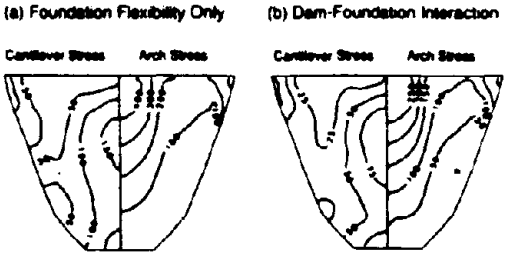

Figure 8. Dam-foundation interaction effects in response of Morrow Point Dam, E_f/E_s = 1/4.

4 ANALYSIS PROCEDURES AND COMPUTER PROGRAMS

A few years ago a procedure was developed to analyze the earthquake response of arch dams (Fok and Chopra, 1986a). Based on the substructure method, this procedure and the implementing computer program EACD-3D (Fok, Hall, and Chopra, 1986) included the effects of dam-water interaction, water compressibility, and reservoir boundary absorption. Recently, the procedure and computer program have been extended to include dam-foundation rock interaction without introducing the common assumption that the foundation rock is massless (Chopra and Tan, 1992). Thus, all the factors known to be significant in the earthquake response of arch dams can now be considered.

By this procedure, it is possible to perform a three-dimensional analysis of a concrete arch dam supported by flexible foundation rock in a canyon and impounding a reservoir of water (Figure 9).

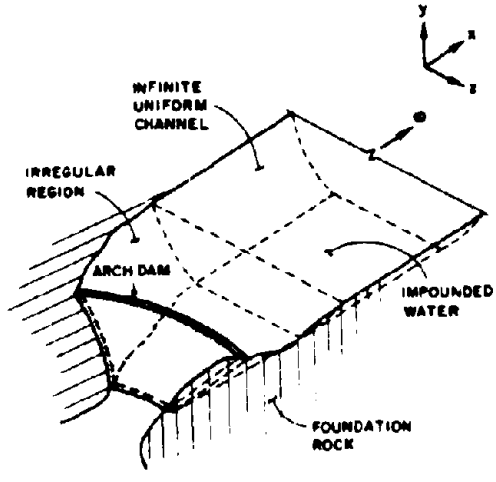

Figure 9. Arch dam-water-foundation rock system (Fok and Chopra 1985).

The system is analyzed under the assumption of linear behavior for the concrete dam, impounded water, and foundation rock. Thus, the possibility of water cavitation, concrete cracking, or opening of the vertical contraction joints of the dam during vibration is not considered.

In earthquake response analysis of dams by the substructure method, the earthquake input is specified as the free-field ground motion at the dam-foundation rock interface. Usually, the same motion is specified over the entire dam-foundation rock interface, an assumption that is inappropriate for arch dams because the dam boundary in contact with the foundation rock extends through the height of the dam and the free-field motion can vary significantly over the height and between the two sides of the canyon. Nonuniform boundary motions can be included in finite-element analysis of structures. The principal difficulty, however, is in rationally defining the variations in motions over the dam-foundation rock interface because few measurements of actual ground motion variations have been obtained at arch dam sites.

5 SEISMIC DESIGN AND SAFETY EVALUATION

The seismic evaluation of an existing dam involves the following phases: (1) selection of earthquake ground motions expected at the site; (2) analysis of the dynamic response of the dam; and (3) evaluation of the results of dynamic response analysis to predict the expected earthquake performance of the dam.

The current practice in the seismic analysis of concrete dams is to assume that the structure is linearly elastic. If the compressive and tensile stresses in the dam predicted by linear analysis procedures summarized in the preceding section do not exceed the compressive and tensile strengths, respectively, of concrete, the dam can be expected to remain undamaged during the selected earthquake ground motions. The concrete strength requirements will be controlled by the tensile stresses because they will be similar in magnitude to the compressive stresses, whereas the tensile strength of concrete is an order of magnitude less than its compressive strength.

Thus, the key property which determines the capacity of concrete dams to withstand earthquakes is the tensile strength of concrete. Among the various types of tests available, the splitting tension test is easiest to accomplish and provides the most reliable estimates of concrete strength. These strength values should be multiplied by about 4/3 to account for the nonlinear behavior of concrete near failure before using it to interpret results of linear finite-element analysis (Raphael, 1984).

Because the tensile strength of concrete depends on the rate of loading, the aforementioned tests should be conducted at loading rates the concrete may experience during earthquake motions of the dam. Lacking the facility to perform dynamic tests, it is recommended that the tensile strength of concrete for judging the seismic safety of a concrete dam should be the static value augmented by a multiplier of about 1.5.

The tensile strength should obviously be determined from appropriate tests on specimens of concrete for the particular dam. However, a preliminary estimate of the tensile strength can be obtained from Figure 10 which presents four plots of tensile strength as a function of compressive strength, to be used depending on need. The lowest two plots, $f_t = 1.7f_c^{2/3}$ and $f_t = 2.3f_c^{2/3}$, are for long-time or static loading. The lowest plot represents actual tensile strength, whereas the second plot takes into account the nonlinearity of concrete and is to be used to interpret the stresses computed by linear finite-element analysis. The third and fourth plots, $f_t = 2.6f_c^{2/3}$ and $f_t = 3.4f_c^{2/3}$, are the actual and "apparent" tensile strengths under seismic loading.

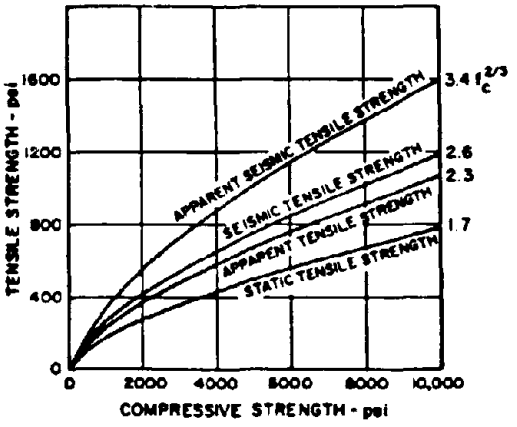

Figure 10. Design chart for tensile strength (Raphael 1984).

Permitting significant tensile stresses, up to the tensile strength of concrete, is of course a major departure from the standard design criteria wherein little tension is permitted. However, evidence is available to support the recommended design criteria that significant dynamic stresses in tension can be carried by sound concrete. In addition to the data from laboratory tests mentioned earlier, evidence of the dynamic tensile strength of concrete was provided by the performance of dams during earthquakes. Dynamic analyses indicated that Pacoima Dam should have developed maximum tensile stresses in the order of 750 psi during the San Fernando earthquake of 1971, yet no evidence of cracking could be found on either face of the dam (Swanson and Sharma, 1979). Elastic analyses of Koyna Dam indicated tensile stresses almost three times the tensile strength of concrete, resulting in significant cracking of the dam. However, the dam survived the earthquake without any sudden release of water (Chopra and Chakrabarti, 1973). Perhaps most interesting is the lack of damage to Crystal Springs Dam--a curved concrete gravity dam located approximately 1,000 ft from the San Andreas fault--during the great San Francisco earthquake of 1906 (Wulff and Van Orden, 1979).

Linear analyses of arch dams subjected to the very intense ground motions expected in highly seismic areas may indicate that the computed tensile stresses exceed the available tensile strength of concrete. While linear analyses can usually predict locations in the dam where cracking will be initiated, they may not reliably predict the extent of cracking or the true nonlinear behavior of dams during intense earthquake motions.

For these reasons nonlinear response of concrete dams has been a subject of increased research activity during recent years, and progress has been made in developing nonlinear analysis procedures (Dowling and Hall, 1989). However, the predictions of the extent of the damage obtained from these analyses are quite sensitive to the assumed nonlinear properties of mass concrete. Thus, the mechanical properties of mass concrete need to be better defined before the extent of damage, and its implications to dam safety can be determined with confidence. Comprehensive testing programs are therefore necessary to determine the constitutive and strength properties of multiaxially loaded mass concrete under dynamic, reversible, cyclic strains and stresses representative of earthquake conditions.

Linear analyses of an arch dam, treated as a monolithic structure, for intense ground shaking may show that dynamic tensile stresses in the arch direction exceed the compressive arch stresses that exist prior to the earthquake. However, arch dams are typically constructed as cantilever monoliths separated by contraction joints which cannot develop tensile stresses. Thus, net tensile arch stresses predicted by linear analysis imply cyclic opening and closing of the vertical contraction joints during an earthquake. This joint-opening mechanism has been included in recently developed nonlinear analysis procedures (Fenves, Mojtahedi, and Reimer, 1992). However, so far it has not been possible to consider effects of water compressibility, reservoir boundary absorption, and dam-foundation rock interaction which are known to be significant in the earthquake response of arch dams.

6 APPLICATIONS TO ENGINEERING PRACTICE

Dam regulatory agencies have revised their design standards and engineering companies have updated their procedures to acknowledge the research accomplishments of the past decade, some of which have been summarized in this paper. Static force methods involving seismic coefficients have given way to dynamic analysis procedures. As shown in this paper, these procedures should consider the following factors: dam-water interaction, reservoir boundary absorption, water compressibility, and dam-foundation rock interaction. In order to produce safe and economical designs of concrete dams, the most reliable techniques considering the above-mentioned factors should be used to evaluate existing dams and proposed design of new dams. The EACD-3D computer program mentioned in this paper was used in recent seismic safety evaluations of Englebright and Pardee dams in California, and Valdecanas dam in Spain.

Since most existing dams were designed by methods that are now considered oversimplified, there is considerable interest in reevaluating the original designs using current procedures. As a result of such safety evaluations, structural modifications have been made to some dams, and restrictions on reservoir water levels have been imposed in some cases. Since the economic impact of such modifications and restrictions is generally substantial, it is important to improve the reliability of present methods of safety evaluation.

Although considerable progress has been made in the last decade, much additional research needs to be done to improve the reliability of present methods for the seismic analysis, design, and safety evaluation of concrete dams. In particular, spatial variability of ground motion around an arch dam canyon needs to be considered in linear analyses, and efficient and reliable procedures need to be developed to predict the damage expected in arch dams during intense ground motions.

ACKNOWLEDGEMENTS

The research studies that lead to the material presented in this paper were sponsored by the National Science Foundation under several grants, including the current grant, BCS-9121943. This support is gratefully acknowledged.

Grateful application is also expressed to the author's students, Dr. K-L. Fok and Mr. H-C. Tan, whose research provided the basis for much of the information presented. In addition, parts of this paper are based on two earlier publications of the author (Chopra, 1987; Chopra, 1988).

REFERENCES

Ahmadi, M.T. and G.Khoshrang 1992. Sefidrud dam's dynamic response to the near field earthquake of June 1990. Dam Engrg. (2):85-116.

Chopra, A.K. 1968. Earthquake behavior of reservoir-dam systems. J. Eng. Mech. Div. ASCE 94(EM6):1475-1500.

Chopra, A.K. 1970. Earthquake response of concrete gravity dams. J. Eng. Mech. Div. ASCE 96(EM4).

Chopra, A.K. 1987. Earthquake analysis, design, and safety evaluation of concrete dams. Proc. 5th Canadian Conf. on Earthq. Engrg., Ottawa, Canada, A. A. Balkema, Rotterdam.

Chopra, A.K. 1988. Earthquake response analysis of concrete dams. Chapt. 15 in Advanced Dam Engineering for Design, Construction and Rehabilitation (R.B. Jansen, ed.), Van Nostrand Reinhold, New York, pp. 416-465.

Chopra, A.K. and P.Chakrabarti 1973. The Koyna earthquake and the damage to Koyna Dam. Bull. Seismol. Soc. Amer. 63(2):381-397.

Chopra, A.K. and H.C.Tan 1992. Modelling of dam foundation interaction in analysis of arch dams. Proc. 10th World Conf. on Earthq. Engrg., Madrid, Spain.

Clough, R.W. 1980. Nonlinear mechanisms in the seismic response of arch dams. Presented at Internat. Conf. on Earthq. Eng., Skopje, Yugoslavia.

Dowling, M.J. and J.F.Hall 1989. Nonlinear seismic analysis of arch dams. J. Engrg. Mech., ASCE 115:768-789.

Fenves, G.L., S.Mojtahedi and R.B.Reimer 1992. Effect of contraction joints on earthquake response of an arch dam. J. Struct. Engrg., ASCE 118:1039-1055.

Fok, K.L., J.F.Hall and A.K.Chopra 1986. EACD-3D: a computer program for three-dimensional earthquake analysis of concrete dams. Report No. UCB/EERC-86/09. Univ. of Calif., Berkeley.

Fok, K.L. and A.K.Chopra 1986. Earthquake analysis of arch dams including dam-water interaction, reservoir boundary absorption, and foundation flexibility. Earthq. Eng. Struct. Dyn. 14(2):155-184.

Fok, K.L. and A.K.Chopra 1986. Hydrodynamic and foundation flexibility effects in earthquake response of arch dams. J. Struct. Eng. ASCE 112(8):1810-1828.

Fok, K.L. and A.K.Chopra 1987. Water compressibility in earthquake response of arch dams. J. Struct. Eng. ASCE, 113(5):958-975.

Hall, J.F. 1986. Study of the earthquake response of Pine Flat Dam. Earthq. Eng. Struct. Dyn. 14(2):281-295.

International Conference of Building Officials 1982. Uniform building code.

Kuo, J.S.H. 1982. Fluid-structure interactions: added mass computations for incompressible fluid.

Report No. UCB/EERC-82/09. Univ. of Calif., Berkeley.

Raphael, J.M. 1984. Tensile strength of concrete. ACI J., Title No. 81-17, pp. 158-165.

Swanson, A.A. and R.P.Sharma 1979. Effects of the 1971 San Fernando earthquake on Pacoima Arch Dam. Transactions, 13th Int. Cong. Large Dams, New Delhi 2:797-824.

Tarbox, G.S., K.Dreher and L.Carpenter 1979. Seismic analysis of concrete dams. Transactions, 13th Internat. Cong. Large Dams, New Delhi 2:963-994.

U.S. Army Corps of Engineers 1958. Gravity dam design. Design Manual EM 1110-2-2200. Washington, D.C.

U.S. Bureau of Reclamation 1965. Arch dams. In Concrete dams (Chapter 1). Design Standards No. 2. Denver: Department of the Interior.

U.S. Bureau of Reclamation 1966. Gravity dams. In Concrete dams (Chapter 2). Design Standards No. 2. Denver: Department of the Interior.

U.S. Bureau of Reclamation 1977. Design of arch dams. Denver: U.S. Government Printing Office.

Westergaard, H.M. 1933. Water pressure on dams during earthquakes. Transactions ASCE, Vol. 98.

Wuliff, J.G. and R.C.Van Orden 1979. Evaluation of the earthquake stability of Lower Crystal Springs Dam. Transactions, 13th Int. Cong. Large Dams, New Delhi 2:747-774.

Zhang, L.P. and A.K.Chopra 1991. Impedance functions for three-dimensional foundations supported on an infinitely long canyon of uniform cross-section in an homogeneous half-space. Earthq. Eng. Struct. Dynam. 20:1011-1028.

Experimental studies of the mechanical characteristics of three types of seismic isolation bearings

Ian D. Aiken, James M. Kelly, and Peter W. Clark
Earthquake Engineering Research Center, University of California at Berkeley, USA

Kazuo Tamura, Masaru Kikuchi, and Tetsuji Itoh
Ohsaki Research Institute, Shimizu Corporation, Tokyo, Japan

ABSTRACT: The results of an extensive series of experimental tests to identify the mechanical characteristics of three types of seismic isolation bearings are presented. Two types of high-damping rubber bearings and one type of lead-rubber bearing were studied. Cyclic horizontal displacement tests, varying the test parameters of shear displacement amplitude, axial load, and loading frequency were performed on all of the bearings. Bearing shear stiffness and damping properties were investigated in terms of the different test parameters. Ultimate-level tests consisted of monotonic shear loading to failure at several different axial loads, and tension failure tests of the bearings with bolted connections. Roll-out instability tests of the doweled bearings were conducted. Comparisons are made between experimental results and available analytical relationships for material and bearing properties.

1 INTRODUCTION

Elastomeric bearings are now the most commonly-used type of system for seismic isolation. Accurately characterizing bearing mechanical properties is a very important aspect of the design process for an isolation system, and this experimental program was aimed at confirming and refining existing analytical models for this purpose.

An extensive series of tests of three types of seismic isolation bearings was carried out with the objective of fully identifying their mechanical characteristics. Two types of high-damping rubber bearings and one type of lead-rubber bearing were studied.

The three types of bearings tested in this program were developed for earthquake simulator tests of a large-scale, reinforced-concrete model of a three-story building located in Sendai, Japan (Saruta et al., 1988, and Kelly et al., 1992). The full-size building was constructed to study the behavior of different isolation systems under real earthquake excitations. Since its completion in 1985, several different systems have been installed under the building. These have included the two types of high-damping bearings studied in this investigation. (At this time, there are no plans for the lead-rubber system to be installed).

2 BEARING DESIGNS

The high-damping A and high-damping B designs described below are both reduced-scale designs of the bearings that have already been installed under the full-size building. The model constructed for the earthquake simulator tests has a (geometric) scale factor of 2.5, and this is the scale factor that was used to determine the size of the reduced-scale bearings. Lead-rubber bearings have not been installed under the full-size building. With no initial bearing design to scale, the design basis for the lead-rubber bearings was selected as providing a bearing with the same stiffness characteristics as the high-damping A bearings.

The reduced-scale bearings under the model structure are subjected to axial loads of approximately 49.0 kN and 78.5 kN. These loads were the basis for defining the axial loads used in this study. With a few exceptions, only the results for the 78.5 kN tests are presented and discussed in this paper.

The designs of the 1/2.5-scale bearings are described in the following sections.

2.1 *Design 1: High-damping A*

These bearings were made from a blend of filled natural rubber and a synthetic rubber. The compound is called KL301 by the manufacturer, Bridgestone Corporation, Ltd., Japan, and is one of a suite of high-damping elastomers that they have developed for seismic isolation applications. KL301 has a shear modulus of about 4300 kPa at very small strains, which decreases to 650 kPa at 50 percent strain, 430 kPa at 100 percent strain, and 340 kPa at 150 percent strain. The bearings consist of twenty layers of 2.2 mm thick rubber at 176 mm diameter (shape factor =

20), nineteen 1.0 mm steel shims, and 12 mm top and bottom plates (Figure 1). The design axial pressure is 3.23 MPa. The bearings were designed with flange-type end plates to permit bolted structure and foundation connections. Fifteen bearings of this design were tested in this study.

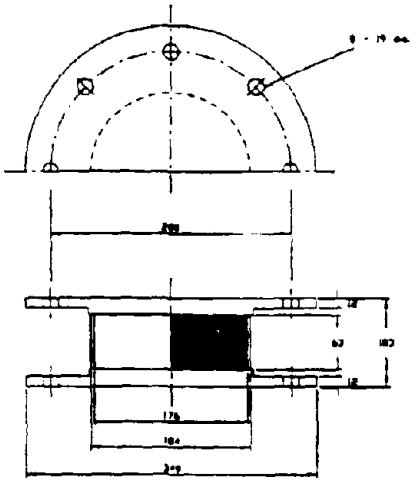

Fig. 1 Bearing design 1: high-damping A

2.2 *Design 2: High-damping B*

These bearings were made from a low-modulus, filled natural rubber compound, designated HDNR-S by the manufacturer, Rubber Consultants, Ltd., England. The shear modulus of this material varies from about 800 kPa at a shear strain of 5 percent to about 480 kPa at 50 percent strain and 400 kPa at 100 percent strain. The bearings consist of twelve layers of 4.0 mm thick rubber at 140 mm diameter (shape factor = 8.75), eleven 1.6 mm steel shims, and 20 mm top and bottom plates (Figure 2). The design axial pressure is 5.10 MPa. Bearing-structure and foundation connections are bolted. Instead of using flange-type end plates, the bearings are connected by bolting directly into the top and bottom end plates. Twelve bearings of this design were tested in this study.

2.3 *Design 3: Lead-rubber*

These bearings were made from an unfilled natural rubber compound, and contain a 25.4 mm diameter lead plug. For design purposes, the rubber shear modulus was assumed to have a constant value of 590 kPa. The bearings consist of 21 layers of 3.0 mm thick rubber at 180 mm diameter (shape factor = 15), twenty 1.0 mm steel shims, and 15 mm top and bottom plates (Figure 3). The design axial pressure is 3.08 MPa. These bearings have shear dowel end plate connections. The bearings were manufactured by Oiles Industries, Ltd., Japan. Fifteen bearings of this design were tested in this study.

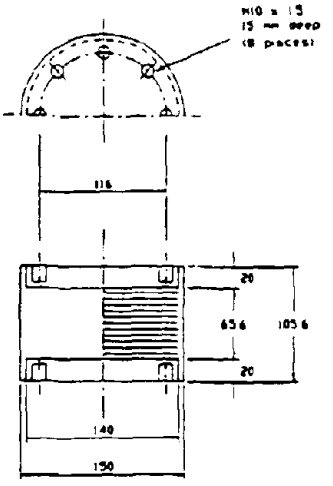

Fig. 2 Bearing design 2: high-damping B

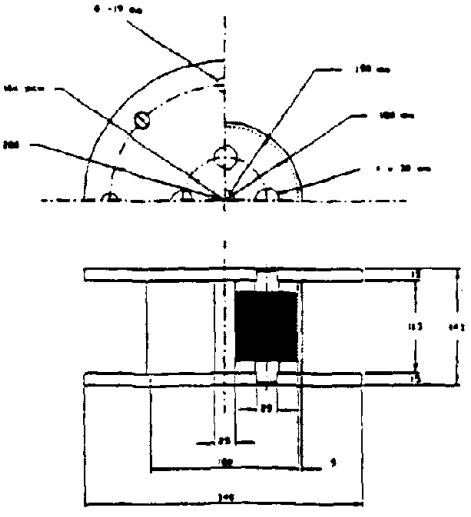

Fig. 3 Bearing design 3: lead-rubber

3 TYPES OF TESTS

All of the bearing tests were performed in a machine developed for general testing of small-to-moderate sized isolation bearings. The machine is capable of

subjecting a bearing to simultaneous generalized horizontal and vertical dynamic loading. It has limits of 1335 kN vertical force, 534 kN horizontal force, and ± 250 mm horizontal displacement.

In addition to the horizontal shear tests, a large number of vertical tests were performed on the bearings. The results of these tests are not discussed in this paper.

3.1 *Characteristic tests*

1. Basic test

The basic type of test performed on all of the bearings of each design was a sinusoidal horizontal displacement-controlled loading, conducted at either 49.0 kN or 78.5 kN constant axial load and for 5 cycles of loading at shear strain amplitudes of 5, 25, 50, 75, and 100 percent. The axial loads selected correspond to the axial loads to which the bearings were subjected in the earthquake simulator tests of the 1/2.5-scale model of the full-size isolated building (Kelly, 1992). The frequency of loading was 1 Hz for all of these tests.

2. Variable axial load

The basic test was also performed at a number of different axial loads. The load was constant during each test, and tests were performed at loads of $3P_{des}$, $2P_{des}$, P_{des}, $P_{des}/2$, 0, and $-P_{des}/10$, where P_{des} was 49.0 kN or 78.5 kN. The rate of loading and the strain increments were otherwise the same as for the basic test described above.

3. Variable frequency

The basic test was also performed at loading frequencies of 0.1, 0.3, 0.5, 1.0, and 2.0 Hz. The other test variables were the same as those for the basic test.

3.2 *Ultimate tests*

1. Large-strain cyclic

Large-strain sinusoidal cycles at strain amplitudes of 100, 150, 200, 250, 300, and 350 percent were performed. (Maximum strain for the design 3 bearings was 200 percent, limited by the onset of roll-out instability; loading frequency was 0.5Hz for the 250, 300, and 350 percent tests).

2. Monotonic shear failure

Two bearings of designs 1 and 2 were failed in shear under monotonic loading. One bearing was tested under zero axial load, and the other at 78.5 kN axial load. The ultimate-level shear tests of the design 3 bearings consisted of determining the roll-out displacement of the bearings under different axial loads. Roll-out tests were performed at axial loads of 0, 49.0, 78.5, and 156.9 kN.

3. Monotonic tension failure

One bearing each of designs 1 and 2 was tested to break under monotonic tension loading. (The doweled connection detail of the design 3 bearings did not permit tension load to be applied to these bearings).

4 TEST RESULTS

Typical hysteresis loops for the three types of bearings under sinusoidal shear displacement loading are presented in Figure 4. The loops shown for the high-damping A bearing are at shear strains of 200, 250, 300, and 350 percent, those for the high-damping B bearing are at strains of 100, 150, 200, and 250 percent, and those for the lead-rubber bearing are at strains of 50, 100, 150, and 200 percent. Beyond a certain strain level, the high-damping bearings exhibit a clear stiffening behavior. Various results are presented and discussed in the following sections.

4.1 *Characteristic tests*

Bearing effective stiffness and damping were calculated from the experimental hysteresis loops using the following relationships:

$$k_{eff} = \frac{F_{max} - F_{min}}{d_{max} - d_{min}} \tag{1}$$

$$\xi = \frac{W_d}{4\pi W_s} \tag{2}$$

where:

F_{max}, F_{min} = peak values of shear force

d_{max}, d_{min} = peak values of shear displacement

W_d = hysteresis loop area

$W_s = \frac{1}{2} F_{max} d_{max}$

These properties are plotted as a function of shear strain for each type of bearing in Figure 5. The design 1 and 3 bearings show very similar effective stiffness-strain relationships. This is to be expected, as the original design intent for these two types of bearings was that their stiffness properties be the same. The design 2 bearings, however, show a much lower stiffness, about one-third of the stiffness of design 1 or 3 over the entire strain range. The damping ratios of the three bearing designs show greater differences. For design 1, the damping ratio decreases gradually from 12 percent at small strains to about 10 percent at strains above 200 percent. The design 2 bearings have an almost constant damping ratio of about 9-10 percent for strains up to 150 percent, which increases to about 14 percent at 250 percent strain. The design 3 bearings have the highest damping ratio: nearly 19

The influence of axial load variation on the shear stiffness of the design 1 and 2 bearings is shown in Figure 7. The curve for the design 3 bearings is very similar to that of the design 1 bearings, with neither design exhibiting any significant stiffness variation with axial load. Using k_{eff} at P = 78.5 kN as the reference stiffness, the stiffness variations at 25 and 100 percent strain for these bearings is only about ±5 percent of the 78.5 kN stiffness. The variation for the design 2 bearings is somewhat greater, being about ±20 percent of the 78.5 kN stiffness. Axial load variations influence damping ratios more than stiffness for all three bearing designs. The design 1 bearing damping ratio varies from 11 to 14 percent at 25 percent strain, and from 10 to 12 percent at 100 percent strain, and the design 3 bearing damping ratio varies from 15 to 21 percent at 25 percent strain, and from 13 to 16 percent at 100 percent strain. The design 2 bearing damping ratio varied more, from 8 to 14 percent at 25 percent strain, and from 6 to 15 percent at 100 percent strain.

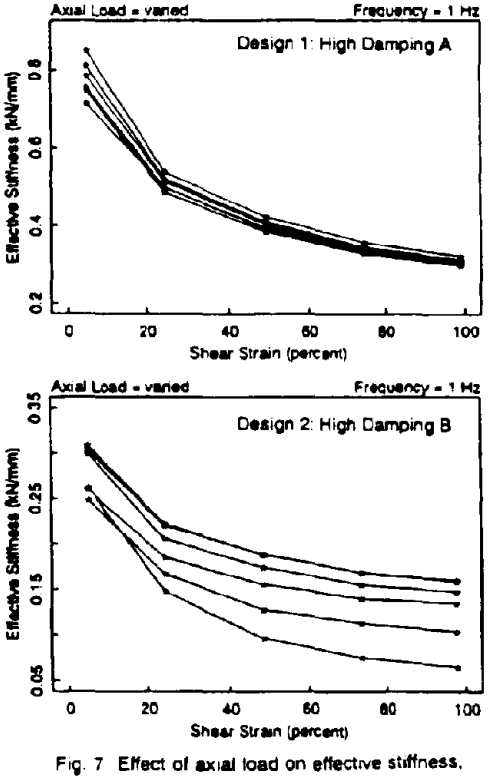

Fig. 7 Effect of axial load on effective stiffness, designs 1 and 2

Loading frequency effects on stiffness and damping ratio are shown in Figure 8 for the design 3 bearings. Stiffness is negligibly affected by the variation in loading frequency for all of the three designs. Using k_{eff} at 0.5 Hz as the reference stiffness, the lead-rubber bearing stiffness variation at 25 and 100 percent shear strain is only about ±2 percent of the 0.5 Hz stiffness. The variation for the high-damping bearings is about ±10 percent, and about ±6 percent of the 0.5 Hz stiffness for designs 1 and 2, respectively. Damping ratio is influenced less by load frequency than by axial load. The variation is about ±5 to 10 percent for all three bearing types, when compared to the damping ratio at 0.5 Hz.

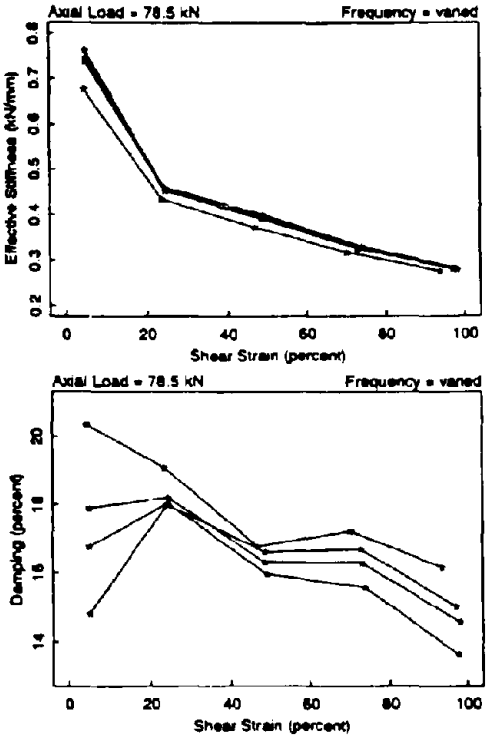

Fig. 8 Effect of loading frequency on bearing properties, design 3

4.2 *Ultimate tests*

1. Large-strain cyclic

Large-strain cyclic tests up to 350 percent shear strain were performed on the design 1 bearings, up to 250 percent on the design 2 bearings, and up to 200 percent on the design 3 bearing. Hysteresis loops for these tests are shown in Figure 4. Both types of high-damping bearings exhibit a stiffening characteristic at large strains. The high-damping A bearings begin to stiffen at about 250 percent and the high-damping B bearings at about 200 percent shear strain. High-strain stiffening is a material property of filled rubbers. The lead-rubber bearing, which is made from unfilled natural rubber and has doweled shear connections (which permit instability in the bearing before it can sustain extreme lateral displacements) does not show this stiffening effect at large strains.

2. Monotonic shear failure

Shear failure force-displacement curves for a design 1 and a design 2 bearing under zero axial load are shown in Figure 9. The design 1 bearing failed at a strain of 739 percent, and the design 2 bearing at about 510 percent. The peak shear forces at failure were 274 kN and 116 kN for the design 1 and 2 bearings, respectively. These forces correspond to shear stresses of 11.2 MPa for the design 1 bearing, and 7.5 MPa for the design 2 bearing. The failure mechanisms for both bearings involved tensile material rupture. Elastomer-shim bond separation was not observed in any of the bearing shear failures.

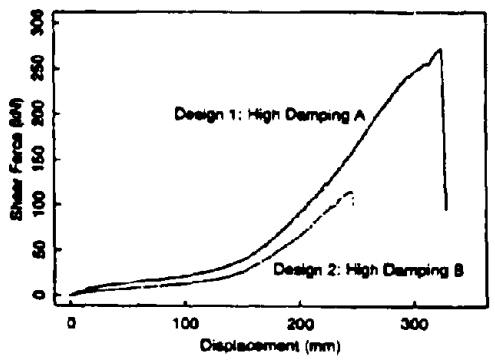

Fig. 9 Monotonic shear failure, designs 1 and 2

Roll-out strains ranged from 133 to 200 percent, reached in the 0 and 78.5 kN axial load tests, respectively. The calculated roll-out displacements for the 49.0 and 78.5 kN axial loads agree well with the experimental results, however, agreement is not so good for the 0 and 156.9 kN loads.

3. Monotonic tension failure

Tensile stress versus tensile strain curves for the failure tests of one design 1 and one design 2 bearing are plotted in Figure 10. The sharp reduction in stiffness in both curves at a stress of about 2 MPa indicates the onset of cavitation in the elastomer. The design 1 bearing reached a stress of 7.7 MPa and a strain of 514 percent at failure, while the design 2 bearing reached a stress of 8.0 MPa and a strain of 408 percent. These failure stresses represent a tension load of about two times the design compression load for the bearings. Future ultimate-level tests under combined large shear deformation and tension loading are planned. This type of test will more closely represent, than the pure tension tests described here, the type of extreme loading condition in which tensile stresses may develop in isolators.

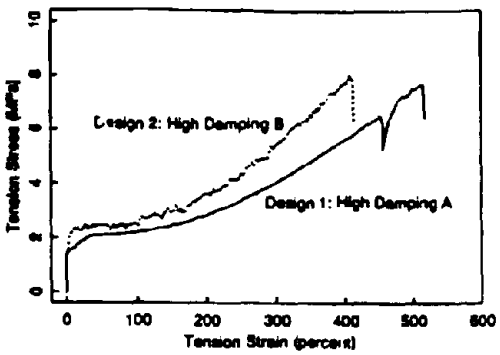

Fig. 10 Tension failure, designs 1 and 2

5 CONCLUSIONS

All of the bearings performed well in the large range of tests conducted. This experimental investigation has provided an extensive database for the confirmation and refinement of existing analytical models for isolation bearing properties.

Fundamental bearing characteristics of stiffness and damping were studied in terms of shear strain, axial load, and rate of loading. In general, it was found that variations in axial load and rate of loading did not significantly affect bearing stiffness and damping properties for moderate shear strain levels. The understanding of the failure mechanisms of seismic isolators has been enhanced by the various ultimate-level tests performed. The ultimate-level shear tests achieved bearing shear strains in excess of 500 percent before failure occurred. The tension failure tests revealed the very large tension capacity of the bolted high-damping bearings.

The results and conclusions will directly benefit the designers of isolation systems utilizing these types of bearings, providing a greater understanding of and confidence in bearing properties and behavior.

REFERENCES

Ministry of Works & Development, 1983. Design of lead-rubber bridge bearings. *CDP 818/A*, Wellington, New Zealand.

Saruta, M., H. Watanabe, & M. Izumi, 1989. Proof test of base-isolated building using high damping rubber bearing. *Proc. SMiRT-10, vol. K:* 631-636, Los Angeles, USA.

Kelly, J.M., 1991. Dynamic and failure characteristics of Bridgestone isolation bearings. *Report No. UCB/EERC-91/04*, EERC, Univ. of Calif. at Berkeley, USA.

Kelly, J.M., I.D. Aiken, P.W. Clark, H. Yamahara, M. Saruta & M. Kikuchi, 1992. Earthquake simulator tests of a scale model of a base-isolated, reinforced-concrete building. *Proc. 10th WCEE*. Madrid, Spain.

Seismic upgrading of existing structures

V.V. Bertero
Earthquake Engineering Research Center, University of California, Berkeley, CA, USA

ABSTRACT: The importance of proper seismic upgrading of existing hazardous structures to reduce seismic risk in urban areas is stressed, followed by a discussion of factors influencing the decision to upgrade and the selection of efficient strategies and techniques. Problems encountered in reliably assessing seismic activity, seismic hazards, and the seismic vulnerability of a given structure are briefly reviewed. Based on an energy balance equation, guidelines for the proper strategies and techniques are formulated.

1. INTRODUCTION

Most human injury and economic loss due to moderate and severe *Earthquake Ground Motions (EQGMs)* are caused by the failure of engineered structures, particularly buildings, which presumably have been designed and constructed to protect their users against expected natural hazards. Recent earthquakes (1988 Armenia, 1990 Iran and 1990 Philippines), in which large numbers of people have been killed and large economic losses have been suffered, confirm this dramatically. The 1989 Loma Prieta earthquake, in spite of the fact that it caused relatively few deaths (67), is considered one of the most costly natural disasters in U.S. history. The economic losses induced by these earthquakes clearly indicate that the level of *"acceptable damage"* should vary with the function and occupancy of the facility. For certain occupancies there is an urgent need to require damage control even under the major expected EQGMs (usually denoted in the literature as the *Maximum Credible EQGMs*).

Improving existing and developing better methods of designing, constructing and maintaining new structures, and particularly of upgrading existing seismically hazardous facilities, is one of the most effective ways to mitigate the destructive effects of EQGMs. This paper aims at the formulation of guidelines for the selection of efficient strategies and techniques for seismic upgrading of existing facilities. The problems encountered in attempts to evaluate seismic risk to an existing facility are discussed, as are the factors in the decision to upgrade a facility, the main concepts in the selection of the proper upgrading strategies and techniques, and the development of guidelines.

2. SEISMIC RISK ASSESSMENT AND CONTROL

Seismic risk to a facility is the probability that social or economic consequences of earthquakes will equal or exceed a specified value during a specified time period. It can be expressed briefly as follows [Dowrick 1987]:

$$\begin{pmatrix} Seismic \\ risk \end{pmatrix} = \begin{pmatrix} Seismic \\ hazard \end{pmatrix} (Vulnerability)\ (Value)$$

The evaluation and thus the control of seismic risk to a facility require evaluation of both the main seismic hazards to the facility, which depend on the seismic activity that can occur at the facility site and its surroundings, and the seismic vulnerability of the whole facility system (soil, foundation, superstructure, and nonstructural components and contents) expressed as a fraction of the value of this system.

2.1 *Assessment of seismic activity and hazards*

Seismic activity can be considered as the function describing the probability of occurrence of EQGMs of various intensities and their effects on the earth's surface at a given site, urban area or region during a given period of time. There are significant uncertainties in forecasting future seismic activity rates and strengths because relevant data are scarce and poor in quality. For reliable seismic activity assessment, it is important to gather as much information as is available regarding future earthquakes in terms of locations, magnitudes, frequencies of occurrence, the attenuations of the intensity of the waves and their energy with distance, and the intensities and durations of the strong EQGMs at the facility site and its surroundings.

Seismic hazard is any physical phenomenon associated with an earthquake which may produce adverse effects on human activities. For a given facility, there are many different types of seismic hazards. *The seismic hazards to which a facility may be exposed depend on (1) the seismic activity at the site and its surrounding area, and (2) on the interaction of the seismic effects originated by seismic activity (fault ruptures, landslides, ground failures, vibrations of the ground, floods, fires, etc.) with the whole facility system's vulnerability to them.*

A comprehensive approach to EQ risk reduction requires that all sources of seismic hazards to structures

be identified. In the U.S. the assessments of seismic activity and hazards are presently based on zonation maps and information supplied in local building codes. The seismic effect emphasized in building code seismic regulations is the vibration of structures as a result of earthquake shaking. The author has questioned the reliability of these code maps and this information (1991b & c).

2.2 *Seismic vulnerability assessment*

Seismic vulnerability is the amount of damage induced by a given degree of hazard, expressed as a fraction of value of the facility. Most methods for conducting seismic vulnerability assessments of existing structures are based on estimates of capacity/demand ratios using current seismic code-specified criteria. In general, this approach is not satisfactory because, even in present seismic regulations, the reliability of the procedures for evaluating seismic demands and capacities are highly questionable. Bertero (1988) and Miranda (1991) have conducted reviews of the available criteria for evaluating the vulnerability of existing structures.

The real problem in assessing the vulnerability of a given facility is in estimating its response to future critical EQGMs. Prediction of seismic response depends on an adequate knowledge of at least: (1) the seismic activity at the site; (2) the sources of seismic hazards, which depend on the seismic activity, local soil conditions, and the type, size, shape and detailing of the foundation, superstructure and nonstructural components of the facility and their mechanical characteristics under dynamic excitation; and (3) the desired level of safety and/or the acceptable level of damage. The difficulties involved in reliably assessing vulnerability were clearly in evidence in the studies assessing the vulnerability of the Cypress Viaduct, of which a large part collapsed during the 1989 Loma Prieta EQ [Miranda & Bertero (1991)]. In spite of the simplicity of the structure, the availability of "as built" drawings and the fact that tests of the structural materials were conducted, it was not possible to estimate the actual strength of the weakest frame, because in the real existing structure the anchorage length of some main bars were not as specified in the "as built" drawings.

2.3 *Concluding remarks*

In spite of progress in the above assessments, considerable uncertainties remain. The importance of reliable assessments of seismic hazards and activity and of the vulnerability of existing facilities cannot be overemphasized. If the expected intensity of EQGMs is greatly overestimated, the costs of new construction and rehabilitation of existing structures may be excessive. On the other hand, if the intensity of EQGMs is seriously underestimated, the result may be costly damage and loss of life such as that seen in the disasters of Tangshan, Mexico City, Armenia, Loma Prieta, and the Philippines.

Until the 1989 Loma Prieta EQ, not only were the assessments of seismic activity, hazards, vulnerability and, consequently, risk, based on the use of building code seismic regulations for *Earthquake-Resistant Design* (EQRD) of new buildings, but also the common philosophy for upgrading existing buildings was to bring them into compliance with such regulations. This approach usually results in inefficient rehabilitation of buildings, and in some cases, prohibitively uneconomical upgrading solutions. For example, many old concrete buildings are condemned because they have structural systems and/or reinforcement detailing which are not ductile enough to be acceptable under present seismic codes, in spite of the fact that they may possess sufficient overstrength over the code required yielding strength (C_y) to remain elastic under the effects of the maximum credible EQGM. The main difficulty in proving that they need not comply with the code is in the evaluation of the their actual dynamic characteristics, i.e., in assessment of their real seismic vulnerability.

In most cases, bringing the building up to compliance with building code seismic regulations does not guarantee good seismic performance, particularly when damage control is desired under the expected future major EQGMs. The basic philosophy of present building code seismic regulations is to protect the public in and about buildings from loss of life and serious injury during major earthquakes. These regulations are not intended to limit damage, maintain functions, or provide for easy repair. Recent EQs, particularly the 1989 Loma Prieta, clearly indicate that seismic codes ought to consider damage control. The level of "*acceptable damage*" should vary with the function (occupancy category) of the building. The need for code specifications which require damage control is urgent for certain occupancies. A comprehensive approach to the upgrading of existing buildings will require that the following three levels of critical upgrading EQGMs be considered: *Service Level; Functional or Operational Level; and Safety Level*. Guidelines for establishing these different levels of design EQGMs are suggested by Bertero (1991b & c) and Miranda (1991).

3. UPGRADING OF HAZARDOUS FACILITIES

The decision to upgrade a facility and the choice of the retrofitting strategy and techniques depend on many factors, including not only assessments of (1) The seismic activity; (2) the sources of seismic hazards; and (3) the main seismic hazards given the vulnerability of the facility's whole system; but also (4) the type, function and age of the facility; (5) the required levels of performance (serviceability, continuous operation, life safety) expected of the upgraded facility for different levels of EQGMs and seismic hazards that can occur during the expected service life of the structure; (6) architectural requirements; (7) the need to minimize disturbance to the occupants and operation of the facility during the upgrading; (8) selection of the best strategy for rehabilitating the whole facility system; (9) development of alternative rehabilitation schemes; (10) the availability of equipment and expertise for the field work; (11) cost vs. benefits of the upgrading work, and the socio-economic impact on the community; (12) assessment of the vulnerability of the alternative upgrading schemes to the identified sources of seismic hazard; and (13) selection of the most efficient solution.

3.1 *Selection of the proper upgrading strategy*

The selection of the most efficient upgrading strategy

requires thorough study of the factors discussed above. There are many uncertainties involved in these studies. Although basic concepts and guidelines for seismic upgrading of structures have been formulated [Bertero & Whittaker (1989); Jirsa & Badoux (1990)], the upgrading of a given facility is a unique problem requiring a customized solution. For two identical buildings with different occupancies or functions and located on sites with different soil conditions, the upgrading strategies can be vastly different.

In selecting the upgrading strategy the designer should examine the two sides of the design equation:

$$\text{DEMANDS} \leq \text{SUPPLIES} \qquad (1)$$

This equation shows that the designer can seismically upgrade an existing facility by: (1) decreasing the seismic hazard demands; (2) improving the facility's supplied mechanical (dynamic) characteristics; or (3) a combination of (1) and (2). A promising methodology for rational selection of upgrading strategies for existing hazardous facilities as well as for EQRD of new structures is one based on an energy approach, specifically on the use of an energy balance equation. Although Uang & Bertero (1988) have shown that two different basic energy equations can be derived from the basic equation of a viscous damped *Single Degree of Freedom System* (SDOFS) subjected to an EQGM, they have also shown that the maximum values of the Energy Input (E_I) are very close in the period range of practical interest for buildings, which is 0.3 to 5.0 secs. Therefore, the two basic energy equations can be rewritten as

$$E_I = E_E + E_D$$

$$E_I = E_K + E_\xi + E_H$$

$$\left(\begin{matrix}\textit{Input}\\ \textit{energy}\end{matrix}\right) \left\{\begin{matrix}\textit{Kinetic}\\ \textit{energy}\end{matrix}\right. \left\{\begin{matrix}\textit{Elastic}\\ \textit{strain}\\ \textit{energy}\end{matrix}\right. \left\{\begin{matrix}\textit{Damping}\\ \textit{energy}\end{matrix}\right. \left\{\begin{matrix}\textit{Hysteretic}\\ \textit{energy}\end{matrix}\right.$$

where E_E *is the stored elastic energy and* E_D *the dissipated energy*. A comparison of this equation with the design equation (1) makes it clear that E_I represents the demands, and the summation of $E_E + E_D$ represents the supplies. From analysis of Eqs. 2a and 2b it is clear that a good estimate of the E_I for the critical EQGM is the first step in selecting an efficient upgrading strategy. Next, the designer has to analyze whether it is possible to meet this demand just by keeping the behavior of the structure in the elastic range, or whether it is convenient to try to dissipate E_I as much as possible, i.e., to increase E_D. As shown in Eq. 2b, there are three ways to increase E_D: one is to increase the linear viscous damping (E_ξ); another is to increase the hysteretic energy (E_H); and the third is to increase both E_ξ and E_H. It is common practice at present to try to increase E_H through inelastic (plastic) behavior alone, which implies damage of the structural members. It has recently been recognized that it is possible to increase E_D significantly with energy dissipation devices such as viscous dampers (visco-elastic shear, or oil) and hysteretic dampers (friction, yielding metals and lead) [Bertero & Whittaker (1989) and Kelly & Aiken (1991)]. Although hysteretic energy dissipation devices by themselves do improve behavior efficiently at safety level, where some level of damage is tolerable, viscous dampers have the great advantage that they can be used to control the behavior of the upgraded structure under both safety and service levels. If technically and/or economically it is not possible to balance the required E_I through either E_E alone or $E_E + E_D$, the designer has the option of attempting to decrease the E_I to the structure with base isolation techniques. Combining base isolation techniques with energy dissipation devices is a very promising strategy both for upgrading existing hazardous structures and for EQRD of new structures. This energy approach requires the reliable selection, for each of the limit states that need to be considered (service, function, and/or safety), the critical design EQGM that controls the design, i.e., which has the largest damage potential for the structure. Most of the parameters used to establish design EQs are unreliable for assessing the damage potential of EQGMs. A promising parameter for this assessment is E_I. However, as discussed by Bertero (1991a & b) and Bertero & Uang (1991), E_I alone does not give a clear picture of the E_D that has to be supplied to balance the E_I for any specified acceptable damage, and the additional information given by E_ξ, E_H, μ_a (*cumulative ductility ratio*) and NYR (*Number of Yielding Reversals*) spectra is needed.

3.2 *Guidelines for selecting efficient upgrading strategy*

From analysis of design Eqs. (1) and (2), it is obvious that, generally, three main strategies can be considered for upgrading a seismically hazardous facility: (1) decreasing the earthquake demands [E_I in Eq. (2)]; (2) improving the facility's supplied mechanical (dynamic) characteristics [E_E and/or E_D in Eq. (2)]; and (3) both (1) and (2). It should be noted that strategies (1) and (2) are not independent, because the demands of seismic excitations depend on the mechanical characteristics supplied to the whole facility system. The following main guidelines should help with the selection of efficient upgrading strategies. In applying these guidelines it should be kept in mind that damage is more a consequence of deformation than of strength, and thus that in order to control damage it is desirable to limit the deformations, particularly the tangential interstory drift.

1. *Decreasing the demands*. If the effects of the expected critical EQGMs at the site at the different limit states are reliably defined by their response spectra [E_I, C_y *(yielding strength) and* S_d *(displacement)*, as illustrated in Fig. 1], the demands on the structure depend on the relation between the period of the structure, T, and the predominant period of the EQGM, T_{GM}. The largest response, and thus the largest demands on E_I and C_y, usually occur when $T/T_{GM} \approx 1$. Thus, one main strategy for decreasing demands is:

1a. *Shifting the T of the whole facility system*. How? By increasing or decreasing T depending on the ratio of T/T_{GM}. If $T \leq T_{GM}$ and the structure is on soft soil, the solution is usually to decrease T, because, as can be seen from Figs. 1(b), 1(d), 1(f) and 1(h), this decreases the demands. If the structure is on firm soil, with a T close to T_{GM}, and its C_y is very small, then the solution is to increase T with base isolation, because, as can be seen from Figs. 1(a), 1(c), 1(e) and 1(g), except for C_y

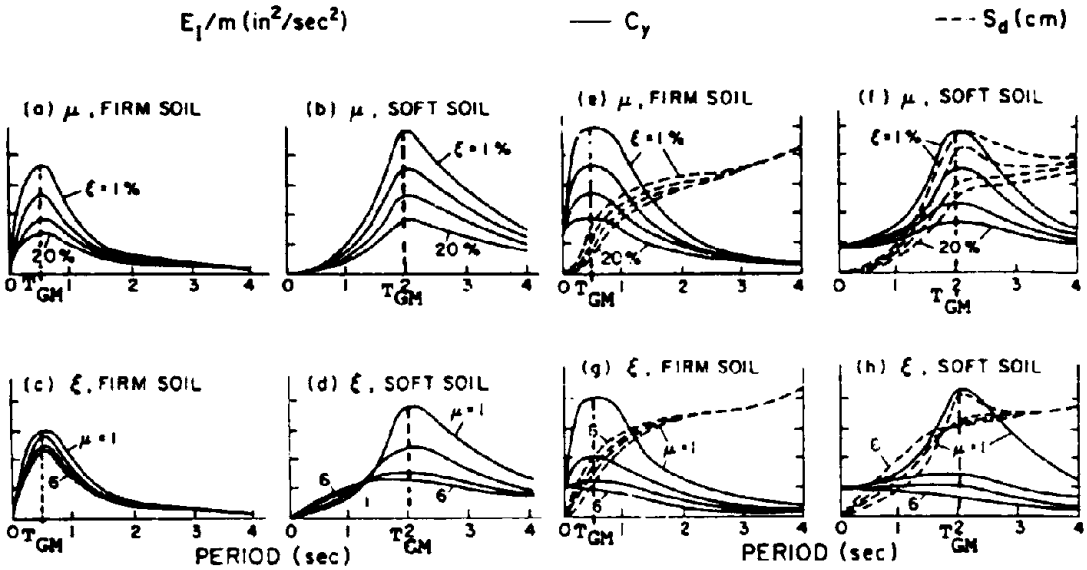

Figure 1. Qualitative illustration of the following response spectra E_I (energy input), C_y (yielding strength coefficient), and S_d (displacement) corresponding to firm and soft soil earthquake ground motions and the variation of these spectra when for: (1) a given ductility ratio, μ, the damping ratio, ξ, varies from 1 to 20%; and (2) a given ξ the μ varies from 1 to 6.

in the case of large μ, this decreases the C_y and E_I demands. However, Figs. 1(e) and 1(g) show that the increase in T can lead to a considerable increase in lateral displacement (S_d) demands - but this increase is concentrated in the base isolation elements, which are specially designed for such large displacements. In general, if base isolation cannot be used, T should be decreased by increasing the supplied stiffness and/or decreasing the mass, because both lead to smaller deformations and therefore to better control of damage. In practical applications of this strategy, the extent to which the T of the original structure has to be shifted depends on the reliability with which T and T_{GM} can be predicted.

1b. Another strategy for decreasing the demands is to *increase the damping ratio ξ [Figs. 1(a), 1(b), 1(e) and 1(f)], and/or to lower the C_y by increasing μ [Figs. 1(c), 1(d), 1(g) and 1(h)].* In the case of soft soils and where $T < T_{GM}$, the increase in μ could lead to larger values of input energy [Fig. 1(d)]. Comparison of Figs. 1(e) and 1(f) with Figs. 1(g) and 1(h) shows that when it is necessary to control deformations (S_d) at either service or safety level, and where $T < T_{GM}$, it is better to increase ξ than to increase μ, because at service level no inelastic deformations are acceptable, and at safety level an increase in μ results in an increase in S_d.

2. *Improving the dynamic characteristics supplied to the existing structure.* The demands depend not only on the dynamic characteristics of the EQGM, but also on the interaction of these characteristics with the dynamic characteristics supplied to the structure. Some guidelines for improving the supplied dynamic characteristics follow. The legitimacy of these guidelines is supported by the plots of Fig. 1.

2(a) *Decrease the reactive mass.* Why? Because it can result in a reduction of EQ inertia forces, and so will reduce the EQ's demand (this is particularly true in the case of $T \leq T_c$). How? By removing unnecessary weight, reducing the weights of walls, partitions, and so on -- in the case of a multistory building, removing one or more of the upper stories.

2(b) *Minimize the distance between the centers of mass, stiffness and resistance.* Why? To reduce torsional effects. How? By modifying the dispositions of reactive mass, stiffness and resistance of the structural elements.

2(c) *For flexible buildings on deep soft soil deposits, reduce the fundamental period.* Why? To avoid resonance problems with long period ground motions. How? By reducing the building's mass or increasing its stiffness or both. The stiffness can be increased efficiently with steel bracing and/or shear walls.

2(d) *For buildings lacking ductility, tie all of the lateral load resisting elements together to maximize the building's yielding and maximum strengths, or increase the damping, or both.* Why? It is difficult to improve the ductility of structural members, but relatively easy to increase a building's strength, reducing its required ductility. How? By a variety of means, e.g., using prestressed rods to tie the roof and floor slabs to the gravity load supporting elements and/or as bracing elements to enhance the building's lateral stiffness and strength. In the case of an isolated building, buttresses and outriggers can be used, as can dampers.

2(e) *For stiff structures lacking the necessary strength and ductility and subject to earthquake shaking with high frequency content, increase the building's fundamental period or increase its damping, or both.* Why? To reduce EQ demand by avoiding engineering resonance and decreasing the dynamic amplification factor. How? By some combination of eliminating infills, isolating nonstructural elements from the structure, adding dampers, using base isolation systems and using energy dissipation devices.

2(f) *For flexible buildings lacking ductility and located on soft soils and where interstory displacements are the major concern, increase the building's stiffness, strength, and damping.* Why? An increase in stiffness will decrease T, which, together with an increase in strength, will reduce deformations and ductility requirements; the increase in damping will reduce the required strength and the deformations. How? Through the use of braces in the form of prestressed rods, concentric braces and/or eccentric braces; or through the use of shear walls and energy dissipation devices. If the T of the building cannot be shifted very much, i.e., the stiffness and/or the reactive mass cannot be changed significantly, the supplied dynamic characteristics can be improved by a change (usually increase) of the: strength (C_y); μ; ξ, or a combination of these. Jirsa and Badoux (1990) formulate redesign strategies based on strength-ductility relationship.

2(g) *In selecting the retrofitting strategy, careful consideration should be given to the entire soil-foundation-superstructure-nonstructural component system, and not just to the superstructure.* Evaluation of the adequacy of the foundation is an essential step in the selection of the most appropriate strategy.

3.3 *Selection of appropriate technique and final design*

After the selection of the proper strategy, schemes by which it can be implemented must be developed and analyzed. The final implementation scheme must consider not only the technical aspects and the total cost of the upgrading, but must also minimize disturbance to the function of the building during upgrading. The latter consideration necessitates upgrading strategies which either (1) involve construction activity only on the external faces of the building or (2) require only minimal reconstruction work inside the building. Generally, the final upgrading strategy is a compromise among the optimal technical strategy, the strategy that demands the smallest construction costs, and the strategy with minimum disturbance to the building's occupants.

The ideal approach for obtaining an efficient upgrading program is, after selecting an efficient upgrading strategy and technique, to conduct the design and estimate the cost for the existing facility according to three alternatives regarding desired future performance: (1) the upgraded structure will realize all of the objectives of the presently accepted philosophy of EQRD for new buildings with a minimum possible extra cost in initial construction and the slightest possible sacrifice of the architectural features which would be required if the building could be designed for just gravity loads; (2) under the maximum credible EQGM, the upgraded building will not only be safe but operational as well; and (3) the structure will not suffer any damage even under safety EQGMs. The advantages and costs of each of these different designs should be explained to the client, and he or she should decide what is affordable.

The final design of the upgrading scheme must include both detailed analyses of the building's performance under all significant levels of EQGM, and complete details and procedures of the field work, because some techniques may be unfamiliar to construction workers.

3.4 *Application of the concepts, strategies and guidelines to the upgrading of existing buildings*

The author and his research associates have conducted a series of detailed studies on the seismic upgrading of existing structures [Gu (1987), Bertero & Whittaker (1989) and Miranda (1991)]. Because of space limitations, only the *main observations* made in the application of the above concepts and guidelines are presented below. The details of the existing buildings and of the upgrading strategies and techniques investigated in these studies, as well as the main observations made in other projects in which the author acted as a consultant, will be illustrated and discussed in the oral presentation of this paper at the 10WCEE.

(1) For very flexible, insufficiently strong, low rise reinforced concrete buildings located on very soft soil, an efficient strategy is to decrease their fundamental periods by increasing stiffness or reducing reactive mass, or both. Usually the increase in lateral stiffness should be accompanied by an increase in the elastic (yielding) strength. Two efficient techniques for increasing stiffness and strength are bracing, usually steel, and RC shear walls. In the design of the bracing or shear walls, the following two approaches should be compared. One approach is to try to keep the response of the upgraded building in its elastic range (i.e., and *elastic solution*); the other is based on an *energy dissipating solution*, i.e., an attempt to dissipate part of the input energy through the use of energy dissipation devices.

(2) Of all the schemes considered, it was found that the elastic solution based on the use of high strength post-tensioned steel cables seems to be the most economical. From the standpoint, of extra safety, the use of steel bracing members incorporating energy dissipating devices appears to be the most promising.

4. CONCLUSIONS FROM SUMMARIZED STUDIES

1. Proper upgrading requires (1) reliable evaluation of the seismic activity at the facility site and its surroundings; (2) identification, by evaluation of both the seismic activity and the built environment around the facility, of the sources of seismic hazards to the facility; and (3) reliable assessment of the vulnerability of the whole facility system (soil-foundation-superstructure and nonstructural components) to the identified sources of seismic hazards, expressed as a fraction of its value.
2. Present seismic codes do not properly identify seismic activity and sources of seismic hazards at a facility site. Their methodology and procedures for evaluating the dynamic characteristics and particularly

the deformation capacity of the facility's whole system and of the response of this system to the expected critical EQGMs are inadequate.

3. There are many uncertainties in conducting vulnerability assessments of an existing whole facility system, even when "as built" drawings exist.

4. The importance of reliable assessment of the seismic risk to an existing facility cannot be overemphasized: If it is greatly overestimated, rehabilitation costs may be prohibitive; underestimation can result in costly damage and loss of life.
5. The commonly used criterion for upgrading seismically hazardous existing facilities is compliance with the building code seismic regulations for EQRD of new buildings. This usually results in inefficient rehabilitation of such buildings, and in some cases in prohibitively uneconomical upgrading solutions.
6. Although basic concepts and general guidelines for upgrading of structures have been formulated, the proper upgrading of a given facility is a unique problem requiring a customized solution.
7. The use of an energy approach, and particularly the use of an energy balance equation, offers a promising basis for rational seismic upgrading of existing hazardous structures.
8. Understanding and simultaneous examination of the basic design equation and the energy balance equation can guide the designer to selection of the most efficient strategy and technique for upgrading a seismically hazardous structure.
9. In developing and selecting an efficient upgrading strategy, it should be kept in mind that damage is more a consequence of deformation than of strength.
10. The first and most difficult problem in upgrading an existing facility is the reliable establishment of the redesign EQGM for each of the limit states that can control the redesign according to the main purpose of the upgrading program, which depends on the performance expected at the service, functional and safety levels. A promising approach for establishing these is the computation, plotting, and analysis of the E_I, E_E, E_H, C_y and S_d response spectra for each of the above levels of expected EQGMs.
11. In selecting the most appropriate retrofitting strategy and technique for improving the supplied dynamic characteristics, careful consideration should be given to the entire soil-foundation-superstructure-and-nonstructural component system rather than just to the superstructure. Stiffening and strengthening the structure may lead to changes which are significant not only in the demands on the existing foundation but also in the soil-structure effects.
12. In the selection of the upgrading technique, the designer should consider not only the design that is the most technically efficient and least expensive in construction costs, but also the one with the minimum disturbance to the function (operation) of the building during the upgrading. Generally, the optimum upgrading strategy and technique are compromises among the ideal technical strategy, the strategy least demanding in construction costs and the one that causes minimum disturbance to building occupants.

5. ACKNOWLEDGEMENTS

Most of the studies summarized in this paper were sponsored by the National Science Foundation, and this support is gratefully acknowledged. The author wishes to express his most sincere thanks to his graduate students, who conducted most of the detailed studies referred to in this paper.

REFERENCES

Bertero, V.V. & C.-M. Uang 1991. Issues and future directions in the use of an energy approach for seismic-resistant design of structures. Essex: Elsevier.

Bertero, V.V. 1991a. Structural engineering aspects of seismic zonation. *Proc 4th International Conference on Seismic Zonation 1:262-321.* Stanford University.

Bertero, V.V., 1991b. Earthquake hazard mitigation: The need for improving earthquake resistant code regulations. *Proc. 5th International Research and Training Seminar on Regional Development Planning for Disaster Prevention.* Nagoya: U.N Center for Regional Development.

Bertero, V.V., 1991c. Earthquake-resistant code regulations: Implications of recent EQs and research. *Proc. Int. Symposium on Building Technology and EQ Hazard Mitigation. 1-35.* Kunming: P.R. China.

Bertero, V.V. 1988. Earthquake hazard reduction: Technical capability - U.S. perspective. *Proc 2nd Japan-US Workshop on Urban EQ Hazards Reduction.* Shimizu: Tokai University.

Bertero, V.V. & A.S. Whittaker 1989. Seismic upgrading of existing buildings. *Proc. 5as Jornadas Chilenas de Sismologia e Ingeniería Antisísmica. I.27-46.* Santiago: Asociacion Chilena de Sismología e Ingeniería Antisísmica.

Dowrick, D.J. 1987. Earthquake-resistant design for engineers and architects. New York: John Wiley & Sons, Ltd.

Gu, T.J. 1987. Seismic upgrading of building structures using post-tensioning. Ph.D dissertation. CE: University of California at Berkeley

Jirsa, T.O. & M. Badoux 1990. Strategies for seismic redesign of buildings. *Proc. 4th US National Conference on EQ Engineering.* 3:343-351. Oakland: EERI.

Kelly, J.M. & I.D. Aiken 1991. Earthquake simulator testing of energy absorbing systems for multistory structures. *Proc. International Meeting on EQ Protection of Buildings:* 3/D-20/D. Ancona: Universitá Degli Studi di Ancona.

Miranda, E. 1991. Seismic evaluation and upgrading of existing buildings. Ph.D dissertation. CE: University of California at Berkeley.

Miranda, E. & V.V. Bertero 1991. Evaluation of the failure of the Cypress viaduct in the Loma Prieta EQ. *Bulletin of the Seismological Society of America 81:2070-2086.*

Uang, C.-M. 1988. Use of energy as a design criterion in earthquake-resistant design. *UCB/EERC-88/18.* University of California at Berkeley: EERC.

Investigation of coupled lateral-torsional response in multistory buildings

R. L. Boroschek
University of California Berkeley, USA

S. A. Mahin
University of California Berkeley, USA

ABSTRACT: The dynamic torsional behavior of an existing building that responded severely during service level earthquakes is presented in this paper. The building is a thirteen story "regular" space frame structure. The recorded responses of the building during different earthquakes were characterised by long duration, narrow banded motions with strong amplitude modulation; by large translational and torsional motions; by large amplification of the input ground motions; and by slow decay of the building's dynamic responses. Records are studied to obtain the building's dynamic properties and response envelopes. The causes for the severe response are identified from these studies. Three dimensional linear and nonlinear models of the building are developed to match the recorded response of the structure. Parametric studies are perform on the analytical models to study the effects of material and geometric nonlinearities, accidental eccentricities, bi-directional input ground motions and energy dissipation capacity in the response of the building. Results indicate that the severity of the torsional response in a eccentric multi-story structure is strongly influenced by the level of inelastic behavior, level of eccentricity, ground motion characteristics and the structure's energy dissipation capacity.

1 INTRODUCTION

The lateral-torsional coupled behavior of structures has been the subject of a large number of studies. Investigations of this behavior have usually been undertaken using highly simplified linear or nonlinear computer models. With the extensive installation of strong motion instruments in structures around the world, it has become possible to monitor the actual three dimensional behavior of buildings during earthquake events and to study lateral-torsional coupling in these structures under different conditions.

A structure that exhibited strong lateral-torsional coupling in its recorded response, among other response characteristics of interest, is an apparently regular thirteen story office building, located in San Jose, California, Fig. 1. This building is instrumented with twenty-two unidirectional strong motion accelerographs, positioned in five different levels (ground, 2, 7, 12 and roof) at the NW, SW and SE corners of the square frame plan (Lines B and 12, Fig. 1). The structural system consists of steel moment resistant space frames. A strong moment resisting frame, Lines 2-12-A-B, is located around a lighter moment resisting frame. A much lighter frame is located outside the strong frame, Lines 12-13 and A-B.

Several earthquake records have been obtained in this structure. The three most intense responses recorded to date are those obtained during the Morgan Hill earthquake of April 24, 1984 (M_l = 6.2), the Mt. Lewis earthquake of March 31, 1986 (M_l = 5.8) and the October 17, 1989 Loma Prieta earthquake (M_l = 7.1). Peak horizontal ground accelerations recorded for these events at the base of the building were 4, 4 and 11 % g, respectively. The building substantially amplified these base motions so that the maximum structural accelerations during the earthquakes were 17, 32 and 36 % g, respectively. Motions of the structure during all the earthquakes caused widespread damage to contents and disruption of services. The response records exhibit a strongly modulated pattern and locally indicate that the structure experienced substantial torsion, Figs. 2, 3 and 4. Another feature of the responses shown in these figures is that the structure continued to vibrate vigorously for more than 80 seconds. The input motion was much shorter in duration and maximum structural responses occurred generally long after the end of the strong motion portion of the base excitation.

2 RESPONSE OF SIMPLE ECCENTRIC FRAMES

Considerable insight on the effects of small eccentricities in nearly regular multi-story space frames can be obtained considering simple three degrees of freedom one story frame systems. The dynamic characteristics of a one story frame can be obtained by formulating the eigenvalue problem at the structure's center of mass (CM) in terms of the total global stiffness at the center of stiffness (CS) and the distance between these centers as follows:

$$\left[\begin{bmatrix} K_x & -K_x e_y & 0 \\ -K_x e_y & (K_\theta + K_x e_y^2 + K_y e_x^2) & K_y e_x \\ 0 & K_y e_x & K_y \end{bmatrix} - m\omega_n^2 \begin{bmatrix} 1 & 0 & 0 \\ 0 & r^2 & 0 \\ 0 & 0 & 1 \end{bmatrix}\right] \begin{bmatrix} v_{xn} \\ v_{\phi n} \\ v_{yn} \end{bmatrix} = \begin{bmatrix} 0 \\ 0 \\ 0 \end{bmatrix} \tag{1}$$

where: K_x is the story translational stiffness in the X direction at the center of stiffness, K_y is the story translational stiffness in the Y direction at the center of stiffness, K_θ is the story torsional stiffness at the center of stiffness, r is the story radius of gyration of the plan, e_x is the distance from the center of mass to the center of stiffness in the global X direction, e_y is the distance from the center of mass to the center of stiffness in the global Y direction, ω_n is the natural frequency form mode "n" and $n = 1, 2, 3$, v_{xn}, $v_{\phi n}$, and v_{yn} are the translational and rotational components of mode n.

The general eigenvalue problem presented here cannot be solved in closed form because of its cubic characteristic equation. Nevertheless, this equation can be solved for the special case of identical translational stiffness in orthogonal directions. Then $K_x = K_y = K$. The solution of this special problem, with a single translational stiffness K, will provide insight into the more general problem.

The eigenvalue solution for this system can be expressed as:

$$\Omega_{1 \text{ or } 3} = \frac{1}{2}\left\{\left(1 + \left(\frac{e_o}{r}\right)^2 + \left(\frac{e}{r}\right)^2\right) \mp \left[\left(1 + \left(\frac{e_o}{r}\right)^2 + \left(\frac{e}{r}\right)^2\right)^2 - 4\left(\frac{e_o}{r}\right)^2\right]^{\frac{1}{2}}\right\}$$

$$\Omega_2 = 1 \tag{2}$$

where: $e^2 = e_x^2 + e_y^2$ is a measure of global eccentricity, $\Omega_n = (\omega_n/\omega)^2$ is ratio of coupled to uncoupled frequencies, $\omega = K/m$, and $e_o^2 = K_\theta/K$ is the ratio of torsional to translational stiffness at the center of stiffness. (Note that $(e_o/r)^2$ is equal to the ratio of translational to torsional periods of an uncouple system.)

After some numerical manipulation it can be shown that:

$$(1 - \Omega_1)(1 - \Omega_3) = -\left(\frac{e}{r}\right)^2 \tag{3}$$

These equations indicate that for similar uncoupled torsional and translational periods (values of e_o/r close to one), and small static eccentricities, the three coupled natural periods of the system could be extremely close.

The mode shapes that correspond to this eigenvalue solution have the following form if $e_x \neq 0$ and $e_y \neq 0$:

$$\Phi = \begin{bmatrix} \frac{e_x/r}{1-\Omega_1} & \frac{e_x}{e} & \frac{e_x/r}{1-\Omega_3} \\ 1 & 0 & 1 \\ \frac{-e_y/r}{1-\Omega_1} & \frac{e_y}{e} & \frac{-e_y/r}{1-\Omega_3} \end{bmatrix} \tag{4}$$

Then the mode that corresponds to Ω_2 (=1) is a pure translational mode: the predominant direction of the mode is skewed relative to the reference axes, in accordance with the global eccentricity.

Close torsional and translational uncoupled periods are typically observed in systems that have uniform distribution of stiffness in plan (Newmark (1969)). For regular space frame structures these periods can then be quite close. It can be shown that for one story frames or multi-story frames with only three degrees of freedom per story (chain system) the ratio of translational to torsional uncoupled periods can be obtained by Equation 5 if the system has the following characteristics: a) multiple columns evenly distributed, b) uniform distribution of mass, c) coincident center of mass and stiffness, d) all columns with the same stiffness in a given direction, e) a shear behavior with three degrees of freedom per story (two horizontal translations and one in-plane rotation at center of mass), d) all vertical elements with negligible torsional stiffness, and e) radio of gyration defined in terms of the external column position and distributed mass.

$$\left(\frac{T_{uc}}{T_{ut}}\right)^2 = \frac{[(\frac{d_x}{d_y})^2(\frac{k_x}{k_y})(N_x^2 - 1) + (N_y^2 - 1)]}{(N_x - 1)^2(\frac{d_x}{d_y})^2 + (N_y - 1)^2} \tag{5}$$

where: $N_{x \text{ or } y}$ is the number of column lines in the x or y direction, $d_{x \text{ or } y}$ is the spacing between two consecutive columns in the X or Y direction, $k_{x \text{ or } y}$ is the stiffness of a individual column in the X or Y direction, T_{uc} is the uncoupled translational period

in the X direction, and $T_{\omega\theta}$ is the uncoupled torsional period.

For the special case of a square building with equal structural systems in both directions, this formula can be simplified as follows:

$N_x = N_y = N$, $d_x = d_y$ and $k_x = k_y$,

so that

$$\left(\frac{T_{\omega x}}{T_{\omega\theta}}\right)^2 = \frac{(N+1)}{(N-1)} \tag{6}$$

It can be seen in Fig. 5 that this ratio quickly approaches one as the number of columns increases.

For regular frames with an even distribution stiffness in plan and small eccentricities the following assumption can be made $(e/r)^2 \ll 1$ and $(e_o/r)^2 \approx 1$. So Equations 2 and 4 can be approximated by:

$$\Omega_1 \approx 1 - \frac{e}{r};\ \ \Omega_2 = 1 \text{ and } \Omega_3 \approx 1 + \frac{e}{r} \tag{7}$$

and

$$\Phi = \begin{bmatrix} \frac{\phi_{1y}}{\sigma\sqrt{2}} & \frac{\phi_{1x}}{\sigma} & -\frac{\phi_{1y}}{\sigma\sqrt{2}} \\ \frac{1}{\sqrt{2}} & 0 & \frac{1}{\sqrt{2}} \\ -\frac{\phi_{3y}}{\sigma\sqrt{2}} & \frac{\phi_{3x}}{\sigma} & \frac{\phi_{3y}}{\sigma\sqrt{2}} \end{bmatrix} = [\Phi_1 \ \ \Phi_2 \ \ \Phi_3] \tag{8}$$

where: the mode shapes are normalized so that $\Phi_i^t \Phi_i = 1$, (see also Kelly (1990)).

Finally, the coupled natural frequencies of the system can be found from Equation 7 making use again of the assumption of small eccentricities:

$$w_1 \approx w\left(1 - \frac{1}{2}\frac{e}{r}\right);\ w_2 = w;\ w_3 \approx w\left(1 + \frac{1}{2}\frac{e}{r}\right) \tag{9}$$

The closeness of the predominant periods and the three dimensional characteristics of the modes shape will produce responses that can increase substantially the severity of the linear response of the coupled system (see Boroschek (1991)). Also the time history responses of this systems are strongly modulated (beating behavior).

3 BUILDING RECORDED RESPONSE

The recorded response of the San Jose building have been studied extensively, for example, Boroschek and Mahin (1989; 1990; 1990; 1991). Basic dynamic properties and response envelopes were obtained directly from the records. The dynamic properties of the building are presented in Table 1. The maximum response envelopes obtained during the three earthquakes studies are presented in Table 2. Figures 2 through 4 show some time histories obtained in the building.

It can be concluded, from the analysis of the response records, that the building presents a rather flexible structural system with relatively low damping. The predominant period was found to be near 2.2 seconds and modal damping is believed to be below 3% of critical. Because of the similar frame structural characteristics in both directions and the even distribution of stiffness in plan, the predominant periods of the system are quite close. The closeness of the periods together with small eccentricities present in the structure produced the strongly coupled lateral-torsional behavior observed in the records. Because of the spatial characteristics of the frame, the coupling affects both directions and the rotation for most of the modes studied. The eccentricity that produce the torsionally coupled response can be associated with the irregular distribution of the mass and framing irregularities caused by a greater number of structural and nonstructural elements on the west and south sides of the building.

The structure responded strongly to these relatively minor earthquakes. It is believed that the intensity of the structural response was caused by the building's relatively low damping, the three-dimensional modes of the building constructively reinforcing one another during portions of the motion, the input duration, the possible resonance effect on

Table 1: Natural periods and damping.

Predominant Direction	Mode	Period (sec)	Damping[a] (%)
EW	First	2.15-2.20	2-3
NS	Second	2.05-2.10	2-4
Torsion	Third	1.70	-
EW	Fourth	0.65-0.75	-
NS	Fifth	0.60-0.70	-

(a) Values based on the appearance of response wave forms.

Table 2: Response maxima.

Response Values	MH 1984	ML 1986	LP 1989
H Base Peak Rec. Acc. (g)	0.04	0.04	0.10
V Base Peak Rec. Acc. (g)	0.02	0.02	0.11
Max Str. Acc. (g)	0.17	0.32	0.34
Max Str. Amp.[a]	4.87	7.05	3.84
Max Str. Drift (cm)[b]	18.64	33.19	38.17
Max Torsional Disp (cm)[c]	7.28	12.22	12.32
Max Drift Index[b]	0.41	0.72	0.85
Input Duration EW (sec.)	55	27	28
Input Duration NS (sec.)	56	32	35
Base Shear EW (V/W)	0.08	0.06	0.18
Base Shear NS (V/W)	0.09	0.15	0.17

(a) Defined as the ratio of the peak acceleration at a location to the corresponding acceleration at the ground. (b) At recording position. (c) Maximum difference between recordings at same building side.

the building caused by the close match of the dynamic characteristics of the site and the structure and the relatively large flexibility of the structure.

4 ANALYTICAL MODELING AND PARAMETRIC STUDIES

Three-dimensional linear and non-linear numerical models of the complete structure were developed to simulate the recorded responses and to perform parametric studies. Static and dynamic analyses were performed. The dynamic analyses consider unidirectional as well as bi-directional input motions with and without torsional input excitations. Several parameters were monitored during the analyses: maximum displacements, interstory drifts, base shear, maximum ductility demands, maximum cumulative ductility and element forces. The final model had 2418 elements.

4.1 *Linear models*

The model was developed using information from building plans and site inspections. A good match was obtained when the models included the center-to-center member dimensions (i.e., no rigid panels were included to model the flexibility of the beam-column joints), mass magnitude and distribution as estimated from structural plans, nominal element properties, and a modal damping ratio typically associated with steel structures responding in the linear range (1-3% of critical). By further adjusting the actual mass distribution and incorporating the deck contribution to the beam stiffness, computed global results were virtually identical to recorded values.

From analyses of different loading conditions it was concluded that in order to reproduce the building's response, both horizontal components of the ground records should be included. Bi-directional effects accounted for nearly 22% of the response in orthogonal directions. Torsional input motion had a small effect on the overall response of the structure.

The damping ratio did have an important effect on the response of the models. Because of the rapid fluctuations of spectral accelerations with periods present in lightly damped systems, the response of the low damping models used in the study were very sensitive to modeling uncertainties that influence the period estimates.

Also the models showed a strong sensitivity to the position of floor center of mass. Increasing the eccentricity by 5% of the building's largest plan dimension reduced displacements and shears in both directions by a maximum of 36% and increased floor rotations by nearly 144% and base torque by 160%. The ratio of maximum base torque to maximum base shear was increased by 180% when this additional eccentricity was included.

The modal coupling was quite sensitive to design model parameters. Small changes of stiffness in one direction reduce the coupling, in some modal components, by nearly 75%. This demonstrates the difficulty in reproducing the coupled behavior of the structure.

The linear models confirmed that the severity of the response was caused in part by the modal interaction of the three dimensional structural modes. Figure 6, for example, shows the response of a model with relatively low damping to the first 40 seconds of the Mt. Lewis earthquake. In part (a) of the figure the response of the analytical model with 1% viscous damping is compared with the recorded motion. Parts (b) and (c) of the figure show the first and second mode contribution to the displacement in the EW direction. Here it can be seen that the first and second modes individually have lightly attenuated responses after about 30 seconds of motion. However, the two modes go in and out of phase, resulting in constructive and destructive interference that produces a large dip in the combined response at second 30 and an increase in response up to second 60.

An analysis was also performed considering 5% viscous damping. Here (Fig. 6d), the response of the individual modes attenuate so quickly that virtually no beating under free vibration can occur and little significant motion occurs after 35 seconds.

4.2 *Nonlinear models*

The building studied did not suffer significant inelastic behavior, so the nonlinear characteristics of the models were not fit to any of the observed responses. Nevertheless the nonlinear model was used to study the effect of nonlinearities, additional eccentricities, damping and ground motion characteristics in the global response of the system. The elements developed by Riahi et al (1978) were used in the analysis. These elements are three dimensional beam-columns with a multidimensional interaction yield surface (P, M_y, M_z, M_s).

Initially a nearly triangular static lateral loading was applied to the structure. The load deformation curve showed that, due to the pattern of yielding, torsional rotations can grow more rapidly than the displacements at the center of mass in the direction of loading, Figs. 7 and 8. Nevertheless, after severe yielding of the system has occurred the displacement grows much faster than torsional rotations (energy dissipating mechanism is mainly translational). In other words, apparent coupling between translations

and rotations in a multi-story structure is highly dependable on the story of loading, inelastic distribution and level of inelastic behavior.

For the dynamic studies five earthquake records were considered: the recorded base building records during the Morgan Hill (1984), Mt. Lewis (1986) and Loma Prieta (1989) events (because of their period characteristics these are considered as a soft site records), as well as the Mexico SCT (1985) and El Centro (1940) events. Both horizontal components of these earthquakes were used in all the analyses. The records were scaled to different values of effective peak acceleration to obtain the response of the structure at different levels of inelastic behavior.

Analyses using different ground motions indicate that the properties of the input motion have a strong effect on the response of the models. These differences are more pronounced for elastic than for inelastic responses.

It was found that the ratio of in-plane torsional rotations to lateral displacements ("apparent coupling") could increase or decrease depending on the level of inelastic behavior and the characteristics of the input ground motion. Nevertheless, some scatter was found from the results. This indicates that more analyses are needed to identify a trend on the response and its relation to the observations regarding decoupling of torsional and lateral motions made on the basis of the static load to collapse studies and the effect of input motion predominant direction observed from the recorded torsional response of the building and simple linear models studied by Boroschek (1991).

Results from the analyses that considered added mass eccentricities indicate that, contrary to what was found for models subjected to unidirectional inputs, displacements at center of mass (or at a fixed point on the story plan) could decrease or increase depending on the building's characteristics and the properties of the input ground motion. An increase in eccentricity, from 0 to 10% of the maximum building dimension, had the effect of increasing the maximum rotational ductility demand on the strong frame girders (maximum increment was 22%) and reducing the cumulative ductility demand on these same elements (maximum reduction was 58%). On the other hand, for the elastic models, the variation of moment ratios for the strong frame girders increased (up to 40%) or decreased (25%) for the different ground motions studied. Similar trends were observed for the inter-story drifts.

Also, the addition of this eccentricity had the effect of redistributing inelastic demands between orthogonal directions. In some cases the maximum ductility demand for a given earthquake changed from one direction to the orthogonal direction, when the additional eccentricity was included.

5 CONCLUDING REMARKS

The results of this investigation agree with findings from the analyses of simple structures developed in other investigations. In general, the existence of torsional behavior in nearly regular space frames has the effect of increasing the stress or ductility demands in elements located far away from the center of rotation and changes the maximum translational displacements. These effects are more severe for elastic structures than inelastic structures and are highly dependent on the characteristics of the input ground motion.

REFERENCES

Boroschek, Mahin, and Zeris (1990). "Seismic response and analytical modeling of three instrumented buildings." 4 US Nat. Conf Earthquake Eng.

Boroschek, R. L. (1991). "Investigation of the seismic response fo a lightly damped torsionally coupled building." PhD thesis, Civil Engineering. U of California Berkeley.

Kelly, J. (1990). "Coupled lateral torsional response of base isolated buildings." Course 290D Notes, U of California, Berkeley.

Mahin, Boroschek, and Zeris (1989). "Engineering interpretation of responses of three instrumented buildings in San Jose." *Seminar on Seismological and Engineering Implications of Recent Strong Motion Data*, SMIP.

Newmark, N. M. (1969). "Torsion in symmetrical buildings." In *Proceedings of Fourth World Conference on Earthquake Engineering*, Chile.

Riahi, A., Row, D. G., and Powell, G. H. (1978). *ANSR-I : INEL-2 & 3. Three Dimensional Inelastic Frame Elements For The ANSR-I Program*, EERC 78-06,.

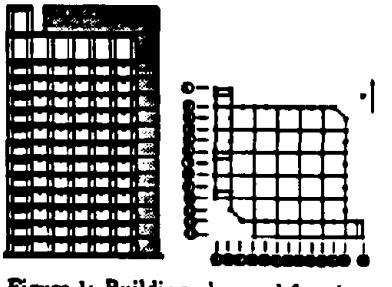

Figure 1: Building plan and framing.

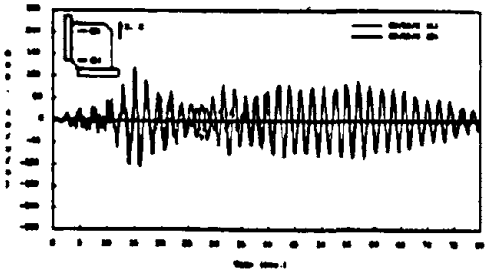

Figure 2: Twelfth floor acceleration records. EW direction. Mt. Lewis earthquake.

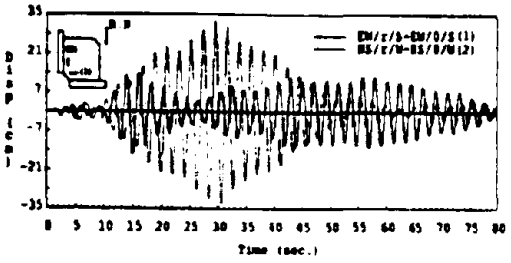

Figure 3: Roof SW corner relative displacements. Mt. Lewis earthquake.

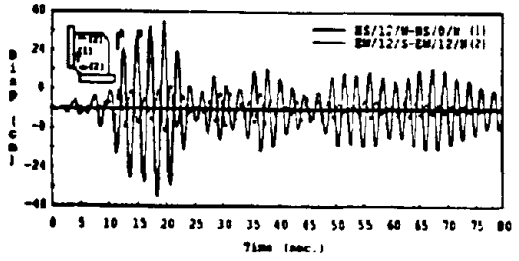

Figure 4: Twelfth floor NS relative displacements (SW corner) and torsion (EW records). Loma Prieta earthquake.

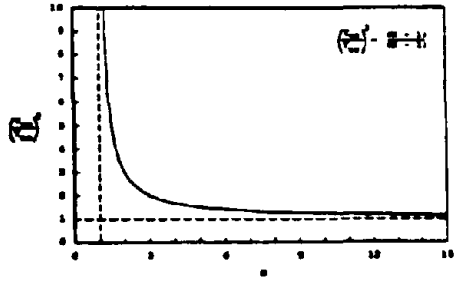

Figure 5: Ratio of uncoupled translational and torsional periods for a regular one story structure.

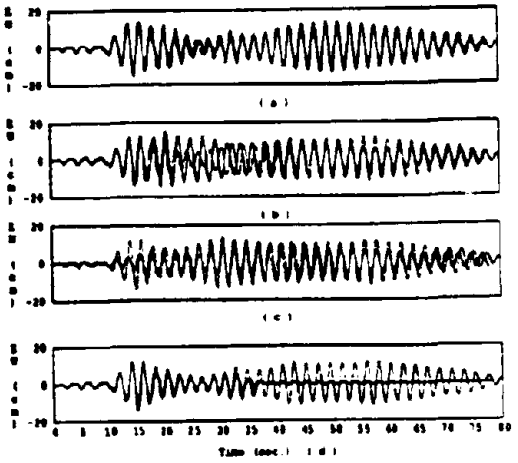

Figure 6: Twelfth floor motion Mt. Lewis event. Input ground motion 0-40 seconds. EW relative displacement, SW corner. a) First three modes, low damping model (1 %). b) First mode, low damping model. c) Second mode, low damping model. d) First three modes, moderate damping model (5 %). Model —— Record ·····.

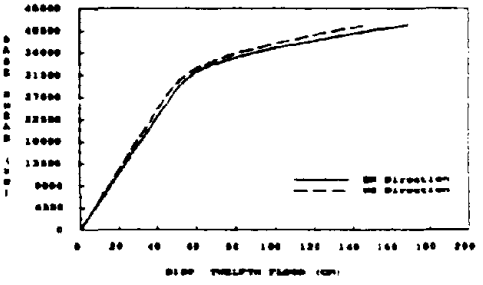

Figure 7: Base shear-twelfth floor displacement. EW and NS directions.

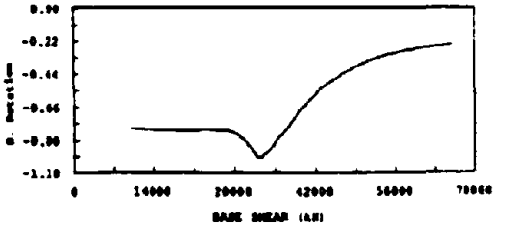

Figure 8: Normalized twelfth floor torsional rotations (θ/Δ_{EW}) at Center of Mass. Static-to-collapse analysis for the EW direction.

Qualitative reasoning about seismic behavior of buildings

Luis M. Bozzo
Department of Civil Engineering, University of California at Berkeley, U.S.A.

Gregory L. Fenves
Department of Civil Engineering, University of California at Berkeley, U.S.A.

ABSTRACT: The use of expert systems to evaluate the seismic performance of buildings is often limited by the shallow level of knowledge included in the rule–base. An alternative methodology, qualitative reasoning, derives exact qualitative solution of physical problems based on representations of fundamental principles. The principles governing the seismic behavior of structures are the conjugate laws of equilibrium and compatibility, and force–displacement relationships of the structural components. A new qualitative reasoning methodology, called the space centered approach, is suitable for the preliminary design of earthquake resistant buildings. The methodology enables the engineer to determine the internal force and deformation distributions in a structure and to detect possible undesirable behavior at a very early stage of the design. Application of the space centered approach to structural systems under lateral loads, implemented using logic programming, provides useful information about the the signs and relative magnitude of forces and deformations in a structure.

1 MOTIVATION

Recent developments in computer software for structural analysis have provided valuable tools for generating and analyzing precise mathematical models of structures subjected to earthquake ground motion. Numerical solutions to governing equations provide detailed information about the structural and non–structural demands. However, the detailed information required for a quantitative analysis may not be available at early stages in the design of a structure. Even if the design is sufficiently refined that detailed information is available for constructing a model, the influence of factors such as material characteristics, soil conditions and influence of non–structural components, may not be investigated. Emphasis on the conceptual seismic design of structures, rather than numerical analysis, is one way to achieve good solutions to the earthquake resistant design task. Given a conceptual design of a structure, knowledgeable engineers can reason, in many cases, the direction and relative magnitude of the internal forces and displacements. The important load transfer characteristics and possible undesired structural behaviors can and should be identified early in the design process. This goal motivates the application of qualitative reasoning to evaluate the behavior of structures using only the limited information available from a preliminary design.

2 INTRODUCTION

Qualitative reasoning attempts to explain in an automated way how the model of a device functions by representing the fundamental or first principles for the domain (Weld and De Kleer 1990). In the context of structural engineering, the function of a building is to transfer safely the seismic and gravity loads to the foundation, and the structural behaviors are the internal mechanisms such as bending moments, torsional moments, shear forces, axial forces, displacements and rotations developed in resistance to loads.

Qualitative reasoning derives behavior from the structure of a model and not from experience or heuristic knowledge. Compared with the shallow level of knowledge represented in most expert systems, qualitative reasoning methodologies are called "deep models," because of the representation of fundamental principles.

There are important differences between quantitative and qualitative models. For quantitative models, the parameters are in a large, usually infinite, range of values such as the set of real numbers. Given complete information about the parameters, a *procedural computation* results in a unique solution which is valid only for the selected parameters. Even a small variation in the model requires a new analysis or at the very least an

evaluation of the sensitivity coefficients. For qualitative models, in contrast, parameters are represented by a small set of values, such as positive, zero, and negative. Given possibly incomplete information about the qualitative values of the parameters, a *search* results in a usually non–unique set of solutions. The set of solutions may include undesirable behaviors.

Various frameworks for the automated reasoning about qualitative models have been developed by researchers. Current qualitative reasoning methodologies, however, primarily apply to one–dimensional initial value problems. This paper presents a newly developed space centered approach for multi–dimensional static boundary value problems applied to structural engineering. The space centered approach is implemented in a program named *Agrippa*. Representing the principles of equilibrium, compatibility and material behavior, and using information about topology and incomplete information about geometry and material characteristics, *Agrippa* provides information about the load transfer characteristics and deformations of a structure. At the present, inelastic behavior and dynamic response are not included in the reasoning capabilities of *Agrippa*.

An optimal design for a building under static loads can be achieved by minimizing an objective function, typically the total weight of construction materials. For earthquake resistant design, however, there is no simple objective function which can be used to achieve an optimal design. Instead engineers select robust designs by criteria such as redundant load paths, ductile failure modes and energy dissipation capacity, among others (Aktan and Bertero 1984). An interpretation of the qualitative structural evaluation performed by *Agrippa* provides the engineer with insights about the loads paths and type of failure modes that may be expected in the structure. The qualitative evaluation of a planar frame and a three–dimensional frame subjected to lateral loads demonstrates the usefulness of the methodology.

3 SUMMARY OF PREVIOUS WORK

Pertinent research can be divided into general qualitative reasoning frameworks and heuristic structural evaluation methodologies. This section briefly presents four qualitative frameworks and four heuristic structural evaluation approaches.

3.1 General frameworks

The four basic methodologies for qualitative reasoning are the component (De Kleer 1984), the process (Forbus 1984) the constraint (Kuipers 1984), and the unifying (Bredeweg 1990) approaches. The component centered approach models physical behavior based on the qualitative states of individual components. The values of the parameters defining the component states are qualitatively represented as positive, zero or negative.

The process centered approach represents physical laws explicitly as primitives which induce changes in the qualitative states of the model. In the process centered approach, parameters have a qualitative value, as in the component centered approach, and they are partially ordered by magnitude. Ordering relations between qualitative parameters are called *parameter relations*. The constraint centered approach models physical laws directly as qualitative equations. The lack of primitives limits its modeling adequacy but increases the inference efficiency. A parameter value is represented by an ordered set of intervals defined by the user, and parameter relations are not used in the constraint centered approach.

The unifying approach represents qualitative states of components as well as processes in a common framework. Changes in the states of the model are caused by processes and individual components. The unifying approach uses parameter relations, as with the process centered approach, but it also enhances the calculus with a specialized algebraic simplifier called *constant elimination* (Bredeweg 1990). Constant elimination reduces ambiguity by deriving new relations based on previous ones. For example, with relations such as $a+b=f$ and $f=g+c$, the constant elimination procedure derives the relation $a+b=g+c$.

3.2 Heuristic structural evaluation

A basic difference between qualitative reasoning and the heuristic methodologies is that qualitative reasoning does not derive conclusions based on experiential knowledge but from the fundamental principles of the domain applied to the specific problem. A methodology to derive the displacements and forces in continuous beams was developed by Slater (1986). Heuristic knowledge about the location of inflection points is used to transform a statically indeterminate structure to a determinate one.

In the earthquake engineering field two knowledge–based expert systems have been recently developed. Both systems represent a shallow level of knowledge and a slight variation from the scope of the rules could give incorrect results. The knowledge base by Subramani (1989) represents building code information for heuristic estimates of structural periods, base shears, story drifts, eccentricities and torsional effects. The knowledge base by Ganguly (1990) evaluates preliminary designs using so–called causal links between selected structural behaviors. Conclusions derived from heuristics are

usually too general to be useful. For example, if a building is asymmetric, an expert system (Ganguly 1990) would conclude that torsion exists, but the elements resisting the torque are not provided. In contrast, *Agrippa* indicates which components develop a torque and the relative values of the internal forces. In this regard, qualitative reasoning provide information of intermediate detail with respect to heuristic methodologies and quantitative analysis.

Recently a framework using kinematic assumptions, similar to Slater (1986), and qualitative reasoning has been developed for analyzing continuous beams under gravity loads (Fuchter 1991). Using a forward chaining inference scheme, this methodology derives displacements and forces based on equilibrium relations. Material characteristics and compatibility are not represented in the aforementioned approaches, consequently they can only be used for standard structures in which the general response characteristics can be described from experience.

4 SPACE CENTERED APPROACH

The space centered approach is a qualitative reasoning methodology suitable for static boundary value problems. As with the component centered approach, components (such as frame members, walls and supports) have a set of valid states for equilibrium, compatibility, and material behavior. As with the process centered approach, equilibrium and compatibility are represented as processes acting upon connections, and parameters are represented by qualitative values and parameter relations. Finally, as with the unifying approach, constant elimination enhances the ambiguity resolution of qualitative calculus. An extension in the space centered approach compared with the earlier general frameworks is that parameters such as frame member directions, stresses and displacements are explicitly represented as vectors.

The quantity space, qualitative calculus, modeling primitives and inference scheme for the space centered approach are discussed in the following subsections.

4.1 Quantity space

Parameters are represented qualitatively by a small set of ordered intervals. A typical quantity space consists of three qualitative values: positive, zero, and negative. This quantity space provides the direction of the forces and displacements, which is the minimum information necessary for conceptual understanding of structural behavior. The quantity space is further restricted by eliminating the zero value, except if a parameter is defined to be zero, to avoid solutions in which a particular geometry and stiffness result in exactly a zero value.

A parameter can be a scalar or a vectorial quantity. For example, length is a scalar which is always positive, but the direction of a frame member is a vector represented as a three tuple (X,Y,Z), where X, Y and Z are scalar parameters for the direction cosines of the member. In contrast, the previous general frameworks would represent a vector as individual parameters interrelated by a process.

4.2 Qualitative calculus

A qualitative calculus is a set of rules that govern the operations on qualitative values. For example Table 1 presents the addition operation as originally used for the process centered approach (Forbus 1984). Qualitative calculus (De Kleer 1984) could lead to physically infeasible solutions. To avoid infeasible solutions, the space centered approach uses parameter relations such as "greater than," "smaller than," and "equal to." The addition of positive and negative values can be disambiguated by the extended addition operation in Table 1. The algebraic sign of a parameter is represented by its qualitative value and the magnitude is ordered with respect to other parameters by parameter relations.

Parameter relations do not eliminate all invalid solutions, so constant elimination is required (Bredeweg 1990). When a new equilibrium equation is obtained, constant elimination derives new equations based on existing equilibrium relations. The generation of all free body diagrams can still be computationally demanding, therefore the algorithm only derives equations within a specified maximum depth criterion.

Table 1. Extended addition operation

EXTENDED ADD R = X + Y		X	X	X
				+, |X| > |Y|
Y	-	-	-	0, |X| = |Y|
				-, |X| < |Y|
Y	0	-	0	+
		+, |X| < |Y|		
Y	+	0, |X| = |Y|	+	+
		-, |X| > |Y|		

4.3 Modeling primitives

The modeling primitives include individual component's qualitative states and connection processes. The structural behavior of a component is represented as a set of qualitative states that

satisfy the fundamental principles of equilibrium, compatibility and force–displacement. A typical component is a frame member, and end connections define the interaction between the frame member and the rest of the structure. The component description includes all possible behaviors of the following types: 1) the qualitative values for the forces, moments, displacements and rotations that satisfy equilibrium, compatibility and material characteristics; and 2) the parameter relations between qualitative values at the two ends of the frame member. Using equilibrium laws it is possible to derive that a planar frame member has seventeen bending states, and in similar manner, other states of structural behavior can be enumerated. Another component is a structural support, such as roller, pinned, or clamped, in which the states are defined by the parameter values transferred by the support.

The conjugate beam analogy shows the similarity between the equilibrium and compatibility laws. The analogy allows the representation of equilibrium and compatibility using similar predicates. In qualitative terms a linear elastic material and an elastic softening material are the same, as illustrated in Fig. 1, using the conjugate beam analogy. For linear material it is possible to conclude that if the moment M_1 is greater than the moment M_2, then the conjugate force F_1 is greater than F_2, and an elastic softening material accentuates this relationship. Similar conclusions could be derived for the relations between displacements because softening translates the center of gravity of the conjugate loads closer to the ends of the member.

Equilibrium and compatibility at the connections are represented by global processes. A valid qualitative description is reached if each component has a valid qualitative state and equilibrium and compatibility at the connections are satisfied, along with equilibrium of all free body diagram specified in the search depth. Equilibrium at the connections means that the addition of qualitative forces and moments applied at a given connection must be zero. Compatibility at the connections means that all components attached at the connection have the same qualitative displacements and rotations. Constant elimination derives new equilibrium relations based on equilibrium at the connections, which correspond to relations for the free body diagrams.

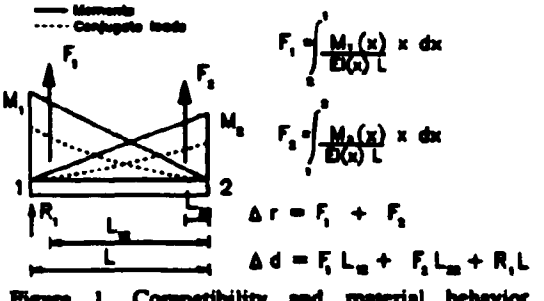

Figure 1. Compatibility and material behavior processes using conjugate beam analogy.

4.4 Inference scheme

The inference scheme is a backward–forward procedure. The process begins by deriving all possible conclusions based on specified parameter values. When no further information can be derived, the backward procedure selects a valid qualitative component state that satisfies global equilibrium and compatibility. From this new information, consistent qualitative values are specified in a forward procedure. New states are assumed until a complete description is achieved.

Figure 2 shows the inference tree for a continuous beam with a concentrated moment applied at the center joint. The inference scheme starts by assuming one out of the three valid component states for member 1. The compatibility process requires member 2 to have the same rotation as member 1 at the common joint, therefore member 2 has only one valid state. From the three possible solutions for member 1, only the first one satisfies equilibrium of the joint.

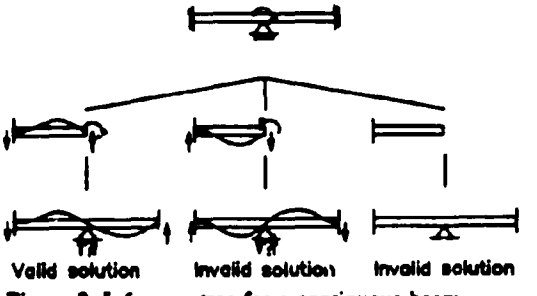

Figure 2. Inference tree for a continuous beam.

5 IMPLEMENTATION

The space centered approach has been implemented in the computer program *Agrippa* using Prolog. Knowledge is represented by a scenario, which has six meta–classes: model name, objects, objects attributes, parameter values, parameter relations, and system structures. The model name is the identifier for a particular problem. The objects are the components such as members, supports and loads, and the object attributes are the topology and geometry. The parameter values are stored as tuples. Parameter values are implemented using N+K trees (O'Keefe 1990) and parameter relations are implemented using AVL–trees. System structures represent information regarding the model itself, such as the class of structure, e.g. planar frame or three–dimensional frame.

6 APPLICATIONS

In this section, two conceptual designs are qualitatively evaluated using *Agrippa*. As a simple example, consider the wall carrying a lateral load and supported by two columns, shown in Fig. 3(a). The material is elastic and the lateral load distribution over height, and the member lengths and the stiffnesses are not known. This structure is modeled with two types of components, a wall and a frame member. *Agrippa* concludes that there is a unique qualitative solution, the internal forces and deflected shape of which are presented in Fig. 3(b) and Fig. 3(c), respectively. The columns are subjected to axial force, shear and flexure and the magnitude of the compressive force in one column is equal to the tension in the other column. Consequently, *Agrippa* derives the behavior that earthquake loads increase or decrease axial loads in columns. An engineering interpretation of the results or an heuristic rule can conclude the possibility of a buckling or a tension failure modes in the columns. Although the sign of the shear force in the column is given, the relation between the magnitude of shear in the columns cannot be derived unless the relative stiffness and length of the members is known and represented.

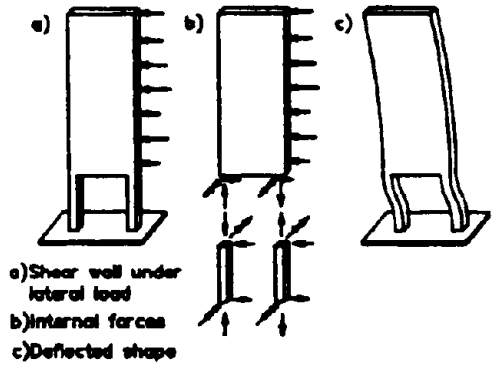

Figure 3. Results of qualitative evaluation of a wall supported on columns.

As a second example, consider the three-dimensional frame supporting lateral loads in the longitudinal direction, as shown in Fig. 4(a). This model represents one upper level bent from the Cypress Street viaduct which tragically collapsed during the October, 1989, Loma Prieta earthquake. The design of the viaduct had various releases to minimize time-dependent effects like creep (in the post-tensioned girders) and differential settlement. These releases also simplified analysis efforts, reduced moments transferred to the foundation and would had eventually facilitated future widening of the viaduct (Bollo 1990). A symmetric model of this bent includes the frame members $b3$ and $b1$ representing the deck perpendicular to the frame and the column, respectively, and the frame members $b2$ and $b4$ representing the girder. The member $b2$ represents the offset of a few inches between the deck and the face of the column.

Agrippa concludes that there is a unique qualitative solution for forces and moments, independent of the member lengths and stiffnesses. The internal forces and moments for the members are shown in Fig. 4(b) and Fig. 4(c), respectively. Member $b2$ is subjected to a complex state of stresses transferring compression, biaxial shear, biaxial flexure and torsion; $b1$ resists compression biaxial shear and biaxial flexure; $b3$ resists compression shear and flexure; and $b4$ resists compression and constant biaxial

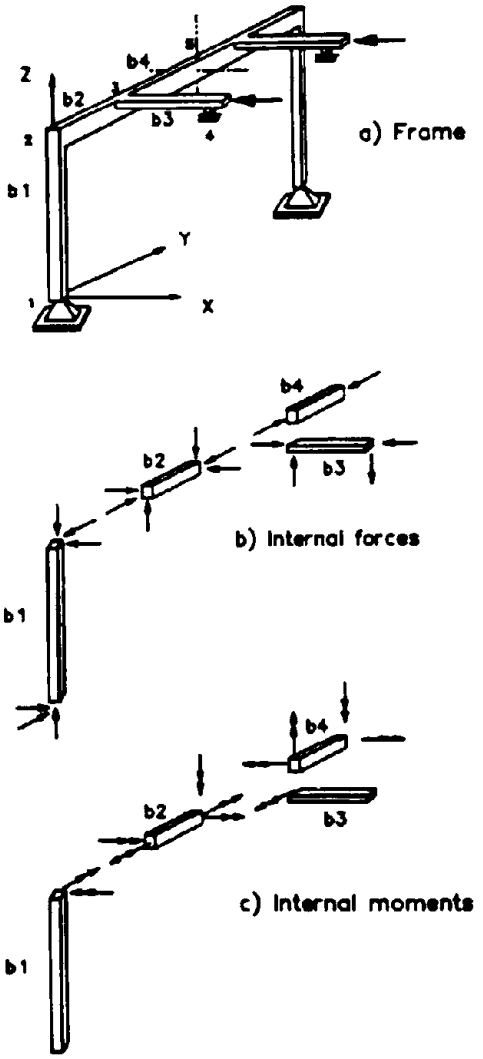

Figure 4. Results of qualitative analysis of the Cypress street viaduct.

flexure. Furthermore, if the goal of zero torsion in member *b*2 is posted, there is no equilibrium solution because shear cannot develop in *b*1. The qualitative analysis indicates a deficiency in the load path for lateral loads in the longitudinal direction because a complex state of forces including torsion must be developed in member *b*2. There is no redundancy in the load path if *b*2 fails to transfer the torque.

Parameter relations are derived in the qualitative analysis, such as the shear force in the column *b*1 equals the lateral load, and the compressive force in the column equals the vertical reaction at the roller support (or shear in the deck member *b*3). There are several qualitative solutions for the displaced shape, which can only be disambiguated if more information about length or stiffness is known. Some general conclusion are still valid such as the symmetry connection 5 always has a vertical displacement downward and support 1 always has a positive rotation about the x–axis.

The collapse of a structure is usually caused by several factors, and the Cypress Street viaduct is not an exception. Site observations after the earthquake and from experimental testing indicate that the collapse was triggered by a joint failure in the transverse direction. However, proposed retrofit schemes for viaducts of this type provide an alternate load path for longitudinal forces besides the torque in member *b*2. It is believed that conclusions derived by *Agrippa* are helpful in assessing the conceptual deficiencies in the seismic behavior of structures of this type.

7 CONCLUSIONS

A new qualitative reasoning methodology, the space centered approach, is useful for evaluating the seismic behavior of preliminary structural designs where limited information about the structure is available. The methodology includes a quantity space, a qualitative calculus, modeling primitives, and an inference scheme. The methodology is implemented in a computer program *Agrippa* that derives load transfer characteristics and displacements for three–dimensional structures under static lateral and gravity loads. Reasoning with knowledge about topology and incomplete knowledge about geometry and material characteristics, *Agrippa* derives conclusions regarding the signs and relative magnitude of parameters such as internal forces, moments, displacements and rotations. Future developments will include application of the method to practical seismic design procedures.

REFERENCES

Aktan, A.E. and Bertero, V.V. 1984. Conceptual seismic design of frame–wall structures. *Journal of structural engineering*, ASCE, 110: 2778–2797.

Bollo M., Mahin S., Moehle J., Stephen R., and Qi X. 1990. Observations and implications of tests on the Cypress street viaduct test structure. *Report* EERC-90/21, Earthquake Engineering Research Center, University of California at Berkeley.

Bredeweg B., Reinders [illegible] Wielinga B. 1990. GARP: A unifying approach to qualitative reasoning. VF-memo 117, Department of social science informatics, University of Amsterdam, Herengracht.

De Kleer J., and Brown J. 1984. A qualitative physics based on confluences. *Artificial Intelligence* 24: 7–83.

Forbus K. 1984. Qualitative process theory. *Artificial Intelligence* 24: 85–168.

Fuchter R., Iwasaki Y., and Law K. 1991. Generating qualitative models for structural engineering analysis and design. *Seventh conference on Computing in Civil Engineering*, ASCE, Washington, D.C.: 268–277.

Ganguly J., Sriram D., and Kausel E. 1991. Integrated framework for deriving behavior from structural descriptions. *Journal of Computing in Civil Engineering*, ASCE, 5: 391–441.

Kuipers B. 1984. Commonsense reasoning about causality: deriving behavior from structure. *Artificial Intelligence* 24: 169–203.

O'Keefe, R. 1990. *The craft of Prolog*. Cambridge: MIT Press.

Slater J. 1986. Qualitative physics and the prediction of structural behavior. *Expert Systems in Civil Engineering*, ASCE, C.N. Kostem and M.L. Maher, eds.: 239–249.

Subramani M., Gergely P., Conley C., Abel J., and Zaghw A. 1989. A knowledge–based approach to structural design of earthquake–resistant buildings. *Report* NCEER-89-0006, National Center for Earthquake Engineering Research, State University of New York at Buffalo.

Weld D. and De Kleer, J. 1990. *Readings in qualitative reasoning about physical systems*. Palo Alto: Morgan Kaufmann.

Modeling of dam-foundation interaction in analysis of arch dams

Anil K. Chopra
University of California at Berkeley, U.S.A.

Hanchen Tan
University of California at Berkeley, U.S.A.

ABSTRACT: The limitations of "standard" earthquake analysis procedures for arch dams in modeling dam-foundation rock interaction effects are identified. Results from recently developed procedures demonstrate that the "standard" procedure fails to recognize the significant reduction in dam response arising from foundation material and radiation damping. The resulting overestimation of stresses in the dam may lead to overly conservative designs of new dams and to the erroneous conclusion that an existing dam is unsafe.

1 INTRODUCTION

Based on the substructure method, a procedure has been developed (Fok and Chopra 1986) to analyze the earthquake response of arch dams (Figure 1). Implemented in the computer program EACD-3D (Fok, Hall, and Chopra 1987), this analytical procedure considers the effects of dam-water interaction, water compressibility, and reservoir boundary absorption. These hydrodynamic effects have been shown to be significant in the earthquake response of arch dams.

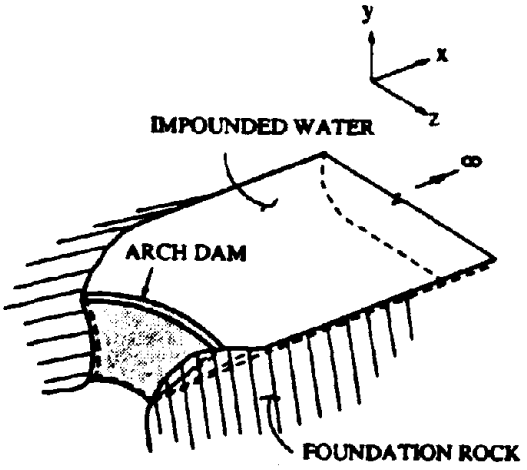

Figure 1. Arch dam-water-foundation rock system.

Required in the substructure method for earthquake analysis of concrete dams is the impedance matrix (or the frequency-dependent stiffness matrix) for the foundation rock region, defined at the finite element nodal points on the dam-foundation rock interface. Computation of this foundation impedance matrix for analysis of arch dams requires solution of a series of mixed boundary value problems governing the steady-state response of the canyon cut in a three-dimensional foundation rock region. Because such analyses are extremely complicated, usually only the foundation flexibility is considered in analysis of arch dams, i.e. material and radiation damping, as well as inertial effects of the foundation rock, are ignored. The objective of this work is to overcome these limitations and analyze the earthquake response of arch dams including dam-foundation rock interaction. Based on the results of such analyses, the significance of dam-foundation rock interaction effects in arch dam response is evaluated.

2 FOUNDATION IMPEDANCE MATRIX

The impedance matrix, $\mathbf{S}_f(\omega)$, where ω is the excitation frequency, relates the interaction forces $\bar{\mathbf{R}}(t)$ at the dam-foundation rock interface, Γ_f, to the corresponding displacements, $\mathbf{r}(t)$, relative to the earthquake-induced displacements in the absence of the dam (Figure 2):

$$\mathbf{S}_f(\omega)\bar{\mathbf{r}}(\omega) = \bar{\mathbf{R}}(\omega) \qquad (1)$$

where the overbar denotes a Fourier transform of the time functions. The square matrix, $\mathbf{S}_f(\omega)$, is of

the order equal to the number of degrees-of-freedom in the finite element idealization of the dam at the interface. The n^{th} column of this matrix multiplied by $e^{i\omega t}$ is the set of complex-valued forces required at the interface DOF to maintain a unit harmonic displacement, $e^{i\omega t}$, in the n^{th} DOF with zero displacements in all other DOF.

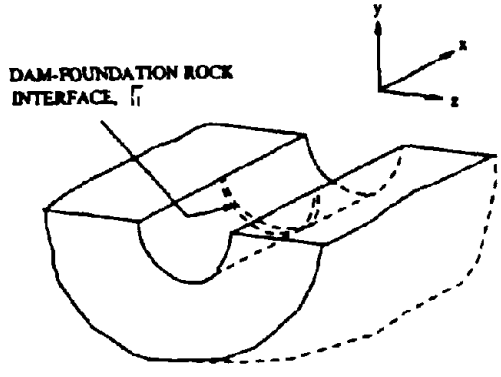

Figure 2. Infinitely-long canyon of arbitrary but uniform cross-section.

Evaluation of these forces requires solution of a series of mixed boundary value problems (BVP) with displacements prescribed at the interface, Γ_I, and tractions outside Γ_I--on the canyon wall and the half-space surface--are prescribed as zero. Instead of directly solving this mixed BVP, it is more convenient to solve a stress BVP in which non-zero tractions are specified at the interface, Γ_I, and the resulting displacements at Γ_I are determined. Assembled from these displacements, the dynamic flexibility influence matrix is inverted to determine the impedance matrix $\underline{S}_I(\omega)$.

A direct boundary element procedure has been developed to determine the impedance matrix associated with the nodal points at the base of a structure supported on a canyon cut in a homogeneous viscoelastic half-space (Zhang and Chopra 1991). The canyon is infinitely long and may be of arbitrary but uniform cross-section. The uniform cross-section of the canyon permits analytical integration along the canyon axis of the three-dimensional boundary integral equation. Thus, the original three-dimensional problem is reduced to an infinite series of two-dimensional problems, each of which corresponds to a particular wave number and involves Fourier transforms of full-space Green's functions. Appropriate superposition of the solutions of these two dimensional boundary problems leads to a dynamic flexibility influence matrix which is inverted to determine the impedance matrix.

3 ANALYTICAL PROCEDURE

The computer program EACD-3D and our earlier results for earthquake response of arch dams were all for spatially-uniform ground motion at the dam-foundation rock interface and massless foundation rock. Analytical procedures have been developed and the computer program extended to use the dynamic stiffness matrix to model dam-foundation rock interaction. Based on the substructure method, this analytical procedure and computer program treats the dam as a finite element system; the fluid domain as a finite element system adjacent to the dam, with a wave-transmitting boundary at the upstream end of this region, and a partially wave-absorptive reservoir bottom to account for the effects of the foundation rock or overlying alluvium and sediments; and the foundation rock region as a homogeneous, viscoelastic half-space less the canyon--assumed as uniform--supporting the dam.

4 SYSTEM CONSIDERED

Numerical results are presented for the dynamic response of Morrow Point Dam, located on the Gunnison River in Colorado. It is a 465 ft. high, approximately symmetric, single-centered arch dam. For the purposes of dynamic analysis the dam is assumed to be symmetric about the x-y plane with the dimensions averaged from the two halves.

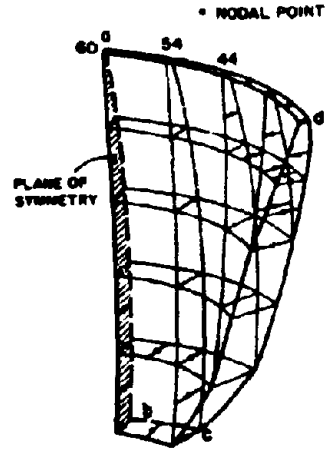

Figure 3. Finite element idealization of one-half of Morrow Point Dam.

The finite element idealization of one-half of the arch dam consists of 8 thick-shell finite elements in the main part of the dam and 8 transition elements in the part of the dam near its junction with the foundation rock, with a total of 61 nodal points (Figure 3). When dam-foundation interaction is considered, this idealization has approximately 300 degrees of freedom. The mass concrete of the dam is assumed to be homogeneous, isotropic, and linearly elastic with the following properties: Young's modulus = 4.0 million psi, unit weight = 155 pcf, and Poisson's ratio = 0.2. The constant hysteretic damping factor selected is 0.10, which corresponds to 5 percent damping in all natural vibration modes of the dam with an empty reservoir on rigid foundation rock.

The arch dam is supported in an infinitely-long canyon of uniform cross-section--defined by the geometry of the dam-foundation rock interface--cut in a homogeneous half-space. The properties of the rock are: Young's modulus = 1.0 million psi, unit weight = 165 pcf, Poisson's ratio = 0.2, and constant hysteretic damping factor = 0.10. The elastic modulus of the foundation rock has been chosen as a fraction of the modulus of dam concrete, an assumption that is appropriate in many practical situations because of joints in the foundation rock.

Because the objective of this paper is to investigate modeling of dam-foundation rock interaction and its effects, the water impounded behind the dam is not included in the system that is analyzed.

5 RESPONSE RESULTS

The dynamic response of the dam-foundation rock system described in the preceding section was analyzed for three conditions:

1. Dam on rigid foundation rock.
2. Dam-foundation rock system considering only foundation flexibility effects.
3. Dam-foundation rock system considering all interaction effects.

For each of these three cases, the complex frequency response functions were determined. These functions presented in Figures 4-6 are dimensionless response factors that represent the radial acceleration at one location at the dam crest due to unit, harmonic, free-field ground acceleration. The response of the dam to upstream or vertical ground motion is plotted at the crown location (nodal point 60 at the plane of symmetry in Figure 3). With the cross-section ground motion as the excitation, the response of the dam is presented at nodal point 54 on the dam crest (Figure 3) defined by $\theta = 13.25°$ measured from the crown. The absolute value of the complex-valued frequency response function for acceleration is plotted in Figures 4-6 against the normalized excitation frequency parameter ω/ω_1, where ω_1 is the fundamental natural vibration frequency of the dam without water on rigid foundation rock; ω_1^s is used as the normalizing factor for symmetric (upstream or vertical) ground motion, and ω_1^a is used for antisymmetric (cross-stream) ground motion.

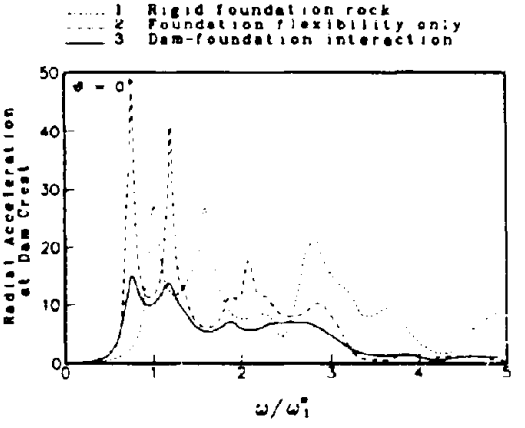

Figure 4. Response of dams to harmonic upstream ground motion for three foundation rock cases.

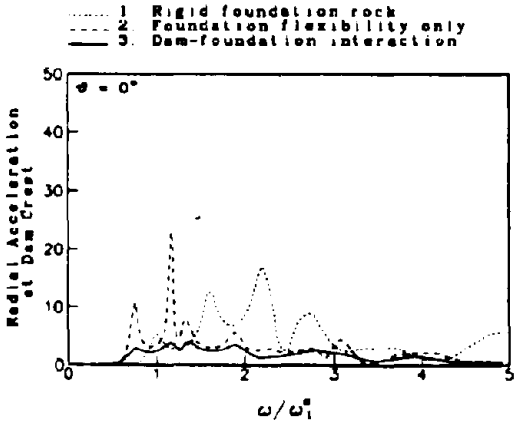

Figure 5. Response of dams to harmonic vertical ground motion for three foundation rock cases.

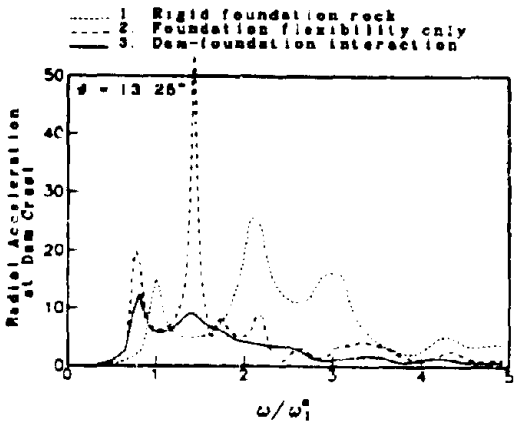

Figure 6. Response of dams to harmonic cross-stream ground motion for three foundation rock cases.

The response of the dam supported on rigid foundation rock (Case 1) is characteristic of a multi-degree-of-freedom system with frequency-independent mass, stiffness, and damping matrices. In particular, the first resonance occurs at the fundamental natural vibration frequency of the dam: ω_1^s of the symmetric vibration mode in the case of upstream or vertical motion, or ω_1^a of the antisymmetric vibration mode in the case of cross-stream ground motion.

Because of foundation flexibility (Case 2), the fundamental resonant frequency of the dam decreases, the response at this frequency increases, and the frequency bandwidth at resonance decreases, implying a decrease in the apparent damping of the structure. The increase in response is, in part, due to the increase in the effective earthquake forces in individual vibration modes arising from modifications in the mode shape due to foundation flexibility. Similar but somewhat smaller effects of foundation flexibility are observed at higher resonant frequencies. These effects of foundation-rock flexibility are qualitatively similar in the response to the three components of ground motion.

When all aspects of dam-foundation rock interaction are considered (Case 3), the decrease in the fundamental resonant frequency is about the same as determined by considering foundation flexibility only. However, dam-foundation rock interaction reduces the amplitude of the fundamental resonant peak and increases the bandwidth at resonance because of material damping of foundation rock and radiation damping resulting from interaction. Similarly, dam-foundation interaction reduces the higher resonant frequencies--although to a lesser degree than the fundamental resonant frequency--and substantially reduces the amplitude of the higher resonant peaks. The above-mentioned effects of dam-foundation rock interaction are qualitatively similar in the response to the three components of ground motion.

6 CONCLUDING REMARKS

It is apparent from the limited response results presented that "standard" analyses of arch dams, wherein only the foundation flexibility is considered, are deficient in a major sense. In particular, the significant reduction in the dam response arising from foundation material and radiation damping is not recognized in the "standard" analyses. The resulting overestimation of stresses in the dam may lead to overconservative designs of new dams and to the erroneous conclusion that an existing dam is unsafe. Additional results showing the response of dams to realistic earthquake ground motion will be presented at the conference in order to quantify the significance of the above-mentioned limitation of "standard" analyses of arch dams.

ACKNOWLEDGEMENTS

This research investigation is supported by the National Science Foundation under Grant No. BCS-8719296. The authors are grateful for this support.

REFERENCES

Fok, K-L. & A.K. Chopra 1986. Earthquake analysis of arch dams including dam-water interaction, reservoir boundary absorption and foundation flexibility. *Earthquake Engineering and Structural Dynamics* 14:155-184.

Fok, K-L., J.F. Hall & A.K. Chopra 1986. *EACD-3D: A computer program for three-dimensional earthquake analysis of concrete dams*, Report No. UCB/EERC-86/09, Earthquake Engineering Research Center, University of California, Berkeley, July, 144 pages.

Zhang, L-P. & A.K. Chopra 1991. Impedance functions for three-dimensional foundations supported on an infinitely long canyon of uniform cross-section in a homogeneous half-space. *Earthquake Engineering and Structural Dynamics* 20:1011-1028.

Response spectrum method for incoherent support motions

Armen Der Kiureghian
University of California, Berkeley, CA 94720, U.S.A.

Ansgar Neuenhofer
Rheinish-Westphalian Technical University, Aachen, Germany

ABSTRACT: A new response spectrum method is developed for seismic analysis of linear multi-degree-of-freedom, multiply-supported structures subjected to spatially varying ground motions. Variations of the ground motion due to wave passage, loss of coherency with distance, and variation of local soil conditions are included. The method is based on fundamental principles of random vibration theory and properly accounts for the effects of correlation between the support motions as well as between the modes of the structure.

1 INTRODUCTION

Observations during recent earthquakes, notably the Loma Prieta earthquake of October 17, 1989, have clearly demonstrated that seismic ground motions can vary significantly over distances which are of the same order of magnitude as the dimensions of some extended structures, such as bridges. Three phenomena are responsible for these variations: (1) the difference in the arrival times of seismic waves at different stations, denoted herein as the "wave passage" effect; (2) the loss of coherency of the motion due to reflections and refractions of the waves in the heterogeneous medium of the ground, as well as due to the difference in the manner of superposition of waves arriving from an extended source at various stations, denoted herein as the "incoherence effect"; and (3) the difference in the local soil conditions at each station and the manner in which they influence the amplitude and frequency content of the bedrock motion, denoted herein as the "local" effect. Recent analyses with array recordings have shed light on the nature of these effects and their relative magnitudes (e.g., Bolt et al. 1982, Harichandran and Vanmarcke 1986, Abrahamson et al. 1991).

The effect of differential support motions on the response of extended structures has been of concern for a long time and studies based on time history or random vibrations analyses have been carried out (e.g., Abdel-Ghaffar and Rubin 1982, Zerva 1990). It is known that, under realistic conditions, the differences in the support motions can significantly influence the internal forces generated in the structure. While in most cases the magnitudes of these forces are reduced, there are situations where differential support motions may actually result in larger internal forces. The failure of several bridges during the Loma Prieta earthquake has highlighted the need for a better understanding of this phenomenon, and for the development of practical analysis tools that can accurately account for its effects.

This paper, based on a report by the authors (Der Kiureghian and Neuenhofer, 1991), describes a new response spectrum method for seismic analysis of structures subjected to multiple support excitations, which properly accounts for the wave passage, incoherence, and local effects. The method is based on the principles of random vibration theory and is an extension of the well known CQC method (Der Kiureghian 1981, 1991) to the case of multiple-support excitations. The method is practical, since it employs information that is normally available in seismic design applications, i.e., peak ground displacements and response spectra at each support degree of freedom, a rough estimate of the duration of motion, and a coherency function. An example, demonstrating an application of the method and characterizing the influence of differential support motions on selected responses of a structure, concludes the paper.

2 EQUATIONS OF MOTION

The equations of motion for a discretized, n-degree-of-freedom linear system subjected to m support motions can be written in the matrix form (Clough and Penzien 1975)

$$\begin{bmatrix} \mathbf{M} & \mathbf{M}_c \\ \mathbf{M}_c^T & \mathbf{M}_g \end{bmatrix} \begin{Bmatrix} \ddot{\mathbf{x}} \\ \ddot{\mathbf{u}} \end{Bmatrix} + \begin{bmatrix} \mathbf{C} & \mathbf{C}_c \\ \mathbf{C}_c^T & \mathbf{C}_g \end{bmatrix} \begin{Bmatrix} \dot{\mathbf{x}} \\ \dot{\mathbf{u}} \end{Bmatrix} + \begin{bmatrix} \mathbf{K} & \mathbf{K}_c \\ \mathbf{K}_c^T & \mathbf{K}_g \end{bmatrix} \begin{Bmatrix} \mathbf{x} \\ \mathbf{u} \end{Bmatrix} = \begin{Bmatrix} \mathbf{0} \\ \mathbf{F} \end{Bmatrix} \quad (1)$$

where $\mathbf{x} = [x_1, \ldots, x_n]^T$ is the n-vector of (total) displacements at the unconstrained degrees of freedom; $\mathbf{u} = [u_1, \ldots, u_m]^T$ is the m-vector of prescribed support displacements; $\mathbf{M}$, $\mathbf{C}$ and $\mathbf{K}$ are the $n \times n$ mass, damping and stiffness matrices associated with the unconstrained degrees of freedom, respectively; $\mathbf{M}_g$, $\mathbf{C}_g$ and $\mathbf{K}_g$ are the $m \times m$ matrices associated with the support degrees of freedom; $\mathbf{M}_c$, $\mathbf{C}_c$ and $\mathbf{K}_c$ are the $n \times m$ coupling matrices associated with both sets of degrees of freedom; and $\mathbf{F}$ is the m-vector

of reacting forces at the support degrees of freedom. Both $\mathbf{x}$ and $\mathbf{u}$ may contain translational as well as rotational components.

Following conventional procedures, we decompose the response into pseudo-static and dynamic components:

$$\mathbf{x} = \mathbf{x}^s + \mathbf{x}^d \tag{2}$$

where the pseudo-static component, $\mathbf{x}^s$, is the solution to Eq. 1 without the inertia and damping terms

$$\mathbf{x}^s = -\mathbf{K}^{-1}\mathbf{K}_c\mathbf{u} = \mathbf{R}\mathbf{u} \tag{3}$$

in which $\mathbf{R} = -\mathbf{K}^{-1}\mathbf{K}_c$ is denoted the influence matrix. Substituting Eqs. 2 and 3 in Eq. 1, the dynamic component of the response is obtained in the differential form

$$\begin{aligned}\mathbf{M}\ddot{\mathbf{x}}^d + \mathbf{C}\dot{\mathbf{x}}^d + \mathbf{K}\mathbf{x}^d &= -(\mathbf{M}\mathbf{R} + \mathbf{M}_c)\ddot{\mathbf{u}} - (\mathbf{C}\mathbf{R} + \mathbf{C}_c)\dot{\mathbf{u}} \\ &\approx -(\mathbf{M}\mathbf{R} + \mathbf{M}_c)\ddot{\mathbf{u}}\end{aligned} \tag{4}$$

The right-hand side is approximated by neglecting the damping forces, which are usually much smaller than the inertia forces on the same side. The above reduction is exact when the damping matrix is proportional to the stiffness matrix. It is noted that $\mathbf{M}_c = \mathbf{0}$ if a lumped mass model is used.

To formulate a response spectrum method, it is necessary to employ the normal mode approach. Let $\Phi = [\boldsymbol{\phi}_1 \cdots \boldsymbol{\phi}_n]$, ω_i and ζ_i, $i = 1, \cdots, n$, denote the modal matrix, natural frequencies and modal damping ratios of the structure with its support points fixed. Using the transformation $\mathbf{x}^d = \Phi\mathbf{y}$, $\mathbf{y} = [y_1, \cdots, y_n]^T$, in Eq. 4 and employing the orthogonality of the mode shapes (assuming classical damping), the decoupled equations of motion are

$$\ddot{y}_i + 2\zeta_i\omega_i\dot{y}_i + \omega_i^2 y_i = \sum_{k=1}^{m} \beta_{ki}\,\ddot{u}_k(t) \quad i = 1, \cdots, n \tag{5}$$

where the index k denotes the degrees of freedom associated with the prescribed support motions, the subscript i denotes the mode number, and β_{ki} is the modal participation factor given by

$$\beta_{ki} = -\frac{\boldsymbol{\phi}_i^T(\mathbf{M}\mathbf{r}_k + \mathbf{M}_c\mathbf{i}_k)}{\boldsymbol{\phi}_i^T\mathbf{M}\boldsymbol{\phi}_i} \tag{6}$$

in which $\mathbf{r}_k$ is the k-th column of $\mathbf{R}$ and $\mathbf{i}_k$ is the k-th column of an $m \times m$ identity matrix. It is convenient to define a normalized modal response $s_{ki}(t)$, representing the response of a single-degree-of-freedom oscillator of unit mass, frequency ω_i and damping ζ_i, which is subjected to the base motion $u_k(t)$. From Eq. 5, $s_{ki}(t)$ satisfies

$$\ddot{s}_{ki} + 2\zeta_i\omega_i\dot{s}_{ki} + \omega_i^2 s_{ki} = \ddot{u}_k(t) \tag{7}$$

Obviously, $y_i(t) = \sum_{k=1}^{m} \beta_{ki}\, s_{ki}(t)$.

A generic response quantity of interest, $z(t)$ (e.g., a nodal displacement, an internal force, stress or strain component), in general can be expressed as a linear function of the nodal displacements $\mathbf{x}$, i.e.,

$$z(t) = \mathbf{q}^T\mathbf{x}(t) = \mathbf{q}^T[\mathbf{x}^s(t) + \mathbf{x}^d(t)] \tag{8}$$

where $\mathbf{q}$ is a response transfer vector that usually depends on the geometry and stiffness properties of the structure. Substituting for the pseudo-static component of $\mathbf{x}$ from Eq. 3 and for the dynamic component in terms of the normalized modal responses, the generic response $z(t)$ is

$$z(t) = \sum_{k=1}^{m} a_k u_k(t) + \sum_{k=1}^{m}\sum_{i=1}^{n} b_{ki}\, s_{ki}(t) \tag{9}$$

in which

$$a_k = \mathbf{q}^T\mathbf{r}_k \quad k = 1, \ldots, m \tag{10}$$

$$b_{ki} = \mathbf{q}^T\boldsymbol{\phi}_i\beta_{ki} \quad k = 1, \ldots, m; \quad i = 1, \ldots, n \tag{11}$$

are denoted effective influence factors and effective modal participation factors, respectively. It is useful to note that a_k and b_{ki} are functions only of the structural properties, and that $s_{ki}(t)$ is dependent only on the i-th modal frequency and damping ratio and the k-th input motion. The first sum on the right-hand side of Eq. 9 represents the pseudo-static component of the response and the double-sum term represents the dynamic component.

3 THE RESPONSE SPECTRUM METHOD

For the response spectrum method, we assume the following information is available: the set of peak ground displacements $u_{k,max}$ for all support points; the set of displacement response spectra $D_k(\omega, \zeta)$ (representing the mean peak response of an oscillator of frequency ω and damping ζ to the base acceleration $\ddot{u}_k$) for each support motion; an estimate of the duration of motion τ; and the coherency function $\gamma_{kl}(\omega)$ characterizing the spatial variability of the ground motion in the region. The coherency function is defined as the normalized cross power spectral density (PSD) of the ground acceleration processes at two stations k and l, i.e.,

$$\gamma_{kl}(\omega) = \frac{G_{\ddot{u}_k\ddot{u}_l}(\omega)}{[G_{\ddot{u}_k\ddot{u}_k}(\omega)\, G_{\ddot{u}_l\ddot{u}_l}(\omega)]^{1/2}} \tag{12}$$

where $G_{xy}(\omega)$ denotes the cross-PSD of processes $x(t)$ and $y(t)$. Empirical models of the coherency function are available from array recordings (Harichandran and Vanmarcke 1986, Abrahamson et al. 1991). This function in general is complex valued, with its modulus characterizing the incoherence effect and the phase angle characterizing the wave passage effect. We note that the response spectrum for each support degree of freedom can be different, thus allowing for the local effects at each station.

The new response spectrum method is based on the superposition rule in Eq. 9 and the fundamental principles of stationary random vibration. The details of the derivation are beyond the scope of this paper. It suffices to say that the method is rigorously derived and properly accounts for the effects of incoherence, wave passage, local site conditions, as well as the correlation between the modes of vibration of the structure. The method works best when the significant

segment of the excitation is quasi-stationary and it is several times longer than the fundamental period of the structure. The combination rule for the mean of the absolute maximum response is given as follows:

$$\mathrm{E}[\max|z(\tau)|] = \left[\sum_{k=1}^{m}\sum_{l=1}^{m} a_k a_l \rho_{u_k u_l} u_{k,\max} u_{l,\max} + 2\sum_{k=1}^{m}\sum_{i=1}^{m}\sum_{j=1}^{n} a_k b_{ij} \rho_{u_k s_{ij}} u_{k,\max} D_i(\omega_j,\zeta_j) + \sum_{k=1}^{m}\sum_{i=1}^{m}\sum_{o=1}^{n}\sum_{j=1}^{n} b_{ki} b_{lj} \rho_{s_{ki} s_{lj}} D_k(\omega_i,\zeta_i) D_l(\omega_j,\zeta_j) \right]^{1/2} \quad (13)$$

In this expression, the double sum represents the square of the pseudo-static response, the quadruple sum represents the square of the dynamic response, and the triple sum represents a coupling term between the pseudo-static and dynamic responses that arises from the covariance between the two components. All terms in this combination rule are readily available, except the three cross-correlation coefficients $\rho_{u_k u_l}$, $\rho_{u_k s_{ij}}$ and $\rho_{s_{ki} s_{lj}}$. These coefficients incorporate the effects of incoherence and wave passage, as well as the correlation between the vibration modes. Interpretation of these coefficients and their evaluation are described in the remainder of this section.

The three cross-correlation coefficients $\rho_{u_k u_l}$, $\rho_{u_k s_{ij}}$ and $\rho_{s_{ki} s_{lj}}$ can be interpreted in terms of two oscillators of frequencies ω_i and ω_j and damping ratios ζ_i and ζ_j, which are subjected to the ground motions $u_k(t)$ and $u_l(t)$, respectively (see Fig. 1). Specifically, $\rho_{u_k u_l}$ denotes the cross-

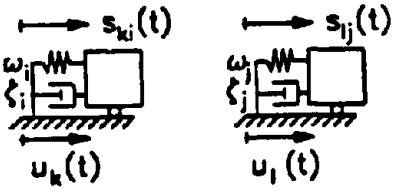

Figure 1. Pair of oscillators

correlation between the two support displacements (at the same time instance), $\rho_{u_k s_{ij}}$ denotes the cross-correlation coefficient between the displacement at support k and the response of the oscillator at support l, and $\rho_{s_{ki} s_{lj}}$ denotes the cross-correlation coefficient between the responses of the two oscillators. Assuming stationary processes and using the definition in Eq. 12, these coefficients can be written in terms of the coherency function and the PSD's of the individual support accelerations as (see Der Kiureghian and Neuenhofer 1991)

$$\rho_{u_k u_l} = \frac{\int_{-\infty}^{\infty} \omega^{-4} \gamma_{kl}(\omega) [G_{\ddot{u}_k \ddot{u}_k}(\omega) G_{\ddot{u}_l \ddot{u}_l}(\omega)]^{1/2} d\omega}{\left[\int_{-\infty}^{\infty} \omega^{-4} G_{\ddot{u}_k \ddot{u}_k}(\omega) d\omega \int_{-\infty}^{\infty} \omega^{-4} G_{\ddot{u}_l \ddot{u}_l}(\omega) d\omega \right]^{1/2}} \quad (14)$$

$$\rho_{u_k s_{ij}} = \frac{\int_{-\infty}^{\infty} \omega^{-2} H_j(-\omega) \gamma_{kl}(\omega) [G_{\ddot{u}_k \ddot{u}_k}(\omega) G_{\ddot{u}_i \ddot{u}_i}(\omega)]^{1/2} d\omega}{\left[\int_{-\infty}^{\infty} \omega^{-4} G_{\ddot{u}_k \ddot{u}_k}(\omega) d\omega \int_{-\infty}^{\infty} |H_j(\omega)|^2 G_{\ddot{u}_i \ddot{u}_i}(\omega) d\omega \right]^{1/2}} \quad (15)$$

$$\rho_{s_{ki} s_{lj}} = \frac{\int_{-\infty}^{\infty} H_i(\omega) H_j(-\omega) \gamma_{kl}(\omega) [G_{\ddot{u}_k \ddot{u}_k}(\omega) G_{\ddot{u}_l \ddot{u}_l}(\omega)]^{1/2} d\omega}{\left[\int_{-\infty}^{\infty} |H_i(\omega)|^2 G_{\ddot{u}_k \ddot{u}_k}(\omega) d\omega \int_{-\infty}^{\infty} |H_j(\omega)|^2 G_{\ddot{u}_l \ddot{u}_l}(\omega) d\omega \right]^{1/2}} \quad (16)$$

in which $H_i(\omega) = [\omega_i^2 - \omega^2 + 2i\zeta_i\omega_i\omega]^{-1}$ are the modal frequency response functions. It is seen that, in addition to the coherency function, it is necessary to know the individual PSD's of ground acceleration at each support degree of freedom. It is quite well known, however, that the PSD of ground acceleration is closely connected to the response spectrum and several approximate relations between the two are available (e.g., Kaul 1978). In the present work, owing to the need to develop the PSD for the entire range of frequencies, a new formula is developed which, omitting the subscript k for the support degree of freedom, is

$$G_{\ddot{u}\ddot{u}}(\omega) = \frac{\omega^{p+2}}{\omega^p + \omega_f^p} \left(\frac{2\zeta\omega}{\pi} + \frac{4}{\pi\tau} \right) \left[\frac{D(\omega,\zeta)}{p_s(\omega)} \right]^2 \qquad \omega \geq 0 \quad (17)$$

in which $p_s(\omega)$ is a peak factor function, τ is the duration of the excitation, and p and ω_f are parameters determined such that the area underneath the PSD matches the mean square ground acceleration. It is important to note that the coefficients in Eqs. 14-16 are not overly sensitive to the shapes of the individual PSD's (due to the integrals involved), and hence a rough estimate of the PSD is sufficient to make good approximations of these coefficients.

Extensive numerical analysis has revealed the following properties of the cross-correlation coefficients(see Der Kiureghian and Neuenhofer 1991) : (a) The cross-correlation coefficient $\rho_{u_k u_l}$ is generally large, especially for soft soil conditions, and its contribution to the pseudo-static component of the response cannot be neglected. (b) The cross-correlation coefficient $\rho_{u_k s_{ij}}$ is usually small, except for frequencies below 0.5 *Hz*. The contribution of this coefficient and, therefore, that of the cross term between the pseudo-static and dynamic components of the response may be neglected without a significant loss of accuracy if the fundamental frequency of the system is greater than about 0.5 *Hz*. (c) The cross-correlation coefficient $\rho_{s_{ki} s_{lj}}$ depends on the separation between the two frequencies and the soil

conditions at the two stations. For firm soil and in absence of the wave passage effect, the correlation is small for well spaced frequencies (as long as they are not far from the range of dominant input frequencies) and tends to further decay with increasing incoherence. For soft soils, or in the presence of the wave passage effect, the correlation coefficient can be significant even for well spaced modes if there is not a strong incoherence effect.

4 EXAMPLE APPLICATION

As an example application of the new response spectrum method, we consider the two-span continuous beam in Fig. 2, which has uniform mass and stiffness properties and simple supports. The beam is discretized into 20 elements along each $L = 50\,m$ span. The system is represented by 38 translational and 41 rotational degrees of freedom, and 3 translational support degrees of freedom (i.e., $m = 3$). Since no mass moments of inertia are associated with the rotational degrees of freedom, the latter are condensed out and the system analyzed has $n = 38$ degrees of freedom. Only the first four modes of vibration are considered in the analysis.

Figure 2. Example structure

Two values of the fundamental period of the beam are considered: $T = 1\,s$ and $T = 1/4\,s$. These are obtained for $EI/m = 2.53 \times 10^6$ and $40.5 \times 10^6\ m^4/s^2$, respectively, where EI denotes the flexural rigidity and m denotes the mass per unit length of the beam. The resulting frequencies of the first four modes are listed in Table 1. We refer to the two beams as the "flexible" and the "stiff" beam, respectively. The modal damping ratio is assumed to be 5 percent in all modes.

Table 1. Modal Frequencies of Example Structures

mode	ω_i, rad/s	
	"flexible" beam	"stiff" beam
1	6.28	25.13
2	9.82	39.30
3	25.13	100.57
4	31.80	127.26

Five response quantities are considered for the analysis: the mid-span deflections u_1 and u_2, the bending moment M at the middle support, and the shear forces V_1 and V_2 at the faces of the middle support. Although the beam is symmetric, the two mid-span deflections and the shear forces on both sides of the middle support are considered, since different results are obtained for these pairs of responses due to the wave passage effect.

The motion at each support is assumed to be vertical and specified by identical response spectra consistent with the design spectrum recommended by the Structural Engineering Association of California for $a_{g,max} = 0.5\,g$. The coherency function is assumed to have the form $\gamma_{kl}(\omega) = \exp[-(\alpha\omega d_{kl}/v_s)^2]\ \exp(i\omega d^L_{kl}/v_{app})$ suggested by Luco and Wong (1986), where α is an incoherence factor, d_{kl} denotes the horizontal distance between stations k and l and d^L_{kl} is its projection along the longitudinal direction of propagation of waves, v_s is the shear wave velocity of the medium, and v_{app} is the surface apparent wave velocity. It is noted that the first exponential term characterizes the effect of incoherence, whereas the second exponential term characterizes the wave passage effect. Five different cases are considered: *Case 1*: Fully coherent (uniform) motions at all three supports, i.e., $\gamma_{kl}(i\omega) = 1$; *Case 2*: Only wave passage effect included (i.e., $\alpha = 0$) with $v_{app} = 400\,m/s$; *Case 3*: Only incoherence effect included (i.e., $v_{app} = \infty$) with $v_s/\alpha = 600\,m/s$; *Case 4*: Both wave passage and incoherence effects included with $v_{app} = 400\,m/s$ and $v_s/\alpha = 600\,m/s$; and *Case 5*: Mutually statistically independent support motions, i.e., $\gamma_{kl}(i\omega) = 0$ for $k \neq l$. For cases 2 and 4, it is assumed that the waves propagate in the direction from support 1 to support 3 and that $d^L_{kl} = d_{kl}$. The results for the various cases are compared to determine the relative influences of the wave passage and incoherence effects, as well as to determine the consequences of assuming uniform excitations (Case 1) or independent excitations (Case 5), which are commonly assumed in the current practice.

The normalized mean values of the peak responses are listed in Table 2 for both the "flexible" and "stiff" beams, respectively. The total response for each case, denoted z, and representing the result obtained from the combination rule in Eq. 13, is listed in the columns 3 and 8. Note that the pair of values for the midspan displacement responses u_1 and u_2, and for the middle support shear forces V_1 and V_2 are identical for Cases 1, 3 and 5 due to the symmetry of the beam and the absence of the wave passage effect. In Cases 2 and 4, these pairs of responses are different, in spite of the symmetry of the beam, due to the directionality of the wave passage effect.

In columns 4 and 9 are listed the ratios of the total response to the total response for Case 1. These ratios indicate the influence of the spatial variability on each of the response quantities. By comparing Cases 2 and 3, it is apparent that the influence of the wave passage effect is greater than that of the incoherence effect for both the "flexi-

Table 2. Mean peak responses of example structures

response $z \times 10^3$ (1)	case (2)	"flexible" beam z_t (3)	"flexible" beam $z_t/z_{t,case\,1}$ (4)	"flexible" beam ss/z_t^2 (5)	"flexible" beam $s\text{-}d/z_t^2$ (6)	"flexible" beam dd/z_t^2 (7)	"stiff" beam z_t (3)	"stiff" beam $z_t/z_{t,case\,1}$ (8)	"stiff" beam ss/z_t^2 (9)	"stiff" beam $s\text{-}d/z_t^2$ (10)	"stiff" beam dd/z_t^2 (11)
$\frac{u_1}{L}$	1	7.86	1	0.950	−0.080	0.130	7.63	1.000	1.006	−0.006	0.001
	2	7.85	0.999	0.948	−0.090	0.142	7.62	0.998	1.006	−0.007	0.000
	3	7.80	0.993	0.960	−0.080	0.120	7.62	0.999	1.006	−0.007	0.001
	4	7.78	0.990	0.962	−0.090	0.128	7.61	0.997	1.006	−0.007	0.001
	5	6.36	0.809	0.938	−0.088	0.150	6.13	0.804	1.006	−0.008	0.001
$\frac{u_2}{L}$	1	7.86	1	0.950	−0.080	0.130	7.63	1.000	1.006	−0.006	0.001
	2	7.71	0.981	0.983	−0.069	0.086	7.62	0.998	1.006	−0.006	0.001
	3	7.80	0.993	0.960	−0.080	0.120	7.62	0.999	1.006	−0.007	0.001
	4	7.73	0.984	0.974	−0.071	0.097	7.61	0.997	1.006	−0.006	0.001
	5	6.36	0.809	0.938	−0.088	0.150	6.13	0.804	1.006	−0.008	0.001
$\frac{LM}{EI}$	1	60.6	1	0	0	1	4.23	1	0	0	1
	2	46.3	0.764	0.001	0.015	0.984	3.60	0.853	0.138	0.269	0.594
	3	51.4	0.848	0.001	0.009	0.990	3.68	0.870	0.184	0.178	0.638
	4	45.4	0.749	0.003	0.022	0.975	4.34	1.027	0.361	0.198	0.441
	5	51.2	0.845	0.302	0.066	0.632	28.5	6.739	0.975	0.015	0.010
$\frac{L^2V_1}{EI}$	1	238	1	0	0	1	16.7	1	0	0	1
	2	212	0.891	0.000	0.004	0.996	11.9	0.714	0.013	0.108	0.880
	3	211	0.884	0.000	0.003	0.997	13.4	0.802	0.014	0.057	0.929
	4	198	0.832	0.000	0.007	0.993	13.6	0.817	0.037	0.088	0.875
	5	180	0.753	0.025	0.026	0.949	31.7	1.902	0.787	0.056	0.157
$\frac{L^2V_2}{EI}$	1	238	1	0	0	1	16.7	1	0	0	1
	2	180	0.753	0.000	0.004	0.996	12.7	0.764	0.011	0.088	0.901
	3	211	0.884	0.000	0.003	0.997	13.4	0.802	0.014	0.057	0.929
	4	181	0.760	0.000	0.004	0.995	13.6	0.814	0.037	0.087	0.876
	5	180	0.753	0.025	0.026	0.949	31.7	1.902	0.787	0.056	0.157

z_t total value of the peak response
$z_{t,case\,1}$ total value of the peak response for Case 1
ss square of the pseudo-static component of response
$s\text{-}d$ cross term between pseudo-static and dynamic components of response
dd square of the dynamic component of response

ble" and "stiff" beams (i.e., the ratios for Case 2 are smaller than the corresponding ratios for Case 3), except for responses u_1 and V_1 of the "flexible" beam. For Case 4, which includes both the wave passage and the incoherence effects, the combined influence in some cases is smaller (i.e., the ratio is closer to 1.0) than in the individual cases just mentioned. In fact, for response M of the "stiff" beam, the ratio for Case 4 is greater than unity (i.e., the response is amplified due to the spatial variability of the ground motion), whereas in Cases 2 and 3 the ratios are smaller than unity. This is due to the elimination of certain negative cross-correlation terms arising from the wave passage effect by the incoherence effect. All ratios for Cases 2-4 are smaller than unity, except the case just mentioned, indicating that the spatial variability tends to reduce the total response for both systems. This reduction is insignificant for responses u_1 and u_2 (the midspan deflections), but rather significant for the responses M, V_1 and V_2. The former is due to the dominance of the pseudo-static component of the displacement response as described below.

As evident from the response M of the "stiff" beam in Case 4, reduction in the response due to the spatial variability effect is not a general rule. One may expect a large pseudo-static response to be generated in a stiff structure when there is a rapid loss of coherency in the ground motion. Such pseudo-static response may lead to a larger total response compared with the response for uniform support motions (Case 1). This is evident for Case 5 with uncorrelated support motions, where the ratios for the responses M, V_1 and V_2 are greater than unity for the "stiff" beam. Nevertheless, from the results in Table 2, one may conclude that the effect of spatial variability is more likely to reduce the response (compared with the uniform motion case) than to amplify it.

Columns 5-7 and 10-12 of Table 2 list ratios of the three terms inside the square brackets in Eq. 13 with respect to the square of the total response. They indicate the relative contributions of the pseudo-static part (the double-sum term), the cross term between the pseudo-static and dynamic

parts (the triple-sum term), and the dynamic part (the quadruple-sum term) to the square of the response. Note that for Case 1 the pseudo-static and cross terms are zero for the internal force responses M, V_1 and V_2, since rigid body motions of the beam do not generate internal forces.

From the results in the columns 5-7 and 10-12 of Table 2, the displacement responses u_1 and u_2 are found to be dominated by the pseudo-static part, especially for the "stiff" beam. It is interesting to note that for these responses the cross term between the pseudo-static and dynamic parts is negative. The bending moment, M, and shear force responses, V_1 and V_2, are primarily dominated by the dynamic part of the response, except in Case 5 for the "stiff" beam. The cross term between the pseudo-static and dynamic parts for these responses is positive and in many cases is greater than the contribution of the pseudo-static component alone. However, in most cases the contribution of the cross term can be neglected with little effect on the total response.

The results for the above example show that the influence of spatial variability of the ground motion on the response of a multiply-supported structure can be significant. In the present case, this influence results in a reduction of the peak response, in some instances by almost 30 percent. However, this trend cannot be generalized since for stiffer structures and in cases of rapid loss of coherence, the response can be amplified due to the increased contribution of the pseudo-static part of the response.

5 SUMMARY AND CONCLUSIONS

A new response spectrum method is developed for seismic analysis of linear multi-degree-of-freedom, multiply-supported structures subjected to spatially varying ground motions. Variations of ground motion due to wave passage, loss of coherency with distance, and variation of local soil conditions are considered. The former two effects are modeled in terms of a coherency function, whereas the local soil effect is considered in terms of its influence on the response spectral shape at each individual support point. The method is based on fundamental principles of random vibration theory and properly accounts for the effects of correlation between the support motions as well as between the modal responses of the structure. The combination rule explicitly accounts for the contributions of the pseudo-static and dynamic components of the response, as well as for their covariance.

An example application is considered, which demonstrates the influence of the spatial variability of the ground motion on selected responses of the structure, and examines the relative contributions of the pseudo-static, dynamic, and their covariance terms to the total response. It is found that in most cases the spatial variability tends to reduce the response (in relation to the case with uniform support motions), often by a significant amount (e.g., close to 30 percent). However, this rule cannot be generalized since, under certain conditions (i.e., stiff structures and rapid loss of coherency), the response may actually amplify due to an increase in the pseudo-static component of the response.

6 ACKNOWLEDGMENT

This study was supported by the National Science Foundation Grant No. BCS-9011112 with Dr. S-C. Liu as Program Director. The second author was supported in part by the German Academic Exchange Service (DAAD) during his studies at the University of California at Berkeley. This support is gratefully acknowledged.

REFERENCES

Abdel-Ghaffar, A., and L.I. Rubin (1982). Suspension bridge response to multiple-support excitations. *J. Eng. Mech.* 108, 419-435.

Abrahamson, N.A., J.F. Schneider, and J.C. Stepp (1991). "Empirical spatial coherency functions for application to soil-structure interaction analysis." *Earthq. Spectra*, 7, 1-28.

Bolt, B.A., C.H. Loh, J. Penzien, Y.B. Tsai and Y.T. Yeh (1982). Earthquake strong motions recorded by a large near-source array of digital seismographs. *Earthq. Eng. Struc. Dynamics*, 10, 561-573.

Clough, R.W., and J. Penzien (1975). *Dynamics of structures*. McGraw-Hill Book Co., New York, NY.

Der Kiureghian, A. (1981). "A response spectrum method for random vibration analysis of MDF systems." *Earthq. Eng. Struct. Dyn.*, 9, 419-435.

Der Kiureghian, A. (1991). "CQC modal combination rule for high-frequency modes." *Trans. 11th Int. Conf. on Struct. Mech. in Reactor Technology*, Tokyo, Japan, August, K. .

Der Kiureghian, A. and A. Neuenhofer (1991). "A response spectrum method for multiple-support excitations." *Report No. UCB/EERC-91/08*, Earthquake Engineering Research Center, University of California, Berkeley, CA.

Harichandran, R.S., and E. Vanmarcke (1986). "Stochastic variation of earthquake ground motion in space and time." *J. Eng. Mechanics*, ASCE, 112, 154-174.

Kaul, M.K. (1978). "Stochastic characterization of earthquakes through their response spectrum." *Earthq. Eng. Struc. Dynamics*, 6, 497-509.

Luco, J.E., and H.L. Wong (1986). "Response of a rigid foundation to a spatially random ground motion." *Earthq. Eng. Struc. Dynamics*, 14, 891-908.

SEAOC (1990). *Recommended lateral force requirements and commentary*. Structural Engineers Association of California, Sacramento, CA.

Zerva, A. (1990). "Response of multi-span beams to spatially incoherent seismic ground motions." *Earthq. Eng. Struct. Dyn.*, 19, 819-832.

Nonlinear earthquake analysis of arch dam/reservoir

Gregory L. Fenves
Department of Civil Engineering, University of California at Berkeley, Berkeley, CA, U.S.A.

Soheil Mojtahedi
Department of Civil Engineering, University of California at Berkeley, Berkeley, CA, U.S.A.

Richard B. Reimer
Department of Civil Engineering, University of California at Berkeley, Berkeley, CA, U.S.A.

ABSTRACT: Concrete arch dams cannot develop significant tensile stresses in the arch direction during an earthquake because the contraction joints separating the cantilever monoliths will open. A dynamic analysis procedure using a nonlinear joint element simulates the joint opening behavior in the response of a typical arch dam to a maximum credible earthquake. The analysis shows that the maximum arch tensile stress of 2000 psi in a model with closed joints reduces to 800 psi when the joints open. The opening of the joints and release of arch action increases the cantilever tensile stresses to a maximum of 1200 psi at the downstream face compared with 1000 psi at the upstream face for the model with closed joints. It is necessary to include at least three contraction joints in the model of an arch dam to represent the effects of joint opening with reasonable accuracy.

1 INTRODUCTION

Concrete arch dams are usually constructed as cantilever monoliths separated by contraction joints. Since the joints cannot transfer substantial tensile stresses in the arch direction, the joints may open as the dam vibrates in response to earthquake ground motion. A seismic safety evaluation of an arch dam often relies on a linear dynamic analysis assuming the dam is a monolithic structure. The joint opening behavior is not represented, and hence a linear analysis can show unrealistically large tensile stresses in the arch direction.

The earthquake response of arch dams is further complicated by the important effects of dam–water interaction, dam–foundation rock interaction, and the spatial variation of the input motion along the interface between the dam and canyon. It is not possible to include these frequency–dependent effects along with the nonlinear joint behavior in an analysis procedure without some approximation.

A recently developed modeling technique and numerical procedure for computing the nonlinear earthquake response of arch dams provide improved understanding about the effects of joint opening (Fenves 1989). The joints are modeled with a nonlinear joint element, a detailed discretization near the joint provides resolution of stress concentrations, and the dam body is modeled with shell elements. A substructure procedure, in conjunction with the fact that only a few contraction joints in the dam have to be included in the model, provides an efficient numerical solution. The impounded water is represented as an incompressible fluid, the foundation rock is represented by a massless finite element model, and uniform free–field motion is specified along the canyon–dam interface.

This paper presents selected results from an extensive parameter study on joint opening behavior in the seismic response of an arch dam. The study specifically investigates Morrow Point dam, Colorado, U.S.A., subjected to a ground motion characteristic of a maximum credible earthquake at the site. The primary question examined in this paper is how the number of contraction joints included in the model of the dam affects the stress distribution.

2 SUMMARY OF ANALYSIS METHOD

The finite element model recognizes that contraction joints separate the cantilever monoliths, as shown in Figure 1. The cantilevers are modeled by sixteen–node three–dimensional shell elements near the abutments, and thick shell elements away from the abutments. The foundation rock is modeled by eight–node solid elements. As illustrated in Figure 2, several joint elements through the thickness of the dam model the opening and closing of a contraction joint.

The region of the dam adjacent to the contraction joints is modeled by three–dimensional solid elements to provide a transition with the shell elements and improve the resolution of the stresses near the joint elements. The number of solid elements through the thickness of the arch is equal to the number of joint elements through the thickness (Figure 2). The nodal points along the interface of the shell elements and the solid elements are kinematically constrained to remain in a plane.

The regions of the model between the contraction joints are substructures. The static and dynamic behavior of the cantilevers is assumed to be linear, so cracking of concrete in the substructures is not represented. The assumption of linear substructures leads to an

efficient numerical solution procedure even with the nonlinear joint elements.

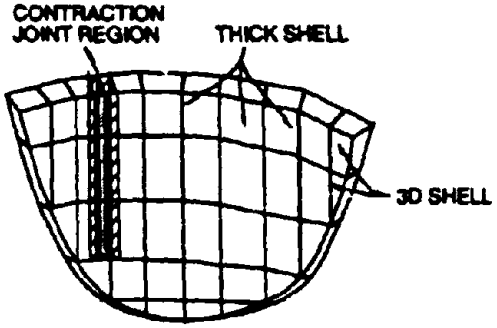

Figure 1. Finite element model of arch dam including contraction joint.

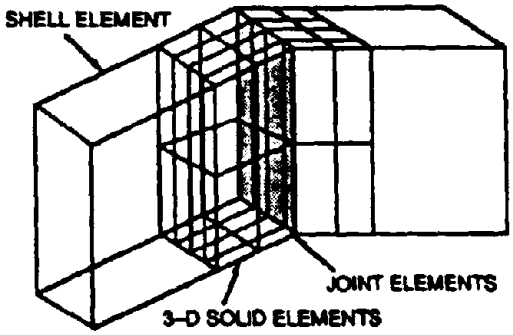

Figure 2. Detail of finite element model for contraction joint region.

2.1 *Nonlinear joint element*

The nonlinear joint element represents the opening and closing of the contraction joints. It is similar to joint elements described by Hohberg (1988). The element develops resisting forces due to relative normal and tangential displacements between two coincident surfaces, as shown in Figure 3(a). The stress–displacement relationship for the element is shown in Figure 3(b). The stresses, q_i, in the joint are a nonlinear function of the relative displacements, v_i. Since the local coordinate system is orthogonal, the assumption is made that displacement in one direction only produces stress in that direction. The joint has a specified tensile strength, q_{0i}, in each direction. Once the strength is reached, the joint unloads and the subsequent tensile strength is zero. In the current study, the tangential displacements are constrained, although this can be relaxed to represent slippage when the joint is open.

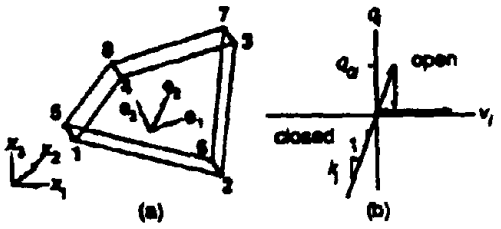

Figure 3. Nonlinear joint element; (a) geometry of element; (b) stress–relative displacement relationship.

The integrals for element tangent stiffness matrix and the restoring force vector are evaluated using Gauss quadrature. For a closed joint, 2x2 Gauss integration exactly evaluates the integrals. In the case of an open joint, 2x2 Gauss integration also produces sufficiently accurate results. The normal to the element surface at the origin is used as an approximation of the normal throughout the element.

2.2 *Substructure analysis procedure*

The equations of motion for a structure with a small number of nonlinear elements may be solved efficiently using a substructure procedure (Clough 1979). Arch dams are an example of such a structure because the cantilevers are assumed to be linear and a small number of joints are nonlinear. In the model of an arch dam, cantilever sections (as defined by the contraction joints in the model) and the foundation rock region are linear substructures, and the set of joint elements is a nonlinear substructure.

The substructure procedure used for the analysis of arch dams (Fenves 1989) is similar to earlier work (Row 1984). The equations of motion for the substructures are coupled by equilibrium and compatibility conditions at the boundaries. The constant–average acceleration method is used for time integration of the equations of motion, and a Newton–Raphson iteration achieves equilibrium in each time step. The substructure solution has several advantages compared with allowing nonlinear behavior in the entire system:

1. An equilibrium iteration during a time step only involves the degrees–of–freedom in the nonlinear substructure, resulting in a substantial reduction of computation for structures with a small number of nonlinear elements.

2. The stiffness matrix for the substructure is computed once because the states of the linear substructures do not change. Only the joint elements are linearized during an iteration.

3. The restoring force for a linear substructure is expressed in terms of the response at the boundaries of the substructure. This also results in a substantial reduction of computation when the number of boundary DOF in a substructure is small compared with the number of interior DOF.

Three static analyses of a dam represent the construction and loading sequence. In the first analysis gravity

is applied to alternate cantilevers acting independently. The remaining cantilevers are loaded by gravity in the second analysis. The third static analysis, for the hydrostatic loads and temperature, uses the complete dam–foundation rock model with joint opening allowed.

2.3 *Dam–Water and Dam–Foundation Interaction*

Water compressibility affects arch dam response (Fok 1987) but the analysis including compressibility requires a frequency domain solution which precludes the nonlinear effect of joint opening. If water compressibility is neglected, dam–water interaction is represented by a frequency–independent added mass matrix and a time domain solution can be used. The added mass matrix can be computed from a finite element model of the impounded water (Kuo 1982).

The added mass matrix is full, however, and it couples all the wet nodes at the upstream face of the dam. This negates a major advantage of the substructure procedure because all substructures are mutually coupled through the impounded water. Since the principal goal of this study is to determine the effects of joint opening on the earthquake response of arch dams, dam–water interaction is simplified by diagonalizing the added mass matrix. The diagonal terms of the added mass matrix are scaled such that the total hydrodynamic force due to rigid body acceleration in each direction is the correct value for the incompressible water in the reservoir.

The modeling of the foundation region is complicated by the three–dimensional geometry of canyons and highly variable properties of the foundation rock. The common practice is to model a foundation region of dimensions approximately equal to the size of the dam. The mass of the foundation rock, and hence wave propagation, is neglected.

The finite element model of the foundation rock region is a massless, linear substructure with uniform support acceleration specified at the far boundaries. The stiffness matrix for the foundation region is statically condensed to the degrees–of–freedom at the dam–foundation rock interface. This matrix could be used in the analysis, but all the interface nodes would have to be included in the boundary partition for the substructure analysis. Numerical studies have shown that it is only necessary to retain the coupling between two adjacent nodes on the dam–foundation interface. Consequently, a cantilever substructure is only coupled to adjacent substructures through the foundation rock.

3 PARAMETER STUDY

Morrow Point dam is a thin double curvature arch dam in a U–shaped canyon. The variable–center dam has an axis radius of 375 ft and the crest length is 724 ft. The thickness of the crown section varies from 52 ft at the base to 12 ft at the crest. Contraction joints between 18 cantilevers are spaced approximately 40 ft at the crest. The dam was selected for the parameter study because:

1. The dam is in a narrow canyon, so the arch action is important in resisting seismic loads.
2. The near symmetry of the dam makes it possible to analyze a symmetric half–model subjected to stream and vertical ground motion components.
3. Previous analytical and experimental studies of the dam are a good basis for interpreting the nonlinear earthquake response.

The parameter study investigates the response of a symmetric half–model of the dam to stream and vertical ground motion components. The response to static loads and symmetric ground motion is symmetric even with joint opening. Further investigation, not described in this paper, examines the effects of the cross–stream ground motion component on the entire dam, because the nonlinear dynamic response is not antisymmetric.

The symmetric half–model of Morrow Point dam includes four contraction joints evenly spaced along the radial direction. This corresponds to seven joints in a model of the full dam, spaced at 90 feet, compared with seventeen joints in the dam. The primary parameter investigated is the number of joints allowed to open in the half–model: zero, one, two, and four joints. For joints that are allowed to open, zero normal tensile strength is specified. Closed joints have a very large tensile strength that prevents opening.

The finite element model of the dam is based on nine design elevations to give 72 shell elements. Three joint elements are used through the thickness at each joint and the transition region has three solid elements in the arch direction. Energy dissipation is represented by Rayleigh damping of 5% in the first and fifth vibration modes. The static analysis includes self–weight and hydrostatic loads, but temperature effects are neglected.

The finite element models of the full reservoir and foundation rock region are developed using the procedures described in Section 2.3.

The acceleration time history used as the input motion is characteristic of a maximum credible earthquake of magnitude 6.5 at a distance of one kilometer. The peak accelerations in the stream and vertical directions are 0.64 g and 0.39 g, respectively. Although the duration is twenty seconds, only the first twelve seconds are used because the peak response of the dam occurs within this time. The analysis uses a time step of 0.01 sec.

4 EARTHQUAKE RESPONSE

Figures 4 to 7 show the envelopes of maximum arch and cantilever stress at the upstream and downstream faces of the dam with full reservoir. The envelopes for the cases with zero (joints closed), one, two, and four joints in the half–model of the dam show the effects of contraction joint opening on stresses in the dam.

When the joints are prevented from opening (zero joints—the dam model is monolithic) the maximum arch tensile stresses are 2000 psi at the upstream face and 1600 psi at the downstream face. The maximum stresses occur at the crown section and at approximately the one–quarter point. Clearly, the contraction joints

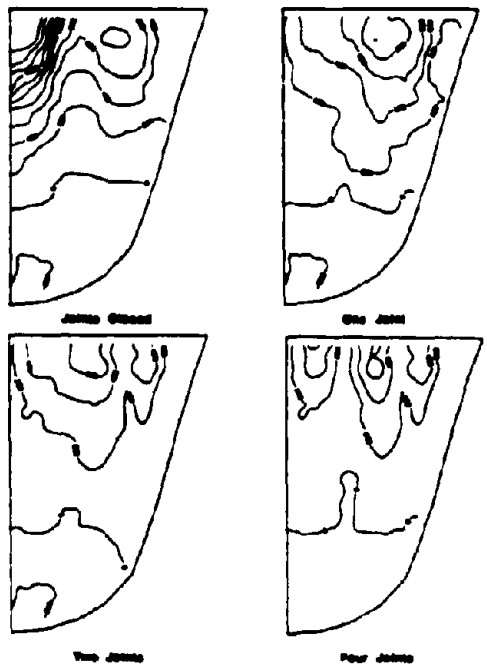

Figure 4. Envelopes of maximum arch stress (in psi) at upstream face of dam with full reservoir.

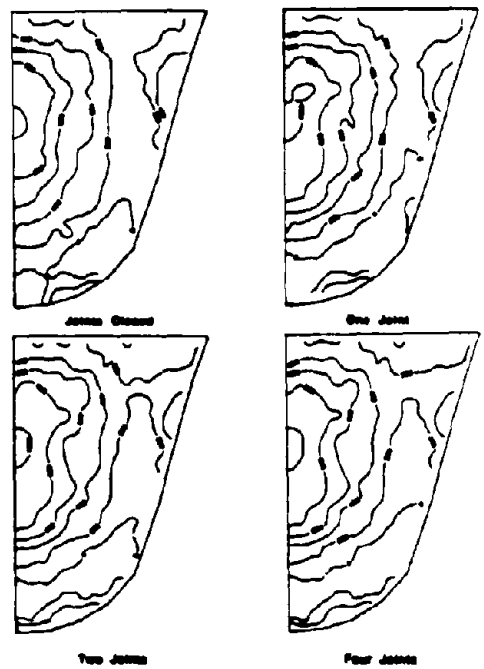

Figure 6. Envelopes of maximum cantilever stress (in psi) at upstream face of dam with full reservoir.

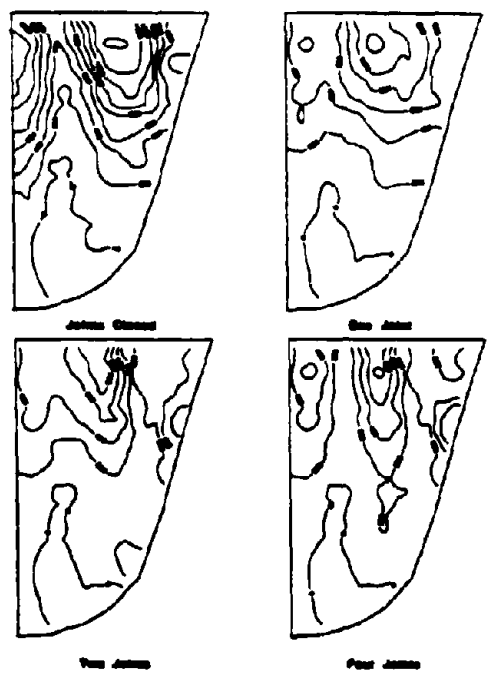

Figure 5. Envelopes of maximum arch stress (in psi) at downstream face of dam with full reservoir.

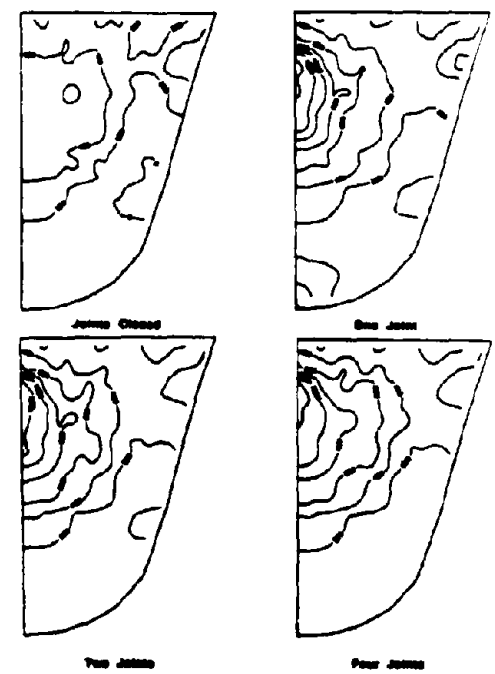

Figure 7. Envelopes of maximum cantilever stress (in psi) at downstream face of dam with full reservoir.

cannot transmit the large tensile analysis predicted by a linear analysis.

Allowing one contraction joint at the crown section to open during the earthquake significantly reduces the arch stresses (Figures 4 and 5). With respect to the model with joints closed, the maximum arch stresses decrease from 2000 psi to 800 psi at the upstream face and from 1600 psi to 1200 psi at the downstream face.

The one contraction joint at the crown does not relieve the arch stresses of 1200 psi at the quarter-point of the downstream face (Figure 5). However, the model with two contraction joints reduces the arch tensile stresses in this region; the maximum arch tensile stress is 800 psi for the two joint model.

The final analysis includes four joints in the symmetric half-model of the dam. The four joint model has a maximum arch stress of about 800 psi and 600 psi at the downstream and upstream faces, respectively. The reduction in arch stresses from two to four joints is less than from one to two joints.

The history of arch stresses at the crown near the crest are shown in Figure 8 for the case with four joints (joints open) and zero joints (joints closed). The tensile stresses that develop in the monolithic model with no joints are eliminated when the joint is allowed to open. The effect of joint opening on the tensile stresses is more important at the upstream face than at the downstream face. The opening, however, does not alter substantially the maximum arch compressive stresses at these locations.

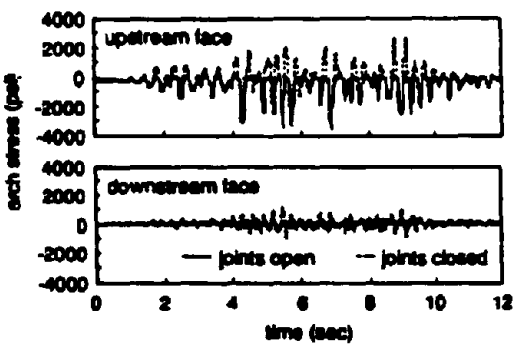

Figure 8. History of arch stress at crest of crown section of dam with four joints and full reservoir.

Joint opening has very little effect on the cantilever stresses at the upstream face. The maximum cantilever tensile stress is about 1000 psi for all cases (Figure 6). However, joint opening does affect the maximum cantilever stresses at the downstream face because the opening transfers the loads from arch action to cantilever bending in the upstream direction. The maximum downstream cantilever stress for the monolithic dam with no joints is 600 psi . As shown in Figure 7, this nearly doubles to a maximum of 1200 psi.

The joints open as the dam displaces in the upstream direction. Figure 9 shows the history of normal displacement at the crest of the crown joint for the four joint model. There are about 20 to 25 cycles of opening, and the maximum opening at the upstream face is one inch for the half-model, which correspond to two inches for the complete dam.

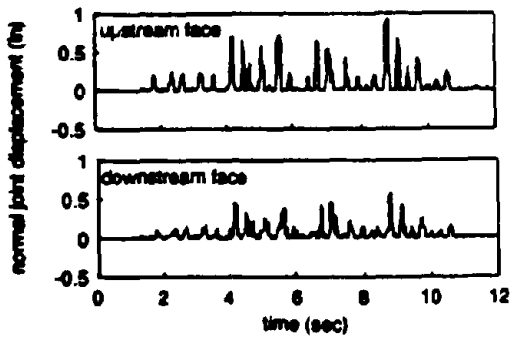

Figure 9. History of normal joint displacement at crest of crown section of dam with four joints and full reservoir.

5 CONCLUSIONS

The nonlinear earthquake analysis of a concrete arch dam with full reservoir shows that joint opening relieves arch tensile stresses typically computed by an analysis of a monolithic dam. For Morrow Point dam subjected to a maximum credible earthquake, the maximum arch stress reduces from 2000 psi to 800 psi when joints are allowed to open. As arch action is relieved, the cantilever stresses increase from a maximum of 1000 psi at the upstream face to a maximum of 1200 psi at the downstream face.

Based on the results of the parameter study, two joints for a half-model (three joints for a complete model) are the minimum necessary to represent the effects of joint opening in arch dams.

ACKNOWLEDGEMENTS

This study was sponsored by the U.S. Bureau of Reclamation, U.S. Corps of Engineers, County of Los Angeles Department of Public Works, and Harza Engineering Company. Alain Placido performed the computer analyses and post-processing of results.

REFERENCES

Clough, R.W., and Wilson, E.L. 1979. Dynamic analysis of large structural systems with local nonlinearities. *Computer methods in applied mechanics and engineering* 17/18: 107–129.

Fenves, G.L., Mojtahedi, S., and Reimer, R.B. 1989. ADAP-88: A computer program for nonlinear earthquake analysis of concrete arch dams. *Report*

No. UCB/EERC-89/12, Earthquake Engineering Research Center, Univ. of Calif. at Berkeley.

Fok, K.-L., and Chopra, A.K. 1987. Water compressibility in earthquake response of arch dams. *Journal of Structural Engineering*, ASCE 113: 958–975.

Hohberg, J.-M., and Bachman, H. 1988. A macro joint element for nonlinear arch dam analysis. *Numerical methods in geomechanics Innsbruck 1988*. G Swoboda, ed., Innsbruck: 829–834.

Kuo, J. 1982. Fluid–structure interactions: added mass computations for incompressible fluid. *Report No. UCB/EERC-82/09*, Earthquake Engineering Research Center, Univ. of Calif. at Berkeley.

Row, D., and Schricker, V. 1984. Seismic analysis of structures with localized nonlinearities. *Eighth world conference on earthquake engineering*. IV: 475–482.

Models of critical regions and their effect on the seismic response of reinforced concrete frames

F.C. Filippou & N. Zulfiqar
University of California, Berkeley, Calif., USA

ABSTRACT: A new approach in describing the hysteretic behavior of inelastic regions in reinforced concrete moment resisting frames is proposed. This approach consists of subdividing the inelastic region into slices called critical regions at locations where cracks form. The response of each critical region to loads or deformations which are applied at the cracked end sections of the region is determined separately and the results combined to yield the response of the inelastic region. The model is used in the analysis of interior and exterior beam-column joints, girder inelastic regions and beam-column subassemblages.

1 INTRODUCTION

Reinforced concrete (RC) structures designed according to present building codes as moment resisting space frames, shear-walls, coupled shear-walls or any combination thereof to withstand strong earthquake motions are expected to deform well into the inelastic range and dissipate the energy input by the base motion through stable hysteretic behavior of structural components. Since inelastic deformations are typically concentrated at certain critical regions within the structure, the accurate prediction of the mechanical behavior of the structure during earthquake excitations depends on the development of reliable analytical models which describe the hysteretic behavior of these regions.

In a typical lower story of a reinforced concrete moment resisting frame, which is designed according to current provisions of earthquake resistant design and is subjected to large lateral displacements, inelastic deformations concentrate at the ends of girders and at beam-column joints (Figure 1). The ideal analytical model of the hysteretic behavior of these inelastic regions should be able to account for all factors which are responsible for the stiffness and strength deterioration of these regions. Among the most important factors is the cyclic bond deterioration along the reinforcing bars, the hysteretic behavior of concrete and reinforcing steel and the effect of shear stress transfer, both, inside the beam-column joint and girder inelastic region and across discrete cracks running through the depth of the member.

2 FORMULATION OF THE MODEL

In this study a rational model of the hysteretic behavior of inelastic regions in RC moment resisting frames is developed. The model accounts for the hysteretic behavior of reinforcing steel and concrete, the cyclic bond deterioration and the transfer of shear within each critical region. The model does not, presently, include the shear transfer across cracks running through the depth of the member.

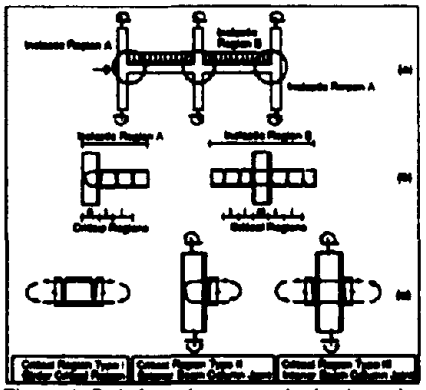

Figure 1. Reinforced concrete inelastic regions
(a) Forces at lower story of moment resisting frame
(b) Subdivision of inelastic region in critical regions
(c) Critical region types I, II and III

In the proposed model each inelastic region is subdivided into elements or slices called critical regions at locations where cracks form. In the presence of low shear stresses, cracks run almost vertically through the depth of reinforced concrete frame members. While well defined cracks are known to form at the beam-column interfaces of the joints (Viwathanatepa et al. 1979) cracks in girder inelastic regions are randomly spaced. To avoid the complications associated with the formation and location of cracks, attention is focused on the final cracking state of the member, when cracks have stabilized at a more or less regular spacing. It is, then, assumed that cracks are vertical, equally spaced and form at predetermined locations in girder inelastic regions.

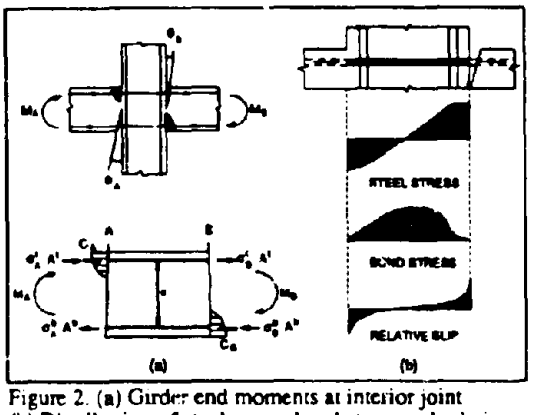

Figure 2. (a) Girder end moments at interior joint (b) Distribution of steel stress, bond stress and relative slip along the top reinforcing bar.

The subdivision of each inelastic region into critical regions is shown in Figure 1 for a typical lower story of a reinforced concrete moment resisting frame. Each inelastic region consists of several critical regions of one or more types. Thus, inelastic region *A* is composed of an exterior beam-column joint (Critical Region Type II) and two girder critical regions (Critical Region Type I), while inelastic region *B* consists of an interior beam-column joint (Critical Region Type III) and four girder critical regions (Critical Region Type I).

After subdividing each inelastic region of the frame into critical regions the inelastic response is determined by following a step-by-step procedure based on the flexibility method. The bending moments at the cracked end sections of each critical region are determined from the moments at the ends of the member by satisfying equilibrium. The bending moments at the end sections of each critical region are resisted by the concrete in compression and the reinforcing steel. The stress in the top and bottom reinforcing bars is partially transferred to the concrete within the region through bond. This process is accompanied by the relative elongation of the top and bottom reinforcing bars with respect to concrete which manifests itself as bar pull-out at the cracks. The pull-out of the top and bottom reinforcing bars is used to calculate the relative rotation at the cracks. Most of the rotation of each critical region can be attributed to this effect with a small contribution coming from the deformation of the concrete within the region. The rotations of all critical regions are then added to obtain the relative rotation at the ends of the member. At the same time the flexibility of the member is updated by summing up the flexibility matrices of the critical regions. The member flexibility matrix is then inverted to obtain the stiffness. If the stiffness has changed during the load step, the end moments which correspond to the new member rotations are not equal to the moments at the beginning of the step and an unbalance results. This unbalance is removed by an iterative solution scheme.

The behavior of each critical region depends on two basic mechanisms which are interrelated: the stress transfer from reinforcing steel to concrete through bond and the equilibrium of forces and moments at the cracked end sections. In order to illustrate the proposed solution process an interior joint is used as an example.

The interior joint is subjected to girder end moments M_A and M_B at the cracked end sections *A* and *B*, respectively, as shown in Figure 2. In this case the location of the cracked end sections is readily established, since well defined cracks are known to form at the beam-column interface of joints. With the forces acting at sections *A* and *B*, as shown in Figure 2a, the equilibrium of horizontal forces at section *A* is given by

$$\sigma'_A A' + \sigma^b_A A^b + C_A = 0 \qquad (1)$$

while the equilibrium of bending moments about the centroid of the bottom reinforcing layer yields

$$\sigma'_A A' d + M_{CA} = M_A \qquad (2)$$

Similarly, the force and moment equilibrium at end section *B* yield the following equations:

$$\sigma'_B A' + \sigma^b_B A^b + C_B = 0 \qquad (3)$$

$$\sigma'_B A' d + M_{CB} = M_B \qquad (4)$$

In Eqs. 1-4 a superscript denotes top or bottom reinforcing layer and a subscript designates the end section. d is the distance between the centroid of the top and bottom reinforcing layer, A is the area of the reinforcing layer and σ is the steel stress. C_A and C_B are the concrete compressive forces, while M_{CA} and M_{CB} are the moments of the concrete compressive stresses about the centroid of the bottom reinforcing layer.

To satisfy the four equilibrium equations (Eqs. 1-4) it is possible to use the steel strain values in sections *A* and *B* as basic unknowns. In this case there are four unknowns, the steel strains at the top and bottom reinforcing layer at sections *A* and *B*, which can be determined from the four available equations. There are, however, two problems with this solution approach. First, the contribution of concrete to the equilibrium of forces and moments depends on the strain distribution. While it is reasonable to assume that plane sections remain plane at an uncracked RC section, such an approximation does not hold true at a cracked section. In addition, the concrete contribution to the section equilibrium reduces to zero at the moment that the crack opens. Since the process of crack opening and closing is related to the relative elongation of reinforcing steel with respect to the surrounding concrete, it is not reasonable to relate crack opening and closing to the steel strains. In order to assess the state of the crack in a realistic way the transfer of steel stresses from section *A* to section *B* needs to be established, since this will yield the relative slip of the reinforcing steel with respect to concrete. Another problem with the solution approach of using the strains at the top and bottom reinforcing steel at sections *A* and *B* as the only unknowns derives from the fact that in this case Eqs. 1 and 2 are rendered independent from Eqs. 3 and 4. This lack of interaction between sections *A* and *B* is a reasonable approximation of the actual behavior, if sections *A* and *B* are far apart and concrete bond is relatively intact in the region between them. Neither fact holds true in critical regions of reinforced concrete frames which are subjected to severe cyclic load reversals and experience considerable cyclic bond deterioration.

It becomes clear from this discussion that Eqs. 1-4 do not suffice to describe the hysteretic behavior of critical regions in RC frames which are subjected to severe cyclic load reversals, since concrete bond in the region between sections *A* and *B* may be severely damaged. In this case the equilibrium of forces and moments at sections *A* and *B* also depends on the stress transfer from reinforcing steel to concrete through bond in the region between sections *A* and *B*. This is, particularly, true in interior beam-column joints.

The proposed model addresses the problem of stress transfer from reinforcing steel to concrete through bond and the associated interaction between the forces and moments of sections *A* and *B* in Figure 2. In this case the four equilibrium equations (Eqs. 1-4) cannot be solved independently, since the stress σ'_A in the top reinforcing steel at section *A* is related to the stress σ'_B at end section *B* and the same holds true for the stresses in the bottom reinforcing steel. The stress transfer problem adds two equations for each reinforcing layer, so that eight coupled nonlinear equations result. Instead of solving the eight nonlinear equations simultaneously an iterative solution approach is adopted in this study. This approach has the advantage that the stress transfer problem is solved separately from the equilibrium equations, so that different solution strategies which are best suited to each case can be used.

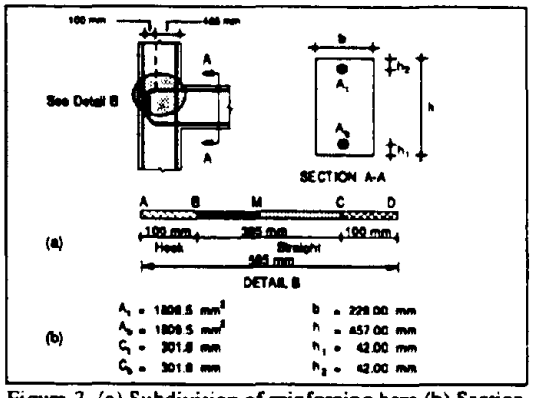

Figure 3. (a) Subdivision of reinforcing bars (b) Section dimensions and details of idealized top and bottom reinforcing layer.

The solution of the stress transfer problem along each reinforcing layer is accomplished by assuming a piecewise linear bond stress distribution between a few control points. The integration of bond stresses between two adjacent cracks yields the steel stress distribution. After obtaining the steel strains from the corresponding stresses the relative slip of the reinforcing bar between two adjacent cracks can be determined by integration of the steel strains. Since the bond stresses at the control points depend on the relative slip between reinforcing steel and concrete at these points, the bond stress distribution which satisfies compatibility, equilibrium and the hysteretic material laws of steel, concrete and bond is found by successive iterations.

3 APPLICATIONS

A number of correlation studies of the hysteretic behavior of interior and exterior beam-column joints, plastic hinge regions and entire beam-column subassemblages under cyclic load reversals are used to test the validity of the proposed model. A few examples are provided below. A very extensive series of correlation studies is presented elsewhere (Zulfiqar and Filippou 1990).

3.1 Exterior beam column joint

The first specimen is an exterior beam-column joint subassembly designed according to the New Zealand Code of practice NZS-3101 (Milburn 1982). In Unit #3 four #8 bars were used as top and bottom beam reinforcement. #2 ties spaced at 100 mm center to center were used as horizontal stirrups in the joint core region and #2 ties spaced at 90 mm center to center were used in the beam inelastic region. The amount of joint shear reinforcement and the presence of the beam stub which provided sufficient anchorage length for the beam flexural reinforcement and also increased the shear resistance of the joint core concrete prevented significant joint shear deformations.

The exterior joint is modeled as shown in Figure 3. An equivalent top and bottom reinforcing layer is derived and the 90° hook of the bars is represented by an equivalent straight portion with modified bond stress-slip relation (Zulfiqar and Filippou 1990). The subdivision of the top and bottom reinforcing bars and the geometry of the model is shown in Figure 3.

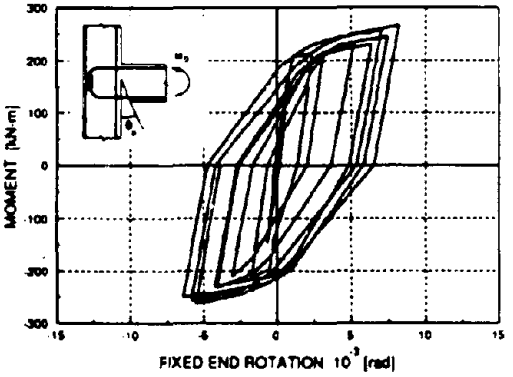

Figure 4. End moment-fixed end rotation relation at the beam-column interface.

The analytical end moment-fixed end rotation relation is shown in Figure 4. The hysteretic behavior is quite stable and the loops show little pinching. Figure 5 shows the steel strain distributions along the top and bottom reinforcing layers for three points of the moment-rotation history. The measured strains are also shown in Figure 5. Very satisfactory agreement between model and measurements is observed.

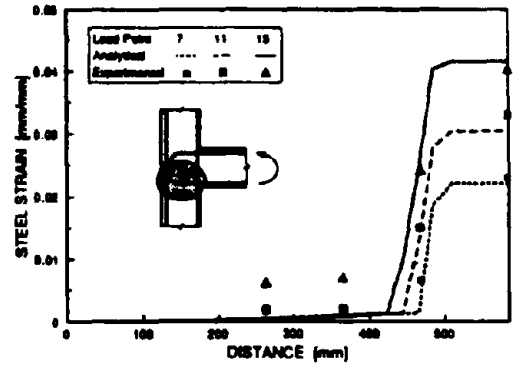

(a) Bottom bars in tension

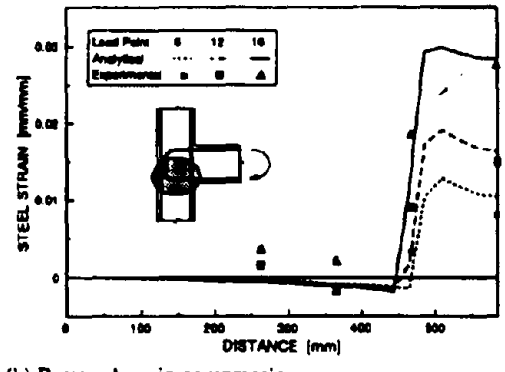

(b) Bottom bars in compression

Figure 5. Distribution of steel strain along the reinforcing bars in the joint.

3.2 Interior beam column joint

The second selected specimen is an interior beam-column joint subassemblage representing a two third scale model of part of the lower story of a typical reinforced concrete moment resisting frame building of 10 to 15 stories height (Beckingsale 1980).

The geometry and reinforcement details of specimen B13 were established so as to ensure that the columns remain elastic and inelastic deformations concentrate at the ends of the girders and in the beam-column joint. The specimen consists of two 356 mm by 610 mm beams and a 457 mm by 457 mm column. The beam was symmetrically reinforced with six D19 (#6) bars in the top and bottom arranged in two layers. The anchorage length of the girder reinforcing bars passing through the joint was 457 mm, which corresponds to about 24 d_b. The column was subjected to an axial load of $0.50f'_cA_g$ and R12.7 (#3) bars spaced at 76 mm were used as horizontal shear reinforcement in the beam-column joint. The high axial load and the sufficient amount of shear reinforcement limited the extent of joint cracking and kept joint shear deformations small.

The interior joint is modeled as shown in Figure 6, which shows the subdivision of the top and bottom reinforcing bars and the geometry of the model. An equivalent top and bottom reinforcing layer is derived (Zulfiqar and Filippou 1990).

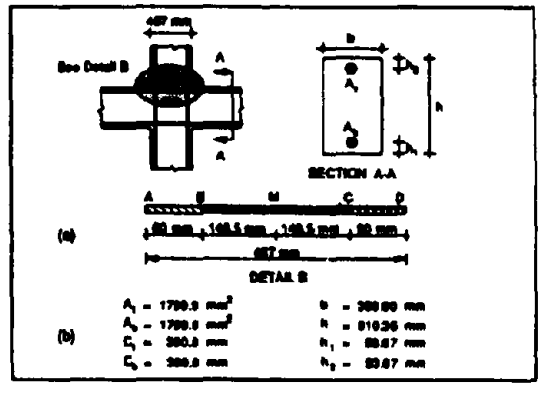

Figure 6. (a) Subdivision of reinforcing bars (b) Section dimensions and details of idealized reinforcing layers

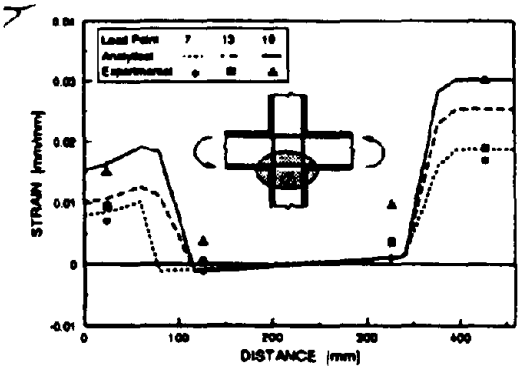

(a) Bottom reinforcing layer

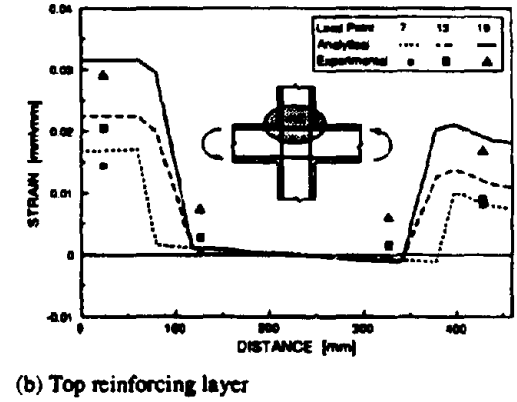

(b) Top reinforcing layer

Figure 7. Distribution of steel strain along the reinforcing bars in the joint

Figure 7 shows the steel strain distributions along the top and bottom reinforcing layers for three points of the moment-rotation history. The measured strains are also shown in Figure 7. Very satisfactory agreement between model and measurements is observed.

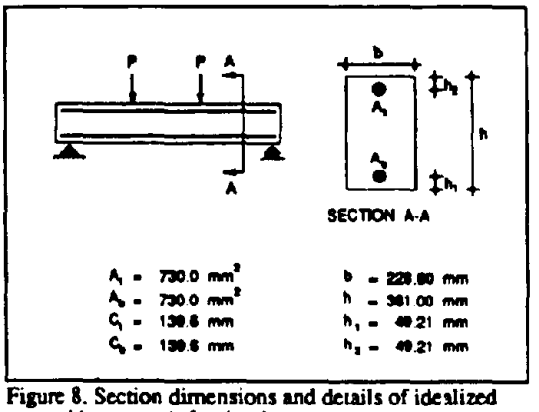

Figure 8. Section dimensions and details of idealized top and bottom reinforcing layer

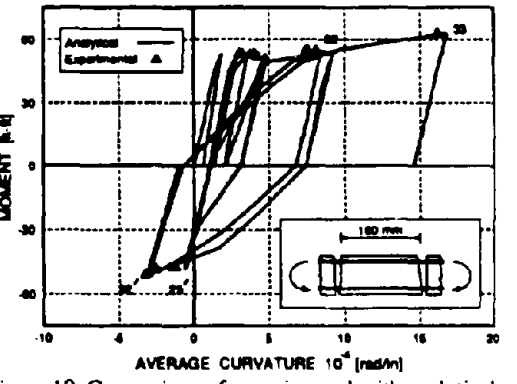

Figure 10. Comparison of experimental with analytical moment-average curvature relation over 180 mm girder length

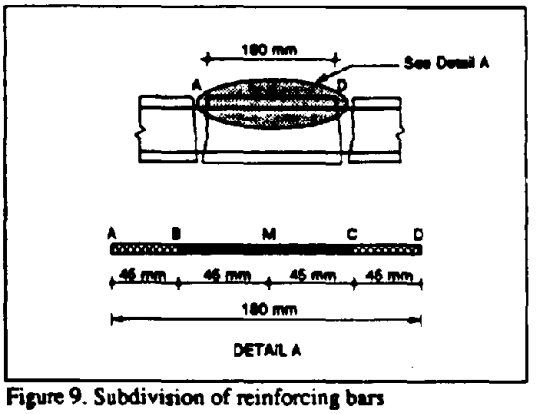

Figure 9. Subdivision of reinforcing bars

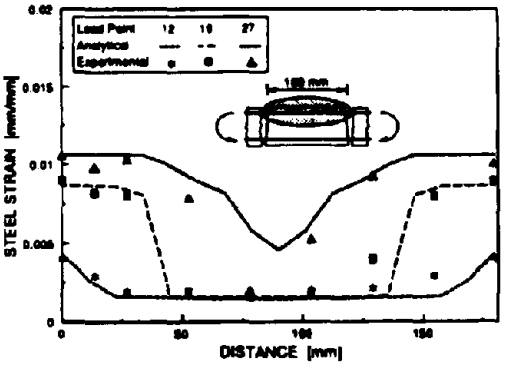

Figure 11. Distribution of steel strain along the top reinforcing layer

3.2 Beam inelastic region

The third selected specimen is a simply supported beam under two point cyclic loading (Bertero et al. 1969). Specimen #4 was a 13 ft. 2 in. long beam with a rectangular cross section measuring 9 in. by 15 in and was reinforced with 2 #7 reinforcing bars at the top and bottom. In the constant moment region between the load application points #2 ties at 6 in. on center provided confinement and prevented buckling of the reinforcing bars under compression. The section dimension and model details are shown in Figures 8 and 9.

The subdivision of the top and bottom reinforcing bars is shown in Figure 9. The length of the girder critical region is set equal to 7 in. (180 mm) based on the recorded crack spacing of the test specimen. The length of regions AB and CD where gradual spalling of the concrete cover takes place is equal to 45 mm which is 1.5 times the clear cover of 30 mm. The confined region BC is divided by point M into two segments of equal length.

The analytical moment-average curvature relation over the measurement length of 180 mm is shown in Figure 10. Figure 11 shows the steel strain distributions along the top reinforcing layer for three points of the moment-rotation history. The measured strains are also shown in Figure 11. Very satisfactory agreement between model and measurements is observed.

3.4 Dynamic response of multistory frames

The effect of models of the hysteretic behavior of inelastic regions on the overall response of well designed frames depends on the characteristics of the earthquake ground motion and on model parameters. Preliminary results with frame models (Filippou and Issa 1988) indicate that the overall response of a multistory frame may not be very sensitive to model selection, as long as the model parameters are selected consistently. It is this consistent selection of model parameters that is very difficult in empirical frame models. The model proposed in this study is based on the material properties and the geometry of the members of interest and can thus help in the rational selection of parameters of simple frame models, which can be economically used in the seismic response analysis of multistory frames. The example of such an analysis of a six story frame which is subjected to a ground motion from the 1977 Bucarest earthquake is shown in Figure 12. It can be seen that the inclusion of the fixed-end rotations between girder and joint does not seem to significantly affect the maximum displacement at the roof of the structure.

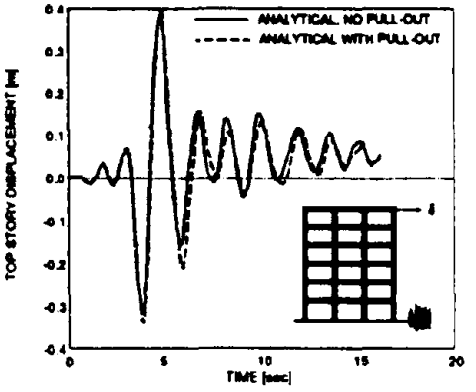

Figure 12. Time history of roof displacement of six story RC moment resisting frame subjected to 1977 Bucarest earthquake.

4 CONCLUSIONS

In this paper a rational model of the hysteretic behavior of inelastic regions in reinforced concrete moment resisting frames is proposed. The model is validated by comparing analytical results with experimental measurements from interior and exterior beam-column joints and girder inelastic regions.

From the correlation studies between analytical and experimental results it is concluded that the proposed model is capable of describing with sufficient accuracy the global and local behavior of interior and exterior beam-column joints provided that the joint shear stress does not exceed the values specified in Chapter 21 of American Concrete Institute Building Code 318-89. The comparison of the analytical moment-fixed end rotation relation of beam-column joints with experimental evidence indicates that the model predicts satisfactorily the hysteretic joint behavior, particularly, the strength, stiffness and energy dissipation capacity of the joint. At the same time the distribution of strains along the reinforcing bars anchored in the joint agrees very well with measured values.

Further studies are required to assess the effect of models of the hysteretic behavior of inelastic regions on the global and local response of reinforced concrete moment resisting frames.

5 ACKNOWLEDGEMENTS

This study was supported by Grant No. ECE-8657525 from the National Science Foundation. This support is gratefully acknowledged. Any opinions expressed in this report are those of the authors and do not reflect the views of the sponsoring agency.

REFERENCES

Beckingsale, C.W. (1980). Post elastic behavior of reinforced concrete beam-column joints. *Research Report 80-20*, University of Canterbury, New Zealand.

Bertero, V.V., Bresler, B., and Liao, H. (1969). Stiffness degradation of reinforced concrete members subjected to cyclic flexural moments. *Report No. EERC 69-12*, University of California, Berkeley.

Filippou, F.C. and Issa, A. (1988) Nonlinear analysis of reinforced concrete frames under cyclic load reversals. *Report No. UCB/EERC-90/06*, University of California, Berkeley.

Milburn, J.R. (1982). Behavior of beam-column joints designed to NZS3101. *Research Report 82-7*, University of Canterbury, 1982.

Viwathanatepa, S., Popov, E.P. and Bertero, V.V. (1979). Seismic behavior of reinforced concrete interior beam-column subassemblages. *Report No UCB/EERC-79/14*, University of California, Berkeley.

Zulfiqar, N. and Filippou, F.C. (1990). Models of critical regions in reinforced concrete frames under earthquake excitations. *Report No. UCB/EERC-90/06*, University of California, Berkeley.

Experimental study of dam-water-foundation interaction

Y.Ghanaat
QUEST Structures, Emeryville, Calif., USA
R.W.Clough
University of California, Berkeley, Calif., USA
B.B.Redpath
Redpath Geophysics, Murphys, Calif., USA

ABSTRACT: This paper describes an experimental study of dam-water-foundation interaction that was conducted on Dongjiang Arch D m in China. In the primary tests, the dam and its retained lake were excited by detonating explosive charges buried in the foundation rock. The system responses to the explosions were recorded by accelerometers, pressure transducers as well as by three-component seismographs. In the secondary test series, the system was excited by shock waves propagated in the lake from small suspended charges. In addition, two approaches based on the seismic refraction and reflection techniques were used to determine the reflection coefficient of the lake-bottom materials. The results obtained indicate that contained explosive detonations appear to be the best means for exciting the dam-water-foundation system in order to predict the dynamic response of the combined system for validation of existing analytical procedures.

1 INTRODUCTION

This paper describes an experimental study of concrete arch dam-water-foundation interaction that was performed in September 1991 on Dong-jiang Dam -- a double curvature structure located in Zixing County, Hunan Province, China. This work was done as the most recent phase of a continuing cooperative research program funded under the U.S.-China Protocol on Earthquake Studies described by Clough et al. (1985). The two collaborating organizations in the present research are QUEST Structures of Emeryville, California and the Institute of Water Conservancy and Hydroelectric Research (IWHR) of Beijing, China. Dr. Yusof Ghanaat of QUEST Structures and Professor H-Q Chen of IWHR are co-principal investigators, while Professor Clough and Dr. C.G. Shen of IWHR have been designated as Project Advisers.

The objectives of the research were to develop new testing procedures for exciting the complete dam-water-foundation system, and to obtain measured data that can be used to validate the existing analytical procedures for predicting the earthquake response of arch dams. The basic concept in this experimental study was to excite the dynamic response of the dam and its retained lake by detonating explosive charges. In the principal program tests, large charges were fired in boreholes drilled into the solid foundation rock at a distance 800 m downstream of the dam; these were intended to excite the dam-water interaction by shock waves travelling through the foundation rock. In a secondary test series, the system was excited by shock waves propagated in the lake water from small explosive charges suspended in the retained lake. A major purpose of the tests was to determine the contribution to the dam-water interaction resulting from reflection and refraction of vibratory waves at the lake bottom, taking account of the sediment deposited there.

The primary instrumentation used in recording the dynamic interaction was a set of dynamic water pressure gages (hydrophones) and its recording system. This equipment was provided by the QUEST team, which was headed by Dr. Ghanaat and included Mr. Bruce Redpath who served as principal geophysicist, as well as Professor Clough. A second instrumentation system consisting of accelerometers and a computer based data acquisition unit was supplied by the U.S. Army Corps of Engineers Waterways Experiment Station (WES) of Vicksburg, Mississippi under the direction of Dr. Robert Hall. The third major response recording system was a set of digital seismograph units together with a computer based data acquisition system; this was provided by IWHR and was under the general supervision of Professor H-Q Chen.

2 TEST STRUCTURE & INSTRUMENTATION

Dongjiang Dam, the highest double curvature arch dam presently in operation in China, is 157 m high and has a crest length of 438 m; it is 7 m and 35 m thick at the crest and base, respectively. The dam structure includes a powerhouse near the toe and four power penstocks; additionally there are three ski-jump spillways, one on the left and two on the right side. Figure 1 is a photograph of the dam taken from downstream.

Fig.1 Downstream view of Dongjiang Dam.

The hydrodynamic pressure recording system supplied by QUEST included a set of 20 Aquasense hydrophones having a cutoff frequency of 3 Hz and a sensitivity of 5.3 Volts/Bar. Each of these gages is encapsulated and provided with a waterproof lead wire; they proved to be completely free of water leakage problems during the entire test program. They were connected to a 24-channel EG&G Geometrics Model-2401 Seismograph, which is a computer based recorder including a 15 bit A/D converter, instantaneous floating point amplifiers, selective sampling ratios from 0.1 to 50 msec, various digital filters and built-in data storage capacity for 4096 data samples per record.

In the major tests of the dam, 9 of the 20 hydrophones were suspended in groups of three from locations at the dam crest; these measured the dynamic pressures at three different elevations at the dam face, as shown in Figure 2. Also shown are the two additional hydrophones suspended similarly that served to sense the dynamic pressures at locations near the abutments. Three additional strings of three sensors each were suspended from a support cable positioned on a vertical plane near the midsection of the dam and oriented normal to the dam face. These strings were attached at distances of 60 m, 110 m, and 210 m from the dam face (measured at the water surface); thus the 9 hydrophones were located on a rectangular grid as shown in Figure 3.

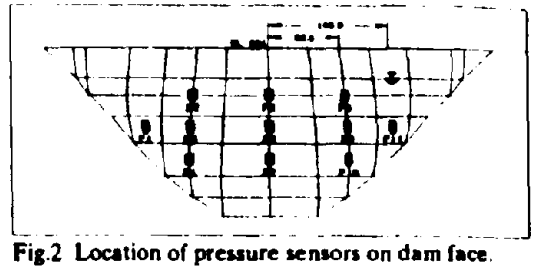

Fig.2 Location of pressure sensors on dam face.

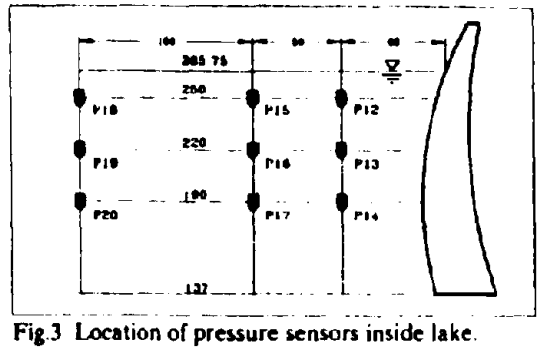

Fig.3 Location of pressure sensors inside lake.

The PC-based digital recording system supplied by WES included a set of 15 Wilcoxon accelerometers and served to record the response of the dam to either the explosive generated ground shock or the lake water shock wave. The accelerometers were positioned on the crest and within the galleries of the dam at the locations shown in Figure 4; all were oriented so as to sense the radial component of dam accelerations.

Also shown in Figure 4 are the positions where the 12 strong motion seismograph units supplied by IWHR were located. It will be noted that 7 of these were at the dam-rock interface, while the other 5 were equally spaced across the dam crest. The abutment positions were intended to give some indication of the shock wave applied to the dam by the foundation rock; of course, their records did not indicate "free-field" motions because of the influence of the dynamic response of the dam. Comparison of the crest location response with that at the dam-rock interface gives an indication of the amplification caused by the dynamic response of the dam.

Two additional seismograph units were positioned along the river bank to record the free-field motions induced by the blasts. One was at the base of the bridge 100 m from the shot array, and the other was placed either at 445 m (S13a) or at 665 m

(S13b) along the line between the shot holes and the dam base as shown in Figure 5. All of these seimographs as well as those on or adjacent to the dam were three component units with their axes oriented to record the acceleration along the main channel, across channel, and vertically.

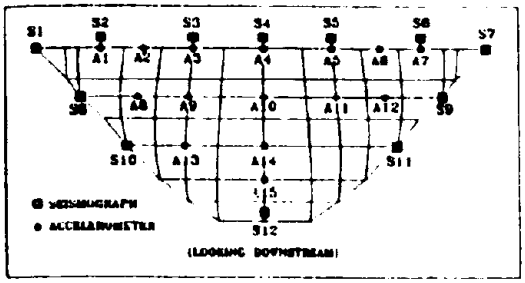

Fig.4 Location of accelerometers and seismographs for measuring dam response.

3 EXPERIMENTAL PROGRAM

This experimental study included two types of explosion tests intended to demonstrate the dam's dynamic performance: those applied to the foundation rock and those detonated in the lake water. Other shock tests were done using small blasting cap charges to evaluate the reflection and refraction properties of the materials at the lake bottom. In addition, supplementary tests were performed to determine the vibration properties of the dam, and the topography of the lake bottom. Descriptions of each part of the test program follow.

3.1 *Blast tests*

A. Ground shock: For the ground shock phase of the testing, an array of 5 boreholes, 15 cm in diameter, were drilled to a depth of 40 m at a distance of 800 m from the dam base. As shown in Figure 5, this array was aligned approximately parallel to the dam axis so the shock wave propagating from simultaneous detonation of the charges would impinge nearly simultaneously along the entire base of the dam. Two preliminary shots of 40 kg each were detonated in hole no. 1 to calibrate the prediction of the resulting ground motion based on empirical equations. This calibration was needed to ensure that the larger charges used later would not damage the highway bridge located only 40 m away (see Figure 5). In addition these shots helped in setting gain ranges on the instrumentation and in establishing communication between recording and detonation sites that was needed for the firing count-down and for the firing impulse signal that gave a common time base for all recorders.

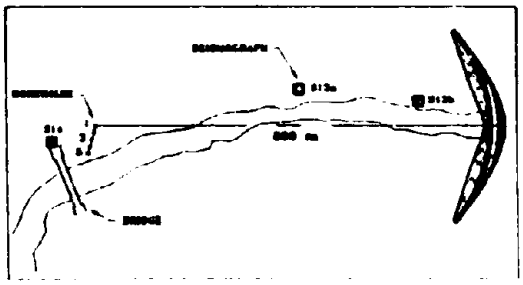

Fig. 5 Plan view showing dam, boreholes, free-field seismographs and highway bridge.

For the first multiple-hole ground shock blast, the five holes of the array were loaded with 120 kg of explosives each, making a total blast weight of 600 kg. The explosive used was a water-resistant ammonium nitrate based slurry supplied in cylinders 20 cm long and 13 cm in diameter; the charges were water stemmed. After the blast, the 4 holes located in competent rock (nos. 1, 2, 4, 5) were found to be undamaged and suitable for a second test. However, hole no. 3 had been drilled through fill material at the surface and thus was severely damaged. Hence for the second multiple blast only holes 1, 2, 4, and 5 could be used, but these were loaded with 150 kg each so the total blast weight again was 600 kg. In planning the test program it had been hoped to use sequential detonation with 100 to 200 ms delays; however such precise delay caps were not available to the project in China, so in both of the multiple blasts all charges were detonated simultaneously.

B. Lake water shock: Additional data on the dam-water interaction mechanism was obtained using as excitation the water shock waves induced by detonation of explosives in the lake. It was well-known from previous experience that such water shock tests could produce response in the dam as great as that caused by ground shock due to explosive charges two orders of magnitude larger; consequently it was important to learn how such water shock tests might be used in the study of dam-water interaction.

In these tests, 4 kg charges were suspended from a cable stretched across the lake parallel to the dam axis at a distance of 210 m from the dam face. The suspension point was about 30 m east of the dam midsection, and the charge was at a depth of 10 m. Three of these blast tests were performed with vary-

ing degrees of success, the variability being due mainly to difficulty in communication between the recording site at the crest of the dam and the detonation point on the lake. The first shot was totally unrecorded because it was detonated before the recorders were turned on; the timing of the second shot was well coordinated but the recording gain for the transducers below the water surface was too great so many transducer signals were saturated. In the third shot again good records were attained only for the accelerometers on the crest, even though the recording gains for the accelerometers in the galleries had been adjusted to measure up to 1g. No hydrophone records were obtained in this final shot.

C. *Refraction and reflection tests:* An additional series of water shock tests was done as a first attempt to develop procedures for measuring the reflection coefficient of the lake-bottom materials, the coefficient that had been used previously by Rosenblueth (1968) and by Hall and Chopra (1980). Two approaches were used, both utilizing a vertical 12-channel array of hydrophones and a blasting cap energy source as shown in Figure 6. In the first approach, the propagation velocity of the bottom materials was measured by means of novel technique described by Hunter and Pullan (1990). While refraction surveys are usually accomplished by recording the times of first arrival from a source of energy at the end of a linear string of detectors placed horizontally along the surface of interest, this is a difficult operation when 100 m of water overlies the surface. The method described by Hunter and Pullan that we employed requires only that a vertical array be suspended just above the bottom and that shots be detonated on the bottom at some horizontal distance away from the array. Knowing the propagation velocity and the density of the bottom sediments then allows a direct computation of the reflection coefficient based on the ratio of the acoustic impedances of the water and the underlying material.

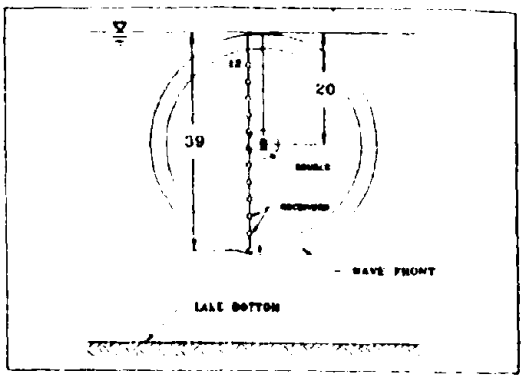

Fig.6 Test set-up for lake-bottom reflection tests

The second approach to obtaining the reflection coefficient was to attempt to measure the amplitude of incident and bottom-reflected pulses directly by recording these signals on the same array of vertical hydrophones as depicted in Figure 6. The array was suspended below the water surface and a cap was detonated few meters away from the center of the hydrophone array. Figure 7 shows a record obtained from one of these experiments. The incident and reflected (both surface and bottom-reflected) pulses are clearly visible on the record. The use of multichannel array of sensors, as opposed to a single sensor, allows the events to be easily identified in the field simply by visual correlation across the record.

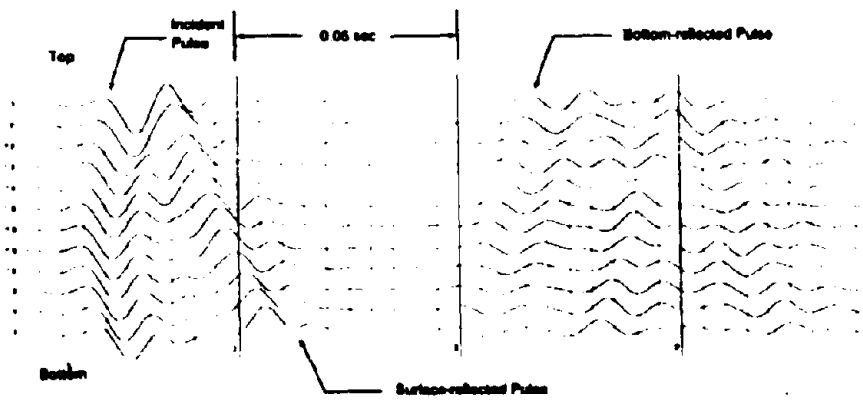

Fig. 7 Reflection record obtained from vertical array of hydrophones suspended in lake.

3.2 Supplementary tests

A. Ambient vibration tests: Although it was not a major purpose of this research program to study the vibration properties of Dongjiang Dam, it was considered important to use measured properties for validation of the mathematical model that was to be employed in subsequent phases of the research. For this reason, the response of hydrophones and accelerometers in the dam to ambient noise were recorded, and these records were then used in evaluating the system vibration properties. To facilitate carrying out this research effort on dam-water interaction, the operators of the dam agreed to turn off the power turbines for a limited period of time so that the blast test data would be relatively pure. Thus it was possible to study the ambient excitation performance of the dam both with and without the turbines running, and it was found that the ambient noise signal was reduced by a factor of 6 when the turbines were turned off.

B. Bottom profile surveys: The lake geometry, especially near the dam, may have some influence on the dam-water interaction mechanism. The actual bottom profiles of dam-retained lakes needed for the dynamic response analysis usually differ from the original canyon topography due to the sediment accumulation and the overburden materials. Thus acoustic surveys were performed to establish the actual bottom profiles for the Dongjiang Lake. The measurements were conducted from a boat moving steadily along three sections across the lake and along two additional sections in the channel direction. The equipment used consisted of a fathometer with both digital display of actual bottom depth at all times as well as a paper recorder, and an electronic compass for determining positions with respect to a fixed reference point. This procedure proved to be very effective and indicated some profile features that had not been noted in the construction drawings.

4 SUMMARY OF MEASURED DATA

This experiment has produced what is probably the most complete set of data now available for the study of dam-water-foundation interaction effects. A total of 20 pressures, 16 accelerations, and 42 components of strong motion seismograph records have been collected. In addition, each reflection and refraction test provided 12 additional pressure records for determining the bottom reflection coefficient. The comprehensive data analysis and interpretation of the recorded signals will take some time and will be presented in our final report to the National Science Foundation. Only a few examples of some of the measured data can be included in this paper mainly due to space limitation. The radial components of seismograph records S14 and S13b which were recorded at 100 m and 665 m distances, respectively, from the boreholes are shown in Figure 8. The most noticeable features in these traces are the reduction in amplitude and the elongation in duration of motions with distance from the energy source.

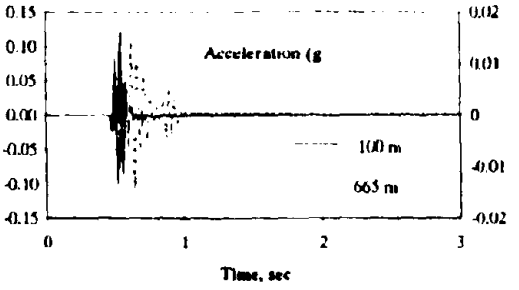

Fig. 8 Radial component of free-field records at 100 m and 665 m from energy source.

Figures 9 and 10 show an example time-history and power spectrum of the dam response recorded at the center of the dam crest (A4 in Fig. 3). This power spectrum clearly indicates identifiable vibration modes that were excited; especially the measured 8 modes below 10 Hz are of particular interest in the response of the dam to earthquake ground motions. The power spectrum for one dynamic pressure transducer (P3) shown in Figure 11 is another example pertinent to the study of dam-water interaction. Information related to the mode of vibrations similar to that identified from the acceleration record can be deduced from this pressure spectrum.

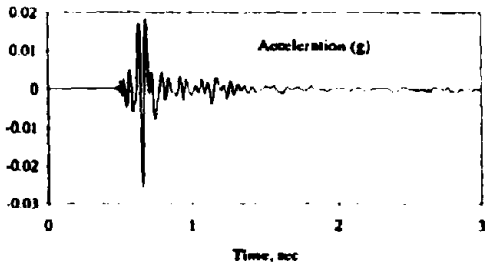

Fig.9 Time-history of dam radial acceleration A4.

The results of ambient measurements (not included in this paper) showed similar and some additional modes, even when the power turbines were off; in particular the hydrophones inside the lake at 210 m away from the dam could still record such ambient noise.

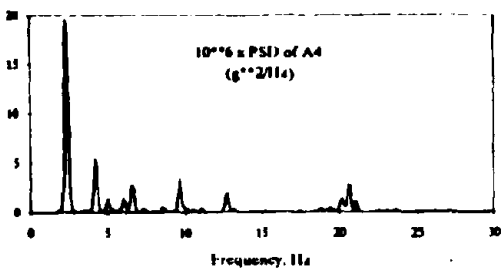

Fig. 10 Power spectrum of dam acceleration A4.

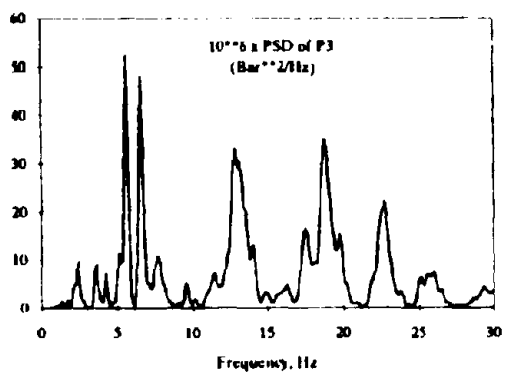

Fig. 11 Power spectrum of dynamic pressure P3.

5 CORRELATION STUDIES

In addition to the experimental aspects of the investigation described in this paper, the field measurements were preceded by several computer analyses of Dongjiang Dam in order to obtain a preliminary understanding of the expected dynamic response behavior. More refined computer analyses of the dam-water-foundation system, both including and ignoring the water compressibility and the lake-bottom absorption effects, are now underway and will be reported later. The main purpose of these analyses is to verify the accuracy of existing analytical procedures by comparing the calculated results with those measured in the field. For this purpose we will attempt to construct a transfer function between the measured dam response and the free-field ground motions. These transfer functions based on the measured accelerations and the dynamic pressures will then be compared with results calculated using the latest computer analysis procedures for the dam-water-foundation interaction.

6 CONCLUSION

This experiment has proved that concrete arch dams and their retained lake can be successfully excited by detonating explosive charges buried in the foundation rock. It also demonstrated that good planning, execution, and appropriate instrumentation are essential for obtaining meaningful signals in the frequency range of interest. Similar to earthquake ground shaking, the complete system was excited by these blast shock waves travelling through the foundation rock; thus they produced more representative data on the dam-water-foundation interaction effects than are given by other test procedures. The seismic refraction and reflection approaches used here for the first time to measure the reflection coefficient of the lake-bottom materials were successful, and thus have provided two procedures for measuring this coefficient in the field.

The acquired data are specially unique because they have provided a first opportunity to construct transfer functions between any measured dam point response and the ground motions measured in the free-field. This information in addition to expressing the measured vibration properties provides the basis for validating existing analytical procedures for predicting the earthquake response of arch dams.

REFERENCES

Clough, R.W. et al. 1985. Dynamic interaction effects in arch dams. University of California Earthquake Eng. Research Center Report No. *UCB/EERC-85/11*.

Hall, J.F. & A.K. Chopra. 1983. Dynamic analysis of arch dams including hydrodynamic interaction. *J. of Eng. Mech. Div.*, ASCE, V. 109, No. EM1:149-167.

Hunter, J.A. and S.E. Pullan 1990. A vertical array method for shallow seismic refraction surveying of the sea floor, *Geophysics*, V.55, No. 1: 92-96.

Rosenblueth, E. 1968. Presion hidrodinamica en presas debida a la aceleracion vertical con refraccion en el fondo. *2nd Congreso Nacional de Ingenieria Sismica*. Veracruz, Mexico.

Evaluation of seismic code provisions for asymmetric-plan systems

Rakesh K. Goel and Anil K. Chopra
University of California, Berkeley, CA 94720

ABSTRACT: The effects of plan asymmetry on the earthquake response of code-designed, one-story systems are identified with the objective of evaluating how well these effects are represented by torsional provisions in building codes. The earthquake-induced deformations and ductility demands on resisting elements of asymmetric-plan systems, are compared with their values if the system plan were symmetric. The presented results demonstrate that the design eccentricity in building codes should be modified in order to achieve the desirable goal of similar ductility demands on asymmetric-plan and symmetric-plan systems. The design eccentricity should be defined differently depending on the design value of the reduction factor R.

1 INTRODUCTION

The evaluation of torsional provisions in building codes based on computed responses of elastic as well as inelastic, asymmetric-plan systems has been the subject of numerous studies in the past. However, the conclusions of these studies may not be generally applicable to code-designed buildings because the assumed plan-wise distribution of stiffness and strength is not representative of code-designed buildings and the strength distribution can significantly influence the inelastic structural response (Chopra and Goel 1991). Thus, the main objective of this work is to investigate the effects of plan-asymmetry on the earthquake response of code-designed, one-story systems and to determine how well these effects are represented by torsional provisions in building codes. For this purpose, the deformation and ductility demands on resisting elements of asymmetric-plan systems are compared with their values if the system plan were symmetric. Based on these results, deficiencies in code provisions are identified and improvements suggested.

2 TORSIONAL PROVISIONS IN SEISMIC CODES

2.1 Method for Computing Design Forces

The design force V specified in building codes is usually much smaller than the strength V_o required for the system to remain elastic during intense ground shaking. Instead of computing the base shear from code formulas which would result in different values according to different codes, the base shear is defined as

$$V = \frac{1}{R} V_o \tag{1}$$

where R is a reduction factor depending on the capacity of the system to safely undergo inelastic deformation during intense ground shaking.

In a one-story, symmetric-plan system, the design force V is applied at the center of stiffness (CS). If the floor diaphragm is rigid, all resisting elements along the direction of ground motion undergo the same lateral displacement u, the lateral resisting force in the elements is $k_j u$, and the total resisting force is $V = K_y u$; k_j and K_y are the lateral stiffness of the j^{th} element and the total system, respectively. Thus, the design force in the j^{th} resisting element is $(k_j/K_y)V$ and the forces are distributed to the elements in proportion to their lateral stiffnesses or rigidities.

In asymmetric-plan systems, the design force V is applied eccentric from the CS at a distance equal to design eccentricity, e_d, which is defined in the next section. Under the action of the resulting torque, $e_d V$, the rigid roof diaphragm will undergo rotation of $e_d V/K_\theta$ where $K_\theta = \sum k_j (x'_j)^2 + \sum k_{xi} y_i^2$ is the torsional stiffness about the CS, in which $x'_j = x_j - e_s$; x_j is the distance of the j^{th} element oriented in the Y-direction from the center of mass (CM); e_s is the stiffness eccentricity, i.e., the distance between the CM and the CS; and y_i defines the location of the i^{th} element oriented in the X-direction. Thus the design force in the j^{th} element along the direction of ground motion is

$$v_j = \frac{k_j}{K_y} V + \frac{e_d V}{K_\theta} (-x'_j) k_j \tag{2}$$

The second term represents the element force associated with its deformation resulting from deck rotation and thus the change in element force due to plan-asymmetry. Obviously, the torsion induced forces are distributed to the various resisting elements in proportion to their torsional

stiffnesses or rigidities.

2.2 Design Eccentricity

Most building codes require that the lateral earthquake force at each floor level of an asymmetric-plan building be applied eccentrically relative to the CS. The design eccentricity e_d specified in most seismic codes is of the form (International 1988)

$$e_d = \alpha e_s + \beta b \tag{3a}$$

$$e_d = \delta e_s - \beta b \tag{3b}$$

where b is the plan dimension of the building perpendicular to the direction of ground motion; and α, β, and δ are specified coefficients. For each element the e_d value leading to the larger design force is to be used. Consequently, Eq. 3a is the design eccentricity for elements located within the flexible-side of the building and Eq. 3b for the stiff-side elements (Fig. 1).

The coefficients, α, β, and δ vary among building codes (International 1988, Tentative 1978). For example, the Uniform Building Code (UBC-88) and Applied Technology Council (ATC-3) provisions specify β=0.05 and α=δ=1, with α=1 implying no dynamic amplification of torsional response; the Mexico Federal District Code (MFDC-77) specifies β=0.1, δ=1, and α=1.5, which implies dynamic amplification; the National Building Code of Canada (NBCC-85) specifies β=0.1, α=1.5, and δ=0.5; and the New Zealand Code (NZC-84) specifies β=0.1 and α=δ=1.

The first term in Eq. 3 involving e_s is intended to account for the coupled lateral-torsional response of the building arising from lack of symmetry in plan, whereas the second term is included to consider torsional effects due to factors not explicitly considered, such as the rotational component of ground motion about a vertical axis; differences between computed and actual values of stiffnesses, yield strengths, and dead-load masses; and unforeseeable unfavorable distribution of live-load masses. This accidental eccentricity, βb, which is a fraction of the plan dimension, b, is obviously considered in design to be on either side of the CS.

3 INELASTIC RESPONSE

From a design point of view, it would be useful to know how the deformations and ductility demands of resisting elements in an asymmetric-plan system differ from those in the corresponding symmetric-plan system. For this purpose, presented in this investigation are the deformations u_i and ductility demands μ_i of resisting elements in the asymmetric-plan system, normalized by u_o and μ_o, the respective response quantities of the corresponding symmetric-plan system -- a system with e_s=0 but mass m, lateral stiffness K_y, torsional stiffness K_θ, about the CS, and element stiffnesses k_{jy} same as in the asymmetric-plan system (Goel and Chopra 1990). The normalized response quantities, u_i/u_o and μ_i/μ_o, for the system of Fig. 1 are presented in the form of response spectra for the first 6.3 secs. of the S00E component of the 1940 El Centro ground motion applied in the Y-direction. This excitation and its response spectra with various frequency regions identified are available elsewhere (Goel and Chopra 1990, Veletsos and Vann 1971). The yield force for the system is defined by Eq. 1 and the element yield forces are determined in accordance with the torsional provisions of UBC-88. In order to focus on effects of plan asymmetry, the accidental eccentricity is not included in computing the design forces for the resisting elements of the asymmetric-plan system and its corresponding symmetric-plan system. Two types of asymmetric-plan systems are considered: in the first system, the code design force for the stiff-side element can be smaller than the design force of the same element in the corresponding symmetric-plan system; and in the second type, such a reduction is precluded. Each resisting element oriented along the ground motion direction is idealized as elastic-perfectly-plastic with its yield force defined by the design force; the perpendicular elements are taken as elastic, an assumption which has little influence on the response (Goel and Chopra 1990). Several parameters of the system are fixed at: stiffness eccentricity normalized by the radius of gyration, e_s/r = 0.5, ratio of the uncoupled torsional and lateral frequencies, Ω_θ = 1, and damping ratio, ξ = 0.05.

The deformations of resisting elements in the system designed according to UBC-88 may be significantly affected by plan-asymmetry, as indicated by the deviation of u_i/u_o or μ_i/μ_o from unity (Fig. 2). Plan-asymmetry tends to reduce the deformation of the stiff-side element in medium-period, velocity-sensitive systems and increase the deformation of the flexible-side element compared to their respective deformations in the corresponding symmetric-plan system. However, the effects of plan-asymmetry on element deformations are small for short-period, acceleration-sensitive systems, and negligible for long-period, displacement-sensitive systems. The increased strength of the system resulting from the restriction that the stiff-side element design force must not fall below its symmetric-plan value affects the response ratio, u_i/u_o, in a manner consistent with the effects of strength increase on the response of SDF systems (Veletsos and Vann 1971).

The ratio μ_i/μ_o of the element ductility demands in an asymmetric-plan system and the corresponding symmetric-plan system are also presented in Fig. 2. If the design force for the stiff-side element is permitted to be smaller than its value in the corresponding symmetric-plan system, over a wide range of periods the element ductility demand is significantly larger due to plan-asymmetry, primarily because the yield deformation of the element is smaller in asymmetric-plan systems if reduction in its design force is permitted (Chopra and Goel 1991). However, if reduction in the element design force is precluded, μ_i/μ_o=u_i/u_o because the yield deformations of this element are identical in the symmetric-plan and asymmetric-plan systems, and the above observations on how deformations are affected by plan-asymmetry also apply to ductility demand. The ductility demand on the flexible-side element is significantly reduced because of plan-

asymmetry, with exceptions at few periods (Fig. 2), because the yield deformation of this element in the code-designed asymmetric-plan system is significantly larger than in the symmetric-plan system (Chopra and Goel 1991). These trends are unaffected by whether the design force reduction for the stiff-side elements is permitted or not (Fig. 2), primarily because the yield deformation of the flexible-side element is unaffected by such reduction (Chopra and Goel 1991).

The preceding results have demonstrated that the response of systems with and without reduction in the stiff-side element design force, arising from plan-asymmetry, may differ significantly. In particular, the ductility demand on the stiff-side element may increase significantly because of plan-asymmetry when reduction in the stiff-side element design force is permitted. Since it is desirable that the element ductility demands be similar whether the plan is symmetric or not, the presented results suggest that seismic codes should preclude reduction in the design forces of the stiff-side elements below their values for symmetric-plan systems.

Several earlier investigations (e.g., Goel and Chopra 1990, Tso and Hongshan 1990) of the earthquake response of asymmetric-plan systems with equal stiffness and strength eccentricities, i.e. $e_p=e_s$, indicate that the largest deformation as well as the largest ductility demand generally occurs in the flexible-side elements, which were therefore interpreted as the most critical elements for design purposes. However, the preceding results for the system of Fig. 1 indicate that, although the largest deformation among all the resisting elements of the code-designed asymmetric-plan systems for which $e_p<<e_s$ occurs in the flexible-side element, the largest ductility demand may occur in the stiff-side element. Thus, additional care is required not only in the design of flexible-side elements for deformation demand, but also in the design of stiff-side elements for ductility demand.

4 'ELASTIC' RESPONSE

It is the intent of most seismic codes that buildings suffer no damage during some, usually unspecified, level of moderate ground shaking. Thus, the elastic response of asymmetric-plan systems designed according to UBC-88 is examined next. The normalized deformation, u_i/u_{o_i}, and ductility demand μ_i, are presented in the form of response spectra for the El Centro ground motion; values for other parameters are fixed: $e_s/r=0.5$, $\Omega_\theta = 1$, $R = 1$, and $\xi=0.05$. $R=1$ implies that the design strength V of the corresponding symmetric-plan system is just sufficient for it to remain elastic during the selected excitation. However, as will be shown in subsequent sections, asymmetric-plan systems designed for the same base shear may not remain elastic.

The deformation of resisting elements may be significantly affected by plan-asymmetry. The deformation of the stiff-side element is reduced because of plan-asymmetry for most short-period, acceleration-sensitive and medium-period, velocity-sensitive systems whereas deformation of the flexible-side element in such systems is considerably increased (Fig. 3). The element deformations of long-period, displacement-sensitive systems are essentially unaffected by plan-asymmetry (Fig. 3).

The ductility demand for stiff-side and flexible-side elements in the asymmetric-plan system exceeds one in some period ranges (Fig. 3) indicating yielding in these elements, which were designed to remain elastic if the building plan were symmetric. The stiff-side element yields more if its design force is permitted to fall below its symmetric-plan value because this results in smaller yield deformation (Chopra and Goel 1991). As a corollary, this element yields less if reduction in its strength is not permitted. The flexible-side element yields primarily because of its significantly larger deformation (Fig. 3) compared to the symmetric-plan system, although its yield deformation is also larger (Chopra and Goel 1991). However, its ductility demand is unaffected whether reduction in the stiff-side element design force is permitted or not because the peak deformation as well as the yield deformation of the flexible-side element is unaffected by such reduction.

5 RESPONSE OF SYSTEMS DESIGNED BY OTHER CODES

The response results presented in this paper are for systems designed by the UBC-88. Similar results generated for systems designed according to other codes -- NBCC-85, MFDC-77, MFDC-87, and NCZ-84 -- are available in Chopra and Goel (1991). These results indicated that the element deformations in systems designed by various codes are essentially identical; however, the ductility demands may differ significantly among these systems. Among these codes, systems designed by UBC-88 experience the largest ductility demand, whereas systems designed by MFDC-87 undergo the smallest ductility demand; response of systems designed by other codes fall in between these two extremes. It was also found that element ductility demands in the MFDC-87-designed systems tends to be significantly reduced because of plan-asymmetry, suggesting that the additional requirements imposed in this code to restrict the strength eccentricity may not be necessary.

6 MODIFICATIONS IN DESIGN ECCENTRICITY

The results of preceding sections indicate that deformations and ductility demands on resisting elements in a code-designed asymmetric-plan system differ from those for the corresponding symmetric-plan system. However, it would be desirable that the responses of the two systems be similar so that the earthquake performance of the asymmetric-plan system would be similar to, and specifically no worse than, that of the symmetric-plan system. In order to investigate this issue further, the responses of asymmetric-plan systems with their element yield forces computed with three different values of $\delta=1$,

0.5, and 0 in Eq. 3 are compared in Fig. 4. The first value, δ=1, is typical of several codes: UBC-88, MFDC-77, and NZC-84; δ=0.5 is specified in NBCC-85; and δ=0 implies no reduction in the stiff-side element design force. In all cases, α=1 and four different values of R -- 1, 2, 4 and 8 -- were considered in Eq. 1. The ductility demand on the stiff-side element is the only response quantity presented because other responses are affected very little by δ. It is apparent that the ductility demand μ_i on the stiff-side element in the asymmetric-plan systems designed with δ=0 is generally below the element ductility demand, μ_o, if the system plan were symmetric. However, for some period values, precluding reduction of stiff-side element design force (δ=0) is not sufficient to keep μ_i below μ_o. In order to achieve this objective, perhaps this design force should be increased relative to its symmetric-plan value, which implies a negative value of δ in Eq. 3b.

Even if such a reduction in the stiff-side element design force is precluded, earlier inelastic response results for systems designed with R=4 have demonstrated that the ductility demand on the flexible-side element may be reduced because of plan-asymmetry (Fig. 2). Thus, the ductility capacity of the flexible-side element is underutilized in an asymmetric-plan system if it is designed for the ductility demand in a symmetric-plan system. In order to better utilize the element ductility capacity, the design eccentricity, e_d, in Eq. 3a should be modified by decreasing α to reduce the strength of this element. On the other hand for systems with R=1, i.e., systems designed to remain elastic if their plan were symmetric and no accidental eccentricity were considered, the ductility demand on the flexible-side element in an asymmetric-plan system may exceed one indicating yielding of the element because of torsional motions (Fig. 3). Thus the strength of this element should be increased by increasing α in Eq. 3a to compute the design eccentricity, e_d.

In order to further investigate these concepts, the responses of asymmetric-plan systems with their element yield forces computed with three different values of α are compared in Fig. 5. In addition to α=1, two larger values are considered for systems designed with R=1 or 2; two smaller values are considered when R=8; and one smaller and another larger value is selected when R=4. The ductility demand on the flexible-side element is the only response quantity presented because other response quantities are affected very little by α. These results demonstrate that, in order to keep the ductility demand on the flexible-side element in the asymmetric-plan system below its symmetric-plan value, α should be selected as follows: α=1 if R=8; α=1.5 if R=2 and 4; and α=2 if R=1. However, the optimal α values may differ with the ground motion. Thus, response results should be generated for several ground motions to determine for code use the coefficient α which should depend on the design value of the reduction factor R.

Even if the asymmetric-plan system can be designed for significant yielding in such a way that the ductility demand on the flexible-side element does not exceed the symmetric-plan value, the element deformation may still be larger because of plan-asymmetry. It may not be possible to reduce this deformation by increasing the strength of the system because, as shown by the responses of SDF systems (Veletsos and Vann 1971), the deformation of a medium-period, velocity-sensitive system is not strongly affected by its strength and it is for such systems that the additional deformation due to plan-asymmetry is most significant (Figs. 2 and 3). Because increasing the strength of a system beyond that required for it to remain elastic would not influence its response if it is within the elastic range, the additional deformations of elastic systems resulting from plan-asymmetry also can not be reduced. Thus, these larger deformations should be provided for in the design of asymmetric-plan structures.

7 CONCLUSIONS

This investigation of the effects of plan-asymmetry on the earthquake response of one-story systems designed by seismic codes and how well these effects are represented by the torsional provisions in building codes has led to the following conclusions:

A stiff-side resisting element with design force smaller than its symmetric-plan value, which is permitted by some codes, experiences increased ductility demand because of plan-asymmetry. However, if the force reduction is precluded, as in some codes, the ductility demand on this element is roughly unaffected by plan-asymmetry. The ductility demand on the flexible-side element is significantly smaller than in the symmetric-plan system, with exceptions at few periods, regardless of whether the design force reduction for the stiff-side element is permitted or not.

Although, symmetric-plan systems designed with R=1 would be expected to remain elastic during the design ground motion, similarly designed asymmetric-plan systems may deform into the inelastic range. Also because of torsional motions, the element deformation may significantly exceed the deformation of the corresponding symmetric-plan system. Thus, asymmetric-plan systems designed with R=1 may experience structural damage due to yielding and nonstructural damage resulting from increased deformations.

Building code provisions do not ensure that the deformation and ductility demands on an asymmetric-plan system are similar to those on a similarly-designed symmetric-plan system. This suggests that the design eccentricity should be modified. This goal can usually be achieved for stiff-side elements by precluding any reduction in their design forces below their symmetric-plan values; δ=0 in the design eccentricity, e_d, is equivalent to this requirement. However, for some period values, this requirement is not sufficient and the design force for this element should be increased relative to its symmetric-plan value, which implies a negative value of δ.

Similarly, the ductility demand on the flexible-side element can be kept below and close to its symmetric-plan value by modifying the coefficient α in the design eccentricity, e_d. The optimal value of α in Eq. 3 depends on the design value of the reduction factor R -- being larger

for smaller R -- and may differ with the ground motion. Thus, response results should be generated for several ground motions to determine the coefficient α appropriate for use in building codes. However, it does not appear possible to reduce the additional element deformations due to plan-asymmetry by modifying the design eccentricity; these larger deformations should be provided for in building design.

8 ACKNOWLEDGMENTS

This research investigation is supported by the National Science Foundation under Grant BCS-8921932. The authors are grateful for this support.

REFERENCES

Chopra, A.K., and Goel, R.K. (1991). "Evaluation of Torsional Provisions in Seismic Codes," *J. Struct. Div.*, ASCE, 117(12), 3762-3782.

Goel, R.K., and Chopra, A.K. (1990). *Inelastic earthquake response of one-story, asymmetric-plan systems*, Report No. UCB/EERC-90/14, Earthquake Engineering Research Center, University of California, Berkeley, California.

Gomez, R. and Garcia-Ranz, F. (1988). "The Mexico earthquake of September 19, 1985 - complementary technical norms for earthquake resistant design," *Earthquake Spectra*, 4(3), 441-460.

International Association for Earthquake Engineering (1988). Earthquake Resistant Regulations, A World List, 1988, Tokyo.

Kan, C.L. and Chopra, A.K. (1981). "Torsional coupling and earthquake response of simple elastic and inelastic systems," *J. Struct. Div.*, ASCE, 107(8), 1569-1588.

Tentative Provisions for the Development of Seismic Regulations for Buildings (1978). ATC3-06, Applied Technological Council, Palo Alto, CA.

Tso, W.K., and Hongshan, Y. (1990). "Additional seismic inelastic deformation caused by structural asymmetry", *J. Earthq. Engrg. Struct. Dyn.*, 19(2), 243-258.

Veletsos, A.S., and Vann, W.P. (1971). "Response of ground-excited elastoplastic systems," *J. Struct. Div.*, ASCE, 97(4), 1257-1281.

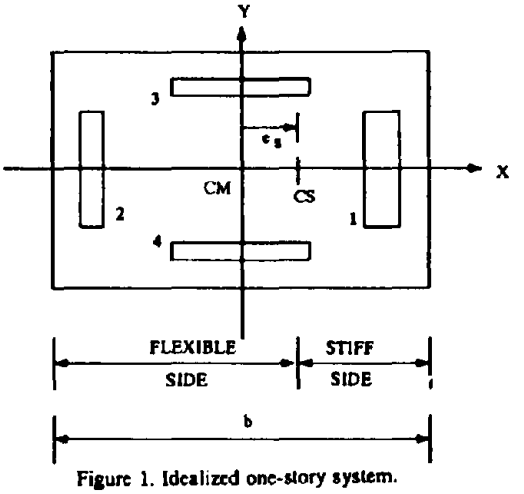

Figure 1. Idealized one-story system.

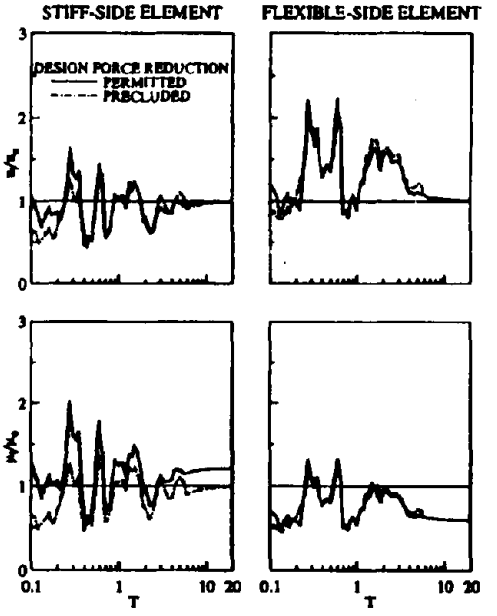

Figure 2. Ratio of element deformations, u_i/u_o, and ductility demands, μ_i/μ_o, for asymmetric-plan and corresponding symmetric-plan systems designed by UBC-88; $R = 4$.

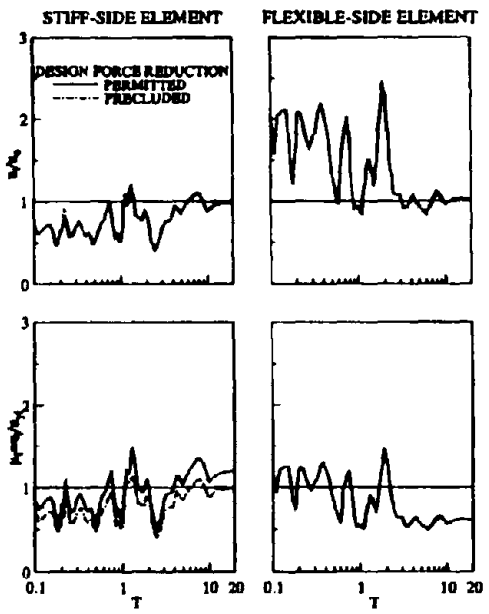

Figure 3. Ratio of element deformations, u_i/u_o, for asymmetric-plan and corresponding symmetric-plan systems, and element ductility demands, μ_i, for asymmetric-plan systems designed by UBC-88; R = 1.

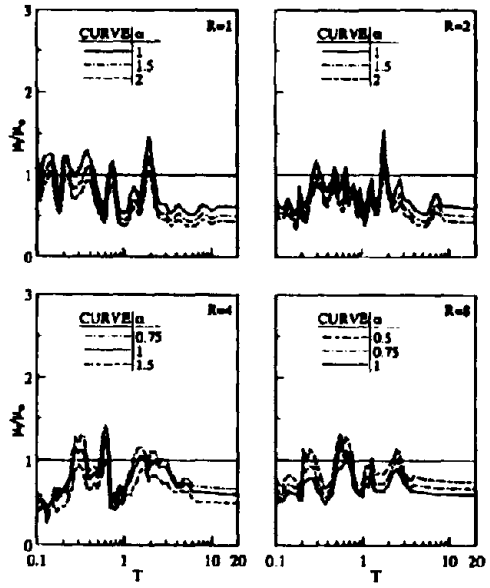

Figure 5. Ratio of flexible-side element ductility demands, μ_i/μ_o, for asymmetric-plan and corresponding symmetric-plan systems; δ=0 and β=0.

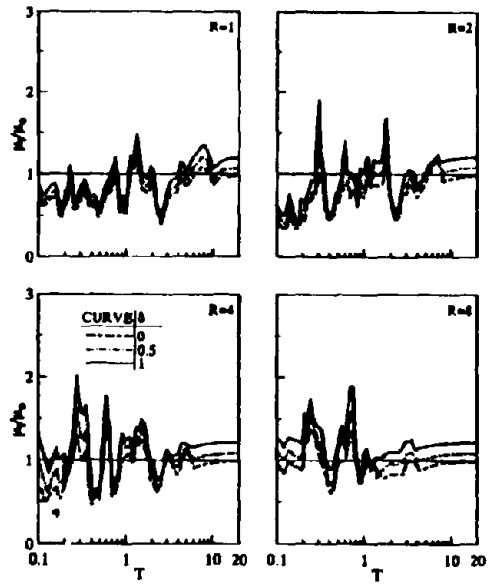

Figure 4. Ratio of stiff-side element ductility demands, μ_i/μ_o, for asymmetric-plan and corresponding symmetric-plan systems; α=1 and β=0.

Optimum damping in base-isolated structures

Jose A. Inaudi & James M. Kelly
University of California at Berkeley, Calif., USA

ABSTRACT: Optimum viscous isolation damping for minimum acceleration response of base-isolated structures subjected to stationary random excitation is investigated. Two linear models are considered to account for the energy dissipation mechanism of the isolation system: a viscous linear element, and a Maxwell element, which are commonly used models for viscodampers. The criterion selected for optimality is the minimization of the peak floor acceleration response. The effects of frequency content of the excitation and superstructure properties on the optimum damping and minimum peak acceleration response are addressed.

1. INTRODUCTION

Base isolation is today an accepted design alternative for earthquake hazard mitigation for structures on firm soil. Superior seismic performance can be achieved by means of the introduction of a flexible set of isolators between a stiff superstructure and its foundation. The benefits of this design approach are not only complete preservation of the structural system but also equipment protection during moderate and strong ground motions. While the failure of the structural system is prevented by guaranteeing a maximum deformation demand on the isolation system, failure of sensitive equipment can be prevented by ensuring low enough levels of floor accelerations.

Ground motion and structural system characteristics determine the deformation demand on the isolation system and the floor acceleration response of the structure subjected to ground excitation. Intensity of the ground shaking, frequency content as well as maximum ground velocity are factors of crucial importance. Natural frequencies of the base-isolated structure and energy dissipation capability in the isolation system are controlling factors for the response. The relative displacement at the isolator level is dominated by the response of the system in its first mode of vibration. The superstructure damping capability has a negligible effect on the damping of the first mode of vibration of a base-isolated structure and consequently, the isolator deformation can not be controlled by an increase of the superstructure damping capability. However, significant damping can be introduced in the first mode of the structure by increasing the energy dissipation capability of the isolation system. Damping, although not essential in the isolation phenomenon, is needed to keep the isolator displacements within limits in case of low frequency ground motion. High-damping rubbers, lead plugs and or added viscous or frictional dampers can give the desired energy dissipation capability to the isolation system and with that, a reduction of the demand on the isolation system can be attained. On the other hand, the energy dissipation mechanism of the isolation system has a significant effect on the floor acceleration response.

Tsai and Kelly (1988) have shown that the response of internal equipment on base-isolated structures in which the damping matrix is non-classical can not be accurately determined by the classical mode method. The high frequency content is distorted by the classical mode method and the use of complex modes is recommended to find equipment response. Constantinou and Tadjbakhsh (1985) have developed studies on the optimum fundamental period of base-isolated structures under random excitation. The work reported herein aims at determining optimal levels of damping induced by viscodampers which will render minimal acceleration response in the structure subjected to ground excitation. A statistical approach and a deterministic approach are followed. For the statistical approach, the ground motion is modelled as a stationary Gaussian random process and optimum damping is defined as that which renders minimum peak floor acceleration. For the deterministic approach, the maximum floor acceleration of base isolated structures subjected to recorded ground motions is evaluated as a function of the isolation energy dissipation capacity by numerical simulation. Simple structural models were analyzed aiming at identifying the main controlling parameters.

2. STRUCTURAL MODELS

The dynamic response of a n-story symmetric isolated building subjected to unidirectional ground excitation can be described using a floor lumped-mass model in terms of relative coordinates by the following equation

$$M\ddot{y} + C\dot{y} + Ky + If = -Mr\ddot{w} \quad (1)$$

where M, C and K are, respectively, the mass, damping and stiffness matrices of the superstructure; y is a vector which contains the relative displacements of basement and floors with respect to the ground, w represents the ground acceleration, $I^T = [1\ 0\ \cdots\ 0]$ and $r^T = [1\ 1\ \cdots\ 1]$. f represents the force that the isolation system applies on the basement of the structure. This term includes both forces resulting from deformation of the isolator and of the energy dissipation devices acting in the isolation system. The floor accelerations can be easily expressed as

$$\ddot{x} = -M^{-1}Ky - M^{-1}C\dot{y} - M^{-1}If \quad (2)$$

Shear building models are used for the analyses in this study. Figure 1 describes a typical structure used in this study. A parametric definition of the structure allows the assessment of the effect of the different parameters in the phenomenon under study. The superstructure stiffness matrix K is characterized by means of a single parameter k which is selected to give a desired frequency to the first fixed-base undamped mode of the superstructure T_{fb}. The flexibility of the superstructure will be varied in this study by changing the value of T_{fb}. The superstructure damping matrix C is defined by assuming modal dampings in the superstructure. In order to simplify this study all modal damping ratios of the superstructure are assumed equal to ξ_m except for the the free-body mode which is taken as zero.

A large variety of devices with a wide range of mechanical behaviors have been proposed to be used as part of the isolation system. Natural rubber bearings made of different rubber compounds, rubber bearings with lead plugs, rubber bearings in combination with viscous dampers, friction dampers or elastoplastic dampers are among the most commonly proposed devices. In the present paper, viscodampers modelled by linear models will be considered. Extrapolating these results and conclusions to highly nonlinear devices is not a recommendable scheme. Series and parallel combinations of linear springs and dashpots can be used then to obtain different viscoelastic models for the mechanical elements under study. At the expense of greater complexity the number of springs and dashpots can be increased seeking a more accurate agreement between the response of the model and the response of the real mechanical device. In order to keep this study as simple as possible the models we will consider include at most three parameters.

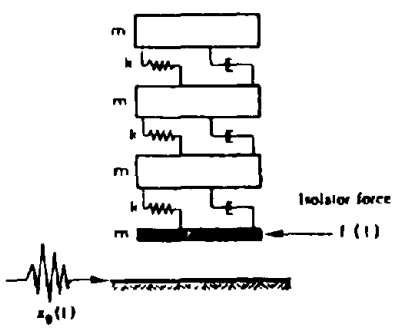

Figure 1. Structural model used in this study.

2.1. Kelvin element and Maxwell element

A Kelvin element, a linear spring in parallel with a pure viscous damper constitutes the first model for this study. The force in a Kelvin element f^I satisfies

$$f^I = k_o y_1 + c_o \dot{y}_1 \quad (3)$$

The dissipation of energy in harmonic excitation is linearly proportional to the frequency of excitation for this model. The parameter c_o will be varied to study the effect of viscous damping in the acceleration response of base-isolated structures. k_o will be selected to give a certain first natural frequency ω_1 to the isolated structure.

The second model for the isolation system to be used in the present study consists of a linear spring in parallel with a of Maxwell element, so called standard solid in mechanics of solids. The element force f^{II} is governed in this case by

$$f^{II} = k_o y_1 + f_e \quad (4)$$

$$\dot{f}_e + \frac{1}{\tau} f_e = g\dot{y}_1 \quad (5)$$

The main mechanical characteristic of a Maxwell model is its relaxation time τ. The energy dissipated in a cycle in this model increases with frequency for frequencies less than $1/\tau$ and monotonically decreases with frequency for frequencies larger than $1/\tau$.

3. ACCELERATION RESPONSE FOR MODEL I

A formulation of the equations of motion in state space form is convenient for developing the analysis. The set of n second order differential equations (1) is converted into a set of $2n$ first order differential equations by defining a suitable state vector $z^T = [y^T\ \dot{y}^T]$. Considering eq.(3), eq.(1) can be expressed in state space as

$$\dot{z} = A^I z + B_w^I w \qquad \ddot{x} = D^I z \quad (6)$$

$$A^I = \begin{bmatrix} 0 & I \\ -M^{-1}\bar{K} & -M^{-1}\bar{C} \end{bmatrix} \qquad D^I = \begin{bmatrix} -M^{-1}\bar{K} & -M^{-1}\bar{C} \end{bmatrix}$$

$$\bar{C} = C + diag\,(c_o, 0, \ldots, 0) \qquad \bar{K} = K + diag\,(k_o, 0, \ldots, 0) \qquad B_w^I = \begin{bmatrix} 0 \\ -r \end{bmatrix}$$

The floor acceleration frequency response can be obtained from eqs.(8 and 9) as

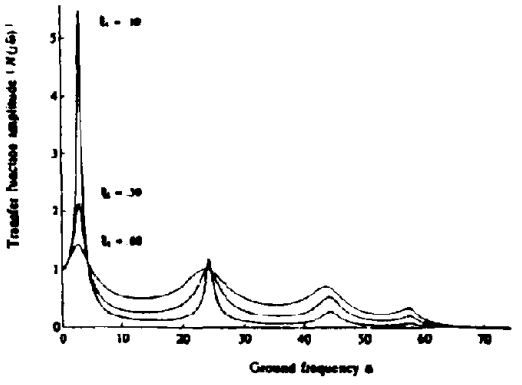

Figure 2. Acceleration frequency response: Model I.

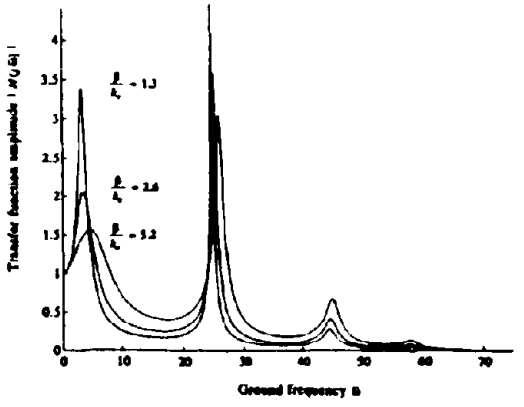

Figure 3. Acceleration frequency response: Model II.

$$H^{I}(j\bar{\omega}) = \frac{\ddot{X}(j\bar{\omega})}{W(j\bar{\omega})} = D^{I}(j\bar{\omega}\, I - A^{I})^{-1} B_{o}^{I} \qquad (7)$$

Figure 2 describes the acceleration frequency response for the top floor of a 4DOF structure ($\omega_1 = \pi$ *rad/s*, $T_{fb} = .6$ *s*) for different values of c_o. The three curves correspond to induced damping ratios in the first mode of $\xi_1 = .10, .30$ and .60. It is worth noticing that only resonant responses are suppressed by means of an increase in the isolation damping. While the transfer function amplitude decreases for higher damping at low frequency, it increases at high frequencies. This effect is very important in the understanding of the phenomenon under consideration. If the ground motion presents dominant low frequency content heavily damped isolation systems will improve the performance of the structure in terms of acceleration response and isolation deformation, however if high frequency is dominant in the ground acceleration signal, a heavily damped isolation system will reduce isolation deformation but will tend to increase the floor acceleration response of the structure.

4. ACCELERATION RESPONSE FOR MODEL II

In order to study the effect that Maxwell viscous dampers introduced in the isolation system have in the floor acceleration response of the structure a state space formulation is developed assuming that a certain number N_e of such devices with identical mechanical characteristics are connected in parallel with the isolators. The force in the i-th Maxwell element is denoted as f_e^i. From eqs.(4 and 5) the force in the isolation system will then satisfy

$$f^{II} = k_o\, y_1 + f_e \qquad f_e = \sum_{i=1}^{N_e} f_e^i \qquad (8)$$

$$\dot{f}_e + \frac{1}{\tau} f_e = \beta\, \dot{y}_1 \qquad \beta = N_e\, g$$

Since for the Maxwell model f_e satisfies a first order differential equation, a suitable definition of an extended state $z_e^T = [z \;\; f_e]$ allows us to put the system in state form

$$\dot{z}_e = A_e^{II} z + B_e^{II} w \qquad \ddot{x} = D_e^{II} z_e \qquad (9)$$

$$A_e^{II} = \begin{bmatrix} O & I & 0 \\ -M^{-1}\bar{K} & -M^{-1}C & M^{-1}l \\ [0..0] & [-\beta\, 0..0] & -\frac{1}{\tau} \end{bmatrix} \qquad B_e^{II} = \begin{bmatrix} O \\ -r \\ 0 \end{bmatrix}$$

$$D_e^{II} = [\, -M^{-1}\bar{K} \;\; -M^{-1}C \;\; -M^{-1}l \,]$$

The poles of the system as a function of β and the relaxation time τ can be obtained by solving for the eigenvalues of $A_e^{II}(\beta,\tau)$. It is interesting to note that the most significant effect in the modal damping ratios is introduced by τ. The smaller the τ the most effectively the poles can be moved into the left half of the complex plane. A change in β can produce a redistribution of negative real parts between the poles but no change in the trace of A_e^{II} and consequently no change in the center of gravity of the poles. An other important characteristic of this model is that it introduces an stiffening effect on all the modes of vibration increasing their natural frequencies.

The acceleration frequency response of the system under Maxwell-type damping can be obtained as

$$H^{II}(j\bar{\omega}) = D_e^{II}(j\bar{\omega}\, I - A_e^{II})^{-1} B_e^{II} \qquad (10)$$

Figure 3 describes the acceleration frequency response of the top floor of a 4DOF structure ($\omega_1 = \pi$ *rad/s*, $T_{fb} = .6$ *s*) for $\tau = .10$ and different values of β. The stiffening effect of the Maxwell elements appears clear in the shifting of the peaks of $|H(j\bar{\omega})|$. While for low frequency range the transfer function magnitude decreases for higher β, for high frequency it increases.

5. RESPONSE TO STATIONARY EXCITATION

The effect of damping in the acceleration response of the base-isolated structure subjected to random excitation is addressed in this section for both models. Optimum damping levels are defined as those which render a minimal peak acceleration response of the base-isolated structure.

Given a linear system as that of eq.(6 or 9) subjected to stationary excitation $w(t)$ with zero mean and power spectral density $S_g(\bar{\omega})$, the power spectral density of the floor acceleration response $S_{\ddot{x}}(\bar{\omega})$ can be obtained as

$$S_{\ddot{x}}(\bar{\omega}) = H(j\bar{\omega})\, S_g(\bar{\omega})\, H^*(j\bar{\omega}) \tag{11}$$

The ground acceleration variance σ_g^2 is given by

$$\sigma_g^2 = \frac{1}{2\pi} \int_{-\infty}^{\infty} S_g(\bar{\omega})\, d\bar{\omega} \tag{12}$$

The floor acceleration covariance matrix can be obtained as

$$E[\ddot{\bar{x}}\, \ddot{\bar{x}}^T] = \frac{1}{2\pi} \int_{-\infty}^{\infty} S_{\ddot{x}}(\bar{\omega})\, d\bar{\omega} \tag{13}$$

The diagonal of the acceleration covariance matrix contains the floor acceleration variances. If we assume that the ground motion is a Gaussian random process the estimation of extreme values of an output signal ν of the excited linear system over a certain period of time T can be done according to the Poisson model for the barrier crossings

$$V_{max} = \sigma_\nu \left[2 \ln \left(-\frac{T\, \sigma_{\dot{\nu}}}{\pi \ln \gamma\ \sigma_\nu} \right) \right]^{\frac{1}{2}} \tag{14}$$

where γ represents the probability that V_{max} will not be exceeded during an interval of duration T of the random process, and σ_ν and $\sigma_{\dot{\nu}}$ are the standard deviations of the signal ν and its time derivative (Vanmarke, 1883). Since we are interested in the floor acceleration response, the evaluation of floor jerks e, time derivative of the floor acceleration, becomes necessary. The floor jerk covariance matrix $E[\dot{\bar{x}}\, \dot{\bar{x}}^T]$ can be obtained as

$$E[\dot{\bar{x}}\, \dot{\bar{x}}^T] = \frac{1}{2\pi} \int_{-\infty}^{\infty} \bar{\omega}^2\, H(j\bar{\omega})\, H^*(j\bar{\omega})\, S_g(\bar{\omega})\, d\bar{\omega} \tag{15}$$

The diagonal of the floor jerk covariance matrix contains the floor jerks variances.

Equations (13), (14) and (15) along with the expressions for the acceleration frequency response of the system can be used then to estimate the peak floor acceleration $\ddot{x}_{peak}$ of a base isolated structure as a function of the different damping models in the isolation system. The optimum values of damping parameter ($c_{o_{opt}}$ or β_{opt}) can now be estimated by minimizing the peak floor acceleration value over the values of the damping parameter.

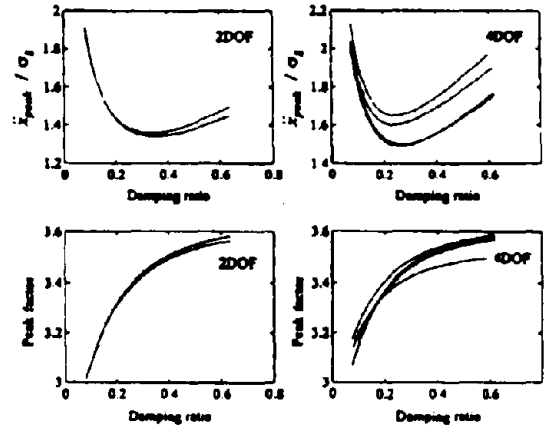

Figure 4. Peak floor acceleration: Model I.

5.1. MDOF systems under band limited excitation

The effect of the number of degrees of freedom of the structural system, the flexibility and damping of the superstructure on the optimum damping is investigated in this section. Two structural models are considered to analyze the effect of number of degrees of freedom: a 2DOF system and a 4DOF system. Their fixed base periods T_{fb} are taken as .15 *s* and .45 *s* respectively. The value values of the first natural frequency of the undamped base-isolated structure is taken as $\omega_1 = 3.1415$ *rad/s*. The power spectral density of the ground motion is assumed as

$$S_g(\bar{\omega}) = S_o \quad -\omega_o < \bar{\omega} < \omega_o \tag{16}$$

with $\omega_o = 80$ *rad/s*. Figures 4 and 5 show the results obtained from for both models. The peak floor acceleration ($\gamma = .5$, $T = 40$ *s*) for the 2DOF and the 4DOF systems are plotted at the top of the figure as a function of the induced first mode damping ratio (Models I and II). As we can notice, the optimum damping decreases with an increase in the number of degrees of freedom for model I while for the maxwell model it does not present high sensitivity to a change in the number of degrees of freedom. Peak acceleration values corresponding to optimum damping levels augment with the number of degrees of freedom. The peak factors (quotient between the peak acceleration and its standard deviation) are shown in the figures for comparison. The peak factor slightly increases with the increase in the damping parameter. The results shown for model II correspond to $\tau = .10s$. Larger values of τ render larger peak acceleration response.

The effect of the superstructure flexibility T_{fb} and superstructure damping ξ_{ss} is analyzed in figures 6 and 7 for models I and II. A 2DOF system is used in the analyses and the optimum damping values are obtained for different

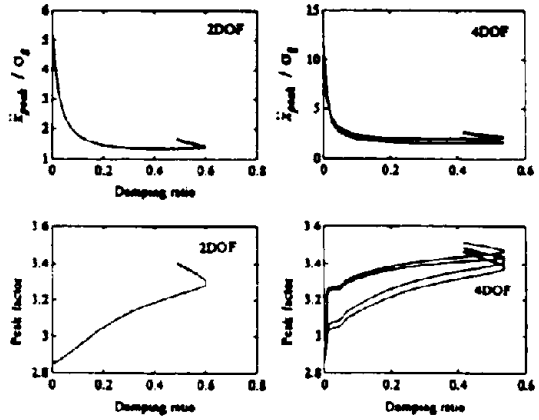

Figure 5. Peak floor acceleration: Model II.

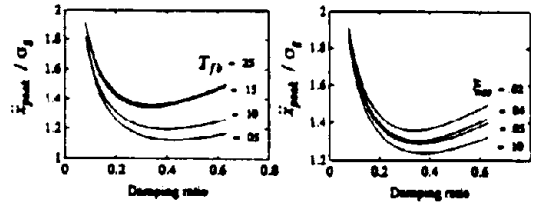

Figure 6. Effect of flexibility and damping: Model I.

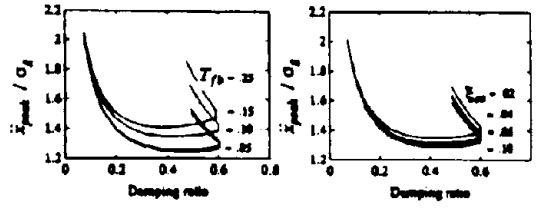

Figure 7. Effect of flexibility and damping: Model II.

Table 1. Recorded signals used for dynamic simulation

Station name	Direction	PGA [g]	PGV [cm/s]
El Centro	S90W	0.21	36.92
Taft	N21E	0.15	15.72
James Road	S40E	0.52	43.99

values of superstructure flexibility T_{fb} = .05, .10, .15, .25 s keeping constant superstructure damping ξ_{ss} = .02 and for different values of superstructure damping ξ_{ss} = .02, .04, .05, .10 keeping T_{fb} = .15 constant. An increase in the flexibility of the superstructure causes a decrease in the value of the optimum damping as well as an increase in the peak acceleration. This effect is particularly noticeable in the viscous model. The effect of superstructure damping has the opposite sense: the higher ξ_{ss} the higher the value of optimum damping and the lower the peak acceleration response.

6. RESPONSE TO RECORDED GROUND MOTIONS

In this section, the effect of isolation damping in the dynamic behavior of base isolated structures is evaluated by numerical simulation of the response of the structure to recorded ground motions. The acceleration response of the structure is computed for several recorded signals under different levels of isolation damping. Optimal levels of damping are defined as those that render minimum maximum floor acceleration response for a particular ground motion. The isolator deformation is also computed. The effects of the type of isolation system, the number of degrees of freedom, the superstructure flexibility, the frequency content of the excitation as well as the frequency content of the excitation are evaluated. The signals used in the study are listed in the following table and correspond to the earthquakes of Imperial Valley (May 18, 1940), Kern County (July 21, 1952) and Imperial Valley (October 15, 1979) respectively.

6.1. Results for Model I and Model II

The effect of isolation damping in the floor acceleration response is basically to reduce it up to a certain value of damping from which an increase in damping determines an increase in acceleration response. For a given structural system and a given ground motion there exist a damping value which minimizes the floor acceleration response while satisfying the constraint imposed by maximum deformability in the isolation system. Deformability of the isolation system determines some bounds on the allowable deformation demand. Once this safety requirement is met, the criterion for defining the optimum energy dissipation capacity of the isolation system should be the minimization of maximum floor accelerations. In order to evaluate the effect of number of degrees of freedom, superstructure flexibility in the optimum damping value, maximum acceleration response spectra were generated for different ground motions and different structural systems ($\omega_1 = \pi$ rad/s and ξ_{ss} = .02). Tables (2) and (3) summarize the results. There is significant variability of the optimum damping values which it is mainly caused by the different characteristics of the ground motions selected for the analysis. This leads us to the first obvious conclusion: the optimum damping value crucially depends on the ground motion characteristics, basically in its frequency content in relation to the fundamental frequency of the base-isolated structure. There exist however some trends that coincide with those obtained in previous sections for the random model of the ground excitation. Those are basically the following: the optimum damping value decreases with an increase in the fundamental period of the base-isolated structure and with an increase in the superstructure flexibility. The higher the frequency content of the ground motion the lower the value of optimum damping and the

Table 2. Optimum damping for model I.

Signal	NDOF	T_{fb} [s]	ξ_1^{opt}	$\max(\ddot{x})$ [cm/s²]	$\max(y_1)$ [cm]
El Centro	8	.7	.33	174	9.6
El Centro	4	.6	.27	153	10.6
Taft	8	.7	.19	77	5.1
Taft	4	.6	.18	69	5.2
James R.	8	.7	.15	281	19.4
James R.	4	.6	.16	262	18.3

Table 3. Optimum damping for model II.

Signal	NDOF	T_{fb} [s]	ξ_1^{opt}	$\max(\ddot{x})$ [cm/s²]	$\max(y_1)$ [cm]
El Centro	4*	.6	.23	153	10.9
El Centro	8*	.7	.24	176	10.4
El Centro	4**	.6	.21	160	9.8
El Centro	8**	.7	.23	171	8.7
Taft	4*	.6	.09	91	6.3
Taft	8*	.7	.16	96	5.2
Taft	4**	.6	.08	100	6.8
Taft	8**	.7	.12	106	5.8
James R.	4*	.6	.17	279	17.0
James R.	8*	.7	.14	298	18.4
James R.	4**	.6	.17	273	15.7
James R.	8**	.7	.16	277	16.2

* $\tau = .10\ s$ ** $\tau = .20\ s$

better the performance of the base-isolated structure. This effect should be expected since both an increase in the flexibility of the superstructure will automatically reduce the efficacy of the isolation system in decoupling higher frequency dynamics. Furthermore, the force induced by the viscodampers on the basement of the structure is "felt" by all the modes of the structure and if the stiffness of those modes is reduced the excitation of those higher modes will increase. Although the results are not shown in the tables, it was found that the optimum damping value increases with an increase in the superstructure damping ξ_m and that the low-pass filter characteristics of a base-isolated structure are deteriorated in presence of a heavily damped isolation system.

7. CONCLUDING REMARKS

A procedure for defining optimum damping in linear isolation systems have been presented. The optimization scheme has as objective function the peak floor acceleration response for the base-isolated structure subjected to stationary Gaussian excitation. Two simple linear elements with different energy dissipation mechanisms have been analyzed. The same procedure can be easily extended to consider more elaborate linear viscoelastic models of viscodampers. Summarizing the most significant findings of this study we conclude the following points:

- The optimum damping has been obtained based on minimum peak acceleration response to Gaussian excitation. The minimization of acceleration variances renders very similar values for the optimum damping values. This is the case since the peak factor is not sensitive to changes in the isolation damping.
- The effect of high frequency content in the excitation is to decrease the optimum viscous damping. For both Kelvin and Maxwell models, superior acceleration reduction can be attained under high frequency excitation and optimum isolation damping design.
- The results have shown that the optimum isolation damping decreases with an increase in the number of degrees of freedom. An increase in the damping of the superstructure produces an increase in the optimum damping value while an increase in the flexibility of the superstructure tends to decrease the optimum damping and amplify the peak floor accelerations.
- The low-pass filter characteristics of a base-isolated structure are deteriorated by a heavily damped isolation system. Special care should be taken in defining the isolation damping when designing an isolated structure for sensitive equipment protection.

REFERENCES

Bhatti M.A. and Pister K.S., "A dual criteria approach for optimal design of earthquake-resistant structural systems", *Earthquake Engineering and Structural Dynamics, Vol. 9, 557-572 (1981).*

Constantinou, A.M., Tadjbakhsh A., "Optimum characteristics of isolated structures", *Journal of Structural Engineering, Vol. 111, No. 12, 2733-2750 (1985).*

Kelly J.M., Tsai H.C., "Non-classical damping in dynamic analysis of base-isolated structures with internal equipment", *Earthquake Engineering and Structural Dynamics, Vol. 16, 29-43 (1988).*

Lai M.L., Soong T.T., "Seismic design considerations for secondary structural systems", *Journal of Structural Engineering, Vol. 117, No. 2, 459-472 (1991).*

Manolis G., Juhn G., Constantinou M., Reinhorn A., "Secondary systems in base-isolated structures: Experimental investigation, stochastic response and stochastic sensitivity", *Tech. Report NCEER-90-0013, July 1990, State University of New York at Buffalo.*

Vanmarke E., "Random Fields: Analysis and Synthesis", *The MIT Press, Cambridge, Massachussets, (1983).*

Finite element analysis of reinforced concrete structures under monotonic and cyclic loads

H.-G. Kwak
Korea Advanced Institute of Technology, Seoul, Korea
F.C. Filippou
University of California, Berkeley, Calif., USA

ABSTRACT: This paper deals with the finite element analysis of the monotonic and cyclic behavior of reinforced concrete beams and beam-column joint subassemblages. It is assumed that the behavior of these members can be described by a plane stress field. Concrete and reinforcing steel are represented by separate material models which are combined together with a model of the interaction between reinforcing steel and concrete through bond-slip to describe the behavior of the composite reinforced concrete material. A new smeared crack finite element model is proposed based on an improved cracking criterion derived from fracture mechanics principles. A new reinforcing steel model which is embedded inside a concrete element, but accounts for the effect of bond-slip is developed. Correlation studies between analytical and experimental results show the validity of the proposed models and identify the significance of various effects on the local and global response of reinforced concrete members.

1 INTRODUCTION

The assessment of the strength and stiffness of existing structures and newly designed critical structures such as offshore platforms, long-span bridges and nuclear power plants requires the development of advanced analytical methods capable of representing the behavior of the structure under all possible loading conditions, both, monotonic and cyclic, its time-dependent behavior, and, especially, its behavior under overloading.

The development of such models for reinforced and prestressed concrete structures is complicated by differences in short- and long-term behavior of the constituent materials, concrete and reinforcing steel. Moreover, reinforcing steel and concrete interact in a complex way through bond-slip and aggregate interlock. A general purpose model of the short- and long-term response of reinforced concrete members and structures should, therefore, be based on separate material models for reinforcing steel and concrete, which are then combined along with models of the interaction between the two constituents to describe the behavior of the composite reinforced concrete material. This is the approach adopted in this study.

2 MATERIAL MODELS

The following assumptions are made in the description of material behavior:

1. The stiffness of concrete and reinforcing steel is formulated separately. The results are then superimposed to obtain the element stiffness;
2. The smeared crack model is adopted in the description of the behavior of cracked concrete;
3. Cracking in more than one direction is represented by a system of orthogonal cracks;
4. The crack direction changes with load history (rotating crack model);
5. The reinforcing steel is assumed to carry stress along its axis only and the effect of dowel action of reinforcement is neglected;
6. The transfer of stresses between reinforcing steel and concrete and the resulting bond-slip is explicitly accounted for in a new discrete reinforcing steel model, which is embedded in the concrete element.

In the following, the material model of each constituent material and their interaction through bond-slip is briefly described. This is followed by examples of the monotonic and cyclic behavior of anchored reinforcing bars, beams and beam-column joints. Details of the models and their implementation can be found elsewhere (Kwak and Filippou 1990).

2.1 Concrete

The orthotropic model is adopted in this study for its simplicity and computational efficiency. The ultimate objective of this work is the response analysis of large structures under cyclic loads for which more rational and sophisticated models are prohibitively expensive.

The behavior of the model depends on the location of the present stress state in the principal stress space. In the biaxial compression region the model remains linear elastic for stress combinations inside the initial yield surface. Both the initial yield and the ultimate load surface are described by Kupfer's model (Figure 1).

For stress combinations outside the initial yield surface but inside the ultimate failure surface the behavior of concrete is described by a nonlinear orthotropic model. This model derives the biaxial stress-strain response from equivalent uniaxial stress-strain relations in the axes of

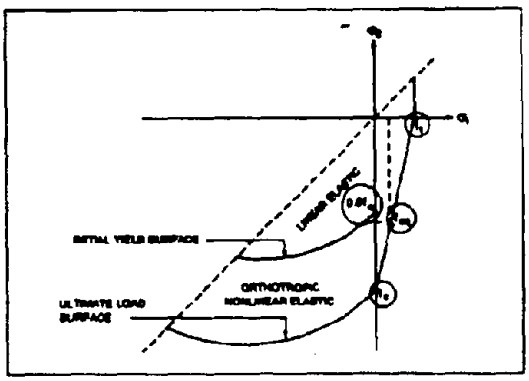

Figure 1. Strength Failure Envelope of Concrete

orthotropy (Darwin and Pecknold 1977). The uniaxial concrete stress-strain relation follows a piecewise linear modification of Hognestad's model.

When the biaxial stresses exceed Kupfer's failure envelope, concrete enters into the strain softening range of behavior where an orthotropic model describes the biaxial behavior (Darwin and Pecknold 1977). In this region failure occurs by crushing of concrete when the principal compressive strain exceeds a limit value. In defining the crushing of concrete under biaxial compressive strains a strain failure surface in complete analogy to Kupfer's stress failure envelope is used.

In the biaxial compression-tension and tension-tension region the following assumptions are adopted in this study: (1) failure takes place by cracking and, therefore, the tensile behavior of concrete dominates the response; (2) the uniaxial tensile strength of concrete is reduced to the value f_{sq}, to account for the effect of the compressive stress; in the tension-tension region the tensile strength remains equal to the uniaxial tensile strength f_t; (3) the concrete stress-strain relation in compression is the same as under uniaxial loading and does not change with increasing principal tensile stress. The last assumption holds true in the compressive stress range which is of practical interest in typically reinforced frame structures.

In the compression-tension and the biaxial tension region the proposed concrete model remains linear elastic for tensile stresses smaller than f_{sq}. Beyond the tensile strength the tensile stress decreases linearly with increasing principal tensile strain. Ultimate failure in the compression-tension and the tension-tension region takes place by cracking, when the principal tensile strain exceeds the value ϵ_u. The value of ϵ_u is derived from fracture mechanics concepts and depends on the finite element mesh size. In this way the analytical results retain objectivity for large finite element mesh size. At the same time this approach allows for the realistic representation of microcrack concentration near the tip of the crack without loss of accuracy for large finite elements. When the principal tensile strain exceeds ϵ_u, the material only loses its tensile strength normal to the crack, while it is assumed to retain its strength parallel to the crack direction.

2.2 Reinforcing steel with bond-slip

The simplest model of the bond-slip interaction between reinforcing steel and concrete is the bond-link element (Ngo and Scordelis 1967). This element connects one steel node with a corresponding concrete node which occupies the same physical location in the undeformed configuration of the structure. Consequently, the use of this element in the finite element analysis of RC structures imposes the following restrictions: (a) the finite element mesh must be arranged so, that a reinforcing bar is located along the edge of a concrete element and (b) a double node is required to represent the relative slip between reinforcing steel and concrete. These restrictions arise from the fact that the stiffness of the bond link element is associated with the relative displacement between steel and concrete. Consequently, the total displacement of, both, reinforcing steel and concrete is required at each node of the finite element mesh, so that the relative displacement and, consequently, the bond stress between steel and concrete can be determined.

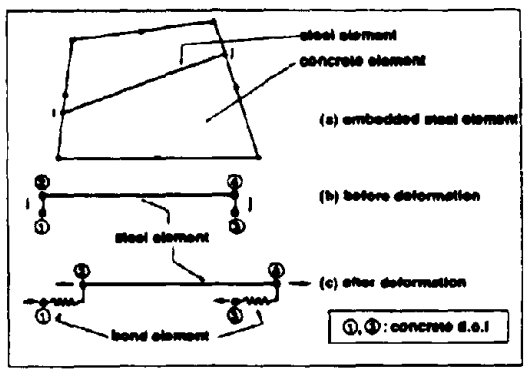

Figure 2. Reinforcing steel element with bond-slip.

In a complex structure, particularly in three-dimensional models, these requirements lead to a considerable increase in the number of degrees of freedom, not only because of the doubling of the number of nodes along the reinforcing steel bars, but also because the mesh has to be refined, so that the bars pass along the edges of concrete elements. The complexity of mesh definition and the large number of degrees of freedom has discouraged researchers from including the bond-slip effect in many studies to date.

To address these limitations of the bond link element a new discrete reinforcing steel model which includes the bond-slip deformation is proposed in this study. In this model the reinforcing bar is modeled by a truss element embedded inside the concrete element, as shown in Figure 2. In this case the finite element mesh configuration does not have to follow the arrangement of the reinforcing bars. At the same time the relative slip between reinforcing steel and concrete is explicitly taken into account in the model. The cyclic stress-slip relation of the bond links follows the modified model of Eligehausen in Figure 3 (Filippou et. al. 1983).

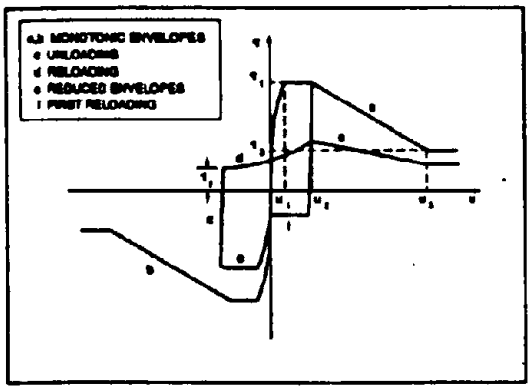

Figure 3. Cyclic stress-slip relation of bond links.

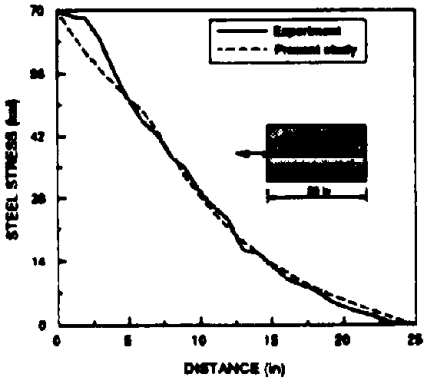

Figure 4. Stress distribution along anchored reinforcing bar for end stress of 70 ksi.

Since the finite element model only includes the concrete displacement degrees of freedom, the degrees of freedom which are associated with the reinforcing steel are condensed out from the element stiffness matrix, before it is assembled into the structure stiffness matrix. A second pass, however, is now required in order to satisfy the equilibrium of each reinforcing bar and determine the steel forces. In the second pass the current concrete displacement increments are imposed on the reinforcing steel-concrete interface. The resulting linearized system of equilibrium equations for the entire reinforcing bar is solved followed by the state determination and calculation of the resisting steel and bond forces. The updated steel and bond link stiffness along with the resisting forces are then transformed to the global concrete degrees of freedom to allow for the iterative solution of the nonlinear equilibrium equations of the entire structure.

3 APPLICATIONS

A number of correlation studies are conducted with the objective of establishing the ability of the proposed model to simulate the response of reinforced concrete beams and beam-column joint subassemblages. In order to independently test the reinforcing steel model with bond-slip, the response of anchored reinforcing bars under monotonic pull-out and cyclic push-pull loads is also studied. The latter study highlights the pronounced effect of cyclic bond-deterioration on the hysteretic response of reinforced concrete members.

3.1 Reinforcing bar under monotonic and cyclic loads

Several anchored reinforcing bars simulating anchorage and loading conditions in interior beam-column joints of moment resisting frames which are subjected to a combination of gravity and high lateral loads were tested (Viwathanatepa, Popov and Bertero 1979b). #6, #8 and #10 reinforcing bars were anchored in well confined concrete blocks and were subjected to monotonic pull-out at one end, monotonic pull-out at one end with simultaneous push-in at the other (called push-pull) and cyclic push-pull.

Two specimens are selected for comparison with the proposed reinforcing steel model with bond-slip. The first specimen is an anchored #8 bar in a well confined block of 25 in. width, which corresponds to an anchorage length of 25 bar diameters. This specimen was subjected to a monotonic pull-out under displacement control at one end only. The second specimen also involves a #8 reinforcing bar with identical dimensions which was subjected to a cyclic push-pull loading with gradually increasing end slip value. Both specimens have been the subject of earlier analytical correlation studies (Viwathanatepa et al. 1979b, Ciampi et al. 1982, Yankelevky 1985). The material properties of concrete and reinforcing steel are as follows (Viwathanatepa et al. 1979b): the concrete cylinder strength is 4,700 psi for the specimen under monotonic pull-out and 4,740 psi for the specimen under cyclic push-pull. The yield strength of the reinforcing steel is 68 ksi and the yield strain is 0.23%.

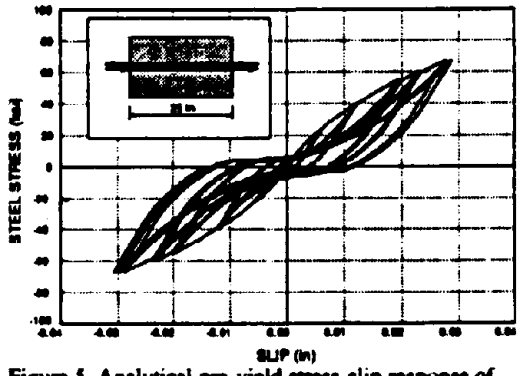

Figure 5. Analytical pre-yield stress-slip response of reinforcing bar under cyclic push-pull loading.

In the monotonic pull-out test a bilinear steel model is used. The strain hardening modulus is equal to 411 ksi, which corresponds to 1.4% of Young's modulus. In the cyclic push-pull test a modified Menegotto-Pinto steel model is used (Filippou et al. 1983). In both specimens the parameters of the bond-slip model in Figure 2 are as follows: $u_1 = 0.028$ in, $u_2 = 0.079$ in, $u_3 = 0.28$ in,

τ_1 = 2350 psi and τ_3 = 870 psi. In a previous study (Ciampi et al. 1982) the bond-slip relation was modified in the outer unconfined portions of the anchorage length. By contrast, in the present study the same bond stress-slip relation is used along the entire anchorage length for the sake of simplicity, since the hysteretic behavior is not the focus of the present study. Under cyclic loading conditions this assumption leads to underestimation of the bond resistance at the push-in end of the reinforcing bar. 25 steel elements of 1 in length each were used in modeling the anchored reinforcing bar.

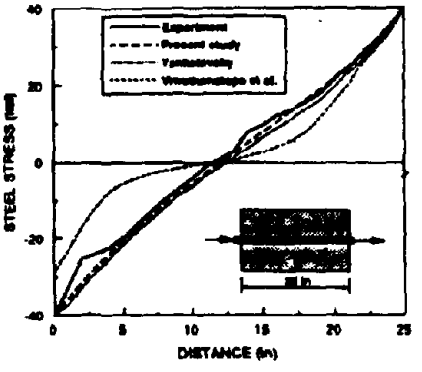

Figure 6. Stress distribution along reinforcing bar at the seventh cyclic push-pull loading cycle.

Figure 4 shows the distribution of steel stresses along the anchorage length of the reinforcing bar under monotonic pull-out for a steel stress of 70 ksi at the loaded end. The analytical results show very good agreement with experimental measurements.

Figure 5 shows the end stress-slip relation of the reinforcing bar under cyclic push-pull loading for load cycles before yielding of the reinforcement. The steel stress distribution along the anchorage length of the reinforcing bar for part of the seventh loading cycle is shown in Figure 6. The experimental results are compared with the results of previous studies (Viwathanatepa et al. 1979b, Yankelevsky 1985) and those of the present study. The results of the proposed model show very good agreement. It should be noted, however, that the reinforcing steel does not yield in the seventh cycle. In latter load cycles the analytical results start to deviate from the measured stress distribution. This is attributed to two factors: (a) the model is tested under load controlled conditions, while the specimen was subjected to displacement controlled testing, and (b) the assumption that the bond stress-slip relation is the same along the anchorage length of the bar is not reasonable for cycles which induce significant bond damage.

3.2 Reinforced concrete beams

Three simply supported reinforced concrete beams have been investigated. In these case studies the concrete was modeled by 8-node serendipity plane stress elements with 3x3 Gauss integration and the reinforcement was modeled by the 2-node truss elements. In all studies the bond-slip effect is taken into account with bond link elements, as described in the previous section.

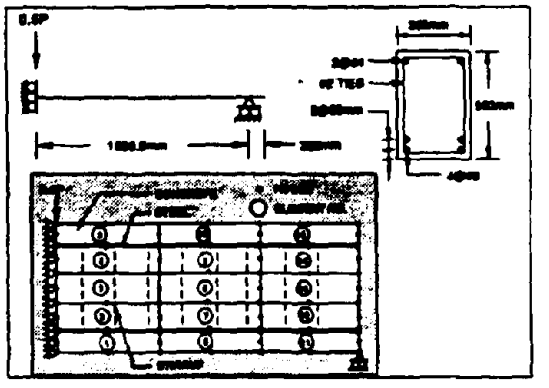

Figure 7. Configuration and finite element idealization of beam A1.

In the following the results for beam A1 (Bresler and Scordelis 1963) are presented. This is a heavily reinforced beam with a longitudinal reinforcing steel ratio of 1.53%. The geometry and cross section dimensions of beam A1 are presented in Figure 7, which also shows the finite element idealization of the beam. The steel material properties of the beam are: (a) for the bottom longitudinal steel (#9 bars) E_s = 29000 ksi and f_y = 80.5 ksi, (b) for the top longitudinal steel (#4 bars) E_s = 29200 ksi and f_y = 50.1 ksi and (c) for the transverse reinforcement (#2 bars) E_s = 27500 ksi and f_y = 47.2 ksi. The concrete material properties of the beam are: E_c = 3370 ksi and f'_c = 3.49 ksi.

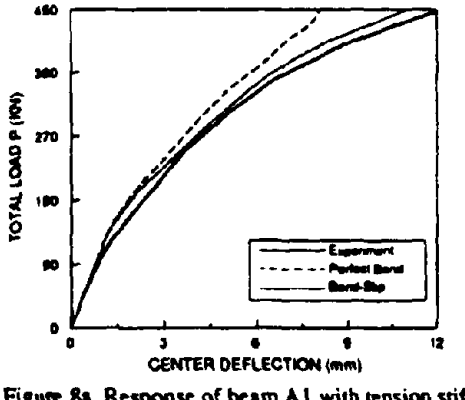

Figure 8a. Response of beam A1 with tension stiffening and bond-slip.

Figure 8a compares the analytical results with the measured load-displacement response of beam A1. Very satisfactory agreement between analysis and experiment is observed.

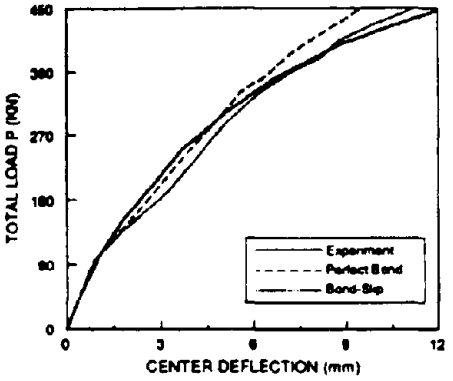

Figure 8b. Response with bond-slip but without tension stiffening.

To identify the relative contribution of tension stiffening and bond-slip four different analyses are performed for this specimen. In Figure 8a the effect of tension stiffening is included in both analytical results. The response depicted by the long-dash line excludes the effect of bond-slip, while the response depicted by the dotted line includes this effect. It is clear from the comparison of the analysis with the experimental data that the inclusion of both effects yields very satisfactory agreement of the model with reality. Figure 8b shows two analytical results which exclude the effect of tension-stiffening. In this case the inclusion of bond-slip (dotted line) produces a slightly more flexible response than the experiment, while the exclusion of bond-slip produces a slightly stiffer response. Figures 8a and 8b show that the contribution of bond-slip to the load-displacement response of the specimen increases with load. Near the ultimate strength of the beam the magnitude of the bond-slip contribution to the load-displacement response is almost twice that of the tension-stiffening effect, which is of opposite sign.

The studies of beam specimen A1 show that the inclusion of, both, tension-stiffening and bond-slip, yields excellent agreement of the analytical results with the experiments. In lightly reinforced beams these two effects are of comparable importance and might cancel each other at certain stages of the load history. This does not happen over the entire response, since gradual bond damage leads to increasing bond-slip contribution with increasing load. The bond-slip effect is more marked in heavily reinforced beams, such as specimen A-1, where it outweighs the effect of tension-stiffening.

3.3 Beam to column joint subassemblage

Experimental studies have shown that bond slip has a pronounced effect on the global deformation of beam-column subassemblages which are subjected to loading simulating the effect of large lateral loads. This happens because the anchorage length of the reinforcing bars in the joint does not suffice to transfer to the concrete the steel forces at the beam-column interfaces of the joint. These forces cause the reinforcing bars to be pulled from one end of the joint and pushed from the other, so that a force equal to almost twice the yield force of the bar needs to be transferred to the concrete within the joint. When lateral load reversals occur, the stress transfer problem is aggravated by bond deterioration under cyclic load reversals.

In order to assess the ability of the proposed finite element model to simulate the behavior of beam-column joint subassemblages specimen BC4 is selected for further study (Viwathanatepa et al. 1979a). The subassemblage consists of two 9 in. by 16 in. girders framing into a 17 in. by 17 in. square column. The column was bolted at the top and bottom to steel clevises for mounting the specimen on the testing frame. The main longitudinal reinforcement of the beams consisted of 4#6 bars at the top and 3#5 bars at the bottom of the section with #2 tied stirrups spaced at 3.5 in. as transverse reinforcement. The longitudinal reinforcement of the column consisted of 12#6 bars with #2 ties spaced 1.6 in. center-to-center along column providing the transverse reinforcement. Seven #2 ties were placed inside the beam-column joint region to satisfy the confinement and shear resistance requirements of the Uniform Building code.

The beam-column subassemblage was subjected to a constant axial load P of 470 kips which simulated the effect of gravity loads and a horizontal load H at the lower column end which was cycled to simulate the effect of lateral loads on the subassemblage. Specimen BC4 was subjected to a very severe, pulse-type loading with a single load reversal in order to study the monotonic behavior of the subassemblage and establish the load-displacement response envelope. Since the load-displacement response of subassemblage BC4 during the first load cycle, which represents a monotonic load test to near failure, was well established during the experiment, it serves as an ideal case study for the proposed model.

The finite element representation of the beam-column subassemblage is shown in Figure 9. Concrete was modeled by 8-node isoparametric elements and the longitudinal and transverse reinforcement was modeled by 2-node truss elements. The bond-slip effect is included in the analysis with bond link elements, as described in the previous section.

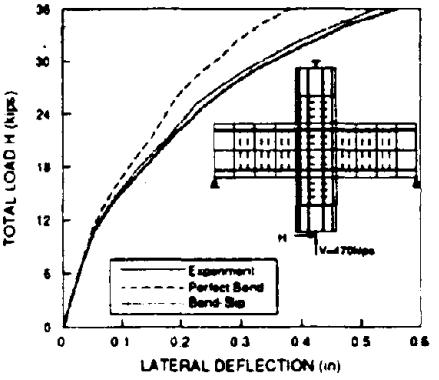

Figure 9. Load-displacement response of beam-column subassemblage with tension stiffening and bond-slip.

Figure 9 compares the analytical results with the measured load-displacement response of the subassemblage. With the effects of tension stiffening and bond-slip the analysis shows excellent agreement with the experimental results. The lateral force of 36 kips closely approximates the ultimate load of the specimen.

Figure 9 shows that the effect of bond slip affects the behavior of the subassemblage much more than tension stiffening. In this case the bond-slip of reinforcing bars in the joint contributes approximately 33% of the total deformation of the subassemblage near the ultimate load of 36 kips. The significance of bond-slip in the response of the beam-column subassemblage agrees with the results of the over-reinforced concrete beam A1, where the interaction of bond and shear plays a significant role in the response. This interaction also has an important effect on the stress transfer in beam-column joints, particularly, when these are subjected to loading simulating the effect of lateral loads. Even though the tension stiffening effect plays a minor role in the response of this beam-column joint, it should always be included in the model, since it helps with numerical instability problems which might arise during crack formation and propagation.

4 CONCLUSIONS

The objective of this study is to develop reliable and computationally efficient finite element models for the analysis of reinforced concrete beams, slabs and beam-column joint subassemblages under monotonic and cyclic loading conditions. Even though the applications in this paper concentrate mostly on the monotonic behavior of reinforced concrete members, the proposed models are general enough to be extended to cyclic loading conditions. A cyclic reinforcing steel model which includes the effect of bond-slip and is embedded in a concrete finite element is presented in this paper.

The correlation studies between analytical and experimental results lead to the following conclusions:

1. The developed finite element model exhibits very satisfactory agreement with experimental results of reinforcing bar anchorages, beams and beam-column joint subassemblages.
2. The effect of tension-stiffening is important in the analysis of monotonic behavior of reinforced concrete beams. Its inclusion is important for the independence of the analytical results from the size of the finite element mesh, but also for avoiding numerical problems in connection with crack formation and propagation.
3. Present smeared crack models are too stiff in connection with large finite elements. A new criterion which limits the effect of tension stiffening to the vicinity of the integration point yields very satisfactory results.
4. The effect of bond-slip is very important in the analysis of reinforced concrete beams and beam-column subassemblages under monotonic, but particularly, under cyclic loads. This effect is more pronounced in heavily reinforced beams and beam-column joints, which are subjected to loads simulating the effect of lateral loads on the structure.
5. Tension-stiffening and bond-slip have opposite effect on the response of reinforced concrete members. While tension-stiffening, which accounts for the concrete tensile stresses between cracks, increases the stiffness of the member, bond-slip leads to a stiffness reduction. In lightly reinforced beams these effects might cancel each other at certain load stages, leading to the erroneous impression that they can be neglected. Since bond-slip increases with loading, while tension-stiffening does not, consistent results can only be obtained when both effects are included. Moreover, the effect of bond-slip clearly outweighs the contribution of tension-stiffening in heavily reinforced beams and beam-column joint subassemblages. In these cases the exclusion of the bond-slip effect can lead to significant overestimation of the stiffness of the structure.

5 ACKNOWLEDGEMENTS

This study was supported by Grant No. ECE-8657525 from the National Science Foundation. This support is gratefully acknowledged. Any opinions expressed in this report are those of the authors and do not reflect the views of the sponsoring agency.

REFERENCES

Bresler, B. and Scordelis, A.C. (1963). Shear strength of reinforced concrete beams. *Journal of ACI*, Vol. 60, No. 1, pp. 51-72.

Ciampi, V., Eligehausen, R., Bertero, V.V. and Popov, E.P. (1982). Analytical model for concrete anchorages of reinforcing bars under generalized excitations. *Report No. EERC 82-23*, University of California, Berkeley.

Darwin, D. and Pecknold, D.A. (1977). Analysis of cyclic loading of plane R/C structures. *Computers & Structures*, Vol. 7, No. 1, pp. 137-147.

Filippou, F.C., Popov, E.P., and Bertero, V.V. (1983). Effects of bond deterioration on hysteretic behavior of reinforced concrete joints. *Report No. UCB/EERC-83/19*, University of California, Berkeley.

Kwak, H.G. and Filippou, F.C., Finite element analysis of reinforced concrete structures under monotonic loads. *Report No. UCB/SEMM-90/14*, University of California, Berkeley.

Ngo, D. and Scordelis, A.C. (1967). Finite element analysis of reinforced concrete beams. *Journal of ACI*, Vol. 64, No. 3, pp. 152-163.

Viwathanatepa, S., Popov, E.P. and Bertero, V.V. (1979a). Seismic behavior of reinforced concrete interior beam-column subassemblages. *Report No. UCB/EERC-79/14*, University of California, Berkeley.

Viwathanatepa, S., Popov, E.P. and Bertero, V.V. (1979b). Effects of generalized loadings on bond of reinforcing bars embedded in confined concrete blocks. *Report No. EERC 79-22*, University of California, Berkeley.

Yankelevsky, D.Z. (1985). New finite element for bond-slip analysis, *Journal of Structural Engineering, ASCE*, Vol. 111, No. 7, pp. 1533-1542.

Nonlinear Response Spectra for Earthquake Resistant Design

Eduardo Miranda
University of California at Berkeley, USA

ABSTRACT: This paper summarizes the results of a comprehensive statistical study of nonlinear response spectra in which 124 ground motions recorded during various earthquakes was considered. Special emphasis is given to the influence of soil conditions on the inelastic strength and deformation demands of single-degree-of-freedom systems. The study included both a deterministic and a probabilistic approach. For each soil group, mean and mean plus one standard deviation spectral ordinates were computed for: inelastic strength demands, strength reduction factors, inelastic displacement demands, and inelastic displacement ratios. The paper also presents an evaluation of the dispersion and distribution of spectral ordinates, as well as probabilistic nonlinear spectra computed from the observed probability distribution. Results and conclusions from this study can be directly used in design of new structures, the evaluation of existing structures and for the evaluation of present seismic design provisions.

1. INTRODUCTION

There is a general consensus that the greatest source of uncertainty in the determination of the response of structures to earthquake ground motions is that associated with the prediction of the intensity and characteristics of the seismic input. Since the concept of response spectrum was developed in the late 30's response spectra have been widely used to estimate strength demands on structures imposed by earthquake ground motions.

A number of statistical studies have been conducted over the years with the purpose of improving the knowledge on design spectra. These studies have been improved in time as more earthquake ground motions have been recorded. Linear elastic response spectra provide a reliable tool to estimate the level of forces and deformations developed in structures responding elastically during the earthquake. There has been a good number of statistical studies that, by considering a large number of recorded ground motions, have investigated the characteristics of linear elastic response spectra (Newmark et al. 1973, Seed et al. 1974, Mohraz et al. 1975, Katayama et al. 1978, Kiremidjian et al. 1980). During strong earthquakes, however, present seismic design philosophy accepts structural and non-structural damage. Thus, buildings designed according to this philosophy are likely to experience significant inelastic excursions which produce deformations and reductions in seismic forces which cannot be predicted with the use of linear elastic models. Typically, statistical studies that have included nonlinear behavior have only considered a small number of recorded ground motions (Veletsos 1969, Ridell et al. 1979). Recently, Ridell et al. (1989) studied strength reductions due to nonlinear behavior by using 53 ground motions, mostly recorded in South America. Similarly, Krawinkler et al. (1990) studied strength reductions by using 33 ground motions recorded during the 1987 Whittier Narrows, California earthquake. However, the effect of soil conditions was not taken into account in any of these two studies. A complete bibliography review on statistical studies of linear and nonlinear spectra has recently been compiled by Miranda (1991).

The objective of this paper is to present a summary of the results of a comprehensive statistical study of inelastic strength and deformations demands of single-degree-of-freedom (SDOF) systems in which a large number of recorded ground motions was considered.

2. SYSTEMS AND MOTIONS CONSIDERD

In order to improve the present knowledge on the characteristics of ground motions and of current methods for estimation of seismic demands on inelastic systems, a comprehensive statistical study of nonlinear was conducted.

2.1 Method of analysis and systems considered

Constant ductility nonlinear spectra were com-

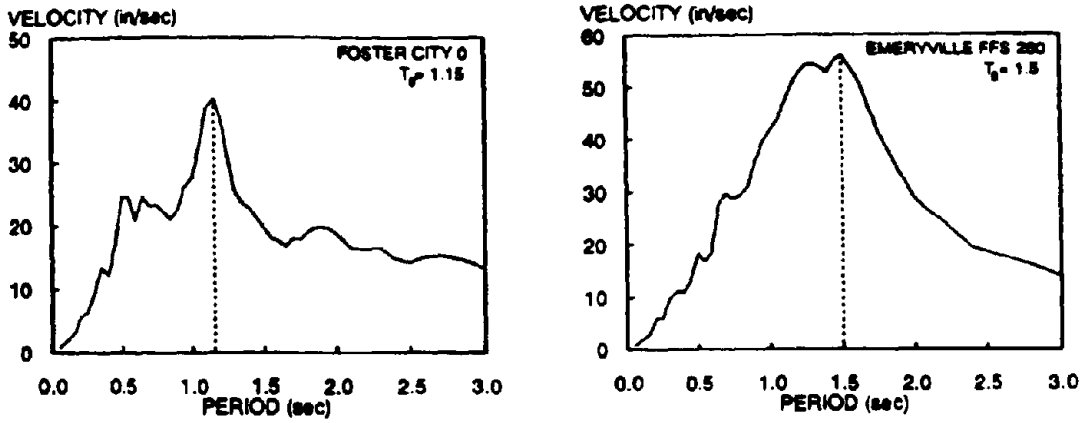

Figure 1. Predominant ground period computed for two soft soil sites in California.

puted for 124 ground motions by iterating on the yielding strength of SDOF systems until the target ductility ratio was reached. The spectra were computed for a set of 50 periods. The following values of displacement ductility, μ, were selected for this study: 1 (elastic), 2, 3, 4, 5 and 6. Iteration was done using the secant method and the iteration was successful when the computed ductility was within 1% of the specified (target) ductility. For cases where multiple roots exist, that is, systems with different yielding strengths exhibit the same ductility demand under a given ground motion, the computer program used in this study yields the root corresponding to the largest strength. This largest strength is the minimum strength required (i.e., strength that needs to be supplied) in order to limit the ductility demand to the target ductility.

Due to the large number of records and the computational effort involved in calculating constant ductility nonlinear spectra, the study was limited to bilinear systems with a post-elastic stiffness of 3% of the elastic stiffness and with a damping ratio of 5% of the critical. On each iteration, response time histories were computed by numerical step-by-step integration using the linear acceleration method with a variable time step to minimize energy equilibrium violations when changes in stiffness occur.

2.2 Ground motions considered

For this study 124 ground motions records were selected, with emphasis on those recorded in California and on those recorded during the last six years. The ground motions were classified into three groups according to the geologic conditions at the recording station. These groups were rock, alluvium and very soft soil. Complete listing of all records and their classification can be found in Miranda (1991).

3. STATISTICAL STUDY

As mentioned above the constant ductility nonlinear spectra were computed for 50 periods. For ground motions recorded on rock or alluvium sites a, fixed set set of periods between 0.05 and 3 seconds was used, while for motions recorded on very soft soil, the spectra were computed for a fixed set of T/T_g ratios, where T_g is the predominant period of the site. For this study T_g is defined as the period corresponding to the maximum spectral velocity of systems responding elastically. Figure 1 shows two examples on the computation of the predominant period for two sites in California.

After computing the constant displacement ductility nonlinear response spectra for all ground motions, statistical studies were conducted on the following parameters:

3.1 Normalized inelastic strength demands

Two sets of normalized inelastic strength demand spectra were computed for each record. The first set used peak ground acceleration (PGA) as normalizing parameter, then the normalized strength demand is given by η which is defined as

$$\eta = \frac{C_y}{\ddot{u}_{g\_\_} / g} \qquad (1)$$

where $\ddot{u}_{g\_\_}$ is the peak ground acceleration, g is the acceleration due to gravity and C_y is the structure's yielding seismic coefficient defined as the yielding strength divided by the weight of the system.

The second set used effective peak ground acceleration, EPA, (as defined in the ATC-3-06 and NEHRP seismic provisions) as normalizing parame-

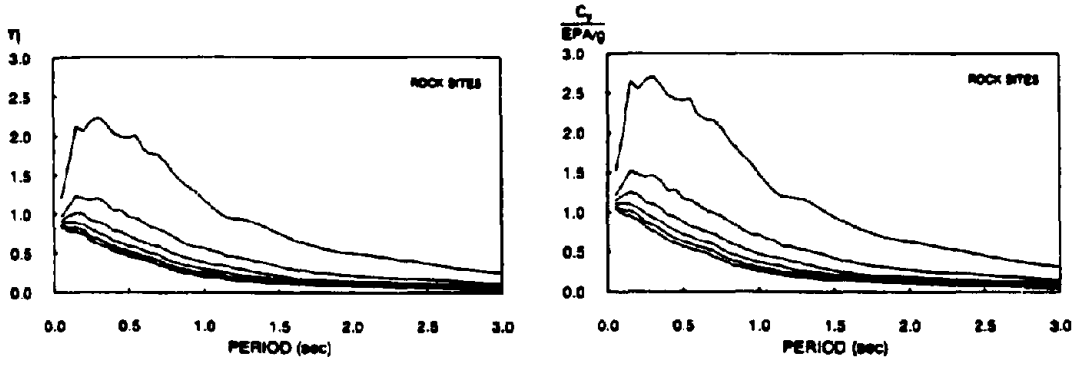

Figure 2. Mean strength demands of ground motions recorded on rock when normalized using PGA and EPA (μ=1,2,3,4,5,6 from top line to bottom line).

ter. Mean normalized spectra were computed for each soil group. Mean inelastic strength demand spectra for ground motions recorded at rock sites are shown in Fig. 2. In order to provide strength demand spectra with a smaller probability of exceedance, mean plus one standard deviation spectra were also computed. Study of the dispersion of the inelastic strength demands was conducted by means of computing coefficients of variation, COV, (defined as the ratio of standard deviation to the mean) for each level of ductility. An example of COV of strength demands (normalized by PGA) for ground motions recorded on rock is presented in Fig. 3.

3.2 Strength reduction factors

For each soil group and for each level of inelastic deformation (i.e. displacement ductility ratio), the strength reduction due to nonlinear hysteretic behavior in the system was computed. This reduction factor, R_μ, is defined as the ratio of the elastic strength demand (strength required to maintain the system elastic) to the strength demand on an inelastic system undergoing a certain ductility demand μ_i,

$$R_\mu = \frac{C_y(\mu=1)}{C_y(\mu=\mu_i)} \qquad (2)$$

For design purposes this reduction factor corresponds to the maximum reduction in strength that can be taken to limit the displacement ductility demand to a certain value μ_i.

This ratio was computed for a total of 31,000 different SDOF systems (the product of 124 ground motions, 50 periods and 5 levels of displacement ductility). Mean spectra were computed for each soil group and each level of ductility. Figure 4 shows mean values for ground motions recorded on rock and very soft soil for six levels of ductility.

In order to study the reliability of the computed strength reduction factors for each soil group and each level of ductility the statistical study included the computation of COV's as well as reduction factors spectra corresponding to mean minus one standard deviation. Examples of COV's for ground motions recorded on alluvium and for ductility ratio of 2 and 5 are shown in Fig. 5.

3.3 Normalized inelastic displacement demands

Using again PGA and EPA as normalizing parameters, mean displacement demands and their dispersion was computed for each soil group and each ductility ratio.

3.4 Inelastic displacement ratio

The inelastic displacement ratio is defined as the ratio of the maximum inelastic deformation of a system undergoing a certain ductility ratio to the max-

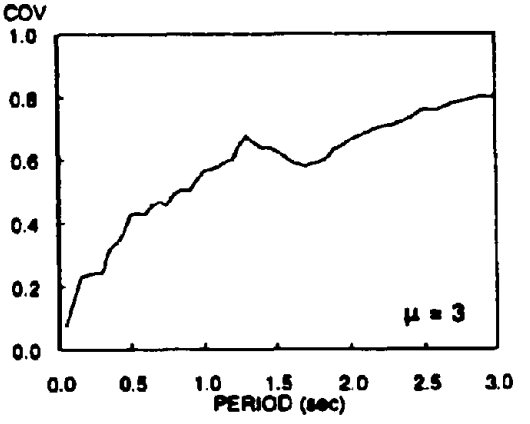

Figure 3. Coefficients of variation of strength demands (normalized by PGA) for ground motions recorded on rock and for μ=3.

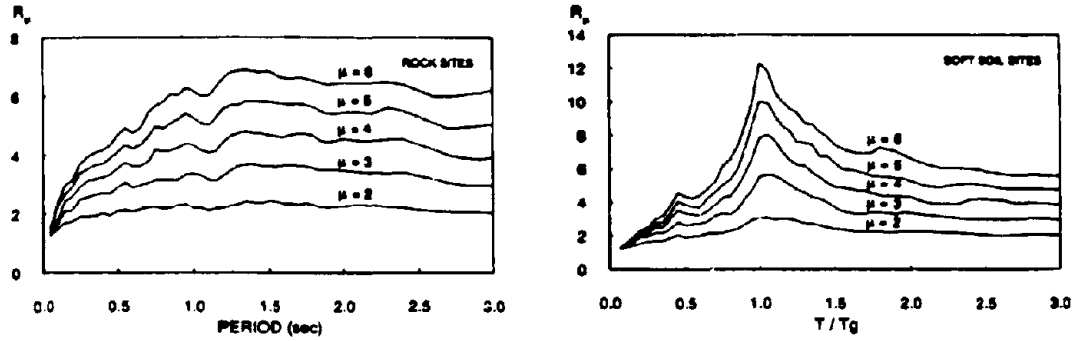

Figure 4. Mean of strength reductions due to nonlinear behavior for rock sites and for soft soil sites.

imum deformation of a system undergoing a ductility ratio of one (i.e., which remains elastic). An example of inelastic displacement ratio spectra corresponding to mean values and ground motions recorded on alluvium and soft soil sites are shown in Fig. 6.

3.5 Probability distribution of spectral ordinates

A more rational consideration of the uncertainty in seismic demands is to look at the frequency distribution of spectral ordinates. For each soil group and each normalizing parameter 300 frequency histograms were computed. Figure 7 shows an example for T=0.3 seconds and ductility of 3 for motions recorded on alluvium.

Attempts to fit the computed statistical data to various theoretical probability density functions were made by plotting the sorted data against the quantiles of five different theoretical probability distribution functions, PDF (Normal, Lognormal, Rayleigh, Gamma and Gumbel type I). An example using the Gamma distribution is shown in Fig. 8.

3.6 Probabilistic nonlinear response spectra (PNRS)

These spectra provide a rational way to design since they allow the designer the option of selecting the confidence level for which a certain response parameter is likely to be exceeded. Murakami and Penzien (1975) and more recently Conte et al.(1990) computed PNRS using artificially-generated accelerograms combined with the use of theoretical PDFs (Gumbel Type I in the former study and Lognormal in the latter study).

A PNRS is computed by obtaining the nonlinear response spectra for different probabilities of non-exceedance of a certain random variable (i.e., response parameter). If the selected random variable is the displacement ductility demand, then the probability of having a ductility demand less than or equal to a certain ductility μ_i is given by

$$P(\mu_i) = P(\mu \leq \mu_i) = \int_{-\infty}^{\mu_i} p(\mu)\, d\mu \qquad (3)$$

where $p(\mu)$ is the PDF of μ. The corresponding pro-

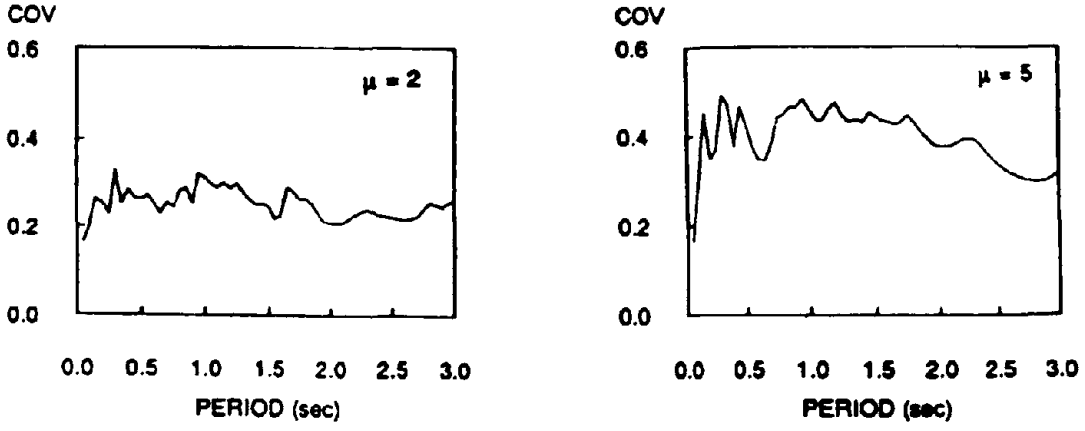

Figure 5. Coefficients of variation of strength reduction factors for alluvium sites and ductilities of 2 and 5.

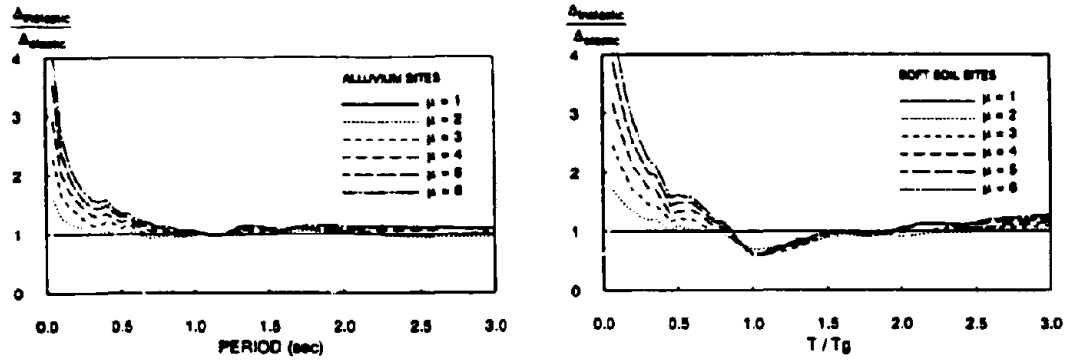

Figure 6. Mean of ratio of inelastic to elastic displacement demands for alluvium sites and for soft soil sites.

bability of exceedance is given by

$$P(\mu>\mu_i) = \int_{\mu_i}^{\infty} p(\mu)\, d\mu = 1-P(\mu_i) \qquad (4)$$

In this study, PNRS were computed using the previously computed constant ductility nonlinear spectra of 124 ground motions and using the actual (observed) probability distribution. The advantage of using the observed probability distribution instead of the a theoretical probability distribution is that the resulting PNRS are based on no assumption on the probability distribution of spectral ordinates. The PNRS were computed for six confidence levels (probability of non-exceedance of a certain ductility demand) namely p = 50, 60, 70, 80, 90, and 95%, which correspond to probabilities of exceedance (probability of ductility demands larger than the maximum specified) of 50, 40, 30, 20, 10, and 5%, respectively. For each period, ductility level, and confidence level the normalized strength demands (quantile) were computed through integration (summation) of the area under the observed PDF (i.e., frequency histogram).

Two sets of PNRS were computed, one for strength demands normalized by PGA, and the other for strength demands normalized by EPA. An example of the former for p=0.8 and ground motions recorded on rock is shown in Fig 9.

4. CONCLUSIONS

Based on the results obtained from the statistical study, a number of general conclusions are made

(i) The shape of nonlinear response spectra differs significantly from the shape of elastic response spectra. Thus, direct scaling by the use of a period-independent factor, of the elastic spectra to obtain

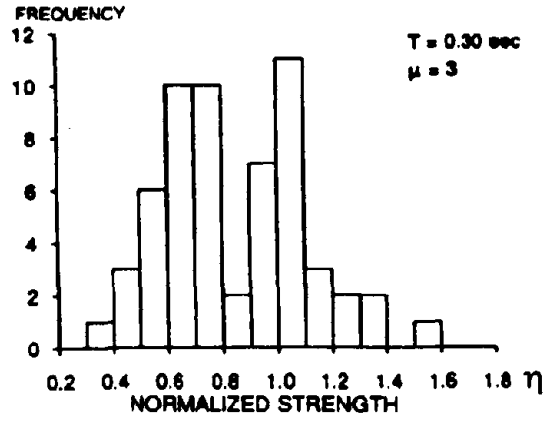

Figure 7. Frequency histogram of normalized strength demands for alluvium sites (T=0.4 sec and μ=3).

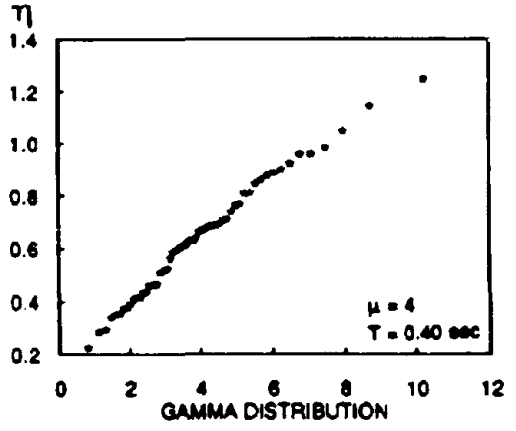

Figure 8. Gamma probability fit of normalized strength demands for alluvium sites (T=0.4 sec and μ=4).

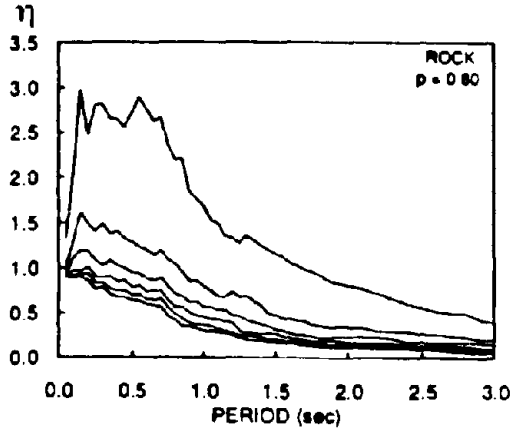

Figure 9. Probabilistic nonlinear spectra for strength demands (normalized by PGA) for rock sites and a 20% probability of exceedance (μ=1,2,3,4,5,6 from top to bottom).

inelastic strength demands is not rational nor conservative.

(ii) The use of either PGA or EPA to normalize inelastic strength demands results in an increase in dispersion (coefficient of variation) with increasing period. In both cases the dispersion was found to be independent of the level of inelastic deformation (i.e., ductility ratio).

(iii) Strength reduction factors were found to be strongly influenced by the level of inelastic deformation, local site conditions, and the period of vibration. Unlike the dispersion of inelastic strength demands, the dispersion of strength reduction factors was observed to be independent of the period of vibration. This dispersion was found to increase as the level of inelastic deformation increased.

(iv) Periods which limit the use of elastic analyses to estimate inelastic displacement demands were observed to depend on the level of inelastic deformation.

(vi) The reliable estimation of inelastic strength and deformation demands of structures on soft soils requires the estimation of the predominant site period.

(vii) It was found that with the exception of the extreme values, inelastic spectral ordinates may be assumed to have a Gaussian probability distribution. An improved fit of extreme values was obtained using a gamma probability distribution.

5. ACKNOWLEDGEMENTS

The work presented in this paper was conducted while the author was a graduate student at the University of California at Berkeley working under the supervision of Professor Vitelmo Bertero whose guidance is appreciated.

6. REFERENCES

Conte, J.P., K.S. Pister, & S.A. Mahin 1990. Influence of the Earthquake Ground Motion Process and Structural Properties on Response Characteristics of Simple Structures. *Report No. UCB/EERC - 90/09*. Earthquake Engineering Research Center, University of California at Berkeley.

Katayama, T., T. Iwasaki, & M. Saeki 1978. Statistical Analysis of Earthquake Acceleration Response Spectra. *Transactions of the Japan Society of Civil Engineering* 10:311-313.

Kiremidjian, A.S. & H.C. Shah 1980. Probabilistic Site-Dependent Response Spectra. *Journal of the Structural Division* 106:69-86.

Krawinkler, H. & A. Nassar 1990. Strength and Ductility Demands for SDOF and MDOF Systems Subjected to Whittier Narrows Earthquake Ground Motions. *Proceedings of the Seminar on Seismological and Engineering Implications of Recent Strong-Motion Data*. SMIP Sacramento.

Miranda, E. 1991. Seismic Evaluation and Upgrading of Existing Buildings. *Ph.D Thesis*. University of California at Berkeley.

Mohraz, B. 1975. A Study of Earthquake Response Spectra for Different Soil Conditions. *Civil and Mechanical Engineering Department*. Southern Methodist University. Dallas.

Murakami, M., & J. Penzien. Nonlinear Response Spectra for Probabilistic Seismic Design and Damage Assessment of Reinforced Concrete Structures. *Report No. UCB/EERC-75-38*. Earthquake Engineering Research Center. University of California at Berkeley.

Newmark, N.M., J.A. Blume, & K.K. Kapur 1973. Seismic Design Spectra for Nuclear Power Plants. *Journal of the Power Division ASCE* 99:287-303.

Riddell, R., & N.M. Newmark 1979. Statistical Analysis of the Response of Nonlinear Systems Subjected to Earthquakes *Structural Research Series No. 468*. University of Illinois, Urbana-Champaign.

Riddell, R., P. Hidalgo, & E. Cruz 1989. Response Modification Factors for Earthquake Resistant Design of Short Structures. *Earthquake Spectra* 5:571-590.

Seed, H.B., C. Ugas & J. Lysmer 1974. Site-Dependent Spectra for Earthquake-Resistant Design. *Report No. EERC 74-12*. Earthquake Engineering Research Center. University of California at Berkeley.

Veletsos, A.S. 1969. Response of Ground-Excited Elastoplastic Systems. *Report No. 6*. Rice University. Houston, Texas.

Displacement based design of RC structures

J. P. Moehle
University of California at Berkeley

ABSTRACT: The importance of structural displacement as a main determinant of structural and nonstructural damage during an earthquake is identified. Methods for estimating displacement amplitude and distribution in simple and complex structures are reviewed. Applications of displacement information to design of nonstructural elements, structural elements, and complete structures is reviewed. It is concluded that a design approach based on structural displacement is viable and effective.

1 INTRODUCTION

The tradition of designing structures to resist externally applied loads has led to earthquake resistant design approaches in which ductility demands are derived based on calculated force demand-capacity ratios. These approaches have focussed design attention away from the importance of structural deformation as a main determinant of damage in structures subjected to earthquakes. This paper develops some fundamental ideas of earthquake resistant design and evaluation using structural displacements directly. It is assumed throughout that design will be based on relatively simple analysis concepts and results. The discussion focuses on applications to reinforced concrete systems, but it is more generally applicable.

2 DISPLACEMENT AS A DESIGN PARAMETER

The idea of using structural displacement information directly in earthquake resistant design and evaluation is not new. Based on a limited analog study, Muto, et al. [1960] wrote that maximum inelastic displacements of SDOF (single-degree-of-freedom) systems are not significantly different from those of elastic systems having the same initial period and damping, and that this tendency "...may suggest employment of a structural design method based upon the maximum displacement." More recent numerical studies indicate that the equal displacement rule is valid only for specific period ranges and demand-capacity ratios [Shimazaki and Sozen, 1985; Qi and Moehle, 1991]. Techniques are proposed in these references for relating inelastic and elastic displacement demands as a function of the strength, period, and ground motion character.

A fundamentally important aspect of these studies is that displacement amplitude of SDOF systems can be estimated using relatively simple elastic models, thereby providing an avenue for design based directly on displacement information. Although the methods presented are generally applicable, in the present paper it will be assumed for clarity of presentation that the equal displacement rule provides an adequate measure of inelastic displacement amplitude. When using the rule for concrete structures, it is suggested that the displacement be read from a displacement spectrum using an initial period based on half the gross-section stiffness (to account for expected stiffness near yield) and damping in the range between two and five percent of the critical value.

3 DISPLACEMENT CONCEPTS FOR MULTI-STORY FRAMES

Numerical and experimental studies of planar frames of moderate height have indicated that displacement response is dominated by response in an apparent first mode [Sozen, 1981; Moehle, 1984]. Saiidi and Sozen [1979] demonstrated that this predominant component of the displacement response could be modeled using a SDOF oscillator having hysteretic properties similar to those of the constituent elements of the frame. This finding suggests that the global displacement maxima of multistory systems may be estimated using simplified response spectrum methods as discussed previously for equivalent SDOF systems. Numerous case studies confirm this view [Moehle, 1984; Qi and Moehle, 1991; Shimazaki and Sozen, 1985].

In a laterally-loaded multistory framed structure having column strengths exceeding the beam strength, the lateral distortion will vary over the height approximately as illustrated in Fig. 1b. For this shape, roof displacement may be estimated as being equal to approximately 1.25 times the equivalent SDOF displacement.

Design requirements will depend not only on total drift but on the drift profile. Elastic analyses may provide insight into drift distribution, but may result in non-conservative estimates due to concentrations of

inelastic action. Based on numerical studies, Qi and Moehle [1991] reported that for five-story frames the maximum interstory drift was approximately 1.5 times the roof value for frames designed to resist lateral load; in contrast, frames having uniform strength over height had maximum drift ratios as high as 1.8. For ten-story frames, the respective ratios were 2.1 and 2.8. Sozen [1981] reported measured drift ratios for earthquake simulation tests of small-scale nine- and ten-story frames ranging from 1.3 (for regular structures) to 2.0 (for irregular frames) times the roof drift. In the analyses and tests reported above, the columns were designed so the sum of column strengths at a joint exceeded the sum of beam strengths at all but the roof level. The composite results suggest that a reasonably conservative approach is to assume interstory drifts in regular structures may be as large as twice the roof drift.

Quantitative information on drift distribution in structures having columns relatively weaker than beams is limited [Schultz, 1990; Kelly, 1977]. Drift in such structures tends to concentrate in a single "weak" story (Fig. 1c). A conservative approach is to assume the maximum interstory displacement is equal to the maximum roof displacement, resulting in a relatively high interstory drift estimate for multistory structures. This approach provides a suitable deterrent for new designs having soft stories, but is unsatisfactory for existing construction where realistic solutions are needed for whatever conditions are encountered. Nonlinear static or dynamic analyses may be required to provided insight into drift profile in such structures, though the results should not be interpreted as being absolute.

4 DISPLACEMENT AND DESIGN

The relation between deformation and damage is a well-established concept in many fields of engineering. Some possible applications of displacement information in earthquake resistant design are discussed below. It is assumed that to some acceptable degree (a) the design earthquake ground motions are known, (b) the resulting global displacement to each motion can be calculated, and (c) the profile of displacement is estimable.

4.1 Nonstructural Elements and Non-Lateral Load Resisting Elements

Nonstructural damage, disrupted operations, and life-safety considerations make protection of nonstructural elements a high priority. Damage to these elements will depend on both drift and nonstructural details [Sakamoto, et al., 1984; Wang, 1987]. Attention need also be paid in design to structural elements that are not considered in design as part of the lateral load resisting system. Examples in the latter category include some floor systems and complete existing framing systems in seismically rehabilitated structures. These "vertical load carrying elements" are susceptible to damage due to earthquake induced lateral deformations, and must be checked to ensure they can continue to support vertical loads under the imposed lateral deformations.

When demand-capacity ratios are used to estimate ductility demands in a structure, the demand and the capacity refer to the lateral load resisting elements. The ratio provides no direct information regarding performance of the non-lateral load resisting elements. Analyses of expected behavior of nonstructural elements and structural elements not considered part of the lateral load resisting system should be carried out by directly considering the expected displacements.

4.2 Lateral Load Resisting Elements

The displacement based approach to design of reinforced concrete structural elements is based on the idealized deformation components of Fig. 2. Flexural deformation is modeled by elastic curvature over height and inelastic curvature concentrated in a plastic hinge of equivalent length l_p at the base. The ultimate displacement capacity with this model is

$$\delta_u = \frac{\phi_y l^2}{3} + (\phi_u - \phi_y) l_p (l - \frac{l_p}{2}) \qquad (1)$$

In Eq. 1, ϕ_y = yield curvature, l = pier height, and ϕ_u = ultimate curvature. Satisfactory correlation with laboratory test results is obtained using $l_p = 0.5h$, where h = the section depth.

The flexural curvature distribution of Fig. 2 can be simplified without significant loss of accuracy as illustrated in Fig. 3. Elastic curvatures outside the plastic hinge zone are ignored, and the curvature near the base is centered at the base (Fig. 3c). The ultimate displacement capacity with this model is

$$\delta_u = \phi_u l_p l \qquad (2)$$

The approximation produces a satisfactory estimate of the ultimate displacement capacity for common ranges of section curvature ductility and member aspect ratio (Fig. 4).

Assuming plane sections remain plane, curvature in Eq. 2 can be expressed as

$$\phi_u = \frac{\epsilon_u}{\beta h} \qquad (3)$$

in which ϵ_u is limiting strain of a point on the cross section located a perpendicular distance βh from the neutral axis. Substituting Eq. 3 in Eq. 2, substituting 0.5h for l_p, and dividing by member length l results in Eq. 4.

$$\frac{\delta_u}{l} = \frac{1}{2\beta}\epsilon_u \qquad (4)$$

Equation 4 directly relates strain in a member to the effective drift ratio for the member.

As an application of Eq. 4, consider an unconfined reinforced concrete beam. Flexural response is

calculated according to ACI 318-89 [1989] except maximum usable concrete compression strain is taken equal to 0.004. Concrete strength is 4000 psi, and yield strength of elasto-plastic Grade 60 reinforcement is assumed equal to 75 ksi. Figure 5 plots results in which drift ratio is defined by Eq. 4. (In a building, the beam drift ratio conservatively may be assumed to be equal to the interstory drift ratio.) The results indicate a maximum drift ratio capacity equal to approximately 0.01 for the permitted range of longitudinal reinforcement ratios. A design that controls interstory drift to this value is likely to result in satisfactory flexural response of the beam.

4.3 Global Response

Pounding between adjacent structures has been identified as a contributor to damage and collapse during earthquakes. In order to determine the likelihood of pounding, it is important that a direct analysis of expected displacements be made. It is not clear that widely used code equivalent lateral force procedures and minimum building separations provide adequate assurance against pounding damage.

Second order (P-delta) effects associated with large displacement response may result in displacement amplitudes exceeding those estimated by conventional analyses, and can therefore increase the potential for damage and collapse [Carr and Moss, 1980]. Considering a SDOF structure consisting of a mass atop a cantilever, it may be shown that the effective lateral load strength is

$$V = \frac{M_p}{l} - P\frac{\delta}{l} \qquad (5)$$

in which M_p = plastic moment strength and P = the vertical load. The effective resistance is most significantly affected when the base shear strength M_p/l is low or the lateral drift ratio δ/l is high. Some studies of inelastic seismic response of frames satisfying current code strength requirements indicate that P-delta effects will not significantly impact response if drift levels (ignoring P-delta effects) are below 0.01 [Carr and Moss, 1980].

In order to effective control pounding and P-delta effects, a design approach should focus on those aspects of design that directly control displacement response. Conventional force-based approaches to design may be unsuitable for this purpose.

5 DRIFT AND DUCTILITY APPROACHES TO DESIGN

The displacement approach to design as described previously utilizes expected structural displacements directly for evaluation of behavior of structural and nonstructural elements. A commonly used alternate and equally simple approach, the ductility based approach, uses displacement information indirectly with information on system strength to derive strength and ductility requirements. The fundamental principal of the approach is illustrated in Figure 6. If in a particular period range it is assumed that the elastic and inelastic displacements are equal, then ductility demand is equal to the ratio of the computed elastic force demands to the force capacity, that is, the demand capacity ratio. Where ductility demands are deemed to be excessive, it is common practice using this method to increase the strength of the structure so as to reduce the demand-capacity ratio, and hence, the ductility demand.

The displacement and ductility based approaches are effectively the same. However, the nature of the information used in the ductility based and displacement based approaches can influence decisions made in the design process. As an example, consider the existing structure illustrated in Fig. 7a. The columns possess a load-deformation behavior represented by curve "a" in Fig. 7b, with yield occurring at a unit displacement and failure occurring at displacement δ_a equal to 3 units, such that the available displacement ductility is $\mu_a = 3$. The structure possesses an initial period T_a, with resulting displacement demand δ_a and acceleration demand A_a read from the linear elastic response spectra of Fig. 7c. For this example, because the fundamental period exceeds the predominant ground motion period it can be expected that the elastic displacement spectrum adequately represents the inelastic displacement maxima. As indicated in Fig. 7b, the displacement demand δ_a exceeds the deformation capacity of the columns, so that redesign (retrofit) of the structure is in order. It will be assumed in the following discussion that the structure will be retrofit by addition of external structural elements rather than by direct modification of the columns.

In a ductility based approach the apparent goal in redesign of the structure (Fig. 7) is to reduce the demand-capacity ratio (because doing so will reduce the nominal ductility demand). This goal may suggest that the successful redesign is one that (a) adds strength and (b) avoids significant stiffness increase because an increase in stiffness results in an increase in "demand." A plausible solution based on this specious goal is illustrated in Fig. 7b and 7c, where the structure strength is increased to V_b and the stiffness is increased only slightly resulting in an initial period T_b. As illustrated in the figure, this solution may not adequately change the deformation demand on the columns and therefore might not provide the desired degree of safety. Specifically, for the period range of the subject structure, modifications that influence strength and not stiffness cannot be effective for protecting the critical columns.

A displacement based approach indicates directly that if the columns are to be protected the structure must be stiffened so as to reduce the displacement demand. A solution satisfying this more realistic goal is illustrated in Fig. 7, where the redesign results in a significant increase in stiffness (load-displacement relation "c"), with corresponding reductions in initial period T_c and displacement demand δ_c.

The example illustrated in the preceding paragraphs is obviously simplified. Seldom can the structure strength and stiffness be modified independently as has been assumed. Furthermore, there are cases (e.g., short period structures situated on soft sites [Qi and Moehle, 1991]) where strength has a significant influence on deformation demand. Nonetheless, the example illustrates the advantage of operating directly with deformation quantities as opposed to demand-capacity ratios. The particular case considered here illustrates further that seismic strengthening frequently is more a matter of stiffening than it is of strengthening.

The ductility based approach is well suited to cases where inelastic response is distributed uniformly over height; in such cases the local demand-capacity ratios provide a reasonably accurate picture of ductility distribution and magnitude. Where inelastic response is not uniformly distributed the local demand-capacity ratios do not provide information on local ductility demands, and the displacement based approach may be preferred. As an example, consider a bridge pier founded on a flexible foundation (Fig. 8). The elastic rotational stiffnesses of the foundation and of the pier are assumed to be equal, and the pier strength is assumed to be one fourth of the elastic force demand. During an earthquake, the maximum displacement of the superstructure is determined by the combined flexibility of the pier and foundation. If the ductility based approach is used, the pier displacement ductility demand may erroneously be estimated to be equal to the demand-capacity ratio (that is, $\mu_\delta = 4$). If displacements are viewed directly, as in Fig. 8, the correct displacement ductility for the pier ($\mu_\delta = 7$) is obtained.

A comprehensive approach to analysis of seismic response requires simultaneous consideration of displacements, forces, and ductilities, regardless of the basic approach used. Lateral displacements result in P-delta effects that may be important. Forces associated with inelastic flexural response determine actions in shear and other less-ductile response modes, and should be used in a capacity design approach to establish required strengths [Park, 1986]. Flexural ductility plays an important role in capacity design where behavior in nonductile modes (e.g., shear in reinforced concrete columns) depends on the ductility level. For these reasons, displacements and forces should be considered when using the ductility based approach, and forces and ductilities should be considered when using the displacement based approach.

6 CONCLUSIONS

Studies of the inelastic response of simple and complex structures have resulted in the development of uncomplicated tools for estimating maximum lateral drift during a strong earthquake. Two approaches to design and evaluation using drift information are available. A ductility based approach uses displacement information indirectly, establishing ductility requirements as a function of the provided strength and the strength required for elastic response. A displacement based approach uses displacement information directly. The latter approach has been the main subject of the present paper.

The displacement based approach can be used to establish proportions and layout that will control drift demand, and to determine structural and nonstructural details that will ensure adequate performance. Several examples illustrating its application have been presented. The examples demonstrate that the displacement based approach is a simple and effective tool for design.

REFERENCES

ACI 318-89, 1989. "Building Code Requirements for Reinforced Concrete (ACI 318-89)

Carr, A., and Moss, P., 1980, "The Effects of Large Displacements on the Earthquake Response of Tall Concrete Frame Structures," *Bltn of the New Zealand Natl Soc for Earthquake Engr*, Vol. 13, No. 4, pp. 317-328.

Kelly, T. E., 1977, "Some Comments on Reinforced Concrete Structures Forming Column Hinge Mechanisms," *Bltn of the New Zealand Natl Soc for Earthquake Engr*, Vol. 10, No. 4, pp. 186-195.

Moehle, J. P., 1984, "Strong Motion Drift Estimates for R/C Structures," *Jrnl of Structural Engr*, ASCE, Vol. 110, No. 9, pp. 1988-2001.

Muto, K., et al., 1960, "Non-linear Response Analyzers and Application to Earthquake Resistant Design," *Proc*, 2WCEE, Vol. 2, Japan, pp. 649-668.

Park, R., 1986, "Ductile Design Approach for Reinforced Concrete Frames," *Earthquake Spectra*, EERI, El Cerrito, CA, Vol. 2, No. 3, pp. 565-619.

Qi, X., and Moehle, J. P., 1991, "Displacement Design Approach for Reinforced Concrete Structures Subjected to Earthquakes," *Report No. UCB/EERC-91/02*, EERC, UC Berkeley, Berkeley, CA, 186 pp.

Saiidi, M. and M. A. Sozen, 1979, "Simple and Complex Models for Nonlinear Seismic Response of Reinforced Concrete Structures," *SRS No. 465*, U of Illinois, Urbana.

Sakamoto, I., H. Itoh and Y. Ohashi, 1984, "Proposals for Aseismic Design Method on Nonstructural Elements," *Proc*, 8WCEE, San Francisco, CA, Vol. 5, pp. 1093-1100.

Schultz, A. E., 1990, "Experiments on Seismic Performance of RC Frames with Hinging Columns," *Jrnl of Structural Engr*, ASCE, Vol. 116, No. 1, pp. 125-145.

Shimazaki, K. and M. A. Sozen, 1985, "Seismic Drift of Reinforced Concrete Structures," Special Research Paper, Hazama-Gumi, Ltd., Tokyo, Japan.

Sozen, M. A., 1981, "Review of Earthquake Response of R.C. Buildings with a View to Drift Control," *State-of-the-Art in Earthquake Engineering - 1981*, Ankara, pp. 383-418.

Wang, M. L., 1987, "Cladding Performance on a Full Scale Test Frame," *Earthquake Spectra*, EERI, El Cerrito, CA, Vol. 3, No. 1, pp. 119-174.

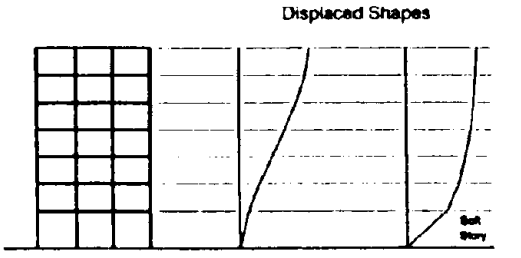

Figure 1 - Building Frame Deformation Modes

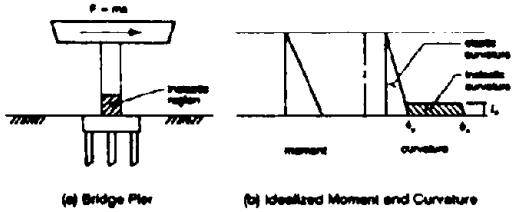

Figure 2 - Idealized Flexural Curvature in Cantilever Bridge Pier

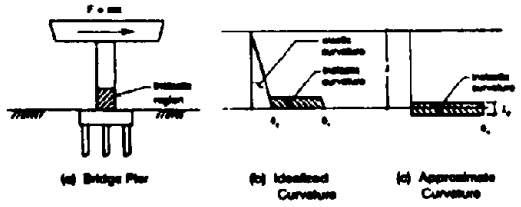

Figure 3 - Simplified Curvature Distribution in Cantilever Bridge Pier

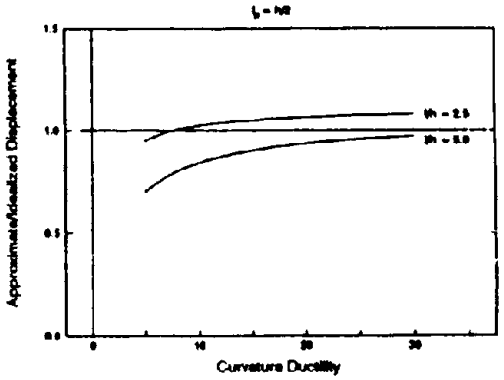

Figure 4 - Comparison of Ultimate Displacement Capacities Calculated Using Idealized (Eq. 1) and Simplified (Eq. 4) Curvature Distributions

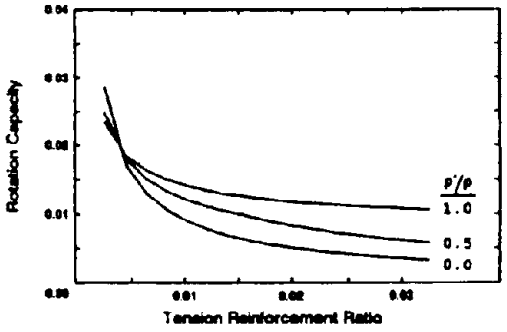

Figure 5 - Rotational Capacity of Reinforced Concrete Beam Sections

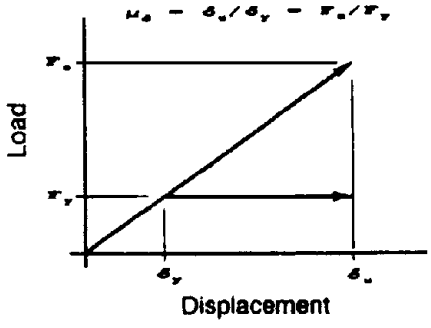

Figure 6 - Displacement Ductility Based on Equal Displacement Rule

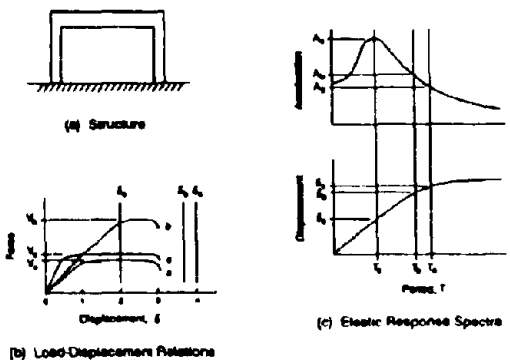

Figure 7 - Example Redesign of Existing Frame

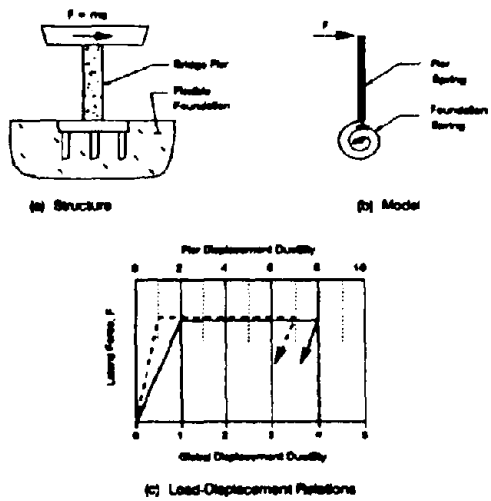

Figure 8 - Bridge Pier with Flexible Foundation

Methodology for optimum EBF link design

E. P. Popov
University of California, Berkeley, California, U.S.A.

J. M. Ricles
University of California, San Diego, California, U.S.A.

K. Kasai
Illinois Institute of Technology, Chicago, Illinois, U.S.A.

ABSTRACT: Eccentrically braced frames (EBFs) designed improperly can develop undesirable large inelastic link deformations where energy is dissipated at only a few floors. This unsatisfactory behavior can be caused by ill proportioning of links in an EBF. Cases are discussed drawn from both analytical and experimental studies to illustrate the unacceptable seismic behavior in EBFs with incorrectly proportioned links. A design procedure for avoiding such behavior is explained, illustrating a correct selection of links and corresponding behavior of the EBFs. Primary emphasis is placed on the link strength distribution along the height of an EBF and its desirable effect on inelastic link deformations throughout the structure.

1 INTRODUCTION

Eccentrically braced frames (EBF) have established themselves as a viable seismically resistant frame system. An EBF is a hybrid system, combining the advantages of a moment resisting frame (MRF) and a concentrically braced frame (CBF). Eccentricities in EBFs are deliberately introduced at joints to provide short portions of beams called "links". During frequently occurring minor earthquakes links remain elastic. In the event of a strong earthquake causing structural overloading, links are designed to deform inelastically and thereby prevent buckling of diagonal bracing. It has been recognized that short links that yield primarily in shear provide excellent energy dissipation under severe cyclic loading. Such links are known as "shear links" [Kasai et al., 1986b,c].

EBF design provisions exist in most major design codes in the United States as well as other countries. It has come to the authors' attention that some of the recent EBF construction, as well as EBF research, is based on an incorrect interpretation of EBF link design method. This stems apparently from a misunderstanding of EBF design philosophy associated with proportioning the links, where not enough attention is given to strength distribution of links over the height of an EBF. An incorrect proportioning of links can result in the EBF becoming susceptible to a concentration of excessive inelastic link deformation at particular story levels.

Analytical and experimental evidence of undesirable seismic behavior of EBFs having incorrectly proportioned links is discussed. The authors' original design philosophy for EBF links for avoiding such behavior is illustrated by a method for proportioning links and the corresponding behavior of EBFs. Emphasis is placed on link inelastic deformation developed with respect to the link strength distribution throughout the height of the EBF.

2 PROPORTIONING OF LINKS

Based on studies by the authors [Kasai et al., 1986a; Popov et al., 1989], an approximate link design shear force V_{link} in an EBF subjected to lateral loads is obtained as follows:

$$V_{link} = V_{story}\left(\frac{h}{L}\right) \qquad (1)$$

in which V_{story}, h, and L are the story shear, floor height, and span length, respectively, at the corresponding story level of the EBF. In general, V_{story}, and therefore V_{link}, calculated from typical code forces, varies parabolically over the height of the EBF when the building is of a regular type. In this paper, V_{story} is chosen to be the required nominal story shear at the yield limit state of the EBF. Thus, the link yield capacity must be equal to or greater than V_{link} obtained from Equation 1. Accordingly, if a shear link is used, the design requirement for the link is:

$$\frac{V_p}{V_{link}} = \alpha \geq 1.0 \qquad (2)$$

where V_p is the nominal shear yield capacity of the shear link, and α is the link strength index [Ricles et al., 1989]. The nominal capacity V_p is calculated as 0.55 times the product of the steel yield stress and web area [AISC, 1992].

It has been established [Kasai et al., 1986a; Ricles et al., 1990] that, if an EBF possesses a uniform value for α throughout the frame height, all links yield almost simultaneously under monotonically increasing lateral load. These EBFs are shown to develop a fairly uniform inelastic deformation, without any concentration of excessive inelastic link deformation at particular story levels. This behavior under static loading is also desirable in an EBF subjected to actual seismic conditions involving earthquake-induced dynamic lateral loads having various histories. A study was conducted

which investigated under dynamic loading the: (1) effect of uniform and variable distributions of α throughout the EBF height, and (2) the effect of static V_{story} distribution throughout the EBF height for which the links are proportioned. This investigation and previous studies involving EBFs with ill proportioned links are discussed below.

3 INCORRECT PROPORTIONING OF LINKS

3.1 U.S.-Japan 6-story EBF

A full-scale 6-story EBF building was tested pseudo-dynamically under Phase II of the U.S.-Japan Cooperative Earthquake Research Program Utilizing Large-Size Testing Facilities [Roeder et al., 1987]. The building was originally designed as a concentrically braced frame (CBF) building for Phase I of the test program, in which the concentric braces were placed at the left bay of the frame shown in Figure 1. Upon completion of the Phase I tests, the concentric braces were removed from the building and the structure was repaired. Then, an eccentric bracing system was installed in the right bay of the frame as shown in Figure 1(b).

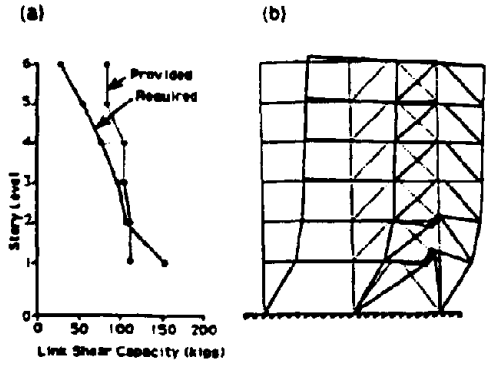

Figure 1. U.S.-Japan EBF Test Structure.

For economic reasons, it was required that for Phase II testing all the beams and columns designed for Phase I be reused. This restricted the EBF design. The beam sections used for the CBF were found inappropriate for a correct design for the EBF, but had to be used. Fortunately, column sections were found sufficiently large for the EBF. Tube brace sizes were selected in order that the braces remain essentially elastic and not buckle.

Using the existing beam sections, shear links were created by maintaining their lengths sufficiently short. Figure 1(a) compares the required V_{link} of the EBF based on the static design loads with the provided link shear capacity V_p. Note that in general V_{link} varies parabolically throughout the EBF height, since V_{story} varies parabolically as noted previously. The exceptional case is seen at the first floor level, where V_{link} increased due to a larger h as compared with the upper story levels (see Equation 1). In contrast to these, the provided link capacity V_p was almost constant throughout the EBF height, resulting in an extremely nonuniform strength index α which varies from 0.7 at the first floor level to 3.3 at the sixth (roof) level. This indicated that the upper story levels of the EBF were over-strengthen whereas the lower story levels were under-strengthen.

In spite of the problem, the EBF generally performed in a superior manner as compared with the CBF [Roeder et al., 1987]. However, the EBF developed the soft story mechanism illustrated in Figure 1(b). This was expected prior to the experiment in view of the extremely nonuniform α explained above (Figure 1(a)). During the final phase of the test, a failure occurred at a diagonal brace-to-beam connection in the first floor. Therefore improved connection details were proposed [Popov et al., 1989] for avoiding this type of damage in a local region. However, it should be noted that a concentration of such damage could have been reduced significantly if the EBF had much larger links at the lower levels, since the links were under-strengthen at these levels.

3.2 13-Story EBF with and without Tied Links

Some seismic designers do not recognize the importance of having a uniform strength index α to avoid concentrations of large inelastic link deformations at particular floor levels. Such was the case in the design of a 13-story EBF by Martini et al [1990] where the links were incorrectly proportioned in the above sense. Compare the V_{link} and V_p shown in Figure 2. Like the frame discussed in Section 3.1, large overstrength of the EBF at the top six levels is evident due to the oversized links. These incorrectly proportioned links resulted in large link inelastic deformations at the lower levels of the EBFs when subjected to a static lateral load (see Figure 2(b)).

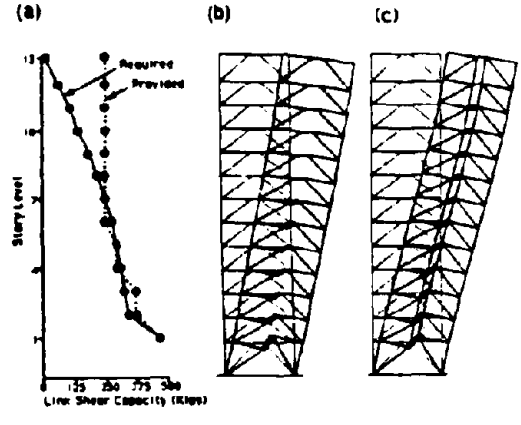

Figure 2. (a) Required Story Shear vs. Designed Capacity, (b) Inelastic Deformation of Untied, and (c) Tied EBF.

As one of the solutions to this problem, Martini et al. proposed a modified EBF connecting the links vertically

with ties (see Figure 2(c)). This type of EBF tends to develop a more uniform distribution of link inelastic deformation, as illustrated in Figure 2(c). However, under the static loading condition considered, the ties would have been unnecessary had the links been proportioned by maintaining a more uniform value for α throughout the EBF height (Section 2). Similar conclusions can be reached for dynamic loading cases, as will be noted below.

4 EBF DESIGN FOR DYNAMIC ANALYSIS

A variety of EBFs were designed and used in a subsequent inelastic time history analyses. The basic configuration of the frame consisted of a three bay dual system: an MRF with an eccentrically braced interior bay (see Figure 3). The frame was designed to represent a parameter frame in a typical office building in seismic Zone 4 (San Francisco). The outer bays of the frame have a 20 ft (6.1. m) column spacing and the inner bays a 30 ft (9 14 m) column spacing. All links were designed as shear links and had a length of 30 in. (762 mm). The height h of the first floor was 15 ft (4.57 m) with all remaining floors 12 ft (3.66 m) high. To study the effect of the building height, EBFs of 4, 6, 10, and 20 stories were designed and analyzed.

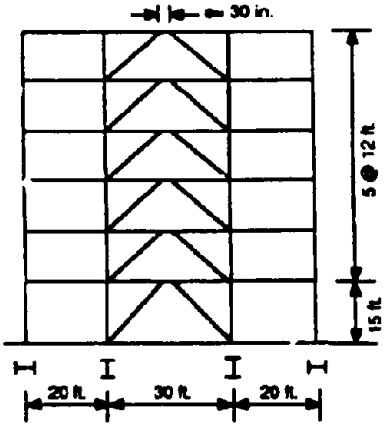

Figure 3. EBF configuration for inelastic time history analysis (6 story EBF shown, 1 ft = 0.305 m, 1 in. = 25.4 mm).

The design of the EBFs was based on the base shear force V_{base} prescribed for a dual EBF system per NEHRP [1988]. V_{base} is plotted as a function of elastic period in Figure 4.

To assess the effect of the distribution of story shear V_{story}, two sets of EBFs were designed and analyzed (Sets A and B). EBFs in Set A included Frames 4A, 6A, 10A, and 20A. The EBFs in Set A were designed for a story shear based on a distribution of V_{base} using the equivalent lateral load distribution per NEHRP, where for floor i the lateral load F_{xi} is:

$$F_{xi} = V_{base} \frac{(w_i h_{xi})^k}{\sum_{i=1}^{n} w_i h_{xi}} \qquad (3)$$

where w_i, h_{xi}, and k are floor weight, height of floor above ground, and a coefficient that varies from 1.0 to 2.0 as a function of frame height, respectively.

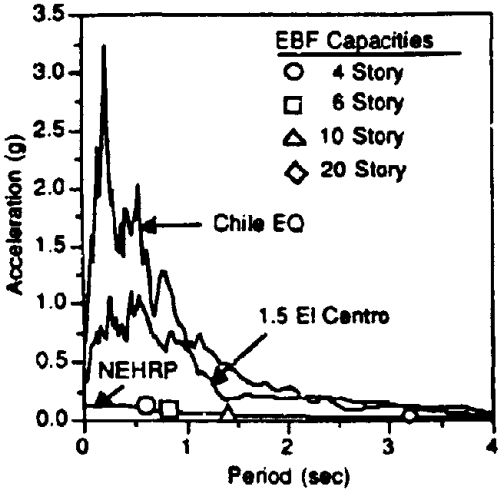

Figure 4. Spectral acceleration corresponding to earthquakes records, NEHRP, and EBFs' base shear.

The second set of EBFs, Set B, was designed using the CQC method [A.Der Kiureghian, 1981], accounting for 90% of the effective modal mass, to generate the story design shears. EBFs belonging to Set B included Frames 4B, 6B, 10B, and 20B. The values for V_{story} for EBFs of both sets are shown in Figure 5, where the nominal story shear capacity based on the nominal link capacity V_p for EBFs in Sets A and B are also given, and calculated by:

$$V_{p,\,story} = \frac{L}{h} V_{p,\,link} \qquad (4)$$

As shown in Figure 5, the EBFs in Set A were designed with a greater link overstrength, and not as uniform a distribution of α throughout the frame as those EBFs in Set B. For the design of EBFs in Set B, emphasis was placed on achieving as uniform a value for α as possible. In the 4, 6, and 10 story EBFs of Set B this was achieved by using fictitious links in the model of the frames whose strengths gave a constant value of α =1.25 at each floor level. In the 20 story EBF, available W-Shape sections were used for the links in the model of the frame. A further examination of V_{story} in Figure 5 based on the static and CQC distributions, respectively, of V_{base} indicates that for the shorter EBFs (particularly the 4 and 6 story) the two distributions are nearly identical. As the frame height increases, a larger discrepancy develops between the two distributions, where the CQC prescribes larger shears in the upper

floors near the roof and smaller shears in the middle and lower floors compared to the static based distribution.

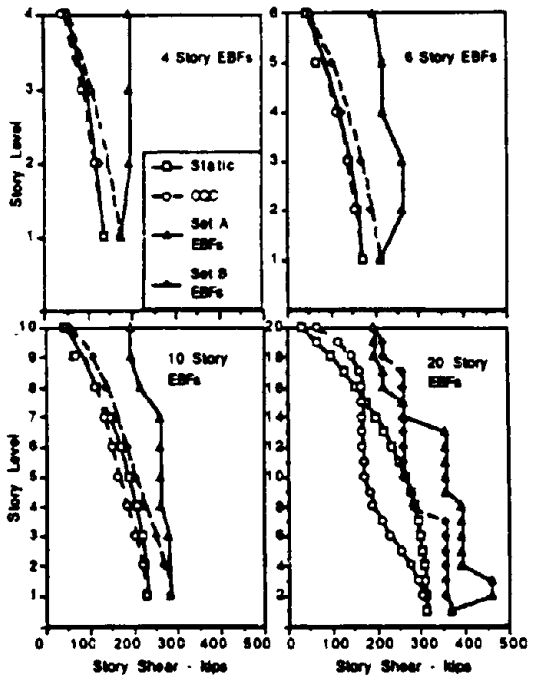

Figure 5. Required and Supplied Story Shear Distributions.

Two earthquake records were used for the inelastic time history analyses. These included the NS component of the 1940 El Centro earthquake, scaled to 0.5 g maximum ground acceleration, and the N10E component of the 1985 Chile earthquake. The latter had a maximum ground acceleration of 0.67 g. The El Centro accelerogram was selected for its common use in other studies and the cyclic yielding caused by the scaled record, whereas the Chile earthquake was used because of the high frequency content in the record and its long duration. The response spectra for these two earthquakes are shown in Figure 4, where they are seen to exceed the NEHRP design base shear and EBFs' strength. Thus, major inelastic response and ductility demand is expected in the time history analysis. The time history analysis was performed using the ANSR-I program [Mondkar, 1975], where the links were modelled by a specially developed link element for random cyclic inelastic loading [Ricles et al., 1987].

5 DYNAMIC ANALYSIS RESULTS

5.1 4-Story EBFs

Figure 6 illustrates the distribution of peak link inelastic deformation, γ_{max}, of Frames 4A and 4B subjected to scaled El Centro earthquake (see Figure 6(a)) and the Chile earthquake (see Figure 6(b)). For both earthquakes, Frame 4A, having a significantly larger α at the upper story levels, developed a soft story mechanism in the lower story levels where a large concentration of γ_{max} developed. In contrast, Frame 4B, having a more uniform α developed a much more uniform distribution of γ_{max} throughout the height of the EBF.

Research has shown that the "relative link deformation" γ_{rel} measured as the sum of the absolute values of positive and negative γ_{max} is a key parameter to measure the ductility demand on the links. It was found that a well-stiffened link can sustain a γ_{rel} up to 0.18 radians [Kasai et al., 1986b]. In Frame 4A, γ_{rel} at the first floor level is 0.20 radians, exceeding the acceptable limit under the scaled El Centro earthquake. In Frame 4B, γ_{rel} at all story levels are well within the acceptable limit for link deformation under both earthquakes.

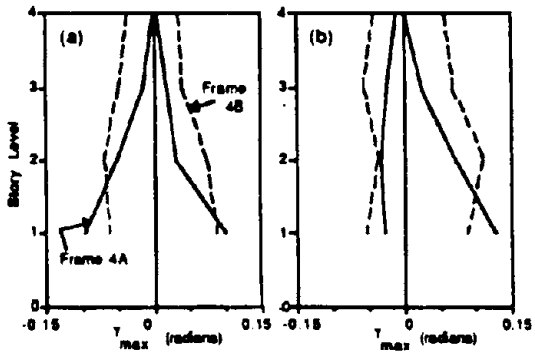

Figure 6. Link Deformation for 4-Story EBFs subjected to (a) 1.5 El Centro and (b) Chile earthquakes.

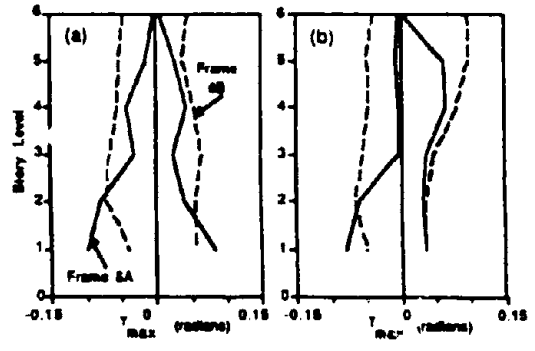

Figure 7. Link Deformation for 6-Story EBFs subjected to (a) 1.5 El Centro and (b) Chile earthquakes.

5.2 6-Story EBFs

Figure 7 illustrates the distribution of γ_{max} for Frames 6A and 6B subjected to the two named earthquakes. Like Frame 4A discussed above, Frame 6A, having a large value for α at the upper story levels, developed a

soft story mechanism with a large γ_{max} concentrated at the lower story levels. In contrast, Frame 6B indicates a much more uniform distribution of γ_{max} throughout the height of the EBF.

In Frame 6A γ_{rel} at the first floor level slightly exceeded the acceptable limit under the scaled El Centro earthquake. In Frame 6B, γ_{rel} at all story levels are well within the acceptable limits under both earthquakes.

Note that γ_{rel} at the first floor level of Frame 6B is 52% of that in Frame 6A under the scaled El Centro earthquake, and 71% under the Chile earthquake. This indicates a considerable reduction of the link deformation demand at the lower level by maintaining a more uniform value for α throughout the height of the EBF.

5.3 10-Story EBFs

Figure 8 illustrates the distribution of γ_{max} for Frames 10A and 10B subjected to the two earthquakes. In both frames, the magnitudes of γ_{max} are generally smaller as compared with the 4-story and 6-story frames discussed above. Unlike Frames 4A and 6A, Frame 10A, having a large α at the upper story levels, did not develop a soft story mechanism at the lower story levels under the scaled El Centro earthquake. It did however develop such a mechanism under the Chile earthquake, but the γ_{rel} at the first floor level was well within the acceptable limit.

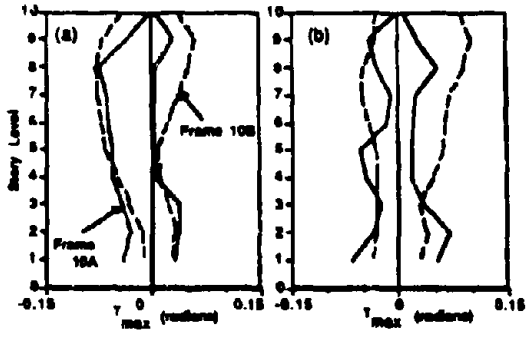

Figure 8. Link Deformation for 10-Story EBFs subjected to (a) 1.5 El Centro and (b) Chile earthquakes.

Like Frames 4B and 6B, Frame 10B, with more uniform values for α throughout the EBF's height, resulted in a considerable reduction of the link deformation demand at the lower level under both earthquakes. Its γ_{rel} at the first floor level is less than 60% of that of the Frame 10A under both earthquakes. It should be noted, however, that Frame 10B developed much larger γ_{max} at the upper story levels as compared with its lower story levels under the two earthquakes. Although the γ_{rel} at the upper levels are still well within the acceptable limit, this suggests the need for further investigation regarding the optimum value for α in order to achieve a uniform γ_{max} throughout the EBF's height. It can be concluded, however, that the EBF with a uniform α throughout its height, as compared with that with larger values of α at the upper story levels, can distribute link inelastic activity well throughout the frame height, thus avoiding excessive inelastic deformation demand at the lower floor levels.

5.4 20-Story EBFs

Figure 9 illustrates the distribution of γ_{max} for Frames 20A and 20B subjected to the two earthquakes. In both frames, the magnitudes of γ_{max} are relatively small at the lower floors compared with the shorter frames discussed earlier.

Frame 20A has links proportioned to the NEHRP static design force by maintaining an approximately constant value for α. Under the simulation of the Chile earthquake, Frame 20A showed an extremely large γ_{max} of -0.2 radians at the 17th story level, and the γ_{rel} exceeded the acceptable limit of 0.18 radians. Similar behavior was observed under the scaled El Centro earthquake, but the magnitudes of γ_{max} were smaller than those under the Chile earthquake. The frame also showed very moderate link deformation below the 13th story level for both earthquakes.

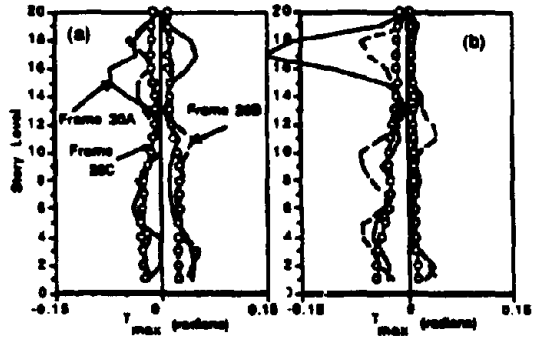

Figure 9. Link Deformation for 20-Story EBFs subjected to (a) 1.5 El Centro and (b) Chile earthquakes.

Frame 20B has the links proportioned to the CQC story shear force, maintaining approximately a constant value for α. Unlike Frame 20A, Frame 20B behaved in an excellent manner showing very moderate and fairly uniform link deformation throughout the frame height under both earthquakes.

The significant difference on performance between Frames 20A and 20B indicates an excessively large γ_{max} at the upper level of tall EBFs that are proportioned to the NEHRP static force. The result also suggests that this problem can be avoided if the CQC story shear force that considers the higher modes of vibration is used for proportioning the links. Although the links in Frame 20A have fairly uniform overstrength with respect to a V_{link} calculated from the NEHRP static force, there is a significant non-uniform distribution of overstrength of Frame 20A's link capacity compared to V_{link} based on the CQC story shear forces. The strength index α for this frame is significantly lower at the 1st, 16th, and 17th levels compared with the other floor levels. This is why a large γ_{max} developed in the vicinity of the 17th story of Frame 20A.

Figure 9 additionally shows the link deformation in a tied EBF, namely Frame 20C, explained earlier in Section 3.2. The purpose for the use of ties is to distribute link inelastic deformation uniformly throughout the EBF story height. As expected, Frame 20C exhibited fairly uniform γ_{max}, but the EBF's performance is no superior to that of Frame 20B. This indicates that even without ties the EBF can be designed to have well distributed link inelastic action throughout the frame height. Other studies by the authors [Ricles et al., 1991], however, indicate some performance advantages in using relatively short tied EBFs.

6 CONCLUSIONS

The following conclusions are given:

(1) An EBF design that typically overstrengthens the links at higher story levels results in a concentration of link deformation at the lower levels, developing large story drift at these floors leading to soft story mechanism.

(2) If the links are proportioned closely to the required link shear force using current static code design forces, an EBF up to 10 stories in height develops inelastic link deformation that is distributed reasonably well throughout the frame height during earthquakes.

(3) If elastic dynamic vibration modes are considered to calibrate the static design force, seismic inelastic performance of taller EBFs can be further improved. The key is to include the contribution of second and third modes of vibration in determining the static story shear design forces.

(4) Link deformation demand on taller EBFs is generally less compared to that of shorter EBFs.

(5) It was observed in this study that the effect of very severe earthquakes on column axial forces in 4 and 6 story EBFs exceeded the commonly specified magnification factor of 1.25 [AISC, 1992]. It was smaller for the higher frames [Ricles et al., 1991].

Short links, a preferred type, were used in the EBF designs. The design can be modified if longer links are needed. These analyses pertain only to seismic loading. In the event that wind loading governs the design, it is still necessary to check the link size for compliance with seismic requirements. It is clear from this study that an EBF having unnecessarily large links at the higher floor levels develops very small link energy dissipation at these levels. Considering this, and since larger links require more expensive detailing as well as large braces and columns, such EBFs are uneconomical. Undoubtedly, the EBF having links of uniform α throughout the height of the structure is a more economical solution.

REFERENCES

AISC Seismic Provisions for Structural Steel Buildings-LRFD and ASD. 1992. *American Institute of Steel Construction*, Chicago.

Der Kiureghian, A. 1981. "A Response Spectrum Method for Random Vibration Analysis of MDF Systems," *Earthq. Eng. and Str. Dynamics*, Vol. 9, pp. 419-435.

Kasai, K., and E.P. Popov. 1986a. "A Study of Seismically Resistant EBFs," *EERC Report No. 86-01*, Earthq. Eng. Res. Center, U. of Calif. Berkeley.

Kasai, K., and E.P. Popov. 1986b. "General Behavior of WF Steel Shear Link Beams," *J. of Str. Eng.*, ASCE, Vol. 112, No. 2.

Kasai, K., and E.P. Popov. 1986c. "Cyclic Web Buckling Control for Shear Link Beams," *J. of Str. Eng.*, ASCE, Vol. 112, No. 3.

Martini , K. et al. 1990. "The Potential Role of Non-linear Analysis in the Seismic Design of Building Structures," *Proc.*, 4th U.S. Nat. Conf. on Earthq. Eng., May, Palm Springs, California, Vol. 2.

Mondkar, D.P.,. and G.H. Powell. 1975. "ANSR-I General Purpose Computer Program for Analysis of Non-linear Structural Response," *EERC Report No. 75-37*, Earthq. Eng. Res. Center, U. of Calif., Berkeley.

National Earthquake Hazards Reduction Program (NEHRP). 1988. " Recommended Provisions for the Development of Seismic Regulations for New Buildings", Building Seismic Safety Council, Washington, D.C.

Popov, E.P., M.D. Engelhardt, and J.M. Ricles. 1989. "Eccentrically Braced Frames: U.S. Practice," *AISC Engineering Journal*, 2nd Quarter 1989, Vol. 26, No. 2.

Ricles,J.M.,. and E.P. Popov. 1987. "Dynamic Analysis of Seismically Resistant Eccentrically Braced Frames," *EERC Report No. 87-07*, Earthq. Eng. Res. Center, U. of Calif., Berkeley, CA.

Ricles, J.M., and S.M. Bolin. 1990. "Energy Dissipation in Eccentricity Braced Frames," *Proc.*, 4th U.S. Nat. Conf. on Earthq. Eng., May, Palm Springs, CA, Vol. 2

Ricles, J.M., and S. Bolin. 1991. "Seismic Performance of Eccentrically Braced Steel Frames,"*Report No. SSRP-91/09*, Str. Sys. Res. Project, Dept. of AMES, U. of Calif., San Diego, December.

Roeder,C.W., D.A. Foutch, and S.C. Goel. 1987. "Seismic Testing of Full-Scale Steel Building - Part 2," *J. of Str. Eng.*, ASCE, Vol. 113, No. 11.

ACKNOWLEDGEMENTS

The authors are grateful for the support by the National Science Foundation and American Institute of Steel Construction of the research program on EBFs over a number of years. The continued encouragement of Dr. S.C. Liu, Dr. Ken Chong, and Dr. Henry Lagorio of the NSF is particularly appreciated. Appreciation is also extended to graduate research assistants Scott Bolin (University of California) and Ashish Goyal (Illinois Institute of Technology) for their contributions. The opinions expressed in this paper are those of the writers and do not necessarily reflect the views of the sponsors.

Behavior and retrofit of bridge outrigger beams

C.R.Thewalt & B.I.Stojadinović
University of California, Berkeley, Calif., USA

ABSTRACT: Many older elevated freeways in California were designed considering lateral seismic loads, but the effects of longitudinal bridge response were in some respects ignored. Consideration of longitudinal response has a significant impact on outrigger beams, which are used when columns cannot be located directly beneath the superstructure. These outrigger beams were designed for shears and flexure resulting from gravity and lateral loads. However, longitudinal bridge excitation introduces biaxial flexure and shear as well as torsion into these members. In addition to problems carrying torsion, the outrigger-column joint connection is often poorly detailed. In this experimental study, three half scale specimens are used to investigate the as-built behavior of the outrigger beam and joint as well as the behavior of two retrofit schemes.

1 INTRODUCTION

Although not a common feature in building structures, outrigger beams and knee joints are fairly common in bridges. In many cases the columns of bridges are offset from the deck, resulting in an outrigger configuration. During seismic excitation, the outrigger must resist flexure from gravity and lateral loads, as well as torsion and flexure due to longitudinal excitation of the bridge. The bent cap details, even in older structures, were capable of some ductility under flexure from lateral loads, but the older torsional details were not ductile. The outrigger-column joints in older bridges typically contain no transverse steel and are unlikely to sustain the complex loads from cyclic bidirectional excitation. In fact, small scale tests (Mazzoni et al 1991) indicate that even the current ACI (1989) provisions may be unconservative for knee joints. For these reasons, an experimental investigation of the complex interaction between the forces on the beam and the joint has been performed.

In this project, the bent cap and joint are investigated under combined loads from gravity, lateral, longitudinal motion of the bridge. These loads induce torsion and biaxial flexure and shear in the cap. A representative outrigger bent was selected from the southern freeway at the Interstate 101/280 interchange in San Francisco. The bent had an outrigger length to depth ratio of two, which was long enough to develop extended torsional cracks while being short enough to be experimentally convenient.

2 EXPERIMENTAL PROGRAM

A series of three half scale models of the selected specimen have been tested. The experiments were performed with the specimen inverted, as shown in Figure 1. In each of the models the amount of transverse steel in the columns was doubled from the actual amount, since the column behavior was not the focus of these tests and a shear failure of the column was undesirable during the retrofit tests. The heavy block that is stressed to the laboratory floor represents the deck. At the top of the specimen, the base of the column, there are two actuators to apply independent longitudinal and lateral displacements. There are two additional actuators which apply vertical loads, that vary during the test to account for

the effects of gravity and framing action under lateral displacement.

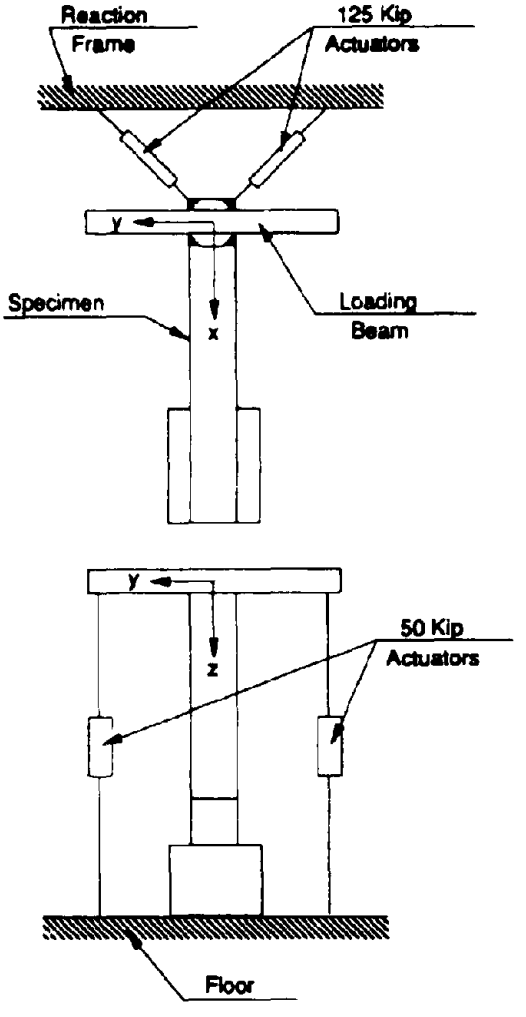

Figure 1: Test Specimen and Loading System

The first specimen represents the as-built condition, typical of 1950's construction in California. The as-built specimen had outrigger stirrups composed of two overlapping U's capped by a tie with two 90 degree hooks. The as-built specimen is shown in the unshaded portion of Figure 2. The cap strength data using ACI (1989) estimates with no interaction is shown in Table 1, and as expected from the open stirrup arrangement the torsional strength after cracking is less than the gross section strength. The column moment capacity was 860 kip-ft in both X and Y directions.

Table 1: Outrigger Beam Capacity

Flexural Capacity (joint closing)	490 kip-foot
Flexural Capacity (joint opening)	920 kip-foot
Torsional Capacity (cracking)	290 kip-foot
Torsional Capacity (nominal)	170 kip-foot

The second specimen is a concrete retrofit of the outrigger beam and joint area. The goal in the retrofit design was to enhance ductility without dramatically increasing capacity. The torsional strength was increased to be about double the cracking capacity. The outrigger retrofit consisted of closed stirrups running above the existing top and bottom beam steel and through added side bolsters. Longitudinal steel was added in the bolsters to increase torsional strength, although the torsional capacity was explicitly designed to be below the load that would cause longitudinal hinging in the column. The joint area was confined by horizontal hoops and external vertical ties.

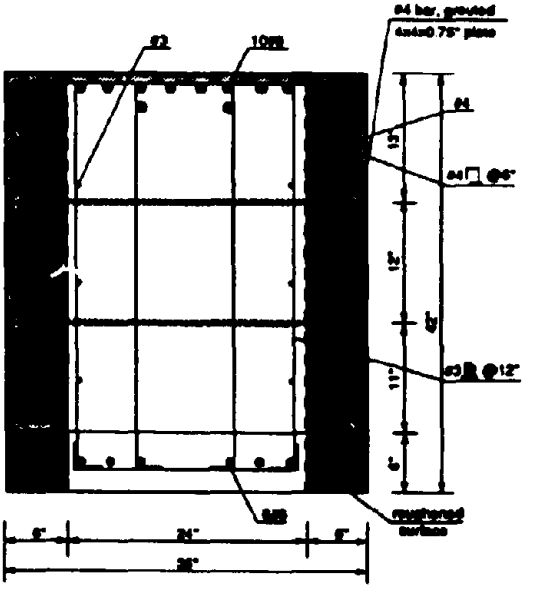

Figure 2: Concrete Retrofit Details

The final retrofit specimen consisted of a half inch thick steel plate jacket around the outrigger and joint, as shown in Figure 3. The plate thickness was selected to be larger than that needed for strength in order to provide adequate confinement between the cross-tie support plates. Additional stiffeners were

added to the outside of the plate in the joint area where compression strut reactions were expected. The steel plates were placed around the specimen and welded at the seams, and high strength half inch diameter steel bolts were used as crossties. The bolts were preloaded with a 15 kip axial load as recommended by AISC (1986). After the bolts were loaded, the space between the old concrete surface and the inside of the plate was injected with high strength epoxy.

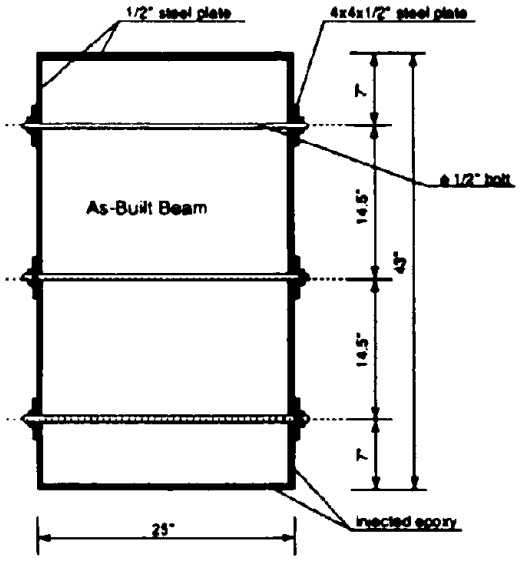

Figure 3: Steel Retrofit Details

Additional specimens are planned to investigate torsion transfer for short outrigger systems, and to test several identical systems under transverse motion only, longitudinal motion only, and combined transverse-longitudinal motion in order to study interaction effects.

The loading history for the specimens is shown in Figure 4. It is a cloverleaf displacement history, with two quadrants applying initial lateral displacements and the other two quadrants applying initial longitudinal displacements. The axial load in the column was forty-five kips plus one half of the applied lateral load. The component proportional to lateral load accounts for the change in axial load due to the lateral response of the frame. The specimen's yield displacement in the longitudinal direction is about 1.5 inches, while in the lateral direction it is 1.0 inch. The initial plan was to use a rectangular cloverleaf representing equal ductility loops, but preliminary analysis showed that the actual ratio of longitudinal to lateral displacements was sensitive to bridge length and abutment conditions, and the longitudinal response could be larger or smaller than the lateral. Since there was no rational reason to impose displacements based on the yield displacements, it was decided to use square loops. The test sequence consists of two complete loops at each displacement level, with a displacement sequence of 0.25 inch, 0.5 inch, 1.0 inch, 2.0 inch, etc., increasing to failure.

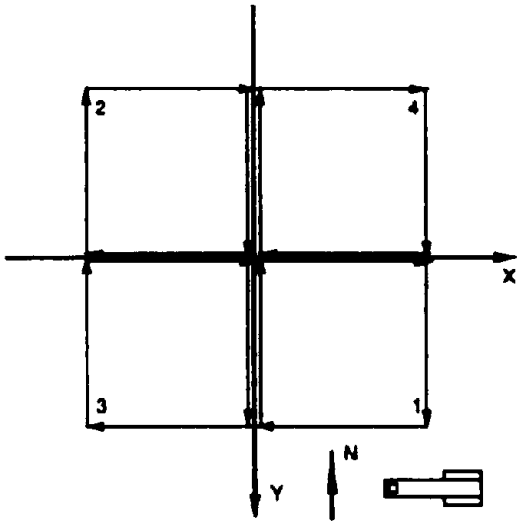

Figure 4: Applied Displacement Pattern

The instrumentation on the specimens includes strain gauges at a variety of locations, as well as potentiometers distributed over the length of the beam to measure the curvature and torsional rotation distribution. The joint was instrumented on two faces to measure axial and shearing deformations.

3 RESULTS

3.1 As-Built Specimen

During the test, response remained fairly linear up to the 1 inch loading level, but significant torsional cracks began to occur at this level. Interestingly, an X pattern of torsional cracks never developed, since the shears produced from gravity and torsion tended to reinforce each other on one side of the beam and

cancel on the other. The effect produced diagonal cracks from the interior of the joint across the beam. This was consistent with observations after the Loma Prieta earthquake.

At increasing displacements, the torsional cracks continued to open on each cycle, but failure occurred within the joint during a joint closing motion. The column bars at the outer face of the joint eventually peeled away from the joint, and the concrete in front of the hooked beam bars at the outer corner of the joint crushed. These effects limited the force that could be developed in the outer bars of the column and beam.

The response during closing action consisted of increasing moment and fairly constant stiffness up until the second half of the first two inch loop. After this point the joint suffered severe damage as described above. It can be seen from the hysteresis loops that the final closing moment was only one sixth of the maximum achieved. The opening moments were more stable, increasing up through the four inch cycle, although there was marked stiffness degradation in the final cycle.

The torsional capacity increased up through the four inch cycle, but the stiffness decreased with each cycle after one inch was reached. The premature joint failure during closing limited the forces that could be transferred from the column through the joint, so extended torsional testing was impossible. Since one of the primary interests of the as-built test was to investigate the torsional behavior of the beam, the joint was repaired so that the test could continue to beam failure. The repair consisted of the removal of the joint concrete and the addition of vertical and horizontal steel in the joint, with additional crossties across the joint to prevent the lateral spreading that was observed during the test. This repair was more conservative than either current ACI (1989) provisions or the ACI-ASCE Committee 352 (1985) provisions, in that both horizontal and vertical shear steel was added in the joint. The goal was to prevent further joint damage and examine the outrigger behavior.

The flexural behavior of the as-built and repaired specimen are shown in Figure 5. It is clear that the joint repair greatly enhanced the flexural capacity of the system. The torsional response of the system is shown in Figure 6. The large diagonal crack in the beam was not repaired when the joint was repaired, so the torsional capacity did not increase. The diagonal crack continued to open on each cycle and ultimately when the gap was wide enough to lose aggregate interlock the stirrups broke in rapid succession and the specimen broke in two.

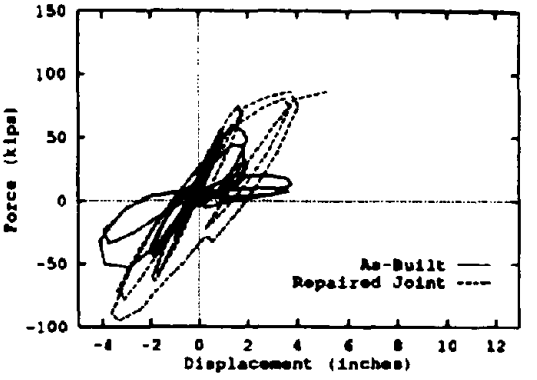

Figure 5: Transverse Response at Top of Column

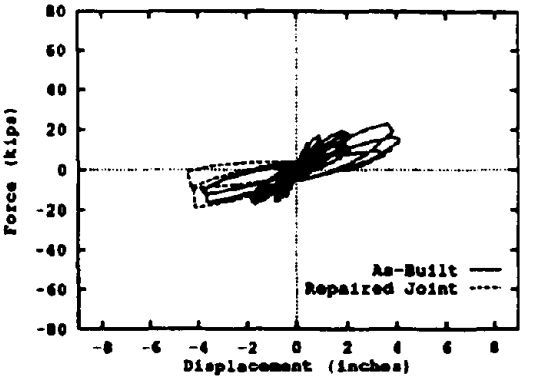

Figure 6: Longitudinal Response at Top of Column

3.2 Concrete Retrofit

The specimen with the concrete retrofit performed well throughout the testing sequence. In fact it never failed, and the test was terminated because the hydraulic actuators had reached their stroke limit.

The flexural capacity was stable through the 8 inch cycles, as shown in Figure 7. The maximum joint closing displacement of around 12 inches represents a ten percent drift. The joint retrofit also performed well, with only minor cracks forming in the joint region throughout the test.

The torsional response, shown in Figure 8, was not as stable and decreased with increasing displacement as the outrigger became more cracked. Unlike the as-built specimen, which concentrated damage along a single inclined crack, the cracks in the concrete retrofit specimen were well distributed throughout the cap beam. The side bolsters began to shift relative to the as-built beam during the four inch loops and by the eight inch loops significant relative displacements were present and the bolsters had separated from the beam at the bottom of the specimen. The behavior would have been enhanced if the new closed stirrups were positioned below the bottom steel but the location shown in Figure 2 was mandated by the research sponsor.

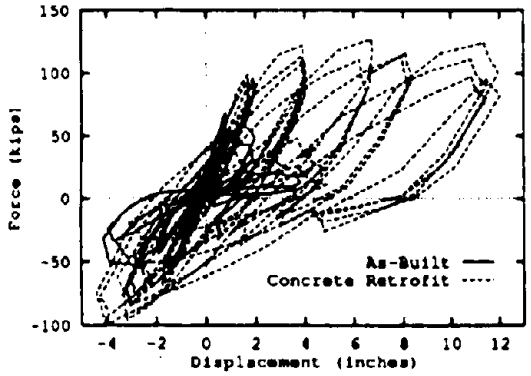

Figure 7: Transverse Response at Top of Column

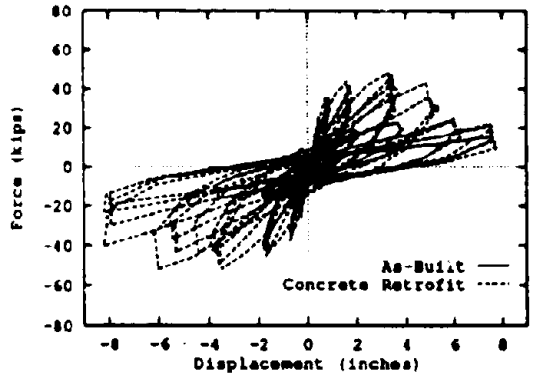

Figure 8: Longitudinal Response at Top of Column

3.3 Steel Retrofit

The steel specimen behavior was quite different than the concrete, in that the relative strengths of the system components were now drastically different. The addition of the half inch thick plate made the entire outrigger extremely strong and rigid relative to the column. Before the test there was some concern that it would be hard to estimate the extent of damage within the concrete under the plates, but the column essentially acted as a fuse, limiting the amount of force that was transmitted into the system.

As the test progressed the base of the column near the outrigger sustained increasing damage. Concrete began to spall at the two inch cycle, and by the four inch cycle significant column bar buckling was already evident near the column base. The column hinged under both transverse and longitudinal loads.

The transfer of torsion from the jacketed beam to the support block worked well, but flexural problems were imminent in the beam's weak direction at the point of attachment to the support block. Had the column been stronger in the longitudinal direction there would have been extensive bar yielding at the outrigger/block interface. Thus, enhancing the column capacity or confinement in the hinge region would not have resulted in a better system.

As can be seen in Figure 9, the flexural response of the system was already decreasing by the second six inch cycle. The torsional response shown in Figure 10 appears to dissipate more energy than the loops for the concrete retrofit. This is because the dissipation in the steel specimen is emanates from the column hinging flexurally. The test was terminated after the six inch cycles because of extensive damage at the base of the column.

4 CONCLUSIONS

The as-built test clearly demonstrated that the outrigger system was deficient in two key areas. First, the essentially unreinforced joint was incapable of developing the strengths of the connected column and beam, especially under cyclic loads. The second problem was that with a repaired joint the outrigger becomes the weak link susceptible to brittle shear failure. The nature of the joint failure, including crushing in front of the lower beam steel hooks and peeling off of the straight column bars influenced

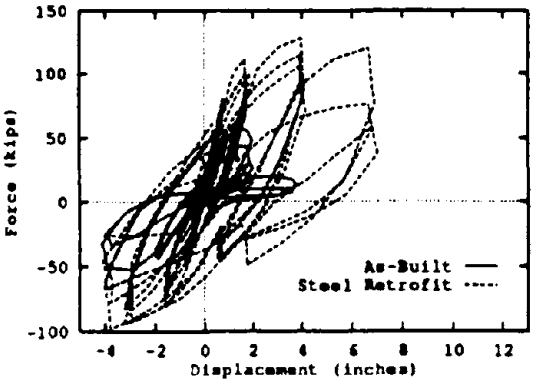

Figure 9: Transverse Response at Top of Column

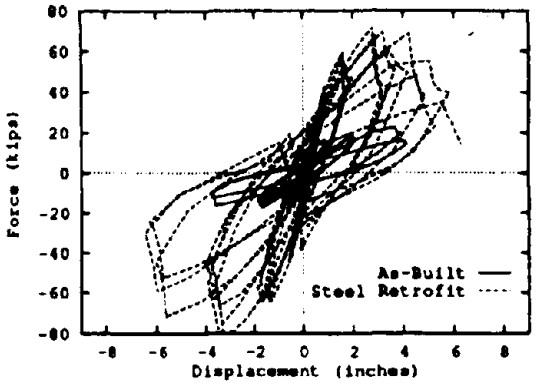

Figure 10: Longitudinal Response at Top of Column

the joint retrofit design.

The concrete retrofit was well behaved, allowing a ten percent lateral drift in the joint closing direction with no noticeable loss in flexural capacity. The torsional retrofit in the outrigger worked well. Its design level of approximately twice the cracking torsional capacity was also well chosen in that it limited the maximum longitudinal load that could be taken by the specimen. The longitudinal load must be controlled to avoid flexural failure in the weak direction of the outrigger beam at the point of attachment to the deck. The joint retrofit, consisting primarily of steel and concrete external to the original joint, performed well, transferring the full loads needed to fail the cap and column.

The steel retrofit certainly limited damage to the cap beam and joint area, but the drift capacity of the system was dramatically reduced because all damage was now forced to the base of the column, for both lateral and longitudinal loads. Simply detailing the plastic hinge region in the column to retain capacity through a larger rotation would have forced the failure to the cap/deck interface through flexure in the weak beam direction, since there was already evidence of bar yielding at this location under the reduced load levels.

The development of a retrofit strategy to achieve desired displacement levels while maintaining loads requires careful consideration of the complete system. It was found that simply strengthening the weak link was not the best thing to do, one must not overload the next weakest link in an undesirable fashion.

5 ACKNOWLEDGEMENTS

The authors would like to thank the Karl Kardel Company of Oakland California who graciously contributed their time and equipment to inject the epoxy into the steel specimen.

REFERENCES

ACI-ASCE Committee 352 1985. "Recommendations for design of beam-column joints in monolithic reinforced concrete structures." *ACI Journal*, 82(23):266-283, May-June.

ACI Committee 318 1989. "Building code requirements for reinforced concrete." ACI 318-89, American Concrete Institute, Detroit.

American Institute of Steel Construction 1986. "Manual of steel construction - load & resistance factor design." First Edition, AISC.

Mazzoni, S., Moehle, J., and Thewalt, C. 1991. "Cyclic response of RC beam-column knee joints: Test and retrofit." UCB/EERC-91/14, University of California, Berkeley, Earthquake Engineering Research Center.

Optimal design of seismic isolation for multistoried buildings

F.L. Zhou
Guangzhou Urban Construction Institute, People's Republic of China
J.M. Kelly
University of California, Berkeley, Calif., USA
K.N.G. Fuller
Tun Abdul Razak Laboratory, Hertford, UK
T.C. Pan
Nanyang Technological University, Singapore

ABSTRACT: This paper suggests the method of quantitative controlling of structural response for earthquake resistant structures with base isolation and energy dissipation system. This method is based on dynamic analysis, shaking table tests for a 1/4 scale steel frame model, and a great number of low cycle fatigue failure tests for energy dissipating elements The comparing theoretical results with testing results was described. A set of calculation formulas for quantitative controlling of structural response of the structures with base isolation and energy dissipation system were derived , and are able to be used in engineering design for earthquake resistant structures.

1 DEVELOPMENT OF CONTROLLING METHOD FOR SEISMIC RESPONSE OF BUILDING STRUCTURE

During earthquake attack, the building structure which fixed on the ground will respond gradually increasing from the building bottom (ground) to the building top liking a "Amplifier" (Figure 1). This will result in damage of structure or building contents due to the large response of structure. In order to reduce the response and avoid the damage of structure, some controlling methods have been developed by Kelly (1986).

1. Increasing the structural stiffness very more, form a " Rigid Structure System "(Figure 2) which structural response may be nearly as same as the ground motion. But this kind of structure system is very expensive and very difficult to realize in some cases.

2. Decreasing the structural stiffness to very small, form a " Flexible Structure System" (Figure 3) which structural response may be very small. But this kind of structure system is not suitable for normal usefulness because it is too flexible in wind load or minor earthquake.

3. Increasing the structural ductility and allowing the structural elements or joins to work in inelastic range to dissipate the energy of structure in earthquake, then reduce the structure response, form a "Inelastic Structure System " (Figure 4), it is the general structure system for earthquake resistance in many countries at present. But its usefulness is limited or not very safe in some cases. First, it is difficult to control the structural damage level due to the inelasticdeformation, and it may be dangerous in severe earthquake which is not predicted before. Second, it is not able to be used in some important structures which elements is not allowed to work in inelastic range, such as some buildings which decoration is very expensive nuclear power plant, museum building, and so on. Third, it is not able to be usedfor some buildings there are precise instruments in it.

4. Making the first story columns very soft and allowing it to deform in inelastic range to dissipate the energy then reduce the response of upper structure, form a "Soft First Story Structure System "(Figure 5) . This system can reduce the upper structure response very effectively, but the building may collapse in severe earthquake because of the large inelastic deformation of first story columns.

The controlling methods described above for seismic response are not very perfect. The " Base Isolation System "(Figure 6) supplies a new method to control the seismic response of building structure and it is very effective, safe, simple and can be used in very wide range. This new method possesses following advantages ,

1. It can reduce the structure response very effectively by keeping the advanteges of " Soft First Story Structure System " , but it changes from the soft first story columns into only a isolation sliding layer. The effect of torsional coupling on the transient response of base isolated structures is insignificant depending on Pan (1981). So it is more effective and safe.

2. It changes from relying the whole

structure to resist the earthquake into only relying the isolating device to isolate the earthquake. So it make the design and construction work very simple and the restore work is very easy.

3. It can keep the structure working in elastic range in earthquake, so it can be used in different kinds of important buildings in different seismic zones.

4. It can be used in new buildings, also can be used in existing buildings to improve its earthquake resistant ability.

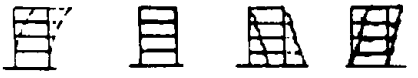

Figure 1 Structural "Amplifier"

Figure 2 Rigid Structure

Figure 3 Flexible Structure

Figure 4 Inelastic Structure

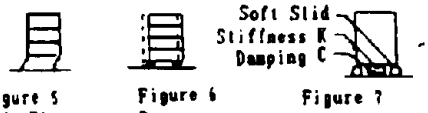

Figure 5 Soft-First Story Structure

Figure 6 Base Isolation

Figure 7 Characters of Base Isolation

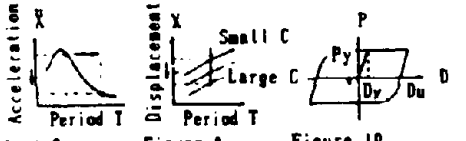

Figure 8 Acceleration Reduce

Figure 9 Displacement Reduce

Figure 10 Load-Displacement Curve

2 CHARACTERS, COMBINATION OF BASE ISOLATION STRUCTURE SYSTEM AND APPLICATION

In general case, the base isolation device requires to possess three basic characters (Figure 7):

1. Soft sliding : The structure can softly slide on the base in severe earthquake. This character can isolate the horizontal vibration from ground motion to structure, make the natural period of structure very long then reduce the acceleration response of structure effectively (Figure 8).

2. Certain amount of damping C, it will dissipate the energy input to the structure then attenuate the response of structure in earthquake (Figure 9).

3. Suitable horizontal stiffness K, it will provide the primary stiffness in wind load or minor earthquake while P < Py (Figure 10)

There are four kinds of combination of bas isolation and energy dissipation system:

1. Rubber pads (steel plates reinforced) as isolator (Figure 11.a).

2. Rubber pads (steel plates reinforced) as isolator combines with lead plug or steel elements as energy dissipator described by Kelly (1988) (Figure 11.b).

3. Roller as isolator combines with steel elements as energy dissipator described by Chow (zhou) (1983) (Figure 11.c).

4. Dry friction layer or sand (or other material) sliding layer as isolator also energy dissipator (Li (1984)), (Fig.11.d).

There are some kinds of buildings with base isolation for investigetion , One 8 stories RC frame building with Rebber Pads (Figure 12.a,b), two 5 stories masonry buildings with sand sliding layer (Figure 12.c,d).

(a) Rubber Pad (b) Rubber Pad with Lamping or Steel Elements (c) Roller with Steel Elements (d) Friction or Sliding Layer

Fig.11 Combination of Base Isolation and Energy Dissipation

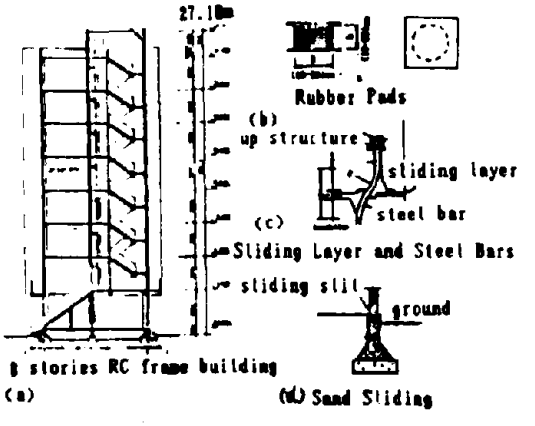

Figure 12 Building with Base Isolation in China

3 SHAKING TABLE TESTS AND ANALYSIS

The tests were carried out on an earthquake shaking table which has a floor dimension of 10ft×10ft in THE UNIVERSITY OF BRITISH COLUMBIA. The overall dimension of four stories steel frame model is 10ft×6. 6ft in plan and 12. 8ft high. The total mass of structure model and loading concrete blocks are 16 kips (Figure 13).

The roller and mild steel curved plates were used as isolating and energy dissipating device . Five kinds of curved plates were fitted and tested in order of priority. A series of pseudo tests were finished for curved plates (Stiemer and Zhou (1984)) before shaking table tests. Four sine-waveforms (Freq. w=1.0, 2.0, 3.0, 4. 0 0Z) and three simulated earthquake records (EL Centro, Sanfernando, Parkfield) were inputted to the shaking table, which predominant Freq. w was found from the Fourier spectra of acceleration record.

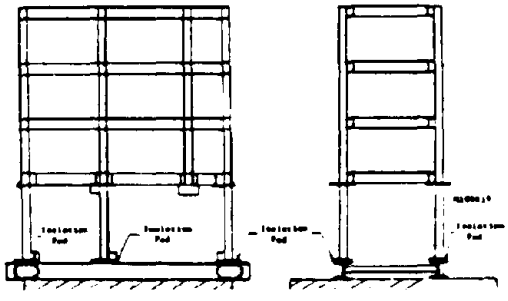

Figure 13 1/4 scale steel frame

The testing results show that :

1. The acceleration responses $\ddot{X}a$ on each stories of structure model are nearly the same. (Figure 14). It means that the elements and joins of structure with base isolation nearly work within elastic rang only.

2. The acceleration response $\ddot{X}a$ on structure with base isolation is only (1/6-1/10) response $\ddot{X}af$ on structure fixed on shaking table. It means the base isolation is more effective to attenuate the structural response in earthquake than any other methods (Figure 14).

3. The acceleration response $\ddot{X}a$ of structure with base isolation depends on the Ratio of exciting frequency W to natural frequency Wn of structural system (W/Wn). In order to attenuate effectively the structure response, it is very important to make both (W and Wn) having more disparity (Figure 15).

4. The relative displacement D between the structure and the shaking table are very close to the displacement $\ddot{X}g$ of shaking table (Figure 16) . It means the horizontal displacement of structure with base isolation are rather large and need to be controlled in design.

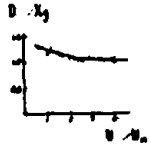

Figure 15 Displacement with (W /Wn)

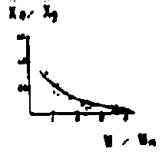

Figure 16 Acceleration Attenuation with (W / Wn)

In order to investigate the effect of base isolating system for highrise building, a 1/15 scale model of 9 stories frame building structure was tested on a shaking table. The isolation device contains the rollers and horizontal spring which provides a certain amount of stiffness and damping of isolating system .Different sine waveforms with frequency W= (1-28) HZ were input to the shaking table, the maximum acceleration of shaking table are $\ddot{X}g$ = (0.2-0.5) g. There are 8 accelerometers used to measure the structural acceleration response $\ddot{X}i$ at each stories of structure model. The testing results for structure model with fixed base and base isolation were recorded and compared. Fig.18 shows the testing records which relates to the shaking table vibration with Freq. W=15. 5 HZ and the maximum acceleration of shaking table $\ddot{X}g$ = 0.49 g.

Analyzing this results (Figure 17), some conclusions can be described below :

1. The acceleration responses at each stories of structure model with base isolation are nearly the same. It means that the elements and joins of structure with base isolation will work within elastic rang during earthquake. The "Amplifier" action resulted from fixed base structure is completely eliminated during severe earthquake.

2. The acceleration response at top story of structure model with base isolation is only 0.885 g, while the acceleration response at the same story with fixed base reaches 1.13 g. The ratio of $\ddot{X}$ (isolation / $\ddot{X}$ (fixed base) = 0.885 g /1.13 g = 1 / 226 . It means the base isolation is so significantly effective to attenuate the structure response for highrise building during severe earthquake.

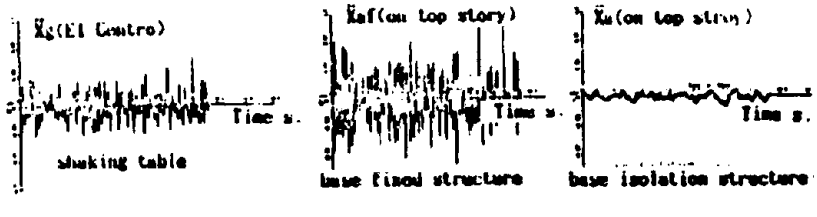

Figure 14 Acceleration response

3. Both theoretical and testing results of acceleration response at each stories in structure model with base isolation are very near, and , the theoretical values are always larger than the testing values. It means the dynamic analysis method for controlling structural response suggested by author for highrise buildings with base isolation system is reasonable and conservative. It may be applied in engineering design.

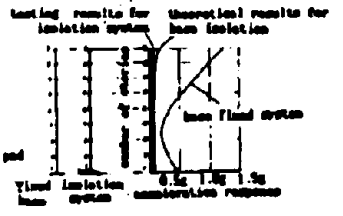

Figure 17 Shaking table with base isolation and base fixed model

4 DYNAMIC ANALYSIS AND CALCULATION FOR ISOLATION AND ENERGY DISSIPATION SYSTEM

4.1 Equivalent damping ratio Ee

From Mathematical model, the basic differential equation of motion is given as;

$$M\ddot{X}a + Ce\dot{X}a + KXa = Ce\dot{X}g + KXg \qquad (1)$$

Where M is the structural mass, Ce is the equivalent viscous damping of isolating and energy dissipating system, K is the elastic stiffness of isolating and energy dissipating system, Xg $\dot{X}g$ $\ddot{X}g$ are the ground response of displacement, velocity and acceleration respectively in earthquake. Xa $\dot{X}a$ $\ddot{X}a$ are the structure response of displacement, velocity and acceleration respectively in earthquake.

Define $Ee=Ce/2MWn$ EQUIVALENT DAMPING RATIO

$Wn=K/M$ NATURAL FREQUENCY of system

Solve Equation (1) with finding transfer function and get ;

$$Ee = \frac{1}{2(W/Wn)}\sqrt{\frac{1-AR^2\,[1-(W/Wn)^2]^2}{AR^2-1}} \qquad (2)$$

Where $AR = \ddot{X}a / \ddot{X}g$ is called ACCELERATION ATTENUATION RATIO of system.

4.2 Maximum relative displacement De

From the basic differential equation of motion can write ;

$$M\ddot{D}u + Ce\dot{D}u + KDu = -M\ddot{X}g$$

Where Du $\dot{D}u$ $\ddot{D}u$ are maximum relative displacement, velocity and acceleration respectively between structure and ground.

Solve this equation with finding transfer function and get ;

$$Du=\frac{Xg}{W^2}\sqrt{\frac{(1-AR^2)(W/Wn)^4}{(W/Wn)^2-2}} = Xg * r \qquad (3)$$

$$\text{Define } r=\sqrt{\frac{(1-AR^2)(W/Wn)^4}{(W/Wn)^2-2}}$$

as DISPLACEMENT FACTOR

Comparing the theoretical value Du with measuring value [Du] from tests show that the $Du / [Du] = 0.98 - 1.67$, Du are almost all greater than [Du]. It means Equation(3) is suitable and conservative in designing.

4.3 Acceleration attenuation ratio AR

The damping ratio Ee is related to the area enclosed by the hysteresis loop and find ;

$$Ee=\frac{Ce}{2MWn} = \frac{2(1-1/U)}{U\Pi}\cdot\frac{1}{(W/Wn)} = B\frac{1}{(W/Wn)} \qquad (4)$$

$$\text{Define } B=\frac{2(1-1/U)}{U\Pi}$$

as ENERGY DISSIPATION DAMPING RATIO

$U = Du/Dy$ as DUCTILITY FACTOR

Where Du and Dy are the relative displacements at utmost point and yield point shown in Figure 18. The Value of B represent the basic of Ee, and depends on the value of U.

Substitute Equation(4) into Equation(2) and finally get ;

$$AR=\frac{\ddot{X}a}{\ddot{X}g}=\sqrt{\frac{1+4B^2}{4B^2+[1-(W/Wn)^2]^2}}\cdot\frac{W}{Wn} \qquad (5)$$

This is the final expression of ACCELERATION ATTENUATION RATIO AR

Now, comparing the theoretical values AR from Equation(5) with the measured values [AR], shown in Figure 18 and know ;

1. The ratio AR/[AR] approaches 1.0, it means that Equation(5) gives reasonable estimation.

2. The theoretical values AR are always larger than measured values [AR], it means that Equation(5) gives conservative results for practical design.

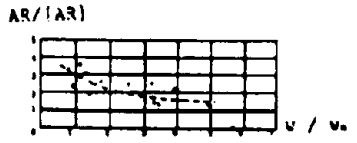

Figure 18 Acceleration Attenuation Ratio AR with (W /Wn)

The isolation and energy dissipation system for highrise building structure can be simplify to a multi degree of f eedom system with isolating pad which is replaced by roller and spring (Figure 19). The stiffness of isolating pad is :

$$K = G A_s / h$$

Where G is the horizontal shear module of isolating pad, As is the area of cross section of isolating pad, h is the height of isolating pad.

For any point i on the structure, the differential equations of motion can be written:

$$Mi\ddot{X}i+\sum_{j=1}^{n}Cij(\dot{X}i-\dot{X}g)+\sum_{j=1}^{n}Kij(Xi-Xg)=0$$

Develop and rearrange the equation above, then get :

$$Mi\ddot{X}i+\sum_{j=1}^{n}Cij\dot{X}i+\sum_{j=1}^{n}Kij Xi=\sum_{j=1}^{n}Cij\dot{X}g+\sum_{j=1}^{n}Kij Xg \qquad (6)$$

Where Mi is the lumped mass at any point i on structure,

$\ddot{X}i$, $\dot{X}i$, Xi are the structural horizontal response of acceleration, velocity and displacement at Mi during earthquake

$\ddot{X}g$, $\dot{X}g$, Xg are the ground horizontal response of acceleration, velocity and displacement during earthquake.

Cij is the damping influence coefficient of point i, the force corresponding to point i due to unit velocity of point j.

Kij is the stiffness influence coefficient of point i, the force corresponding to point i due to unit displacement of point j .

Then the matrix formulation of differential equation for multi degree of freedom system can be written below :

$$[M]\{\ddot{X}\}+[C]\{\dot{X}\}+[K]\{X\}=\dot{X}g[C]\{1\}+Xg[K]\{1\} \qquad (7)$$

That is the Differential Equation of Motion of base isolation system of multi degree freedom for highrise building structures. Where [M] is the mass matrix of system, [C] is the damping matrix of system, [K] is the stiffness matrix of system, $\{\ddot{X}\}$, $\{\dot{X}\}$, $\{X\}$ are the structural horizontal response vectors of acceleration, velocity and displacement of structural system during earthquake, $\dot{X}g$, Xg are the ground horizontal response of velocity and displacement during earthquake, {1} is the unit vector.

Here the characters of structure and isolation devices were decided during design then [M], [C], [K] can be got. And $\dot{X}g$, Xg can be found from the possible maximum spectrum values of ground motion for a certain seismic zone. Solving Equation(6) and (7), the responses $\{\ddot{X}\}$, $\{\dot{X}\}$, $\{X\}$ at any story of highrise building can be controlled to be a suitable level by selecting a reasonable base isolating and energy dissipating device. Authors have compiled a set of computer programs EBIS-1 for design in engineering application.

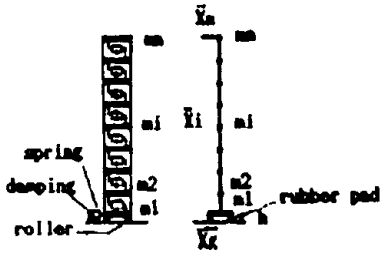

Figure 19

Model of highrise building with base isolation

5 TESTS AND ANALYSTS OF LOW CYCLE FATIGUE FAILURE OF STEEL DISSIPATOR

Because the steel elements were used as energy dissipater, these may deform into plastic regions withstanding large number of cyclic loads, and may fail due to the low cyclic fatigue in earthquake. The permanence of resisting low cycle fatigue failure can be represented by a parameter --Number of loading cycles to fail N. Many works indicate that N mainly depends on the absolute maximum strain value ε on the surface of mild steel elements in cyclic loads (Zhou (1987)). So, the relationship between ε and N is the key to predict the low cycle fatigue failure for mild steel elements.

In order to get the accurate results, a series of X - shaped plates made of mild steel were chosen as main specimens to be tested, because the vertical strain of section is nearly uniformly distributed during horizontal bending under horizontal loads at top or bottom of specimen (Figure 20)

There are 36 pieces of X-shaped mild steel plates with different thickness t and length L cyclically loaded to fail under certain strain ε on surface. The tests were carried out on the " MTS Model 904. 55 Structure Testing System ". Tests were displacement controlled. The loading cyclic frequency is 0.1 HZ. The number of loading cycles to fail N was recorded by recorder automatically. The strain ε was measured at 4 pieces of strain gauges placed on each

side of the X-shaped plate. The testing results of values ε and N were plotted in Figure 21.

From statistic analysis, A theoretical curve (Figure 21) to represent the relationship between ε and N was expressed by equation :

$$\varepsilon = 0.22 / N \qquad (8)$$

Where ε -- The maximum strain on surface of steel elements.
N -- The number of loading cycles to fail

The results of tests and analysis indicate :

1. The theoretical curve is very close to the testing records, especially in the strain range ε = (0.5 - 3.0)% which covers the general cases. The theoretical N values from theoretical curve are always smaller than the testing values. It means the appropriate conservative results can be got from Equation(8) for design.

2. The ability of resisting low cycle fatigue failure for mild steel elements under bending is very great. If yielding strain for mild steel is ε = 0.15%, while maximum strain ε on surface of elements in earthquake is about ε = 1.5 %(equivalently ductile factor U = 10 about), then the allowed number of cyclic loading N reaches more 200 from Equation(8). It means this energy dissipator can reliably withstand tens of severe earthquake attack continuously.

3. The designer can use Equation(8) to predict the permanence of resisting low cycle fatigue failure by controlling the strain value ε on the surface of steel elements very simply.

6 CONCLUSION

1. This base isolation and energy dissipation system is a very hopeful way for controlling structure response in earthquake It is more effective, reasonable and simple than other traditional way used at present.

2. The ability of resisting low cycle fatigue failure for mild steel elements under bending is very great. Using mild steel elements as energy dissipator is reliable.

3. A series of calculating formulas for controlling the structure response and low cycle fatigue failure in base isolation and energy dissipation system derived by authors in this paper have been proofed by a great number of tests. The reasonable and conservative results can be got from these formulas and can be used in engineering design.

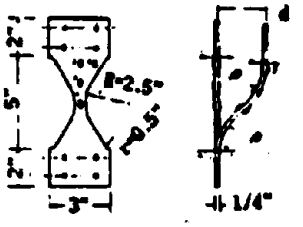

Figure 20 Strain gauges on X shaped plate

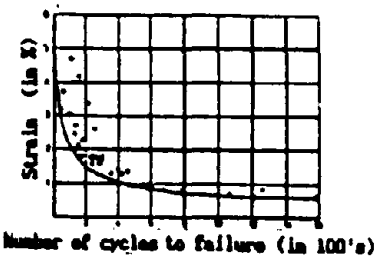

Figure 21 Relation of strain and loading cycles up to failure

REFERENCES

Chow F.L.(Zhou Fu Lin), Stiemer S.F. and Cherry S. 1983. Experimental Investigation of Solid State Steel Energy Absorbers for Earthquake Resistant Structures. The Dept. of Civil Eng., The University of British Columbia, Canada

Kelly K.L.1986. Progress and Prospects in Seismic Isolation, Seminar on Base Isolation and Passive Energy Dissipation. San Francisco.

Kelly J.M.,.Skinner M.S.and Beucke K.E. 1980. Experimental Testing of and Energy Absorbing Base Isolation System. Report No. UCB/EERC--80/35.

Li L. 1984. Base Isolation Measure for A Seismic Buildings in China, Proc. of 8WCEE, San Francisco.

Pan T. C. and Kelly J.M. , 1983. Seismic Response of Torsionally Coupled Base Isolated structures.Earthquake Engineering and Structural Dynamics. Vol.11.

Stiemer S.F.and Zhou F.L. 1984.Curved Plate Energy Absorbers for Earthquake Resistant Structures.Proc.of 8WCEE Vol.5.SanFrancisco

Zhou F.L.,Stiemer S.F. and Cherry S. 1987. Prediction of Low Cycle Fatigue Failure for Mild Steel Structural Components. Proc. of International Conference on Structural Failure, Singapore.

Lessons of the 1990 Manjil-Iran earthquake

A. Astaneh-Asl
University of California at Berkeley, USA

ABSTRACT: On June 20, 1990, a strong earthquake occurred in Iran causing widespread death and destruction in one of the well developed areas of the country. Most of the death occurred due to collapse of adobe, unreinforced stone or brick masonry homes. The damage to modern engineered facilities was minimal and was in the form of cracking of reinforced concrete structures and in one case collapse of a major elevated water tank which probably had design deficiancies. Several poorly constructed 6-8 story steel and reinforced concrete buildings completely collapsed. Throughout the area, damage to unreinforced hollow infill walls and the equipment was widespread.

1 INTRODUCTION

The areas affected by the Manjil-Iran earthquake are shown in Figure 1. The quake measured 7.7 by the United States Geological Survey (USGS 1990). According to unofficial statistics (Zargar 1991), about 200,000 residential, commercial and industrial units were damaged where about 60,000 of them were totally demolished. About 400 hospitals and health units were damaged and 7500 classrooms were rendered useless. The initial monetary damage was estimated at 800 billion Iranian Rials (about 8 to 11 billion U.S. dollars).

The damage caused by the Manjil-Iran earthquake has been reported by A. Astaneh (1990), M. Ghalibafian (1991), M. R. Maheri (1991), M. Mehrain (1990), A. A. Moinfar (1990), M. Niazi (1992) and M.K. Yegian (1990) among others. The purpose of this paper is to summarize the earthquake engineering aspects of this major event and discuss the lessons that were learned and could be learned.

2 GENERAL EARTHQUAKE ENGINEERING ASPECTS

The Manjil earthquake occurred in a developed part of Iran affecting many modern and engineered facilities in urban areas as well as many remote villages with thousands of traditional adobe houses. Most of the non-engineered adobe or unreinforced masonry houses in the area were severely damaged or collapsed. Damage to the engineered facilities was in the form of extensive rock slides over the highways, collapse of portions of the tunnels, minor damage to abutments of modern bridges, some damage to a major dam, minor damage to a modern grain silo, some damage to foundations in a major power plant, extensive damage to equipment in many industrial facilities and damage to unreinforced hollow tile or concrete block infill walls in many buildings.

In the following sections more field data on the performance of man-made facilities are provided and lessons that were learned or could be learned are discussed.

3. NON-ENGINEERED TRADITIONAL CONSTRUCTION

In small towns and villages throughout the affected area, the majority of buildings were non-engineered one or two-story buildings with adobe and unreinforced stone or brick masonry construction. These buildings are usually built by local masons to resist gravity loads but with limited or no seismic considerations. The walls are usually load bearing masonry walls constructed by using sun-dried mud bricks, stone or brick masonry with mud, lime-mud, or sand cement mortar.

The roof of an adobe building is usually flat earthen roof built by mud layers placed on the wood mattings which in turn are supported on a series of round wood logs. The round wood logs are supported on the adobe walls. The roof structure in stone or brick masonry buildings consists of a series of steel I-beams spaced at about one meter intervals and ten centimeter thick brick jack arches span the two adjacent I-beams. On top of the brick arch light-weight gravel and about 2 centimeters of cement mortar and 2 centimeters of terrazzo tiles are placed.

The adobe and unreinforced masonry building have been built for many years in the rural areas throughout the central and eastern portion of the Alpine-Himalayan seismic belt. During past moderate or strong earthquakes, these relatively heavy, weak and brittle buildings have sustained heavy damage or completely collapsed killing thousands of

their occupants in each earthquake. In Iran alone, over the last 30 years, more than 70,000 people have perished in these hazardous buildings.

However, brick masonry buildings that were seismically reinforced by using vertical and horizontal tie columns and tie beams have survived strong earthquakes including the Manjil earthquake. The survival of brick masonry buildings with seismic ties, even those with only horizontal ties, signifies the importance of tying the load carrying elements of the building to each other as well as ensuring that the walls will not fall apart.

The poor seismic performance of the adobe and unreinforced masonry buildings has been well known for many years and is not a new lesson to be learned. The frequent collapse of these buildings during earthquakes is related to several factors including the heavy weight, low natural period, existence of no continuous load path for seismic forces, brittleness, lack of ductility, relatively low strength to weight ratio of the material, lack of significant tension capacity of the elements and usually poor foundations.

Several studies on earthen and low strength masonry buildings (for example, Erdik 1987) have discussed seismic performance and have proposed technologies for improving seismic behavior of these hazardous buildings. However, actual implementation of these solutions appears to be a challenge. The adobe houses are mostly located in the remote villages and towns which are not easily accessible. The delivery of the material, equipment and technical man-power is very difficult and expensive if not impossible. Also, it appears that the volume of the buildings that need to be retrofitted is so great that the government agencies and communities involved are unable to provide the necessary financial support.

As a result, thousands of these "death trap" buildings are standing on the seismically active Alpine-Himalayan belt waiting for another fault to slip and thousands of lives to be perished.

4 PERFORMANCE OF ENGINEERED BUILDINGS

During Manjil earthquake, a few six to eight story, presumably engineered buildings in the city of Rasht, totally collapsed. The buildings had reinforced concrete or welded steel structures. Initial investigations of the wreckage indicated that poor performance of concrete structures was most likely due to the poor quality of the concrete and lack of proper seismic detailing in the joints. In steel structures, the cause of the collapse was related to the inadequacy and poor execution of fillet welds in the connections (Ghalibafian, 1991).

A lesson to be noted here is that due to the existence of factor of safety in design of structures for gravity loads, in some cases, poorly constructed structures can still withstand gravity loads. However, strong earthquakes push the structures to their limit and damage the poorly constructed areas of the structures. If these areas are critical to the overall stability and integrity of the structure, the damage usually results in partial or total collapse with tragic consequences.

Other than the few poorly constructed buildings that collapsed during the earthquake, the remaining engineered buildings in the affected areas performed very well. There was almost no critical structural damage. The quality of the design as well as construction of the modern engineered facilities, visited by the author, appeared to be good and in general compliance with the the currently available earthquake engineering technology. However, unreinforced infill walls and equipment inside the well-built structures sustained considerable damage during the earthquake.

The use of unreinforced masonry infill walls with hollow clay tiles or cement blocks was very common in the area. These walls usually were not reinforced and were not attached to the structure by any mechanical means. As a result, during the earthquake, these relatively stiff but brittle walls had failed. The falling debris resulting from the failure of the infill walls occasionally had caused serious damage to the nearby equipment. In most cases, due to cracking and partial failure of these walls, a number of buildings were evacuated and costly repairs were being undertaken.

Iran has a relatively modern seismic design code (BHRC 1988) that has been initiated in 1962 and is currently maintained by a committee of earthquake engineers at the Ministry of Housing and Urban Development. According to the law, compliance with the code is mandatory. However, most non-engineered and some engineered buildings do not fully comply with the code. Sometimes, particularly in the remote areas, the buildings do not have any seismic design considerations and are not subjected to rigorous construction inspections. As a result, during the earthquakes these seismically hazardous buildings are severely damaged or collapse.

5 PERFORMANCE OF MAJOR ENGINEERED FACILITIES

Numerous important residential, commercial and industrial facilities were located within the affected areas. Most of these facilities have been built during the last 30 years and were designed to withstand varying levels of seismic forces. In the following, a discussion of performance of these facilities and lessons learned are provided.

5.1 Geotechnical Aspects

In the town of Masooleh several boulders, approximately 3x3x3m in size, had been released from the mountains overlooking the town and rolled down the slopes. The boulders had

completely demolished several homes and caused death of ten people and injuries to others. Some evidence of liquefaction was observed in and around the town of Astaneh-Ashrafieh where sand-boils had completely filled up some wells and several houses were unevenly uplifted and settled. According to Ghalibafian, (1991) major damage due to failure of soil was almost total burial of two villages built on the downslope due to landslides above the villages.

5.2 Bridges, Tunnels and Highways

Numerous rockslides were observed along the major highway between the cities of Gazvin and Rasht. The rockslides had closed the highway during the main shock and continued to do so during the aftershocks. The entrances to three tunnels on this highway had collapsed. A sixteen meter long segment of the Shirinsoo tunnel had collapsed twice, once during the main shock and again two days later due to the aftershocks. The bridges in the affected areas even in the epicentral areas had performed well. Two major steel truss bridges had no visible damage. Two major concrete bridges had sustained minor damage in their abutment and one bridge had a horizontal crack in one of its piers. Two old brick masonry bridges with multiple arch spans damaged and one had lost half of its deck width in one span.

5.3 Hospitals

A major hospital in Rostamabad, a town near the epicenter had totally collapsed during the earthquake as shown in Figure 2. The modern facilities had been completed only two years prior to the earthquake. The hospital complex consisted of several one story unreinforced concrete block masonry buildings where unreinforced walls and a number of steel columns were carrying the gravity load. Probably the collapse was due to sliding of the poor supporting soil and lack of seismic considerations in design and construction of such a critical facility.

5.4 Dams

The Manjil dam over the Sefidrood river, built in 1967, sustained some minor damage in the form of a horizontal crack and some hair cracks at the top of the dam and in the buttresses. According to Moinfar (1991) after the reservoir was drained, some cracks at the base of the dam on the upstream side were also observed. According to engineers at the dam site, the dam was designed for 0.25g horizontal equivalent static force. The operating facilities and staff housing near the dam were severely damaged or collapsed. The seismic behavior of this major buttress dam provides a unique and very valuable opportunity for seismic studies to advance the technology of earthquake engineering of major concrete dams.

5.5 Power plants and a cement factory

A major fossil-fueled power plant was located within 30km of the likely epicenter. The structures of the power plant, which were mostly reinforced concrete frames had very minor damage. The most important damage in this facility was collapse of a heavy non-structural exterior wall panel above the gate where the main power transmission lines were exiting the building. The falling debris has demolished the power line conduits making the power transmission impossible. Also, in this facility, the foundation of one of the generators showed uneven settlement of about 5cm.

The modern Khazar cement factory with 2000 ton daily cement production is located within the 15km of the likely location of the epicenter. The structures of this plant, which were reinforced concrete frames with shear walls, reinforced concrete silos or steel gable frames, had no significant visible damage. However, considerable damage had been inflicted on the equipment either due to failure of equipment supports or due to collapse of the adjacent non-structural walls on the equipment.

5.6 A major silo and water tanks

A major reinforced concrete grain silo with 120,000 ton capacity sustained some minor damage at the base of columns of its elevator shaft. The damage was primarily a horizontal crack developed at the construction cold joint. The grain-loading equipment at the top floor of the silo were displaced and damaged. the damage was easily repaired and operation of silo resumed in about a week after the quake.

An elevated water tank in the City of Rasht had totally collapsed and two others, which had just been constructed, Figure 4, were damaged. The quality of construction in these reinforced concrete water tanks appeared to be good. It is possible that the damage might have been due to deficiency in the seismic design. An older reinforced concrete elevated water tank in the town of Astaneh-Ashrafieh had also collapsed. In this case, the seismic design, detailing as well as construction appeared to be poor.

Studies of the behavior and causes of damage in these important structures, can provide very valuable information to improve their seismic design in the future as well as in the retrofit of existing ones.

6 SUMMARY

The performance of the man made facilities during Manjil Iran earthquake and the lessons learned from this earthquake could be summarized as follows.

1. The non-engineered facilities or engineered facilities with poor construction collapsed or were heavily damaged causing most of the deaths and injuries. The large number of fatalities once again emphasizes an urgent need for practical and inexpensive retrofit systems that can be implemented to reduce the risk of collapse of these hazardous buildings.

2. The engineered facilities designed and constructed in accordance with the current earthquake engineering technology performed very well with minor structural damage. The good performance of these facilities emphasized the benefits of implementing sound earthquake engineering in the design of structures as well as the importance of quality control in construction.

3. Damage to the equipment in the industrial facilities was extensive indicating deficiencies in the seismic design and detailing of the supports of the equipment.

4. In some cases damage to the equipment was caused by the collapse of the structural or nonstructural elements on them.

5. The performance of unreinforced hollow clay tile infill walls was poor.

6. Finally, all buildings and other facilities that collapsed, without exception, were either not designed according to the current seismic code provisions or were poorly constructed.

An important lesson that one can learn from this earthquake is that in order to survive major earthquakes with minimum or at least tolerable damage, it is necessary that the structure, non-structural elements and equipment comply with at least the provisions of the current seismic codes and all components of a facility be constructed properly.

REFERENCES

Ambraseys, N. N. & C.P. Melville 1982. A history of Persian earthquakes. London: Cambridge. U.K. 1982.

Astaneh A. & M. Ghafory-Ashtiany 1990. The Manjil Iran earthquake of June 21, 1990. Newsletter, Earthquake Engrg. Research Ins.

Berberian, M., M. Ghorashi, J.A. Jackson, K. Priestly, and T. Wallace 1991. The Rudbar-Tarom earthquake of June 20 1990 in NW Persia: preliminary field and seismological observations and its tectonic significance. Preprint.

BHRC 1988a. Iranian code for seismic resistant design of buildings. Tehran: Ministry of Housing and Urban Development. (in Farsi)

Erdik, M.O. 1987 (ed.). Earthen and low-strength masonry buildings in seismic areas. proc., Mid. East Tech. Univ. Turkey

Gharibafian, M. 1991. Lessons of Manjil earthquake. Proc., Conf. on the 20th June 1990 Manjil earthquake :17-100. Tehran: Ministry of Housing and Urban Development. (in Farsi).

Maheri, M.R. 1991 Response of large structures to Manjil Earthquake of June 1990. Proc., Seism. & earthq. engrg. Conf. 1018-1028. Tehran:IIEES

Mehrain M. 1990. Reconnaissance report on the northern Iran earthquake of June 21, 1990, Rep. NCEER-90-0017. Buffalo, N.Y.

Moinfar A.A. & A. Naderzadeh 1990. The Manjil, Iran earthquake of 20 June 1990. Pub. No. 119, BHRC, Tehran: Ministry of Housing and Urban Development. (in Farsi)

Moinfar, A.A. 1991. General report on 31 Khordad 1369 earthquake. Proc., Conf. on the 20th June 1990 Manjil earthquake :17-

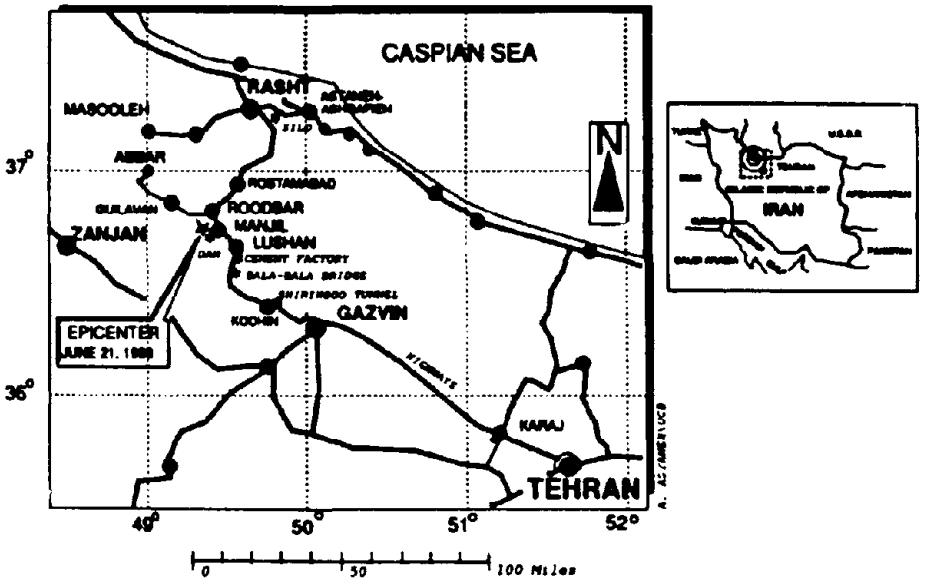

Figure 1. Map of the affected areas

Figure 2. Collapsed hospital in Rostamabad

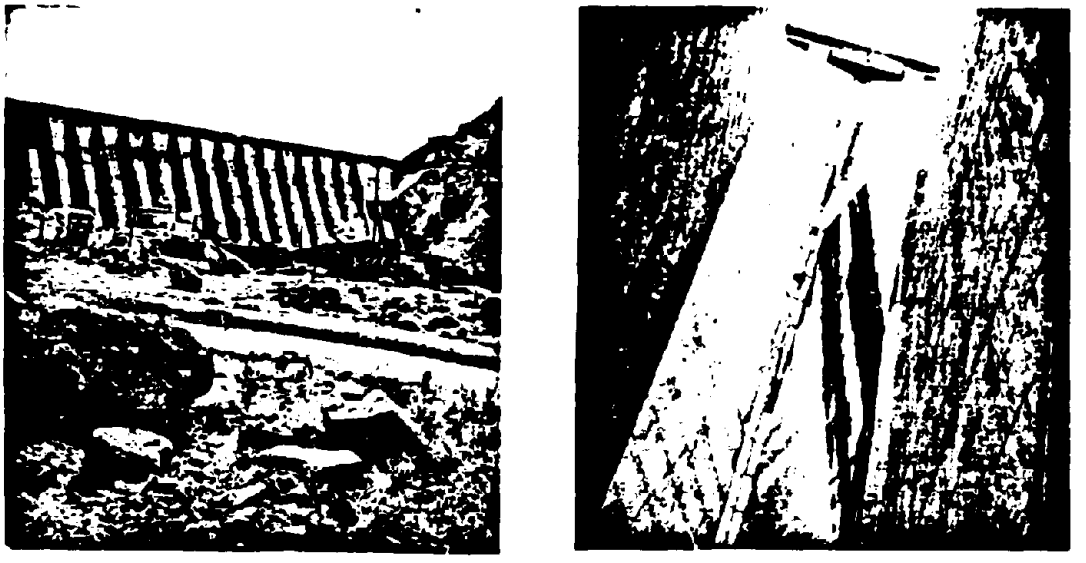

Figure 3. Manjil dam and observed damage

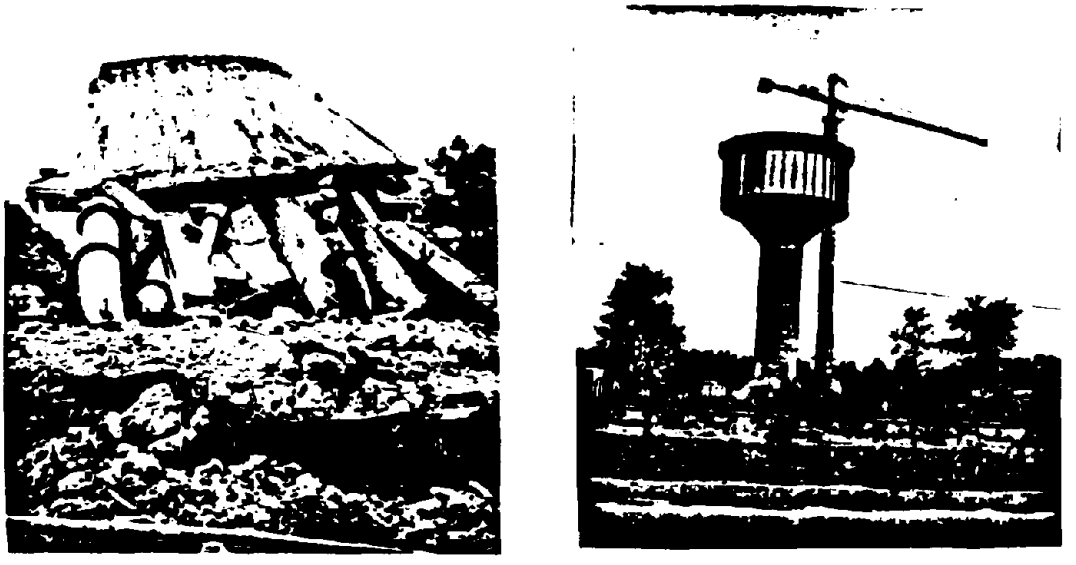

Figure 4 Damaged and collapsed elevated water tanks

The Loma Prieta, California earthquake of October 17, 1989

J. Penzien
International Civil Engineering Consultants, Inc., Berkeley, California, USA

C. Stepp
Electric Power Research Institute, Palo Alto, California, USA

The Loma Prieta earthquake, Richter Magnitude 7.1, originated on the San Andreas Fault system approximately 90 km south of the city of San Francisco. This earthquake produced the strongest shaking in the city since the 1906 San Francisco earthquake that was generated by fault slipping from a point approximately 100 miles south of San Francisco and extending to a point approximately 100 miles north of San Francisco, thus passing a few miles west of the city (see Figure 1). The metropolitan area, with approximately 5 million people, is spread around San Francisco Bay. The major portion of the population is on the San Francisco peninsula, the Oakland city region, and the San Jose city region.

The people and the city governments were aware of the earthquake hazard because of the 1906 earthquake and also the knowledge that the metropolitan area lies between two major faults, the San Andreas Fault to the west and the Hayward Fault to the east, both of which are known to have generated large earthquakes in the past. A modern building code is in effect and new buildings are designed and constructed according to the seismic requirements in the code. However, seismic requirements have been in the code only for about 50 years so that many buildings in San Francisco and Oakland were constructed before 1945 and these have less seismic resistance than modern buildings. The early seismic requirements were improved as we learned from each destructive earthquake: 1933 Long Beach M6.2, 1952 Tehachapi M7.5, 1971 San Fernando M6.5, and other smaller earthquakes; thus, structures designed under the early requirements in the code do not have a resistance to earthquakes as great as buildings designed more recently. It is thus clear that California, one of the leaders in seismic research and design, still has weaknesses and efforts are now underway to minimize these weaknesses by a program of retrofitting.

RECORDED GROUND MOTIONS

Many strong-motion accelerographs were in the region affected by strong ground shaking and much was learned from the recorded accelerograms. On firm ground, in the near-field the peak accelerations were in the range of 50–60% g; and in San Francisco, at a distance of 60 km on firm ground, the peak accelerations averaged approximately 10% g but with a considerable spread in values.

The nature of the ground shaking at a site depends upon the source mechanism, the travel path of the seismic waves, and the local soil conditions; and these effects were clearly illustrated by records obtained during the earthquake. In California earthquakes the expected fault slip originates at one point and then progresses along the fault to the other extremity of the slipped area; but in the Loma Prieta earthquake the fault slip started at the hypocenter and then progressed in both directions. This had the effect of reducing the duration of strong shaking and increasing the intensity. At 10 km from the fault the Gilroy No. 1 record had a duration of strong shaking of approximately 4 seconds and the Corralitos record at 5 km from the fault had a duration of strong shaking of approximately 7 seconds; these durations are much less than would have been expected from a magnitude 7.1 earthquake (Figure 3). An effect of travel path is shown in the Santa Cruz record at 20 km from the site. This record has a much higher frequency content than the Corralitos record, for example, and has a longer duration of strong shaking. A pronounced effect of local site conditions on ground shaking is illustrated in Figure 5. Over the years, filled ground was built up around the edge of the Bay and these areas are underlain by soft Bay mud. The ground shaking recorded on these sites was much affected by a reduction in high frequency content and an amplification of longer period content. This is illustrated in Figure 6 which compares the motions recorded on a rock island with the motions recorded on an adjacent man-made island. The peak accelerations were amplified by a factor of approximately 2.5; similar ground motions were recorded on filled ground overlying Bay mud at several other locations around the shore of the Bay.

A disasterous earthquake not only causes deaths, injuries and suffering but also can have a long-

...sting economic depression because of the impact ... the functioning of the city because industry and ...ommerce have been negatively impacted.

RECORDED BUILDING MOTIONS

The Embarcadero Four building in San Francisco, a 47-story, steel-frame structure, had been well-instrumented prior to the earthquake. The peak recorded acceleration in the base of the building was approximately 10% g and the motion recorded on the 47th floor had a peak acceleration of 46% g (Figure 7). This acceleration came from the motion of the third mode of vibration; the accelerations of the first mode (5 seconds) were relatively small because the duration of strong ground motion was relatively short. The high accelerations in the upper parts of several high-rise buildings were sufficiently strong to cause damage to architectural features. On the roof of a 4-story, shear-wall building in Watsonville, a peak acceleration of 1.25 g was recorded; no significant damage.

FREEWAY STRUCTURE AND BRIDGES

The Golden Gate Suspension Bridge was designed in the 1930's before dynamic analysis was possible. No significant damage was sustained but after the earthquake thorough dynamic analyses were made of the bridge and a retrofit program was initiated to strengthen weak points that had been identified. The San Francisco-Oakland Bridge is composed of two suspension spans going from San Francisco to Yerba Buena Island and a multispan steel-truss structure going from Yerba Buena Island to Oakland. This bridge was also designed in the 1930's for 10% g static force. Some damage was sustained by the truss segment of the bridge and dynamic analyses are being made to ascertain what retrofit is needed.

The Cypress Viaduct was a reinforced concrete, two-story structure in Oakland. That portion that passed over the filled ground underlain by Bay mud was subjected to ground shaking having approximately 25% g peak acceleration. The structure had been designed in 1950 and was relatively weak and brittle so that approximately one mile of the upper deck collapsed onto the lower deck. Following the earthquake, the Governor directed the Department of Transportation to undertake a retrofit program to ensure that no bridge in California would collapse in future earthquakes and that major bridges and important freeway structures should survive an earthquake and remain functional. This program is now underway.

SEISMOLOGICAL FEATURES

The San Andreas Fault, together with its related faults, forms the boundary between the Pacific Ocean crustal plate and the North American crustal plate. The movement of the Pacific plate relative to the Continental plate is at a rate of about 4 cm per year. The strains produced by this movement build up shear stresses which produce a sudden slip on the fault. In 1906 the slip occurred over a length of about 220 miles centered approximately on San Francisco. The maximum relative slip across the fault, just north of San Francisco, was about 6 meters. A large earthquake is expected to occur on the San Andreas Fault and adjacent to San Francisco. Such an earthquake could produce ground shaking in San Francisco three times as intense as during the Loma Prieta earthquake and with three times the duration of strong shaking. Had the Loma Prieta earthquake been this expected event the damage and loss of life would have been much greater.

A large earthquake (estimated magnitude 7.1) occurred on the Hayward Fault in 1868, so a similar earthquake could occur in the future. Such an earthquake would produce strong ground shaking in San Francisco and very strong ground shaking in Oakland.

The Loma Prieta earthquake occurred on a segment of the fault that slipped in 1906. The area of the 1989 slip is well defined by the locations of aftershocks (see Figure 2). The length of slipped fault was approximately 50 km. The fault slip did not reach the surface of the ground so it is inferred that in 1906 the fault slip extended only a few kilometers beneath the ground surface. The area of fault slip is consistent with a magnitude 7.1 earthquake. The Loma Prieta earthquake made the public aware that an earthquake of magnitude 6.5, or greater, can produce a disaster if it is sufficiently close to a city that is not prepared and in California the average return period for such earthquakes is four years, based on twentieth century data.

NON-ENGINEERING IMPACTS

The death toll was relatively small with only 67 casualties, of which 42 were killed in the collapse of the Cypress Viaduct. 3,757 people were injured during the earthquake. These are relatively small numbers for such an earthquake but, on the other hand, the damage to property was estimated to be $6 billion and the total impact of the earthquake was estimated to be as much as $10 billion. Approximately 1.4 million customers temporarily lost electricity after the earthquake. Approximately 1,000 single family residences were destroyed and 23,000 were damaged. Approximately 64,000 people were given temporary shelter by the Red Cross, and one year later 3,000 people were still homeless.

The earthquake had an impact on business activities and on industrial activities (Silicon Valley) but these impacts have not been quantified. Few data of this type have been collected in California earthquakes because of a relectance to provide information.

Before the earthquake, the San Francisco-Oakland Bridge carried 240,000 vehicles on a typical weekday and for the one month that the bridge was closed for repairs traffic was diverted to other crossings. This shift in traffic pattern affected the Bay Area cities and had a noticeable effect on businesses. This made it clear that the functioning of the Bay Area cities was dependent on the six bridges plus the sub-bay rapid transit tube and if several of the major bridges collapsed during an earthquake there would be a very severe impact on the Bay Area cities.

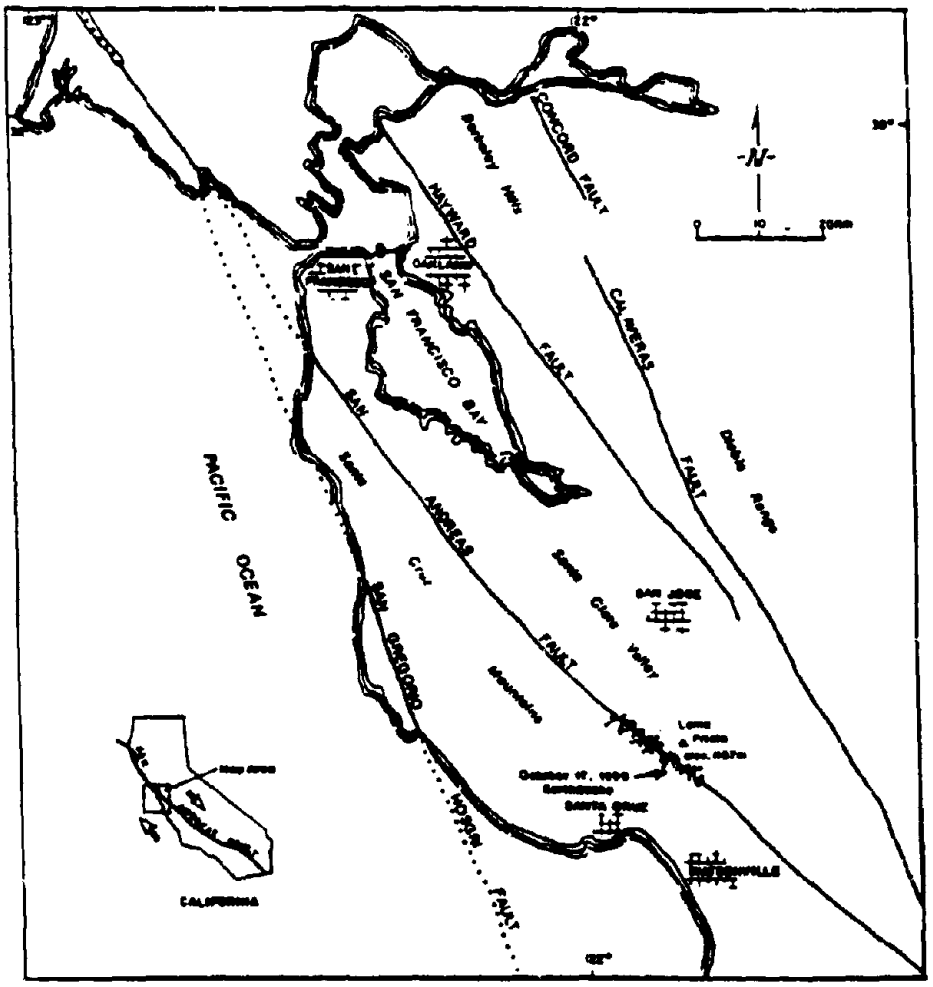

Figure 1. Map of the Loma Prieta–San Francisco region of California. The San Andreas Fault and the Hayward Fault have produced major earthquakes in the last 150 years. The ground motions were amplified and higher frequencies were filtered out at sites near San Francisco and Oakland where filled ground was underlain by Bay mud along the shore of the Bay. The metropolitan area of 5 million inhabitants is flanked by the San Andreas Fault to the west and the Hayward Fault to the east, so it is very likely that one or both faults will generate a large earthquake in the next one hundred years.

Figure 2. Plot of small aftershocks following the Loma Prieta earthquake. Seismic instruments were installed in the vicinity of the fault and the hypocenters thus determined depict the slipped area of the fault. The slip did not extend to the surface of the ground. During the 1906 earthquake a relatively small slip occurred at this location. This information, provided by seismological research was valuable to engineers by explaining the source mechanism of the quake and helping to assess past and future seismic hazards. (From Plafker 1989)

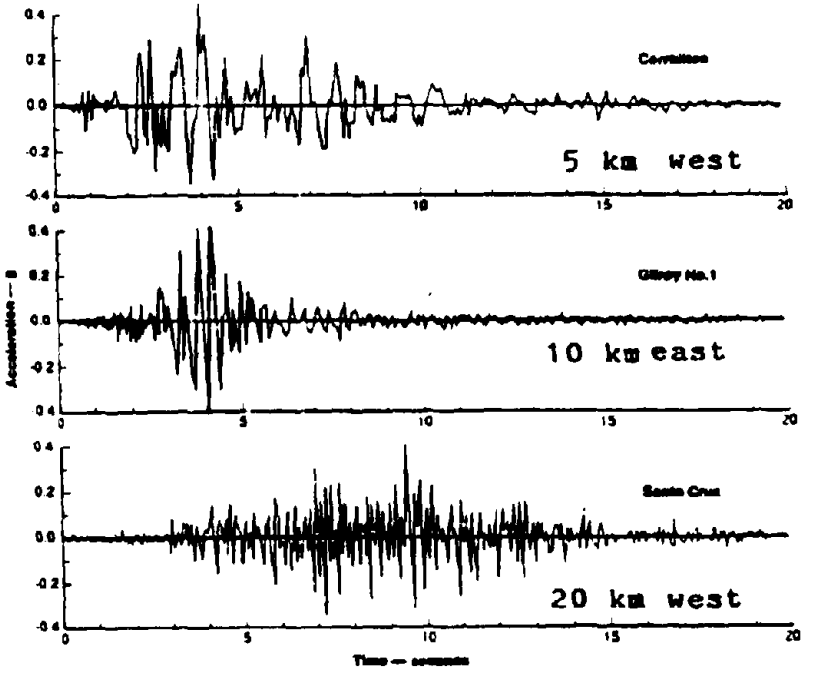

Figure 3. East-west accelerations recorded at sites 5, 10, and 20 km from the fault, recorded on firm ground. The remarkable differences are attributed to travel-paths of the seismic waves. The peak accelerations are the same on the three accelerograms but the frequency characteristics and the duration of strong shaking differ.

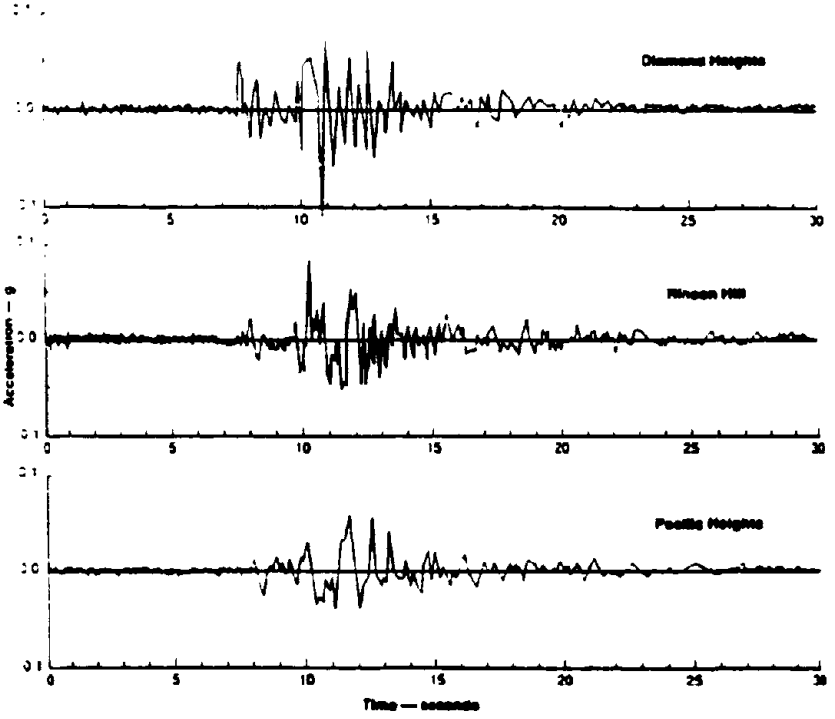

Figure 4. East-west accelerations recorded on three different rock sites in San Francisco. Peak accelerations on firm ground in San Francisco were approximately 10% g. The attenuation of shaking on firm soil was consistent with past experience. (Housner 1990)

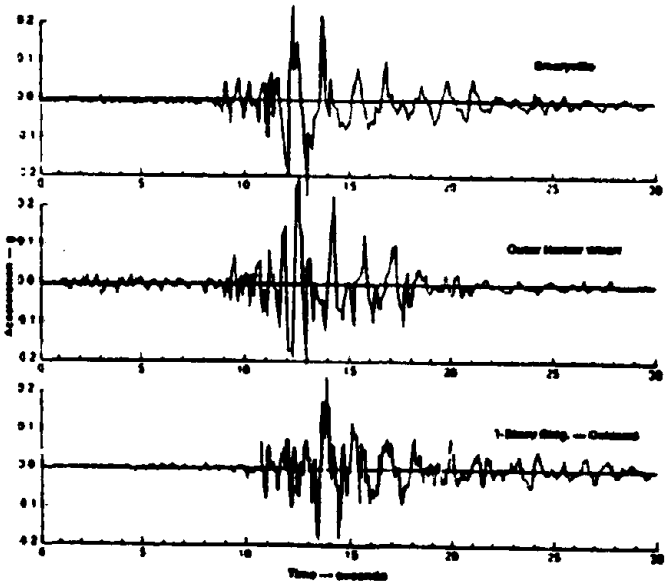

Figure 5. East-west accelerations recorded on three sites in the Oakland area on filled ground underlain by Bay mud.

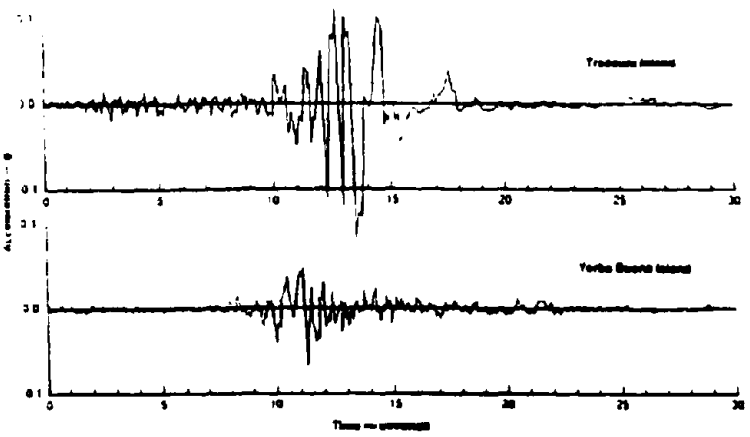

Figure 6. East-west accelerations on Yerba Buena Island (rock) between San Francisco and Oakland, and on Treasure Island (filled ground underlain by Bay mud), which is an extension of Yerba Buena Island. (Housner 1990)

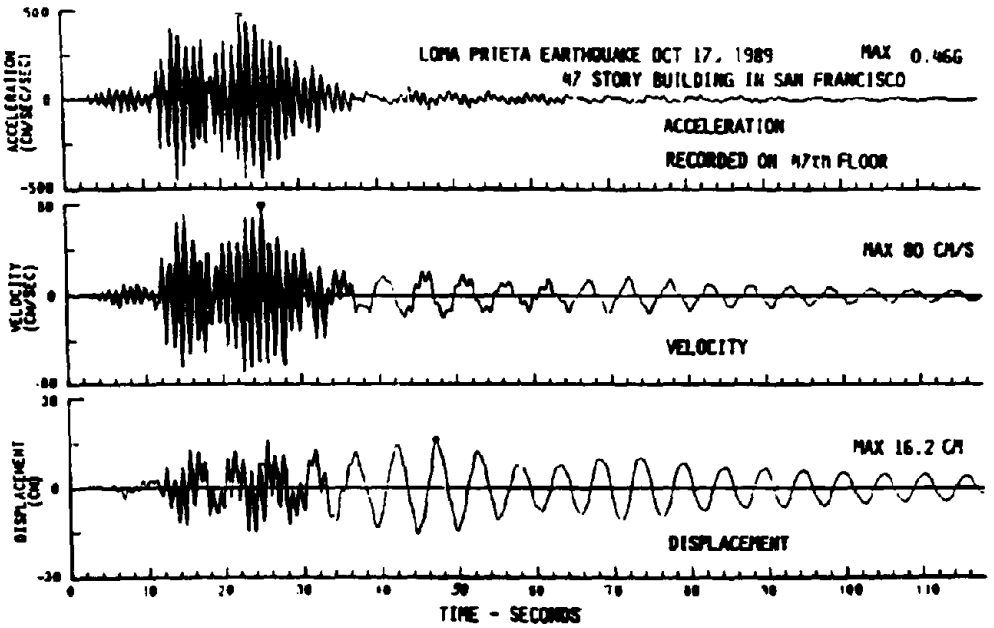

Figure 7. Motion recorded on the top floor of the 47-story Embarcadero Four building in San Francisco. The peak acceleration at the base of the building was 11% g and on the 47th floor 48% g. The acceleration was dominated by the 3rd mode of vibration (1 sec period); the first mode of vibration (5 sec period) is prominant in the displacement.

REFERENCES

Division of Mines and Geology 1990. The Loma Prieta, California earthquake of 17 October 1989. Department of Conservation.

Earthquake Engineering Research Institute 1989. Loma Prieta Earthquake 17 October 1989.

Housner, G. W. 1990. Competing against time - report to the governor on the 1989 Loma Prieta earthquake. State of California.

Seismic Safety Commission 1991. Loma Prieta's call to action. State of California.

Seismic Safety Commission 1992. California at risk - reducing earthquake hazards 1992-1996. State of California.

Seismological Society of America - Bulletin 1991. The 1989 Loma Prieta, California, earthquake and its effects.

Structural Engineers Association of California 1991. Reflections on the Loma Prieta earthquake.

CONCLUSIONS

Important lessons were learned from the Loma Prieta earthquake because of the following features: 1) modern cities were in the shaken area; 2) many strong motion accelerographs recorded the strong shaking; 3) modern seismic requirements were in the building code; 4) numerous pre-code buildings were in the region; 5) many earthquake engineers and researchers were in the region; 6) the Seismological Branch of the U.S. Geological Survey was stationed in the shaken area. Thus, the earthquake generated many data and these were studied by numerous people, so it can be expected that many new things were learned. Almost every major earthquake teaches us something new and brings to our attention complexities of which we were not aware, so that it often seems — The more we "learn", the less we "know". The principal lessons learned from the Loma Prieta earthquake are:

1. Buildings designed according to the modern code requirements performed well. However, the intensity of ground shaking in the metropolitan area was not exceptionally strong and a few modern buildings did receive damage, so it is necessary to re-think the seismic requirements of the code.

2. Older buildings not designed according to "modern" code requirements performed less well and buildings constructed before there were requirements in the building code exhibited dangerous weaknesses. When very strong ground shaking occurs in the metropolitan region there will be many collapsed buildings if an appropriate retrofit program is not undertaken.

3. The metropolitan area lies between two major faults each of which has generated a large earthquake (1868 and 1906) in the past and will certainly generate earthquakes in the future. When a large earthquake occurs on either of these faults the intensity of ground shaking will be perhaps three times greater than during the Loma Prieta earthquake and the duration of strong shaking will be three times longer. The damage potential of these earthquakes is much greater than the damage potential of the Loma Prieta earthquake.

4. The populace and the city and state governments must recognize that strong earthquakes will come and that the region should be prepared to respond appropriately.

5. Seismological and geological data greatly improved the understanding of the Loma Prieta earthquake and the seismic hazard faced in the future.

6. The network of strong-motion accelerographs provided data of great value to earthquake engineers. Characteristics of ground shaking that had never been observed before were obtained. However, major bridges, traffic tube, etc., had not been instrumented and, therefore, it is not known what motions and stresses these structures underwent.

7. Accelerograms obtained during the Loma Prieta earthquake showed unusual effects of the source mechanism, the travel path geology, and the local soil conditions. The duration of strong shaking was shorter and the intensity of ground shaking was somewhat greater than would have been expected from an earthquake of magnitude 7.1. Near-field accelerograms showed markedly different characteristics of ground shaking attributable to the travel path geology. Around the border of San Francisco Bay there were locations where filled ground was underlain by bay mud and this amplified the intensity of shaking and filtered out higher frequencies of ground motion.

8. Bridges not designed according to modern seismic codes are susceptible to damage and collapse if subjected to strong ground shaking. This was demonstrated by the collapse of the Cypress Viaduct and by the damage to the San Francisco-Oakland Bridge. Following the earthquake, the Governor of California directed the Department of Transportation to check all bridges in the state and to retrofit them as required to prevent collapse and important bridge and freeway structures were to be retrofitted so as to remain functional. There are about 40 major bridges and major freeway interchange structures and 24,000 other bridges in California. A retrofit program is underway but will require a number of years to complete.

9. Very strong accelerations were experienced in the upper parts of some high-rise buildings from higher modes of vibration (two, three, four). Although such motions do not threaten to collapse the structure, they do cause damage that is objectionable to the tenants.

10. Soil liquefaction occurred in a number of places where filled ground was underlain by bay mud. And also in other locations where there was soft ground with high water table. Liquefaction does not produce life-threatening damage but it can be costly to repair the effects.

11. Some modern buildings did experience structural damage. This indicates that the seismic requirements in the building code and their implementation need some improvements. The improvements to the building code should be made with reference to the fact that much stronger ground shaking in San Francisco will occur in future earthquakes.

12. Retrofit of older buildings is needed. The old pre-code buildings pose a great hazard to life and limb. Also, investigations should be made of the seismic resistance of engineered buildings that were constructed in the early decades of the seismic requirements in the code. These buildings do not meet the modern requirements in the building code and the effect of the deficiencies should be determined and structures should be strengthened as required.

13. The impact of the Loma Prieta earthquake was costly ($6 to $10 billion) but not as costly as if it had been a magnitude 8 earthquake adjacent to San Francisco ($50 billion, or more); and the number of deaths and injuries would have been much greater. The disaster relief activities and the disaster recovery measures performed quite well, with a few exceptions; however, when a large earthquake occurs on a fault close to the metropolitan region a much greater demand will be put on relief and recovery measures. It will be important now to use the Loma Prieta experience as a base from which to estimate the relief and recovery measures needed in the event of a large, close earthquake.

EARTHQUAKE ENGINEERING RESEARCH CENTER REPORT SERIES

EERC reports are available from the National Information Service for Earthquake Engineering (NISEE) and from the National Technical Information Service (NTIS). Numbers in parentheses are Accession Numbers assigned by the National Technical Information Service; these are followed by a price code. Contact NTIS, 5285 Port Royal Road, Springfield Virginia, 22161 for more information. Reports without Accession Numbers were not available from NTIS at the time of printing. For a current complete list of EERC reports (from EERC 67-1) and availablity information, please contact University of California, EERC, NISEE, 1301 South 46th Street, Richmond, California 94804.

UCB/EERC-82/01 "Dynamic Behavior of Ground for Seismic Analysis of Lifeline Systems," by Sato, T. and Der Kiureghian, A., January 1982, (PB82 218 926)A05.

UCB/EERC-82/02 "Shaking Table Tests of a Tubular Steel Frame Model," by Ghanaat, Y. and Clough, R.W., January 1982, (PB82 220 161)A07.

UCB/EERC-82/03 "Behavior of a Piping System under Seismic Excitation: Experimental Investigations of a Spatial Piping System supported by Mechanical Shock Arrestors," by Schneider, S., Lee, H.-M. and Godden, W. G., May 1982, (PB83 172 544)A09.

UCB/EERC-82/04 "New Approaches for the Dynamic Analysis of Large Structural Systems," by Wilson, E.L., June 1982, (PB83 148 080)A05.

UCB/EERC-82/05 "Model Study of Effects of Damage on the Vibration Properties of Steel Offshore Platforms," by Shahrivar, F. and Bouwkamp, J.G., June 1982, (PB83 148 742)A10.

UCB/EERC-82/06 "States of the Art and Practice in the Optimum Seismic Design and Analytical Response Prediction of R/C Frame Wall Structures," by Aktan, A.E. and Bertero, V.V., July 1982, (PB83 147 736)A05.

UCB/EERC-82/07 "Further Study of the Earthquake Response of a Broad Cylindrical Liquid-Storage Tank Model," by Manos, G.C. and Clough, R.W., July 1982, (PB83 147 744)A11.

UCB/EERC-82/08 "An Evaluation of the Design and Analytical Seismic Response of a Seven Story Reinforced Concrete Frame," by Charney, F.A. and Bertero, V.V., July 1982, (PB83 157 628)A09.

UCB/EERC-82/09 "Fluid-Structure Interactions: Added Mass Computations for Incompressible Fluid," by Kuo, J.S.-H., August 1982, (PB83 156 281)A07.

UCB/EERC-82/10 "Joint-Opening Nonlinear Mechanism: Interface Smeared Crack Model," by Kuo, J.S.-H., August 1982, (PB83 149 195)A05.

UCB/EERC-82/11 "Dynamic Response Analysis of Techi Dam," by Clough, R.W., Stephen, R.M. and Kuo, J.S.-H., August 1982, (PB83 147 496)A06.

UCB/EERC-82/12 "Prediction of the Seismic Response of R/C Frame-Coupled Wall Structures," by Aktan, A.E., Bertero, V.V. and Piazzo, M., August 1982, (PB83 149 203)A09.

UCB/EERC-82/13 "Preliminary Report on the Smart 1 Strong Motion Array in Taiwan," by Bolt, B.A., Loh, C.H., Penzien, J. and Tsai, Y.B., August 1982, (PB83 159 400)A10.

UCB/EERC-82/14 "Seismic Behavior of an Eccentrically X-Braced Steel Structure," by Yang, M.S. September 1982, (PB83 260 778)A12.

UCB/EERC-82/15 "The Performance of Stairways in Earthquakes," by Roha, C., Axley, J.W. and Bertero, V.V., September 1982, (PB83 157 693)A07.

UCB/EERC-82/16 "The Behavior of Submerged Multiple Bodies in Earthquakes," by Liao, W.-G., September 1982, (PB83 158 709)A07.

UCB/EERC-82/17 "Effects of Concrete Types and Loading Conditions on Local Bond-Slip Relationships," by Cowell, A.D., Popov, E.P. and Bertero, V.V., September 1982, (PB83 153 577)A04.

UCB/EERC-82/18 "Mechanical Behavior of Shear Wall Vertical Boundary Members: An Experimental Investigation," by Wagner, M.T. and Bertero, V.V., October 1982, (PB83 159 764)A05.

UCB/EERC-82/19 "Experimental Studies of Multi-support Seismic Loading on Piping Systems," by Kelly, J.M. and Cowell, A.D., November 1982, (PB90 262 684)A07.

UCB/EERC-82/20 "Generalized Plastic Hinge Concepts for 3D Beam-Column Elements," by Chen, P. F.-S. and Powell, G.H., November 1982, (PB83 247 981)A13.

UCB/EERC-82/21 "ANSR-III: General Computer Program for Nonlinear Structural Analysis," by Oughourlian, C.V. and Powell, G.H., November 1982, (PB83 251 330)A12.

UCB/EERC-82/22 "Solution Strategies for Statically Loaded Nonlinear Structures," by Simons, J.W. and Powell, G.H., November 1982, (PB83 197 970)A06.

UCB/EERC-82/23 "Analytical Model of Deformed Bar Anchorages under Generalized Excitations," by Ciampi, V., Eligehausen, R., Bertero, V.V. and Popov, E.P., November 1982, (PB83 169 532)A06.

UCB/EERC-82/24 "A Mathematical Model for the Response of Masonry Walls to Dynamic Excitations," by Sucuoglu, H., Mengi, Y. and McNiven, H.D., November 1982, (PB83 169 011)A07.

UCB/EERC-82/25 "Earthquake Response Considerations of Broad Liquid Storage Tanks," by Cambra, F.J., November 1982, (PB83 251 215)A09.

UCB/EERC-82/26 "Computational Models for Cyclic Plasticity, Rate Dependence and Creep," by Mosaddad, B. and Powell, G.H., November 1982, (PB83 245 829)A08.

UCB/EERC-82/27 "Inelastic Analysis of Piping and Tubular Structures," by Mahasuverachai, M. and Powell, G.H., November 1982, (PB83 249 987)A07.

UCB/EERC-83/01 "The Economic Feasibility of Seismic Rehabilitation of Buildings by Base Isolation," by Kelly, J.M., January 1983, (PB83 197 988)A05.

UCB/EERC-83/02 "Seismic Moment Connections for Moment-Resisting Steel Frames.," by Popov, E.P., January 1983, (PB83 195 412)A04.

UCB/EERC-83/03 "Design of Links and Beam-to-Column Connections for Eccentrically Braced Steel Frames," by Popov, E.P. and Malley, J.O., January 1983, (PB83 194 811)A04.

UCB/EERC-83/04 "Numerical Techniques for the Evaluation of Soil-Structure Interaction Effects in the Time Domain," by Bayo, E. and Wilson, E.L., February 1983, (PB83 245 605)A09.

UCB/EERC-83/05 "A Transducer for Measuring the Internal Forces in the Columns of a Frame-Wall Reinforced Concrete Structure," by Sause, R. and Bertero, V.V., May 1983, (PB84 119 494)A06.

UCB/EERC-83/06 "Dynamic Interactions Between Floating Ice and Offshore Structures," by Croteau, P., May 1983, (PB84 119 486)A16.

UCB/EERC-83/07 "Dynamic Analysis of Multiply Tuned and Arbitrarily Supported Secondary Systems," by Igusa, T. and Der Kiureghian, A., July 1983, (PB84 118 272)A11.

UCB/EERC-83/08 "A Laboratory Study of Submerged Multi-body Systems in Earthquakes," by Ansari, G.R., June 1983, (PB83 261 842)A17.

UCB/EERC-83/09 "Effects of Transient Foundation Uplift on Earthquake Response of Structures," by Yim, C.-S. and Chopra, A.K., June 1983, (PB83 261 396)A07.

UCB/EERC-83/10 "Optimal Design of Friction-Braced Frames under Seismic Loading," by Austin, M.A. and Pister, K.S., June 1983, (PB84 119 288)A06.

UCB/EERC-83/11 "Shaking Table Study of Single-Story Masonry Houses. Dynamic Performance under Three Component Seismic Input and Recommendations," by Manos, G.C., Clough, R.W. and Mayes, R.L., July 1983, (UCB/EERC-83/11)A08.

UCB/EERC-83/12 "Experimental Error Propagation in Pseudodynamic Testing," by Shing, P.B. and Mahin, S.A., June 1983, (PB84 119 270)A09.

UCB/EERC-83/13 "Experimental and Analytical Predictions of the Mechanical Characteristics of a 1/5-scale Model of a 7-story R/C Frame-Wall Building Structure," by Aktan, A.E., Bertero, V.V., Chowdhury, A.A. and Nagashima, T., June 1983, (PB84 119 213)A07.

UCB/EERC-83/14 "Shaking Table Tests of Large-Panel Precast Concrete Building System Assemblages," by Oliva, M.G. and Clough, R.W., June 1983, (PB86 110 210/AS)A11.

UCB/EERC-83/15 "Seismic Behavior of Active Beam Links in Eccentrically Braced Frames," by Hjelmstad, K.D. and Popov, E.P., July 1983, (PB84 119 676)A09.

UCB/EERC-83/16 "System Identification of Structures with Joint Rotation," by Dimsdale, J.S., July 1983, (PB84 192 210)A06.

UCB/EERC-83/17 "Construction of Inelastic Response Spectra for Single-Degree-of-Freedom Systems," by Mahin, S. and Lin, J., June 1983, (PB84 208 834)A05.

UCB/EERC-83/18 "Interactive Computer Analysis Methods for Predicting the Inelastic Cyclic Behaviour of Structural Sections," by Kaba, S. and Mahin, S., July 1983, (PB84 192 012)A06.

UCB/EERC-83/19 "Effects of Bond Deterioration on Hysteretic Behavior of Reinforced Concrete Joints," by Filippou, F.C., Popov, E.P. and Bertero, V.V., August 1983, (PB84 192 020)A10.

UCB/EERC-83/20 "Correlation of Analytical and Experimental Responses of Large-Panel Precast Building Systems," by Oliva, M.G., Clough, R.W., Velkov, M. and Gavrilovic, P., May 1988, (PB90 262 692)A06.

UCB/EERC-83/21 "Mechanical Characteristics of Materials Used in a 1/5 Scale Model of a 7-Story Reinforced Concrete Test Structure," by Bertero, V.V., Aktan, A.E., Harris, H.G. and Chowdhury, A.A., October 1983, (PB84 193 697)A05.

UCB/EERC-83/22 "Hybrid Modelling of Soil-Structure Interaction in Layered Media," by Tzong, T.-J. and Penzien, J., October 1983, (PB84 192 178)A08.

UCB/EERC-83/23 "Local Bond Stress-Slip Relationships of Deformed Bars under Generalized Excitations," by Eligehausen, R., Popov, E.P. and Bertero, V.V., October 1983, (PB84 192 848)A09.

UCB/EERC-83/24 "Design Considerations for Shear Links in Eccentrically Braced Frames," by Malley, J.O. and Popov, E.P., November 1983, (PB84 192 186)A07.

UCB/EERC-84/01 "Pseudodynamic Test Method for Seismic Performance Evaluation: Theory and Implementation," by Shing, P.-S.B. and Mahin, S.A., January 1984, (PB84 190 644)A08.

UCB/EERC-84/02 "Dynamic Response Behavior of Kiang Hong Dian Dam," by Clough, R.W., Chang, K.-T., Chen, H.-Q. and Stephen, R.M., April 1984, (PB84 209 402)A08.

UCB/EERC-84/03 "Refined Modelling of Reinforced Concrete Columns for Seismic Analysis," by Kaba, S.A. and Mahin, S.A., April 1984, (PB84 234 384)A06.

UCB/EERC-84/04 "A New Floor Response Spectrum Method for Seismic Analysis of Multiply Supported Secondary Systems," by Asfura, A. and Der Kiureghian, A., June 1984, (PB84 239 417)A06.

UCB/EERC-84/05 "Earthquake Simulation Tests and Associated Studies of a 1/5th-scale Model of a 7-Story R/C Frame-Wall Test Structure," by Bertero, V.V., Aktan, A.E., Charney, F.A. and Sause, R., June 1984, (PB84 239 409)A09.

UCB/EERC-84/06 "Unassigned," by Unassigned, 1984.

UCB/EERC-84/07 "Behavior of Interior and Exterior Flat-Plate Connections Subjected to Inelastic Load Reversals," by Zee, H.L. and Moehle, J.P., August 1984, (PB86 117 629/AS)A07.

UCB/EERC-84/08 "Experimental Study of the Seismic Behavior of a Two-Story Flat-Plate Structure," by Moehle, J.P. and Diebold, J.W., August 1984, (PB86 122 553/AS)A12.

UCB/EERC-84/09 "Phenomenological Modeling of Steel Braces under Cyclic Loading," by Ikeda, K., Mahin, S.A. and Dermitzakis, S.N., May 1984, (PB86 132 198/AS)A08.

UCB/EERC-84/10 "Earthquake Analysis and Response of Concrete Gravity Dams," by Fenves, G.L. and Chopra, A.K., August 1984, (PB85 193 902/AS)A11.

UCB/EERC-84/11 "EAGD-84: A Computer Program for Earthquake Analysis of Concrete Gravity Dams," by Fenves, G.L. and Chopra, A.K., August 1984, (PB85 193 613/AS)A05.

UCB/EERC-84/12 "A Refined Physical Theory Model for Predicting the Seismic Behavior of Braced Steel Frames," by Ikeda, K. and Mahin, S.A., July 1984, (PB85 191 450/AS)A09.

UCB/EERC-84/13 "Earthquake Engineering Research at Berkeley - 1984," by EERC, August 1984, (PB85 197 341/AS)A10.

UCB/EERC-84/14 "Moduli and Damping Factors for Dynamic Analyses of Cohesionless Soils," by Seed, H.B., Wong, R.T., Idriss, I.M. and Tokimatsu, K., September 1984, (PB85 191 468/AS)A04.

UCB/EERC-84/15 "The Influence of SPT Procedures in Soil Liquefaction Resistance Evaluations," by Seed, H.B., Tokimatsu, K., Harder, L.F. and Chung, R.M., October 1984, (PB85 191 732/AS)A04.

UCB/EERC-84/16 "Simplified Procedures for the Evaluation of Settlements in Sands Due to Earthquake Shaking," by Tokimatsu, K. and Seed, H.B., October 1984, (PB85 197 887/AS)A05.

UCB/EERC-84/17 "Evaluation of Energy Absorption Characteristics of Highway Bridges Under Seismic Conditions - Volume I (PB90 262 627)A16 and Volume II (Appendices) (PB90 262 635)A13," by Imbsen, R.A. and Penzien, J., September 1986.

UCB/EERC-84/18 "Structure-Foundation Interactions under Dynamic Loads," by Liu, W.D. and Penzien, J., November 1984, (PB87 124 889/AS)A11.

UCB/EERC-84/19 "Seismic Modelling of Deep Foundations," by Chen, C.-H. and Penzien, J., November 1984, (PB87 124 798/AS)A07.

UCB/EERC-84/20 "Dynamic Response Behavior of Quan Shui Dam," by Clough, R.W., Chang, K.-T., Chen, H.-Q., Stephen, R.M., Ghanaat, Y. and Qi, J.-H., November 1984, (PB86 115177/AS)A07.

UCB/EERC-85/01 "Simplified Methods of Analysis for Earthquake Resistant Design of Buildings," by Cruz, E.F. and Chopra, A.K., February 1985, (PB86 112299/AS)A12.

UCB/EERC-85/02 "Estimation of Seismic Wave Coherency and Rupture Velocity using the SMART 1 Strong-Motion Array Recordings," by Abrahamson, N.A., March 1985, (PB86 214 343)A07.

UCB/EERC-85/03 "Dynamic Properties of a Thirty Story Condominium Tower Building," by Stephen, R.M., Wilson, E.L. and Stander, N., April 1985, (PB86 118965/AS)A06.

UCB/EERC-85/04 "Development of Substructuring Techniques for On-Line Computer Controlled Seismic Performance Testing," by Dermitzakis, S. and Mahin, S., February 1985, (PB86 132941/AS)A08.

UCB/EERC-85/05 "A Simple Model for Reinforcing Bar Anchorages under Cyclic Excitations," by Filippou, F.C., March 1985, (PB86 112 919/AS)A05.

UCB/EERC-85/06 "Racking Behavior of Wood-framed Gypsum Panels under Dynamic Load," by Oliva, M.G., June 1985, (PB90 262 643)A04.

UCB/EERC-85/07 "Earthquake Analysis and Response of Concrete Arch Dams," by Fok, K.-L. and Chopra, A.K., June 1985, (PB86 139672/AS)A10.

UCB/EERC-85/08 "Effect of Inelastic Behavior on the Analysis and Design of Earthquake Resistant Structures," by Lin, J.P. and Mahin, S.A., June 1985, (PB86 135340/AS)A08.

UCB/EERC-85/09 "Earthquake Simulator Testing of a Base-Isolated Bridge Deck," by Kelly, J.M., Buckle, I.G. and Tsai, H.-C., January 1986, (PB87 124 152/AS)A06.

UCB/EERC-85/10 "Simplified Analysis for Earthquake Resistant Design of Concrete Gravity Dams," by Fenves, G.L. and Chopra, A.K., June 1985, (PB87 124 160/AS)A08.

UCB/EERC-85/11 "Dynamic Interaction Effects in Arch Dams," by Clough, R.W., Chang, K.-T., Chen, H.-Q. and Ghanaat, Y., October 1985, (PB86 135027/AS)A05.

UCB/EERC-85/12 "Dynamic Response of Long Valley Dam in the Mammoth Lake Earthquake Series of May 25-27, 1980," by Lai, S. and Seed, H.B., November 1985, (PB86 142304/AS)A05.

UCB/EERC-85/13 "A Methodology for Computer-Aided Design of Earthquake-Resistant Steel Structures," by Austin, M.A., Pister, K.S. and Mahin, S.A., December 1985, (PB86 159480/AS)A10.

UCB/EERC-85/14 "Response of Tension-Leg Platforms to Vertical Seismic Excitations," by Liou, G.-S., Penzien, J. and Yeung, R.W., December 1985, (PB87 124 871/AS)A08.

UCB/EERC-85/15 "Cyclic Loading Tests of Masonry Single Piers: Volume 4 - Additional Tests with Height to Width Ratio of 1," by Sveinsson, B., McNiven, H.D. and Sucuoglu, H., December 1985, (PB87 165031/AS)A08.

UCB/EERC-85/16 "An Experimental Program for Studying the Dynamic Response of a Steel Frame with a Variety of Infill Partitions," by Yanev, B. and McNiven, H.D., December 1985, (PB90 262 676)A05.

UCB/EERC-86/01 "A Study of Seismically Resistant Eccentrically Braced Steel Frame Systems," by Kasai, K. and Popov, E.P., January 1986, (PB87 124 178/AS)A14.

UCB/EERC-86/02 "Design Problems in Soil Liquefaction," by Seed, H.B., February 1986, (PB87 124 186/AS)A03.

UCB/EERC-86/03 "Implications of Recent Earthquakes and Research on Earthquake-Resistant Design and Construction of Buildings," by Bertero, V.V., March 1986, (PB87 124 194/AS)A05.

UCB/EERC-86/04 "The Use of Load Dependent Vectors for Dynamic and Earthquake Analyses," by Leger, P., Wilson, E.L. and Clough, R.W., March 1986, (PB87 124 202/AS)A12.

UCB/EERC-86/05 "Two Beam-To-Column Web Connections," by Tsai, K.-C. and Popov, E.P., April 1986, (PB87 124 301/AS)A04.

UCB/EERC-86/06 "Determination of Penetration Resistance for Coarse-Grained Soils using the Becker Hammer Drill," by Harder, L.F. and Seed, H.B., May 1986, (PB87 124 210/AS)A07.

UCB/EERC-86/07 "A Mathematical Model for Predicting the Nonlinear Response of Unreinforced Masonry Walls to In-Plane Earthquake Excitations," by Mengi, Y. and McNiven, H.D., May 1986, (PB87 124 780/AS)A06.

UCB/EERC-86/08 "The 19 September 1985 Mexico Earthquake: Building Behavior," by Bertero, V.V., July 1986.

UCB/EERC-86/09 "EACD-3D: A Computer Program for Three-Dimensional Earthquake Analysis of Concrete Dams," by Fok, K.-L., Hall, J.F. and Chopra, A.K., July 1986, (PB87 124 228/AS)A08.

UCB/EERC-86/10 "Earthquake Simulation Tests and Associated Studies of a 0.3-Scale Model of a Six-Story Concentrically Braced Steel Structure," by Uang, C.-M. and Bertero, V.V., December 1986, (PB87 163 564/AS)A17.

UCB/EERC-86/11 "Mechanical Characteristics of Base Isolation Bearings for a Bridge Deck Model Test," by Kelly, J.M., Buckle, I.G. and Koh, C.-G., November 1987, (PB90 262 668)A04.

UCB/EERC-86/12 "Effects of Axial Load on Elastomeric Isolation Bearings," by Koh, C.-G. and Kelly, J.M., November 1987.

UCB/EERC-87/01 "The FPS Earthquake Resisting System: Experimental Report," by Zayas, V.A., Low, S.S. and Mahin, S.A., June 1987, (PB88 170 287)A06.

UCB/EERC-87/02 "Earthquake Simulator Tests and Associated Studies of a 0.3-Scale Model of a Six-Story Eccentrically Braced Steel Structure," by Whittaker, A., Uang, C.-M. and Bertero, V.V., July 1987, (PB88 166 707/AS)A18.

UCB/EERC-87/03 "A Displacement Control and Uplift Restraint Device for Base-Isolated Structures," by Kelly, J.M., Griffith, M.C. and Aiken, I.D., April 1987, (PB88 169 933)A04.

UCB/EERC-87/04 "Earthquake Simulator Testing of a Combined Sliding Bearing and Rubber Bearing Isolation System," by Kelly, J.M. and Chalhoub, M.S., December 1990.

UCB/EERC-87/05 "Three-Dimensional Inelastic Analysis of Reinforced Concrete Frame-Wall Structures," by Moazzami, S. and Bertero, V.V., May 1987, (PB88 169 586/AS)A08.

UCB/EERC-87/06 "Experiments on Eccentrically Braced Frames with Composite Floors," by Ricles, J. and Popov, E., June 1987, (PB88 173 067/AS)A14.

UCB/EERC-87/07 "Dynamic Analysis of Seismically Resistant Eccentrically Braced Frames," by Ricles, J. and Popov, E., June 1987, (PB88 173 075/AS)A16.

UCB/EERC-87/08 "Undrained Cyclic Triaxial Testing of Gravels-The Effect of Membrane Compliance," by Evans, M.D. and Seed, H.B., July 1987, (PB88 173 257)A19.

UCB/EERC-87/09 "Hybrid Solution Techniques for Generalized Pseudo-Dynamic Testing," by Thewalt, C. and Mahin, S.A., July 1987, (PB 88 179 007)A07.

UCB/EERC-87/10 "Ultimate Behavior of Butt Welded Splices in Heavy Rolled Steel Sections," by Bruneau, M., Mahin, S.A. and Popov, E.P., September 1987, (PB90 254 285)A07.

UCB/EERC-87/11 "Residual Strength of Sand from Dam Failures in the Chilean Earthquake of March 3, 1985," by De Alba, P., Seed, H.B., Retamal, E. and Seed, R.B., September 1987, (PB88 174 321/AS)A03.

UCB/EERC-87/12 "Inelastic Seismic Response of Structures with Mass or Stiffness Eccentricities in Plan," by Bruneau, M. and Mahin, S.A., September 1987, (PB90 262 650/AS)A14.

UCB/EERC-87/13 "CSTRUCT: An Interactive Computer Environment for the Design and Analysis of Earthquake Resistant Steel Structures," by Austin, M.A., Mahin, S.A. and Pister, K.S., September 1987, (PB88 173 339/AS)A06.

UCB/EERC-87/14 "Experimental Study of Reinforced Concrete Columns Subjected to Multi-Axial Loading," by Low, S.S. and Moehle, J.P., September 1987, (PB88 174 347/AS)A07.

UCB/EERC-87/15 "Relationships between Soil Conditions and Earthquake Ground Motions in Mexico City in the Earthquake of Sept. 19, 1985," by Seed, H.B., Romo, M.P., Sun, J., Jaime, A. and Lysmer, J., October 1987, (PB88 178 991)A06.

UCB/EERC-87/16 "Experimental Study of Seismic Response of R. C. Setback Buildings," by Shahrooz, B.M. and Moehle, J.P., October 1987, (PB88 176 359)A16.

UCB/EERC-87/17 "The Effect of Slabs on the Flexural Behavior of Beams," by Pantazopoulou, S.J. and Moehle, J.P., October 1987, (PB90 262 700)A07.

UCB/EERC-87/18 "Design Procedure for R-FBI Bearings," by Mostaghel, N. and Kelly, J.M., November 1987, (PB90 262 718)A04.

UCB/EERC-87/19 "Analytical Models for Predicting the Lateral Response of R C Shear Walls: Evaluation of their Reliability," by Vulcano, A. and Bertero, V.V., November 1987, (PB88 178 983)A05.

UCB/EERC-87/20 "Earthquake Response of Torsionally-Coupled Buildings," by Hejal, R. and Chopra, A.K., December 1987.

UCB/EERC-87/21 "Dynamic Reservoir Interaction with Monticello Dam," by Clough, R.W., Ghanaat, Y. and Qiu, X-F., December 1987, (PB88 179 023)A07.

UCB/EERC-87/22 "Strength Evaluation of Coarse-Grained Soils," by Siddiqi, F.H., Seed, R.B., Chan, C.K., Seed, H.B. and Pyke, R.M., December 1987, (PB88 179 031)A04.

UCB/EERC-88/01 "Seismic Behavior of Concentrically Braced Steel Frames," by Khatib, I., Mahin, S.A. and Pister, K.S., January 1988, (PB91 210 898/AS)A11.

UCB/EERC-88/02 "Experimental Evaluation of Seismic Isolation of Medium-Rise Structures Subject to Uplift," by Griffith, M.C., Kelly, J.M., Coveney, V.A. and Koh, C.G., January 1988, (PB91 217 950/AS)A09.

UCB/EERC-88/03 "Cyclic Behavior of Steel Double Angle Connections," by Astaneh-Asl, A. and Nader, M.N., January 1988, (PB91 210 872)A05.

UCB/EERC-88/04 "Re-evaluation of the Slide in the Lower San Fernando Dam in the Earthquake of Feb. 9, 1971," by Seed, H.B., Seed, R.B., Harder, L.F. and Jong, H.-L., April 1988, (PB91 212 456/AS)A07.

UCB/EERC-88/05 "Experimental Evaluation of Seismic Isolation of a Nine-Story Braced Steel Frame Subject to Uplift," by Griffith, M.C., Kelly, J.M. and Aiken, I.D., May 1988, (PB91 217 968/AS)A07.

UCB/EERC-88/06 "DRAIN-2DX User Guide.," by Allahabadi, R. and Powell, G.H., March 1988, (PB91 212 530)A12.

UCB/EERC-88/07 "Theoretical and Experimental Studies of Cylindrical Water Tanks in Base-Isolated Structures," by Chalhoub, M.S. and Kelly, J.M., April 1988, (PB91 217 976/AS)A05.

UCB/EERC-88/08 "Analysis of Near-Source Waves: Separation of Wave Types Using Strong Motion Array Recordings," by Darragh, R.B., June 1988, (PB91 212 621)A08.

UCB/EERC-88/09 "Alternatives to Standard Mode Superposition for Analysis of Non-Classically Damped Systems," by Kusainov, A.A. and Clough, R.W., June 1988, (PB91 217 992/AS)A04.

UCB/EERC-88/10 "The Landslide at the Port of Nice on October 16, 1979," by Seed, H.B., Seed, R.B., Schlosser, F., Blondeau, F. and Juran, I., June 1988, (PB91 210 914)A05.

UCB/EERC-88/11 "Liquefaction Potential of Sand Deposits Under Low Levels of Excitation," by Carter, D.P. and Seed, H.B., August 1988, (PB91 210 880)A15.

UCB/EERC-88/12 "Nonlinear Analysis of Reinforced Concrete Frames Under Cyclic Load Reversals," by Filippou, F.C. and Issa, A., September 1988, (PB91 212 589)A07.

UCB/EERC-88/13 "Implications of Recorded Earthquake Ground Motions on Seismic Design of Building Structures," by Uang, C.-M. and Bertero, V.V., November 1988, (PB91 212 548)A06.

UCB/EERC-88/14 "An Experimental Study of the Behavior of Dual Steel Systems," by Whittaker, A.S., Uang, C.-M. and Bertero, V.V., September 1988, (PB91 212 712)A16.

UCB/EERC-88/15 "Dynamic Moduli and Damping Ratios for Cohesive Soils," by Sun, J.I., Golesorkhi, R. and Seed, H.B., August 1988, (PB91 210 922)A04.

UCB/EERC-88/16 "Reinforced Concrete Flat Plates Under Lateral Load: An Experimental Study Including Biaxial Effects," by Pan, A. and Moehle, J.P., October 1988, (PB91 210 856)A13.

UCB/EERC-88/17 "Earthquake Engineering Research at Berkeley - 1988," by EERC, November 1988, (PB91 210 864)A10.

UCB/EERC-88/18 "Use of Energy as a Design Criterion in Earthquake-Resistant Design," by Uang, C.-M. and Bertero, V.V., November 1988, (PB91 210 906/AS)A04.

UCB/EERC-88/19 "Steel Beam-Column Joints in Seismic Moment Resisting Frames," by Tsai, K.-C. and Popov, E.P., November 1988, (PB91 217 984/AS)A20.

UCB/EERC-88/20 "Base Isolation in Japan, 1988," by Kelly, J.M., December 1988, (PB91 212 449)A05.

UCB/EERC-89/01 "Behavior of Long Links in Eccentrically Braced Frames," by Engelhardt, M.D. and Popov, E.P., January 1989, (PB92 143 056)A18.

UCB/EERC-89/02 "Earthquake Simulator Testing of Steel Plate Added Damping and Stiffness Elements," by Whittaker, A., Bertero, V.V., Alonso, J. and Thompson, C., January 1989, (PB91 229 252/AS)A10.

UCB/EERC-89/03 "Implications of Site Effects in the Mexico City Earthquake of Sept. 19, 1985 for Earthquake-Resistant Design Criteria in the San Francisco Bay Area of California," by Seed, H.B. and Sun, J.I., March 1989, (PB91 229 369/AS)A07.

UCB/EERC-89/04 "Earthquake Analysis and Response of Intake-Outlet Towers," by Goyal, A. and Chopra, A.K., July 1989, (PB91 229 286/AS)A19.

UCB/EERC-89/05 "The 1985 Chile Earthquake: An Evaluation of Structural Requirements for Bearing Wall Buildings," by Wallace, J.W. and Moehle, J.P., July 1989, (PB91 218 008/AS)A13.

UCB/EERC-89/06 "Effects of Spatial Variation of Ground Motions on Large Multiply-Supported Structures," by Hao, H., July 1989, (PB91 229 161/AS)A08.

UCB/EERC-89/07 "EADAP - Enhanced Arch Dam Analysis Program: Users's Manual," by Ghanaat, Y. and Clough, R.W., August 1989, (PB91 212 522)A06.

UCB/EERC-89/08 "Seismic Performance of Steel Moment Frames Plastically Designed by Least Squares Stress Fields," by Ohi, K. and Mahin, S.A., August 1989, (PB91 212 597)A05.

UCB/EERC-89/09 "Feasibility and Performance Studies on Improving the Earthquake Resistance of New and Existing Buildings Using the Friction Pendulum System," by Zayas, V., Low, S., Mahin, S.A. and Bozzo, L., July 1989, (PB92 143 064)A14.

UCB/EERC-89/10 "Measurement and Elimination of Membrane Compliance Effects in Undrained Triaxial Testing," by Nicholson, P.G., Seed, R.B. and Anwar, H., September 1989, (PB92 139 641/AS)A13.

UCB/EERC-89/11 "Static Tilt Behavior of Unanchored Cylindrical Tanks," by Lau, D.T. and Clough, R.W., September 1989, (PB92 143 049)A10.

UCB/EERC-89/12 "ADAP-88: A Computer Program for Nonlinear Earthquake Analysis of Concrete Arch Dams," by Fenves, G.L., Mojtahedi, S. and Reimer, R.B., September 1989, (PB92 139 674/AS)A07.

UCB/EERC-89/13 "Mechanics of Low Shape Factor Elastomeric Seismic Isolation Bearings," by Aiken, I.D., Kelly, J.M. and Tajirian, F.F., November 1989, (PB92 139 732/AS)A09.

UCB/EERC-89/14 "Preliminary Report on the Seismological and Engineering Aspects of the October 17, 1989 Santa Cruz (Loma Prieta) Earthquake," by EERC, October 1989, (PB92 139 682/AS)A04.

UCB/EERC-89/15 "Experimental Studies of a Single Story Steel Structure Tested with Fixed, Semi-Rigid and Flexible Connections," by Nader, M.N. and Astaneh-Asl, A., August 1989, (PB91 229 211/AS)A10.

UCB/EERC-89/16 "Collapse of the Cypress Street Viaduct as a Result of the Loma Prieta Earthquake," by Nims, D.K., Miranda, E., Aiken, I.D., Whittaker, A.S. and Bertero, V.V., November 1989, (PB91 217 935/AS)A05.

UCB/EERC-90/01 "Mechanics of High-Shape Factor Elastomeric Seismic Isolation Bearings," by Kelly, J.M., Aiken, I.D. and Tajirian, F.F., March 1990.

UCB/EERC-90/02 "Javid's Paradox: The Influence of Preform on the Modes of Vibrating Beams," by Kelly, J.M., Sackman, J.L. and Javid, A., May 1990, (PB91 217 943/AS)A03.

UCB/EERC-90/03 "Earthquake Simulator Testing and Analytical Studies of Two Energy-Absorbing Systems for Multistory Structures," by Aiken, I.D. and Kelly, J.M., October 1990, (PB92 192 988)A13.

UCB/EERC-90/04 "Damage to the San Francisco-Oakland Bay Bridge During the October 17, 1989 Earthquake," by Astaneh-Asl, A., June 1990.

UCB/EERC-90/05 "Preliminary Report on the Principal Geotechnical Aspects of the October 17, 1989 Loma Prieta Earthquake," by Seed, R.B., Dickenson, S.E., Riemer, M.F., Bray, J.D., Sitar, N., Mitchell, J.K., Idriss, I.M., Kayen, R.E., Kropp, A., Harder, L.F., Jr. and Power, M.S., April 1990, (PB 192 970)A08.

UCB/EERC-90/06 "Models of Critical Regions in Reinforced Concrete Frames Under Seismic Excitations," by Zulfiqar, N. and Filippou, F.C., May 1990.

UCB/EERC-90/07 "A Unified Earthquake-Resistant Design Method for Steel Frames Using ARMA Models," by Takewaki, I., Conte, J.P., Mahin, S.A. and Pister, K.S., June 1990.

UCB/EERC-90/08 "Soil Conditions and Earthquake Hazard Mitigation in the Marina District of San Francisco," by Mitchell, J.K., Masood, T., Kayen, R.E. and Seed, R.B., May 1990, (PB 193 267/AS)A04.

UCB/EERC-90/09 "Influence of the Earthquake Ground Motion Process and Structural Properties on Response Characteristics of Simple Structures," by Conte, J.P., Pister, K.S. and Mahin, S.A., July 1990, (PB92 143 064)A15.

UCB/EERC-90/10 "Experimental Testing of the Resilient-Friction Base Isolation System," by Clark, P.W. and Kelly, J.M., July 1990, (PB92 143 072)A08.

UCB/EERC-90/11 "Seismic Hazard Analysis: Improved Models, Uncertainties and Sensitivities," by Araya, R. and Der Kiureghian, A., March 1988.

UCB/EERC-90/12 "Effects of Torsion on the Linear and Nonlinear Seismic Response of Structures," by Sedarat, H. and Bertero, V.V., September 1989, (PB92 193 002/AS)A15.

UCB/EERC-90/13 "The Effects of Tectonic Movements on Stresses and Deformations in Earth Embankments," by Bray, J. D., Seed, R. B. and Seed, H. B., September 1989.

UCB/EERC-90/14 "Inelastic Seismic Response of One-Story, Asymmetric-Plan Systems," by Goel, R.K. and Chopra, A.K., October 1990.

UCB/EERC-90/15 "Dynamic Crack Propagation: A Model for Near-Field Ground Motion," by Seyyedian, H. and Kelly, J.M., 1990.

UCB/EERC-90/16 "Sensitivity of Long-Period Response Spectra to System Initial Conditions," by Blasquez, R., Ventura, C. and Kelly, J.M., 1990.

UCB/EERC-90/17 "Behavior of Peak Values and Spectral Ordinates of Near-Source Strong Ground-Motion over a Dense Array," by Niazi, M., June 1990.

UCB/EERC-90/18 "Material Characterization of Elastomers used in Earthquake Base Isolation," by Papoulia, K.D. and Kelly, J.M., 1990.

UCB/EERC-90/19 "Cyclic Behavior of Steel Top-and-Bottom Plate Moment Connections," by Harriott, J.D. and Astaneh-Asl, A., August 1990. (PB91 229 260/AS)A05.

UCB/EERC-90/20 "Seismic Response Evaluation of an Instrumented Six Story Steel Building," by Shen, J.-H. and Astaneh-Asl, A., December 1990. (PB91 229 294/AS)A04.

UCB/EERC-90/21 "Observations and Implications of Tests on the Cypress Street Viaduct Test Structure," by Bollo, M., Mahin, S.A., Moehle, J.P., Stephen, R.M. and Qi, X., December 1990.

UCB/EERC-91/01 "Experimental Evaluation of Nitinol for Energy Dissipation in Structures," by Nims, D.K., Sasaki, K.K. and Kelly, J.M., 1991.

UCB/EERC-91/02 "Displacement Design Approach for Reinforced Concrete Structures Subjected to Earthquakes," by Qi, X. and Moehle, J.P., January 1991.

UCB/EERC-91/03 "A Long-Period Isolation System Using Low-Modulus High-Damping Isolators for Nuclear Facilities at Soft-Soil Sites," by Kelly, J.M., March 1991.

UCB/EERC-91/04 "Dynamic and Failure Characteristics of Bridgestone Isolation Bearings," by Kelly, J.M., April 1991.

UCB/EERC-91/05 "Base Sliding Response of Concrete Gravity Dams to Earthquakes," by Chopra, A.K. and Zhang, L., May 1991.

UCB/EERC-91/06 "Computation of Spatially Varying Ground Motion and Foundation-Rock Impedance Matrices for Seismic Analysis of Arch Dams," by Zhang, L. and Chopra, A.K., May 1991.

UCB/EERC-91/07 "Estimation of Seismic Source Processes Using Strong Motion Array Data," by Chiou, S.-J., July 1991.

UCB/EERC-91/08 "A Response Spectrum Method for Multiple-Support Seismic Excitations," by Der Kiureghian, A. and Neuenhofer, A., August 1991.

UCB/EERC-91/09 "A Preliminary Study on Energy Dissipating Cladding-to-Frame Connection," by Conen, J.M. and Powell, G.H., September 1991.

UCB/EERC-91/10 "Evaluation of Seismic Performance of a Ten-Story RC Building During the Whittier Narrows Earthquake," by Miranda, E. and Bertero, V.V., October 1991.

UCB/EERC-91/11 "Seismic Performance of an Instrumented Six Story Steel Building," by Anderson, J.C. and Bertero, V.V., November 1991.

UCB/EERC-91/12 "Performance of Improved Ground During the Loma Prieta Earthquake," by Mitchell, J.K. and Wentz, Jr., F.J., October 1991.

UCB/EERC-91/13 "Shaking Table - Structure Interaction," by Rinawi, A.M. and Clough, R.W., October 1991.

UCB/EERC-91/14 "Cyclic Response of RC Beam-Column Knee Joints: Test and Retrofit," by Mazzoni, S., Moehle, J.P. and Thewalt, C.R., October 1991.

UCB/EERC-91/15 "Design Guidelines for Ductility and Drift Limits: Review of State-of-the-Practice and State-of-the-Art in Ductility and Drift-Based Earthquake-Resistant Design of Buildings," by Bertero, V.V., Anderson, J.C., Krawinkler, H., Miranda, E. and The CUREe and The Kajima Research Teams., July 1991.

UCB/EERC-91/16 "Evaluation of the Seismic Performance of a Thirty-Story RC Building," by Anderson, J.C., Miranda, E., Bertero, V.V. and The Kajima Project Research Team,, July 1991.

UCB/EERC-91/17 "A Fiber Beam-Column Element for Seismic Response Analysis of Reinforced Concrete Structures," by Taucer, F., Spacone, E. and Filippou, F.C., December 1991.

UCB/EERC-91/18 "Investigation of the Seismic Response of a Lightly-Damped Torsionally-Coupled Building," by Boroschek, R. and Mahin, S.A., December 1991.

UCB/EERC-92/01 "Studies of a 49-Story Instrumented Steel Structure Shaken During the Loma Prieta Earthquake," by Chen, C.-C., Bonowitz, D. and Astaneh-Asl, A., February 1992.

UCB/EERC-92/02 "Response of the Dumbarton Bridge in the Loma Prieta Earthquake," by Fenves, G.L., Filippou, F.C. and Sze, D.T., January 1992.

UCB/EERC-92/03 "Models for Nonlinear Earthquake Analysis of Brick Masonry Buildings," by Mengi, Y., McNiven, H.D. and Tanrikulu, A.K., March 1992.

UCB/EERC-92/04 "Shear Strength and Deformability of RC Bridge Columns Subjected to Inelastic Cyclic Displacements," by Aschheim, M. and Moehle, J.P., March 1992.

UCB/EERC-92/05 "Parameter Study of Joint Opening Effects on Earthquake Response of Arch Dams," by Fenves, G.L., Mojtahedi, S. and Reimer, R.B., April 1992.

UCB/EERC-92/06 "Seismic Behavior and Design of Semi-Rigid Steel Frames," by Nader, M.N. and Astaneh-Asl, A., May 1992.

UCB/EERC-92/07 "A Beam Element for Seismic Damage Analysis," by Spacone, E., Ciampi, V. and Filippou, F.C., August 1992.

UCB/EERC-92/08 "Nonlinear Static and Dynamic Analysis of Reinforced Concrete Subassemblages," by Filippou, F.C., D'Ambrisi, A. and Issa, A., August 1992.

UCB/EERC-92/09 "Evaluation of Code Accidental-Torsion Provisions Using Earthquake Records from Three Nominally Symmetric-Plan Buildings," by De la Llera, J.C. and Chopra, A.K., September 1992.

UCB/EERC-92/10 "Slotted Bolted Connection Energy Dissipators," by Grigorian, C.E., Yang, T.-S. and Popov, E.P., July 1992.

UCB/EERC-92/11 "Mechanical Characteristics of Neoprene Isolation Bearings," by Kelly, J.M. and Quiroz, E., August 1992.

UCB/EERC-92/12 "Application of a Mass Damping System to Bridge Structures," by Hasegawa, K. and Kelly, J.M., August 1992.

UCB/EERC-92/13 "Earthquake Engineering Research at Berkeley - 1992," October 1992.